ORIGINAL ARTICLE

Cetuximab-Induced Anaphylaxis and IgE Specific for Galactose-α-1,3-Galactose

Christine H. Chung, M.D., Beloo Mirakhur, M.D., Ph.D., Emily Chan, M.D., Ph.D., Quynh-Thu Le, M.D., Jordan Berlin, M.D., Michael Morse, M.D., Barbara A. Murphy, M.D., Shama M. Satinover, M.S., Jacob Hosen, B.S., David Mauro, M.D., Ph.D., Robbert J. Slebos, Ph.D., Qinwei Zhou, Ph.D., Diane Gold, M.D., Tina Hatley, M.D., Daniel J. Hicklin, Ph.D., and Thomas A.E. Platts-Mills, M.D., Ph.D.

ABSTRACT

BACKGROUND

Cetuximab, a chimeric mouse–human IgG1 monoclonal antibody against the epidermal growth factor receptor, is approved for use in colorectal cancer and squamous-cell carcinoma of the head and neck. A high prevalence of hypersensitivity reactions to cetuximab has been reported in some areas of the United States.

METHODS

We analyzed serum samples from four groups of subjects for IgE antibodies against cetuximab: pretreatment samples from 76 case subjects who had been treated with cetuximab at multiple centers, predominantly in Tennessee, Arkansas, and North Carolina; samples from 72 control subjects in Tennessee; samples from 49 control subjects with cancer in northern California; and samples from 341 female control subjects in Boston.

RESULTS

Among 76 cetuximab-treated subjects, 25 had a hypersensitivity reaction to the drug. IgE antibodies against cetuximab were found in pretreatment samples from 17 of these subjects; only 1 of 51 subjects who did not have a hypersensitivity reaction had such antibodies ($P<0.001$). IgE antibodies against cetuximab were found in 15 of 72 samples (20.8%) from control subjects in Tennessee, in 3 of 49 samples (6.1%) from northern California, and in 2 of 341 samples (0.6%) from Boston. The IgE antibodies were shown to be specific for an oligosaccharide, galactose-α-1,3-galactose, which is present on the Fab portion of the cetuximab heavy chain.

CONCLUSIONS

In most subjects who had a hypersensitivity reaction to cetuximab, IgE antibodies against cetuximab were present in serum before therapy. The antibodies were specific for galactose-α-1,3-galactose.

From the Division of Hematology/Oncology, Department of Medicine (C.H.C., E.C., J.B., B.A.M.), the Department of Cancer Biology (C.H.C., R.J.S.), and the Department of Otolaryngology (R.J.S.), Vanderbilt University School of Medicine, Nashville; Bristol-Myers Squibb, Plainsboro, NJ (B.M., D.M.); Stanford University School of Medicine, Menlo Park, CA (Q.-T.L.); the Department of Medicine, Duke University Medical Center, Durham, NC (M.M.); Asthma and Allergic Diseases Center, University of Virginia, Charlottesville (S.M.S., J.H., T.A.E.P.-M.); ImClone Systems, Branchburg, NJ (Q.Z., D.J.H.); Channing Institute, Harvard University, Boston (D.G.); and Allergy and Asthma Clinic of Northwest Arkansas, Bentonville (T.H.). Address reprint requests to Dr. Platts-Mills at the Asthma and Allergic Disease Center, University of Virginia Medical School, Box 801355, Charlottesville, VA 22908, or at tap2z@virginia.edu.

Drs. Chung and Mirakhur contributed equally to this article.

N Engl J Med 2008;358:1109-17.
Copyright © 2008 Massachusetts Medical Society.

CSPC Exhibit 1004
Page 1 of 336
The New England Journal of Medicine
Downloaded from nejm.org at US PATENT & TRADEMARK OFFICE on March 19, 2019. For personal use only. No other uses without permission.
Copyright © 2008 Massachusetts Medical Society. All rights reserved.

Recombinant monoclonal antibodies have an increasing role in the treatment of cancers, inflammatory bowel disease, rheumatoid arthritis, and asthma.[1-3] These agents can cause rapidly developing, severe hypersensitivity reactions.[4-7] Cetuximab (Erbitux, Bristol-Myers Squibb and ImClone Systems), a chimeric mouse–human IgG_1 monoclonal antibody against the epidermal growth factor receptor (EGFR), is approved for use in metastatic colorectal cancer and squamous-cell carcinoma of the head and neck.[2,6,8-10] According to the drug's product label, severe hypersensitivity reactions to cetuximab occur in 3% of patients. However, higher rates and clusters of cases have been reported in North Carolina, Arkansas, Missouri, Virginia, and Tennessee.[6,9,11] A recent study showed that 22% of patients who were treated with cetuximab in Tennessee and North Carolina had severe hypersensitivity reactions.[11] In contrast, rates of hypersensitivity reactions were lower (<1%) in most centers in the Northeast.[11] A review of case reports on hypersensitivity reactions to cetuximab revealed that many such reactions occurred within minutes after the patient's first exposure to the drug and were compatible with IgE-mediated anaphylaxis.[11-13]

We investigated the hypothesis that severe hypersensitivity reactions occurring during the initial infusion of cetuximab are mediated by preexisting IgE antibodies against cetuximab. Using a recently developed assay,[14] we found such IgE antibodies in serum samples from case subjects and control subjects. Our results indicate that these antibodies, which are present before treatment, are a cause of severe hypersensitivity reactions to cetuximab. The antibodies are specific for an oligosaccharide, galactose-α-1,3-galactose, which is present on the Fab portion of the cetuximab heavy chain. Such IgE antibodies also bind to a range of mammalian proteins, a finding that is consistent with the expression of galactose-α-1,3-galactose on proteins from most nonprimate mammals. We also found that there is a high prevalence of the IgE antibody in areas of the United States where anaphylactic reactions to cetuximab have occurred.

METHODS

STUDY SUBJECTS

In addition to the samples from subjects who had received cetuximab therapy, we analyzed samples from three distinct locations in the United States to investigate the geographic differences in rates of hypersensitivity reaction (Table 1). In group 1, serum samples were available from 76 subjects with cancer who had received cetuximab and whose clinical response had been documented. The case reports were retrospectively evaluated in a blinded manner at Vanderbilt University Medical Center (VUMC), in Nashville. We used a prespecified case definition to determine the presence or absence of a hypersensitivity reaction within 2 hours after the administration of cetuximab and, if present, to score the severity of the reaction. The serum samples that we evaluated included 35 pretreatment samples from VUMC. These samples were obtained from all subjects who had been treated at VUMC for colorectal cancer or cancer of the head and neck between June 2005 and December 2006; of these subjects, 10 had a hypersensitivity reaction that met our case definition.

Group 1 also included 41 samples from subjects at the other centers, including subjects with a history of an adverse event after cetuximab treatment and a nonrandom selection of subjects with no such report. Fourteen of the subjects with an adverse event did not meet our case definition of a hypersensitivity reaction and were categorized as having had no hypersensitivity reaction. The serum samples included those from five subjects at Duke University Medical Center, in Durham, North Carolina (three of whom had a hypersensitivity reaction), and from nine subjects at the Allergy and Asthma Clinic of Northwest Arkansas, in Bentonville, Arkansas (four of whom had a hypersensitivity reaction). Medical reports and serum samples from 27 subjects (8 of whom had a hypersensitivity reaction) were collected from Bristol-Myers Squibb clinical trials at multiple sites.

Groups 2, 3, and 4 were the source of the control serum samples. Group 2 consisted of 72 healthy volunteers at a yearly cancer-screening event held at VUMC, who were matched with subjects with cancer at VUMC for age, sex, race or ethnic group, and smoking status. Group 3 consisted of 49 subjects with cancer of the head and neck (3 of whom had received cetuximab) who had presented at the Stanford University Medical Center, in Stanford, California. Group 4 consisted of 341 female control subjects who were mothers of children in a large cohort study in Boston.[15] Cohorts 3 and 4 were included as representative samples from areas in which there had been a low

CSPC Exhibit 1004
The New England Journal of Medicine
Page 2 of 336
Downloaded from nejm.org at US PATENT & TRADEMARK OFFICE on March 19, 2019. For personal use only. No other uses without permission.
Copyright © 2008 Massachusetts Medical Society. All rights reserved.

Table 1. **Characteristics of the Study Groups.***

Variable	Group 1		Group 2	Group 3	Group 4	Total
	Tennessee Case Subjects (N=35)	Other Case Subjects (N=41)	Tennessee Control Subjects (N=72)	California Control Subjects (N=49)	Boston Control Subjects (N=341)	All Groups (N=538)
Age (yr)						
Median	58	63	58	58	NA	58
Range	43–93	41–81	32–82	36–97		32–97
Sex						
Male:female ratio	22:13	22:19	40:32	37:12	0:341	121:417
Male (%)	63	54	56	76	0	22
Race or ethnic group (no.)†						
White	33	35	65	23	236	392
Black	2	5	7	2	54	70
Other	0	1	0	2	32	35
Unknown	0	0	0	22	19	41
Tobacco use (no.)						
Total						197
Current	18	14	16	0	NA	48
Former	3	11	25	0	NA	39
Never	13	16	31	0	NA	60
Unknown	1	0	0	49	341	391
Tumor site (no.)			NA		NA	
Total						125
Head and neck	18	5		49		72
Colorectal	17	35		0		52
Lung	0	1		0		1
Clinical stage (no.)			NA	NA	NA	
Total						76
I or II	9	4				13
III	8	6				14
IV	14	25				39
Unknown	4	6				10
Hypersensitivity reaction (no.)			NA	NA	NA	
Total						26
Rated by investigators						
Low-grade	6	7				13
High-grade	4	8				12
Late response	1	0				1
Rated retrospectively‡						
Low-grade	0	2				2
High-grade	11	13				24

* NA denotes not available.
† Race or ethnic group was reported by the subjects.
‡ Retrospective scoring of the severity of hypersensitivity reactions was performed by blinded analysis of case reports.

CSPC Exhibit 1004
Page 3 of 336
The New England Journal of Medicine
Downloaded from nejm.org at US PATENT & TRADEMARK OFFICE on March 19, 2019. For personal use only. No other uses without permission.
Copyright © 2008 Massachusetts Medical Society. All rights reserved.

prevalence (<1%) of hypersensitivity reactions during cetuximab treatment. The screening of 21 subjects with recurrent anaphylaxis who had presented at the University of Virginia Allergy Clinic identified 11 subjects with positive results on testing for IgE antibodies against cetuximab; serum from 6 of these subjects was used to develop the assays and evaluate specificity.

Representatives of Bristol-Myers Squibb and ImClone Systems reviewed the manuscript, which was written by Drs. Chung, Mirakhur, and Platts-Mills. The study was approved by the institutional review board at each center. Each subject provided written informed consent.

CASE DEFINITION AND GRADING SYSTEM

Our case definition and grading of hypersensitivity reactions were based on documented symptoms listed in the National Cancer Institute Common Toxicity Criteria, version 3.[11,16] The characteristics of a grade 1 reaction were transient flushing or rash with a fever of less than 38°C (100.4°F); those of a grade 2 reaction were rash or flushing, urticaria, and dyspnea with or without a fever of more than 38°C; and those of a grade 3 reaction were rash, dyspnea, and hypotension. A grade 4 reaction was anaphylaxis. Among 25 subjects who were judged to have had a hypersensitivity reaction, investigators identified 13 mild reactions (grade 1 or 2) and 12 severe reactions (grade 3 or 4) (Table 1). All treatment decisions were made by the local physicians before the serum samples were assayed for IgE antibodies.

EVALUATION OF ANTIGENS

Cetuximab, which is produced by expressing clone C225 in the mouse myeloma cell line SP2/0, was provided by ImClone Systems.[8,17] A variant of cetuximab, CHO-C225, which is produced in Chinese hamster ovary (CHO) cell lines, was also obtained from ImClone. CHO cells do not produce α-1,3-galactosyltransferase and, for this reason, have a pattern of glycosylation that differs from that of cetuximab.[17,18] This monoclonal antibody, which was purified by means of the techniques used for cetuximab, had the same affinity for EGFR as did cetuximab. The F(ab′)2 and Fc fragments of cetuximab were prepared by digestion with pepsin and papain, respectively, followed by purification over a protein A column. The molecular weights of these molecules were confirmed by sodium dodecyl sulfate–polyacrylamide-gel electrophoresis. Antigens were biotinylated with the use of sulfosuccinimidyl 6-(biotinamido) hexanoate (EZ-Link, Pierce Biotechnology).[14]

Rituximab (Genentech), an anti-CD20 monoclonal antibody, and infliximab (Centocor), a monoclonal antibody against tumor necrosis factor α, were obtained commercially. The reagent galactose-α-1,3-galactose-β-1,4-*N*-acetylglucosamine-β-spacer-biotin was purchased from GlycoTech. Mouse IgG was obtained from Immunology Consultants. Fel d 1, a cat allergen, was purified by affinity chromatography with the use of the monoclonal antibody clone 6F9.[19]

IMMUNOCAP IgE ASSAYS

ImmunoCAP is a variation of the radioallergosorbent test in which IgE antibodies that have bound to antigen on the solid phase are detected with a secondary enzyme-labeled anti-IgE antibody.[14,20] Total and specific IgE antibodies were measured with the use of either ImmunoCAP (Phadia U.S.) or the modified assay with streptavidin-coated ImmunoCAP.[14] All assays on serum samples from subjects who had received cetuximab were performed at the University of Virginia and analyzed in a fashion that was blinded to the scoring of subjects' hypersensitivity reactions. Cetuximab was biotinylated, and approximately 5 μg was added to each streptavidin-coated ImmunoCAP before serum was added. The assays were performed with the ImmunoCAP250 instrument, and the results were expressed as international units (IU) per milliliter (with 1 IU equivalent to approximately 2.4 ng). The threshold value for a positive reaction was 0.35 IU per milliliter. The streptavidin ImmunoCAP technique was also used to measure IgE antibodies against CHO-C225, the F(ab′)2 and Fc fragments, galactose-α-1,3-galactose, mouse IgG, rituximab, infliximab, and Fel d 1. ImmunoCAP assays were used to test selected serum samples for IgE antibodies against allergens from dust mites, cats, dogs, German cockroaches, grass pollen, ragweed pollen, beef, pork, and cow's milk.

STATISTICAL ANALYSIS

The limiting factor in our study was the number of serum samples available from subjects who had a hypersensitivity reaction. Using consistent grading criteria, we identified 25 such subjects, who were matched with sequential controls (for subjects

CSPC Exhibit 1004
The New England Journal of Medicine
Page 4 of 336
Downloaded from nejm.org at US PATENT & TRADEMARK OFFICE on March 19, 2019. For personal use only. No other uses without permission.
Copyright © 2008 Massachusetts Medical Society. All rights reserved.

from Tennessee) or with nonrandom controls (for subjects from centers in other states). We compared the results for IgE antibodies in these 25 subjects with results in 51 subjects who did not have a hypersensitivity reaction, using chi-square analysis, and expressed the results as the natural logarithm of the odds ratio. We compared quantitative measures of IgE antibodies against cetuximab and IgE antibodies against galactose-α-1,3-galactose and cat, beef, grass, pollen, and dust-mite allergens with the use of Spearman's rank-order correlation. Statistical analyses were performed with SPSS software, version 13.0 (SPSS). A two-sided P value of less than 0.05 was considered to indicate statistical significance.

RESULTS

SERUM ASSAYS FOR IgE ANTIBODIES

Serum samples that were positive for IgE antibodies against cetuximab had antibody titers ranging from 0.38 to 140.00 IU per milliliter. Table 2 shows results for 6 subjects who had anaphylaxis after receiving cetuximab, 11 subjects who had no reaction to cetuximab, and 6 who had recurrent anaphylaxis or angioedema unrelated to cetuximab

Table 2. IgE Antibodies against Cetuximab and the Fragments of the Molecule for 12 Subjects Who Had a Severe Hypersensitivity Reaction.*

Type of Reaction and Subject No.	Total IgE	Cetuximab†	Fragment of Cetuximab Molecule†		Rituximab†	Depletion with Anti-IgE Antibody‡	
			F(ab′)2	Fc		Total IgE Remaining	IgE Antibodies Remaining†
	international units per milliliter					*percent*	
Hypersensitivity reaction							
Anaphylaxis related to cetuximab							
1§	3161.0	41.6	40.9	0.35	0.35	1.3	1.0
2	887.0	38.8	52.3	ND	0.35	8.9	12.0
3§	374.0	20.2	26.0	0.35	0.35	3.4	3.2
4§	348.0	11.1	13.2	0.35	0.35	9.1	5.2
5	58.5	4.9	5.7	0.35	0.35	29.0	21.0
6§	22.2	4.2	6.6	0.35	0.35	15.0	8.4
Recurrent anaphylaxis unrelated to cetuximab¶							
7	1081.0	131.0	158.0	2.90	1.75	4.9	4.0
8	243.0	69.2	86.8	1.20	0.35	0.9	4.0
9	242.0	55.1	99.6	0.35	0.35	9.6	6.7
10	188.0	43.5	45.8	0.35	0.35	11.1	5.9
11	538.0	81.1	100.0	0.35	0.35	1.4	5.7
12	63.6	13.0	17.9	0.57	0.35	11.0	4.9
Mean	315.0‖	26.7	33.4	1.26**	NA	5.7	5.3
No hypersensitivity reaction	17.4††	0	0	0	0	NA	NA

* NA denotes not applicable, and ND not determined.
† The assay was performed with biotinylated antigen on streptavidin ImmunoCAP.
‡ Omalizumab (monoclonal anti-IgE antibody) that was bound to protein A agarose beads was incubated overnight at 4°C at a 1:5 bead-to-serum volume ratio.
§ The subject had grade 4 anaphylaxis.
¶ Subjects presented to the University of Virginia Allergic Disease Clinic with recurrent angioedema or anaphylaxis and had a positive test for IgE cetuximab-binding antibodies. Subjects 7 through 10 had severe episodes of anaphylaxis, and Subjects 11 and 12 had severe episodes of angioedema.
‖ The IgE value is the geometric mean for 12 cetuximab-treated subjects who had a hypersensitivity reaction (95% CI, 130.0 to 760.0).
** The mean is for results from 3 of 10 subjects.
†† The IgE value is the geometric mean for 11 cetuximab-treated subjects who did not have a hypersensitivity reaction (95% CI, 6.8 to 45.0).

CSPC Exhibit 1004
Page 5 of 336
The New England Journal of Medicine
Downloaded from nejm.org at US PATENT & TRADEMARK OFFICE on March 19, 2019. For personal use only. No other uses without permission.
Copyright © 2008 Massachusetts Medical Society. All rights reserved.

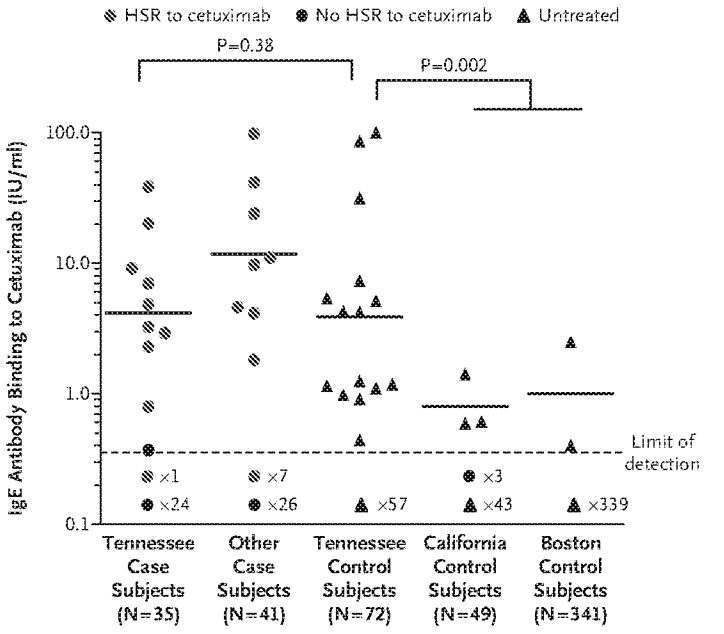


Figure 1. IgE Antibodies Binding to Cetuximab in Serum Samples from 76 Case Subjects and 462 Control Subjects.

Results are shown according to whether the treating physician reported a hypersensitivity reaction (HSR) to cetuximab or no HSR reaction. Results are also shown for pretreatment serum samples from control subjects and from subjects who had not received cetuximab. The horizontal lines indicate geometric mean values for the positive results. Values with multiplication signs indicate the number of negative values for each symbol.

treatment. Evidence that the assay detected IgE antibodies against cetuximab included the detection of these antibodies by the monoclonal anti-IgE antibody used with the ImmunoCAP assay, the demonstration that more than 95% of the IgE antibodies bound to the F(ab′)2 portion of cetuximab, and the finding that absorption of the serum with the use of a monoclonal anti-IgE antibody depleted binding to cetuximab and total levels of IgE in parallel (Table 2).

PREEXISTING IgE ANTIBODIES

Of a total of 538 serum samples from the four groups, 38 contained IgE antibodies against cetuximab (Fig. 1). Among the 76 selected subjects who had received cetuximab, 25 had a hypersensitivity reaction; of these subjects, 17 had a positive test for IgE antibodies against cetuximab in pretreatment serum, whereas only 1 of 51 subjects who did not have a hypersensitivity reaction had such antibodies before treatment with cetuximab ($\log_e$ of the odds ratio, 4.7; P<0.001). The sensitivity and specificity of a positive assay for IgE antibodies for any hypersensitivity reaction were 68% and 98%, respectively. For severe hypersensitivity reaction, these values were 92% and 90%, respectively. Subjects with IgE antibodies against cetuximab had a higher rate of severe hypersensitivity reaction than did subjects without such antibodies (P=0.03 by Fisher's exact test). Among the eight subjects who were reported to have had a hypersensitivity reaction but had negative results on the IgE assay, seven had grade 1 or 2 reactions, and only one subject had a grade 3 reaction. Five of the eight subjects were rechallenged; of these subjects, one had a second hypersensitivity reaction, and four completed treatment without further reactions. Of the subjects who were subsequently found to have IgE antibodies against cetuximab, 17 had discontinued therapy.

Among control subjects in Tennessee, 15 of 72 serum samples (20.8%) had positive results on testing for IgE antibodies against cetuximab. In these samples, both the prevalence and titers of IgE antibodies against cetuximab were similar to those in samples from the treated subjects (Fig. 1). Among subjects with cancer of the head and neck in California and female control subjects in Boston, 3 of 49 serum samples (6.1%) and 2 of 341 (0.6%), respectively, had IgE antibodies against cetuximab (Fig. 1). These low rates in cohorts 3 and 4 parallel the low rates of hypersensitivity reactions that were reported with cetuximab treatment in those regions.[11]

CHARACTERIZATION OF THE EPITOPE ON CETUXIMAB

Given that the IgE antibodies were specific for the Fab portion of the heavy chain of cetuximab, the relevant epitope could be a mouse amino acid sequence or an oligosaccharide on this segment of the molecule (Fig. 2). The absence of binding to other chimeric monoclonal antibodies (e.g., rituximab and infliximab) and the absence of IgE antibodies against cetuximab in 25 samples from allergic subjects who had IgE antibodies against mouse proteins[21] argue against the role of a mouse amino acid sequence (Table 3). The Fab portion of the cetuximab heavy chain is glycosylated at N88 with a range of sugars, including galactose-α-1,3-galactose and a sialic acid, *N*-glycolylneuraminic acid (NGNA).[17] To test whether the IgE antibodies were specific for the oligosaccharides, samples containing IgE antibodies against cetuximab were assayed for IgE antibodies that could bind to CHO-C225. These assays were negative for 11 cetuximab-treated subjects and for 5 of the 6 subjects

CSPC Exhibit 1004
Page 6 of 336
The New England Journal of Medicine
Downloaded from nejm.org at US PATENT & TRADEMARK OFFICE on March 19, 2019. For personal use only. No other uses without permission.
Copyright © 2008 Massachusetts Medical Society. All rights reserved.

who had an anaphylactic reaction after receiving cetuximab (Table 3). In addition, in 150 samples from groups 1 and 2, as well as those listed in Table 3, assays for IgE antibodies against galactose-α-1,3-galactose correlated with results for antibodies that bound to cetuximab ($r=0.92$, $P<0.001$). Most of the positive samples also contained IgE antibodies against cat, dog, and beef proteins but not against mite allergens or pollens (Table 3, and Table 1 of the Supplementary Appendix, available with the full text of this article at www.nejm.org).

The correlation with IgE antibodies against mammalian proteins is consistent with the presence of galactose-α-1,3-galactose on proteins of most nonprimate mammals. To confirm the specificity of the reaction, we showed that the binding of IgE antibodies against cat, dog, beef, and pork proteins and cetuximab was inhibited by soluble galactose-α-1,3-galactose and could be absorbed out of the serum with porcine thyroglobulin, which is glycosylated with galactose-α-1,3-galactose (Table 2 of the Supplementary Appendix).

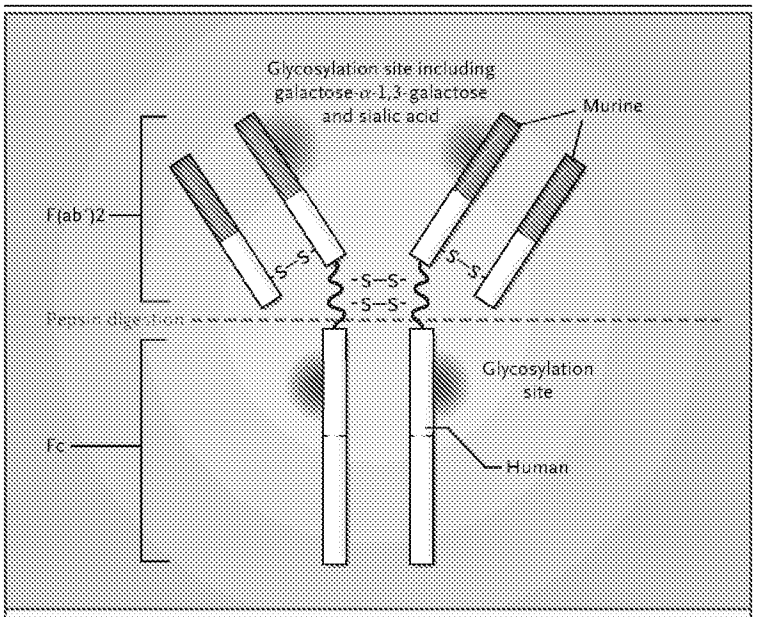


Figure 2. **Structure of Cetuximab.**

The amino acid sequence of cetuximab has potential glycosylation sites at Asn43 of the light chain and at Asn88 and Asn299 of the heavy chain. The sugars on the Fab portion include galactose-α-1,3-galactose and the sialic acid *N*-glycolylneuraminic acid. In contrast, the glycosylation site at Asn43 is not glycosylated, and glycosylation of the Fc portion of the heavy chain includes only oligosaccharides that are commonly present on human proteins.[17,18] S–S denotes a disulfide bond.

DISCUSSION

Severe anaphylactic reactions have been reported after treatment with several different monoclonal antibodies, but the mechanism of these reactions has not been defined, and their rates have generally been less than 1%.[1-5,7,8,22] Our results show that most of the severe hypersensitivity reactions to cetuximab in the subjects we studied were associated with IgE antibodies against galactose-α-1,3-galactose that were present before treatment with cetuximab. The assay we used identified 17 of the 21 subjects whose treatment had to be discontinued after the first infusion because of a hypersensitivity reaction.

Unlike most other monoclonal antibodies, cetuximab is produced in the mouse cell line SP2/0, which expresses the gene for α-1,3-galactosyltransferase.[17,18] The evidence that IgE antibodies that are specific for the post-translational modification of a molecule can cause severe infusion reactions may have relevance for an understanding of allergic responses to other recombinant molecules.

It is now recognized that all humans have IgG antibodies specific for the oligosaccharide galactose-α-1,3-galactose, which is closely related to substances in the ABO blood group.[23-25] This oligosaccharide is one of the major barriers to the transplantation of organs from other mammals in humans and has prompted the development of a strain of pigs in which the gene for α-1,3-galactosyltransferase has been knocked out.[24,26]

Natural exposure to galactose-α-1,3-galactose appears to induce the production of IgE antibodies against galactose-α-1,3-galactose in some people. The presence of such IgE antibodies before treatment may put patients who receive monoclonal antibodies containing galactose-α-1,3-galactose at risk for hypersensitivity reactions. The rapid reactions to cetuximab may be explained by intravenous injection, and the presence of galactose-α-1,3-galactose on both Fab segments of the cetuximab antibody allows for the efficient cross-linking of IgE on mast cells (Fig. 2). Patients who have such antibodies do not report a rapid onset of allergic symptoms after the ingestion of beef, pork, or cow's milk. However, we have identified a series of patients with IgE antibodies against galactose-α-1,3-galactose who reported having had episodes of anaphylaxis or severe angioedema 1 to 3 hours after eating beef or pork (unpublished data). The explanation for such a delayed reaction is not clear, but a similar delay has been reported in patients with IgE antibodies against carbohydrate epitopes of plant proteins.[27,28] In addition, it has recently been reported that some

CSPC Exhibit 1004
Page 7 of 336
The New England Journal of Medicine
Downloaded from nejm.org at US PATENT & TRADEMARK OFFICE on March 19, 2019. For personal use only. No other uses without permission.
Copyright © 2008 Massachusetts Medical Society. All rights reserved.

Table 3. **Specificity of the IgE Antibodies That Cross-React with Cetuximab.***

Type of Reaction and Subject No.	Type of Cetuximab†		Galactose-α-1,3-Galactose‡§	Mammalian Allergens				
	SP2/0‡	CHO‡		Mouse IgG‡	Cat	Dog	Fel d 1‡	Beef
	international units per milliliter							
Hypersensitivity reaction								
Anaphylaxis related to cetuximab								
1	41.6	0.35	13.8	0.35	3.16	2.60	0.35	3.02
2	38.8	0.35	35.2	0.35	13.20	12.30	0.35	12.46
3	20.2	0.35	12.6	0.35	9.34	9.77	0.35	6.92
4	11.1	0.35	2.9	0.35	1.94	1.86	0.35	1.82
5	4.9	0.35	2.0	0.35	0.35	0.35	0.35	0.35
6	4.2	0.35	2.7	0.35	1.54	1.50	0.35	1.66
Recurrent anaphylaxis unrelated to cetuximab¶								
7	131.0	1.89	38.9	1.75	41.50	34.50	3.64	32.90
8	69.2	0.35	42.1	1.19	27.70	32.00	0.35	26.20
9	55.1	0.35	32.2	0.43	22.20	25.10	0.35	13.80
10	43.5	0.35	32.3	0.35	37.30	29.40	0.35	3.48
11	81.1	0.35	100.0	0.35	14.30	14.70	0.35	8.75
12	13.0	0.35	9.0	0.78	8.86	8.84	0.35	8.90
Mean	27.7	NA	25.5	ND	10.30	9.93	NA	7.16
No hypersensitivity reaction‖	0	0	0	0	0	0	0	0

* NA denotes not applicable, and ND not determined.

† Cetuximab is produced by expressing clone C225 in the mouse myeloma cell line SP2/0. A variant of cetuximab is produced in Chinese hamster ovary (CHO) cell lines. Since CHO cells do not produce α-1,3-galactosyltransferase, they have a pattern of glycosylation that differs from that of SP2/0.

‡ The assay was performed with biotinylated antigen on streptavidin ImmunoCAP.

§ The assay was performed with galactose-α-1,3-galactose-β-1,4-*N*-acetylglucosamine-β-spacer-biotin, which binds to streptavidin ImmunoCAP.

¶ Subjects presented to the University of Virginia Allergic Disease clinic with recurrent angioedema or anaphylaxis and had a positive test for IgE antibodies against cetuximab. Subjects 7 through 10 had severe episodes of anaphylaxis, and Subjects 11 and 12 had severe episodes of angioedema.

‖ For statistical analysis of the positive and negative relationships with other allergens, additional data are available in the Supplementary Appendix, available with the full text of this article at www.nejm.org.

patients with cat allergy have IgE antibodies that bind to a carbohydrate epitope on cat IgA.[29]

The high prevalence of hypersensitivity reactions to cetuximab in the Southeast is supported by our own data from the Tennessee group and in other recent studies.[11] The striking difference in the prevalence of the IgE antibodies against cetuximab provides an explanation for the difference in rates of clinical hypersensitivity reaction between subjects in Boston or northern California and those in Tennessee, Arkansas, or North Carolina.[6,11,30] A high prevalence of IgE antibodies against neuromuscular blocking agents in Norway was found to be associated with anaphylaxis, and the difference in incidence between Norway and Sweden was attributed to suxamethonium, an ingredient in a commonly used cough syrup in Norway.[31,32] The explanation for the regional distribution of IgE antibodies against galactose-α-1,3-galactose in the United States is not clear. Most humans have IgG antibodies against galactose-α-1,3-galactose,[24-26] but we do not know why people in one area of the country have IgE antibodies against galactose-α-1,3-galactose, whereas in other areas the incidence of such IgE antibodies is very low. The regional exposures that could be relevant include histoplasmosis, ameba, tick bites, coccidioidomycosis, nematodes, or cestodes. The effect does not appear to be a nonspecific enhancement of IgE production, since we found little or no association with IgE antibodies against allergens other than those derived from mammals.

In conclusion, we have identified a mechanism underlying a hypersensitivity reaction to cetuximab, preexisting IgE antibodies against an oligo-

CSPC Exhibit 1004
The New England Journal of Medicine
Page 8 of 336
Downloaded from nejm.org at US PATENT & TRADEMARK OFFICE on March 19, 2019. For personal use only. No other uses without permission.
Copyright © 2008 Massachusetts Medical Society. All rights reserved.

saccharide present on the recombinant molecule. Our results have implications for evaluating the risks associated with antibody-based therapeutics and for understanding the relevance of IgE antibodies specific for post-translational modifications of natural and recombinant molecules.

Supported by Bristol-Myers Squibb and ImClone Systems; by the Damon Runyon Clinical Investigator Award (CL-28-05), by the Robert J. and Helen C. Kleberg Foundation, and by a grant (R01-DE-017982) from the National Institutes of Health (NIH) — all to Dr. Chung; by grants from the Vanderbilt University GI SPORE (P50-CA-95103) to Dr. Berlin and from the NIH (R01-CA-118582) to Dr. Le; by a grant (AI/EHS-35796) from the NIH to Dr. Gold; and by grants from the NIH (AI-20565) and from the National Institute of Allergy and Infectious Diseases (AI-AAD-CRC-U19-070364) to Dr. Platts-Mills.

Drs. Chung, Chan, Berlin, Hatley, and Platts-Mills report receiving honoraria for attending advisory meetings and lecture fees from Bristol-Myers Squibb; Drs. Mirakhur and Mauro, being full-time employees of Bristol-Myers Squibb; Dr. Morse, receiving grant support from Bristol-Myers Squibb; and Drs. Zhou and Hicklin, being full-time employees of ImClone. No other potential conflict of interest relevant to this article was reported.

We thank the many nurses, assistants, and physicians who participated in the care of the patients in the study; Dr. Dale Ludwig and Dr. Paul Balderes for providing cetuximab variant CHO-C225; Dr. Wendell Yarbrough for supporting the Vanderbilt Head and Neck Tissue Bank; and Dr. Staffan Ahlstedt for providing streptavidin ImmunoCAP and advising us on its use.

REFERENCES

1. Edwards JC, Szczepanski L, Szechinski J, et al. Efficacy of B-cell-targeted therapy with rituximab in patients with rheumatoid arthritis. N Engl J Med 2004;350:2572-81.
2. Bonner JA, Harari PM, Giralt J, et al. Radiotherapy plus cetuximab for squamous-cell carcinoma of the head and neck. N Engl J Med 2006;354:567-78.
3. Holgate S, Casale T, Wenzel S, Bousquet J, Deniz Y, Reisner C. The anti-inflammatory effects of omalizumab confirm the central role in IgE in allergic inflammation. J Allergy Clin Immunol 2005;115:459-65.
4. Cheifetz A, Smedley M, Martin S, et al. The incidence and management of infusion reactions to infliximab: a large center experience. Am J Gastroenterol 2003;98:1315-24.
5. Cook-Bruns N. Retrospective analysis of the safety of Herceptin immunotherapy in metastatic breast cancer. Oncology 2001;61:Suppl 2:58-66.
6. Chung KY, Shia J, Kemeny NE, et al. Cetuximab shows activity in colorectal cancer patients with tumors that do not express the epidermal growth factor receptor by immunohistochemistry. J Clin Oncol 2005;23:1803-10.
7. Omalizumab (marketed as Xolair) information. Rockville, MD: Food and Drug Administration, Center for Drug Evaluation and Research, 2007. (Accessed February 19, 2008, at http://www.fda.gov/cder/drug/infopage/omalizumab/default.htm.)
8. Erbitux (cetuximab). New York: ImClone Systems Incorporated and Bristol-Myers Squibb, 2007 (drug product label).
9. Cunningham D, Humblet Y, Siena S, et al. Cetuximab monotherapy and cetuximab plus irinotecan in irinotecan-refractory metastatic colorectal cancer. N Engl J Med 2004;351:337-45.
10. Saltz LB, Meropol NJ, Loehrer PJ Sr, Needle MN, Kopit J, Mayer RJ. Phase II trial of cetuximab in patients with refractory colorectal cancer that expresses the epidermal growth factor receptor. J Clin Oncol 2004;22:1201-8.
11. O'Neil BH, Allen R, Spigel DR, et al. High incidence of cetuximab-related infusion reactions in Tennessee and North Carolina: association with atopic history. J Clin Oncol 2007;25:3644-8.
12. Sampson HA, Muñoz-Furlong A, Bock SA, et al. Symposium on the definition and management of anaphylaxis: summary report. J Allergy Clin Immunol 2005;115:584-91.
13. Joint Task Force on Practice Parameters. The diagnosis and management of anaphylaxis: an updated practice primer. J Allergy Clin Immunol 2005;115:Suppl 2:S483-S523.
14. Erwin EA, Custis NJ, Satinover SM, et al. Quantitative measurement of IgE antibodies to purified allergens using streptavidin linked to a high-capacity solid phase. J Allergy Clin Immunol 2005;115:1029-35.
15. Lewis SA, Weiss ST, Platts-Mills TA, Burge H, Gold DR. The role of indoor allergen sensitization and exposure in causing morbidity in women in asthma. Am J Respir Crit Care Med 2002;165:961-6.
16. Cancer Therapy Evaluation Program. Common Terminology Criteria for Adverse Events, v3.0 (CTCAE). Bethesda, MD: National Cancer Institute, 2006. (Accessed February 19, 2008, at http://ctep.cancer.gov/forms/CTCAEv3.pdf.)
17. Qian J, Liu T, Yang L, Daus A, Crowley R, Zhou Q. Structural characterization of N-linked oligosaccharides on monoclonal antibody cetuximab by the combination of orthogonal matrix-assisted laser desorption/ionization hybrid quadrupole-quadrupole time-of-flight tandem mass spectrometry and sequential enzymatic digestion. Anal Biochem 2007;364:8-18.
18. Jefferis R. Glycosylation of human IgG antibodies: relevance to therapeutic applications. BioPharm 2002;14:19-26.
19. Chapman MD, Aalberse RC, Brown MJ, Platts-Mills TA. Monoclonal antibodies to the major feline allergen Fel d 1. J Immunol 1988;140:812-8.
20. Cavalier E, Carlisi A, Chapelle JP. Evaluation of the analytical performance of the ImmunoCap 250 (Sweden Diagnostics). Ann Biol Clin (Paris) 2006;64:91-4. (In French.)
21. Platts-Mills TAE, Satinover SM, Naccara L, et al. Prevalence and titer of IgE antibodies to mouse allergens. J Allergy Clin Immunol 2007;120:1058-64.
22. Cheifetz A, Mayer L. Monoclonal antibodies, immunogenicity, and associated infusion reactions. Mt Sinai J Med 2005;72:250-6.
23. Landsteiner K. The specificity of serological reactions. Rev. ed. New York: Dover Publications, 1990.
24. Galili U. The alpha-Gal epitope and the anti-Gal antibody in xenotransplantation and in cancer immunotherapy. Immunol Cell Biol 2005;83:674-86.
25. Koike C, Uddin M, Wildman D, et al. Functionally important glycosyltransferase gain and loss during catarrhine primate emergence. Proc Natl Acad Sci U S A 2007;104:559-64.
26. Milland J, Sandrin MS. ABO blood group and related antigens, natural antibodies and transplantation. Tissue Antigens 2006;68:459-66.
27. Paschinger K, Fabini G, Schuster D, et al. Definition of immunogenic carbohydrate epitopes. Acta Biochim Pol 2005;52:629-32.
28. van der Veen MJ, van Ree R, Aalberse RC, et al. Poor biologic activity of cross-reactive IgE directed to carbohydrate determinants of glycoproteins. J Allergy Clin Immunol 1997;100:327-34.
29. Adédoyin J, Grönlund H, Oman H, Johansson SG, van Hage M. Cat IgA, representative of new carbohydrate cross-reactive allergens. J Allergy Clin Immunol 2007;119:640-5.
30. Needle MN. Safety experience with IMC-C225, an anti-epidermal growth factor receptor antibody. Semin Oncol 2002;29:Suppl 14:55-60.
31. Florvaag E, Johansson SG, Oman H, et al. Prevalence of IgE antibodies to morphine: relation to the high and low incidences of NMBA anaphylaxis in Norway and Sweden, respectively. Acta Anaesthesiol Scand 2005;49:437-44.
32. Johansson SG, Nopp A, Florvaag E, et al. High prevalence of IgE antibodies among blood donors in Sweden and Norway. Allergy 2005;60:1312-5.

Copyright © 2008 Massachusetts Medical Society.

CSPC Exhibit 1004
Page 9 of 336
The New England Journal of Medicine
Downloaded from nejm.org at US PATENT & TRADEMARK OFFICE on March 19, 2019. For personal use only. No other uses without permission.
Copyright © 2008 Massachusetts Medical Society. All rights reserved.

VOLUME 26 · NUMBER 35 · DECEMBER 10 2008

JOURNAL OF CLINICAL ONCOLOGY

ORIGINAL REPORT

Wild-Type *BRAF* Is Required for Response to Panitumumab or Cetuximab in Metastatic Colorectal Cancer

Federica Di Nicolantonio, Miriam Martini, Francesca Molinari, Andrea Sartore-Bianchi, Sabrina Arena, Piercarlo Saletti, Sara De Dosso, Luca Mazzucchelli, Milo Frattini, Salvatore Siena, and Alberto Bardelli

From the Laboratory of Molecular Genetics, The Oncogenomics Center, Institute for Cancer Research and Treatment, University of Torino Medical School, Candiolo; The Falck Division of Medical Oncology, Ospedale Niguarda Ca' Granda, Italian Foundation for Cancer Research–Institute of Molecular Oncology, Milan, Italy; Laboratory of Molecular Diagnostic, Istituto Cantonale di Patologia, Locarno; and Oncology Institute of Southern Switzerland, Ospedale San Giovanni, Bellinzona, Switzerland.

Submitted June 3, 2008; accepted August 28, 2008; published online ahead of print at www.jco.org on November 10, 2008.

Supported by the Italian Association for Cancer Research, Italian Ministry of Health, Regione Piemonte, Italian Ministry of University and Research, Association for International Cancer Research, EU FP6 MCSCs Contract No. 037297, CRT Progetto Alfieri, Oncosuisse Grant No. OCS-01921-08-2006, Fondazione Ticinese per la Ricerca sul Cancro, and Oncologia Ca' Granda Onlus Fondazione.

F.D.N., M.M., and F.M. contributed equally to this work.

M.F., S.S., and A.B. are co-senior authors.

Terms in blue are defined in the glossary, found at the end of this article and online at www.jco.org.

Authors' disclosures of potential conflicts of interest and author contributions are found at the end of this article.

Corresponding author: Alberto Bardelli, PhD, Laboratory of Molecular Genetics, The Oncogenomics Center, Institute for Cancer Research and Treatment, University of Torino, Medical School, Str prov 142 Km 3.95, 10060 Candiolo, Torino, Italy; e-mail: a.bardelli@unito.it.

The Appendix is included in the full-text version of this article, available online at www.jco.org. It is not included in the PDF version (via Adobe® Reader®).

© 2008 by American Society of Clinical Oncology

0732-183X/08/2635-5705/$20.00

DOI: 10.1200/JCO.2008.18.0786

ABSTRACT

Purpose

Cetuximab or panitumumab are effective in 10% to 20% unselected metastatic colorectal cancer (CRC) patients. *KRAS* mutations account for approximately 30% to 40% patients who are not responsive. The serine-threonine kinase BRAF is the principal effector of KRAS. We hypothesized that, in *KRAS* wild-type patients, *BRAF* mutations could have a predictive/prognostic value.

Patients and Methods

We retrospectively analyzed objective tumor responses, time to progression, overall survival (OS), and the mutational status of *KRAS* and *BRAF* in 113 tumors from cetuximab- or panitumumab-treated metastatic CRC patients. The effect of the *BRAF* V600E mutation on cetuximab or panitumumab response was also assessed using cellular models of CRC.

Results

KRAS mutations were present in 30% of the patients and were associated with resistance to cetuximab or panitumumab ($P = .011$). The *BRAF* V600E mutation was detected in 11 of 79 patients who had wild-type *KRAS*. None of the *BRAF*-mutated patients responded to treatment, whereas none of the responders carried *BRAF* mutations ($P = .029$). *BRAF*-mutated patients had significantly shorter progression-free survival ($P = .011$) and OS ($P < .0001$) than wild-type patients. In CRC cells, the introduction of *BRAF* V600E allele impaired the therapeutic effect of cetuximab or panitumumab. Treatment with the BRAF inhibitor sorafenib restored sensitivity to panitumumab or cetuximab of CRC cells carrying the V600E allele.

Conclusion

BRAF wild-type is required for response to panitumumab or cetuximab and could be used to select patients who are eligible for the treatment. Double-hit therapies aimed at simultaneous inhibition of epidermal growth factor receptor and BRAF warrant exploration in CRC patients carrying the V600E oncogenic mutation.

J Clin Oncol 26:5705-5712. © 2008 by American Society of Clinical Oncology

INTRODUCTION

Patients with metastatic colorectal cancer (mCRC) have a 5-year survival rate of less than 10%.[1] Cetuximab and panitumumab, two monoclonal antibodies (MoAb) targeting epidermal growth factor receptor (EGFR), have recently entered clinical practice and have proven to be effective in providing clinical benefit in approximately 10% to 20% of patients.[2-5] Both molecules bind to the extracellular domain of EGFR, thus leading to inhibition of its downstream signaling. EGFR is a transmembrane tyrosine kinase receptor that, on ligand binding, triggers two main signaling pathways. These include the RAS-RAF-MAPK axis, which is mainly involved in cell proliferation, and the PI3K-PTEN-AKT pathway, which is mainly involved in cell survival and motility.[6] Cetuximab and panitumumab are registered for mCRC patients whose tumors express EGFR protein as determined by immunohistochemistry. However, it has been clearly demonstrated that this method is not predictive of treatment efficacy.[2,3,7] On the contrary, recent data indicate that *EGFR* gene status evaluated by fluorescent in situ hybridization or chromogenic in situ hybridization may predict response to these MoAbs.[8-12] We and others have previously shown, at the preclinical[13] and clinical[8-10,14-18] level, that the presence of mutated *KRAS* alleles is an independent predictive marker of anti-EGFR MoAb resistance. On the basis of these results, the European Union drug regulatory body, the European Medicines Agency, has approved the use of panitumumab only for mCRC patients whose tumors display wild-type *KRAS*. However, the occurrence of *KRAS* mutations only accounts for approximately 30% to 40% of

CSPC Exhibit 1004
Page 10 of 336

Downloaded from ascopubs.org by US PATENT TRADEMARK OFF SCI & TECH INFO Center on March 19, 2019 from 151.207.250.071
Copyright © 2019 American Society of Clinical Oncology. All rights reserved.

nonresponsive patients.[8-10,14,15] Therefore, the identification of additional genetic determinants of primary resistance to EGFR-targeted therapies in colorectal cancers (CRCs) is important at least for two reasons. The first is to prospectively identify patients who should not receive either cetuximab or panitumumab, thus avoiding their exposure to ineffective and expensive therapy. Second, understanding the molecular basis of primary resistance to EGFR-targeted MoAb therapies could allow the rationale design of alternative treatment strategies. We hypothesized that, in the absence of *KRAS* mutations, resistance to anti-EGFR treatments could be caused by alterations of other members of the RAS-RAF-MAPK pathway. Using genetic analysis of mCRCs from cetuximab- or panitumumab-treated patients and cellular models of CRC, we assessed whether *BRAF* mutations affect the response to therapies based on EGFR-targeted MoAbs. Because *BRAF* mutations are linked to microsatellite instability (MSI), a condition generally associated with better prognosis and resistance to standard chemotherapy,[19] we also investigated MSI in our cohort of treated patients.

PATIENTS AND METHODS

Patient Population and Treatment Regimens

We retrospectively analyzed 113 patients with histologically confirmed mCRC either at Ospedale Niguarda Ca' Granda (Milan, Italy) or at the Institute of Pathology (Locarno, Switzerland). Patients evaluated in this study were selected based on evidence that treatment outcome could be attributable only to administration of either panitumumab or cetuximab. Patients were enrolled onto clinical trials (64 of 113 patients; see Appendix, online only)[3,5,20-23] or received panitumumab or cetuximab as per label indication. For patients who experienced progression on irinotecan-based chemotherapy, cetuximab was administered in combination with irinotecan at the same dose and schedule previously used. In all patients, refractoriness to irinotecan was defined as documented disease progression by comparison of computed tomography or magnetic resonance imaging scans during or within 3 months of receiving an irinotecan regimen (administered for at least 6 weeks). Besides the earlier mentioned inclusion criteria, the availability of a tumor sample qualitatively and quantitatively suitable for molecular analyses was also a requirement for being considered in the present study. All patients had EGFR expression in their tumor specimens in ≥ 1% of malignant cells assessed by immunohistochemistry with the Dako EGFR PharmDx kit (DakoCytomation, Glostrup, Denmark). Patients' baseline characteristics, disease stage, and number of previous lines of therapy are listed in Table 1. Treatment was continued until progressive disease (PD) or toxicity occurred, according to the standard criteria.[24]

Clinical Evaluation and Tumor Response Criteria

Clinical response was assessed every 6 to 8 weeks with radiologic examination (computed tomography or magnetic resonance imaging). The Response Evaluation Criteria in Solid Tumors[24] were adopted for evaluation, and objective tumor response was classified as partial response (PR), stable disease (SD), or PD. Patients with SD or PD were defined as nonresponders.[24] Two independent oncologists and radiologists verified, in a blinded manner, the clinical response for all patients.

Molecular Analyses

Formalin-fixed, paraffin-embedded tumor blocks were reviewed for quality and tumor content, and a single representative tumor block from each patient, containing at least 70% of neoplastic cells, was selected. Genomic DNA was extracted as previously described.[8]

MSI

The status of MSI was assessed by the analysis of the microsatellite loci included in the panel of Bethesda (BAT25, BAT26, D2S123, D5S346, and D17S250), as previously reported.[25] MSI was confirmed by the presence of an additional peak in tumor sample compared with normal paired tissue. MSI was defined as being present when more than 30% of loci showed instability.

Mutational Analysis of KRAS and BRAF in Tumor Samples

We searched for *KRAS* and *BRAF* point mutations in exons 2 and 15, respectively. These two exons include codons 12 and 13 of *KRAS* and codon

Table 1. Baseline Patient Characteristics by *KRAS* and *BRAF* Status

Characteristic	Mutant *KRAS*		Mutant *BRAF*		Wild-Type *KRAS* and *BRAF*		Total	
	No. of Patients	%	No. of Patients	%	No. of Patients	%	No. of Patients	%
No. of patients	34	30	11	10	68	60	113	100
Male sex	16	14	8	7	56	50	80	71
Baseline age, years								
Median	64		63		62		63	
Range	48-82		43-68		26-85		26-85	
Site of primary disease								
Colon	21	19	10	9	39	35	70	62
Rectum	13	12	1	1	29	26	43	38
Anti-EGFR MoAb								
Cetuximab	12	11	3	3	21	19	36	32
Cetuximab plus chemotherapy	12	11	2	2	37	33	51	45
Panitumumab	10	9	6	5	10	9	26	23
Received prior adjuvant chemotherapy*	31	27	10	9	59	52	100	88
No. of prior lines of chemotherapy								
1	4	4	2	2	6	5	12	11
2	14	12	4	4	35	31	53	47
3	11	10	3	3	15	13	29	26
4	2	2	1	1	2	2	5	4
5	0	0	0	0	1	1	1	1

Abbreviations: EGFR, epidermal growth factor receptor; MoAb, monoclonal antibody.
*Thirteen patients received cetuximab as front-line therapy.

 © 2008 by American Society of Clinical Oncology

CSPC Exhibit 1004
Page 11 of 336

Downloaded from ascopubs.org by US PATENT TRADEMARK OFF SCI & TECH INFO Center on March 19, 2019 from 151.207.250.071
Copyright © 2019 American Society of Clinical Oncology. All rights reserved.

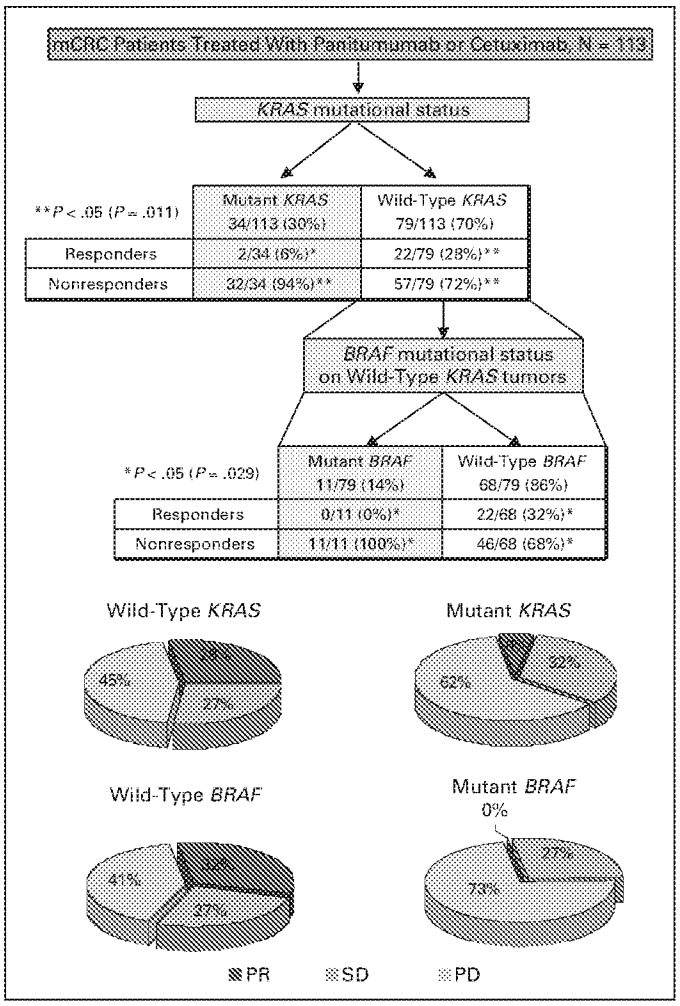


Fig 1. *KRAS* and *BRAF* mutations correlate with lack of response to treatment with monoclonal antibodies targeting epidermal growth factor receptor. The number of responders and nonresponders (stable disease [SD] + progressive disease [PD]) is indicated according to *KRAS* or *BRAF* mutational status. The percentage of patients displaying partial response (PR), SD, or PD is shown in the pie charts. mCRC, metastatic colorectal cancer.

600 of *BRAF*, where the large majority of the mutations in these genes occur, as already reported.[8,25] The list of primers used for mutational analysis is available from the authors on request. All samples were subjected to automated sequencing by ABI PRISM 3730 (Applied Biosystems, Foster City, CA). All mutated samples were confirmed twice, starting from independent polymerase chain reactions.

Cellular Models, Cell Viability, Bromodeoxyuridine, and Apoptosis Assays

Experimental procedures involving the use of cellular models have been described in the Appendix.

Statistical Analysis

The objective tumor response was the end point of our exploratory study. Qualitative comparisons of objective response to therapy (responders [PR] *v* nonresponders [PD + SD]) and gene mutations as predictors were performed by the two-tailed Fisher's exact test to check possible significance. The level of significance was set at $P < .05$. The progression-free survival (PFS) and overall survival (OS) analysis were determined according to the Kaplan-Meier method, and survival curves were compared using the log-rank test. PFS was defined as the time from start of treatment (see Patient Population and Treatment Regimens) until first documented tumor progression or death. Data were analyzed using the Stata 9.1 package (Stata Corp, College Station, TX).

RESULTS

Mutational Profiling of KRAS and Response of Patients Treated With Cetuximab or Panitumumab

The mutational status of *KRAS* was assessed in a cohort of 113 patients (41 females and 72 males, with a mean age 63 years) who had received either panitumumab- or cetuximab-based chemotherapy. Twenty-four patients (21%) achieved PR, and the median duration of response was 25 weeks (range, 10 to 128 weeks). Patient characteristics by *KRAS* mutational status are listed in Table 1. *KRAS* exon 2 mutations were found in 34 (30%) of 113 analyzed patients. *KRAS* mutations were detected in two (8%) of 24 responsive patients but in 32 (35%) of 89 nonresponders (Fig 1). The data confirm that the presence of *KRAS* mutations correlates with lack of response to anti-EGFR MoAb therapy (two-tailed Fisher's exact test, $P = .011$). The follow-up analyses indicated that patients carrying a *KRAS*-mutated tumor displayed a shorter PFS (log-rank test, $P = .0275$; Fig 2A). No statistically significant differences were observed by OS analysis ($P = .0869$; Fig 2B).

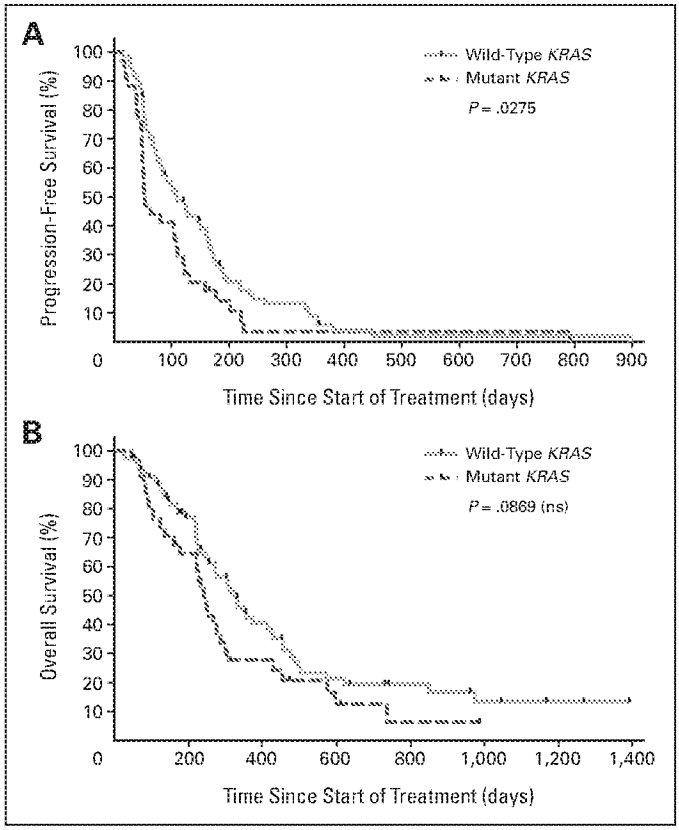


Fig 2. *KRAS* mutations are associated with shorter progression-free survival (PFS). (A) Patients with wild-type *KRAS* tumors displayed a better PFS than patients with *KRAS*-mutated tumors (log-rank test, $P = .0275$). (B) Patients carrying *KRAS*-mutated tumors tended to have shorter overall survival. However, this difference did not reach statistical significance (log-rank test, $P = .0869$). ns, not significant.

© 2008 by American Society of Clinical Oncology

CSPC Exhibit 1004
Page 12 of 336

Downloaded from ascopubs.org by US PATENT TRADEMARK OFF SCI & TECH INFO Center on March 19, 2019 from 151.207.250.071
Copyright © 2019 American Society of Clinical Oncology. All rights reserved.

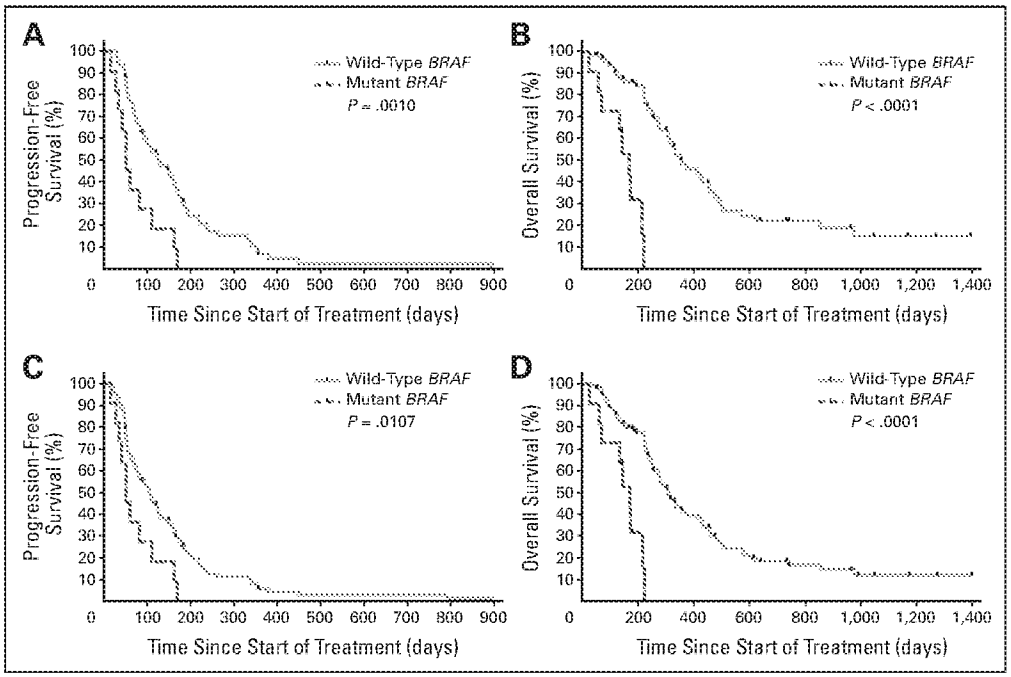


Fig 3. (A and B) In wild-type *KRAS* patients, those carrying a *BRAF*-mutated tumor had a shorter progression-free survival (PFS) and overall survival (OS) than wild-type *BRAF* patients (log-rank test, $P = .0010$ and $P < .0001$, respectively). (C and D) In the entire cohort of patients, individuals with wild-type *BRAF* tumors still displayed longer PFS and OS than patients with *BRAF*-mutated tumors ($P = .0107$ and $P < .0001$, respectively).

Mutational Profiling of BRAF *in Wild-Type* KRAS *Patients Treated With Cetuximab or Panitumumab*

We and others have previously reported that *KRAS* and *BRAF* mutations are mutually exclusive in CRCs.[26,27] This relationship was experimentally verified in our sample set, and we found that none of the *KRAS*-mutated samples carried concomitant *BRAF* mutations, or vice versa. The only type of *BRAF* mutation found in our cohort was the previously described V600E substitution, which was detected in 11 patients (13%). In all patients, the amino acid change was a result of the classic GTG→GAG mutation at position 1799 of the *BRAF* nucleotide sequence. Patient characteristics by *BRAF* mutational status are listed in Table 1.

BRAF *V600E Allele Impairs the Response to Cetuximab or Panitumumab*

The presence of *BRAF* mutations was inversely associated with response to therapy (Fig 1). Significantly, none of 22 *KRAS* wild-type patients who experienced PR displayed *BRAF* mutations, whereas 11 (14.0%) of 79 nonresponder patients carried the *BRAF* V600E mutation (two-tailed Fisher's exact test, $P = .029$). These data indicate that occurrence of oncogenic *BRAF* alleles negatively interferes with the clinical response to MoAbs targeting EGFR.

BRAF *Mutations Are Associated With Shorter PFS and OS*

We assessed how the occurrence of *BRAF* mutations affected clinical parameters such as PFS and OS. The follow-up analyses indicated that within the subgroup of *KRAS* wild-type patients, those carrying a *BRAF*-mutated tumor had a shorter PFS and OS than *BRAF* wild-type patients (log-rank test, $P = .0010$ and $P < .0001$, respectively; Figs 3A and 3B). In the entire cohort of patients, independently from *KRAS* mutational status, individuals with *BRAF*-mutated tumors still displayed shorter PFS and OS than patients with *BRAF* wild-type tumors (log-rank test, $P = .0107$ and $P < .0001$, respectively; Figs 3C and 3D). This significant association indicates that the presence of *BRAF* V600E mutation correlates with a worse prognosis. MSI has been linked both to the occurrence of *BRAF* mutation and to improved prognosis in sporadic CRC patients treated with fluorouracil-based regimens.[19,28-30] MSI was assessed in a subset of patients, including 10 with *BRAF*-mutated samples, 24 with *KRAS*-mutated samples, and 41 with samples that were wild type for both genes. We identified MSI in one (1.3%) of these 75 patients, and this patient had a sample that was wild type for both *KRAS* and *BRAF*. Importantly, none of the tested *BRAF*-mutated tumors displayed MSI, indicating that this factor is unlikely to affect the OS results and the effect on the efficacy of EGFR-targeted therapies presented earlier.

BRAF *V600E Allele Impairs the Response of CRC Cells to Cetuximab or Panitumumab*

The genetic profiling of CRCs showed that the presence of mutated *BRAF* negatively interferes with clinical response to EGFR-targeted MoAbs. We hypothesized that oncogenic activation of *BRAF* by the V600E mutation could bypass (short circuit) the EGFR-initiated signaling cascade. To assess the effect of the *BRAF* V600E mutation on response to cetuximab or panitumumab, we used cellular models of CRC. Specifically, we used a CRC line, DiFi, carrying amplification of the *EGFR* gene.[8] We and others have previously shown that the proliferation of DiFi cells is inhibited by nanomolar concentration of cetuximab, and therefore, this line can be exploited to understand the molecular and cellular basis of sensitivity to anti-EGFR MoAb therapy.[8,31] We verified that DiFi cells do not show mutations in either *KRAS* or *BRAF* (data not shown), thus allowing further functional experiments. We found that DiFi cells expressing the mutated *BRAF* V600E allele (DiFi-BRAF) were less sensitive to either cetuximab or panitumumab compared with parental cells transduced with an empty vector (Figs 4A and 4B). These data indicate that the presence of oncogenic *BRAF* (such as the V600E mutant)

 © 2008 by American Society of Clinical Oncology

CSPC Exhibit 1004
Page 13 of 336

Downloaded from ascopubs.org by US PATENT TRADEMARK OFF SCI & TECH INFO Center on March 19, 2019 from 151.207.250.071
Copyright © 2019 American Society of Clinical Oncology. All rights reserved.

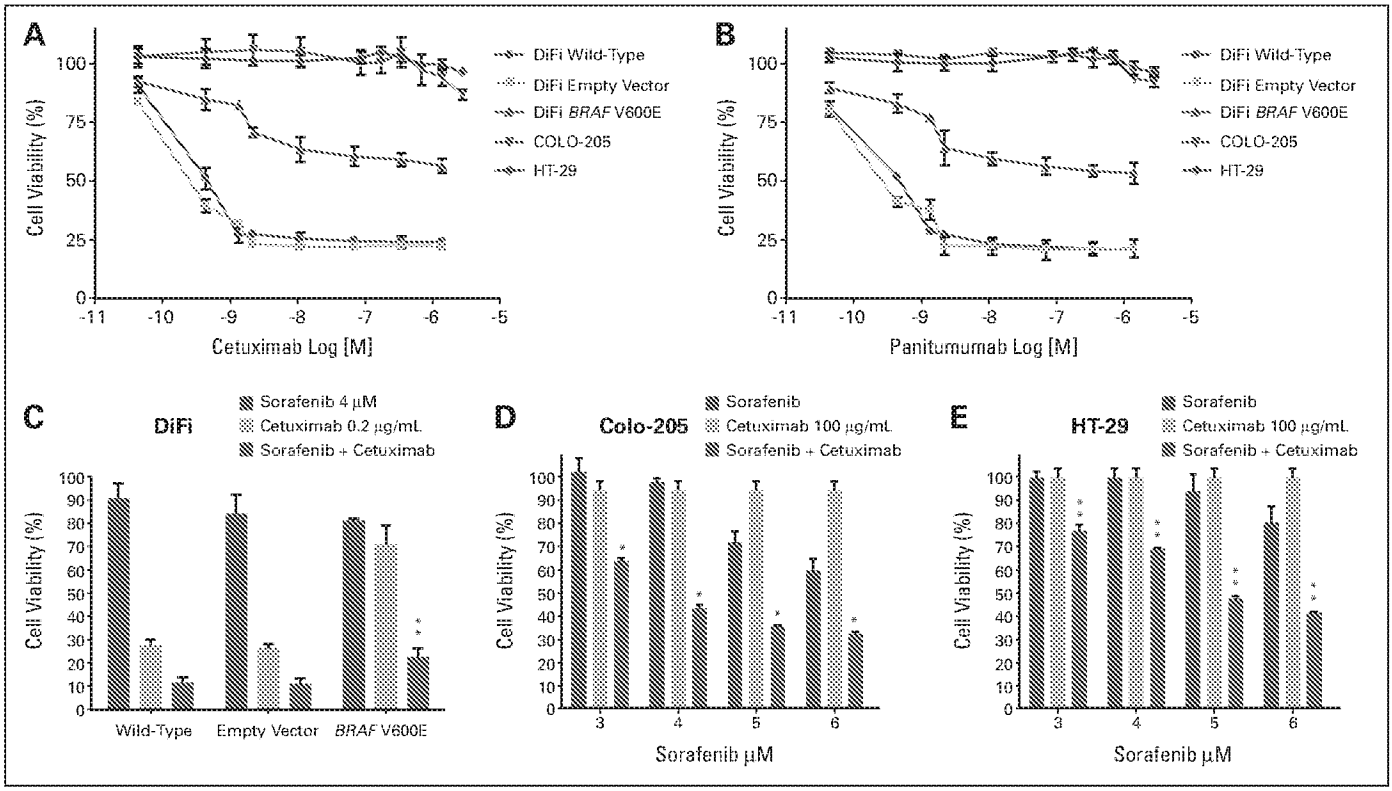


Fig 4. (A and B) The colorectal cancer cell line DiFi was transduced with either an empty vector or a *BRAF* V600E–encoding lentiviral vector. Cell viability was measured after treatment with either cetuximab or panitumumab. (C to E) Viability of DiFi, COLO-205, and HT-29 cells after combinatorial treatment with cetuximab plus sorafenib. Results (average ± standard deviation) were normalized to untreated cells. (*) $P < .05$ and (**) $P < .01$ by Bonferroni multiple comparison test.

impairs the therapeutic potential of cetuximab and panitumumab in CRC cells.

To assess whether this finding could be replicated in cancer cells in which the *BRAF* V600E was naturally present, we used HT-29 and COLO-205, which are two cell lines derived from colorectal tumors in which the mutation had been previously detected. After independently verifying that both lines carried the *BRAF* V600E allele (and were wild type for *KRAS*), we found that HT-29 and COLO-205 are highly refractory to cetuximab and panitumumab treatment (Figs 4A and 4B).

Combinatorial Targeting of EGFR and BRAF in CRC Cells Carrying the BRAF *V600E Allele*

The mutational profiling of CRCs showed that the presence of *BRAF* mutations renders cancer cells unresponsive to EGFR-targeted MoAb therapies. We hypothesized that the pharmacologic inhibition of *BRAF* might restore the sensitivity to cetuximab or panitumumab in CRC cells carrying the V600E mutation. Sorafenib, a clinically approved small-molecule kinase inhibitor, was used to pharmacologically target *BRAF*.[32]

When DiFi-BRAF, COLO-205, and HT-29 cells were treated with a combination of cetuximab and sorafenib, we found a dramatically reduced viability in all three cellular models (Figs 4C, 4D, and 4E), whereas single agents, alone, had limited effects. To dissect the mechanism through which the combinatorial treatment synergistically affected cancer cells carrying the *BRAF* V600E mutation, we measured its effects both on cell cycle and on apoptosis. The combination of cetuximab and sorafenib limitedly affected proliferation compared with sorafenib alone (Fig 5A), whereas it showed a prominent proapoptotic effect, as demonstrated by the massive increase of caspase 3/7 activation observed in HT-29 and COLO-205 cells (Fig 5B).

DISCUSSION

Cetuximab and panitumumab have shown efficacy in approximately 10% to 20% of mCRC patients. It is now emerging that genetic alterations of *EGFR* and its downstream signaling effectors may predict the efficacy of EGFR-targeted MoAbs.[8-15] In particular, the role of oncogenic *KRAS* has been extensively analyzed, leading to the conclusion that the occurrence of *KRAS* mutations represents a predictive marker of anti-EGFR MoAb resistance.[8-10,13-17] However, *KRAS* mutations only account for 30% to 40% of nonresponsive patients. Therefore, the identification of additional genetic determinants of primary resistance to EGFR-targeted therapies in CRC is clearly a priority. Genetic and biochemical evidence indicates that BRAF is the principal downstream effector of KRAS.[33,34] Whether and to what extent the oncogenic activation of BRAF (a serine-threonine kinase mutated in approximately 10% of CRCs) affects the response to anti-EGFR MoAbs has been only marginally investigated.[13] By analyzing a larger cohort of mCRCs patients, we found that *BRAF* mutations are associated with resistance to EGFR-targeted MoAb therapies. Our data indicate that the role of *BRAF* mutations in patients treated with EGFR-targeted drugs is similar to that played by mutated *KRAS*. We propose that the combined mutational analysis of both *KRAS* and

© 2008 by American Society of Clinical Oncology

CSPC Exhibit 1004
Page 14 of 336

Downloaded from ascopubs.org by US PATENT TRADEMARK OFF SCI & TECH INFO Center on March 19, 2019 from 151.207.250.071
Copyright © 2019 American Society of Clinical Oncology. All rights reserved.

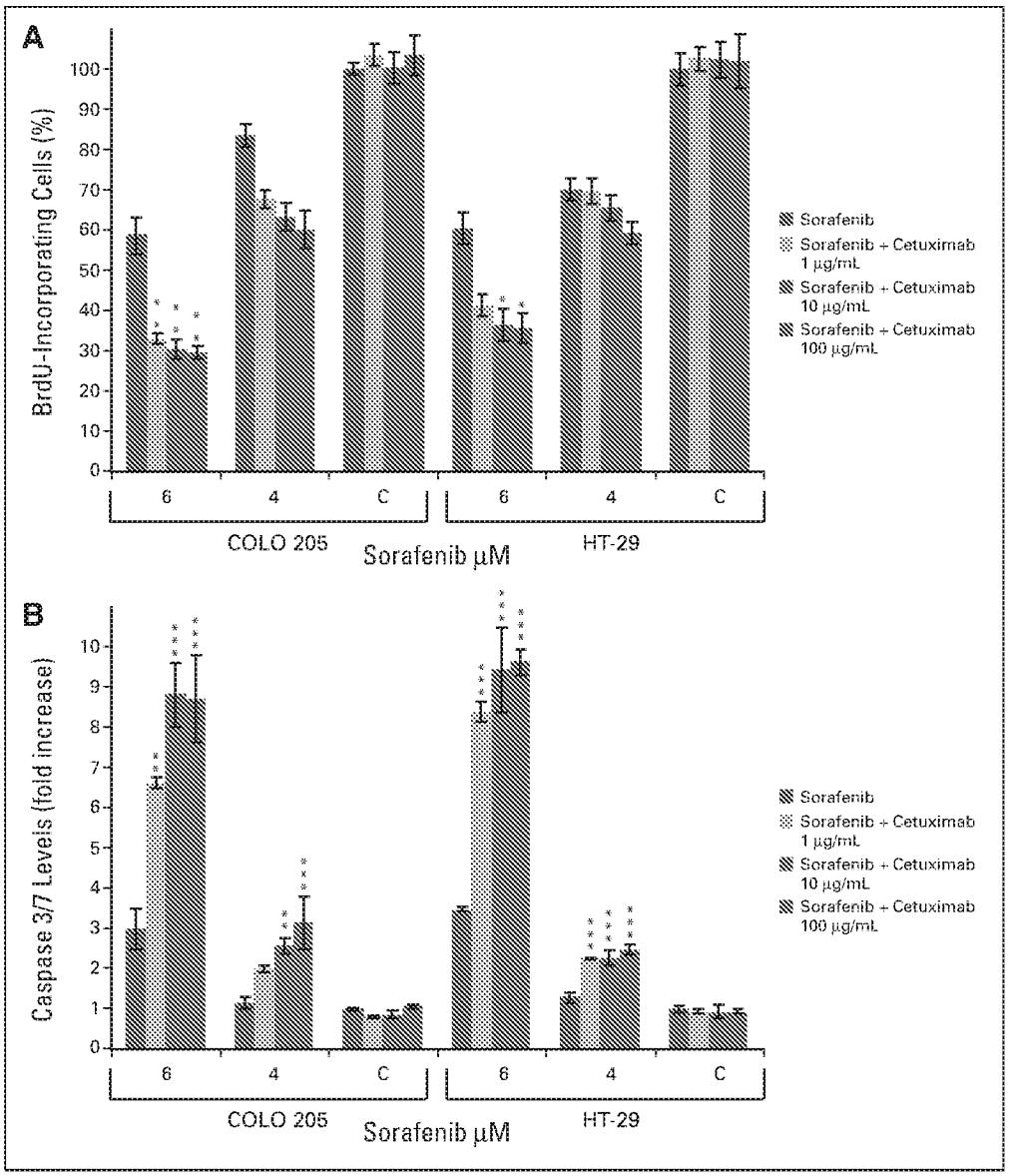


Fig 5. (A) Effects of combinatorial sorafenib plus cetuximab on proliferation by measuring bromodeoxyuridine (BrdU) incorporation in HT-29 and COLO-205 cells. (B) Levels of activated caspases 3/7 (apoptotic markers) after combinatorial treatment. Results (average ± standard deviation) were normalized to untreated cells. C indicates values for vehicle-treated (blue bars) or cetuximab-treated (yellow, gray, and red bars) cells. (*) $P < .05$; (**) $P < .01$; and (***) $P < .001$ by Bonferroni multiple comparison test.

BRAF could be used to prospectively select mCRC patients eligible for EGFR-targeted MoAb treatment, with evident medical and economic implications. However, our findings need to be formally confirmed in a randomized clinical trial comparing an experimental arm containing cetuximab or panitumumab with a control arm without this targeted therapy.

Despite the predictive value of both *KRAS* and *BRAF* mutations, in our cohort, there was still a significant percentage of nonresponsive patients (41%) who did not have mutations in either gene. Therefore, further molecular markers are needed to better define patients who are unlikely to benefit from EGFR-targeted MoAb treatment.

The present study also shows that patients carrying a *BRAF* point mutation have a shorter PFS and OS. This is in accordance with previous data indicating that CRCs with *BRAF* mutations have a more aggressive phenotype.[28] It has been previously reported that *BRAF* mutations are more frequently detected in MSI-sporadic CRC compared with microsatellite-stable CRC (up to 50% *v* up to 12%, respectively).[28-30] Considering that MSI is a condition generally associated with better prognosis and with resistance to standard chemotherapies,[19] we investigated this marker in our series. The tumors in which we detected *BRAF* mutations did not show MSI, thus excluding that the results could be a result of a general mechanism of MSI-dependent drug resistance. Therefore, the prognostic and predictive value of *BRAF* mutations in anti-EGFR–treated mCRC patients does not depend on the MSI status. The frequency of MSI in our cohort of advanced CRC patients is significantly lower (1.3%) with respect to the expected rate (at least 15%) when all stages of sporadic CRC are analyzed. We analyzed 30 additional mCRC patients (not treated with EGFR-targeted therapies), none of whom showed MSI. Therefore, our cumulative results indicate that only one of 105 advanced CRC patients showed MSI. A stage selection may account for these results because our cohort included only metastatic patients. In fact, our frequency is similar to that reported in a previous study that found only five patients (2.7%) with MSI in 190 mCRC patients.[35] Thus, our results are well in accordance with the notion that the MSI phenotype

 © 2008 by American Society of Clinical Oncology

CSPC Exhibit 1004
Page 15 of 336

Downloaded from ascopubs.org by US PATENT TRADEMARK OFF SCI & TECH INFO Center on March 19, 2019 from 151.207.250.071
Copyright © 2019 American Society of Clinical Oncology. All rights reserved.

is associated with better prognosis[19] and with a reduced likelihood of metastasis in patients with CRC.[36]

Although our study suggests a strong correlation of *BRAF* mutations in mCRC with a worse prognosis, further studies are needed to fully evaluate this marker with and without EGFR-targeted therapies, similar to what has been done for *KRAS*.[18]

To assess, at the molecular level, how the *BRAF* mutation could influence the response to anti-EGFR MoAbs, we exploited cellular models of CRC. We found that the occurrence or the exogenous introduction of the *BRAF* V600E allele in CRC cells dramatically impairs their response to cetuximab or panitumumab. These results have two relevant implications. First, they show that the presence of the V600E allele directly affects the response to EGFR-targeted MoAbs at the cellular level. Second, they suggest that the correlation between the occurrence of *BRAF* mutation and the ineffective clinical response to cetuximab or panitumumab is not generically a result of the poorer prognosis of *BRAF*-mutated tumors. Our cell-based analysis also shows that even *BRAF*-mutated CRC cells can potentially respond to EGFR-targeted MoAbs if the *BRAF* inhibitor sorafenib is administered concomitantly with cetuximab or panitumumab. Of note, either drug alone had limited activity, indicating that they act synergistically. These data indicate that in *BRAF*-mutated tumors, the therapeutic effect of cetuximab or panitumumab could be restored by two-hit approaches aimed at blocking the EGFR pathway at multiple locations. In addition to sorafenib, other compounds targeting either *BRAF* (PLX4032) or its downstream effectors (ARRY-162, AZD6244, and PD0325901) are in clinical development[37] and could be exploited in combination with EGFR-targeted MoAb therapy.

Overall, the present study has at least two implications that could be relevant for the therapy of mCRC. The first is that patients whose tumors bear the *BRAF* V600E allele are not likely to experience significant clinical benefit on either cetuximab or panitumumab treatment. Therefore, *BRAF* mutation analysis could be used as an additional tool for the selection of mCRC patients who might benefit from EGFR-targeted MoAb therapies. The second is that clinical trials designed to test multiple therapies with EGFR and BRAF/MAPK inhibitors should be conceived for mCRC patients in whom the KRAS/BRAF pathway is oncogenically activated. Because cetuximab, panitumumab, and sorafenib are already approved for clinical use, the data presented here could find immediate clinical evaluation in phase II trials in patients who have *BRAF*-mutated tumors.

AUTHORS' DISCLOSURES OF POTENTIAL CONFLICTS OF INTEREST

The author(s) indicated no potential conflicts of interest.

AUTHOR CONTRIBUTIONS

Conception and design: Federica Di Nicolantonio, Miriam Martini, Francesca Molinari, Andrea Sartore-Bianchi, Piercarlo Saletti, Luca Mazzucchelli, Milo Frattini, Salvatore Siena, Alberto Bardelli
Financial support: Milo Frattini, Salvatore Siena, Alberto Bardelli
Provision of study materials or patients: Federica Di Nicolantonio, Francesca Molinari, Andrea Sartore-Bianchi, Piercarlo Saletti, Sara De Dosso, Luca Mazzucchelli, Milo Frattini, Salvatore Siena, Alberto Bardelli
Collection and assembly of data: Federica Di Nicolantonio, Miriam Martini, Francesca Molinari, Andrea Sartore-Bianchi, Sabrina Arena, Piercarlo Saletti, Sara De Dosso, Luca Mazzucchelli, Milo Frattini, Salvatore Siena, Alberto Bardelli
Data analysis and interpretation: Federica Di Nicolantonio, Miriam Martini, Francesca Molinari, Andrea Sartore-Bianchi, Piercarlo Saletti, Sara De Dosso, Luca Mazzucchelli, Milo Frattini, Salvatore Siena, Alberto Bardelli
Manuscript writing: Federica Di Nicolantonio, Francesca Molinari, Andrea Sartore-Bianchi, Piercarlo Saletti, Luca Mazzucchelli, Milo Frattini, Salvatore Siena, Alberto Bardelli
Final approval of manuscript: Federica Di Nicolantonio, Miriam Martini, Francesca Molinari, Andrea Sartore-Bianchi, Piercarlo Saletti, Sara De Dosso, Luca Mazzucchelli, Milo Frattini, Salvatore Siena, Alberto Bardelli

REFERENCES

1. Venook AP: Epidermal growth factor receptor-targeted treatment for advanced colorectal carcinoma. Cancer 103:2435-2446, 2005
2. Saltz LB, Meropol NJ, Loehrer PJ Sr, et al: Phase II trial of cetuximab in patients with refractory colorectal cancer that expresses the epidermal growth factor receptor. J Clin Oncol 22:1201-1208, 2004
3. Cunningham D, Humblet Y, Siena S, et al: Cetuximab monotherapy and cetuximab plus irinotecan in irinotecan-refractory metastatic colorectal cancer. N Engl J Med 351:337-345, 2004
4. Meyerhardt JA, Mayer RJ: Systemic therapy for colorectal cancer. N Engl J Med 352:476-487, 2005
5. Van Cutsem E, Peeters M, Siena S, et al: Open-label phase III trial of panitumumab plus best supportive care compared with best supportive care alone in patients with chemotherapy-refractory metastatic colorectal cancer. J Clin Oncol 25:1658-1664, 2007
6. Baselga J: The EGFR as a target for anticancer therapy: Focus on cetuximab. Eur J Cancer 37:S16-S22, 2001 (suppl 4)
7. Chung KY, Shia J, Kemeny NE, et al: Cetuximab shows activity in colorectal cancer patients with tumors that do not express the epidermal growth factor receptor by immunohistochemistry. J Clin Oncol 23:1803-1810, 2005
8. Moroni M, Veronese S, Benvenuti S, et al: Gene copy number for epidermal growth factor receptor (EGFR) and clinical response to antiEGFR treatment in colorectal cancer: A cohort study. Lancet Oncol 6:279-286, 2005
9. Lièvre A, Bachet JB, Le Corre D, et al: KRAS mutation status is predictive of response to cetuximab therapy in colorectal cancer. Cancer Res 66:3992-3995, 2006
10. Frattini M, Saletti P, Romagnani E, et al: PTEN loss of expression predicts cetuximab efficacy in metastatic colorectal cancer patients. Br J Cancer 97:1139-1145, 2007
11. Sartore-Bianchi A, Moroni M, Veronese S, et al: Epidermal growth factor receptor gene copy number and clinical outcome of metastatic colorectal cancer treated with panitumumab. J Clin Oncol 25:3238-3245, 2007
12. Cappuzzo F, Finocchiaro G, Rossi E, et al: EGFR FISH assay predicts for response to cetuximab in chemotherapy refractory colorectal cancer patients. Ann Oncol 19:717-723, 2008
13. Benvenuti S, Sartore-Bianchi A, Di Nicolantonio F, et al: Oncogenic activation of the RAS/RAF signaling pathway impairs the response of metastatic colorectal cancers to anti-epidermal growth factor receptor antibody therapies. Cancer Res 67:2643-2648, 2007
14. Di Fiore F, Blanchard F, Charbonnier F, et al: Clinical relevance of KRAS mutation detection in metastatic colorectal cancer treated by cetuximab plus chemotherapy. Br J Cancer 96:1166-1169, 2007
15. De Roock W, Piessevaux H, De Schutter J, et al: KRAS wild-type state predicts survival and is associated to early radiological response in metastatic colorectal cancer treated with cetuximab. Ann Oncol 19:508-515, 2008
16. Khambata-Ford S, Garrett CR, Meropol NJ, et al: Expression of epiregulin and amphiregulin and K-ras mutation status predict disease control in metastatic colorectal cancer patients treated with cetuximab. J Clin Oncol 25:3230-3237, 2007
17. Lièvre A, Bachet JB, Boige V, et al: KRAS mutations as an independent prognostic factor in patients with advanced colorectal cancer treated with cetuximab. J Clin Oncol 26:374-379, 2008
18. Amado RG, Wolf M, Peeters M, et al: Wild-type KRAS is required for panitumumab efficacy in patients with metastatic colorectal cancer. J Clin Oncol 26:1626-1634, 2008

© 2008 by American Society of Clinical Oncology

CSPC Exhibit 1004
Page 16 of 336

Downloaded from ascopubs.org by US PATENT TRADEMARK OFF SCI & TECH INFO Center on March 19, 2019 from 151.207.250.071
Copyright © 2019 American Society of Clinical Oncology. All rights reserved.

19. Locker GY, Hamilton S, Harris J, et al: ASCO 2006 update of recommendations for the use of tumor markers in gastrointestinal cancer. J Clin Oncol 24:5313-5327, 2006

20. Borner M, Koeberle D, Von Moos R, et al: Adding cetuximab to capecitabine plus oxaliplatin (XELOX) in first-line treatment of metastatic colorectal cancer: A randomized phase II trial of the Swiss Group for Clinical Cancer Research SAKK. Ann Oncol 19:1288-1292, 2008

21. Pessino A, Artale S, Scialiero S, et al: First-line single-agent cetuximab in patients with advanced colorectal cancer. Ann Oncol 19:711-716, 2008

22. Van Cutsem E, Siena S, Humblet Y, et al: An open-label, single-arm study assessing safety and efficacy of panitumumab in patients with metastatic colorectal cancer refractory to standard chemotherapy. Ann Oncol 19:92-98, 2008

23. Wilke H, Glynne-Jones R, Thaler J, et al: MABEL: A large multinational study of cetuximab plus irinotecan in pretreated metastatic colorectal cancer progressing on irinotecan. J Clin Oncol [epub ahead of print on October 14, 2008]

24. Therasse P, Arbuck SG, Eisenhauer EA, et al: New guidelines to evaluate the response to treatment in solid tumors: European Organization for Research and Treatment of Cancer, National Cancer Institute of the United States, National Cancer Institute of Canada. J Natl Cancer Inst 92:205-216, 2000

25. Frattini M, Ferrario C, Bressan P, et al: Alternative mutations of BRAF, RET and NTRK1 are associated with similar but distinct gene expression patterns in papillary thyroid cancer. Oncogene 23: 7436-7440, 2004

26. Frattini M, Balestra D, Suardi S, et al: Different genetic features associated with colon and rectal carcinogenesis. Clin Cancer Res 10:4015-4021, 2004

27. Rajagopalan H, Bardelli A, Lengauer C, et al: Tumorigenesis: RAF/RAS oncogenes and mismatch-repair status. Nature 418:934, 2002

28. Samowitz WS, Sweeney C, Herrick J, et al: Poor survival associated with the BRAF V600E mutation in microsatellite-stable colon cancers. Cancer Res 65:6063-6069, 2005

29. Deng G, Bell I, Crawley S, et al: BRAF mutation is frequently present in sporadic colorectal cancer with methylated hMLH1, but not in hereditary nonpolyposis colorectal cancer. Clin Cancer Res 10:191-195, 2004

30. Wang L, Cunningham JM, Winters JL, et al: BRAF mutations in colon cancer are not likely attributable to defective DNA mismatch repair. Cancer Res 63:5209-5212, 2003

31. Lu Y, Li X, Liang K, et al: Epidermal growth factor receptor (EGFR) ubiquitination as a mechanism of acquired resistance escaping treatment by the anti-EGFR monoclonal antibody cetuximab. Cancer Res 67:8240-8247, 2007

32. Wilhelm SM, Carter C, Tang L, et al: BAY 43-9006 exhibits broad spectrum oral antitumor activity and targets the RAF/MEK/ERK pathway and receptor tyrosine kinases involved in tumor progression and angiogenesis. Cancer Res 64:7099-7109, 2004

33. Yan J, Roy S, Apolloni A, et al: Ras isoforms vary in their ability to activate Raf-1 and phosphoinositide 3-kinase. J Biol Chem 273:24052-24056, 1998

34. Zhang BH, Guan KL: Activation of B-Raf kinase requires phosphorylation of the conserved residues Thr598 and Ser601. Embo J 19:5429-5439, 2000

35. Haddad R, Ogilvie RT, Croitoru M, et al: Microsatellite instability as a prognostic factor in resected colorectal cancer liver metastases. Ann Surg Oncol 11:977-982, 2004

36. Malesci A, Laghi L, Bianchi P, et al: Reduced likelihood of metastases in patients with microsatellite-unstable colorectal cancer. Clin Cancer Res 13:3831-3839, 2007

37. Friday BB, Adjei AA: Advances in targeting the Ras/Raf/MEK/Erk mitogen-activated protein kinase cascade with MEK inhibitors for cancer therapy. Clin Cancer Res 14:342-346, 2008

Acknowledgment

We thank Chris Torrance, Luca Cardone, and Fonnet Bleeker for critically reading the manuscript; Simona Lamba for assistance with sequencing; Silvio Veronese and Marcello Gambacorta for pathology assessments; Salvatore Artale for clinical care; and Giovanna Marrapese and Ines Andreotti for data management.

Glossary Terms

BRAF V600E: The V600E is the most common oncogenic mutation of BRAF in cancer. The V600E aminoacid change results in constitutive activation of the BRAF kinase and promotes cell transformation.

PI3K-PTEN-AKT pathway: Signal transduction pathways involving the signaling molecules phosphatidylinositol-3 kinase (PI3K), PTEN and Akt. PI3K generates phosphorylated inositides at the cell membrane which are required for the recruitment and activation of the serine kinase Akt. PTEN is a lipid phosphatase which counteracts the effect of PI3K. Accordingly mutated PI3K and AKT act as dominant oncogenes while PTEN is a tumor suppressor gene.

Cetuximab: Also called Erbitux or C225, cetuximab is a monoclonal antibody that is designed to target EGFR and block its signaling activity by initiating receptor activation.

Panitumumab: Also known as ABX-EGF, panitumumab is a fully human immunoglobulin G2 monoclonal antibody against EGFR and inhibits ligand-induced activation of the EGFR. This antibody is generated from mouse strains engineered to be deficient in mouse antibody production and to produce fully human antibodies.

KRAS: The gene that encodes K-Ras, a protein that is a member of the small GTPase superfamily, in which a single amino acid substitution results in an activating mutation. Alternative splicing gives rise to variants encoding two isoforms that differ in the C-terminal region.

BRAF: BRAF is an isoform of RAF. Raf proteins (Raf-1, A-Raf, B-Raf) are intermediate to Ras and MAPK in the cellular proliferative pathway. Raf proteins are typically activated by Ras via phosphorylation, and activated Raf proteins in turn activate MAPK via phosphorylation. However, Raf proteins may also be independently activated by other kinases.

Sorafenib: A substance belonging to the family of drugs called raf kinase inhibitors and anti-VEGF that is being studied in the treatment of cancer.

MAPK (mitogen-activated protein kinase): MAPKs are a family of enzymes that form an integrated network influencing cellular functions such as differentiation, proliferation, and cell death. These cytoplasmic proteins modulate the activities of other intracellular proteins by adding phosphate groups to their serine/threonine amino acids.

MSI (microsatellite instability): Microsatellites are repeating units of 1-4 DNA base pairs that are distributed widely throughout the genome and have a high degree of repeat length variation in the population. Their length remains stable with cell division and inheritance so they may be used as molecular markers of cell lineage, in population genetic studies or paternity testing. Defects in the genes involved in DNA mismatch repair result in genomic instability that may be detected as MSI, an alteration in the length of the microsatellites from cell to cell.

 © 2008 by American Society of Clinical Oncology

CSPC Exhibit 1004
Page 17 of 336

Downloaded from ascopubs.org by US PATENT TRADEMARK OFF SCI & TECH INFO Center on March 19, 2019 from 151.207.250.071
Copyright © 2019 American Society of Clinical Oncology. All rights reserved.

R. V. J. Chari et al.

DOI: 10.1002/anie.201307628

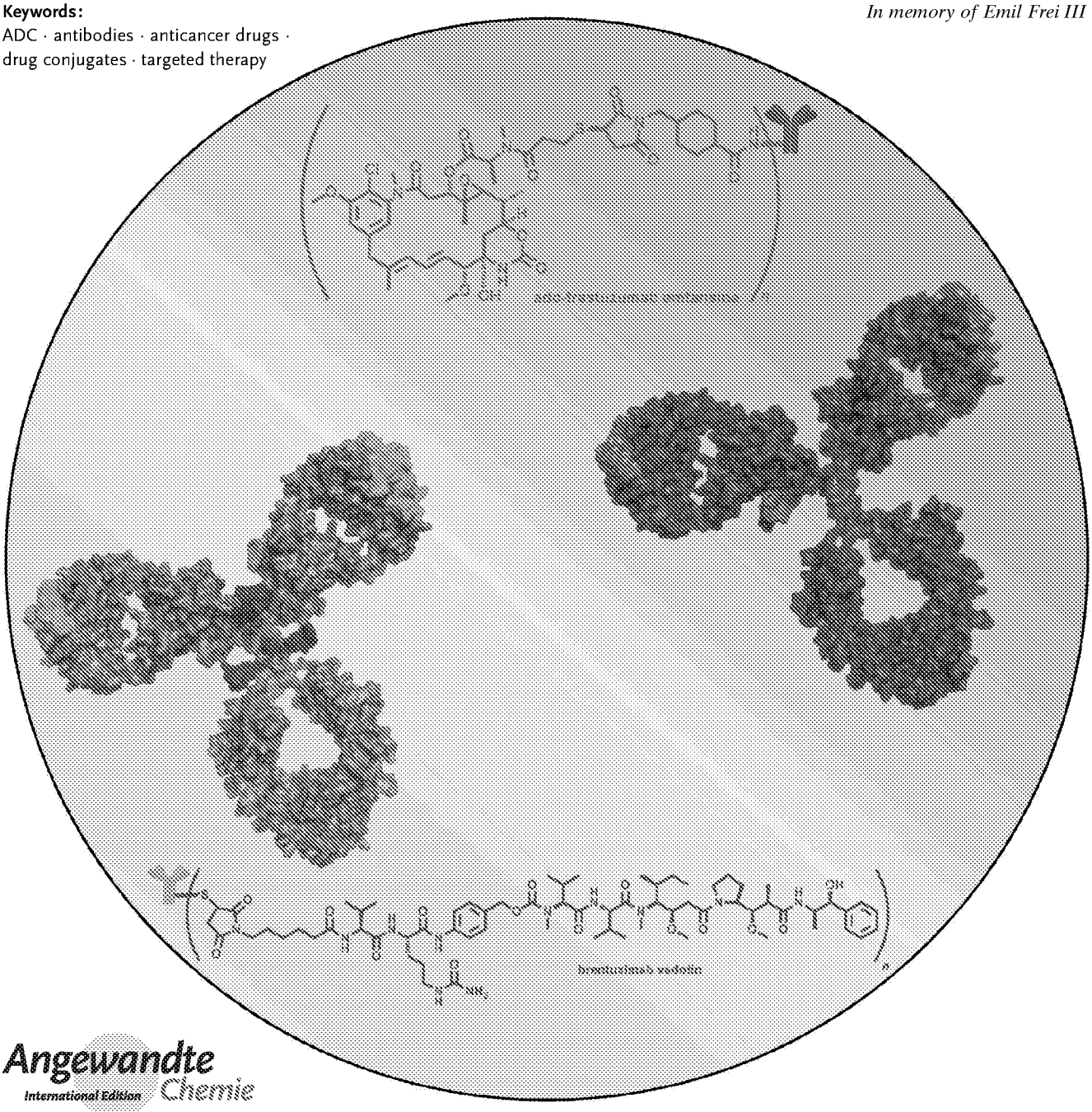
Targeted Cancer Therapy

Antibody–Drug Conjugates: An Emerging Concept in Cancer Therapy

Ravi V. J. Chari, Michael L. Miller, and Wayne C. Widdison*

Keywords:
ADC · antibodies · anticancer drugs · drug conjugates · targeted therapy

In memory of Emil Frei III



© 2014 Wiley-VCH Verlag GmbH & Co. KGaA, Weinheim

CSPC Exhibit 1004
Page 18 of 336

Angewandte International Edition Chemie

Traditional cancer chemotherapy is often accompanied by systemic toxicity to the patient. Monoclonal antibodies against antigens on cancer cells offer an alternative tumor-selective treatment approach. However, most monoclonal antibodies are not sufficiently potent to be therapeutically active on their own. Antibody–drug conjugates (ADCs) use antibodies to deliver a potent cytotoxic compound selectively to tumor cells, thus improving the therapeutic index of chemotherapeutic agents. The recent approval of two ADCs, brentuximab vedotin and ado-trastuzumab emtansine, for cancer treatment has spurred tremendous research interest in this field. This Review touches upon the early efforts in the field, and describes how the lessons learned from the first-generation ADCs have led to improvements in every aspect of this technology, i.e., the antibody, the cytotoxic compound, and the linker connecting them, leading to the current successes. The design of ADCs currently in clinical development, and results from mechanistic studies and preclinical and clinical evaluation are discussed. Emerging technologies that seek to further advance this exciting area of research are also discussed.

From the Contents

1. Introduction 3797
2. Targeted Therapies 3799
3. First-Generation Antibody–Drug Conjugates 3801
4. Improved Antibody–Drug Conjugates: Key Requirements 3802
5. Antimitotic Agents as ADC Payloads 3803
6. DNA Agents as ADC Payloads 3813
7. Clinical Results 3818
8. Emerging Technologies 3819
9. Summary and Outlook 3823

1. Introduction

For the better part of the twentieth century, chemotherapy, or "treatment with chemicals" was the predominant modality for cancer treatment.[1,2] The use of chemotherapeutic agents for the treatment of cancer is based on the premise that these agents would preferentially kill rapidly dividing cancer cells, while sparing normal cells. The first class of chemotherapeutic agents to be tested in humans were the nitrogen mustards, chlorambucil and cyclophosphamide, which exert cellular cytotoxicity by alkylation of DNA. Although success was short lived, the initial promise spurred the development of a steady stream of new anticancer agents with improved activity. The recognition that folic acid stimulates cancer cell growth led to the synthesis of antifolates, such as methotrexate, as antitumor agents. The elucidation of the structure of DNA led to compounds that interfered with DNA synthesis and caused cell death. These included nucleoside analogues, such as thioguanine, 5-fluoruracil, and cytosine arabinoside (ara-C). Subsequently, DNA-interacting agents, such as cisplatin, and antitumor antibiotics derived from bacterial fermentation, such as actinomycin D and the anthracyclines entered the foray of drugs to treat cancer. Chemotherapeutic agents targeting tubulin (e.g. the *Vinca* alkaloids from plants) also entered clinical evaluation.

Although by the late 1980s, there was a plethora of drugs in the anticancer armamentarium, their effectiveness continued to be plagued by the lack of tumor selectivity, resulting in the killing of proliferating normal cells, such as those of the bone marrow and gastrointestinal tract. Most anticancer drugs had to be used near their maximum tolerated dose (MTD) to achieve a clinically meaningful therapeutic effect. A significant milestone in cancer chemotherapy was the introduction of the concept of drug combinations.[3] It was realized that cancer drugs with non-overlapping toxicity profiles and different mechanisms of action could often be combined at full doses with resultant additive or synergistic effect and improved antitumor activity. Thus, multidrug therapy became a standard modality for the treatment of most cancers. With such intensive chemotherapy, systemic toxicity to the host remains a major drawback of cytotoxic drugs in cancer, and cures are achieved only in a small set of cancers.

The limited clinical efficacy of anticancer drugs, whether used alone or in combination, could be attributed to the insufficient therapeutic window of these compounds, that is, the inability to kill a sufficient number of cancer cells without causing toxicity. For example, it has been estimated that more than 99% of the cells in the tumor have to be killed to achieve a complete remission in the patient, with significantly greater degree of cell kill required to achieve tumor eradication.[3] In order to improve the therapeutic index of cancer drugs, either the potency of the cytotoxic agent had to be improved to lower the minimum effective dose (MED), or the tumor selectivity improved to increase the maximum tolerated dose (Figure 1). An ideal solution would be the development of agents that would both decrease the MED and increase the MTD, thus increasing the overall therapeutic index of the cancer drug.

The recognition that many anticancer drugs were derived from natural sources, such as plants and marine or microbial organisms, stimulated active research in the area of natural

[*] Dr. R. V. J. Chari, Dr. M. L. Miller, Dr. W. C. Widdison
ImmunoGen, Inc.
830 Winter St, Waltham, MA 02451 (USA)
E-mail: ravi.chari@immunogen.com
Homepage: http://www.immunogen.com

 © 2014 Wiley-VCH Verlag GmbH & Co. KGaA, Weinheim

CSPC Exhibit 1004
Page 19 of 336

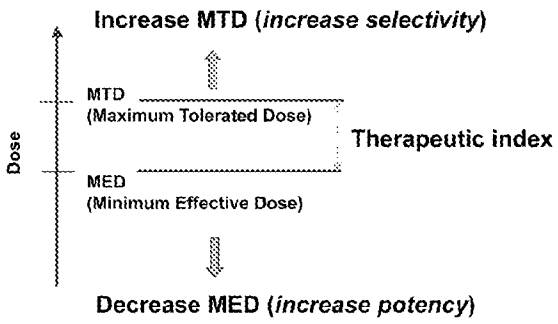


Figure 1. Approach to optimize the therapeutic index.

products by medicinal chemists seeking to discover new cytotoxic compounds with much higher potency than the known anticancer drugs. One of the first such compounds that garnered a lot of excitement was maytansine (**1**), a macrocyclic molecule belonging to the family of compounds termed maytansinoids, which were isolated from the Ethiopian shrub *Maytenus ovatus* by Kupchan et al.[4,5] Maytansine was found to be a strong inhibitor of tubulin polymerization, and thus a highly potent mitotic inhibitor.[6] It was one of the first compounds to kill cancer cells with IC_{50} values in the picomolar range, and thus was several orders of magnitude more cytotoxic than clinically used anticancer agents, such as doxorubicin, methotrexate, and 5-flurouracil. Maytansine was rapidly advanced into human clinical evaluation. However, after Phase II clinical studies, the development of maytansine was discontinued because of insufficient antitumor activity. Consistent with its high in vitro potency, the MTD achieved in humans (2 $mg\,m^{-2}$) was much lower than that of anticancer drugs, such as doxorubicin (dose 60–75 $mg\,m^{-2}$).[7] The main dose-limiting toxicities associated with maytansine treatment were effects on the gastrointestinal tract and peripheral neuropathy.

Subsequently, a few other potent tubulin-interacting agents were discovered and advanced to clinical evaluation (Figure 2). Pettit and co-workers isolated a family of cytotoxic peptides, termed the dolastatins, from the marine shell-less mollusk *Dolabella auricularia*. The most studied members of this family are the linear peptides dolastatin 10 (**2a**) and dolastatin 15 (**2b**).[8,9] Like maytansine, these compounds are also potent inhibitors of tubulin polymerization and induced cancer cell death in vitro at picomolar concentrations. In Phase I clinical studies, the MTD of **2a** was found to be 0.4 $mg\,m^{-2}$, which was even lower than that of maytansine.[10] Dose-limiting toxicities were mainly of haematologic nature and included neutropenia and granulocytopenia. Phase II clinical trials in a number of cancer indications, including melanoma, renal cancer, sarcomas, and breast cancer, failed to demonstrate clinical benefit, and the development of dolastatin 10 was discontinued.[11] The dolastatin 15 analogue cemadotin (**2c**) and the next-generation analogue tasidotin (**2d**), which was designed to be metabolically stable through its resistance to hydrolysis by prolyl oligopeptidases, were also evaluated in human clinical trials and failed to demonstrate meaningful activity. The lack of therapeutic benefit of these compounds did not deter the development of another class of potent tubulin agents, the cryptophycins, a family of macrolides found in the blue-green alga *Nostoc* sp. (cyanobacteria). Cryptophycin 1 (**3a**) was the main component of the algal extract and was responsible for most of the cytotoxic activity. The synthetic analogue cryptophycin 52 (**3b**), which bears a gem-dimethyl substituent at C6 of the C subunit, was found to kill cancer cells in vitro at picomolar concentrations, and was advanced to clinical evaluation.[12] However, the dose achieved was very low (MTD of 1.5 $mg\,m^{-2}$) and sufficient therapeutic activity was not attained.[13] Thus, the cryptophycins joined the ranks of the other highly potent tubulin agents that failed to live up to the promise that higher potency would translate to improved clinical activity. One exception to this trend is the recent approval of eribulin mesylate (**3c**) for the treatment of metastatic breast cancer. This drug is a fully synthetic analogue of halichondrin, a tubulin polymerization inhibitor derived from the marine sponge *Halichondria okadai*.[14]

While clinical success with these cytotoxic agents was elusive, it was not clear whether the lack of therapeutic activity was due to the extremely high potency of these drugs, leading to toxicity at low doses, or their mechanism of action, with all of them being inhibitors of tubulin polymerization. Results from clinical testing of potent drugs (Figure 3) with an alternative mechanism of cell killing could provide some insight. The isolation and structure elucidation of the microbial natural product CC-1065 (**4a**), a highly cytotoxic, sequence-selective DNA-minor-groove binder and DNA-alkylating agent, initiated the synthesis of a panel of simpler analogues.[15] These compounds retained the picomolar in vitro potency of the parent compound toward cancer cells. Several of these compounds, including adozelesin (**4b**), a prodrug form carzelesin (**4c**), an even more potent dimeric



Ravi V. J. Chari received his Ph.D. degree in Chemistry from the University of Detroit. He then pursued postdoctoral work at the School of Medicine of Yale University. Subsequently, he joined the Dana-Farber Cancer Institute/Harvard Medical School as a research scientist. In 1988, he joined ImmunoGen where he began research on antibody–drug conjugates for cancer. He is currently Executive Director, Chemistry & Biochemistry.



Michael L. Miller received his B.S. in 1994 from Memphis State University and his Ph.D. in 1998 at the University of Memphis. He pursued his postdoctoral research with Professor Iwao Ojima at the State University of New York at Stony Brook. In 2000, he joined the Chemistry Department at ImmunoGen, Inc., focusing his efforts on the development of potent compounds for use in antibody–drug conjugates.

© 2014 Wiley-VCH Verlag GmbH & Co. KGaA, Weinheim

CSPC Exhibit 1004
Page 20 of 336

compound bizelesin (**4d**), and the synthetic duocarmycin analogue KW-2189 (**4e**), were evaluated in human clinical trials.[16–19] These DNA-alkylating agents suffered the same fate as the potent tubulin agents described above, with very low clinically achievable doses (ranging from 0.001 $mg\,m^{-2}$ for **4d** to 0.4 $mg\,m^{-2}$ for **4e**) and insufficient activity. Recently, the pyrrolobenzodiazepine dimer SJG-136 (**4f**), a highly cytotoxic DNA crosslinker, has completed Phase I clinical evaluation, and again a low MTD (0.045 $mg\,m^{-2}$) was achieved.[20] This drug is currently undergoing Phase II clinical evaluation. Thus, with few exceptions, merely increasing the cell-killing power of cytotoxic drugs does not appear to increase the therapeutic index of chemotherapy.

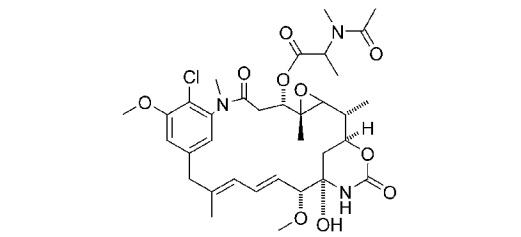
2. Targeted Therapies

Targeted therapy approaches seek to specifically interfere with molecular targets and pathways that are important for the proliferation of cancer cells. These targets are preferentially expressed either intracellularly or on the surface of tumor cells. Thus, targeted therapy offers the potential to generate agents that will be selectively cytotoxic to tumor cells, coupled with lower toxicity to the host, resulting in a larger therapeutic index. The major areas of focus include a) inhibitors of receptor tyrosine kinases, b) monoclonal antibodies, c) antibody–drug conjugates (ADCs), d) small targeting molecule–drug conjugates, and e) antisense and siRNA approaches. The initial clinical success of the targeted therapy approach has led to a burgeoning effort in these areas of cancer drug development. In the one-year period from October 2011 to October 2012, four of the seven cancer drugs approved by the FDA are targeted agents, further validating the promise of this approach.

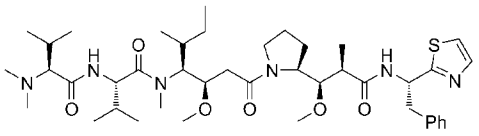
One of the most popular targets for medicinal chemists in the field of cancer research are tyrosine kinases, enzymes that catalyze the transfer of the terminal phosphate group from adenosine triphosphate to the target protein. In cancer cells, some key tyrosine kinases are not properly regulated resulting in excessive phosphorylation of target proteins causing sustained signal transduction and cell proliferation. Additionally, tyrosine kinase may be over-expressed in tumor cells or exist in an aberrant (mutant) form that stimulates cancer cell growth.[21,22] A majority of these kinase inhibitors are heterocyclic compounds that compete with ATP for binding to the active conformational form of the enzyme. Imatinib mesylate was the first compound in this class to be approved by the FDA in 2001 for the treatment of chronic myelogenous leukemia (CML). Imatinib was designed to target the BCR-ABL protein, a mutant fusion protein that is present in leukemic cells in almost all CML patients. Imatinib competitively inhibits the binding of ATP to the BCR-ABL tyrosine kinase and specifically inhibits the proliferation of CML cells.



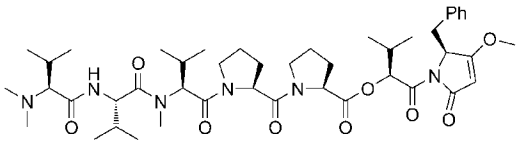
Wayne C. Widdison received his Ph.D. degree in Organic Chemistry with Professor John F. Baldwin at Syracuse University in 1991. He then pursued postdoctoral work at Stanford University. He joined the chemistry department at ImmunoGen in 1993, where he is currently a Principal Scientist. His research is focused on the development of maytansinoids and linkers for the preparation of antibody–drug conjugates.



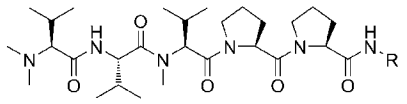
Maytansine (**1**)



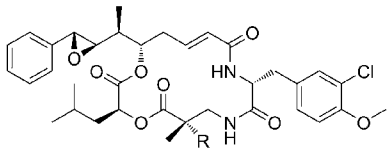
Dolastatin 10 (**2a**)



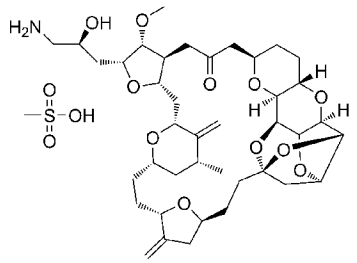
Dolastatin 15 (**2b**)



Cemadotin (R = Bn) (**2c**)
Tasidotin (R = *t*Bu) (**2d**)



Cryptophycin 1 (R = H) (**3a**)
Cryptophycin 52 (R = Me) (**3b**)



Eribulin mesylate (**3c**)

Figure 2. Structures of tubulin-binding cytotoxic agents.

© 2014 Wiley-VCH Verlag GmbH & Co. KGaA, Weinheim

CSPC Exhibit 1004
Page 21 of 336

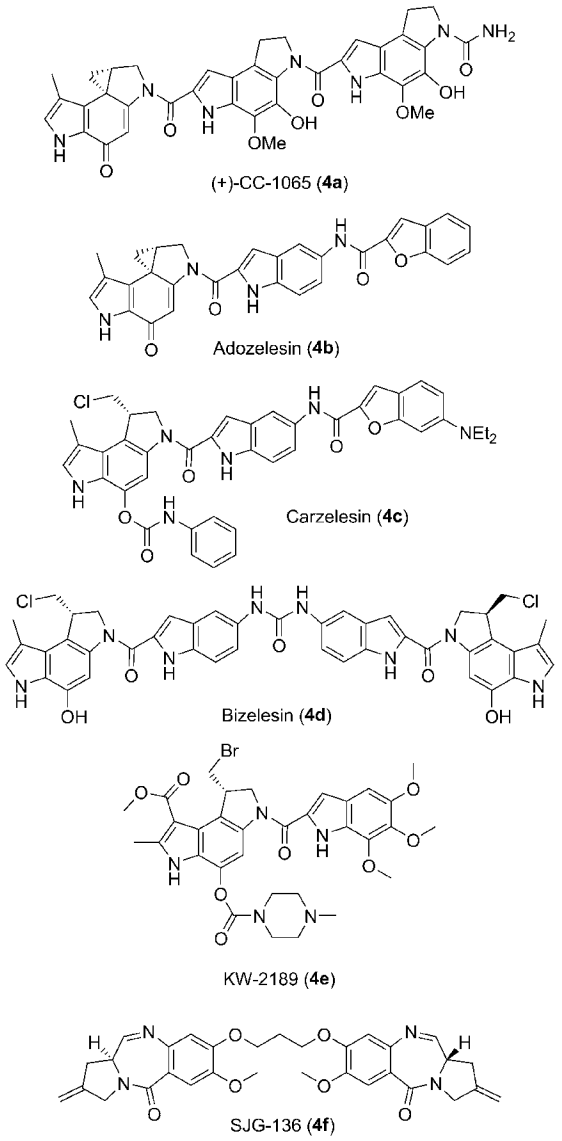


Figure 3. Structures of DNA-alkylating/cross-linking cytotoxic agents.

Success with imatinib was followed two years later with the approval of gefitinib, a selective inhibitor of the epidermal growth factor receptor tyrosine kinase. Thus far, at least 20 kinase inhibitors targeting different tumor indications have been approved. Many of the early kinase inhibitors exert their cytotoxic effect by targeting a specific kinase. In order to increase the treatment population, inhibitors that hit more than one target (multitargeted) are actively being pursued. It is not yet clear whether the lower selectivity of these types of agents would lead to greater adverse effects.

Another emerging targeted therapy approach is the use of small molecules that selectively bind to the surface of tumor cells to deliver a cytotoxic compound.[23] The most advanced compound in this class is a folate–Vinca alkaloid conjugate. In this conjugate, the tumor-targeting element, folic acid, binds with high affinity to the folate receptor that is over-expressed on the surface of a number or tumors, notably ovarian and non-small-cell lung cancers. The construct consists of folic acid linked through a disulfide bond to desacetylvinblastine monohydrazide with a pentapeptide spacer. The folate conjugate showed good dose-dependent antitumor activity in a folate-receptor-positive tumor xenograft model, and was significantly more active than the unconjugated Vinca drug. Co-administration of an excess of unconjugated folic acid abrogated the antitumor activity of the conjugate, demonstrating tumor specificity.[24,25] This conjugate is currently in advanced clinical trials.

2.1. Monoclonal Antibodies in Cancer

The recognition that cancer cells possess specific molecular markers that play a role in tumor growth or progression has opened the door to specifically target these markers. These markers, also known as antigens, are typically cell-surface proteins, glycoproteins, or carbohydrates. Ideally, they are selectively expressed on the surface of tumor cells with minimal expression in normal human tissues. In many cases, the antigen may be overexpressed or present in mutated form on cancer cells. Immunization of mice with human cancer cells or purified antigens elicits a target-specific antibody response in the sera of these animals. While these antibodies could specifically bind to the target antigen, they are often obtained in low yield and as a mixture containing antibodies to nonspecific targets. The advent of the hybridoma technology pioneered by Kohler and Milstein in 1975[26] represented a significant advancement enabling production of large amounts of a single purified antibody to the antigen of interest. In this technique, antibody-producing B lymphocytes are isolated from the mice and immortalized by fusion with a mouse myeloma cell line. The resulting clonal cells, also known as hybridomas, can be cultured in vitro in tissue culture flasks or bioreactors to produce the specific monoclonal antibody (mAb). The efficiency of tumor cell kill by monoclonal antibodies can range widely, from poor to high depending on the nature of the target antigen. Antibodies can induce cancer cell death by a multitude of mechanisms, including a) immune-mediated functions, such as antibody-dependent cellular cytotoxicity (ADCC), b) complement-dependent cytotoxicity (CDC), c) antibody-dependent phagocytosis, d) interference with tumor-cell signaling pathways, often achieved through receptor blockage, e) depletion of circulating tumor cells by direct binding to the antibody, f) apoptosis, and g) immune modulation of T-cell function.[27,28]

The first human clinical trial with a monoclonal antibody was conducted in 1980 when a lymphoma patient was treated with the murine monoclonal antibody AB 89.[29] In the ensuing years, clinical trials with a number of murine monoclonal antibodies were conducted. An emerging theme from these trials was the development of an immune response to the murine monoclonal antibody, a foreign protein, with the generation of human anti-mouse antibodies (HAMA), resulting in rapid clearance of the murine antibody from circulation. Advances in recombinant DNA technology have

© 2014 Wiley-VCH Verlag GmbH & Co. KGaA, Weinheim

CSPC Exhibit 1004
Page 22 of 336

enabled the generation of engineered antibodies in which protein sequences of the murine antibody are replaced by sequences naturally occurring in human antibodies, without affecting the specific binding of the antibody to its target antigen. In the first of these constructs, molecular biologists merely replaced the entire constant regions of the murine antibody with the corresponding human constant region sequences, while retaining the murine variable domains (Fv) responsible for antigen binding (Figure 4). These "chimeric" antibodies still contained a significant number of murine residues, so further antibody engineering advancements led to new "humanization" methods that facilitated the replacement of murine Fv sequences with the human antibody Fv sequences. In the humanized antibody, only the essential antigen recognition murine residues encompassing the complementarity determining regions (CDRs) within the Fv domains are preserved, while the remainder of the murine Fv is replaced with human Fv sequences. The advent of phage display technology and transgenic mice bearing the human repertoire introduced new avenues for generating fully human antibodies requiring no additional engineering for human therapeutic development.[30] With these advances, it has been possible to reduce or eliminate the immune response previously noted with murine antibodies. In addition, the circulation half-life of these new constructs is significantly longer ($T_{1/2}$ up to three weeks) than that of their murine counterparts (typically two to three days).

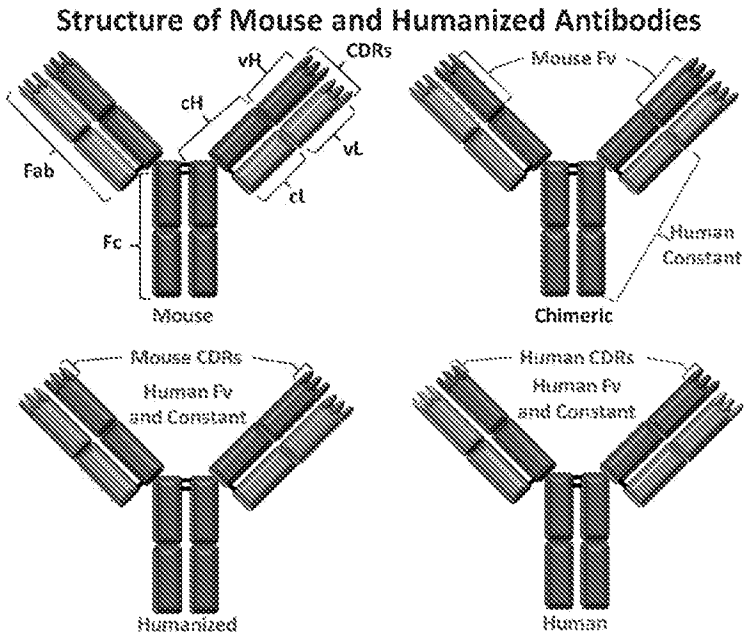


Figure 4. A cartoon representation of mouse (green), chimeric, humanized, and human (blue) antibodies. The antibody subdomains are marked, including Fab, Fc, heavy-chain variable (vH), light-chain variable (vL), heavy-chain constant (cH), light-chain constant (cL), and the complementarity determining regions (CDRs).

The first monoclonal antibody for the treatment of cancer, rituximab, was approved by the U.S. FDA in 1997 for use in patients with relapsed or refractory, CD-20 positive, B-cell, low-grade or follicular non-Hodgkin's lymphoma.[31] Rituximab is a chimeric antibody that binds to the CD20 antigen expressed on the surface of a majority of B-cell lymphomas. Subsequently, the anti-CD52 antibody alemtuzumab, and the anti-CD20 antibody ofatumumab were approved for the treatment of chronic lymphocytic leukemia. While the three approved antibodies for hematologic malignancies are used as single agents, the FDA-approved antibodies for solid tumors often display only modest antitumor activity and are typically used together with chemotherapeutic agents. Thus, the humanized antibodies trastuzumab and pertuzumab targeting the HER-2 antigen, which is over-expressed on a subset of breast cancers and also some gastric tumors, are often used with chemotherapy. Similarly, the anti-EGF receptor antibodies cetuximab and panitumumab are used in combination with chemotherapy for the treatment of colorectal and head and neck cancers. Bevacizumab, an anti-angiogenic antibody that binds to vascular endothelial growth factor A, has been approved for treatment in combination with chemotherapy in a number of solid tumor indications. Such combination therapy has the drawback of preserving the toxic side effects of the cytotoxic drug. Recently, ipilimumab, an antibody that activates the immune system by targeting CTLA-4, has been approved for the treatment of patients with late-stage melanoma. Ipilimumab represents one of the few antibodies with sufficient activity to be used as a single agent in the treatment of solid tumors. In the 32 years since the first monoclonal antibody was evaluated in the clinic, only eight have been approved thus far for the treatment of cancer, and only two cell-surface targets, two members of the ErbB receptor family (HER2 and EGFR), have been successfully targeted by antibodies for treating solid tumors.

3. First-Generation Antibody–Drug Conjugates

The concept of antibody–drug conjugates (ADCs) first evolved from the need to improve the tumor selectivity of clinically used anticancer drugs. While the role of monoclonal antibodies in cancer was still being defined, it was clear that many antibodies displayed preferential binding to tumor cells and could serve as a vehicle for selective delivery of the anticancer drug to the tumor. Thus, in the first set of ADCs to be prepared and tested, the anticancer drugs methotrexate, vinblastine, doxorubicin, and melphalan were linked to monoclonal antibodies. It was recognized early on, that the nature of the linker connecting the monoclonal antibody and drug was important. Once internalized into a target cell, some intracellular release mechanism should cleave the linker to

 © 2014 Wiley-VCH Verlag GmbH & Co. KGaA, Weinheim

CSPC Exhibit 1004
Page 23 of 336

release the active drug. Among the utilized linkers were acid-labile linkers that relied on the acidic pH value (≈ 5) of the intracellular compartment, the endosome, and enzyme-labile linkers that relied on lysosomal enzymes, such as peptidases and esterases, for cleavage.

In vitro evaluation of these first-generation conjugates on target tumor cell lines showed that, in most cases, these conjugates were only moderately potent and often less active than the parent drug. Target-selective potency was rarely demonstrated in vitro, suggesting that the choice of linkers in these conjugates was not appropriate. Nevertheless, researchers pursued the evaluation of antitumor activity of these conjugates in human xenograft models in mice. Significant localization of an antibody–methotrexate conjugate at the tumor was demonstrated. Within 3 h after administration, as much as 15% of the injected dose of conjugate had accumulated per gram of tumor.[32] Researchers were eager to see whether the impressive tumor localization would lead to significant antitumor activity in vivo. The in vivo antitumor activity of vinblastine and doxorubicin, linked to antibodies through acid-labile bonds, was shown to be superior to that of the corresponding unconjugated drugs.[33,34]

These encouraging preclinical results led to the clinical evaluation of four candidates (Figure 5). A conjugate of the murine KS1/4 antibody with the cytotoxic drug methotrexate (**6a**), linked through an amide bond, was evaluated in two Phase I clinical trials in patients with NSCLC.[35] Immunohistochemical (IHC) staining of carcinoma biopsies of the patients (post-treatment) provided convincing evidence of tumor localization of the conjugate. However, little evidence of therapeutic benefit or clinical response was observed in either study. Since the antibody that was used was of murine origin, the conjugate elicited an immune response in a majority of patients with HAMA observed in circulation within three weeks of treatment. The development of a HAMA response posed the risk of faster clearance of the ADC from circulation during repeat dosing. The murine KS1/4 antibody was also linked to desacetylvinblastine, through an esterase-labile hemisuccinate link (KS1/4-DAVLB, **6b**) or an acid-labile hydrazone bond (KS1/4-DAVLBH, **6c**). Both constructs were evaluated in human clinical trials.[36,37] In addition, in one part of the study, patients with adenocarcinoma of the lung or colon were treated with the radiolabeled version of conjugate **6b**. This radiolabeled conjugate provided definitive evidence of tumor localization in patients. Nevertheless, therapeutic activity was not noted with either of these conjugates. Also, a majority of patients in these trials developed an immune response both to the murine antibody and the Vinca component.

Unlike the conjugates described above, which were discontinued after Phase I evaluation, the antibody–doxorubicin conjugate BR96-Dox (**6d**), in which doxorubicin is linked to the chimeric BR96 antibody through an acid-labile hydrazone bond, was advanced to a Phase II human clinical trial in metastatic breast cancer.[38] In this randomized trial, patients were treated either with conjugate **6d** or with free doxorubicin. The toxicity profile of the conjugate was markedly different from that of the unconjugated doxorubicin, suggesting that antibody-mediated delivery can indeed

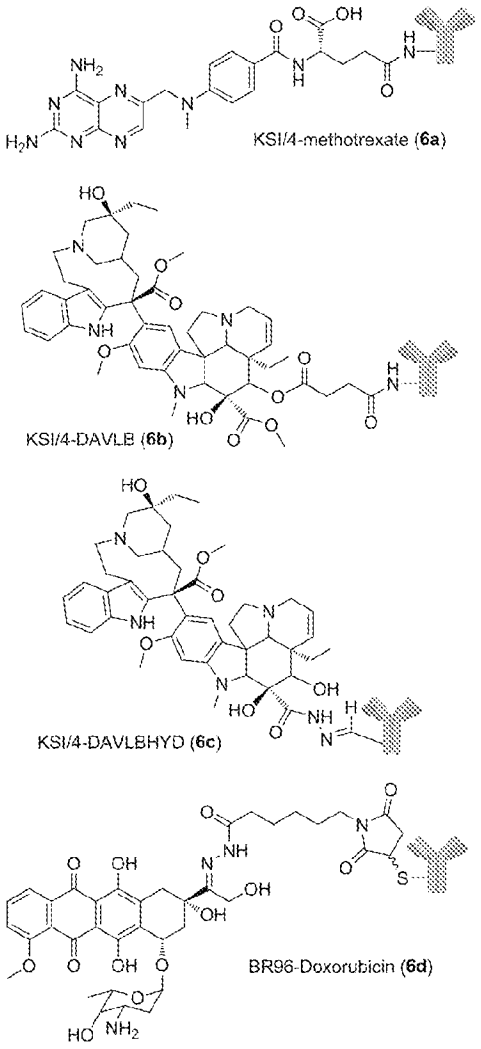


Figure 5. Structures of the first-generation antibody–drug conjugates.

alter the biodistribution of the drug. However, despite the strong preclinical data, wherein the conjugated doxorubicin was shown to be superior to free doxorubicin, the conjugate failed to demonstrate clinically meaningful therapeutic activity. Although BR96 was a chimeric antibody, the conjugate elicited an immune response in about 50% of the evaluable patients

4. Improved Antibody–Drug Conjugates: Key Requirements

The lack of clinical success with early ADCs, all of which used existing anticancer drugs as the "payload", initially dampened enthusiasm in this area of research. However, a careful analysis of each component of these early ADCs led to the identification of several factors that may have led to their failure.

© 2014 Wiley-VCH Verlag GmbH & Co. KGaA, Weinheim

CSPC Exhibit 1004
Page 24 of 336

4.1. The Cytotoxic Molecule

A key feature of the early ADCs was their lack of sufficient in vitro potency, and the finding that conjugation often led to decreased potency compared to the parent free drug. For example the conjugate **6c** was reported to be eight times less potent than the unconjugated desacetylvinblastine drug.[33] Similarly, conjugate **6d** was about eight times less potent than doxorubicin.[34] The diminished potency upon conjugation can be attributed to the different modes of cellular uptake of the unconjugated and conjugated drug. A hydrophobic drug, such as vinblastine, can freely diffuse into the cell and get concentrated at its intracellular target (tubulin), resulting in cell death. The number of molecules of a moderately potent cytotoxic drug required to effect cell kill could be very high ($>10^6$ molecules/cell). Delivery of the cytotoxic molecule by an antibody is limited by two factors: a) moderate number of antigen molecules on the cell surface to which the antibody can bind (typically $\approx 10^5$ receptors/cell), and b) internalization of cell-surface bound antigen–antibody complex, or intracellular processing to release the active drug moiety, may not be efficient. Thus, for an ADC to be therapeutically active, the number of molecules of the cytotoxic agent required to kill a cell has to be below, preferably well below, the number that is deliverable intracellularly by the antibody. Based on these calculations, cytotoxic molecules with potency in the picomolar range are required. Also, dosimetry studies with radiolabeled antibodies in cancer patients have revealed that uptake by the tumor was quite low (ranging from 0.003 to 0.01% injected dose/gram of tumor).[39] In addition to high potency, an important requirement that is often overlooked is that cytotoxic molecules for use in ADCs have to be stable and adequately soluble in the aqueous milieu of the antibody. Another challenge is to be able to chemically modify the drug to introduce functional groups that are amenable to conjugation reactions with antibodies. The site and nature of the modification has to be carefully selected so as to preserve the potency of the parent drug.

4.2. The Linker

In the first ADCs that entered clinical evaluation, the drug (methotrexate or desacetylvinblastine) bearing a carboxy group was merely mixed with the antibody in aqueous solution in the presence of the coupling agent EDC (*N*-ethyl-*N*′-(3-dimethylaminopropyl)carbodiimide hydrochloride) to enable amide bond formation with amino groups of the antibody. As antibodies possess amino acid residues with free carboxy groups (aspartate, glutamate) and free amino groups (lysine), EDC-mediated coupling can result in both intra- and intermolecular amide bond formation between amino acid residues of the antibody. Analytical tools were not available at that time to evaluate the biochemical characteristics of these conjugates prior to clinical evaluation. The first improvement in linker design came from the recognition that the linker should be cleaved upon internalization of the ADC into the targeted cell to release the active drug. In two of the ADCs that entered the clinic, the drug (des-acetylvinblastine hydrazide and doxorubicin) was linked to the antibody through acid-labile hydrazone bonds to take advantage of the acidic pH value (≈ 5) of the endosomes and lysosomes. Upon incubation of the ADC in acidic buffer, efficient release of the drug was demonstrated. However, incubation of the ADC under physiological conditions (pH 7.4, 37 °C) resulted in a time-dependent slow release of drug.[33] Premature release of drug in circulation could lead to systemic toxicity and a lower therapeutic index. Thus, it was reasoned that an effective linker design has to balance the need of good stability during several days in circulation and efficient cleavage upon delivery into the target cell.

4.3. The Antibody

The key function of the antibody is to preferentially bind to antigens on the target cell and thus concentrate the linked cytotoxic agent at the tumor site. Ideally, the antibody should be selected to cell-surface targets wherein the antigen is expressed in high copy numbers ($>10^5$/cell). In addition, it is desirable for the antigen to be expressed homogenously on all cells of the tumor, as determined by IHC staining of tumor tissue biopsies. The desired binding affinity of the antibody to its antigen is an issue of some debate. A high binding affinity ($K_D < 1$ nM) may ensure good tumor localization, but some in vivo studies have suggested that antibodies with lower binding affinity may be able to penetrate solid tumors to a greater extent.[40] The relevance of these studies performed in mice bearing subcutaneous tumor xenografts to human cancers is not known. In addition to binding to the surface of tumor cells, the ability of the antibody–antigen complex to internalize into the cell to enable intracellular delivery of the linked payload is an important factor. This internalization process, called receptor-mediated endocytosis, is dependent on the nature of the antigen, with some growth factor receptors such as the epidermal growth factor receptor (EGFR) known to be well-internalized.[41] Thus, the efficiency of internalization is an important factor to consider in the selection of an antigen target for ADCs. While the ADC approach does not require that the antibody itself possesses functional activity, this feature of the antibody may confer additional therapeutic benefit. The problem of immunogenicity noted with early ADCs that used murine antibodies can be solved with the use of "humanized" or fully human antibodies that are now readily available.

5. Antimitotic Agents as ADC Payloads

Microtubule-acting compounds are antimitotic agents that interfere with the ability of mitotic spindles to segregate chromosomes and also alter the cytoskeletal architecture of cells, causing cell death.[42] The Vinca alkaloids (e.g. vincristine and vinblastine) are examples of tubulin-binding agents, which act by disrupting normal microtubule formation and dynamics, whereas the taxoids (e.g. paclitaxel and docetaxel) stabilize altered microtubule structures, thus interfering with

 © 2014 Wiley-VCH Verlag GmbH & Co. KGaA, Weinheim

CSPC Exhibit 1004
Page 25 of 336

their normal degradation during cell division.[43] Because of their effect on mitosis, antimitotic agents are especially cytotoxic to cancer cells, which typically divide faster than most noncancerous cells. However, rapidly dividing noncancerous cells, such as the cells lining the intestines, cells in hair follicles, and myeloid cells, can also be killed, resulting in nausea, hair loss, and myelosuppression, respectively, as common side effects. Antimitotic agents that interfere with microtubule dynamics have also been found to impair the function of peripheral neurons, resulting in neuropathy.[44,45]

Most monoclonal antibodies and ADCs utilized for anticancer therapy target antigens that are over-expressed on the surface of cancer cells. However, the target antigens are also often expressed, to a lesser extent, on the surface of noncancerous cells. In addition, several types of noncancerous cells may also take up antibody or ADC by nonspecific pinocytosis or through cell surface Fc receptors.[46] It is therefore desirable to select a cytotoxic payload that shows some inherent selectivity toward killing cancerous cells versus noncancerous cells. Use of antimitotic agents as ADC payloads may partially achieve this goal by being less toxic toward slowly dividing or nondividing noncancerous cells that may be exposed to the conjugate.

The maytansinoid and auristatin microtubule binding agents possess the desired high potency for use in ADCs. Compounds from both classes have been successfully used as payloads for clinically approved ADCs, and are being tested in many ADCs in clinical trials.

5.1. Maytansinoids as ADC Payloads

Maytansine (**1**) is a benzoansamacrolide that was first isolated from the bark of the Ethiopian shrub *Maytenus ovatus* by Kupchan et al. in 1972.[4] Maytansine, and maytansinoids in general, bind to tubulin near the Vinca alkaloid binding site, and are thought to have a high affinity for tubulin located at the ends of microtubules, but lower affinity to sites distributed throughout the microtubules.[47] This binding results in the suppression of microtubule dynamics, causing cells to arrest in the G2/M phase of the cell cycle, resulting ultimately in cell death by apoptosis.

Maytansine was extensively evaluated in human clinical trials, but failed to demonstrate a therapeutic benefit at tolerable doses.[48] However, the unusually high cytotoxic activity of the maytansinoids makes them attractive candidates for antibody-targeted delivery. In addition, maytansine met other key criteria, such as good aqueous stability and reasonable aqueous solubility, for use as a payload for ADCs. Maytansine, however, does not possess an obvious functional group that can be used to link it to an antibody.

5.1.2. Developing Linkable Maytansinoids

It was desired to link maytansinoids to antibodies in a manner that the resulting conjugate would be stable in circulation, yet cleavable in targeted cells. Disulfide linkages fit this criterion because they can be cleaved by thiols in the cytoplasm of the cell, which contains high levels of free thiol, mainly in the form of glutathione (1–10 mM),[49] while blood contains much lower levels of free thiol ($\approx 5\,\mu M$).[50] Structure–activity relationship (SAR) studies on maytansinoids showed that several pharmacophores were required to maintain in vitro cytotoxicity.[51] The carbinolamide at C9 and the double bonds at C11 and C13 were required for activity. Also, loss of the epoxide moiety resulted in diminished activity. The ester side chain at C3 was required for biological activity, but the structure of this side chain could be varied without loss of potency. Since, the C3 position was amenable to modification, it was chosen for the incorporation of new ester side chains bearing a terminal thiol group to enable linkage to antibodies.[52]

Maytansinol (**7b**) is the hydrolysis product of **1** formed from cleavage of the ester group at C3. Maytansinol can be esterified with different side chains to produce maytansinoids of interest. Total syntheses of **7b** have been described that could potentially be adapted for the preparation of thiol-bearing maytansinoids.[53–55] However, this would be difficult, as the stereochemistry at several positions has to be maintained, and final yields from such multi-step syntheses are generally low. Thiol-bearing maytansinoids, such as DM1 (**7d**), are instead typically prepared through semisynthesis. The precursor, ansamitocin P-3 (**7a**), is obtained by fermentation of the microorganism *Actinosynnema pretiosum* (Figure 6).[52] Controlled reduction of **7a** with $LiAl(OMe)_3H$ gives maytansinol (**7b**). Esterification with a carboxylic acid that contains a disulfide, in the presence of a coupling agent (EDC) and a Lewis acid (zinc chloride) provides maytansi-

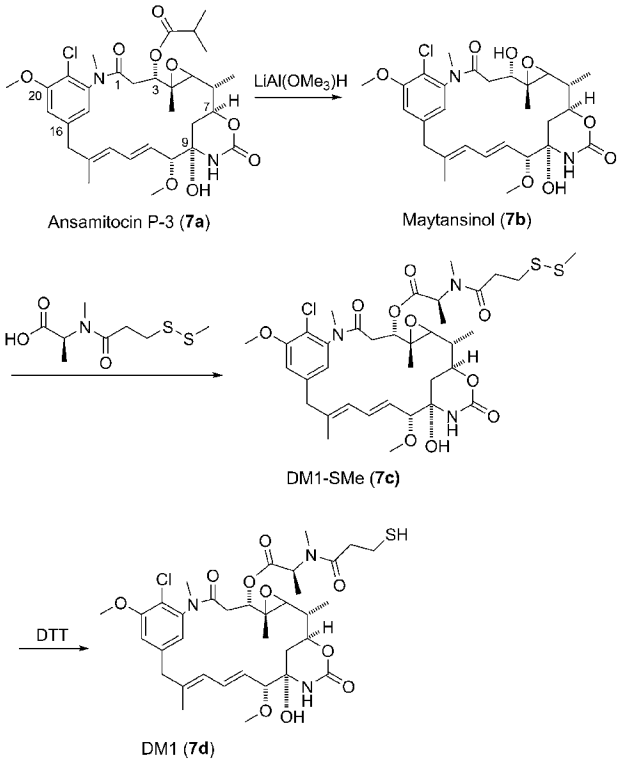
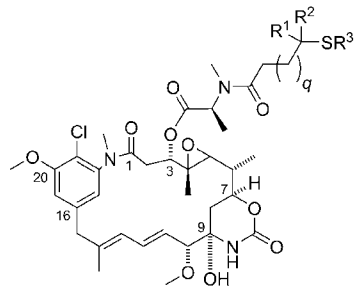


Figure 6. Semi-synthesis of DM1 from ansamitocin P-3.

© 2014 Wiley-VCH Verlag GmbH & Co. KGaA, Weinheim

CSPC Exhibit 1004
Page 26 of 336



DM1, **7d** (q = 0, R^1,R^2,R^3 = H)
DM1-SMe, **7c** (q = 0, R^1,R^2 = H, R^3 = SMe)
DM3, **7e** (q = 1, R^1= Me, R^2,R^3 = H)
DM3-SMe, **7f** (q = 1, R^1= Me, R^2= H, R^3 = SMe)
DM4, **7g** (q = 1, R^1,R^2 = Me, R^3 = H)
DM4-SMe, **7h** (q = 1, R^1,R^2 = Me, R^3 = SMe)

Figure 7. Disulfide- and thiol-bearing maytansinoids.

noid disulfides (**7c**, **7f**, **7h**), which were reduced with dithiothreitol (DTT) to give the desired thiol-bearing maytansinoids (Figure 7, **7d**, **7e**, **7g**).

Typically, the in vitro cytotoxicity of maytansinoids is not determined on compounds that contain a thiol moiety, as these compounds can undergo thiol–disulfide exchange reactions with components of cell culture media, such as cystine. Instead, maytansinoid disulfide derivatives were used for cytotoxicity measurements. The maytansinoids DM1-SMe (**7c**), DM3-SMe (**7f**), and DM4-SMe (**7h**) had potencies (IC_{50} of 0.029 nM, 0.011 nM, and 0.0011 nM, respectively) that were comparable to, or higher than, that of maytansine (IC_{50} = 0.024 nM) against KB cells. Similar results were also reported for the SK-Br-3 cell line.

5.1.3. *Preparation of ADCs with Maytansinoids*

Maytansinoid ADCs or antibody–maytansinoid conjugates (AMCs), wherein the maytansinoids are linked to antibodies through disulfide bonds, are generally prepared from a monoclonal antibody, a heterobifunctional linker, and a thiol-bearing maytansinoid, as shown in Figure 8.[52] Lysine residues of the antibody are reacted with the activated ester of a heterobifunctional linker to give a modified antibody that contains a reactive disulfide. The extent of modification can be varied by adjusting the molar equivalents of added linker. Typically, on average, three to four lysine residues on the antibody are modified. A thiol-bearing maytansinoid is then added to displace 2-thiopyridine to give the conjugate. The bond strength of the disulfide linkage can be varied by using maytansinoids or linkers that bear unhindered or sterically hindered thiols. AMCs can also be prepared by first reacting the thiol-bearing maytansinoid with the linker under highly concentrated conditions, and then reacting the resulting product with an antibody in aqueous solution. This second method is especially advantageous for forming AMCs bearing highly hindered disulfide bonds. AMCs with thioether linkages are prepared by reacting the antibody with a bifunctional linker composed of an activated ester and a maleimido group,

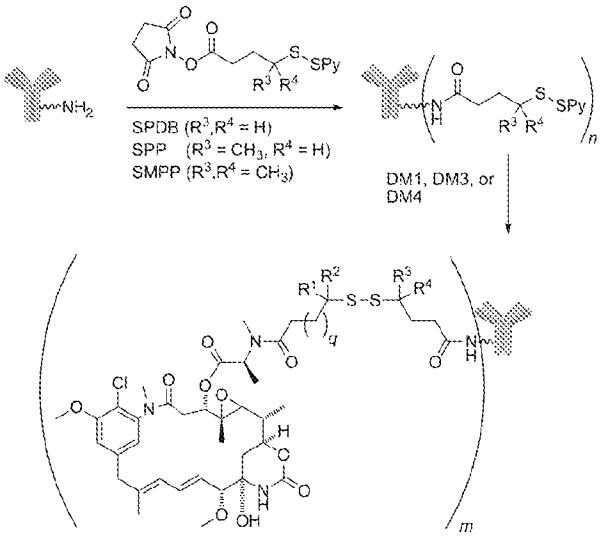


Figure 8. Conjugation of maytansinoids to antibodies by disulfide linkers.

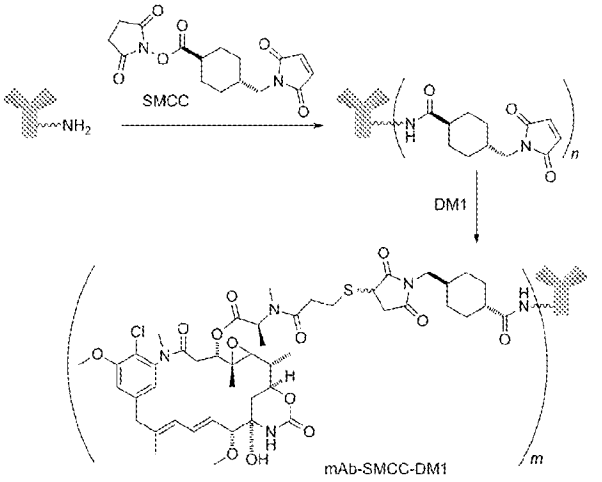


Figure 9. Conjugation of maytansinoids to antibodies by maleimide linkers.

such as SMCC, followed by reaction of the modified antibody with the thiol-containing maytansinoid (Figure 9).

In order to determine how the degree of steric hindrance of the disulfide bond would affect pharmacokinetics, several conjugates of the humanized C242 antibody were prepared.[56] Each conjugate was incubated with DTT at pH 6.5, 37 °C to determine the relative rates of thiol-induced maytansinoid release in vitro. As expected, the more-hindered disulfide conjugates released maytansinoid at a slower rate than the less-hindered ones (Table 1). The most hindered AMC **8g** released maytansinoid over 22000 times more slowly than **8a**, the least-hindered conjugate.

 © 2014 Wiley-VCH Verlag GmbH & Co. KGaA, Weinheim

CSPC Exhibit 1004
Page 27 of 336

Table 1: Effect of hindrance on huC242 AMCs linker stability.[a]

Substituents									
mAb side		DM side				Disulfide	Disulfide reduction	Relative	In vivo PK
R1	R2	R3	R4	*q*	ADC	hindrance	rate[b] (k [M^{-1} min^{-1}])	stability	$t_{1/2}$ [h]
H	H	H	H	0	**8a**	0:0	14	1	15
Me	H	H	H	0	**8b**	1:0	2	7	47
Me	Me	H	H	0	**8c**	2:0	0.8	16	n.d.
H	H	Me	Me	1	**8d**	0:2	1.0	14	87
Me	H	Me	H	1	**8e**	1:1	0.8	170	n.d.
Me	H	Me	Me	1	**8f**	1:2	0.014	980	218
Me	Me	Me	Me	1	**8g**	2:2	< 0.00064	> 22 000	n.d.
H	H	Me	H	1	**8h**	0:1	n.d.	n.d.	n.d.
–	–	–	–	–	**8i**	thioether	n.d.	n.d.	n.d.

[a] n.d. = not determined; –: no disulfide present. [b] Conjugate disulfide reduction by DTT at pH 6.5, 37 °C. Structures of disulfide AMCs are shown in Figure 8.

5.1.4. *In Vitro Cytotoxicity of AMCs*

The in vitro cytotoxicity of a panel of conjugates of the huC242 antibody targeting the CanAg antigen, linked to maytansinoids using different disulfide linkers or a noncleavable thioether linker (Table 1), were tested against antigen-positive COLO 205 cells.[56] All of these conjugates were highly potent, regardless of linker structure, with IC_{50} values between 3.5–15 pM, thus disulfide cleavage was not required to kill these cells in vitro. The AMCs displayed poor potency toward antigen-negative cells, demonstrating the antigen specificity of the cytotoxic effect. A bystander killing assay was then performed, wherein a representative set of huC242 conjugates prepared with different linkers were incubated with antigen-negative (Namalwa) cells in the presence of different numbers of antigen-positive (COLO 205) cells. The AMCs with the disulfide linkers were able to kill the antigen-negative cells (also known as bystander cells) as long as enough antigen-positive cells were present (Figure 10). AMCs with steric hindrance on the maytansinoid side of the disulfide bond gave a higher degree of bystander killing. The AMCs **8h** and **8d** with hindrance on the maytansinoid side of the disulfide bond were found to have similar degrees of bystander killing. The AMC **8i** with the noncleavable thioether linker, however, had no bystander killing, as it could not kill antigen-negative cells, even when large amounts of antigen-positive cells were added.[57]

Although for huC242-AMCs, the nature of the linker did not affect in vitro potency against antigen-positive cells, this was often not the case for AMCs targeting other antigens. The in vitro potencies of AMCs prepared from an antibody against the folate receptor alpha (anti-FOLR1), illustrate this point (Figure 11).[58] The anti-FOLR1 conjugates with the thioether linker or disulfide linkers had similar in vitro potencies on antigen-positive KB cells, which express at least 2×10^6 receptors per cell. Conjugates with disulfide linkers however were more potent than the AMC with the thioether linker against JEG-3 cells, which have lower levels of target antigen expression (about 4×10^4 per cell).[58] Potency differences of disulfide-linked versus thioether-linked anti-FOLR1 AMCs therefore appear to be dependent on cell line and antigen expression levels. EGFR AMCs with a disulfide and thioether linker displayed similar potency

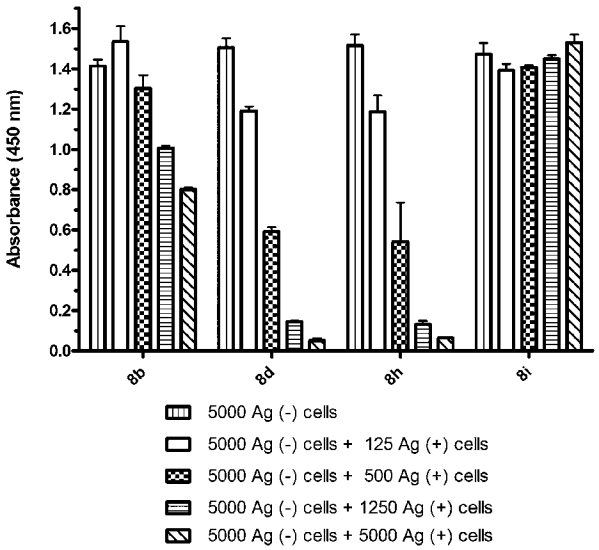


Figure 10. The effect of an AMC linkage on the killing bystander cells. Absorbance at 450 nm is a measure of cell viability. Cells were exposed to 1 nM conjugate for 5 days. Ag (–) = antigen-negative, Ag (+) = antigen-positive.

toward MDA-MB-468 cells, while the former was more than 20 times more potent toward A-431 cells, despite similar levels of antigen expression in this case.[59]

5.1.5. *Cellular Catabolism of AMCs*

In order to understand the cytotoxicity and bystander killing data and to improve the design of AMC linkage systems, studies were conducted to elucidate the mechanism(s) of how AMCs are processed by antigen-positive cells.[60] Antigen-positive COLO 205 cells were treated in vitro with huC242-[^{3}H]-maytansinoid conjugates prepared using different linkers (disulfide linkers: SPP, SPDB; thioether linker: SMCC; Figure 12). All conjugates gave lysine-bearing catabolites that had an intact linkage with the unaltered maytansinoids. The lysine-bearing catabolites were detected predominantly in the cell lysates and in smaller levels in the supernatants ($\approx 10\%$ or less of the lysate level),

© 2014 Wiley-VCH Verlag GmbH & Co. KGaA, Weinheim

CSPC Exhibit 1004
Page 28 of 336

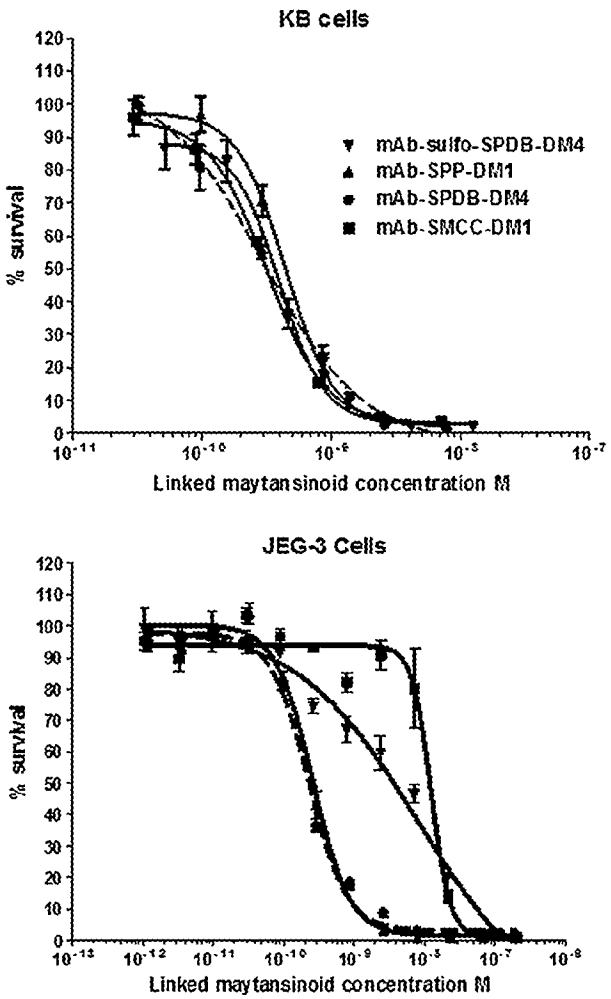


Figure 11. Cell-line dependency of the relative potency of Anti-FOLR1 AMCs in vitro.

suggesting that the antibody portion of the AMCs was fully degraded until only the lysine residue remained, and that these catabolites had some propensity to pass through cell membranes by either active or passive transport. The conjugate with a noncleavable thioether linker gave lysine-linker-maytansinoid as the sole catabolite, while the conjugates with disulfide linkers produced additional catabolites. The disulfide-linked DM1 conjugates generated DM1 and small amounts of *S*-methyl-DM1, which was presumably formed from DM1. Both DM1 and *S*-methyl-DM1 were detected in the cell culture medium as well as in the cell lysate. Likewise, the disulfide-linked DM4 conjugates generated DM4 and *S*-methyl-DM4 (the latter being the major species), which were also detected in both the culture medium and the cell lysate. No alteration of the macrocycle was detected in any of the catabolites, indicating that maytansinoids, even with their epoxide, ester, and cyclic carbamate moieties, are stable in lysosomes.

The proposed mechanism for the metabolism of each conjugate is shown Figure 13. After binding to the surface of tumor cells and internalization, the antibody portion of the AMC is proteolytically degraded in the lysosome until only a residual lysine amino acid remains. The catabolite would then be passively or actively transported from the lysosome to the cytoplasm. In the case of AMCs with the noncleavable linker, the sole lysine-linker-maytansinoid catabolite produced can bind to tubulin in the cytoplasm to disrupt microtubule dynamics and induce cell killing, or it can be effluxed from the cell. Because lysine-bearing catabolites are charged, they would not be expected to diffuse into neighboring bystander cells to induce G2/M arrest and cell death. For AMCs with disulfide linkers, some of the initially generated lysine-bearing catabolite is cleaved by reduction in the cytoplasm to release the thiol-containing maytansinoids DM1 or DM4, which can be further *S*-methylated by an endogenous *S*-methyl transferase enzyme. Since these metabolites are uncharged, they are able to efflux out of the cell and diffuse into bystander cells to kill them. Bystander killing may be advantageous in several situations. It is suggested that ADCs may have poor penetration into tumors so that cancer cells that are progressively further away from a blood vessel may take up less conjugate.[61] However, noncharged low molecular weight metabolites may be able to penetrate deeper into tumors, thus killing tumor cells that are less accessible to the conjugate. Bystander killing may also be essential for killing heterogeneous tumors, which express high levels of target antigen on only a portion of the cells.

5.1.6. Cytotoxicity of AMCs against MDR-1$^+$ Cells

There are several mechanisms by which tumor cells can become resistant to anticancer treatments. For example, multidrug-resistant (MDR) proteins can transport the chemotherapeutic agent out of the cells. One of the more prevalent MDR pumps is MDR-1. AMCs have been tested against cells that express the MDR-1 protein (also known as P-glycoprotein, or Pgp).[62] AMCs utilizing non-charged or non-polar linkers had lower in vitro potency against MDR-1$^+$ cells than against MDR-1$^-$ cells. MDR-1 is known in general to preferentially transport hydrophobic compounds more efficiently than hydrophilic compounds. Consequently, charged or hydrophilic linkers were developed and the AMCs prepared from them were shown to produce highly charged or polar metabolites, resulting in improved potency against MDR-1$^+$ cells. Sulfo-SPDB and Mal-PEG4-NHS are examples of polar linkers (Figure 14).[62,63]

5.1.7. Preclinical Pharmacokinetics, Tolerability, and Efficacy of AMCs

The AMCs prepared with cleavable disulfide linkers and noncleavable thioether linker were evaluated in vivo to determine their pharmacokinetic (PK) parameters.[56] The circulation half-life of AMCs with disulfide linkers was dependent on the degree of steric hindrance of the disulfide linkage; as hindrance was increased, the clearance rate was progressively decreased (Table 1). For example, the highly hindered AMC **8f** had a half-life of about 218 hours, which was comparable to that of the noncleavable AMC **8i** and that

 © 2014 Wiley-VCH Verlag GmbH & Co. KGaA, Weinheim

CSPC Exhibit 1004
Page 29 of 336

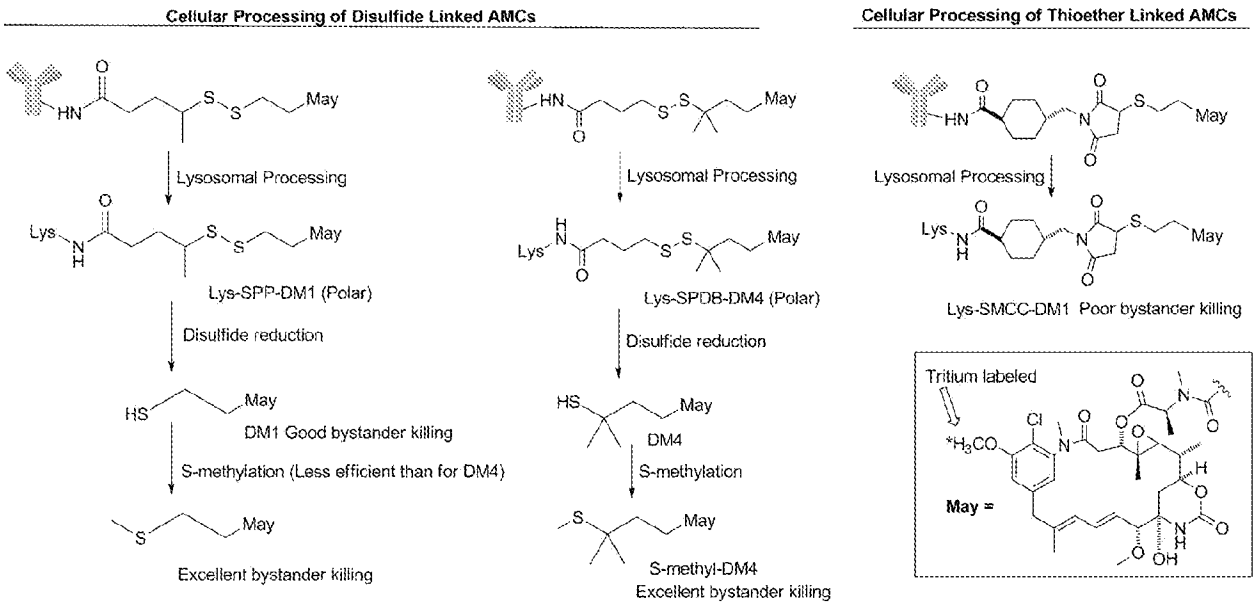


Figure 12. Cellular processing of AMCs.

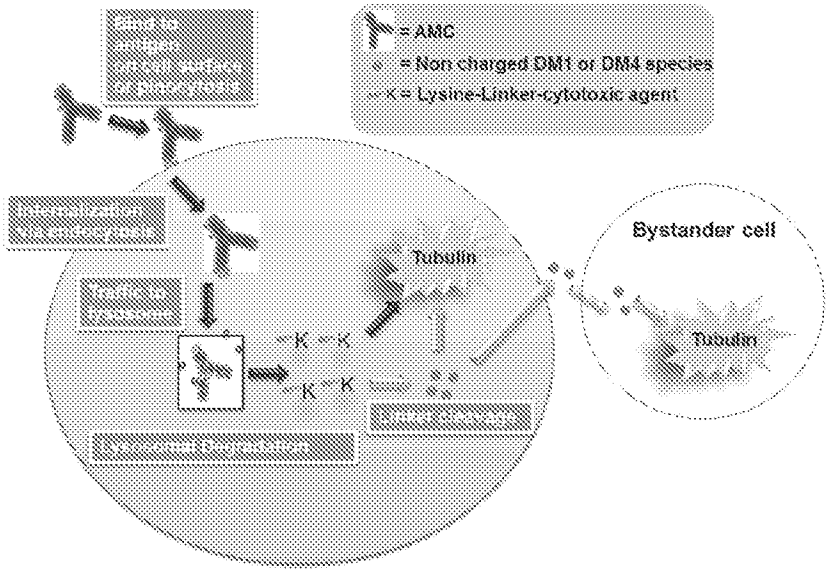


Figure 13. Proposed mechanism for AMC catabolism and potential bystander cell killing.

of unmodified human IgG_1 in mice. The half-life of **8f** was 14.5 times longer than that of the unhindered AMC **8a** in vivo. Tolerability of AMCs with disulfide linkers in mice, however, was not greatly affected by hindrance of the disulfide linker, because the different disulfide-linked AMCs had similar MTDs of about 50 mg kg^{-1} (antibody dose at a typical maytansinoid loading of 3.5 to 4 per antibody).[56] AMCs made with noncleavable linkers were better tolerated in mice, with MTDs that were 2 to 3 times higher than those of AMCs with disulfide linkers.[62]

In vivo experiments with AMCs linked through thioether or disulfide bonds showed that efficacy often does not correlate with in vivo stability. The antitumor activity of huC242–maytansinoid conjugates with varying steric hindrance in the disulfide link (**8b**, **8e**, **8f**) was compared in mice bearing COLO 205 xenografts (Figure 15). In this model, the AMC **8b** showed the best efficacy. At the tested dose, AMCs with less readily cleavable linkages had little or no efficacy advantage over mice dosed with a phosphate-buffered saline (PBS) control. In a second experiment, groups of mice bearing COLO 205 xenografts were treated with another set of AMCs (Figure 16). The AMC **8d** was the most efficacious, followed by **8h**, while **8b** and **8c** were the least efficacious. These two sets of experiments indicate that extensive disulfide hindrance could be detrimental to AMC efficacy, and that the location of the hindrance also affected efficacy. In particular, hindrance on the maytansinoid side of the disulfide bond gave improved efficacy as compared to hindrance on the antibody side. This improved activity can be attributed to the generation of a more potent maytansinoid metabolite, although some differences in AMC processing and pharmacokinetics may also play a role.

Although in a majority of cases an AMC with the optimal disulfide linker is more active in vivo than the corresponding conjugate with a noncleavable linker,[56,64] there may be some

 © 2014 Wiley-VCH Verlag GmbH & Co. KGaA, Weinheim

CSPC Exhibit 1004
Page 30 of 336

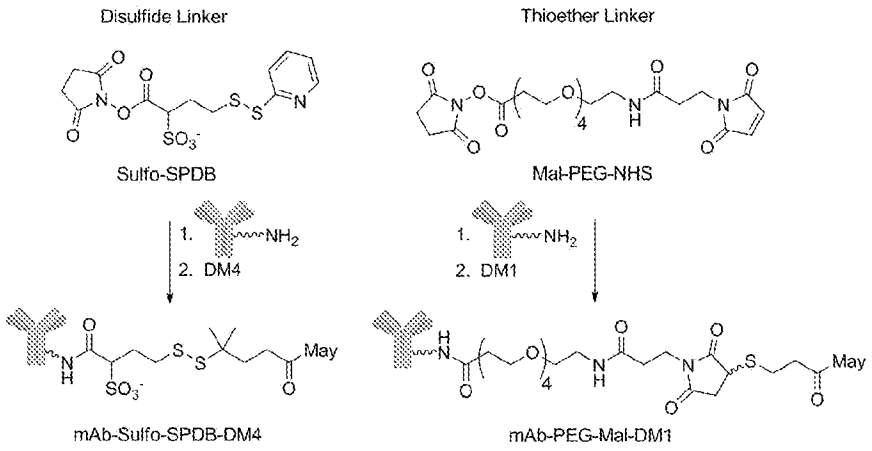


Figure 14. Polar sulfo-SPDB and mal-PEG4-OSu linkers, and the AMCs prepared from them.

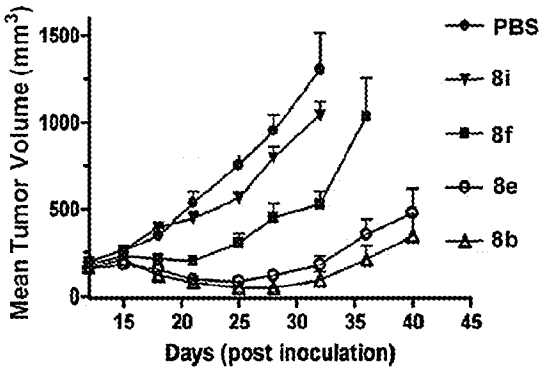


Figure 15. Effect of disulfide hindrance on the in vivo efficacy of huC242 conjugates on COLO 205 xenografts.

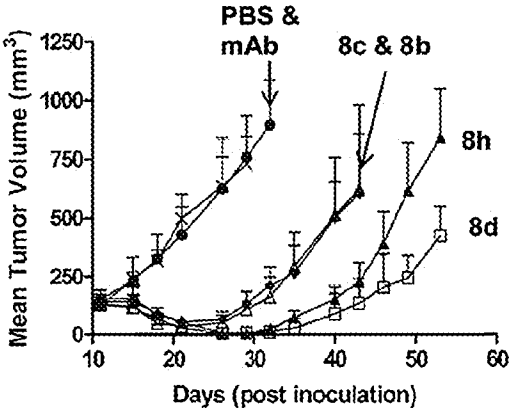


Figure 16. Effect of hindrance at different sides of the AMC disulfide linkage on in vivo efficacy.

target dependency. For example, conjugates of the anti-HER2 antibody trastuzumab linked to the maytansinoid DM1 through a disulfide linker or a thioether linker showed similar in vivo efficacy.[65]

5.1.8. Studies on the In Vivo Metabolism of AMCs and Cytotoxicity of Catabolites

For in vivo investigations, tumor-bearing mice were separately dosed with huC242-[^{3}H]maytansinoid conjugates that were prepared using different linkers (disulfide linkers: SPP, SPDB; thioether linker: SMCC).[66] The mice were sacrificed after intervals of between 2 hours and 7 days post-dosing, then the tumors and livers were excised and homogenized, and the radiolabeled species were analyzed by HPLC. As noted with the in vitro metabolism experiments, lysine–linker–maytansinoid (Lys-SMCC-DM1) was the sole catabolite detected for the conjugate with the noncleavable linker (mAb-SMCC-DM1) at any time point. The lack of new catabolites in liver or bile indicated that no phase I or phase II liver metabolism occurred to any significant extent. In mice treated with conjugates that bear the disulfide linkers, the catabolite profile from the tumors matched that seen in the in vitro studies. In liver, additional catabolites that consist of the oxidation products *S*-methyl-DM1 sulfoxide and *S*-methyl-DM1 sulfone were formed from DM1 disulfide-linked AMCs, while *S*-methyl-DM4 sulfoxide and *S*-methyl-DM4 sulfone were formed from DM4 disulfide-linked AMCs (Figure 17).[66] Again, no phase II metabolites were detected in these liver homogenates.

The catabolites and the liver-oxidized metabolites, which are formed from AMCs in vivo, can potentially contribute to systemic toxicity. It is therefore desirable to know the cytotoxicity of each species and determine if liver metabolism effectively detoxifies catabolites. All of the lysine-bearing catabolites had relatively poor cytotoxic potency in vitro (Table 2). However, these catabolites appear to be highly potent if delivered into a cell by AMC processing. The noncharged catabolites DM1 (**7d**), *S*-methyl-DM1, DM4 (**7g**), and *S*-methyl-DM4 were highly cytotoxic compounds, while the sulfoxides and sulfones of *S*-methyl DM1 and *S*-methyl DM4 had relatively weak cytotoxicities, suggesting that mouse liver efficiently detoxifies these catabolites through oxidation. Also, the lysine-bearing catabolites generated from AMCs with noncleavable linkers are not altered in the liver, thus retaining their relatively poor cytotoxicity.

5.2. Auristatin Analogues as ADC Payloads

The small linear peptide dolastatin 10 (**2a**) (Figure 2) is a highly potent antimitotic agent that was isolated from the marine shell-less mollusk *Dolabella auricularia* found in the Indian Ocean and the coastal waters of Japan.[67] Dolastatin 10 and its derivatives have been shown to inhibit tubulin-

 © 2014 Wiley-VCH Verlag GmbH & Co. KGaA, Weinheim

CSPC Exhibit 1004
Page 31 of 336

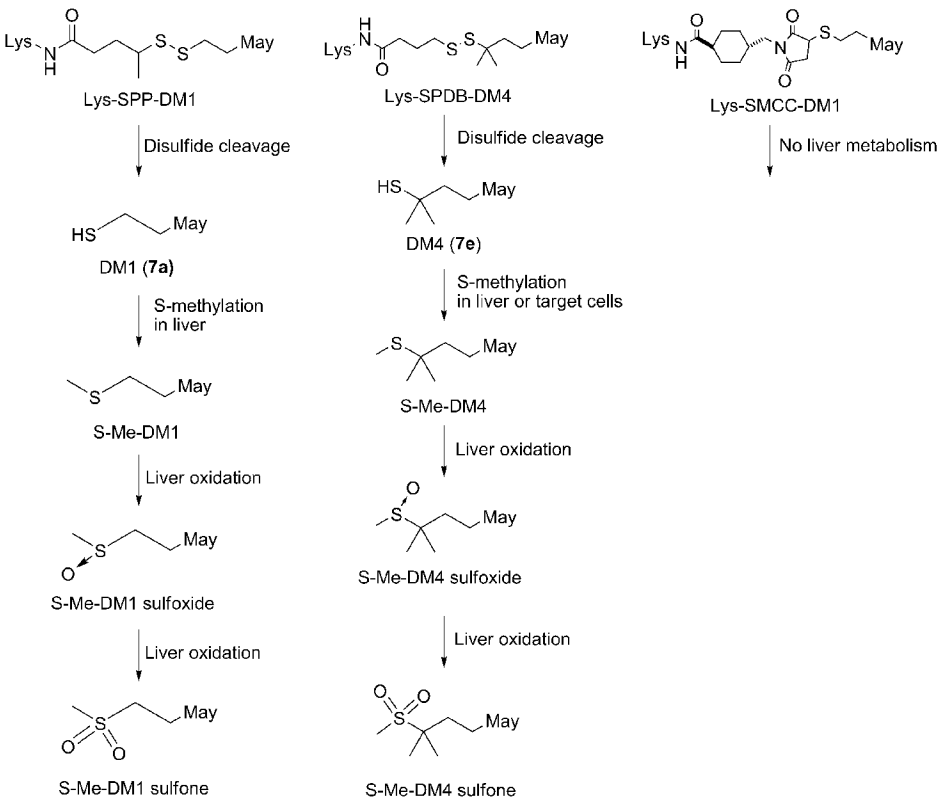


Figure 17. Liver metabolism of the lysosomal and S-methylated catabolites of AMCs.

dependent GTP binding, cause noncompetitive inhibition of vincristine binding to tubulin, and inhibit microtubule dynamics. Some dolastatins, such as dolastatin 15 (**2b**) and the synthetic analogue Cemadotin (**2c**) are known to be labile to proteases and esterases, as shown in Figure 18. Such labile dolastatins may not be desirable for use as ADC payloads, as they could be fully or partially inactivated when processed in the lysosomes of targeted cells.

5.2.1. *Developing Linkable Auristatins*

The auristatin series of antimitotic agents are fully synthetic compounds that were identified by SAR studies based on dolastatin 10.[68] The dolaphenine residue of **2a** could be replaced with phenethyl amine or substituted phenethyl amine moieties without loss of potency. It was also found that potency was retained when the terminal tertiary amine moiety of dolastatin was replaced with a primary or secondary amine. Monomethyl auristatin E (MMAE, **9a**) and monomethyl auristatin F (MMAF, **9b**) were prepared from such SAR studies and then derivatized for use as payloads for ADC (Figure 19).

MMAF is approximately 100 times less cytotoxic in vitro than MMAE.[69] Nevertheless, the methyl ester derivative of MMAF (MMAF-OMe) is one of the most cytotoxic auristatin compounds and is approximately 100 times more cytotoxic than MMAE on most of the tested cell lines. It is believed that MMAF-OMe can diffuse into cells where esterases in the cytoplasm convert it into MMAF. Thus it is suggested that MMAF has low cytotoxicity because its charged carboxy group hinders diffusion into cells,

Table 2: In vitro cytotoxicity of AMC catabolites and liver oxidation products.

ADC catabolite	IC_{50} [M] (KB)	liver metabolite(s) formed from AMC catabolites	IC_{50} [M] (KB)	Decrease in potency[c]
S-Me-DM1	6.6×10^{-11}	*S*-Me-DM1 sulfoxide	1.3×10^{-8}	196
		S-Me-DM1 sulfone	3.5×10^{-9}	53
S-Me-DM4	2.6×10^{-11}	*S*-Me-DM4 sulfoxide	1.9×10^{-9}	73
		S-Me-DM4 sulfone	8.0×10^{-10}	31
DM1	1.0×10^{-9}[b]	DM1 sulfinic acid	n.d.	n.d.
		DM1 sulfonic acid	4.0×10^{-8}	40
DM4	3.0×10^{-10}[b]	DM4 sulfinic acid	n.d.	n.d.
		DM4 sulfonic acid	2.7×10^{-8}	90
Lys-SPP-DM1	2.9×10^{-8}	–	–	–
Lys-SPDB-DM4	3.3×10^{-8}	–	–	–
Lys-SMCC-DM1	6.2×10^{-8}	–	–	–

[a] ND: Not determined; the compound has not been synthesized. – Indicates no value because parent compounds were not metabolized. (KB) indicates that the cytotoxicity of the various maytansinoids was determined on the KB cell line. [b] In vitro cytotoxicity varies due to thiol reactivity with cystine and other disulfide-containing components present in the cell media. [c] Fold decrease in potency = (IC_{50} liver metabolite)/(IC_{50} primary metabolite).

© 2014 Wiley-VCH Verlag GmbH & Co. KGaA, Weinheim

CSPC Exhibit 1004
Page 32 of 336

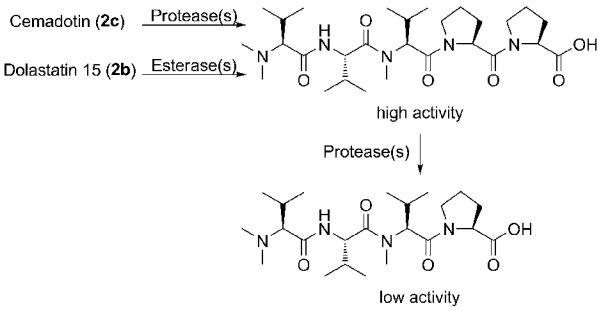


Figure 18. Proteolytic inactivation of the active moiety derived from cemadotin (**2c**) and dolastatin 15 (**2b**).

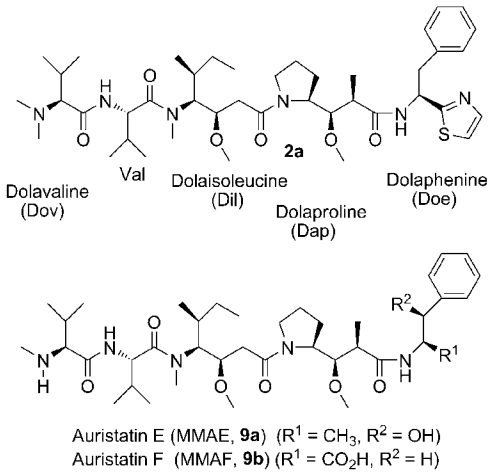


Figure 19. Named moieties for SAR studies on dolastatin 10 (**2a**) and structures of MMAE and MMAF.

but once inside a cell, it would be very potent. MMAE and MMAF were selected and modified for linkage to antibodies.

MMAE is typically modified at its terminal amine so that it can be linked to an antibody through a dipeptide attached to a *para*-aminobenzyl (PAB) moiety (Figure 20). The maleimide moiety of the derivative allows the compound to be linked to a thiol group on a targeting agent. Valine–citrulline–PAB constructs are known to be cleaved by cathepsin B, and all of the auristatin E ADCs presently in clinical trials utilize valine–citrulline (val-cit) as the dipeptide linker. Auristatin E analogues that do not contain a peptide linker have also been reported, but ADCs of these compounds have not yet advanced to the clinic. MMAF has been derivatized on the terminal secondary amine with the same mal-caproyl-val-cit linkage system and also with a noncleavable maleimide-caproyl linker. Auristatin F analogues that bear a terminal dimethyl amine substituent have also been modified at the carboxy terminus for linkage to antibodies, but these will not be discussed here.[70]

5.2.2. *Preparation of Auristatin-ADCs*

Free thiol moieties on the antibody are required to enable conjugation to maleimide-bearing auristatin derivatives. However, antibodies do not generally contain free thiols, but they do contain endogenous cysteine residues that exist as disulfide pairs with other cysteines to form 4 interchain and 12 intrachain disulfide bonds (for a human IgG_1 antibody). The interchain disulfides can be reduced and maintained in a reduced state more easily than the intrachain disulfides.[71] The interchain disulfide bonds can be fully or partially reduced by a mild reducing agent such as DTT to give a distribution of antibody

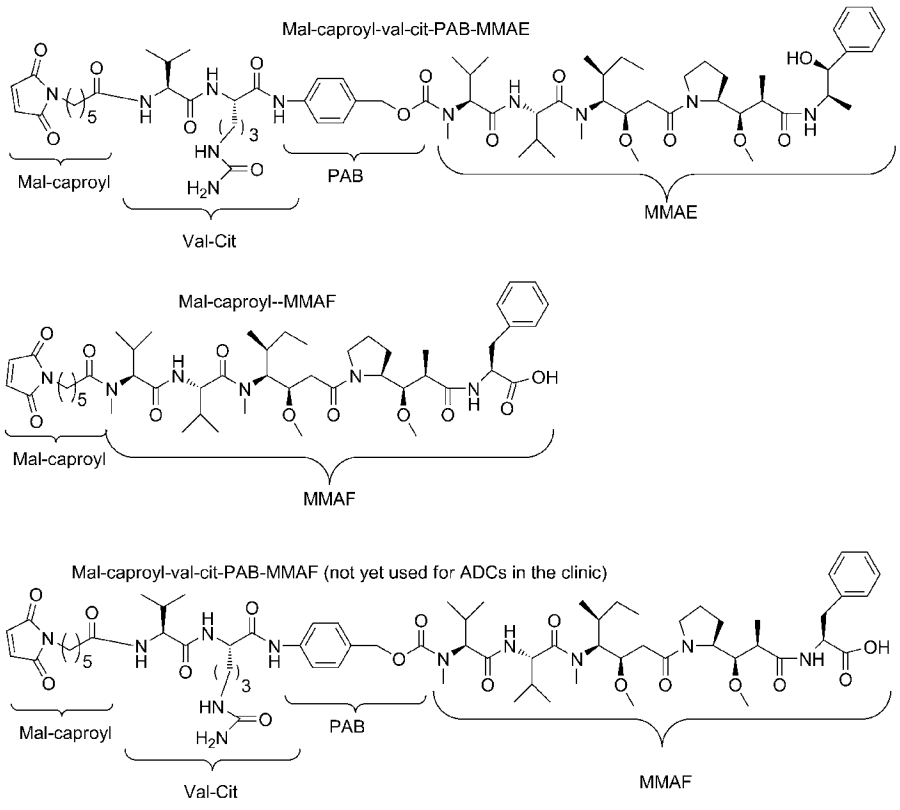


Figure 20. Selected linkable derivatives of MMAE and MMAF.

© 2014 Wiley-VCH Verlag GmbH & Co. KGaA, Weinheim

CSPC Exhibit 1004
Page 33 of 336

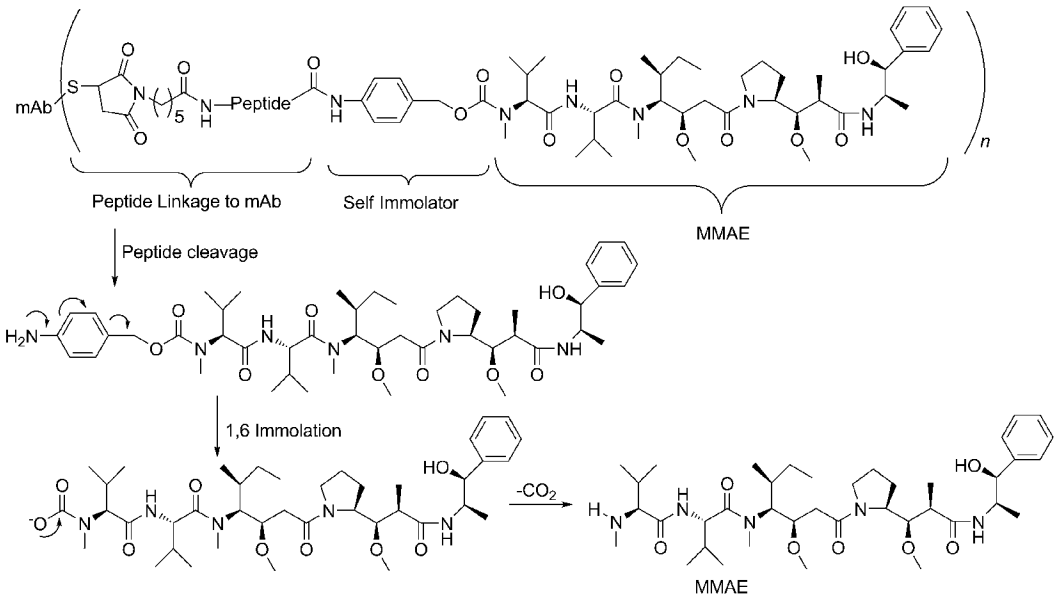


Figure 21. Cellular metabolism of self-immolative ADCs containing auristatin E.

species with two to eight free thiol groups. The reduced antibody with its newly freed thiol groups can then be purified to remove reducing agent and reacted with a maleimide-containing auristatin derivative. Conjugates with a varying distribution of auristatin molecules per antibody were obtained, with an average of four auristatins linked per antibody.[72] Conjugates of MMAE utilizing the val-cit linkage have also been purified by hydrophobic-interaction chromatography (HIC) to separate individual species with two, four, or eight MMAEs per antibody.[73] The separated species have been used for research, but have not yet been evaluated in the clinic.

5.2.3. *Cytotoxicity of Auristatin-ADCs*

Studies were conducted to determine how the load of MMAE on an antibody would affect the in vitro and in vivo potency of the resulting conjugate, as well as pharmacokinetic parameters.[73] Anti-CD30 antibody–MMAE conjugates that bear the separated species with two, four, or eight MMAE molecules per antibody retained full binding affinity to the antigen. Cytotoxicity assays indicated a small increase in the in vitro potency as the MMAE load increased.

ADCs of MMAF have also been reported to be highly cytotoxic to antigen-positive cells. The anti-CD30 antibody cAC10 was separately conjugated to mal-caproyl-vc-PAB-MMAF and mal-caproyl-MMAF to give an ADC with a protease cleavable linkage and an ADC with a noncleavable linkage, respectively. The two ADCs displayed a similar level of potency against a panel of CD30-positive cell lines. However, the val-cit-linked ADC was reported to be up to 10 times more potent on some cell types. It was proposed that MMAF ADCs utilizing val-cit linkages may, in some cases, release catabolite more efficiently than MMAF ADCs using the noncleavable linker.[69]

5.2.4. *Cellular Catabolism of Auristatin ADCs*

As is the case with AMCs, auristatin ADCs are also catabolized by target cells. The proposed mechanism for the catabolism of MMAE ADCs is shown in Figure 21. The antibody component of auristatin ADCs binds to a targeted antigen on the surface of cells, after which the conjugate is internalized and routed to a proteolytic compartment. Cleavage of the amide bond between the peptide and the aromatic amine followed by self-immolation of the *para*-aminobenzyl (PAB) moiety with loss of carbon dioxide gives MMAE. MMAF is most often conjugated to an antibody through a noncleavable linker, thus the linker moiety of these ADCs is not cleaved in catabolic vesicles of cells (Figure 22). Instead, the antibody portion of the resulting ADC is degraded to release a catabolite that contains MMAF linked to cysteine (cys-mal-caproyl-MMAF).

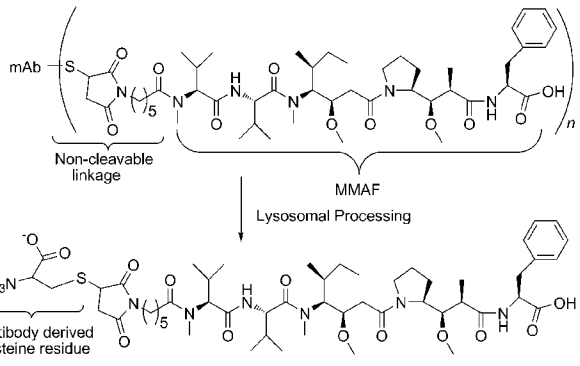


Figure 22. Cellular metabolism of ADCs containing noncleavably linked auristatin F.

© 2014 Wiley-VCH Verlag GmbH & Co. KGaA, Weinheim

CSPC Exhibit 1004
Page 34 of 336

Protease-labile self-immolative conjugates of MMAE ADCs can induce bystander killing presumably by releasing membrane permeable MMAE, which can diffuse into and kill proximal cells.[74] However, MMAF conjugates linked through a noncleavable linker do not induce bystander killing, presumably because they release the charged cys-caproyl-MMAF catabolite, which is poorly membrane permeable.

The efficiency of ADC internalization is expected to impact potency, but the route by which an ADC is internalized appears to also determine if potent catabolites are released. Smith et al. conducted a study with the ADC L49-MMAF, in which the antimelanotransferrin monoclonal antibody (L49) was linked to MMAF by a noncleavable linker.[75] The ADC was readily internalized by several antigen-positive cell lines, which had high target antigen expression. The cell lines were also sensitive to membrane-permeable auristatins, so it was expected that the L49 ADC would be highly cytotoxic to all of these targeted cells. Some cell lines, however, were resistant to the L49–MMAF. It was later determined that insensitive cells were internalizing L49 into vesicles known as caveolae, and the ADC apparently was never routed to catabolic vesicles. Without ADC degradation, cytotoxic catabolites could not be released to kill the cells.

5.2.5. Preclinical Pharmacokinetics, Tolerability, and Efficacy of Auristatin ADCs

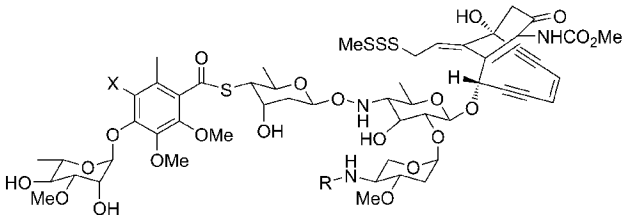
Since, the cAC10 conjugate that bears eight MMAE was more potent in vitro than conjugates with a lower MMAE load, an in vivo evaluation was conducted. However, the ADC with eight MMAE per antibody was found to clear from circulation substantially faster than the conjugates containing four or fewer MMAE molecules per antibody.[73] This is often referenced as proof that ADCs with a high drug load will be cleared rapidly. However, interchain disulfide bonds covalently hold together the heavy and light chains of the antibody, thus contributing to antibody stability, so the cleavage of all these disulfide bonds to provide attachment sites for a higher load of MMAE has the potential to alter the stability of the conjugate and the in vivo clearance rate. More studies with different linkage systems or cytotoxic molecules may be required to determine if high-drug-load ADCs can be prepared without compromising in vivo clearance rates. The cAC10 ADCs that bear four MMAE molecules per antibody have an MTD of between 30–40 $mg\,kg^{-1}$ (antibody protein dose) in SCID mice.[71]

Conjugates of cAC10 with val-cit-linked MMAF or mal-caproyl-MMAF had similar in vivo efficacy against Karpas 299 xenografts in nude mice. However, the ADC with the noncleavable mal-caproyl linker had an MTD in mice of greater than 150 $mg\,kg^{-1}$, while the ADC linked by the cleavable val-cit linker was three times more toxic, with an MTD of 50 $mg\,kg^{-1}$, with an MMAF load of four per antibody. SGN-75 is an anti-CD70 antibody linked to MMAF by a noncleavable linker. For in vivo studies, a version of SGN-75 that was dual radiolabeled ([^{14}C]-MMAF and [^{3}H]-anti-CD70 antibody) was prepared.[76] Biodistribution studies in tumor-bearing mice were conducted with this conjugate and accumulation of ^{14}C from MMAF or ^{3}H from antibody were determined for tumor and various normal tissues. Radioactivity derived from MMAF was found to preferentially accumulate in the tumor (82% injected dose/g after 2 days). Also, similar to maytansinoid conjugates, the radiolabeled MMAF ADC was highly accumulated in tissues that catabolize antibodies.

6. DNA Agents as ADC Payloads

6.1. Calicheamicins

The calicheamicins are a class of enediyne-containing antitumor antibiotics that are recognized as being among the most potent antitumor agents ever discovered. They were first identified in 1986 as a fermentation product of the bacterium *Micromonospora echinospora* ssp. *calichensis* through a screening effort to discover new DNA-damaging agents.[77,78] Calicheamicin γ_1^{Br} (**10a**) and γ_1^{Br} (**10b**) were the first members of this class to be isolated, followed by calicheamicin γ_1^{I} (**10c**; Figure 23) and other calicheamicins.[79]



Calicheamicin γ_1^{Br}, **10a** (X = Br; R = $(CH_3)_2CH$)
Calicheamicin γ_1^{Br}, **10b** (X = Br; R = CH_3CH_2)
Calicheamicin γ_1^{I}, **10c** (X = I; R = CH_3CH_2)

Figure 23. Structures of calicheamicins.

Calicheamicin γ_1^{I}, the most prominent member of this family, is structurally complex, possessing a highly functionalized bicyclic enediyne unit with a methyl trisulfide moiety bridged through a series of unusual linkages to an extended sugar residue, which possesses a fully substituted benzene ring. It was found to possess exquisite potency in vivo against a variety of tumor types at doses as low as 0.15 $\mu g\,kg^{-1}$.[80] In spite of the molecular complexity, all of these elements work together to give the calicheamicins a fascinating mechanism of action (Figure 24).[81,82] The aryl tetrasaccharide of **10c** serves to direct the molecule by binding tightly within the minor groove of DNA in a relatively sequence-specific manner, thus positioning the enediyne warhead within the DNA double helix. In this position, the methyl trisulfide is available to undergo nucleophilic attack (e.g. glutathione) ultimately releasing a free thiol, which spontaneously cyclizes into the α,β-unsaturated ketone bridgehead of the enediyne. The resulting angular strain imposed on the enediyne through this addition is relieved through a cycloaromatization (Bergman type)[83] reaction, which generates a 1,4-benzene dirad-

© 2014 Wiley-VCH Verlag GmbH & Co. KGaA, Weinheim

CSPC Exhibit 1004
Page 35 of 336

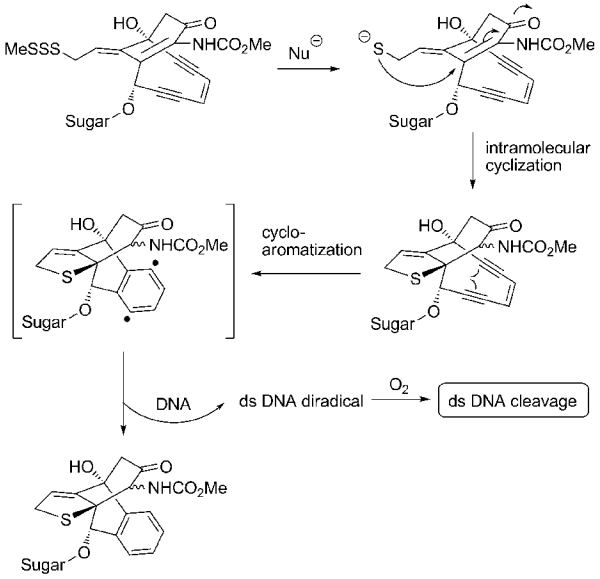


Figure 24. Mechanism of DNA cleavage by calicheamicin.

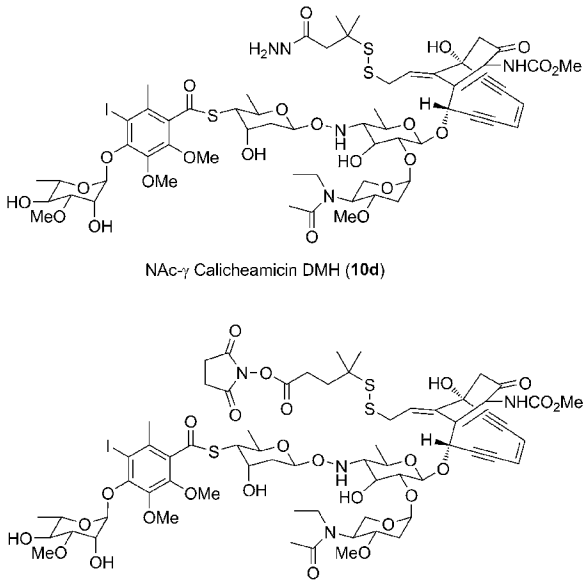


Figure 25. Structures of linkable NAc-γ calicheamicin DMH (**10d**) and DMA, OSu ester (**10e**).

ical. The diradical thus formed abstracts hydrogen atoms from both strands of the duplex DNA, resulting in a double-stranded DNA diradical, which in the presence of oxygen leads to cleavage of DNA double strands and subsequent cell death.

As a result of this unique mechanism of action and high potency, multiple analogues of the calicheamicins have been explored as potential anticancer agents in preclinical models. However, because of the prevalence of associated toxicities upon treatment with these compounds, calicheamicin therapies as single agents have not been developed. In spite of this, their high potency makes them ideal candidates for ADCs, particularly where antigen expression is limited.

6.1.1. *Calicheamicins as ADC Payloads*

Calicheamicin γ_1^I was considered too toxic for use in an antibody–drug conjugate because of its high potency and toxicity, which eventually led to the development of *N*-acetyl γ calicheamicin, a 20 times less potent analogue, as the choice for the calicheamicin core.[84] Additionally, the natural trisulfide found in the calicheamicin structure was converted to a disulfide, thus incorporating a functional group that allows conjugation to an antibody. Efforts to prepare calicheamicin–antibody conjugates primarily focused on using either a hydrazone or an amide linkage.[85]

Conjugates with linkable forms of calicheamicin (Figure 25) have been prepared with the anti-MUC1 and anti-CD33 antibodies with strikingly different outcomes.[85–88] In one method of conjugation, NAc-γ calicheamicin-DMH (**10d**) was linked to the antibody through an acid-labile hydrazone bond. Formation of this bond was accomplished by oxidizing carbohydrate residues of the antibody with periodate to generate aldehyde groups, followed by reaction with **10d** to generate a "carbohydrate conjugate". Alternatively, an "amide conjugate" was prepared by linking NAc-γ calicheamicin-DMA (**10e**) by a lysine group on the antibody, thus creating a more stable linkage. While each of these linkages is different, both forms retain the hindered disulfide with *gem*-dimethyl substitution, thus offering an additional method for drug release through disulfide cleavage. In general, these conjugation methods provide conjugates with loadings of an average of two to three molecules of calicheamicin per antibody.

Anti-MUC1 conjugates[86,87] with the IgG1 antibody CTM01 linked to calicheamicin using the two different linkages were evaluated in vitro, and both conjugates were potent and specific in a one-hour-exposure assay. However, the carbohydrate conjugate lost virtually all specificity in a continuous-exposure assay (4 days), probably because of extracellular hydrolytic cleavage of the less stable hydrazone bond to release calicheamicin. This lack of in vitro specificity is consistent with the slightly increased toxicity of the hydrazone-linked conjugate over that of the amide-linked conjugate. In vivo, the amide conjugate was also found to be at least as active as the hydrazone conjugate against a number of different tumor models, while showing enhanced activity against tumors overexpressing PgP multidrug resistance. This data seems to suggest, at least within the context of this anti-MUC1 conjugate, that the hindered disulfide of the amide conjugate allows sufficient release of intracellular calicheamicin through glutathione reduction. In light of this data, an anti-MUC1 calicheamicin amide conjugate, CMB-401, was pursued in clinical trials against ovarian and lung cancers, however, only limited evidence of activity was observed.[87]

Calicheamicin was also linked through either a carbohydrate or amide linkage, as described above, to prepare anti-

 © 2014 Wiley-VCH Verlag GmbH & Co. KGaA, Weinheim

CSPC Exhibit 1004
Page 36 of 336

CD33 conjugates using the murine antibody P67.6.[85,88] Interestingly, unlike for the anti-MUC1 conjugates, there was a clear preference in vitro for the acid-labile conjugate, as it was found to be almost 7000 times more potent than the corresponding amide conjugate toward antigen-positive HL-60 cells. These results suggest a different mechanism of cellular processing for the two targets. The P67.6 amide conjugates, while active, did not produce long-term durable responses upon in vivo evaluation in xenograft models, whereas the carbohydrate conjugate was found to eradicate most tumors (9/10) at doses of both 150 and 300 $\mu g\,kg^{-1} \times 3$. In light of these contrasting results between antibody (anti-MUC1 versus anti-CD33) and linkage type, it is apparent that a single conjugate-linkage design is not necessarily optimal for all antibody conjugates.

While the process of oxidizing the murine form of the P67.6 antibody with sodium periodate had been successful in preparing hydrazone-linked calicheamicin conjugates, similar attempts with a humanized form of the antibody were accompanied by a loss in binding affinity and drug loading.[88] Thus, the conjugate was redesigned with the goal of preserving the hydrazone link but conjugating through the lysine residues of the antibody, thus avoiding the need for antibody oxidation. From a set of 36 different hybrid linkers (representative set shown in Figure 26) that were evaluated,[88] the AcBut linker (linker B) was chosen, as it showed good stability at pH 7.4 (94%) and almost complete hydrolysis at pH 4.5 (97%) at 37 °C for 24 hours, thus indicating that this linker should have good stability during circulation in blood plasma, yet be readily cleaved once in the acidic lysosomes. The hP67.6-NAc-γ calicheamicin DMH AcBut conjugate (**10f**) was found to be very potent toward antigen-positive HL-60 cells and over 100000 times more potent than the nontargeting MOPC-21 conjugate, thus indicating high conjugate selectivity. In vivo, the conjugate was found to induce complete tumor regressions in HL-60 tumor xenografts. In addition, ex vivo experiments indicated moderate inhibition of colony formation in a variety of leukemic marrow specimens from AML (acute myeloid leukemia) patients. In light of these data, **10f** (CMA-676, gemtuzumab ozogamicin) was advanced to human clinical trials.[88]

CMC-544 (**10g**) is a second NAc-γ calicheamicin–DMH conjugate, which was prepared in a similar manner through the utilization of the AcBut hydrazone linker.[89] CMC-544 is a humanized IgG4 antibody calicheamicin conjugate that targets CD22, which is expressed on a majority of B-cell malignancies. CMC-544 was found to be stable, highly potent, and specific in vitro, and active in vivo, producing complete tumor regression in mice that bear human lymphoma xenografts, with animals reported to be tumor-free for more than 100 days.[90] Currently, **10g** (inotuzumab ozogamicin) is being evaluated in numerous clinical trials, including a phase III trial in acute lymphoblastic leukemia (ALL).[91]

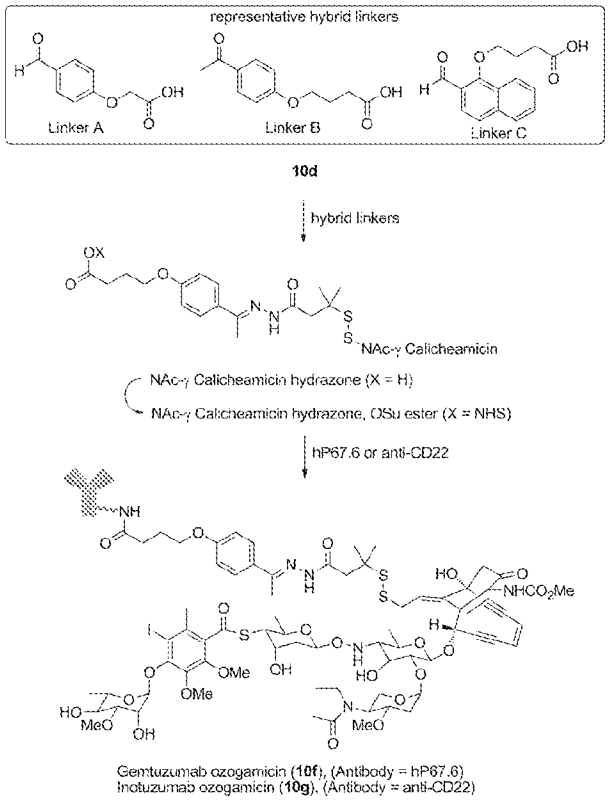


Figure 26. Synthesis of ADCs with calicheamicin.

6.2. (+)-CC-1065 and the Duocarmycins as ADC Payloads

The duocarmycins, such as duocarmycin A (**11a**) and SA (**11b**; Figure 27), are a family of naturally occurring antibacterial agents initially isolated in the late 1970s from the bacterial cultures of *Streptomyces zelensis*.[92] The chemical structure of (+)-CC-1065 (**4a**), a member of the duocarmycin family, was confirmed in 1980 and shown to include a series of three connected pyrroloindole subunits with one of them containing an unprecedented spirocyclic cyclopropapyrrolo-

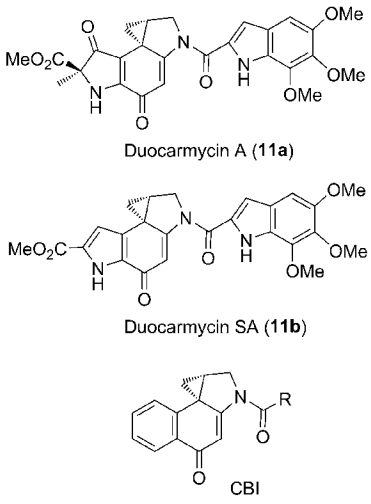


Figure 27. Structures of duocarmycins A and SA, and the cyclopropabenzindole (CBI) moiety.

 © 2014 Wiley-VCH Verlag GmbH & Co. KGaA, Weinheim

CSPC Exhibit 1004
Page 37 of 336

indole (CPI) moiety.[93] At the time of its discovery, **4a** was among the most potent antitumor antibiotics known.[94] The duocarmycins, and **4a** in particular, exert their high potency through a sequence-specific alkylation of DNA, preferring a five-base-pair AT-rich sequence that better accommodates the central pyrroloindole subunit. Thus, within the minor groove of DNA, the N3 of adenine attacks the cyclopropane moiety at the least substituted carbon atom of **4a**, as shown in Figure 28, thus forming a DNA adduct. The DNA alkylation ultimately results in cell death.[95]

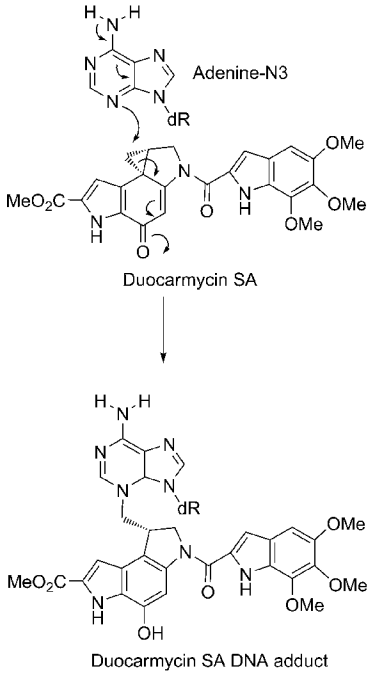


Figure 28. Mechanism of DNA alkylation for duocarmycin SA.

Clinical development of **4a** was not pursued, as it was shown to produce delayed toxicity in mice. The effort to circumvent this problem eventually led to the synthesis of molecules such as adozelesin (**4b**), carzelesin (**4c**), and bizelesin (**4d**; Figure 3). While these molecules circumvented the associated concerns regarding delayed toxicity, they were all found to possess only limited therapeutic activity in the clinic.[96,97] However, the resulting lessons learned through these efforts led to a better understanding of the structure of duocarmycins and provided insight that was useful for the development of the duocarmycins as ADC payloads. For instance, the use of a chloromethyl substituent as a precursor to the reactive cyclopropyl group only slightly decreased in vitro and in vivo activity, thus indicating that ring closure, either chemically or enzymatically, occurred quickly (Figure 29).[96,98] As a result, the CPI moiety could be derivatized in its ring open chloromethyl form in the phenolic state, which allowed the preparation of various types of prodrugs, such as carbamoyl, glycosyl, peptidyl, and carbonate derivatives. The incorporation of such a prodrug functional group could help to control the rate of formation of the DNA-reactive cyclopropyl group, improve the overall chemical stability, and increase the water solubility. Finally, Boger and co-workers described the synthesis of a synthetically more accessible cyclopropabenzindole (CBI, Figure 27) as a way to replace the alkylating CPI subunit, thus resulting in compounds that were still potent, but about four times more stable.[99–101]

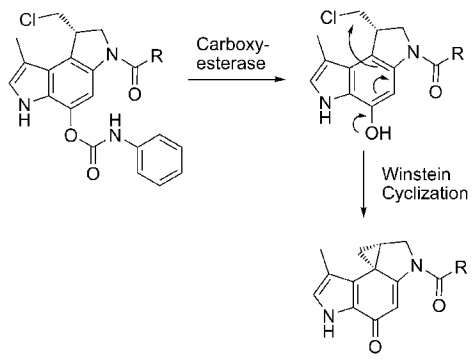


Figure 29. Mechanism for the conversion of carzelesin to its activated form through the Winstein cyclization.

Efforts to utilize these findings were initially realized in the synthesis of the analogue DC1, which incorporated the more stable chloromethyl surrogate, the CBI alkylating subunit, and a thiol-containing linker incorporated into the terminal pyrroloindole subunit for conjugation to an antibody (Figure 30).[102] Antibody-DC1 conjugates that contained about three to four DC1 molecules per antibody and were linked by disulfide bonds, were prepared and shown to be highly cytotoxic with IC_{50} values in the low picomolar range, and with a greater than 1000-fold selectivity for antigen-positive cells. While the lead conjugate, anti-B4-DC1, was active in human tumor xenograft models, its poor solubility and instability in the aqueous buffered solution precluded further development.

In order to circumvent these issues, analogues of DC1 were prepared in which a phosphate prodrug was incorporated into the phenol group of the CBI subunit. This incorporation resulted in compounds (DC4 and DC44; Figure 30) with significantly better solubility (3000 times better than DC1) under the required aqueous conjugation conditions, and greatly improved aqueous stability.[103] Incorporation of the phosphate prodrug did not alter the in vitro potency or specificity of the huB4-DC conjugates, thus indicating that cancer cells possessed the needed phosphatases to activate the prodrug intracellularly.[103]

Additional efforts to expand upon the information gained from duocarmycin research can be found in the ADC MDX-1203. This conjugate contains a synthetic duocarmycin derivative that is conjugated to a human anti-CD70 antibody (Figure 30). The duocarmycin analogue incorporates the chloromethyl surrogate, a piperazino carbamate prodrug at the phenol moiety of the CBI unit, and a modified terminal pyrroloindole subunit that bears a substituted aniline. The

 © 2014 Wiley-VCH Verlag GmbH & Co. KGaA, Weinheim

CSPC Exhibit 1004
Page 38 of 336

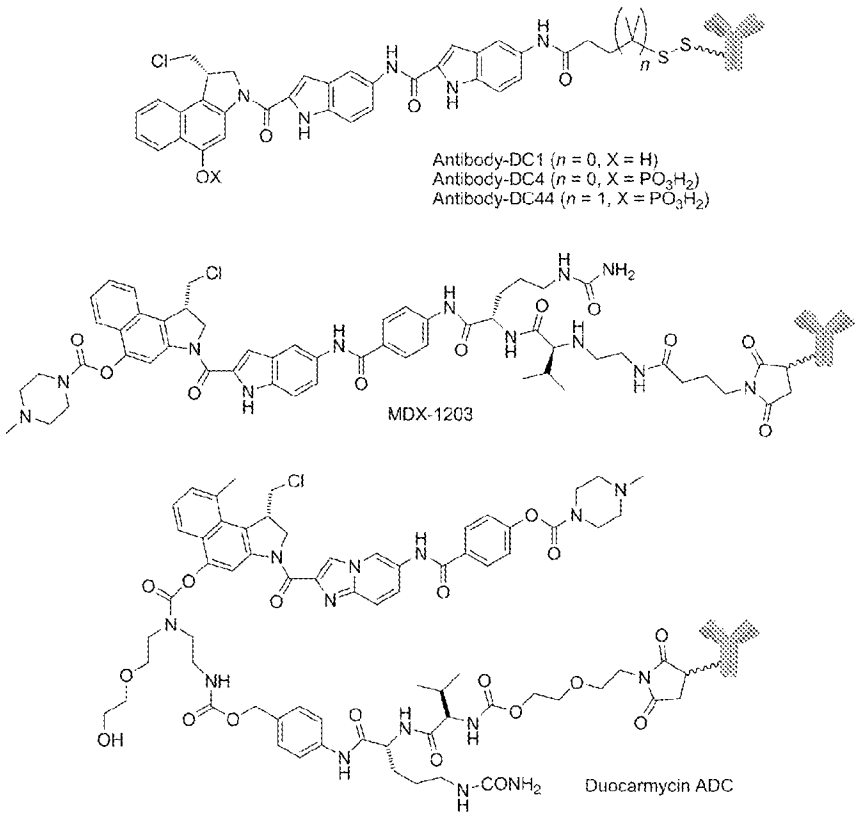


Figure 30. Structures of second-generation duocarmycin ADCs.

substituted aniline allows linkage to the antibody by a linker containing a valine–citrulline dipeptide (val-cit). Once the conjugate is internalized, the dipeptide is cleaved, thus releasing the aniline-bearing duocarmycin, which is then activated by carbamate cleavage, presumably by carboxyl esterase. MDX-1203 was shown to possess potent antigen-specific activity both in vitro and in vivo and was subsequently advanced to clinical trials against renal cell carcinoma and non-Hodgkin's lymphoma.

An alternative way to link duocarmycins is shown in Figure 30. In this case, a methyl piperazine carbamate was incorporated at the terminal pyrroloindole, while a peptide-containing linker was connected through the phenol moiety of the CBI unit.[104] The linker employs a cleavable peptide, which releases a *p*-amino benzyl group that undergoes a series of self-immolations, ultimately releasing the active duocarmycin. These conjugates have been linked to trastuzumab by thiol groups, which were generated through the reduction of interstrand cystines of the antibody, thus providing conjugates with an average of two duocarmycins linked per antibody. Modulation of the linker length was shown to effect conjugate stability in human plasma, and the conjugates were found to be potent in vitro. In vivo antitumor activity was shown to depend on the length of the linker and choice of drug.

6.3. SN-38 and the Camptothecins

Camptothecin (CPT, **12a**), a pentacyclic quinolone-based plant alkaloid, was first isolated from the deciduous Asian tree *Camptotheca acuminata* in 1966 by Wani and Wall (Figure 31).[105] CPT was shown to possess potent antitumor activity by selectively inhibiting DNA topoisomerase I, thus effectively stalling DNA replication in S-phase arrest and resulting in the apoptotic cell death of tumor cells.[106] Like the duocarmycins, **12a** suffered from drawbacks that prevented its clinical development, such as poor water solubility and the ease of physiological conversion of the lactone to its inactive ring-opened carboxylate form. Research that aimed at improving these attributes led to the development of topetecan (**12b**) and irinotecan (**12c**), which have been approved by the FDA as anticancer drugs.[107,108] While the conversion to a water-soluble piperazine prodrug form, as in **12c**, was sufficient to render it clinically effective, it did so with reduced potency as a result of inefficient carboxylesterase-catalyzed hydrolysis of the prodrug to its active metabolite, SN-38 (**12d**), in patients.

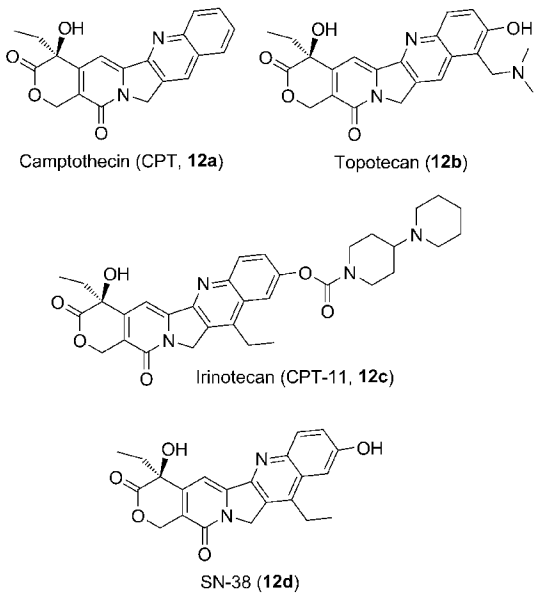


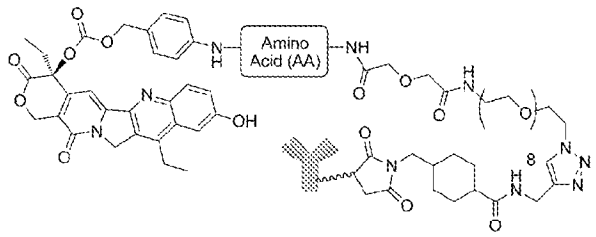
Figure 31. Chemical structures of camptothecin (CPT) and its clinically relevant analogues.

© 2014 Wiley-VCH Verlag GmbH & Co. KGaA, Weinheim

CSPC Exhibit 1004
Page 39 of 336

In an effort to conjugate **12d** to an antibody, linkage of the molecule through its hydroxy group at C20 has been evaluated.[109–114] This approach effectively serves the dual purpose of a) providing a handle for linker incorporation, and b) helping to minimize lactone ring opening under physiological conditions. Current efforts have focused on the use of either the CL2 linker, which contains a solubilizing spacer connected to a pH-sensitive *p*-aminobenzyl carbonate by a lysine-phenylalanine dipeptide,[109] or the CL2A linker, which possesses a single lysine residue.[110,111] Using these linkers, **12d** was conjugated to cysteine residues, obtained through reduction of the antibody, by thioether bonds to give conjugates with an average of about six molecules of SN-38 per antibody. These conjugates have been shown to be somewhat unstable in human serum, thus releasing about 50% of the active metabolite **12a** per day.[112] However, because of the targeting nature of the antibody, the majority of metabolite is released locally at the tumor and it has been suggested that internalization may not be required for activity.[110]

The clinically most advanced SN-38 conjugate, labetuzumab-SN-38 (Figure 32), consists of the humanized hMN-14 antibody, which targets carcinoembryonic antigen (CD66e),



Labetuzumab-SN-38 (Antibody = huMN-14, AA = Lys-Phe (CL2))
hRS7-SN-38 (Antibody = huRS7, AA = Lys (CL2A))

Figure 32. Structures of labetuzumab-SN-38 and hRS7-SN-38 ADCs.

linked to **12d** using the CL2 type linker. In preclinical studies, labetuzumab-SN-38 (IMMU-130) was shown to significantly extend the median survival time of nude mice that bear a variety of different human colorectal and pancreatic carcinomas, compared to both non-targeting controls and CPT-11.[113] Currently, IMMU-130 is being evaluated in two different Phase I clinical trials for patients with relapsed/refractory colorectal cancers. hRS7-SN-38 (IMMU-132) is a conjugate of **12a** connected by the CL2A linker with the humanized Trop-2 antibody, which targets the human trophoblast cell-surface antigen expressed on a variety of human carcinomas, including many epithelial cancers. Preclinical studies with IMMU-132 demonstrated antitumor effects superior to nontargeting controls at nontoxic doses in mice that bear a variety of different tumor types.[114] Currently, IMMU-132 is in a Phase I study for patients with advanced epithelial cancers. Preclinical work for SN38 conjugates directed to two other target antigens, milatuzumab-SN-38[112] and epratuzumab-SN-38,[110] has also been described.

7. Clinical Results

The first ADC to gain marketing approval from the U.S. FDA was gemtuzumab ozogamicin (**10f**; Figure 26), which consists of the highly cytotoxic DNA-strand-breaking calicheamicin compound linked by a hydrazone linker to a CD33 antibody. Its accelerated approval in 2000 was based on single-arm Phase II clinical trials, and was indicated for the treatment of patients who were 60 years and older in first relapse with CD33+ AML and who were not considered candidates for chemotherapy.[115] Subsequently, gemtuzumab ozogamicin was withdrawn from the market in 2010, when a confirmatory clinical trial, in combination with chemotherapy, raised toxicity concerns and did not show sufficient clinical benefit (improvement in survival time).[116,117] Recent reports from other studies suggest that the ADC may well provide clinical benefit with modified dosing regimens.[117]

Currently, two ADCs are approved for cancer therapy: CD30-targeting brentuximab vedotin for use in Hodgkin lymphoma and anaplastic large cell lymphoma (ALCL), and HER2-targeting ado-trastuzumab emtansine (T-DM1) for use in metastatic breast cancer (Figure 33). The two ADCs employ different microtubule-disrupting agents as the payload.

Brentuximab vedotin consists of monomethyl auristatin E (MMAE), a synthetic analogue of dolastatin-10, linked to the chimeric CD30 antibody cAC10 at cysteine residues by a valine-citrulline dipeptide linker that contain a *p*-aminobenzylcarbamate (PABC) self-immolative spacer. The valine-citrulline dipeptide is designed to be cleaved in lysosomes (by cathepsin B), leading to self-immolation of the PABC moiety and release of MMAE.[74,118] The unconjugated anti-CD30 antibody cAC10 was previously tested in the clinic, but did not show sufficient activity as a single agent to progress beyond phase I and II clinical trials (8% overall response rate).[119] In contrast, the compelling clinical activity of its MMAE conjugate, brentuximab vedotin, led to accelerated approval by the FDA in 2011.[120,121] In a pivotal phase II trial in relapsed or refractory Hodgkin lymphoma, brentuximab vedotin given at 1.8 mg kg^{-1} every three weeks showed an overall response rate (ORR) of 75%, with 34% and 40% of patients achieving complete response (CR) and partial response (PR), respectively. In relapsed or refractory systemic ALCL, the ORR was 86%, with CR in 53% of patients.[120,122]

The first approved ADC for the treatment of solid tumors, ado-trastuzumab emtansine, is a conjugate of the anti-HER2-antibody trastuzumab linked at lysine residues with the maytansinoid DM1 by the noncleavable SMCC thioether linker. Release of the active species, the lysine-linked maytansinoid, occurs once the ADC is internalized and routed to lysosomes, where the antibody moiety is completely degraded to its constituent amino acids. Intracellular release of the lysine-linked maytansinoid leads to cell-cycle arrest and ultimately to target cell death.[65] The safety and effectiveness of ado-trastuzumab emtansine was evaluated in a Phase III clinical study in 991 patients randomly assigned to receive ado-trastuzumab emtansine at 3.6 mg kg^{-1} every three weeks, or an established regimen of lapatinib plus capecitabine. In

© 2014 Wiley-VCH Verlag GmbH & Co. KGaA, Weinheim

CSPC Exhibit 1004
Page 40 of 336

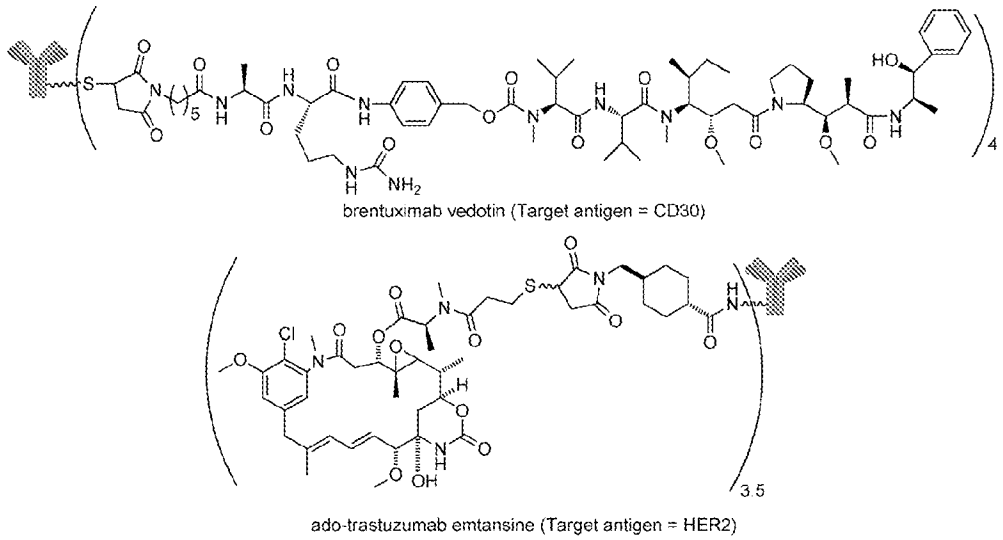


Figure 33. Structures of brentuximab vedotin and ado-trastuzumab emtansine.

these HER2+ metastatic breast cancer patients who had previously been treated with trastuzumab plus a taxane, ado-trastuzumab emtansine showed an improved median progression-free survival of 9.6 months and median overall survival of 30.9 months, versus median progression-free survival (PFS) of 6.4 months and median overall survival of 25.1 months for the combination of lapatinib plus capecitabine. Ado-trastuzumab emtansine also demonstrated a favorable safety profile compared to that of the chemotherapeutic combination of lapatinib and capecitabine.[123] These data led to ado-tratuzumab emtansine receiving full marketing approval by the FDA in 2013[123,124] for treatment of HER2+ positive metastatic breast cancer patients who had previously received trastuzumab and a taxane, the first ADC to receive such full approval.

A number of ADCs are in various stages of clinical evaluation (Table 3). A majority of them employ microtubule-disrupting compounds (maytansinoids or auristatins) as the payload. The two approved ADCs ado-trastuzumab emtansine and brentuximab vedotin are undergoing additonal clinical trials to broaden the treatment indications. For example, in a phase II trial, patients ($N=137$) with HER2-positive metastatic breast cancer or recurrent locally advanced breast cancer were randomly assigned to trastuzumab plus docetaxel ($n=70$) or T-DM1 ($n=67$) as first-line treatment. The T-DM1 arm showed an overall response rate of 69.2% compared to 58.0% for the comparator arm. T-DM1 also showed a significantly improved PFS compared to the trastuzumab plus docetaxel (14.2 months versus 9.2 months). Furthermore, T-DM1 had a favorable safety profile over standard first-line treatment with fewer grade ≥ 3 adverse events (46.4% versus 90.9%).[125] Based on these promising results, a randomized Phase III clinical trial is ongoing.

Brentuxiamb vedotin is being tested in three different Phase III trials, including front line treatment in combination with chemotherapy in Hodgkins lymphoma and CD30+ mature T-cell lymphoma. The ADC, inotuzumab ozogamicin (**10g**; Figure 26), which consists of an anti-CD22 antibody linked to NAc-γ calicheamicin via a hydrazone linker, is currently undergoing a Phase III study in CD22+ adult ALL.[126] This ADC was recently withdrawn from a Phase III study in CD22+ non-Hodgkin lymphoma because of a lack of improvement in overall survival.

8. Emerging Technologies

8.1. New Effector Molecules

8.1.1. Benzodiazepine Dimers

The pyrrolobenzodiazepine (PBD) class of molecules was first discovered in the 1960s, when anthramycin (**13a**) was isolated as the active constituent from the fermentation broth of *Streptomyces refuineus var. thermotolerans*.[127,128] As a result of its promising antibiotic and antitumor activity, the search for additional PBDs led to the discovery of 13 different natural PBD monomer types and a diverse range of synthetic analogues (Figure 34).[129] These PBD monomers are differentiated in the substitution patterns that are present in their A and C rings and the saturation level of the C ring, with an increased unsaturation typically rendering the PBD monomers biologically more active. Mechanistically, the PBDs exert their biological activity through their ability to react through the N10–C11 imine/carbinolamine functionality with the amino group in C2 position of a guanine residue within the minor groove of DNA, as shown in Figure 35.

PBD monomers were shown to prefer a three-base-pair sequence in which the guanine residue was flanked by purines on both sides. As a result of this, Thurston and co-workers sought to further explore this sequence selectivity in the form of PBD dimers that would form irreparable DNA cross-links.[130] A PBD dimer, DSB-120 (**13e**), was prepared by linking two molecules of the natural product DC-81 (**13d**) by

 © 2014 Wiley-VCH Verlag GmbH & Co. KGaA, Weinheim

CSPC Exhibit 1004
Page 41 of 336

Table 3: List of antibody–drug conjugates currently in clinical trials.

Candidate	Drug	Antigen	Lead Indication[a]	Developer/Partner
FDA-Approved				
ado-Trastuzumab emtansine (Kadcyla)	DM1	HER2	Breast Cancer	Roche/Genentech/ImmunoGen
Brentuximab vedotin (Adcetris)	MMAE	CD30	HL/ALCL	Seattle Genetics
Phase III				
Inotuzumab ozogamicin (CMC-544)	Calicheamicin	CD22	ALL	Pfizer
Gemtuzumab ozogamicin (CMA-676)	Calicheamicin	CD33	AML	Pfizer
Phase II				
SAR3419	DM4	CD19	B-Cell malignancies	Sanofi/ImmunoGen
RG7593	MMAE	CD22	B-Cell malignancies	Roche/Genentech/Seattle Genetics
RG7596	MMAE	CD79b	B-Cell malignancies	Roche/Genentech/Seattle Genetics
Glembatumumab vedotin (CDX-011)	MMAE	GPNMB	Breast Cancer, Melanoma	Celldex Therapeutics/Seattle Genetics
PSMA-ADC	MMAE	PSMA	Prostate Cancer	Progenics Pharma/Seattle Genetics
Phase I				
Lorvotuzumab mertanisine	DM1	CD56	SCLC	ImmunoGen
IMGN529	DM1	CD37	B-Cell malignancies	ImmunoGen
IMGN853	DM4	FRα	Solid Tumors	ImmunoGen
IMGN289	DM1	EGFR	Solid Tumors	ImmunoGen
SAR566658	DM4	CA6	Solid Tumors	Sanofi/ImmunoGen
BT-062	DM4	CD138	Multiple Myeloma	Biotest/ImmunoGen
BAY 94-9343	DM4	mesothelin	Solid Tumors	Bayer/ImmunoGen
AMG 595	DM1	EGFRvIII	Gliomas	Amgen/ImmunoGen
AMG 172	DM1	CD27L	ccRCC	Amgen/ImmunoGen
SGN-CD19A	MMAF	CD19	NHL/ALL	Seattle Genetics
AGS-22ME	MMAE	Nectin 4	Solid Tumors	Astellas Pharma/Seattle Genetics
RG7450	MMAE	STEAP1	Prostate Cancer	Roche/Genentech/Seattle Genetics
RG7458	MMAE	MUC16	Ovarian Cancer	Roche/Genentech/Seattle Genetics
RG7599	MMAE	NaPi2b	NSCLC, Ovarian Cancer	Roche/Genentech/Seattle Genetics
MLN0264	MMAE	GCC	GI Malignancies	Takeda/Seattle Genetics
SGN-CD33A	PBD	CD33	AML	Seattle Genetics
MDX-1203	Duocarmycin	CD70	NHL, RCC	Bristol-Myers Squibb
Labetuzumab-SN-38	SN-38	CD66e	CRC	Immunomedics
IMMU-132	SN-38	Trop-2	Epithelial Cancers	Immunomedics
Milatuzumab Doxorubicin	Doxorubicin	CD74	Multiple Myeloma	Immunomedics
RG7598, RG7600, RG7636	Undisclosed	Undisclosed	Various	Roche/Genentech/Seattle Genetics

[a] HL: Hodgkin's Lymphoma; ALCL: Anaplastic Large Cell Lymphoma; NHL: Non-Hodgkin's Lymphoma; AML: Acute Myelogenous Leukemia; SCLC: Small-Cell Lung Cancer; ccRCC: Clear Cell Renal Cell Carcinoma; RCC: Renal Cell Carcinoma; ALL: Acute Lymphoblastic Leukemia; NSCLC: Non-Small-Cell Lung Cancer; GI: Gastrointestinal; CRC: Colorectal Carcinoma.

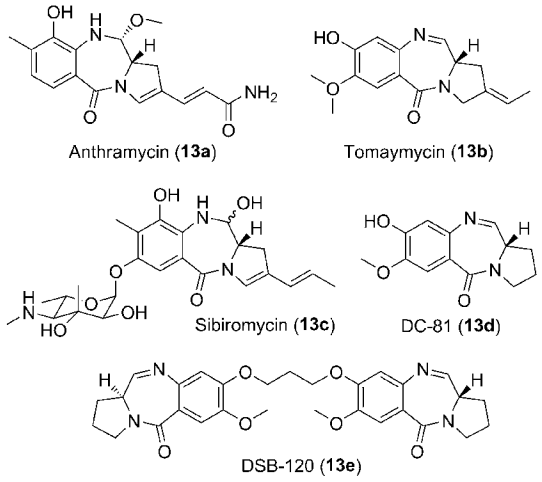


Figure 34. Pyrrolobenzodiazepine (PBD) monomers and DSB-120.

a propyldioxy ether linkage. Dimer formation resulted in significant increase in potency, with **13e** being 600 times more cytotoxic than **13d** in vitro. DSB-120 was shown to form DNA cross-links that spanned six base pairs with a preference for a central GATC sequence. At the time of its discovery it was among the most efficient DNA cross-linking agents known. Further elaboration of the PBD dimers eventually led to the synthesis of SJG-136 (**4f**; Figure 3) in which additional unsaturation was incorporated into the C rings of **13e**.[131,132] As a result, **4f** was shown to demonstrate significantly better DNA cross-linking efficiency and exquisite in vitro potency and good in vivo antitumor activity.[133] Currently, SJG-136 is being evaluated in Phase II clinical studies against solid tumors and hematologic malignancies.[134]

Because of their high potency and DNA-interacting mechanism of action, the PBD dimers are attractive effector molecules for use in ADCs. In 2009, a new class of potent compounds (IGNs) was described, consisting of two indolino-benzodiazepine monomers linked by an anilino-benzyldioxy

© 2014 Wiley-VCH Verlag GmbH & Co. KGaA, Weinheim

CSPC Exhibit 1004
Page 42 of 336

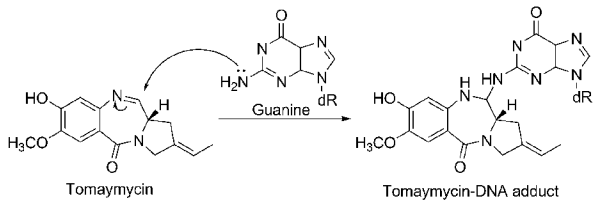


Figure 35. Mechanism of action of pyrrolobenzodiazepine (PBD).

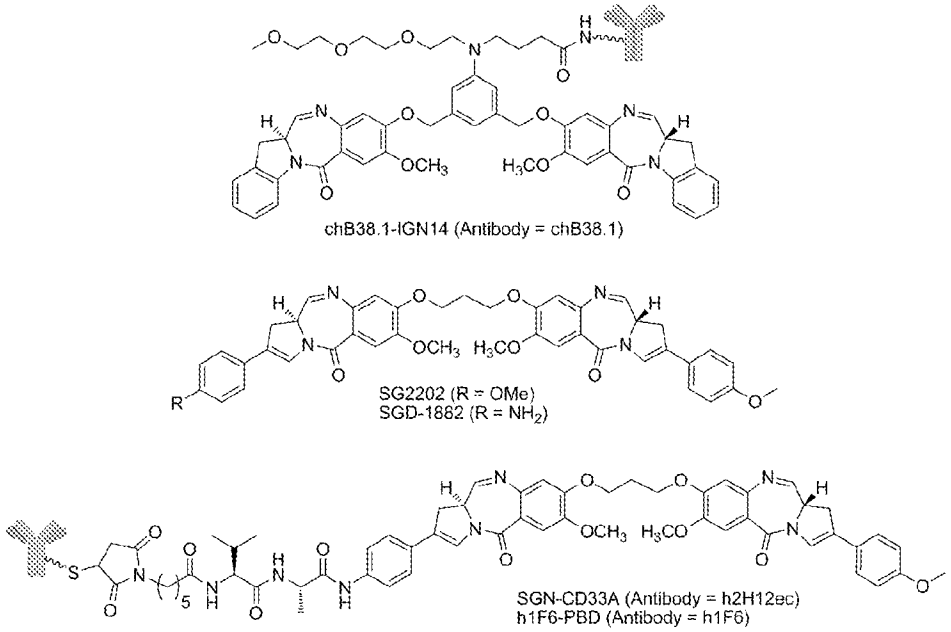


Figure 36. Indolinobenzodiazepine (IGN) and pyrrolobenzodiazepine (PBD) dimer conjugates.

spacer (Figure 36).[135] The parent compound of this class displayed potent sequence-specific DNA–adduct formation in double-stranded DNA and was extremely potent (1–10 pM) against a variety of cancer cell types. The incorporation of the anilino group into the spacer results in a suitable site for the incorporation of a linker for conjugation to an antibody. Incorporation of a short PEG group provided the necessary solubility in water for conjugation in aqueous media. ADCs of these IGNs containing an average of three molecules linked per antibody were prepared and found to be highly potent in vitro against both normal and multi-drug-resistant cancer cell lines (IC_{50} = 5–20 pM). Even cell lines that express low levels of antigen ($\approx$7000 molecules per cell) were efficiently killed by the conjugate (IC_{50} value of 4 pM). In addition, the cytotoxic effect of the conjugate was found to be antigen-specific, as the conjugate was considerably less cytotoxic to an antigen-negative cell line (IC_{50} > 1 nM). Dose-dependent antigen-specific antitumor activity in vivo was also reported.

Recently, two ADCs that utilize the PBD dimer SG2202,[134] which possesses an exocyclic phenyl substituent attached to the C ring (Figure 36), were described.[136,137] The incorporation of styryl groups was found to further increase the in vitro potency of the PBD dimer, while also providing the opportunity to introduce substituents for linking the PBD dimer to an antibody. In the ADC design, one of the monomer units is modified with an anilino substituent, thus generating an unsymmetrical PBD dimer, which was then modified with a valine-alanine dipeptide connected to a maleimide. Conjugates containing 1.9 PBD molecules per antibody were then prepared by linkage through engineered cysteine residues introduced into the antibody sequence.[136,137] ADCs that target the CD70 antigen, expressed on renal cell carcinoma (RCC) and non-Hodgkin lymphoma (NHL), and the CD33 antigen, expressed in acute myeloid leukemia (AML), were found to be potent and specific on a number of antigen-expressing cell lines in vitro. In vivo, both ADCs displayed dose-dependent antitumor activity in xenograft models in mice. In light of these data, an anti-CD33-PBD conjugate has recently been advanced to clinical evaluation in AML.[137]

8.1.2. Amanitin

The amanitins are mushroom toxins derived from the genus *Amanita*. The main component, α-amanitin, is a bicyclic octapeptide that has been shown to be a potent RNA polymerase II inhibitor. α-Amanitin is not therapeutically useful as it is efficiently transported to mature hepatocytes in vivo where it causes high liver toxicity. α-Amanitin has been linked to trastuzumab, and the conjugate displays antigen-specific potency toward HER2+ cell lines (IC_{50}: 8–180 pM).[138] In vivo, complete tumor regressions were obtained at low doses (0.05 mg kg^{-1} linked amanitin) and liver toxicity was not noted at the tested doses. Information about the MTD and therapeutic index of this conjugate were not reported.

8.2. Site-Specific-Conjugation Technology

ADCs that are currently in clinical evaluation take advantage of functional groups (primary amino group of lysines, thiol groups from reduction of cystines) in antibodies that are amenable to chemistry in aqueous solutions. A humanized antibody contains a large number of lysine groups (80–90), therefore allowing the modification of a few lysine groups without affecting the native disulfide bonds and

 © 2014 Wiley-VCH Verlag GmbH & Co. KGaA, Weinheim

CSPC Exhibit 1004
Page 43 of 336

without causing any significant changes in the stability and biophysical or binding properties of the antibody. Mass spectral analysis of a maytansinoid ADC, with an average load of 3.5–4 molecules per antibody, shows a distribution of peaks corresponding to a range of 0–7 maytansinoid molecules per antibody, which approximately fits a binomial distribution.[139] The lysine sites of maytansinoid attachment are consistent from batch to batch under controlled conjugation conditions. Antibody–lysine site modification is used for ado-trastuzumab emtansine, as well as for all other maytansinoid conjugates currently undergoing clinical evaluation. Antibody–lysine site modification is also employed for calicheamicin conjugates.

The cysteine conjugation site used in ADCs is generated by reducing native interchain cystine disulfide bonds, and the drug load is determined by the extent of the reduction. Typically, a fully reduced IgG_1 antibody has about eight cysteine residues. Partial disulfide reduction and loading of about four molecules of a cytotoxic agent per antibody at the cysteine sites also leads to a distribution of several species with 0, 2, 4, 6, and 8 molecules of the cytotoxic agent attached, with species with a load of 4 and 2 molecules being predominant.[140,141] Brentuximab vedotin and other auristatin-based ADCs are conjugated by cysteines that were generated by such partial reduction of native interchain disulfide bonds. An advantage of lysine or reduced-disulfide cysteine sites for the attachment of cytotoxic agents is that any antibody can be conjugated without re-engineering the antibody to introduce specific sites of attachment.

In order to increase the drug load in the ADC, one recently reported approach involves the use of a dendrimeric carrier for the drug. The basis of this method is the use of a hydrophilic, fully degradable polyacetal carrier that bears two orthogonal linkers. One linker was used to connect the carrier to an antibody by cysteine residues, derived from reduction of native cystine bridges in the hinge region of the antibody. The second linker was used to conjugate a dolastatin analogue. A conjugate of trastuzumab with 3–4 polyacetal carriers bearing a total of 20 dolastatin molecules was shown to display good antigen-specific potency in vitro and significant antitumor activity in vivo.[142]

Several approaches are currently evaluated to effect "site-specific" conjugation where sites of attachment of the cytotoxic agent to the antibody are defined. In addition, this approach is expected to give a single ADC species instead of a distribution. In the first described approach, cysteine residues were engineered in antibodies, for example by replacing serine 442 with cysteine in the cH3 domain of the heavy chain, resulting in the generation of two thiol groups per antibody.[143] Antibodies that did not interfere with antigen binding ("thiomabs") and contained engineered cysteines at various positions were conjugated with maleimido-MMAE to give homogeneous ADCs with two linked MMAEs per antibody. The site of cysteine incorporation was important, because thiol-maleimide linkages that were unstable in plasma were formed at some cysteine sites.[139,144] A homogeneously conjugated anti-MUC16 conjugate with two MMAEs per antibody (one per heavy chain), linked by an engineered cysteine in each heavy chain, showed similar efficacy in xenograft models and improved tolerability in rat and monkey preclinical models compared to a conjugate with an average of 3.1 MMAEs per antibody, derived from reduced interchain disulfide conjugation.[141] Cysteine-engineered antibodies require additional manufacturing steps compared to traditional antibodies because of their initial generation from cell culture as mixed disulfides, which require partial reduction and reoxidation.[141] One ADC derived from an engineered cysteine antibody has recently entered into clinical evaluation.[137]

Four other approaches to generate site-specific ADCs through antibody engineering and other techniques are underway. These include: a) The incorporation of an unnatural amino acid through genetic engineering.[145] In this elegant approach, the appropriate tRNA/aminoacyl-tRNA synthetase pair was used to replace an alanine residue in the heavy chain of the trastuzumab antibody with the unnatural amino acid *para*-acetylphenylalanine. The incorporation of an amino acid with a carbonyl moiety, a functional group that is not present in any of the 20 natural amino acids, provides orthogonal chemical reactivity. The antibody mutant was conjugated to an auristatin derivative through a stable oxime link to provide a homogenous ADC with two molecules of drug linked in a site-specific manner (Figure 37). The resulting conjugate displayed good in vitro potency and in vivo antitumor activity, along with favorable pharmacokinetics. b) The incorporation of engineered glutamine residues and coupling of amino groups of the cytotoxic agent by amide linkage using microbial transglutaminase (mTG).[146] This approach takes advantage of the finding that mTG does not recognize naturally occurring glutamine residues in the constant regions of glycosylated antibodies. Thus, glutamine residues were engineered at selected sites in three different antibodies. Treatment with mTG in the presence of an acyl acceptor payload (AcLys-vc-monomethylauristatin D) resulted in the incorporation of around two drug molecules per antibody in a site-specific manner. In one example, ADCs that bear 1.74 and 1.87 drug molecules per antibody were shown to be potent in vitro, and displayed similar in vivo antitumor activity when compared to a traditional conjugate that bears 3.6 auristatin molecules per antibody. c) The site-specific modification of heavy-chain C termini by intein fusion;[147] and d) the incorporation of engineered cysteines at the N terminus and coupling of 1,2-aminothiol to an aldehyde group of a cytotoxic agent by a thiazolidine linkage.[148] Thus far, it was possible to link about two molecules of a cytotoxic agent to an antibody using these approaches. It is not clear whether this load will be sufficient to affect cell killing when the antigen density is not very high. Higher drug loading without affecting the biochemical characteristics of the conjugate has not yet been demonstrated with any of the site-specific approaches. It is not yet known whether site-specific conjugation will actually improve the therapeutic index of ADCs in the clinic. Also, the potential immunogenicity of ADCs that bear antibodies with unnatural amino acids can only be determined through human clinical trials.

© 2014 Wiley-VCH Verlag GmbH & Co. KGaA, Weinheim

CSPC Exhibit 1004
Page 44 of 336

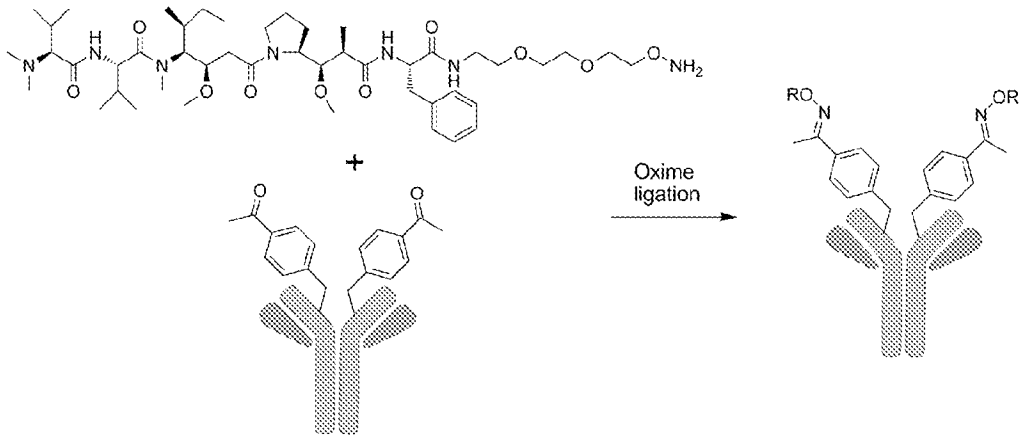


Figure 37. Site-specific conjugation of alkoxyamine-derivatized auristatin.

8.3. Optimizing ADC Activity

Further optimization of ADC design continues to be an active area of research. Use of smaller scaffold proteins or antibody fragments, instead of whole IgGs, may offer the advantage of greater tumor penetration in view of their smaller size. A direct comparison of the in vivo tumor localization of antibody fragments (sFv, Fab′, F(ab)′$_2$) with the intact IgG showed that the rate and degree of tumor penetration correlated with the size.[149] The smallest fragment, sFv, demonstrated maximal tumor penetration at 0.5 hours, while the intact IgG took 48 to 96 hours to achieve the same level of penetration. In addition, the sFv was more evenly distributed throughout the tumor mass as compared to the forms with higher molecular weights. Despite the availability of this data for over twenty years, drug conjugates of antibody fragments have not advanced beyond the preclinical stage. The faster clearance of these fragments and the propensity to accumulate in kidneys requires half-life extension strategies, such as conjugation to poly(ethylene glycol)s, thus making the technology more complex. In one study, a diabody–auristatin conjugate was shown to clear around 30 times faster than the corresponding IgG conjugate, and was four times less potent in vitro and in vivo.[150]

Other considerations for successful ADC development include greater attention to the selection of antibodies and linkers, and more thorough preclinical evaluation prior to advancement to the clinic. It is commonly believed that antibodies have to be efficiently internalized to achieve good ADC activity. A recent report with a vascular-targeting ADC suggests that this may not always be a necessary feature.[151] The linker between the antibody and the drug determines the nature of the metabolite produced in vitro and in vivo. Recent clinical data suggests that the toxicity profile of the ADC is linker-dependent. Thus, changes in linker design would alter the metabolite profile, which in turn would influence clinical toxicity. For ADC therapy, preclinical models for efficacy studies have to be carefully selected such that the antigen expression on the xenograft reflects the clinical population to be treated. In addition, it is important to demonstrate antitumor activity in vivo at doses achievable in the clinic (2–7 mg kg^{-1} for most ADCs). Setting such higher preclinical bars may mitigate the chance of failure in the clinic.

9. Summary and Outlook

The concept of targeted delivery of anticancer drugs originated from the desire of oncologists to improve the tumor selectivity of anticancer drugs in order to lower their systemic toxicity. By these means, the drugs could be administered at higher doses, thus providing greater therapeutic benefit to their patients. The tumor selectivity of antibodies offered an avenue to achieve this goal by using them as vehicles to direct the drug to the tumor. This seemingly simple concept, called antibody–drug conjugates, garnered tremendous attention from researchers at academic institutions and in the pharmaceutical industry. A flurry of research and development activity in the 1980s and early 1990s led to clinical trials of several ADCs. However, disappointing clinical results led to diminishing interest in this approach.

Nevertheless, some research groups persisted and carefully analyzed the possible causes of the failures. From the lessons learned, almost every aspect of the technology was improved. The current breed of ADCs uses antibodies that are humanized, and thus not immunogenic, and linkers that are designed to be stable in circulation, but are cleaved upon delivery into a cell. Medicinal chemists are now able to harness the potency of drugs that were once too toxic to be useful on their own. The recent FDA approvals of the two ADCs, brentuximab vedotin and ado-trastuzumab emtansine, have provided proof-of-concept for this approach, and have generated tremendous excitement. There are over 30 ADCs currently in clinical evaluation and almost every major pharmaceutical company has embraced this technology. There is active research by medicinal chemists to develop new linkers and discover new potent effector molecules suitable for use in ADCs, while biologists have focused on identifying cell-surface targets suitable for antibody development.

 © 2014 Wiley-VCH Verlag GmbH & Co. KGaA, Weinheim

CSPC Exhibit 1004
Page 45 of 336

Acknowledgement

The early and enthusiastic support of RVJC's work on ADCs by the late Dr. Emil (Tom) Frei III, former Physician-in-Chief of the Dana-Farber Cancer Institute, is greatly appreciated. The authors sincerely thank Dr. Daniel Tavares for his creative illustrations, and Dr. John Lambert for his critical review of this manuscript and valuable comments.

Received: August 29, 2013
Published online: February 20, 2014

[1] V. T. DeVita, Jr., E. Chu, *Cancer Res.* **2008**, *68*, 8643 – 8653.
[2] B. C. Baguley in *Anticancer Drug Development* (Eds.: B. C. Baguley, D. J. Kerr), Academic Press, San Diego, **2002**, pp. 1 – 11.
[3] E. Frei III, *Cancer Res.* **1972**, *32*, 2593 – 2607.
[4] S. M. Kupchan, Y. Komoda, W. A. Court, G. J. Thomas, R. M. Smith, A. Karim, C. J. Gilmore, R. C. Haltiwanger, R. F. Bryan, *J. Am. Chem. Soc.* **1972**, *94*, 1354 – 1356.
[5] S. M. Kupchan, Y. Komoda, A. R. Branfman, A. T. Sneden, W. A. Court, G. J. Thomas, H. P. Hintz, R. M. Smith, A. Karim, G. A. Howie, A. K. Verma, Y. Nagao, R. G. Dailey, Jr., V. A. Zimmerly, W. C. Sumner, Jr., *J. Org. Chem.* **1977**, *42*, 2349 – 2357.
[6] S. Remillard, L. I. Rebhun, G. A. Howie, S. M. Kupchan, *Science* **1975**, *189*, 1002 – 1005.
[7] B. F. Issell, S. T. Crooke, *Cancer Treat. Rev.* **1978**, *5*, 199 – 207.
[8] G. R. Pettit, Y. Kamano, C. L. Herald, A. A. Tuinman, F. E. Boettner, H. Kizu, J. M. Schmidt, L. Baczynskyj, K. B. Tomer, R. J. Bontems, *J. Am. Chem. Soc.* **1987**, *109*, 6883 – 6885.
[9] G. R. Pettit, Y. Kamano, C. Dufresne, R. L. Cerny, C. L. Herald, J. M. Schmidt, *J. Org. Chem.* **1989**, *54*, 6005 – 6006.
[10] H. C. Pitot, E. A. McElroy, Jr., J. M. Reid, A. J. Windebank, J. A. Sloan, C. Erlichman, P. G. Bagniewski, D. L. Walker, J. Rubin, R. M. Goldberg, A. A. Adjei, M. M. Ames, *Clin. Cancer Res.* **1999**, *5*, 525 – 531.
[11] U. Vaishampayan, M. Glode, W. Du, A. Kraft, G. Hudes, J. Wright, M. Hussain, *Clin. Cancer Res.* **2000**, *6*, 4205 – 4208.
[12] R. S. Al-awar, J. E. Ray, R. M. Schultz, S. L. Andis, J. H. Kennedy, R. E. Moore, J. Liang, T. Golakoti, G. V. Subbaraju, T. H. Corbett, *J. Med. Chem.* **2003**, *46*, 2985 – 3007.
[13] M. J. Edelman, D. R. Gandara, P. Hausner, V. Israel, D. Thornton, J. DeSanto, L. A. Doyle, *Lung Cancer* **2003**, *39*, 197 – 199.
[14] S. Jain, L. T. Vahdat, *Clin. Cancer Res.* **2011**, *17*, 6615 – 6622.
[15] M. A. Warpehoski, I. Gebhard, R. C. Kelly, W. C. Krueger, L. H. Li, J. P. McGovren, M. D. Prairie, N. Wicnienski, W. Wierenga, *J. Med. Chem.* **1988**, *31*, 590 – 603.
[16] M. Cristofanilli, W. J. Bryan, L. L. Miller, A. Y. Chang, W. J. Gradishar, D. W. Kufe, G. N. Hortobagyi, *Anticancer Drugs* **1998**, *9*, 779 – 782.
[17] N. Pavlidis, S. Aamdal, A. Awada, H. Calvert, P. Fumoleau, R. Sorio, C. Punt, J. Verweij, A. van Oosterom, R. Morant, J. Wanders, A. R. Hanauske, *Cancer Chemother. Pharmacol.* **2000**, *46*, 167 – 171.
[18] H. C. Pitot, J. M. Reid, J. A. Sloan, M. M. Ames, A. A. Adjei, J. Rubin, P. G. Bagniewski, P. Atherton, D. Rayson, R. M. Goldberg, C. Erlichman, *Clin. Cancer Res.* **2002**, *8*, 712 – 717.
[19] S. N. Markovic, V. J. Suman, A. M. Vukov, T. R. Fitch, D. W. Hillman, A. A. Adjei, S. R. Alberts, J. S. Kaur, T. A. Braich, J. M. Leitch, E. T. Creagan, *Am. J. Clin. Oncol.* **2002**, *25*, 308 – 312.
[20] D. Hochhauser, T. Meyer, V. J. Spanswick, J. Wu, P. H. Clingen, P. Loadman, M. Cobb, L. Gumbrell, R. H. Begent, J. A. Hartley, D. Jodrell, *Clin. Cancer Res.* **2009**, *15*, 2140 – 2147.
[21] J. Zhang, P. L. Yang, N. S. Gray, *Nat. Rev. Cancer* **2009**, *9*, 28 – 39.
[22] A. Arora, E. M. Scholar, *J. Pharmacol. Exp. Ther.* **2005**, *315*, 971 – 979.
[23] P. S. Low, W. A. Henne, D. D. Doorneweerd, *Acc. Chem. Res.* **2008**, *41*, 120 – 129.
[24] J. A. Reddy, R. Dorton, E. Westrick, A. Dawson, T. Smith, L. C. Xu, M. Vetzel, P. Kleindl, I. R. Vlahov, C. P. Leamon, *Cancer Res.* **2007**, *67*, 4434 – 4442.
[25] I. R. Vlahov, C. P. Leamon, *Bioconjugate Chem.* **2012**, *23*, 1357 – 1369.
[26] G. Köhler, C. Milstein, *Nature* **1975**, *256*, 495 – 497.
[27] R. K. Oldham, R. O. Dillman, *J. Clin. Oncol.* **2008**, *26*, 1774 – 1777.
[28] A. M. Scott, J. D. Wolchok, L. J. Old, *Nat. Rev. Cancer* **2012**, *12*, 278 – 287.
[29] L. M. Nadler, P. Stashenko, R. Hardy, W. D. Kaplan, L. N. Button, D. W. Kufe, K. H. Antman, S. F. Schlossman, *Cancer Res.* **1980**, *40*, 3147 – 3154.
[30] J. C. Almagro, J. Fransson, *Front. Biosci.* **2008**, *13*, 1619 – 1633.
[31] D. G. Maloney, A. J. Grillo-Lopez, C. A. White, D. Bodkin, R. J. Schilder, J. A. Neidhart, N. Janakiraman, K. A. Foon, T. M. Liles, B. K. Dallaire, K. Wey, I. Royston, T. Davis, R. Levy, *Blood* **1997**, *90*, 2188 – 2195.
[32] P. Uadia, A. H. Blair, T. Ghose, *Cancer Res.* **1984**, *44*, 4263 – 4266.
[33] B. C. Laguzza, C. L. Nichols, S. L. Briggs, G. J. Cullinan, D. A. Johnson, J. J. Starling, A. L. Baker, T. F. Bumol, J. R. F. Corvalan, *J. Med. Chem.* **1989**, *32*, 548 – 555.
[34] P. A. Trail, D. Willner, S. J. Lasch, A. J. Henderson, S. Hofstead, A. M. Casazza, R. A. Firestone, I. Hellstrom, K. E. Hellstrom, *Science* **1993**, *261*, 212 – 215.
[35] D. J. Elias, L. E. Kline, B. A. Robbins, H. C. Johnson, Jr., K. Pekny, M. Benz, J. A. Robb, L. E. Walker, M. Kosty, R. O. Dillman, *Am. J. Respir. Crit. Care Med.* **1994**, *150*, 1114 – 1122.
[36] D. Schneck, F. Butler, W. Dugan, D. Littrell, B. Petersen, R. Bowsher, A. DeLong, S. Dorrbecker, *Clin. Pharmacol. Ther.* **1990**, *47*, 36 – 41.
[37] B. H. Petersen, S. V. DeHerdt, D. W. Schneck, T. F. Bumol, *Cancer Res.* **1991**, *51*, 2286 – 2290.
[38] A. W. Tolcher, S. Sugarman, K. A. Gelmon, R. Cohen, M. Saleh, C. Isaacs, L. Young, D. Healey, N. Onetto, W. Slichenmyer, *J. Clin. Oncol.* **1999**, *17*, 478 – 484.
[39] H. H. Sedlacek, *Antibodies as Carriers of Cytotoxicity*, Karger, Basel, **1992**.
[40] S. I. Rudnick, J. Lou, C. C. Shaller, Y. Tang, A. J. Klein-Szanto, L. M. Weiner, J. D. Marks, G. P. Adams, *Cancer Res.* **2011**, *71*, 2250 – 2259.
[41] J. D. Orth, E. W. Krueger, S. G. Weller, M. A. McNiven, *Cancer Res.* **2006**, *66*, 3603 – 3610.
[42] C. Dumontet, M. A. Jordan, *Nat. Rev. Drug Discovery* **2010**, *9*, 790 – 803.
[43] M. Abal, J. M. Andreu, I. Barasoain, *Curr. Cancer Drug Targets* **2003**, *3*, 193 – 203.
[44] K. E. Gascoigne, S. S. Taylor, *J. Cell Sci.* **2009**, *122*, 2579 – 2585.
[45] J. A. Hadfield, S. Ducki, N. Hirst, A. T. McGown, *Prog. Cell Cycle Res.* **2003**, *5*, 309 – 325.
[46] W. I. Lencer, R. S. Blumberg, *Trends Cell Biol.* **2005**, *15*, 5 – 9.
[47] M. Lopus, E. Oroudjev, L. Wilson, S. Wilhelm, W. Widdison, R. Chari, M. A. Jordan, *Mol. Cancer Ther.* **2010**, *9*, 2689 – 2699.
[48] R. H. Blum, T. Kahlert, *Cancer Treat. Rep.* **1978**, *62*, 435 – 438.
[49] G. Wu, Y. Z. Fang, S. Yang, J. R. Lupton, N. D. Turner, *J. Nutr.* **2004**, *134*, 489 – 492.
[50] B. J. Mills, C. A. Lang, *Biochem. Pharmacol.* **1996**, *52*, 401 – 406.

 © 2014 Wiley-VCH Verlag GmbH & Co. KGaA, Weinheim

CSPC Exhibit 1004
Page 46 of 336

[51] J. M. Cassady, K. K. Chan, H. G. Floss, E. Leistner, *Chem. Pharm. Bull.* **2004**, *52*, 1–26.
[52] C. W. Wayne, D. W. Sharon, E. C. Emily, R. W. Kathleen, A. L. Barbara, Y. Kovtun, S. G. Victor, H. Xie, M. S. Rita, J. L. Robert, R. Zhao, L. Wang, A. B. Walter, V. J. C. Ravi, *J. Med. Chem.* **2006**, *49*, 4392–4408.
[53] M. Bénéchie, F. Khuong-Huu, *J. Org. Chem.* **1996**, *61*, 7133–7138.
[54] A. I. Meyers, P. J. Reider, A. I. Campbell, *J. Am. Chem. Soc.* **1980**, *102*, 6597–6598.
[55] M. Kitamura, M. Isobe, Y. Ichikawa, T. Goto, *J. Am. Chem. Soc.* **1984**, *106*, 3252–3257.
[56] B. A. Kellogg, L. Garrett, Y. Kovtun, K. C. Lai, B. Leece, M. Miller, G. Payne, R. Steeves, K. R. Whiteman, W. Widdison, H. Xie, R. Singh, R. V. Chari, J. M. Lambert, R. J. Lutz, *Bioconjugate Chem.* **2011**, *22*, 717–727.
[57] Y. V. Kovtun, C. A. Audette, Y. Ye, H. Xie, M. F. Ruberti, S. J. Phinney, B. A. Leece, T. Chittenden, W. A. Blattler, V. S. Goldmacher, *Cancer Res.* **2006**, *66*, 3214–3221.
[58] O. Ab, L. Rui, J. Coccia, H. A. Johnson, K. R. Whiteman, B. Kellog, L. Clancy, X. Sun, V. S. Goldmacher, *American Association for Cancer Research 102nd Annual Meeting abstract 4576, Vol. Supplement 1*, Orlando, **2011**.
[59] E. Maloney, N. Fishkin, R. Chari, R. Singh, *Mol. Cancer Ther.* **2009**, *8*, B120.
[60] H. K. Erickson, P. U. Park, W. C. Widdison, Y. V. Kovtun, L. M. Garrett, K. Hoffman, R. J. Lutz, V. S. Goldmacher, W. A. Blattler, *Cancer Res.* **2006**, *66*, 4426–4433.
[61] M. Heine, B. Freund, P. Nielsen, C. Jung, R. Reimer, H. Hohenberg, U. Zangemeister-Wittke, H. J. Wester, G. H. Luers, U. Schumacher, *PLoS One* **2012**, *7*, e36258.
[62] Y. V. Kovtun, C. A. Audette, M. F. Mayo, G. E. Jones, H. Doherty, E. K. Maloney, H. K. Erickson, X. Sun, S. Wilhelm, O. Ab, K. C. Lai, W. C. Widdison, B. Kellogg, H. Johnson, J. Pinkas, R. J. Lutz, R. Singh, V. S. Goldmacher, R. V. Chari, *Cancer Res.* **2010**, *70*, 2528–2537.
[63] R. Zhao, S. Wilhelm, C. Audette, G. Jones, B. Leece, A. Lazar, V. Goldmacher, R. Singh, Y. Kovtun, W. Widdison, J. Lambert, R. Chari, *J. Med. Chem.* **2011**, *54*, 3606–3623.
[64] R. K. Kelly, D. L. Olson, Y. Sun, D. Wen, K. A. Wortham, G. Antognetti, A. E. Cheung, O. E. Orozco, L. Yang, V. Bailly, M. Sanicola, *Eur. J. Cancer* **2011**, *47*, 1736–1746.
[65] H. K. Erickson, G. D. L. Phillips, D. D. Leipold, C. A. Provenzano, E. Mai, H. A. Johnson, B. Gunter, C. A. Audette, M. Gupta, J. Pinkas, J. Tibbitts, *Mol. Cancer Ther.* **2012**, *11*, 1133–1142.
[66] X. Sun, W. Widdison, M. Mayo, S. Wilhelm, B. Leece, R. Chari, R. Singh, H. Erickson, *Bioconjugate Chem.* **2011**, *22*, 728–735.
[67] R. K. Pettit, G. R. Pettit, K. C. Hazen, *Antimicrob. Agents Chemother.* **1998**, *42*, 2961–2965.
[68] G. R. Pettit, J. K. Srirangam, J. Barkoczy, M. D. Williams, M. R. Boyd, E. Hamel, R. K. Pettit, F. Hogan, R. Bai, J. C. Chapuis, S. C. McAllister, J. M. Schmidt, *Anticancer Drug Des.* **1998**, *13*, 243–277.
[69] S. O. Doronina, B. A. Mendelsohn, T. D. Bovee, C. G. Cerveny, S. C. Alley, D. L. Meyer, E. Oflazoglu, B. E. Toki, R. J. Sanderson, R. F. Zabinski, A. F. Wahl, P. D. Senter, *Bioconjugate Chem.* **2006**, *17*, 114–124.
[70] C. L. Law, K. A. Gordon, B. E. Toki, A. K. Yamane, M. A. Hering, C. G. Cerveny, J. M. Petroziello, M. C. Ryan, L. Smith, R. Simon, G. Sauter, E. Oflazoglu, S. O. Doronina, D. L. Meyer, J. A. Francisco, P. Carter, P. D. Senter, J. A. Copland, C. G. Wood, A. F. Wahl, *Cancer Res.* **2006**, *66*, 2328–2337.
[71] S. O. Doronina, B. E. Toki, M. Y. Torgov, B. A. Mendelsohn, C. G. Cerveny, D. F. Chace, R. L. DeBlanc, R. P. Gearing, T. D. Bovee, C. B. Siegall, J. A. Francisco, A. F. Wahl, D. L. Meyer, P. D. Senter, *Nat. Biotechnol.* **2003**, *21*, 778–784.
[72] S. Kaur, K. Xu, O. M. Saad, R. C. Dere, M. Carrasco-Triguero, *Bioanalysis* **2013**, *5*, 201–226.
[73] K. J. Hamblett, P. D. Senter, D. F. Chace, M. M. Sun, J. Lenox, C. G. Cerveny, K. M. Kissler, S. X. Bernhardt, A. K. Kopcha, R. F. Zabinski, D. L. Meyer, J. A. Francisco, *Clin. Cancer Res.* **2004**, *10*, 7063–7070.
[74] N. M. Okeley, J. B. Miyamoto, X. Zhang, R. J. Sanderson, D. R. Benjamin, E. L. Sievers, P. D. Senter, S. C. Alley, *Clin. Cancer Res.* **2010**, *16*, 888–897.
[75] L. M. Smith, A. Nesterova, S. C. Alley, M. Y. Torgov, P. J. Carter, *Mol. Cancer Ther.* **2006**, *5*, 1474–1482.
[76] S. C. Alley, X. Zhang, N. M. Okeley, M. Anderson, C. L. Law, P. D. Senter, D. R. Benjamin, *J. Pharmacol. Exp. Ther.* **2009**, *330*, 932–938.
[77] M. D. Lee, T. S. Dunne, M. M. Siegel, C. C. Chang, G. O. Morton, D. B. Borders, *J. Am. Chem. Soc.* **1987**, *109*, 3464–3466.
[78] M. D. Lee, T. S. Dunne, C. C. Chang, G. A. Ellestad, M. M. Siegel, G. O. Morton, W. J. McGahren, D. B. Borders, *J. Am. Chem. Soc.* **1987**, *109*, 3466–3468.
[79] M. D. Lee, G. A. Ellestad, D. B. Borders, *Acc. Chem. Res.* **1991**, *24*, 235–243.
[80] A. L. Smith, K. C. Nicolaou, *J. Med. Chem.* **1996**, *39*, 2103–2117.
[81] K. C. Nicolaou, C. R. H. Hale, C. Nilewski, *Chem. Rec.* **2012**, *12*, 407–441.
[82] N. Zein, A. M. Sinha, W. J. McGahren, G. A. Ellestad, *Science* **1988**, *240*, 1198–1201.
[83] R. G. Bergman, *Acc. Chem. Res.* **1973**, *6*, 25–31.
[84] L. M. Hinman, P. R. Hamann, R. Wallace, A. T. Menendez, F. E. Durr, J. Upeslacis, *Cancer Res.* **1993**, *53*, 3336–3342.
[85] P. R. Hamann, L. M. Hinman, C. F. Beyer, D. Lindh, J. Upeslacis, D. A. Flowers, I. Bernstein, *Bioconjugate Chem.* **2002**, *13*, 40–46.
[86] P. R. Hamann, L. M. Hinman, C. F. Beyer, L. M. Greenberger, C. Lin, D. Lindh, A. T. Menendez, R. Wallace, F. E. Durr, J. Upeslacis, *Bioconjugate Chem.* **2005**, *16*, 346–353.
[87] P. R. Hamann, L. M. Hinman, C. F. Beyer, D. Lindh, J. Upeslacis, D. Shochat, A. Mountain, *Bioconjugate Chem.* **2005**, *16*, 354–360.
[88] P. R. Hamann, L. M. Hinman, I. Hollander, C. F. Beyer, D. Lindh, R. Holcomb, W. Hallett, H. R. Tsou, J. Upeslacis, D. Shochat, A. Mountain, D. A. Flowers, I. Bernstein, *Bioconjugate Chem.* **2002**, *13*, 47–58.
[89] J. F. DiJoseph, M. M. Dougher, D. Y. Evans, B. B. Zhou, N. K. Damle, *Cancer Chemother. Pharmacol.* **2011**, *67*, 741–749.
[90] F. Kratz, P. Senter, H. Steinhagen, *Drug Delivery in Oncology: From Basic Research to Cancer Therapy*, Wiley-VCH, Weinheim, **2012**.
[91] A. Advani, B. Coiffier, M. S. Czuczman, M. Dreyling, J. Foran, E. Gine, C. Gisselbrecht, N. Ketterer, S. Nasta, A. Rohatiner, I. G. Schmidt-Wolf, M. Schuler, J. Sierra, M. R. Smith, G. Verhoef, J. N. Winter, J. Boni, E. Vandendries, M. Shapiro, L. Fayad, *J. Clin. Oncol.* **2010**, *28*, 2085–2093.
[92] M. Ichimura, T. Ogawa, S. Katsumata, K. Takahashi, I. Takahashi, H. Nakano, *J. Antibiot.* **1991**, *44*, 1045–1053.
[93] L. J. Hanka, A. Dietz, S. A. Gerpheide, S. L. Kuentzel, D. G. Martin, *J. Antibiot.* **1978**, *31*, 1211–1217.
[94] B. K. Bhuyan, K. A. Newell, S. L. Crampton, D. D. Von Hoff, *Cancer Res.* **1982**, *42*, 3532–3537.
[95] D. L. Boger, D. S. Johnson, *Proc. Natl. Acad. Sci. USA* **1995**, *92*, 3642–3649.
[96] L. H. Li, T. F. DeKoning, R. C. Kelly, W. C. Krueger, J. P. McGovren, G. E. Padbury, G. L. Petzold, T. L. Wallace, R. J. Ouding, M. D. Prairie, I. Gebhard, *Cancer Res.* **1992**, *52*, 4904–4913.

© 2014 Wiley-VCH Verlag GmbH & Co. KGaA, Weinheim

CSPC Exhibit 1004
Page 47 of 336

[97] C. S. Lee, G. P. Pfeifer, N. W. Gibson, *Biochemistry* **1994**, *33*, 6024 – 6030.
[98] R. Baird, S. Winstein, *J. Am. Chem. Soc.* **1957**, *79*, 4238 – 4240.
[99] D. L. Boger, C. W. Boyce, R. M. Garbaccio, J. A. Goldberg, *Chem. Rev.* **1997**, *97*, 787 – 828.
[100] D. L. Boger, W. Yun, B. R. Teegarden, *J. Org. Chem.* **1992**, *57*, 2873 – 2876.
[101] D. L. Boger, J. A. McKie, *J. Org. Chem.* **1995**, *60*, 1271 – 1275.
[102] R. V. Chari, K. A. Jackel, L. A. Bourret, S. M. Derr, B. M. Tadayoni, K. M. Mattocks, S. A. Shah, C. Liu, W. A. Blattler, V. S. Goldmacher, *Cancer Res.* **1995**, *55*, 4079 – 4084.
[103] R. Y. Zhao, H. K. Erickson, B. A. Leece, E. E. Reid, V. S. Goldmacher, J. M. Lambert, R. V. Chari, *J. Med. Chem.* **2012**, *55*, 766 – 782.
[104] W. Dokter, P. Beusker, G. Verheijden, R. Ubink, M. v. d. Lee, D. v. d. Dobbelsteen, P. Goedings, J. Lemmens, V. d. Groot, M. Timmers, *AACR National Meeting (Washington, D. C.)* **2013**, Abstr. 4329.
[105] M. E. Wall, M. C. Wani, C. E. Cook, K. H. Palmer, A. T. McPhail, G. A. Sim, *J. Am. Chem. Soc.* **1966**, *88*, 3888 – 3890.
[106] Y. H. Hsiang, R. Hertzberg, S. Hecht, L. F. Liu, *J. Biol. Chem.* **1985**, *260*, 14873 – 14878.
[107] R. H. Mathijssen, R. J. van Alphen, J. Verweij, W. J. Loos, K. Nooter, G. Stoter, A. Sparreboom, *Clin. Cancer Res.* **2001**, *7*, 2182 – 2194.
[108] W. D. Kingsbury, J. C. Boehm, D. R. Jakas, K. G. Holden, S. M. Hecht, G. Gallagher, M. J. Caranfa, F. L. McCabe, L. F. Faucette, R. K. Johnson, R. P. Hertzberg, *J. Med. Chem.* **1991**, *34*, 98 – 107.
[109] S. J. Moon, S. V. Govindan, T. M. Cardillo, C. A. D'Souza, H. J. Hansen, D. M. Goldenberg, *J. Med. Chem.* **2008**, *51*, 6916 – 6926.
[110] R. M. Sharkey, S. V. Govindan, T. M. Cardillo, D. M. Goldenberg, *Mol. Cancer Ther.* **2012**, *11*, 224 – 234.
[111] R. Stein, M. J. Mattes, T. M. Cardillo, H. J. Hansen, C. H. Chang, J. Burton, S. Govindan, D. M. Goldenberg, *Clin. Cancer Res.* **2007**, *13*, 5556s – 5563s.
[112] S. V. Govindan, T. M. Cardillo, R. M. Sharkey, F. Tat, D. V. Gold, D. M. Goldenberg, *Mol. Cancer Ther.* **2013**, *12*, 968 – 978.
[113] S. V. Govindan, T. M. Cardillo, S. J. Moon, H. J. Hansen, D. M. Goldenberg, *Clin. Cancer Res.* **2009**, *15*, 6052 – 6061.
[114] T. M. Cardillo, S. V. Govindan, R. M. Sharkey, P. Trisal, D. M. Goldenberg, *Clin. Cancer Res.* **2011**, *17*, 3157 – 3169.
[115] P. F. Bross, J. Beitz, G. Chen, X. H. Chen, E. Duffy, L. Kieffer, S. Roy, R. Sridhara, A. Rahman, G. Williams, R. Pazdur, *Clin. Cancer Res.* **2001**, *7*, 1490 – 1496.
[116] S. H. Petersdorf, K. J. Kopecky, M. Slovak, C. Willman, T. Nevill, J. Brandwein, R. A. Larson, H. P. Erba, P. J. Stiff, R. K. Stuart, R. B. Walter, M. S. Tallman, L. Stenke, F. R. Appelbaum, *Blood* **2013**, *121*, 4854 – 4860.
[117] J. M. Rowe, B. Lowenberg, *Blood* **2013**, *121*, 4838 – 4841.
[118] M. S. Sutherland, R. J. Sanderson, K. A. Gordon, J. Andreyka, C. G. Cerveny, C. Yu, T. S. Lewis, D. L. Meyer, R. F. Zabinski, S. O. Doronina, P. D. Senter, C. L. Law, A. F. Wahl, *J. Biol. Chem.* **2006**, *281*, 10540 – 10547.
[119] S. M. Ansell, S. M. Horwitz, A. Engert, K. D. Khan, T. Lin, R. Strair, T. Keler, R. Graziano, D. Blanset, M. Yellin, S. Fischkoff, A. Assad, P. Borchmann, *J. Clin. Oncol.* **2007**, *25*, 2764 – 2769.
[120] J. Katz, J. E. Janik, A. Younes, *Clin. Cancer Res.* **2011**, *17*, 6428 – 6436.
[121] A. Younes, A. K. Gopal, S. E. Smith, S. M. Ansell, J. D. Rosenblatt, K. J. Savage, R. Ramchandren, N. L. Bartlett, B. D. Cheson, S. de Vos, A. Forero-Torres, C. H. Moskowitz, J. M. Connors, A. Engert, E. K. Larsen, D. A. Kennedy, E. L. Sievers, R. Chen, *J. Clin. Oncol.* **2012**, *30*, 2183 – 2189.
[122] A. Younes, N. L. Bartlett, J. P. Leonard, D. A. Kennedy, C. M. Lynch, E. L. Sievers, A. Forero-Torres, *N. Engl. J. Med.* **2010**, *363*, 1812 – 1821.
[123] S. Verma, D. Miles, L. Gianni, I. E. Krop, M. Welslau, J. Baselga, M. Pegram, D. Y. Oh, V. Dieras, E. Guardino, L. Fang, M. W. Lu, S. Olsen, K. Blackwell, *N. Engl. J. Med.* **2012**, *367*, 1783 – 1791.
[124] H. A. Burris III, H. S. Rugo, S. J. Vukelja, C. L. Vogel, R. A. Borson, S. Limentani, E. Tan-Chiu, I. E. Krop, R. A. Michaelson, S. Girish, L. Amler, M. Zheng, Y. W. Chu, B. Klencke, J. A. O'Shaughnessy, *J. Clin. Oncol.* **2011**, *29*, 398 – 405.
[125] S. A. Hurvitz, L. Dirix, J. Kocsis, G. V. Bianchi, J. Lu, J. Vinholes, E. Guardino, C. Song, B. Tong, V. Ng, Y. W. Chu, E. A. Perez, *J. Clin. Oncol.* **2013**, *31*, 1157 – 1163.
[126] H. Kantarjian, D. Thomas, J. Jorgensen, E. Jabbour, P. Kebriaei, M. Rytting, S. York, F. Ravandi, M. Kwari, S. Faderl, M. B. Rios, J. Cortes, L. Fayad, R. Tarnai, S. A. Wang, R. Champlin, A. Advani, S. O'Brien, *Lancet Oncol.* **2012**, *13*, 403 – 411.
[127] W. Leimgruber, A. D. Batcho, F. Schenker, *J. Am. Chem. Soc.* **1965**, *87*, 5793 – 5795.
[128] W. Leimgruber, V. Stefanovic, F. Schenker, A. Karr, J. Berger, *J. Am. Chem. Soc.* **1965**, *87*, 5791 – 5793.
[129] D. Antonow, D. E. Thurston, *Chem. Rev.* **2011**, *111*, 2815 – 2864.
[130] D. S. Bose, A. S. Thompson, J. Ching, J. A. Hartley, M. D. Berardini, T. C. Jenkins, S. Neidle, L. H. Hurley, D. E. Thurston, *J. Am. Chem. Soc.* **1992**, *114*, 4939 – 4941.
[131] S. J. Gregson, P. W. Howard, J. A. Hartley, N. A. Brooks, L. J. Adams, T. C. Jenkins, L. R. Kelland, D. E. Thurston, *J. Med. Chem.* **2001**, *44*, 737 – 748.
[132] J. A. Hartley, V. J. Spanswick, N. Brooks, P. H. Clingen, P. J. McHugh, D. Hochhauser, R. B. Pedley, L. R. Kelland, M. C. Alley, R. Schultz, M. G. Hollingshead, K. M. Schweikart, J. E. Tomaszewski, E. A. Sausville, S. J. Gregson, P. W. Howard, D. E. Thurston, *Cancer Res.* **2004**, *64*, 6693 – 6699.
[133] M. C. Alley, M. G. Hollingshead, C. M. Pacula-Cox, W. R. Waud, J. A. Hartley, P. W. Howard, S. J. Gregson, D. E. Thurston, E. A. Sausville, *Cancer Res.* **2004**, *64*, 6700 – 6706.
[134] J. A. Hartley, A. Hamaguchi, M. Coffils, C. R. Martin, M. Suggitt, Z. Chen, S. J. Gregson, L. A. Masterson, A. C. Tiberghien, J. M. Hartley, C. Pepper, T. T. Lin, C. Fegan, D. E. Thurston, P. W. Howard, *Cancer Res.* **2010**, *70*, 6849 – 6858.
[135] M. Miller, N. Fishkin, W. Li, B. Leece, M. Mayo, G. Jones, E. Reid, K. Archer, E. Maloney, Y. Kovtun, J. Pinkas, R. Singh, R. Chari, *Mol. Cancer Ther.* **2009**, *8*, B126.
[136] S. C. Jeffrey, P. J. Burke, R. P. Lyon, D. W. Meyer, D. Sussman, M. Anderson, J. H. Hunter, C. I. Leiske, J. B. Miyamoto, N. D. Nicholas, N. M. Okeley, R. J. Sanderson, I. J. Stone, W. Zeng, S. J. Gregson, L. Masterson, A. C. Tiberghien, P. W. Howard, D. E. Thurston, C. L. Law, P. D. Senter, *Bioconjugate Chem.* **2013**, *24*, 1256 – 1263.
[137] M. S. Kung Sutherland, R. B. Walter, S. C. Jeffrey, P. J. Burke, C. Yu, H. Kostner, I. Stone, M. C. Ryan, D. Sussman, R. P. Lyon, W. Zeng, K. H. Harrington, K. Klussman, L. Westendorf, D. Meyer, I. D. Bernstein, P. D. Senter, D. R. Benjamin, J. G. Drachman, J. A. McEarchern, *Blood* **2013**, *122*, 1455 – 1463.
[138] J. Anderl, C. Muller, B. Heckl-Ostreicher, R. Wehr, *Cancer Res.* **2011**, *71*, 3616.
[139] A. C. Lazar, L. Wang, W. A. Blattler, G. Amphlett, J. M. Lambert, W. Zhang, *Rapid Commun. Mass Spectrom.* **2005**, *19*, 1806 – 1814.
[140] A. Wakankar, Y. Chen, Y. Gokarn, F. S. Jacobson, *MABS* **2011**, *3*, 161 – 172.
[141] J. R. Junutula, H. Raab, S. Clark, S. Bhakta, D. D. Leipold, S. Weir, Y. Chen, M. Simpson, S. P. Tsai, M. S. Dennis, Y. Lu, Y. G. Meng, C. Ng, J. Yang, C. C. Lee, E. Duenas, J. Gorrell, V. Katta, A. Kim, K. McDorman, K. Flagella, R. Venook, S. Ross, S. D. Spencer, W. L. Wong, H. B. Lowman, R. Vandlen, M. X.

 © 2014 Wiley-VCH Verlag GmbH & Co. KGaA, Weinheim

CSPC Exhibit 1004
Page 48 of 336

Sliwkowski, R. H. Scheller, P. Polakis, W. Mallet, *Nat. Biotechnol.* **2008**, *26*, 925 – 932.
[142] A. Yurkovetskiy, N. Bodyak, M. Yin, J. Thomas, P. Conlon, C. Stevenson, A. Uttard, L. Qin, A. Campbell, D. Gumerov, E. Ter-Ovanesyan, M. DeVit, T. Lowinger, in *AACR National Meeting (Washington, D. C.)* **2013**, Abstr. 4331.
[143] J. B. Stimmel, B. M. Merrill, L. F. Kuyper, C. P. Moxham, J. T. Hutchins, M. E. Fling, F. C. Kull, Jr., *J. Biol. Chem.* **2000**, *275*, 30445 – 30450.
[144] B. Q. Shen, K. Xu, L. Liu, H. Raab, S. Bhakta, M. Kenrick, K. L. Parsons-Reponte, J. Tien, S. F. Yu, E. Mai, D. Li, J. Tibbitts, J. Baudys, O. M. Saad, S. J. Scales, P. J. McDonald, P. E. Hass, C. Eigenbrot, T. Nguyen, W. A. Solis, R. N. Fuji, K. M. Flagella, D. Patel, S. D. Spencer, L. A. Khawli, A. Ebens, W. L. Wong, R. Vandlen, S. Kaur, M. X. Sliwkowski, R. H. Scheller, P. Polakis, J. R. Junutula, *Nat. Biotechnol.* **2012**, *30*, 184 – 189.
[145] J. Y. Axup, K. M. Bajjuri, M. Ritland, B. M. Hutchins, C. H. Kim, S. A. Kazane, R. Halder, J. S. Forsyth, A. F. Santidrian, K. Stafin, Y. Lu, H. Tran, A. J. Seller, S. L. Biroc, A. Szydlik, J. K. Pinkstaff, F. Tian, S. C. Sinha, B. Felding-Habermann, V. V. Smider, P. G. Schultz, *Proc. Natl. Acad. Sci. USA* **2012**, *109*, 16101 – 16106.
[146] P. Strop, S. H. Liu, M. Dorywalska, K. Delaria, R. G. Dushin, T. T. Tran, W. H. Ho, S. Farias, M. G. Casas, Y. Abdiche, D. Zhou, R. Chandrasekaran, C. Samain, C. Loo, A. Rossi, M. Rickert, S. Krimm, T. Wong, S. M. Chin, J. Yu, J. Dilley, J. Chaparro-Riggers, G. F. Filzen, C. J. O'Donnell, F. Wang, J. S. Myers, J. Pons, D. L. Shelton, A. Rajpal, *Chem. Biol.* **2013**, *20*, 161 – 167.
[147] S. Möhlmann, P. Bringmann, S. Greven, A. Harrenga, *BMC Biotechnol.* **2011**, *11*, 76.
[148] G. Casi, N. Huguenin-Dezot, K. Zuberbuhler, J. Scheuermann, D. Neri, *J. Am. Chem. Soc.* **2012**, *134*, 5887 – 5892.
[149] T. Yokota, D. E. Milenic, M. Whitlow, J. Schlom, *Cancer Res.* **1992**, *52*, 3402 – 3408.
[150] K. M. Kim, C. F. McDonagh, L. Westendorf, L. L. Brown, D. Sussman, T. Feist, R. Lyon, S. C. Alley, N. M. Okeley, X. Zhang, M. C. Thompson, I. Stone, H. P. Gerber, P. J. Carter, *Mol. Cancer Ther.* **2008**, *7*, 2486 – 2497.
[151] G. J. Bernardes, G. Casi, S. Trussel, I. Hartmann, K. Schwager, J. Scheuermann, D. Neri, *Angew. Chem.* **2012**, *124*, 965 – 968; *Angew. Chem. Int. Ed.* **2012**, *51*, 941 – 944.

 © 2014 Wiley-VCH Verlag GmbH & Co. KGaA, Weinheim

KRAS Mutation Status Is Predictive of Response to Cetuximab Therapy in Colorectal Cancer

Astrid Lièvre,[1,3] Jean-Baptiste Bachet,[3] Delphine Le Corre,[1] Valérie Boige,[4] Bruno Landi,[2] Jean-François Emile,[3] Jean-François Côté,[1,2] Gorana Tomasic,[4] Christophe Penna,[3] Michel Ducreux,[4] Philippe Rougier,[3] Frédérique Penault-Llorca,[5] and Pierre Laurent-Puig[1,2]

[1]Université Paris-Descartes, Institut National de la Sante et de la Recherche Medicale UMR-775; [2]Assistance Publique-Hôpitaux de Paris, Hôpital Européen Georges Pompidou, Paris, France; [3]Assistance Publique-Hôpitaux de Paris, Hôpital Ambroise Paré, Boulogne Billancourt, France, Université de Versailles Saint-Quentin-en-Yvelines, Versailles, France; [4]Institut Gustave Roussy, Villejuif, France; and [5]Centre Jean Perrin, Clermont-Ferrand, France, Université Auvergne, Clermont-Ferrand, France

Abstract

The anti-epidermal growth factor receptor (anti-EGFR) cetuximab has been proven to be efficient in metastatic colorectal cancer. The molecular mechanisms underlying the clinical response to this drug remain unknown. Genetic alterations of the intracellular effectors involved in EGFR-related signaling pathways may have an effect on response to this targeted therapy. In this study, tumors from 30 metastatic colorectal cancer patients treated by cetuximab were screened for *KRAS*, *BRAF*, and *PIK3CA* mutation by direct sequencing and for EGFR copy number by chromogenic *in situ* hybridization. Eleven of the 30 patients (37%) responded to cetuximab. A *KRAS* mutation was found in 13 tumors (43%) and was significantly associated with the absence of response to cetuximab (*KRAS* mutation in 0% of the 11 responder patients versus 68.4% of the 19 nonresponder patients; $P = 0.0003$). The overall survival of patients without *KRAS* mutation in their tumor was significantly higher compared with those patients with a mutated tumor ($P = 0.016$; median, 16.3 versus 6.9 months). An increased *EGFR* copy number was found in 3 patients (10%) and was significantly associated with an objective tumor response to cetuximab ($P = 0.04$). In conclusion, in this study, *KRAS* mutations are a predictor of resistance to cetuximab therapy and are associated with a worse prognosis. The *EGFR* amplification, which is not as frequent as initially reported, is also associated with response to this treatment. (Cancer Res 2006; 66(8): 3992-5)

Introduction

Colorectal cancer is one of the most common human malignancies with >300,000 cases both in the United States and in the European Union each year. In the past decade, survival of metastatic colorectal cancer patients has approximately doubled. This significant improvement is mainly due to the development of new combinations of standard chemotherapy, including 5-fluorouracil, irinotecan, and oxaliplatin, and also to the introduction of new targeted therapies, such as monoclonal antibodies against epidermal growth factor receptor (EGFR) or monoclonal antibodies against vascular endothelial growth factor. The addition of such targeted therapies to standard chemotherapy regimens results in an increase of toxicity and treatment costs (1) and therefore requires the identification of decision-making tools to select patients who are likely to benefit from them. The chimeric IgG1 monoclonal antibody cetuximab has been proven efficient in irinotecan-resistant metastatic colorectal cancer expressing the EGFR by immunohistochemistry, with response rates ranging between 8.8% when used in monotherapy and 22.9% when combined with irinotecan (2, 3). However, the molecular mechanisms underlying the clinical response or resistance to this drug remain unknown. Recently, a 25% objective response rate was obtained in a series of colorectal cancers that did not express EGFR by immunohistochemistry (4), highlighting the potential existence of other predictive markers of response to cetuximab.

Recent progresses have been made in the understanding of the EGFR pathway involved in colorectal carcinogenesis. The binding of a ligand on the extracellular part of EGFR results in the phosphorylation of the tyrosine kinase domain located in its intracellular part. Then, the activation of the receptor leads to the activation of intracellular effectors involved in intracellular signaling pathways, such as the G protein K-ras, the protein kinase RAF [Ras/mitogen-activated protein kinase (MAPK) pathway], and phosphoinositide 3-kinase (PI3K/Akt pathway). Cetuximab binds to EGFR with a high specificity and blocks ligand-induced phosphorylation of the receptor. Consequently, we hypothesized that mutation in the *KRAS*, *BRAF*, and *PI3KCA* coding genes could affect the clinical response to this monoclonal antibody. An analysis of the *EGFR* copy number was simultaneously done as a correlation between *EGFR* amplification and response to anti-EGFR therapy was recently reported (5).

Patients and Methods

Patients. We assessed 30 metastatic colorectal cancer patients (19 males and 11 females; mean age, 62.3 ± 10.9 years) treated by antibodies against EGFR cetuximab (Erbitux, Merck, Lyon, France) in three centers (Hôpital Ambroise Paré, Boulogne Billancourt; Hôpital Européen Georges Pompidou, Paris; Institut Gustave Roussy, Villejuif). All these patients had a metastatic colorectal adenocarcinoma histologically proved and underwent a surgical resection of their primary tumor. An analysis of EGFR expression was done by immunohistochemistry on each primary tumor that was considered EGFR positive if at least 1% malignant cells stained for EGFR (Zymed Laboratories, Inc., San Francisco, CA or DakoCytomation, Glostrup, Denmark). Patients' inclusion in this study was based on the availability of sufficient frozen tumor tissues and the existence of a signed informed consent.

One patient received cetuximab monotherapy, 25 received cetuximab combined with irinotecan alone, and four received cetuximab combined with irinotecan plus 5-fluorouracil and folinic acid (FOLFIRI regimen;

Note: A. Lièvre and J-B. Bachet equally contributed to the work.

Requests for reprints: Pierre Laurent-Puig, Institut National de la Sante et de la Recherche Medicale U775, Molecular Basis of Response to Xenobiotics, 45 rue des Saints-Pères, 75006 Paris, France. Phone: 33-1-4286-2081; Fax: 33-1-4286-2072; E-mail: pierre.laurent-puig@univ-paris5.fr.

©2006 American Association for Cancer Research.

doi:10.1158/0008-5472.CAN-06-0191

CSPC Exhibit 1004

Downloaded from cancerres.aacrjournals.org on March 19, 2019. © 2006 American Association for Cancer Research.

Table 1). Cetuximab was given as first-line treatment in three cases (EMR 62202-010 phase II trial), as second-line in three cases, and as third-line or more in 24 cases after disease progression under irinotecan-based chemotherapy.

Tumor response was evaluated by computerized tomodensitometry according to the Response Evaluation Criteria in Solid Tumors criteria and classified in complete response, partial response, stable disease, and progressive disease. For the analysis, complete and partial responder patients were grouped in responder; patients with a stable and a progressive disease were grouped in nonresponder patients.

DNA extraction and mutation analysis. DNA was extracted from frozen colorectal cancer samples using QIAmp DNA Mini kit (Qiagen,

Table 1. Clinical characteristics, tumor mutation analysis, and *EGFR* copy number analysis in metastatic colorectal cancer patients treated by cetuximab

Sex	Age (y)	Previous chemotherapy regimens for metastastic disease	Anti-EGFR treatment	Tumor response		*KRAS* mutation	*PIK3CA* mutation	*EGFR* copy number*
				Best response	Duration (wk)			
M	77	FOLFIRI	Cetuximab and irinotecan	CR	58.1	WT	WT	20
M	61	NA	Cetuximab and FOLFIRI	PR	34.1	WT	WT	11
M	76	NA	Cetuximab and FOLFIRI	PR	33.9	WT	WT	2.6
M	67	NA	Cetuximab and FOLFIRI	PR	20.9	WT	WT	3.7
M	71	LV5FU2, FOLFOX, capecitabine and mitomycin, capecitabine and irinotecan, irinotecan	Cetuximab and irinotecan	PR	46.0	WT	WT	3
F	44	LV5FU2 IV and oxaliplatin IAH, FOLFOX IV and Adriamycin IAH, FOLFIRI, irinotecan	Cetuximab and irinotecan	PR	62.9	WT	WT	3
M	72	LV5FU2, LV5FU2 IV and oxaliplatin IAH, FOLFIRI, capecitabine and irinotecan	Cetuximab and irinotecan	PR	44.0	WT	WT	2.1
M	48	LV5FU2, FOLFOX, raltitrexed and oxaliplatin, FOLFIRI, phase I trial, capecitabin and mitomycin	Cetuximab and irinotecan	PR	17.1	WT	WT	11
F	55	FOLFIRI, FOLFOX, irinotecan,	cetuximab	PR	23.7	WT	WT	3.4
F	64	FOLFOX, FOLFIRI	Cetuximab and irinotecan	PR	17.1	WT	WT	2.5
M	62	LV5FU2 IV and oxaliplatin IAH, FOLFOX, FOLFIRI	Cetuximab and irinotecan	PR	32.0	WT	WT	2.8
M	50	FOLFIRI, FOLFIRI IV and oxaliplatin IAH, irinotecan	Cetuximab and irinotecan	SD	14.7	WT	WT	2.9
M	54	FOLFOX, FOLFIRI	Cetuximab and FOLFIRI	SD	20.0	G12S	WT	2.6
F	73	LV5FU2, FOLFIRI, FOLFOX	Cetuximab and irinotecan	SD	19.3	G12D	E542K	2.75
M	71	raltitrexed and oxaliplatin, raltitrexed and irinotecan	Cetuximab and irinotecan	SD	16.0	G13D	WT	2.8
F	53	FOLFOX, FOLFIRI, irinotecan	Cetuximab and irinotecan	SD	20.0	G12A	WT	2.25
F	73	FOLFOX	Cetuximab and irinotecan	SD	20.0	WT	WT	2.25
M	78	FOLFOX, FOLFIRI	Cetuximab and irinotecan	PD		WT	WT	2.4
F	51	FOLFIRI, FOLFOX	Cetuximab and irinotecan	PD		G12D	WT	3.2
F	75	FOLFIRI, oxaliplatin and capecitabine	Cetuximab and irinotecan	PD		G12V	E542K	2.3
M	69	LV5FU2 and oxaliplatin and irinotecan, FOLFIRI	Cetuximab and irinotecan	PD		G13D	WT	3.3
M	72	LV5FU2, FOLFOX, FOLFIRI IV and oxaliplatin IAH	Cetuximab and irinotecan	PD		WT	WT	3.8
F	61	LV5FU2 and oxaliplatin and irinotecan, irinotecan	Cetuximab and irinotecan	PD		WT	WT	2.3
M	53	FOLFOX, FOLFIRI, raltitrexed and oxaliplatin, capecitabine, irinotecan	Cetuximab and irinotecan	PD		G12D	WT	2.3
M	59	FOLFIRI, FOLFOX	Cetuximab and irinotecan	PD		G12D	WT	2.9
M	75	FOLFOX, FOLFIRI	Cetuximab and irinotecan	PD		G12D	WT	2.7
F	58	FOLFOX, FOLFIRI, LV5FU2 and mitomycin, FOLFOX, phase I trial	Cetuximab and irinotecan	PD		G12C	WT	3.7
M	47	LV5FU2, FOLFOX, FOLFIRI	Cetuximab and irinotecan	PD		WT	WT	3.3
M	41	capecitabine and oxaliplatin	Cetuximab and irinotecan	PD		G12C	WT	3.6
F	60	FOLFIRI, FOLFOX, irinotecan	Cetuximab and irinotecan	PD		G13D	WT	2.7

Abbreviations: M, male; F, female; IAH, intra-artery hepatic infusion; IV, i.v. infusion; CR, complete response; PR, partial response; SD, stable disease; PD, progressive disease; NA, not applicable; FOLFOX, oxaliplatin, fluorouracil, and folinic acid; FOLFIRI, irinotecan, fluorouracil, and folinic acid; WT, wild type.

*Gene copy number per nucleus.

CSPC Exhibit 1004
Page 5 of 16

Downloaded from cancerres.aacrjournals.org on March 19, 2019. © 2006 American Association for Cancer Research.

Courtaboeuf, France) after a histologic control of the presence of tumor cells (>70%) in each tumor fragment by HES coloration.

Exon 1 of the *KRAS* gene, exons 11 and 15 of the *BRAF* gene, and exons 1, 2, 9, and 20 of the *PIK3CA* gene were selected for mutation analysis because they were frequently found mutated in colorectal cancer (6). These exons were sequenced after PCR amplification. Primers used for the amplification and sequencing of exon-specific region of each gene and the PCR conditions are available upon request. Direct sequencing was done using a Big Dye Terminator cycle sequencing kit (Applied Biosystems, Foster City, CA) and analyzed on an ABI Prism 3900 DNA Analyzer automated sequencer (Applied Biosystems). All somatic mutations found were further validated by a new independent amplification and sequencing.

Analysis of EGFR amplification by chromogenic *in situ* hybridization. Chromogenic *in situ* hybridization (CISH) EGFR experiments were done according to the protocol given by the manufacturer (Invitrogen-Zymed, Carlsbad, CA) on formalin-fixed, paraffin-embedded tumor specimens. Codenaturation of EGFR SPOT-Light probe and DNA target and hybridization were made on a HYBrite instrument (Vysis-Abbott Diagnostic, Baar, Switzerland). CISH results were evaluated with a light microscope using a ×40 dry objective or a ×60 oil objective.

Statistical analysis. Fischer's exact test was used to calculate p value for association between *KRAS*, *BRAF*, and *PIK3CA* mutation and response to cetuximab. A logistic regression was done to estimate the hazard ratio of response according to the *KRAS* mutation status. The survival rates were calculated with the Kaplan-Meier method. Survival curves were compared using the log-rank test. Analysis was carried out using the STATA software package (College Station, TX). The level of significance was set at $P = 0.05$. *P*s were not corrected for multiple comparisons.

Results and Discussion

Eleven of the 30 patients (37%) responded to cetuximab (Table 1). The median duration of response to cetuximab was 33.9 months (range, 17.1-62.9 months). In the six patients with stable disease under cetuximab treatment, the median duration of stabilization was 18.3 months (range, 14.7-20.0 months).

A *KRAS* mutation was found in the tumor of 13 patients (43%; Fig. 1*A* and *B*). No tumor had a *BRAF* mutation, which is consistent with the absence of microsatellite instability determined by the genotyping of five microsatellites in all the tumors included in our series. A *PIK3CA* mutation, located in the exon 9, was found in two tumors (7%), which also had a *KRAS* mutation.

No *KRAS* mutation was found in the tumor from 11 patients with a clinical response to cetuximab [0%; 95% confidence interval (95% CI), 0-28.5%], whereas 13 tumors from the 19 nonresponder patients (68.4%; 95% CI, 43.5-87.5%) were found mutated in this gene ($P = 0.0003$). Therefore, the presence of *KRAS* mutation was significantly associated with the absence of response to cetuximab. This difference remained significant even if the three responder patients treated with the association of cetuximab and FOLFIRI regimen as first-line treatment were removed from the analysis (*KRAS* mutation: 0 of 8 responders versus 13 of 19 nonresponders; $P = 0.002$). In this group of 27 patients, the overall survival of patients without *KRAS* mutation in their tumor was significantly higher compared with those patients with a mutated tumor ($P = 0.016$; median, 16.3 versus 6.9 months; Fig. 2). No significant correlation was found between *PIK3CA* mutation and response to cetuximab. In our series, an increased *EGFR* copy number was found by CISH in 3 of 30 (10%) patient tumors (Table 1; Fig. 1*C*). Amplification was defined as six or more signals per nucleus in >50% of cancer cells, or when a large gene copy cluster was seen. At least 30 nuclei were counted per slide. Slides were scored in a blinded manner by two pathologists. All the patients with *EGFR* amplification were responders, leading to a significant association between *EGFR* amplification and response to cetuximab (*EGFR* amplification in responder versus nonresponder patients: 27% versus 0%; $P = 0.04$).

One study had previously assessed the mutation status of the *EGFR* catalytic domain and its downstream intracellular effectors *PIK3CA*, *KRAS*, and *BRAF* and found no significant correlation with response to cetuximab (5). However, a potential trend toward higher response rates was seen in cetuximab-treated colorectal cancer patients whose tumors were of *KRAS* wild-type status. When our results were pooled with those of Moroni et al., the predictive value of *KRAS* mutation remained significant with a *KRAS* mutation frequency of 52.5% in nonresponders compared with 9.5% in responders ($P = 0.001$). When considering these pooled data, the probability to have no response to cetuximab was 91.3% in the presence of *KRAS* mutation. Moreover, the probability to be responder was 50% when no *KRAS* mutation was identified. The relative risk to obtain a response to cetuximab was 10-fold higher for nonmutated patients compared with that of patients with *KRAS* mutation (hazard ratio, 10.5; 95% CI, 2.1-51.1). Thus, these data suggest that the wild-type *KRAS* status might identify patients with metastatic colorectal cancer who are likely to respond to cetuximab and to have a longer overall survival.

Moroni et al. showed that the gene copy number for *EGFR* determined by fluorescence *in situ* hybridization (FISH) on tumor samples was significantly associated with clinical response to this targeted therapy (5). However, the prevalence of *EGFR* amplification in their series (31%) was much higher than the prevalence we

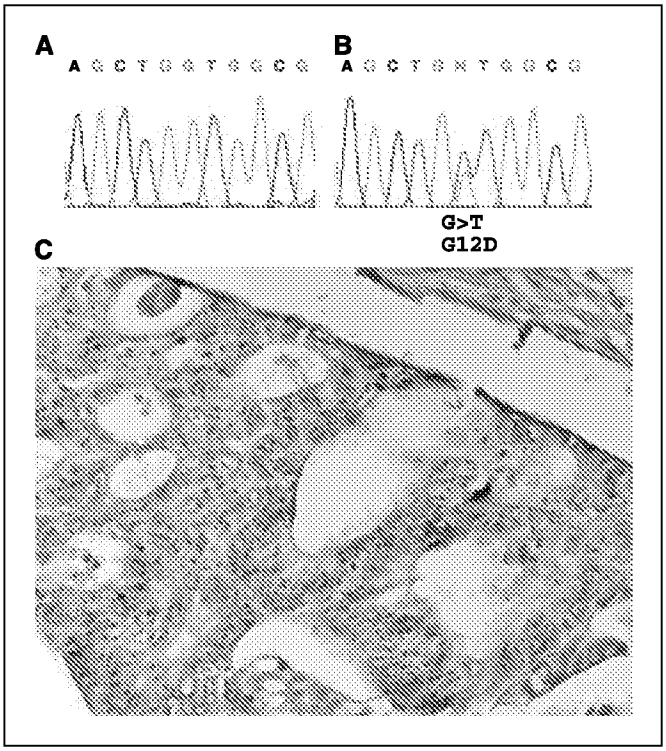


Figure 1. Example of different genetic alterations studied. *A* and *B*, electrophoregram from normal (*A*) and tumor tissue (*B*). A G12D *KRAS* mutation is observed in tumor tissue compared with normal tissue. *C*, an example of high *EGFR* amplification by chromogenic in situ hybridization. Original magnification, ×100. One brown spot corresponds to one *EGFR* gene copy.

CSPC Exhibit 1004
Page 52 of 336

Downloaded from cancerres.aacrjournals.org on March 19, 2019. © 2006 American Association for Cancer Research.

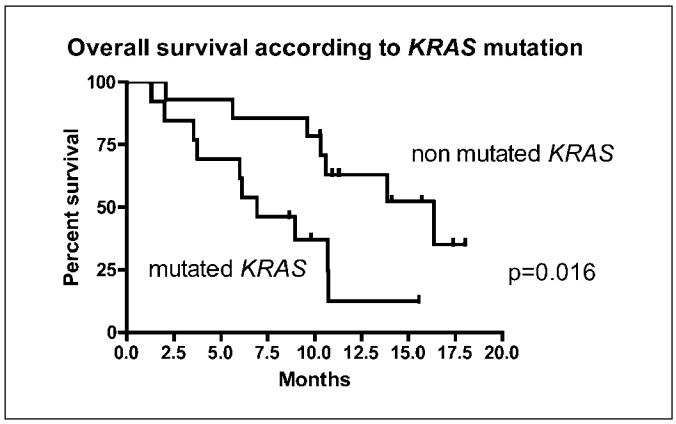


Figure 2. Overall survival curves of patients with a *KRAS*-mutated and nonmutated tumor.

observed. Our results are in accordance with a recent report by Shia et al. (7), showing a copy gain in only 11.5% of 147 colorectal cancers tested by CISH. Furthermore, Sauer et al. (8) reported a prevalence of 15% in a series of 48 rectal cancers tested by FISH. These discrepancies question the prevalence of increased *EGFR* copy number in colorectal cancer and its relevance for the prediction of response to cetuximab. However, it is interesting to note that the unique complete responder patient in our series is the one who have the higher level of *EGFR* amplification. This is in good agreement with the *in vitro* proliferation inhibition observed with a low dose of cetuximab in the DiFi tumor cell line that has the highest copy number of *EGFR* of the different tested cell lines (5).

Our results suggest that cetuximab should not be proposed to ~40% of all metastatic colorectal cancer patients having *KRAS*-mutated tumor cells. Previous studies have shown a lack of correlation between EGFR expression on immunohistochemical analysis and response to cetuximab with a 22.9% maximal response rate in EGFR-expressing colorectal cancer (2). The presence of a *KRAS* mutation in EGFR-positive colorectal cancers might partially explain why one part of these tumors does not respond to cetuximab. K-ras is a G protein that plays a key role in the Ras/MAPK signaling pathway located downstream of many growth factor receptors, including EGFR, and involved in colorectal carcinogenesis. The recruitment of K-ras by the activated EGFR is responsible for the activation of a cascade of serine-threonine kinases from the cell surface to the nucleus. The Ras/MAPK pathway is one of the most important pathways for cell proliferation by inducing the synthesis of cyclin D1 and mutation of the *KRAS* proto-oncogene, which are found in 36% of colorectal cancers (9), leading to the activation of this pathway. Consequently, we can hypothesize that whatever the expression level of EGFR is, the presence of a *KRAS* mutation is associated with a downstream activation of the Ras/MAPK pathway, leading to cell proliferation that cannot be significantly inhibited by cetuximab that acts upstream of the K-ras protein. In accordance with our results, *KRAS* mutations were found to be associated with resistance to EGFR kinase inhibitors gefitinib and erlotinib in lung adenocarcinomas (10). A similar trend was recently observed in a series of 30 colorectal cancers treated with gefitinib, among which the response rate for tumors with and without *KRAS* mutation was 33% and 47%, respectively (11).

In conclusion, we have shown that *KRAS* mutation is associated with resistance to cetuximab and a shorter survival in EGFR-positive metastatic colorectal cancer patients treated with this therapy. Thus, *KRAS* mutation status might allow the identification of patients who are likely to benefit from cetuximab and avoid a costly and potentially toxic administration of this treatment in nonresponder patients. Prospective randomized study is needed to validate this result that bring a new possibility of targeted therapy adapted to each patient according to its *KRAS* mutation status.

Acknowledgments

Received 1/17/2006; revised 1/18/2006; accepted 2/16/2006.

Grant support: Ligue Nationale de Lutte contre le Cancer and the ADEBIOPHARM ER 48 association.

The costs of publication of this article were defrayed in part by the payment of page charges. This article must therefore be hereby marked *advertisement* in accordance with 18 U.S.C. Section 1734 solely to indicate this fact.

We thank Anne Cayre for the CISH test assistance and Françoise Gary for technical assistance.

References

1. Schrag D. The price tag on progress: chemotherapy for colorectal cancer. N Engl J Med 2004;351:317–9.
2. Cunningham D, Humblet Y, Siena S, et al. Cetuximab monotherapy and cetuximab plus irinotecan in irinotecan-refractory metastatic colorectal cancer. N Engl J Med 2004;351:337–45.
3. Saltz LB, Meropol NJ, Loehrer PJ, Sr., Needle MN, Kopit J, Mayer RJ. Phase II trial of cetuximab in patients with refractory colorectal cancer that expresses the epidermal growth factor receptor. J Clin Oncol 2004;22:1201–8.
4. Chung KY, Shia J, Kemeny NE, et al. Cetuximab shows activity in colorectal cancer patients with tumors that do not express the epidermal growth factor receptor by immunohistochemistry. J Clin Oncol 2005;23:1803–10.
5. Moroni M, Veronese S, Benvenuti S, et al. Gene copy number for epidermal growth factor receptor (EGFR) and clinical response to antiEGFR treatment in colorectal cancer: a cohort study. Lancet Oncol 2005;6:279–86.
6. Samuels Y, Wang Z, Bardelli A, et al. High frequency of mutations of the PIK3CA gene in human cancers. Science 2004;304:554.
7. Shia J, Klimstra DS, Li AR, et al. Epidermal growth factor receptor expression and gene amplification in colorectal carcinoma: an immunohistochemical and chromogenic *in situ* hybridization study. Mod Pathol 2005;18:1350–6.
8. Sauer T, Guren MG, Noren T, Dueland S. Demonstration of EGFR gene copy loss in colorectal carcinomas by fluorescence *in situ* hybridization (FISH): a surrogate marker for sensitivity to specific anti-EGFR therapy? Histopathology 2005;47:560–4.
9. Andreyev HJ, Norman AR, Cunningham D, Oates JR, Clarke PA. Kirsten ras mutations in patients with colorectal cancer: the multicenter "RASCAL" study. J Natl Cancer Inst 1998;90:675–84.
10. Pao W, Wang TY, Riely GJ, et al. KRAS mutations and primary resistance of lung adenocarcinomas to gefitinib or erlotinib. PLoS Med 2005;2:e17.
11. Ogino S, Meyerhardt JA, Cantor M, et al. Molecular alterations in tumors and response to combination chemotherapy with gefitinib for advanced colorectal cancer. Clin Cancer Res 2005;11:6650–6.

CSPC Exhibit 1004

Downloaded from cancerres.aacrjournals.org on March 19, 2019. © 2006 American Association for Cancer Research.

AACR American Association for Cancer Research

Cancer Research

The Journal of Cancer Research (1916–1930) | The American Journal of Cancer (1931–1940)

KRAS Mutation Status Is Predictive of Response to Cetuximab Therapy in Colorectal Cancer

Astrid Lièvre, Jean-Baptiste Bachet, Delphine Le Corre, et al.

Cancer Res 2006;66:3992-3995.

Updated version	Access the most recent version of this article at: http://cancerres.aacrjournals.org/content/66/8/3992

Cited articles	This article cites 11 articles, 4 of which you can access for free at: http://cancerres.aacrjournals.org/content/66/8/3992.full#ref-list-1
Citing articles	This article has been cited by 100 HighWire-hosted articles. Access the articles at: http://cancerres.aacrjournals.org/content/66/8/3992.full#related-urls

E-mail alerts	Sign up to receive free email-alerts related to this article or journal.
Reprints and Subscriptions	To order reprints of this article or to subscribe to the journal, contact the AACR Publications Department at pubs@aacr.org.
Permissions	To request permission to re-use all or part of this article, use this link http://cancerres.aacrjournals.org/content/66/8/3992. Click on "Request Permissions" which will take you to the Copyright Clearance Center's (CCC) Rightslink site.

Downloaded from cancerres.aacrjournals.org on March 19, 2019. © 2006 American Association for Cancer Research.

(12) INTERNATIONAL APPLICATION PUBLISHED UNDER THE PATENT COOPERATION TREATY (PCT)

(19) World Intellectual Property Organization
International Bureau

(43) International Publication Date
8 January 2015 (08.01.2015)

WIPO | PCT

(10) International Publication Number
WO 2015/000062 A1

(51) International Patent Classification:
C07K 16/28 (2006.01) *A61P 35/00* (2006.01)
A61K 47/48 (2006.01)

(21) International Application Number:
PCT/CA2014/000543

(22) International Filing Date:
4 July 2014 (04.07.2014)

(25) Filing Language: English

(26) Publication Language: English

(30) Priority Data:
61/843,113 5 July 2013 (05.07.2013) US
61/944,157 25 February 2014 (25.02.2014) US

(71) Applicant: **AVIDBIOLOGICS INC.** [CA/CA]; 101 College Street, Suite 218, Toronto, Ontario, M5G 1L7 (CA).

(72) Inventor: **TIKHOMIROV, Ilia Alexandre**; 954 The Queensway, Toronto, Ontario, M8Z 1P5 (CA).

(74) Agent: **PIASETZKI NENNIGER KVAS LLP**; 120 Adelaide Street West, Suite 2308, Toronto, Ontario, M5H 1T1 (CA).

(81) Designated States *(unless otherwise indicated, for every kind of national protection available)*: AE, AG, AL, AM, AO, AT, AU, AZ, BA, BB, BG, BH, BN, BR, BW, BY, BZ, CA, CH, CL, CN, CO, CR, CU, CZ, DE, DK, DM, DO, DZ, EC, EE, EG, ES, FI, GB, GD, GE, GH, GM, GT, HN, HR, HU, ID, IL, IN, IR, IS, JP, KE, KG, KN, KP, KR, KZ, LA, LC, LK, LR, LS, LT, LU, LY, MA, MD, ME, MG, MK, MN, MW, MX, MY, MZ, NA, NG, NI, NO, NZ, OM, PA, PE, PG, PH, PL, PT, QA, RO, RS, RU, RW, SA, SC, SD, SE, SG, SK, SL, SM, ST, SV, SY, TH, TJ, TM, TN, TR, TT, TZ, UA, UG, US, UZ, VC, VN, ZA, ZM, ZW.

(84) Designated States *(unless otherwise indicated, for every kind of regional protection available)*: ARIPO (BW, GH, GM, KE, LR, LS, MW, MZ, NA, RW, SD, SL, SZ, TZ, UG, ZM, ZW), Eurasian (AM, AZ, BY, KG, KZ, RU, TJ, TM), European (AL, AT, BE, BG, CH, CY, CZ, DE, DK, EE, ES, FI, FR, GB, GR, HR, HU, IE, IS, IT, LT, LU, LV, MC, MK, MT, NL, NO, PL, PT, RO, RS, SE, SI, SK, SM, TR), OAPI (BF, BJ, CF, CG, CI, CM, GA, GN, GQ, GW, KM, ML, MR, NE, SN, TD, TG).

Declarations under Rule 4.17:

— *as to applicant's entitlement to apply for and be granted a patent (Rule 4.17(ii))*

— *of inventorship (Rule 4.17(iv))*

Published:

— *with international search report (Art. 21(3))*

(54) Title: EGFR ANTIBODY CONJUGATES

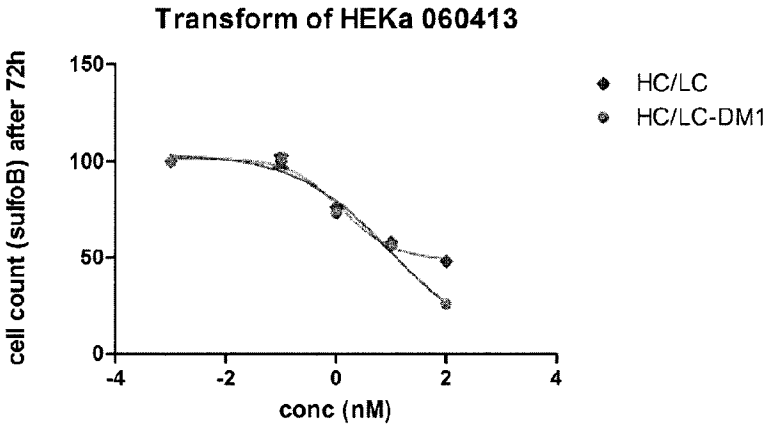


Figure 6

(57) Abstract: A maytansinoid is covalently linked through a non-cleavable linker to an EGFR antibody that is a full EGFR antagonist, such as cetuximab or panitumumab. The result is an anti-cancer agent having cytotoxicity that is potentiated in cancer cells but not normal cells. This benefit is not seen with EGFR antibodies that are partial antagonists, or with toxins that are not processed by lysosomes.

WO 2015/000062 A1

TITLE OF THE INVENTION

EGFR Antibody Conjugates

FIELD OF THE INVENTION

The present invention relates to an immunoconjugate that targets EGFR-expressing cancer cell populations and comprises an anti-EGFR antibody, such as panitumumab or cetuximab, conjugated to a microtubule damaging agent such as a maytansinoid.

BACKGROUND TO THE INVENTION

The conjugation of cell-binding proteins, such as antibodies, to potent cell-killing agents to enhance their anti-cancer activity, and provide the so-called "magic bullets" has had mixed clinical results.

Relative to naked antibodies, immunoconjugates often show enhanced cell-killing potency, and this increases their activity against cancer cells expressing the antibody-targeted antigen. The same increase in potency is also seen, however, in normal cells that express that same antigen. Of particular concern is the increased cytotoxicity against the rapidly proliferating tissues, such as skin. For example, a CD44v6-targeting immunoconjugate consisting of a maytansinoid and CD44v6 antibody was very active against cancer cells but was discontinued because of severe skin toxicities, such as toxic epidermal necrolysis, which occurred as a result of enhanced activity of the immunoconjugate against skin cells also expressing CD44v6 (Tijink *et al.*, Clin Cancer Res, 2006, 12:6064).

Another cell surface protein, epidermal growth factor receptor, or EGFR, is an attractive target for the development of anti-cancer immunoconjugates because of the antigen's expression by many tumors and its rapid internalization. However, because EGFR is also expressed by skin tissues, EGFR-targeting agents, such as the antibodies cetuximab and panitumumab, also show levels of skin toxicities that either demand dose reduction or in some cases are so severe as to warrant discontinuation of treatment.

With immunoconjugates, the toxicity of these antibodies is amplified through conjugation to a potent cell toxin. This exacerbates the problem for antibodies that are already inherently toxic to normal cells. For instance, conjugation with a toxic maytansinoid caused severe toxicity against skin cells when delivered via a CD44v6 antibody. As a result, development of anti-EGFR immunoconjugates based on approved anti-EGFR antibodies has not been pursued because of concerns over enhanced skin toxicity of such immunoconjugates. Alternative strategies are being pursued for the development of anti-EGFR immunoconjugates.

Anti-EGFR immunoconjugates are now being designed specifically to address these safety concerns. These conjugates are based on antibodies that target a mutated but naturally occurring version of EGFR, known as EGFRvIII, or on conformational forms of the EGFR, both of which predominate on tumour cells and not on skin cells (US 7628986, and US 7589180, respectively). For example, anti-EGFR antibody MAb806 is an antibody that targets an EGFR epitope found only on cancer cells, and potentially offers an advantage over the current EGFR antibodies, which all display significant binding to normal organs such as skin in humans. With this specificity, it is recognized that "the most important advantage of MAb 806 compared to current EGFR antibodies, is that MAb 806 can be directly conjugated to cytotoxic agents", an approach not feasible with other EGFR antibodies since the "cytotoxic conjugation would almost certainly induce severe toxicity" (US 7589180). An immunoconjugate comprising EGFR MAb 806 linked to an anti-microtubule payload is currently in phase I clinical testing in patients with advanced solid tumours.

Efforts continue through screening for naked anti-EGFR antibodies, and immunoconjugates thereof, to identify those with partial antagonistic activity against EGFR and reduced activity against keratinocytes (see US 2012/0156217), immunoconjugates based on "masked" anti-EGFR antibodies that are preferentially activated in the tumour microenvironment (WO 2009/025846), and immunoconjugates based on antibodies with medium affinity that preferentially accumulate in the tumor and

not normal tissues (WO 2012/100346). All of these strategies are aimed at reducing toxicities toward skin and other organs expressing EGFR, because currently approved anti-EGFR antibodies were deemed unsuitable for development as immunoconjugates.

An object of the present invention is to provide an immunoconjugate useful to treat EGFR+ disease cells including EGFR+ cancer cells and tumours comprising them. Another object of the present invention is to provide a method for potentiating the cytotoxicity of an EGFR antibody toward disease cells selectively. By this method, potentiation of toxicity toward normal cells is essentially avoided.

SUMMARY OF THE INVENTION

The present invention draws from the unexpected initial finding that conjugation of the anti-EGFR antibody cetuximab to a toxic maytansinoid through a non-cleavable linker yields an immunoconjugate that displays enhanced cytotoxicity against cancer cells without a corresponding increase in cytotoxicity against skin cells. The inventor demonstrates that the activity of some anti-EGFR antibodies against both cancer and keratinocytes is strongly potentiated by linking to maytansinoids and other cell-killing agents, whereas the activity of maytansinoid-conjugated cetuximab is potentiated only against cancer cells and not against keratinocytes. In these studies, conjugates of cetuximab with cell-killing agents other than anti-microtubule toxins, such as saporin, were found, as expected, to have an attendant and significantly enhanced toxicity toward keratinocytes.

It is further demonstrated that another antibody having full antagonist activity at EGFR, i.e. panitumumab, also demonstrates selective potentiation at EGFR+ cells when conjugated to an anti-microtubule payload such as a maytansinoid, in showing toxicity to EGFR+ cancer cells while sparing EGFR+ normal cells such as keratinocytes.

On the basis of these and other findings herein disclosed, the present invention enables the selection of components essential to yield an immunoconjugate that comprises an EGFR antibody and a toxic payload that potentiates antibody activity toward cancer cells

but not toward normal cells such as keratinocytes. Immunoconjugates having this property require the selection of an EGFR antibody that is a full antagonist, a toxin that is an anti-microtubule agent, and a linker that most desirably is not cleavable. By applying these criteria, there is provided an EGFR antibody-based immunoconjugate that has significant therapeutic activity against EGFR+ cancer cells without a corresponding increase in toxicity against EGFR+ normal cells including skin cells such as keratinocytes. Lack of additional potentiation of the toxicity against skin cells is critical because naked EGFR-targeting antibodies are already characterized by high prevalence dermatologic toxicities and it is beneficial not to potentiate these side effects.

Accordingly, in a general aspect, there is provided an immunoconjugate comprising an antibody having full antagonist activity at EGFR, and a toxin conjugated therewith through a non-cleavable linker, the immunoconjugate having a cytotoxic effect relative to a naked form of the antibody that is essentially not potentiated with respect to EGFR+ keratinocytes. The cytotoxic effect of the immunoconjugate with respect to EGFR+ cancer cells desirably is potentiated. The toxic payload desirably is an anti-microtubule toxin.

Also in a general aspect, there is provided a method useful to potentiate the anti-cancer activity of an EGFR antibody without potentiating the effect thereof on normal EGFR+ cells, the method comprising:

(i) selecting, for conjugation, an EGFR antibody that is a full EGFR antagonist and competes with cetuximab for binding to EGFR;

(ii) selecting, for delivery by the EGFR antibody, an anti-microtubule toxin;

(iii) selecting, for coupling the selected EGFR antibody and the anti-microtubule toxin, a linker; and

producing an immunoconjugate that incorporates the linker between the antibody and the toxin, thereby providing an immunoconjugate having a cytotoxicity that is potentiated against EGFR+ disease cells and essentially not potentiated against normal EGFR+ keratinocyte cells.

In one particular aspect, there is provided an immunoconjugate comprising cetuximab and a toxin conjugated therewith, the immunoconjugate having a cytotoxic effect relative to naked cetuximab that is (1) enhanced with respect to EGFR+ cancer cells, and (2) substantially not enhanced with respect to EGFR+ keratinocytes, wherein the immunoconjugate comprises cetuximab and an anti-microtubule toxin such as maytansinoid DM-1 conjugated by a non-cleavable linker. In alternative embodiments, the cetuximab is an equivalent of cetuximab, such as an EGFR-binding fragment of cetuximab, or an EGFR-binding variant of cetuximab that incorporates one or two or more benign substitutions in the antibody constant region or framework region without affecting the antibody binding to the receptor or antibody conjugate-mediated cell killing. For example, chimeric cetuximab can be further humanized using standard methods to create a more human-like version of the antibody. Alternatively, a fully human anti-EGFR antibody, such as necitumumab also known as IMC-11F8, which is considered to be functionally equivalent to cetuximab can be developed by screening of a human Fab library for an antibody that can bind and strongly inhibit EGFR and competes with cetuximab for receptor binding (Li S., Kussie P., Fergusson KM, Structural basis for EGF receptor inhibition by the therapeutic antibody IMC-11F8. Structure. 2008 Feb;16(2):216-27).

In another particular aspect, there is provided an immunoconjugate comprising panitumumab and a toxin conjugated therewith, the immunoconjugate having a cytotoxic effect relative to naked panitumumab that is (1) enhanced with respect to EGFR+ cancer cells, and (2) substantially unaltered with respect to EGFR+ keratinocytes, wherein the immunoconjugate comprises panitumumab and an anti-microtubule toxin such as maytansinoid DM-1 conjugated by a non-cleavable linker. In alternative embodiments, the panitumumab is an EGFR-binding fragment of panitumumab, or is a variant of panitumumab that incorporates one, two, or more benign substitutions yet maintains EGFR binding and inhibitory characteristics of the panitumumab parent.

In preferred embodiments, conjugation of the antibody and toxin is achieved using a non-cleavable linker. With non-cleavable linkers, release of the cytotoxic payload occurs by

intracellular destruction of the drug conjugate by lysosomes. A non-cleavable linker is substantially resistant to acid-induced cleavage, light-induced cleavage, peptidase-induced cleavage, esterase-induced cleavage, or disulfide bond cleavage, whereas cleavable linkers, which can be used optionally but less desirably, are linkers that can be cleaved by one or more of these recited cleaving agents. Examples of such non-cleavable linkers include those that are or can be derived from a haloacetyl-based moiety selected from the group consisting of N-succinimidyl-4-(iodoacetyl)-aminobenzoate (SIAB), N-succinimidyl iodoacetate (SIA), N-succinimidyl bromoacetate (SBA), and N-succinimidyl 3-(bromoacetamido)propionate (SBAP). Alternatively, the non-cleavable linker is or is derived from a maleimido-based moiety selected from the group consisting of N-succinimidyl 4-(maleimidomethyl)cyclohexanecarboxylate (SMCC), N-succinimidyl-4-(N-maleimidomethyl)-cyclohexane-1-carboxy-(6-amidocaproate) (LC-SMCC), κ-maleimidoundecanoic acid N-succinimidyl ester (KMUA), γ-maleimidobutyric acid N-succinimidyl ester (GMBS), ε-maleimidcaproic acid N-hydroxysuccinimide ester (EMCS), m-maleimidobenzoyl-N-hydroxysuccinimide ester (MBS), N-(α-maleimidoacetoxy)-succinimide ester (AMAS), succinimidyl-6-(β-maleimidopropionamido)hexanoate (SMPH), N-succinimidyl 4-(p-maleimidophenyl)-butyrate (SMPB), and N-(p-maleimidophenyl)isocyanate (PMPI); another non-cleavable linker is maleimidocaproyl. (See US 2005/0169933; , Yoshitake et al, 101 Eur. J. Biochem. 395-399 (1979); Hashida et al, J. Applied Biochem. 56-63 (1984); and Liu et al, 18 690-697 (1979), and Doronina et al,. Bioconjugate Chem., 2006 Jan-Feb;17(1):114-24 for additional details.)

In a preferred embodiment, conjugation is achieved using a non-cleavable cross-linking reagent as linker such as succinimidyl 4-(N-maleimidomethyl)-cyclohexane-1-carboxylate (SMCC). Other useful forms of non-cleavable linkers include N-Succinimidyl iodoacetate (SIA), sulfo-SMCC, m-maleimidobenzoyl-N-hydroxysuccinimide ester (MBS), sulfo-MBS and succinimidyl-iodoacetate, as described in the literature, which introduce 1-10 reactive groups. (see, Yoshitake et al, 101 Eur. J. Biochem. 395-399 (1979); Hashida et al, J. Applied Biochem. 56-63 (1984); and Liu et al, 18 690-697 (1979)). Particularly useful for linking auristatins as anti-microtubule

toxin are the non-cleavable maleimidocaproyl linkers described by Doronina et al, in Bioconjugate Chem., 2006 Jan-Feb;17(1):114-24).

In another aspect, there is provided a pharmaceutical composition comprising the present EGFR antibody-based immunoconjugate in an amount cytotoxic to EGFR+ cancer cells, and a pharmaceutically acceptable carrier.

In a further aspect, there is provided the use of the present pharmaceutical composition for the treatment of EGFR+ cancer cells. In a related aspect, there is provided a method for treating a subject presenting with an EGFR+ cancer cell, comprising administering the present immunoconjugate to the subject in an amount cytotoxic to the EGFR+ cancer cell.

These and other aspects of the present invention are now described in greater detail with reference to the accompanying drawings in which:

BRIEF DESCRIPTION OF THE DRAWINGS

Figure 1 is a graph showing cytotoxic activity against keratinocytes of naked anti-EGFR antibodies and maytansinoid conjugates thereof. About 2-3,000 cells/well were seeded in a flat bottom 96-well tissue culture plate, and incubated with various concentrations of test article in culture media for 5 days at 37°C. Viability of the remaining cells was determined by WST-8 based colorimetric assay.

Figure 2 is a graph showing cytotoxic activity against cancer cell line of naked anti-EGFR antibodies and maytansinoid conjugates thereof. About 2-3,000 cells/well were seeded in a flat bottom 96-well tissue culture plate, and incubated with various concentrations of test article in culture media for 5 days at 37°C. Viability of the remaining cells was determined by WST-8 based colorimetric assay.

Figures 1 and 2 herein are reproductions of figures presented in US 2012/0156217.

Figure 3 is a graph showing cytotoxic activity against H226 cancer cell line of naked anti-EGFR antibody cetuximab and maytansinoid conjugates thereof. About 2-3,000 cells/well were seeded in a flat bottom 96-well tissue culture plate, and incubated with various concentrations of test article in culture media for 72 h at 37°C. Viability of the remaining cells was determined via alamar blue cell viability assay.

Figure 4 is a graph showing cytotoxic activity against A431 cancer cell line of naked anti-EGFR antibody cetuximab and maytansinoid conjugates thereof. About 2-3,000 cells/well were seeded in a flat bottom 96-well tissue culture plate, and incubated with various concentrations of test article in culture media for 72 h at 37°C. Viability of the remaining cells was determined via alamar blue cell viability assay.

Figure 5 is a graph showing the cytotoxic activity of naked anti-EGFR antibody cetuximab and maytansinoid conjugates thereof against normal keratinocyte cell line HaCaT. About 2-3,000 cells/well were seeded in a flat bottom 96-well tissue culture plate, and incubated with various concentrations of test article in culture media for 5 days at 37°C. Viability of the remaining cells was determined via alamar blue cell viability assay.

Figure 6 is a graph showing the cytotoxic activity of naked anti-EGFR antibody cetuximab and maytansinoid conjugates thereof against primary keratinocytes. 2-3,000 cells/well were seeded in a flat bottom 96-well tissue culture plate, and incubated with various concentrations of test article in culture media for 72 h or 5 days at 37°C. Viability of the remaining cells was determined via alamar blue cell viability assay.

Figure 7 is a graph showing the cytotoxic activity of naked anti-EGFR antibody panitumumab and maytansinoid conjugates thereof against primary keratinocytes. 2-3,000 cells/well were seeded in a flat bottom 96-well tissue culture plate, and incubated with various concentrations of test article in culture media for 72 h or 5 days at 37°C. Viability of the remaining cells was determined via alamar blue cell viability assay.

Figure 8 is a graph showing the cytotoxic activity of naked anti-EGFR antibody panitumumab and maytansinoid conjugates thereof against primary keratinocytes. 2-3,000 cells/well were seeded in a flat bottom 96-well tissue culture plate, and incubated with various concentrations of test article in culture media for 72 h or 5 days at 37°C. Viability of the remaining cells was determined via alamar blue cell viability assay.

Figures 9-13 show results with immunoconjugates that incorporate elements not selected according to the criteria prescribed herein, as discussed in Example 4.

Figure 9 shows that panitumumab and cetuximab are very strong EGFR activation blockers and thus will not be potentiated on normal keratinocytes by conjugation, whereas partially antagonistic antibodies such as J2898A is potentiated (See Figure 10, and 11).

Figure 10 shows that partially antagonistic anti-EGFR antibody by IMGN (J2989A) is potentiated by conjugation (IMGN289) on normal keratinocytes (see also Setiady et al, Proceedings of the 104th Annual Meeting of the American Association for Cancer Research; 2013 Apr 6-10; Washington, DC. Philadelphia (PA): AACR; Cancer Res 2013;73(8 Suppl):Abstract nr 5463).

Figure 11 shows the toxicity of cetuximab mutant antibody, 6-LC, (having reduced affinity to make it a partially antagonistic against EGFR) is potentiated by conjugation to payload via non-cleavable linker (6LC-DM1).

Figure 12 shows panitumumab, and panitumumab-DM1 effects on keratinocytes, and reveals that conjugation of panitumumab via non-cleavable linker to DM1 (Avid300-DM1) does not increase its activity against normal cells; 2C9-DM1 is cetuximab-DM1 conjugate used as a control.

Figure 13 shows that conjugation of cetuximab to MMAE anti-microtubule payload by a cleavable linker (valine-citruline) potentiates its toxicity against both normal cells and

MDA-MB-468 cancer cells (Cetux 2C9-MMAE), whereas conjugation via non-cleavable linker (SMCC) only (Cetux2C9-DM1) potentiates anti-cancer activity, thus demonstrating a favorable therapeutic window.

DETAILED DESCRIPTION OF THE PREFERRED EMBODIMENTS

The present immunoconjugates are based on antibodies that bind to the human epidermal growth factor receptor (hEGFR), a protein that is presented on the surface of many different cell types including particularly skin cells such as keratinocytes. As used herein, the term "hEGFR" refers to any protein that comprises the expressed and processed product of the human *her-1* gene, wherein the protein is designated as UniProtKB/Swiss-Prot P00533. The term EGFR is used generically herein, and refers to the wild type protein and all naturally occurring variants thereof. The term "wtEGFR" is used more specifically with reference only to the wild type form of human EGFR. The term "EGFRvIII" refers to the EGFR variant protein that comprises the expressed and processed product of a variant of the *her-1* gene lacking exons 2-7, and thus includes only the polypeptide sequence encoded by exons 1 and 8 of *her-1*. The term "domain III" is not related to EGFRvIII, and instead refers to a location within EGFR, and represents an extracellular site that is key for EGF ligand binding, and binding of highly antagonistic antibodies cetuximab and panitumumab (Voigt et al, 2012 November; 14(11): 1023–1031).

The present immunoconjugates comprise an EGFR antibody that is a full antagonist at the EGFR. An EGFR antibody that is a "full antagonist" is an antibody that blocks completely or nearly so the transmission of a signal that is stimulated, in the normal course, by the EGF ligand through wtEGFR to the wtEGFR-coupled tyrosine kinase. EGFR antibodies that are full antagonists are particularly EGFR antibodies that bind directly to EGFR domain III. EGFR antibodies having these properties and an EGFR binding affinity of 5 nanomolar (nM) or less are particularly preferred for inclusion in the present immunoconjugates. By this measure, and as shown in Figure 9, at least the following known antibodies are not suitable for use in the present immunoconjugates:

J2898A, intellimab 6-LC (a cetuximab variant taught in WO 2012/100346), nimotuzumab, and matuzumab.

It is found that when a full antagonist EGFR antibody is selected to deliver a toxic payload, the killing effect is potentiated only on EGFR+ cancer cells and not on EGFR+ normal cells such as keratinocytes. This is not the case when the EGFR antibody is a partial antagonist, i.e., an antibody that allows transmission of some EGF-mediated signal. When conjugated to a toxin, these partial antagonist antibodies show a potentiation of the killing effect at both normal cells that are EGFR+ and cancer cells that are EGFR+.

The present immunoconjugates are based more particularly, and in one embodiment, on the hEGFR antibody known as cetuximab, now commercially available from Eli Lilly and Company under the trade name Erbitux®. Cetuximab is a recombinant, human/mouse chimeric IgG1 antibody that binds specifically to the extracellular domain of wtEGFR. The amino acid sequences of the CDRs for both the heavy chain of cetuximab (SEQ ID Nos.1-3) and the light chain of cetuximab (SEQ ID Nos. 4-6) are listed herein. Also listed are the amino acid sequences of the heavy chain variable region (SEQ ID No.7) and of the light chain variable region (SEQ ID No.8) of cetuximab, together with the amino acid sequences of the complete heavy chain (SEQ ID No. 9) and complete light chain (SEQ ID No.10) of cetuximab.

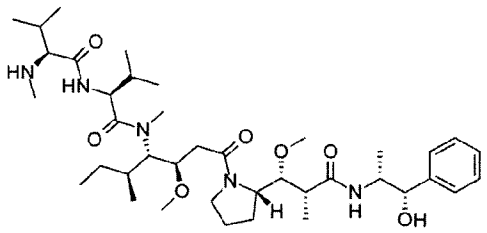
Cetuximab variants useful herein are highly antagonistic EGFR-binding agents that compete with cetuximab for binding to human EGFR. Useful cetuximab variants have been mentioned hereinabove, and include fragments of cetuximab comprising the EGFR binding sites of cetuximab, such as all of the light chain and heavy chain CDRs herein recited. Other cetuximab variants useful here in are cetuximab variants that incorporate one, two or more substitutions outside the antigen binding domains, such as in the framework region or in the constant region (Fc). Such substitutions are benign in the sense that they do not reduce cytotoxicity relative to cetuximab per se.

In another embodiment, the present immunoconjugates are based on the EGFR antibody known as panitumumab, now commercially available and sold under the trade name Vectibix®. Panitumumab is a recombinant, fully human IgG2 antibody that binds specifically to the extracellular domain of wtEGFR. The amino acid sequences of the heavy and light chains of panitumumab are listed in US 6,235,883 and US 7,807,798. A useful alternative to panitumumab is an EGFR binding variant thereof that competes with panitumumab for EGFR binding, such as a fragment of panitumumab that incorporates its antigen binding sites but has an otherwise lost or altered constant region.

The present immunoconjugates can also be based on still other EGFR antibodies provided they show full antagonist activity as defined above, such as EGFR antibodies that bind selectively to domain III of EGFR, and any other EGFR antibodies that compete with EGF and block fully or nearly so the transmission of EGF-stimulated downstream signalling.

In the present immunoconjugates, the full antagonist EGFR antibody, such as cetuximab or panitumumab, is conjugated to an anti-microtubule toxin such as maytansinoid toxin. By "anti-microtubule toxin" is meant an agent having cell toxicity mediated by interference with the microtubule structures important for cell mitosis, such as by inhibiting the formation of tubulin or by inhibiting the organization thereof.

Included within this toxin family are the maytansinoids and auristatins, and many other agents developed more recently and having the same mechanism of action. The auristatins in particular block cell replication by inhibiting polymerization of tubulin and are thus anti-mitotic. The structure of an auristatin useful herein and known as MMAE, or vedotin, is shown below:



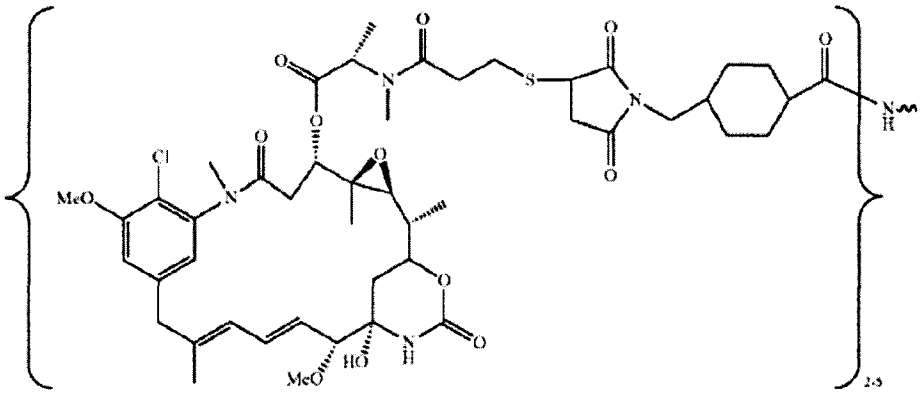
There are various forms of maytansinoids that are useful. These are all based on the complex structure of a natural molecule, maytansine.

Particularly useful are the maytansinoids including DM-1 and DM-4. In a specific embodiment, the toxin coupled to the EGFR MAb is DM-1 having the structure shown *infra*.

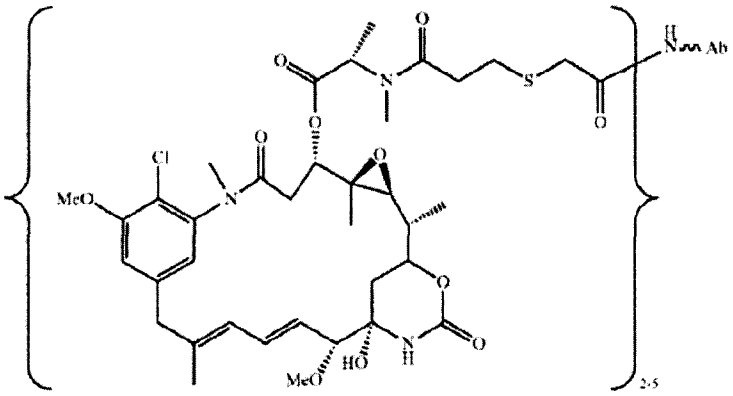
Also useful as anti-microtubule toxins are dolostatins, auristatins, tubulysins and cryptophycins. Specific examples of useful species within each genus include dolostatin 10, monomethyl dolostatin 10, auristatin E, monomethyl auristatin E (MMAE), auristatin F, monomethyl auristatin F, HTI-286, tubulysin M, as well as the tubulin binders such as tubulysin IM-1, tubulysin IM-2, tubulysin IM-3, colchicine DA, and maytansinoids AP-3, DM-1 and DM-4.

Conjugates of a full antagonist EGFR antibody such as cetuximab or panitumumab, and an anti-microtubule toxin such as a maytansinoid or auristatin can be formed using any technique presently known or later developed that couples a linker that is "non-cleavable". These linkers remain intact, and retain the antibody and toxin in covalent association, throughout conditions normally encountered following administration to a subject, including extracellular environments. More specifically, non-cleavable linkers result in ADC constructs for which release of the cytotoxic payload is achieved by destruction of the antibody by intracellular lysosomes.

Methods of linker integration are described for instance in US 5,208,020; US 8,088,387; and US 6,441,163. A preferred method is to modify the EGFR antibody, e.g., cetuximab, with succinimidyl 4-(N-maleimidomethyl)-cyclohexane-1-carboxylate (SMCC) to introduce maleimido groups followed by reaction of the modified antibody with a thiol-containing maytansinoid to give a thioether-linked conjugate. The resulting chemical structures are shown below. Conjugates with 1 to 10 drug molecules per antibody molecule result.



Ab-SMCC-DM1
Ab = Antibody



Ab-SIA-DM1
Ab = Antibody

Other useful forms of non-cleavable linkers include N-Succinimidyl iodoacetate (SIA), sulfo-SMCC, m-maleimidobenzoyl-N-hydroxysuccinimide ester(MBS), sulfo-MBS and succinimidyl-iodoacetate, as described in the literature, to introduce 1-10 reactive groups. (see, Yoshitake et al, 101 Eur. J. Biochem. 395-399 (1979); Hashida et al, J. Applied Biochem. 56-63 (1984); and Liu et al, 18 690-697 (1979)). Particularly useful for linking auristatins as anti-microtubule toxin are the non-cleavable maleimidocaproyl linkers described by Doronina et al, in Bioconjugate Chem., 2006 Jan-Feb;17(1):114-24).

In a specific embodiment, the immunoconjugate comprises cetuximab linked to DM-1 by an SMCC linker.

In another specific embodiment, the immunoconjugate comprises panitumumab linked to DM-1 by an SMCC linker.

Thus, in a general aspect, the invention provides a method useful to potentiate the anti-cancer activity of an EGFR antibody without potentiating the effect thereof on normal EGFR+ cells, the method comprising:

(i) selecting, for conjugation, an EGFR antibody that is a full EGFR antagonist;

(ii) selecting, for delivery by the EGFR antibody, an anti-microtubule toxin;

(iii) selecting, for coupling the selected EGFR antibody to the anti-microtubule toxin, a linker that is non-cleavable; and

incorporating the linker between the antibody and the toxin to provide an immunoconjugate having a cytotoxic activity that is potentiated against EGFR+ disease cells but not against normal EGFR+ cells.

As will be appreciated from the preceding disclosure, the full antagonist EGFR antibody is preferably cetuximab or panitumumab. The anti-microtubule toxin is preferably an auristatin or a maytansinoid, and is most preferably DM-1. The non-cleavable linker is preferably SMCC.

In another specific embodiment, there is the proviso that the full antagonist EGFR antibody is not cetuximab. In a further specific embodiment, there is the proviso that the full antagonist EGFR antibody is not panitumumab.

Therapeutic formulations of the conjugate are prepared for therapeutic use directly or for storage by mixing the conjugate having the desired degree of purity with optional pharmaceutically acceptable carriers, excipients or stabilizers (Remington's Pharmaceutical Sciences, 16th edition, Osol, A. Ed. [1980]), in the form of lyophilized formulations or aqueous solutions. Acceptable carriers, excipients, or stabilizers are nontoxic to recipients at the dosages and concentrations employed, and include buffers such as phosphate, citrate, and other organic acids; antioxidants including ascorbic acid

and methionine; preservatives (such as octadecyldimethylbenzyl ammonium chloride; hexamethonium chloride; benzalkonium chloride, benzethonium chloride; phenol, butyl, or benzyl alcohol; alkyl parabens such as methyl or propyl paraben; catechol; resorcinol; cyclohexanol; 3-pentanol; and m-cresol); low molecular weight (less than about 10 residues) polypeptides; proteins such as serum, albumin, gelatin, or immunoglobulins; hydrophilic polymers such as polyvinylpyrrolidone; amino acids such as glycine, glutamine, asparagines, histidine, arginine or lysine; monosaccharides, disaccharides, and other carbohydrates including glucose, mannose, or dextrins; chelating agents such as EDTA; sugars such as sucrose, mannitol, trehalose or sorbitol; salt-forming counter-ions such as sodium; metal complexes (e.g., Zn-protein complexes); and/or non-ionic surfactants such as TWEEN, PLURONICS or polyethylene glycol (PEG).

The active ingredients to be used for *in vivo* administration must be sterile. This is readily accomplished by filtration through sterile membranes.

Sustained-release preparations may be prepared. Suitable examples of sustained-release include semipermeable matrices of solid hydrophobic polymers containing the conjugate, which matrices are in the form of shapes articles, e.g., films or microcapsules. Examples of sustained-release matrices include polyesters, hydrogels (for example, poly (2-hydroxyethyl-methacrylate), polylactides (U.S. Pat. No. 3,773,919), copolymers of L-glutamic acid and ethyl-L-glutamate, non-degradable ethylene-vinyl acetate, degradable lactic acid-glycolic acid copolymers such as injectable microspheres composed of lactic acid-glycolic acid copolymer and leuprolide acetate, and poly-D-(-)-3-hydroxybutyric acid. While polymers such as ethylene-vinyl acetate and lactic acid-glycolic acid enable release of molecules for over 100 days, certain hydrogels release proteins for shorter time periods.

The conjugates are useful to treat EGFR+ disease cells. Such treatment results in a reduction in the number, size or distribution of such disease cells in subjects presenting with them. In embodiments, the conjugates are used to treat EGFR+ disease cells that are EGFR+ cancer cells and tumours comprising them. Such treatment results preferably in a

reduction in the number, size, volume or distribution of such cancer cells and tumours comprising them, or at least in a reduction in the rate at which such disease cells increase in number, size, volume or distribution of such cells and tumours in subjects presenting with them.

Subjects presenting with EGFR+ cancer cells can be identified with the aid of assays that detect the receptor, as protein or as nucleic acid precursor (DNA or RNA) in physiological samples such as biopsied tissue. A suitable test for EGFR protein is the commercially available and FDA approved Dako EGFR pharmDx® test kit.

For the treatment of subjects presenting with EGFR+ cancer cells, the appropriate dosage of the conjugate will depend on the type of disease to be treated, as defined above, the severity and course of the disease, whether the agent is administered for preventative or therapeutic purposes, previous therapy, the patients clinical history and response to the agent, and the discretion of the attending physician. The agent is suitably administered to the patient at one time or over a series of treatments.

For example, depending on the type and severity of the disease, about 1 μg/kg to 15 mg/kg (e.g., 0.1-20 mg/kg) of conjugate is a candidate dosage for administration to the patient, whether, for example, by one or more separate administrations, or by continuous infusion. A typical daily dosage might range from about 1 μg/kg to 500 mg/kg or more, depending on the factors mentioned above. For repeated administrations over several days or longer, depending on the condition, the treatment is sustained until a desired suppression of disease symptoms occurs. However, other dosage regimens may be useful. The progress of this therapy is easily monitored by conventional techniques and assays.
It will thus be appreciated that an effective amount of the immunoconjugate is an amount effective alone or as part of a treatment regimen that retards or inhibits the rate of growth or proliferation of EGFR+ disease cells.

An EGFR+ disease cell is a disease cell that presents EGFR on its surface as detectable for instance by EGFR antibody binding, or by detection of intracellular mRNA encoding

her-1. Particular EGFR+ disease cells include those having on their surface an abnormally high density and/or activity of EGFR molecules, or the presence of the EGFRvIII variant of EGFR.

It may be useful to administer to administer the present conjugates by intravenous infusion first as loading dose, followed by maintenance dose, such as at an initial dose of 4mg/kg over 90 minutes, then 2 mg/kg over 30 minutes, once weekly for as many as 52 weeks, with follow up as required. In the specific case of the panitumumab conjugate, dosing might be based on that utilized for panitumumab per se, which comprises 6mg/kg given once every two weeks as a one hour infusion.

The conjugates are useful in the treatment of a variety of cancers, to inhibit the growth or proliferation of EGFR+ cancer cells and tumours comprising them, including hematopoietic cell cancers and solid tumours. Conditions or disorders to be treated include benign or malignant tumors (e.g., renal, liver, kidney, bladder, breast, gastric, ovarian, colorectal, prostate, pancreatic, lung, vulva, and thyroid); hepatic carcinomas; sarcomas; glioblastomas; and various head and neck tumors; leukemias and lymphoid malignancies. In particular embodiments, the antibody or bivalent fragment are used in the treatment of such cancer cells that express EGFRvIII, as determined by the screening assays herein described. In particular embodiments, the cancer cells are EGFR+-presenting cancer cells that include head and neck cancers and especially squamous cell carcinoma of the head and neck, colorectal cancers, gastrointestinal cancers, brain tumours including glioblastomas, and tumours of the lung including non-small-cell lung carcinoma, and of the breast, pancreas, esophagus, kidney, ovary, cervix and prostate. In specific embodiments, the EGFR+ cancer is one for which cetuximab has received FDA marketing approval, such as squamous cell carcinoma of the head and neck and colorectal cancers.

It will be appreciated that subjects who could benefit from the present method include mammals including humans as well as livestock, and pets.

Other therapeutic regimens may be combined with the administration of the conjugates of the instant invention. For example, the patient to be treated may also receive radiation therapy, such as external beam radiation. Alternatively, or in addition, a chemotherapeutic agent may be administered to the patient. Preparation and dosing schedules for such chemotherapeutic agents may be used according to manufacturers' instructions or as determined empirically by the skilled practitioner. Preparation and dosing schedules for such chemotherapy are also described in Chemotherapy Service Ed., M. C. Perry, Williams & Wilkins, Baltimore, Md. (1992). The chemotherapeutic agent may precede, or follow administration or the conjugate or may be given simultaneously therewith. The conjugate may be combined with any anti-cancer toxins, or any other suitable drug particularly including irinotecan (CPT-11), cisplatin, cyclophosphamide, melphalan, dacarbazine, doxorubicin, daunorubicin, and topotecan, as well as tyrosine kinase inhibitors, including particularly EGFR kinase inhibitors such as AG1478 ((4-(3-chloroanilino-6,7-dimethoxyquinazoline), gefitinib (Iressa®), erlotinib (Tarceva®), lapatinib (Tykerb®), canertinib (PD183805, Pfizer), PKI-166 (Novartis), PD158780 and pelitinib.

It may also be desirable to administer antibodies or conjugates against other tumor associated antigens or their ligands, such as antibodies which bind to the ErbB2 (including trastuzumab marketed as Herceptin®, and pertuzumab marketed as Omnitarg®), ErbB3, ErbB4, or vascular endothelial factor (VEGF), and/or antibodies that bind to EGF or TGFα.

In another embodiment of the invention, an article of manufacture containing conjugate in an amount useful for the treatment of the disorders described herein is provided. The article of manufacture comprises a container and a label. Suitable containers include, for example, bottles, vials, syringes, and test tubes. The containers may be formed from a variety of materials such as glass or plastic. The container holds a composition which is effective for treating the condition and may have a sterile access port (for example the container may be an intravenous solution bag or vial having a stopper pierceable by a hypodermic injection needle). The label on or associated with the container indicates that

the composition is used for treating a cancer condition. The article of manufacture may further compromise a second container compromising a pharmaceutically-acceptable buffer, such as phosphate-buffered saline, Ringer's solution and dextrose solution. It may further include other matters desirable from a commercial and use standpoint, including other buffers, diluents, filters, needles, syringes, and package inserts with instructions for use.

An anti-cancer immunoconjugate according to the invention may be administered with a pharmaceutically-acceptable diluent, carrier, or excipient, in unit dosage form. Unit doses of the conjugate are suitably 50mgs, 100mgs, 150mgs, 200mgs, 250mgs, 300mgs and 400mgs. The drug can be formulated in single use vials at a concentration such as 20mg/mL, for instance 100mg in 5mL vehicle such as 0.9% saline, 200mg in 10mL or 400mg in 20mL.

Any appropriate route of administration can be employed, for example, parenteral, intravenous, subcutaneous, intramuscular, intracranial, intraorbital, ophthalmic, intraventricular, intracapsular, intraspinal, intracisternal, intraperitoneal, intranasal, aerosol, pulmonary, or oral administration.

Example 1 – Preparation of Cetuximab-SMCC-DM1 conjugate (A-H)

A. PREPARATION AND MEASUREMENT OF CETUXIMAB ANTIBODY

Cetuximab is obtained from the open market, or is produced as described in WO 2012/100346, for conjugation to DM1 using the non-cleavable heterobifunctional cross-linking reagent SMCC.

Cetuximab antibody was then buffer exchanged into 50 mM potassium phosphate, 50 mM sodium chloride, 2 mM EDTA; pH 6.5 buffer (Buffer A). All buffers in this experiment were tested to be free of endotoxin using a chromogenic Limulus amoebocyte lysate (LAL) method (Cambrex). The concentration of antibody was measured using an extinction coefficient of 1.45 mL/mg/cm at 280 nm and a molecular weight of 145,781g.

B. PREPARATION AND MEASUREMENT OF SMCC STOCK SOLUTION

A 20 mM solution of SMCC (6.69 mg/mL) (Concortis Biosystems Corp.) was prepared in DMSO. The solution was diluted 1/40 in Assay Buffer and the absorbance of the samples was measured at 302 nm. The concentration of the stock solution was calculated using a molar extinction coefficient of 602/M/cm.

C. PREPARATION AND MEASUREMENT OF DM1 STOCK SOLUTION

A 10 mM solution of DM1 (free thiol form; Concortis Biosystems Corp.) was prepared in DMA (7.37 mg/mL). The absorbance of dilutions of the stock solution in ethanol was measured at 280 nm. The concentration of stock DM1 was calculated by using a molar extinction coefficient of 5700/M/cm at 280 nm. The concentration of free —SH in the stock DM1 preparation was measured using Elman's reagent (DTNB). Dilutions of the stock solution were prepared in Assay buffer made to 3% (v/v) DMA, and then 100 mM DTNB in DMSO (1/100th volume) was added. The increase in absorbance at 412 nm was measured against a reagent blank and the concentration was calculated using an extinction coefficient of 14150/M/cm. The concentration of —SH resulting from the Elman's assay was used to represent the DM1 stock concentration in calculations for conjugation conditions.

D. MODIFICATION OF CETUXIMAB WITH SMCC CROSSLINKER

The antibody was modified using a 7.5-fold molar excess of SMCC at 20 mg/mL antibody. The reaction was carried out in Buffer A (95% v/v) with DMSO (5% v/v) for 2 hours at room temperature with stirring.

E. G25 CHROMATOGRAPHY TO REMOVE EXCESS SMCC

The cetuximab-SMCC reaction mixture was gel-filtered through a 1.5×4.9 cm pre-packed column of Sephadex G25 resin equilibrated in Buffer A. The load and elution volumes were according to manufacturer's instructions (Amersham Biosciences). The concentration of the modified antibody solution was assayed spectrophotometrically using the extinction co-efficient described above.

F. CONJUGATION OF CETUXIMAB-SMCC WITH DM1

The modified antibody was reacted with a 1.7-fold excess of DM1 over linker (assuming 5 linkers per antibody). The reaction was carried out at 10 mg/mL antibody concentration in Buffer A (94% v/v) with DMA (6% v/v). After addition of DM1, the reaction was incubated at room temperature for 16.5 hours with stirring.

G. CONJUGATION PURIFICATION BY G25 CHROMATOGRAPHY

The conjugation reaction mixture was gel-filtered through a 1.5×4.9 cm pre-packed column of Sephadex G25 resin equilibrated in 1× phosphate buffered saline (PBS), pH 6.5 (Buffer B). The load and elution volumes were according to manufacturer's instructions (Amersham Biosciences). The number of DM1 molecules linked per mole of cetuximab was determined by measuring absorbance at both 252 nm and 280 nm of the eluted material. The DM1/antibody ratio was found to be 2 and 4. The resulting conjugate was analyzed for binding and cytotoxicity.

H. TESTING OF CETUXIMAB-SMCC-DM1

The cell lines used in these studies have the following characteristics:

A431: human epithelial carcinoma of vulva cell line; available from ATCC; plated at 4000 cells/well in DMEM-10%FBS, 100µl/well in 96 well plate.

H226: lung squamous cell carcinoma cell line; available at ATCC; plated at 4000 cells/well in RPMI-10%FBS, 100µl/well in 96-well culture plate.

MDA-MB-468: mammary gland/breast; derived from metastatic site: pleural effusion; available from ATCC; plated at 4000 cells/well in ATCC-formulated Leibovitz's L-15 Medium (Catalog No. 30-2008) with added fetal bovine serum to a final concentration of 10%; 100µl/well in 96 well plate.

HaCaT: in vitro spontaneously transformed keratinocytes from histologically normal skin; available from Chinese Center for Type Culture Collection of Wuhan University; plated at 2000 cells/well in DMEM-10%FBS, 100µl/well in 96-well culture plate.

HEKa: Normal Human Primary Epidermal Keratinocytes, adult; available from PromoCell GmbH; plated at 4000cells/well in EpiLife media 100µl/well, EpiLife medium #MEP1500CA, Invitrogen +HKGS human keratinocyte growth supplement (#S-001-5)

Binding studies showed that the conjugation of antibody to DM1 did not affect the K_D; both naked cetuximab antibody and cetuximab-SMCC-DM1 conjugate had the same binding affinity to EGFR by surface plasmon resonance (~0.3 nM, Table 1). Evaluation of the *in vitro* cytotoxicity of the sample showed that the cetuximab-SMCC-DM1 conjugate is significantly more cytotoxic compared to cetuximab against cancer cell lines (Figs 3&4), but that surprisingly cetuximab-SMCC-DM1 and naked cetuximab have the same cytotoxic activity against keratinocytes (Figs 5&6).

Table 1: effects of conjugation to DM1 on cetuximab KD

Sample	# of experiments	EGFR ecd KD (nM)
Commercial cetuximab	3	0.27 +/- 0.02
Cetuximab-SMCC-DM1	3	0.28 +/- 0.02

The effect of DM1 conjugation on different EGFR MAbs (huML66 and huEGFR-7R) is demonstrated in ImmunoGen's published US patent application 2012/0156217, and Figures 1 and 2 herein are reproductions of figures appearing in that application. More particularly, as shown in Figure 1, conjugation of anti-EGFR antibodies huML66-SMCC-DM1 and huEGFR-7R to maytansinoids to create huML66-SMCC-DM1 and huEGFR-7R-SMCC-DM1 immunoconjugates increases cytotoxic activity of against normal keratinocytes. Similarly, and as expected, conjugation of anti-EGFR antibodies huML66 and huEGFR-7R to maytansinoids to create huML66-SMCC-DM1 and huEGFR-7R-SMCC-DM1 immunoconjugates significantly potentiates cytotoxic activity of the antibodies against H226 cancer cell line (Figure 2).

As shown in Figures 3 and 4, DM1 conjugation of anti-EGFR antibody cetuximab (HC-LC) to create cetuximab-SMCC-DM1 immunoconjugate (HC-LC/DM1) significantly potentiates cytotoxic activity of the antibody against cancer cells, as expected and shown in Figure 3. As shown in Figure 4, and also as expected, conjugation of anti-EGFR antibody cetuximab (HC-LC) to maytansinoids to create cetuximab-SMCC-DM1 immunoconjugate (HC-LC/DM1) significantly potentiates cytotoxic activity of the antibody against cancer cells.

However, and quite surprisingly, as shown in Figures 5 and 6, conjugation of anti-EGFR antibody cetuximab (HC-LC) to maytansinoids to create cetuximab-SMCC-DM1 immunoconjugate (HC-LC/DM1) did not increase cytotoxicity against the keratinocytes as is reflected in substantially the same IC_{50} values for these agents (IC_{50} of 0.8269 for conjugate vs. IC_{50} of 0.4324 for naked antibody; Fig 5, HaCaT - normal human keratinocytes cell line & IC_{50} of 2.210 for conjugate vs. IC_{50} of 0.9348 for naked antibody, Fig 6; HEKa- primary human keratinocyte cells). As used herein, IC_{50} refers to the concentration of drug required to kill 50% of cells.

The measure of whether cytotoxicity is increased or not is determined above by comparing IC_{50} values produced using the alamar blue cell viability assay (each experiment performed in triplicates in a 96-well plate). A difference within one log order is deemed not significant and is considered to reveal no change in cytotoxicity, whereas a difference greater than one log order reveals a significant change in cytotoxicity.

Example 2 - Evaluation in Primates

Cynomolgus monkey species has been previously demonstrated to be a valuable and highly predictive model for evaluating anti-EGFR antibodies toxicities, including dermatologic side-effects. The high level of correlation between Cynomolgus monkey and human toxicity data for EGFR-targeting antibodies is in part due high homology between the monkey and human EGFR receptors that results in very similar K_D values for the antibodies:

Table 1: Binding affinity of cetuximab and panitumumab to human and cynomologus EGFR is consistent across the species. Apparent antibody affinity defined as the antibody concentration (picomolar, pM) required to achieve half-maximal binding in ELISA with recombinant extracellular domains of human EGFR (huEGFR), and Cynomolgus monkey EGFR (cyEGFR).Adapted from Koefoed et al, MABs. 2011 Nov-Dec; 3(6):584-595.

Apparent affinity, ELISA assay		
	Domain IIIB Binding	
Antigens	cetuximab	panitumumab
human sEGFR (pM)	12	32
cynomolgus sEGFR (pM)	14	32

The cetuximab-SMCC-DM1 immunoconjugate was tested in primates particularly to identify any significant potentiation of antibody side-effects by the conjugated toxin on normal cells. In particular, close attention was paid to dermatologic side-effects that are qualitatively different and/or significantly exacerbated relative to what is expected with the naked fully antagonistic anti-EGFR antibody.

The study initially made use of two Cynomolgus macaques, all males that were sedated with ketamine and anesthetized with isoflurane to facilitate IV administration of the antibody-drug conjugate administered at 10mg/kg. Animals were then observed for 5 days prior to sacrifice for general signs of acute toxicity, and examined further.

The detailed histopathology analysis revealed no severe dermatologic toxicities or other severe and qualitatively new dermatologic side-effects other than those that are expected as a result of naked cetuximab treatment. Also, no other severe on-target toxicities were observed in these animals demonstrating safety of ADCs of present invention and absence of significant exacerbation of the naked antibody toxicities.

Subsequent to successful completion of the acute primate study, repeat-dose safety study has been initiated in additional animals. The ADC was administered once every three weeks at 10mg/kg dose over 4 cycles. This dose and schedule was selected based on dosing schedules commonly used with other ADCs in primates and humans (Poon KA et al, Preclinical safety profile of trastuzumab emtansine (T-DM1): mechanism of action of its cytotoxic component retained with improved tolerability. Toxicol Appl Pharmacol. 2013 Dec 1;273(2):298-313; FDA Package Insert for Kadcyla™, accessed February 24, 2014: http://www.accessdata.fda.gov/drugsatfda_docs/label/2013/125427lbl.pdf).

With the exception of reversible liver enzyme elevations which is an expected class side-effect of ADCs, no other severe and/or qualitatively new dermatologic or other on-target side-effects other than those that are already expected as a result of naked cetuximab treatment (cetuximab cynomolgus monkey data available at: http://www.accessdata.fda.gov/drugsatfda_docs/bla/2004/125084_ERBITUX_PHARMR_P3.PDF) have been observed in the ongoing study to date. Severe skin toxicity and toxic epidermal necrolysis previously reported with anti-CD44v6 ADC (which also uses SMCC-DM1 payload technology and targets an antigen expressed by normal keratinocytes) has not been observed in this study (Tijink *et al.*, Clin Cancer Res, 2006, 12:6064). These safety data further validates *in vitro* results that on-target toxicities of fully antagonist naked anti-EGFR antibodies is not significantly potentiated as result of conjugation to the cytotoxic payloads.

Example 3 – Preparation of Panitumumab-SMCC-DM1 conjugate (A-H)

A DM-1 conjugated panitumumab was prepared essentially as described above for the cetuximab counterpart. More particularly,

A. PREPARATION AND MEASUREMENT OF PANITUMUMAB ANTIBODY

Panitumumab is obtained from the open market, or is produced as described in US 6,235,883 or US 7,807,798 for conjugation to DM1 using the non-cleavable heterobifunctional cross-linking reagent SMCC.

Panitumumab antibody was then buffer exchanged into 50 mM potassium phosphate, 50 mM sodium chloride, 2 mM EDTA; pH 6.5 buffer (Buffer A). All buffers in this experiment were tested to be free of endotoxin using a chromogenic Limulus amoebocyte lysate (LAL) method (Cambrex). The concentration of antibody was measured using an extinction coefficient of 1.45 mL/mg/cm at 280 nm and a molecular weight of 145,781g.

B. PREPARATION AND MEASUREMENT OF SMCC STOCK SOLUTION

A 20 mM solution of SMCC (6.69 mg/mL) (Concortis Biosystems Corp.) was prepared in DMSO. The solution was diluted 1/40 in Assay Buffer and the absorbance of the samples was measured at 302 nm. The concentration of the stock solution was calculated using a molar extinction coefficient of 602/M/cm.

C. PREPARATION AND MEASUREMENT OF DM1 STOCK SOLUTION

A 10 mM solution of DM1 (free thiol form; Concortis Biosystems Corp.) was prepared in DMA (7.37 mg/mL). The absorbance of dilutions of the stock solution in ethanol was measured at 280 nm. The concentration of stock DM1 was calculated by using a molar extinction coefficient of 5700/M/cm at 280 nm. The concentration of free —SH in the stock DM1 preparation was measured using Elman's reagent (DTNB). Dilutions of the stock solution were prepared in Assay buffer made to 3% (v/v) DMA, and then 100 mM DTNB in DMSO (1/100th volume) was added. The increase in absorbance at 412 nm was measured against a reagent blank and the concentration was calculated using an extinction coefficient of 14150/M/cm. The concentration of —SH resulting from the Elman's assay was used to represent the DM1 stock concentration in calculations for conjugation conditions.

D. MODIFICATION OF PANITUMUMAB WITH SMCC CROSSLINKER

The antibody was modified using a 7.5-fold molar excess of SMCC at 20 mg/mL antibody. The reaction was carried out in Buffer A (95% v/v) with DMSO (5% v/v) for 2 hours at room temperature with stirring.

E. G25 CHROMATOGRAPHY TO REMOVE EXCESS SMCC

The panitumumab-SMCC reaction mixture was gel-filtered through a 1.5×4.9 cm pre-packed column of Sephadex G25 resin equilibrated in Buffer A. The load and elution volumes were according to manufacturer's instructions (Amersham Biosciences). The concentration of the modified antibody solution was assayed spectrophotometrically using the extinction co-efficient described above.

F. CONJUGATION OF PANITUMUMAB-SMCC WITH DM1

The modified antibody was reacted with a 1.7-fold excess of DM1 over linker (assuming 5 linkers per antibody). The reaction was carried out at 10 mg/mL antibody concentration in Buffer A (94% v/v) with DMA (6% v/v). After addition of DM1, the reaction was incubated at room temperature for 16.5 hours with stirring.

G. CONJUGATION PURIFICATION BY G25 CHROMATOGRAPHY

The conjugation reaction mixture was gel-filtered through a 1.5×4.9 cm pre-packed column of Sephadex G25 resin equilibrated in 1× phosphate buffered saline (PBS), pH 6.5 (Buffer B). The load and elution volumes were according to manufacturer's instructions (Amersham Biosciences). The number of DM1 molecules linked per mole of panitumumab was determined by measuring absorbance at both 252 nm and 280 nm of the eluted material. The DM1/antibody ratio was found to be 2 and 4. The resulting conjugate was analyzed for binding and cytotoxicity.

H. TESTING OF PANITUMUMAB-SMCC-DM1

The cell lines used in these studies have the following characteristics:

MDA-MB-468: mammary gland/breast; derived from metastatic site: pleural effusion; available from ATCC; plated at 4000 cells/well in ATCC-formulated Leibovitz's L-15 Medium (Catalog No. 30-2008) with added fetal bovine serum to a final concentration of 10%; 100µl/well in 96 well plate.

HaCaT: in vitro spontaneously transformed keratinocytes from histologically normal skin; available from Chinese Center for Type Culture Collection of Wuhan University; plated at 2000 cells/well in DMEM-10%FBS, 100µl/well in 96-well culture plate.

In vitro studies with keratinocytes demonstrate that conjugation of panitumumab to an anti-microtubule toxin via non-cleavable linker does not potentiate the toxicity of the antibody. The resulting ADC has a similar safety profile on keratinocytes as the naked panitumumab, as well as another ADC based on a fully antagonistic antibody, cetuximab. On MDA-MB-468 cancer cells, significant potentiation of anticancer activity of panitumumab is observed as a result of conjugating the antibody to anti-microtubule toxin via non-cleavable linker. Similar to toxicity observations, panitumumab-based ADC was similarly active as cetuximab-based ADC.

Example 4 – Results with partial antagonist EGFR MAb conjugates

The effect of selecting immunoconjugate components different from those recommended herein is shown in accompanying drawings. Figure 9 shows that a partial antagonist EGFR antibody, designated J2989A has an activity that is potentiated on normal keratinocytes when conjugated to DM-1. Figure 10 shows, similarly, that another partial antagonist antibody, designated 6-LC (a substitution variant of cetuximab having lower relative affinity for EGFR) has an activity that is also potentiated at normal keratinocytes when conjugated to DM-1. Figure 11 shows that the effect of panitumumab of keratinocytes is not potentiated on keratinocytes when conjugated to DM1, while the anti-cancer effect of the conjugate is potentiated dramatically (Figure 12). And, Figure 13 shows that conjugation of cetuximab to MMAE by a cleavable linker (valine-citrulline) potentiates its toxicity against normal cells and MDA-MB-468 cancer cells, whereas conjugation via non-cleavable linker (SMCC) potentiates anti-cancer activity.

Thus, in these studies, only fully antagonistic anti-EGFR antibodies were not potentiated on normal cells by payload conjugation via non-cleavable linkers, whereas toxicity against normal cells of partial antagonist EGFR antibodies was potentiated by the conjugation. Moreover, we subsequently tested the effect on this activity profile of the

cleavable vs. non-cleavable linkers, while maintaining payload mechanism of action the same (i.e. anti-microtubule agent). The antibodies were conjugated via cleavable linker to anti-microtubule payload, MMAE as described by Doronina et al, Nature Biotechnology Nov 7, 2003, Vol 21: pp 778-784. Cleavable linker data demonstrate that when the fully antagonistic antibodies are conjugated to their payloads via cleavable linkers, their toxicity against normal cells is potentiated. Thus, a safe anti-EGFR ADC should incorporate a strongly antagonistic anti-EGFR antibody linked to an anti-microtubule payload by a non-cleavable linker.

The scope of the claims should not be limited by the preferred embodiments set forth in the examples, but should be given the broadest interpretation consistent with the description as a whole.

Referenced Sequences

SEQ ID No. Description

1 Cetuximab heavy chain CDR1

NYGVH

2 Cetuximab heavy chain CDR2

VIWSGGNTDYNTPFTS

3 Cetuximab heavy chain CDR3

ALTYYDYEFAY

4 Cetuximab light chain CDR1

RASQSIGTNIH

5 Cetuximab light chain CDR2

ASESIS

6 Cetuximab light chain CDR3

QQNNNWPTT

7 Cetuximab heavy chain variable region (V_H)

QVQLKQSGPGLVQPSQSLSITCTVSGFSLTNYGVHWVRQSPGKGLEWLGVIWSGGNTDYNTPFTS
RLSINKDNSKSQVFFKMNSLQSNDTAIYYCARALTYYDYEFAYWGQGTLVTVSA

8 Cetuximab light chain variable region (V_L)

DILLTQSPVILSVSPGERVSFSCRASQSIGTNIHWYQQRTNGSPRLLIKYASESISGIPSRFSGS
GSGTDFTLSINSVESEDIADYYCQQNNNWPTTFGAGTKLELK

9 Cetuximab complete heavy chain

QVQLKQSGPGLVQPSQSLSITCTVSGFSLTNYGVHWVRQSPGKGLEWLGVIWSGGNTDYNTPFTS
RLSINKDNSKSQVFFKMNSLQSNDTAIYYCARALTYYDYEFAYWGQGTLVTVSAASTKGPSVFPL
APSSKSTSGGTAALGCLVKDYFPEPVTVSWNSGALTSGVHTFPAVLQSSGLYSLSSVVTVPSSSL
GTQTYICNVNHKPSNTKVDKRVEPKSCDKTHTCPPCPAPELLGGPSVFLFPPKPKDTLMISRTPE
VTCVVVDVSHEDPEVKFNWYVDGVEVHNAKTKPREEQYNSTYRVVSVLTVLHQDWLNGKEYKCKV
SNKALPAPIEKTISKAKGQPREPQVYTLPPSRDELTKNQVSLTCLVKGFYPSDIAVEWESNGQPE
NNYKTTPPVLDSDGSFFLYSKLTVDKSRWQQGNVFSCSVMHEALHNHYTQKSLSLSPGK

10 Cetuximab complete light chain

DILLTQSPVILSVSPGERVSFSCRASQSIGTNIHWYQQRTNGSPRLLIKYASESISGIPSRFSGS
GSGTDFTLSINSVESEDIADYYCQQNNNWPTTFGAGTKLELKRTVAAPSVFIFPPSDEQLKSGTA
SVVCLLNNFYPREAKVQWKVDNALQSGNSQESVTEQDSKDSTYSLSSTLTLSKADYEKHKVYACE
VTHQGLSSPVTKSFNRGE

WE CLAIM:

1. A method useful to potentiate the cytotoxicity of an EGFR antibody or an EGFR-binding fragment thereof on EGFR+ disease cells without potentiating the cytotoxicity thereof on normal EGFR+ cells, the method comprising:

(i) selecting, for conjugation, an EGFR antibody that is a full EGFR antagonist and competes with cetuximab for binding to EGFR, or an EGFR-binding fragment of said antibody;

(ii) selecting, for delivery by the EGFR antibody or fragment thereof, an anti-microtubule toxin;

(iii) selecting, for coupling the selected EGFR antibody and the anti-microtubule toxin, a linker; and

producing an immunoconjugate that incorporates the linker between the antibody and the toxin, thereby providing an immunoconjugate having a cytotoxicity that is potentiated against EGFR+ disease cells and essentially not potentiated against EGFR+ keratinocyte cells.

2. The method according to claim 1, wherein the selected full antagonist EGFR antibody is cetuximab or panitumumab.

3. The method according to claim 1 or claim 2, wherein the selected anti-microtubule toxin is a maytansinoid.

4. The method according to claims 1, 2 or 3, wherein the selected linker is a non-cleavable linker, preferably SMCC.

5. An immunoconjugate comprising (i) a full antagonist EGFR antibody that binds to an EGFR epitope to which cetuximab binds, or an EGFR binding fragment of said antibody or single chain polypeptide based on said antibody, and (ii) an anti-microtubule toxin conjugated therewith, the immunoconjugate having a cytotoxic effect relative to a naked form of said antibody that is (1) potentiated with respect to EGFR+ cancer cells,

and (2) substantially unaltered with respect to EGFR+ keratinocytes, wherein the antibody and toxin are conjugated by a linker.

6. The immunoconjugate according to claim 5, wherein the antibody is cetuximab or cetuximab variant comprising one, two or more benign substitutions in the constant region.

7. The immunoconjugate according to claim 5, wherein the antibody is panitumumab.

8. The immunoconjugate according to claims 5, 6 or 7 wherein the anti-microtubule toxin is a maytansinoid.

9. The immunoconjugate according to claim 8, wherein the anti-microtubule toxin is DM-1.

10. The immunoconjugate according to claims 5-9, wherein the linker is a non-cleavable linker, preferably succinimidyl 4-(N-maleimidomethyl)-cyclohexane-1-carboxylate (SMCC).

11. The immunoconjugate according to claim 5, which is cetuximab-SMCC-DM1.

12. The immunoconjugate according to claim 5, which is panitumumab-SMCC-DM1.

13. A pharmaceutical composition comprising the immunoconjugate of claims 5-12 in an amount cytotoxic to EGFR+ disease cells, and a pharmaceutically acceptable carrier.

14. A method for producing an anti-cancer composition, comprising the step of combining a pharmaceutically acceptable carrier, and an EGFR antibody that is conjugated to an anti-microtubule toxin to form an immunoconjugate, the immunoconjugate having an effect on cancer cells that is potentiated and an effect on

keratinocytes that is essentially not potentiated, relative to the effects of the naked antibody on such cells.

15. The use of a pharmaceutical composition according to claim 13, for the treatment of EGFR+ disease cells.

16. A method for treating a subject presenting with an EGFR+ disease cell, comprising administering to the subject an amount an immunoconjugate according to claims 5-12 that is cytotoxic to the EGFR+ disease cell.

17. The method according to claim 16, wherein the EGFR+ disease cell is an EGFR+ cancer cell, such as a head and neck or colorectal cancer cell.

18. A method for potentiating the effect of a full antagonist EGFR antibody on EGFR+ disease cells without potentiating the effect thereof on normal EGFR+ cells, comprising linking the antibody to an anti-microtubule toxin by a non-cleavable linker.

19. In a method for treating a subject presenting with a tumour that responds to treatment with a full antagonist EGFR antibody, wherein treatment therewith elicits an EGFR antibody-mediated adverse response by keratinocytes, the improvement comprising treating said subject with the full antagonist EGFR antibody in a form conjugated with an anti-microtubule toxin, whereby the tumour response to treatment with conjugated antibody is enhanced essentially without enhancing the adverse keratinocyte response to treatment, relative to treatment with naked antibody alone.

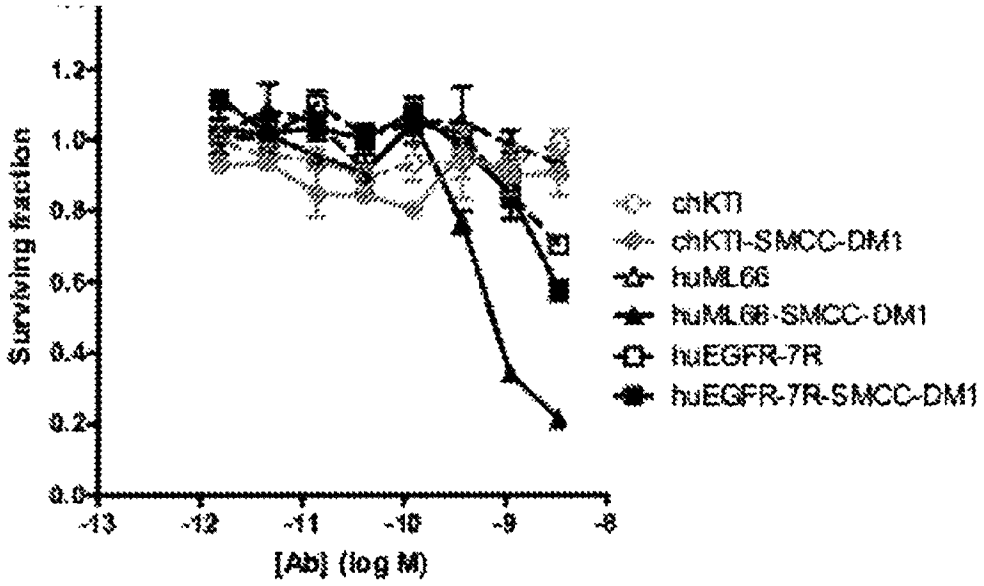


Figure 1

totox assay in cell lines independent of EGFR pathwa

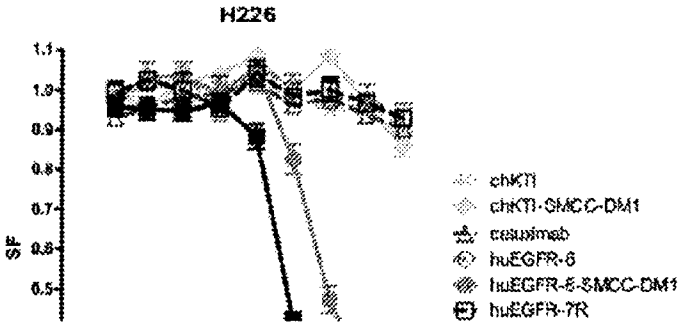


Figure 2

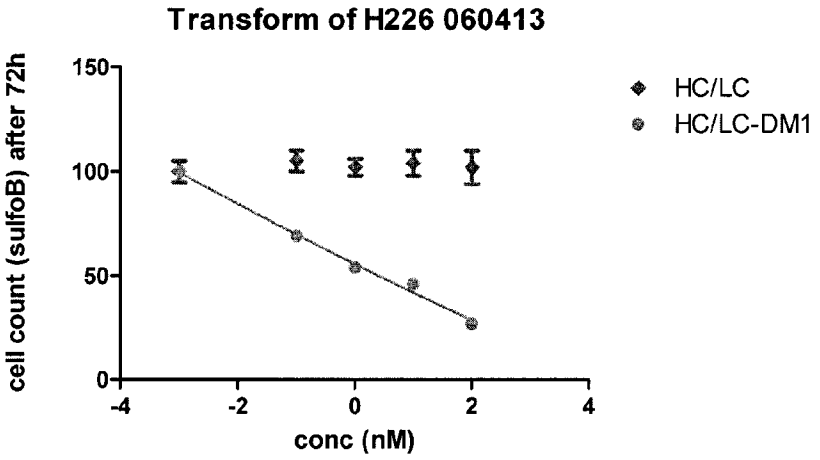


Figure 3

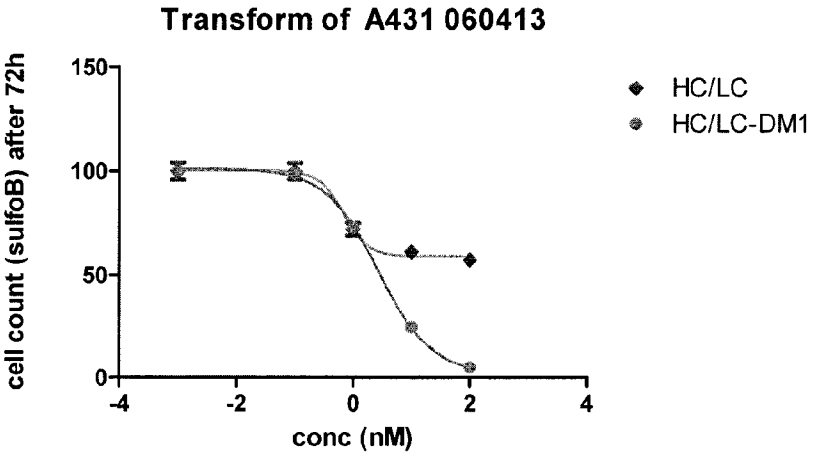


Figure 4

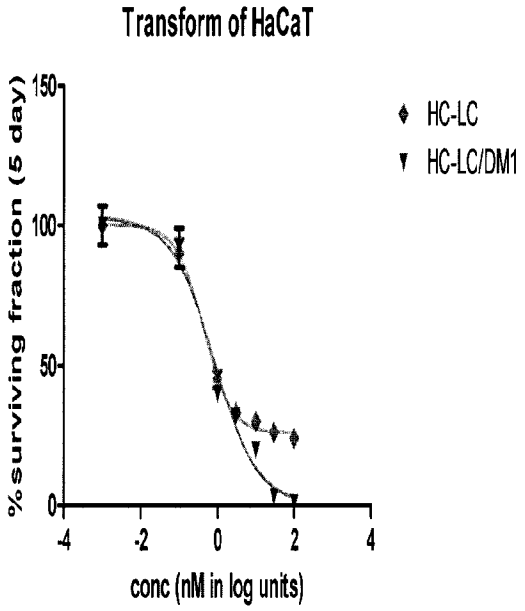


Figure 5

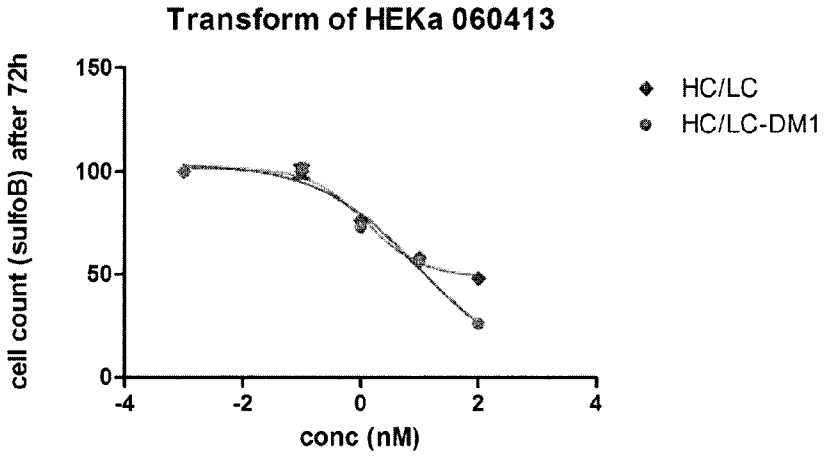


Figure 6

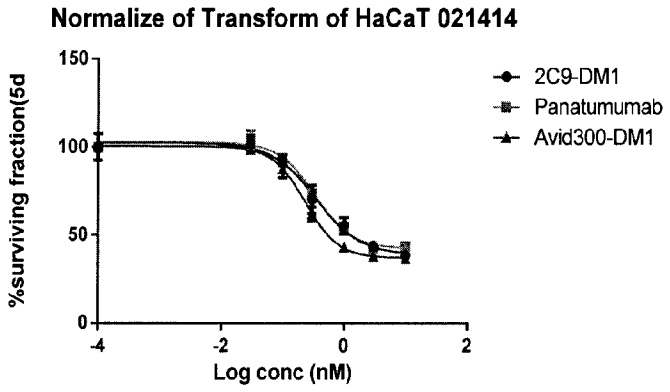


Figure 7

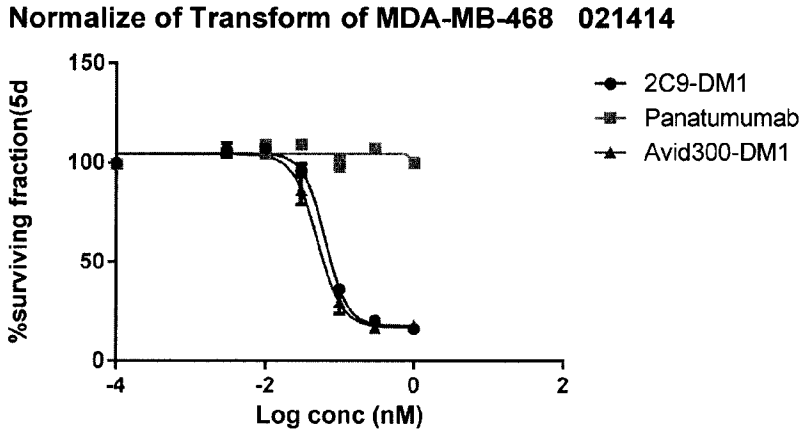


Figure 8

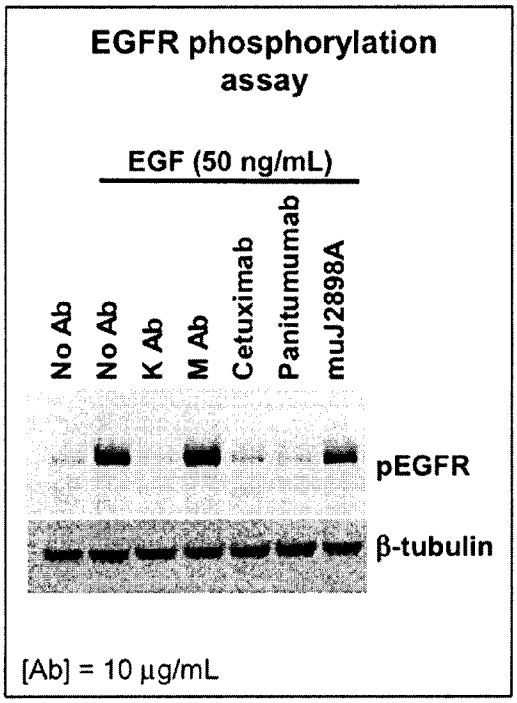


Figure 9

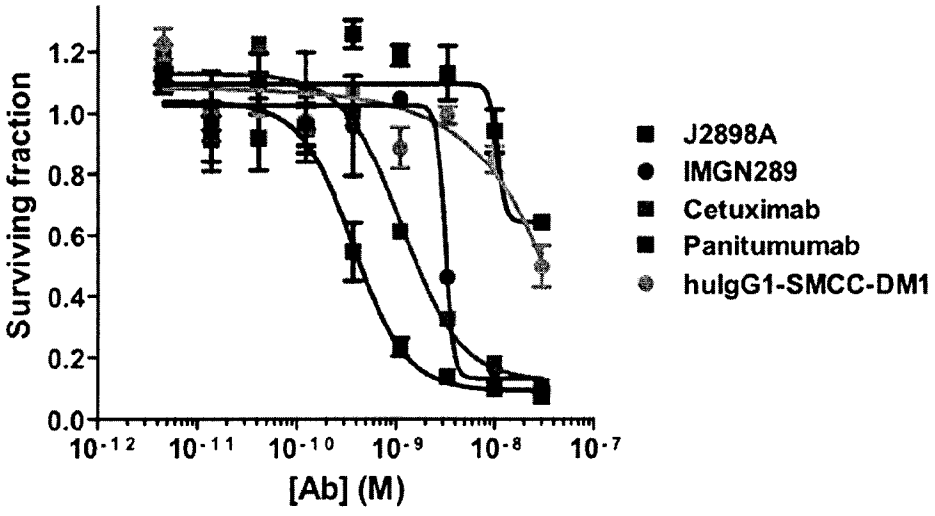


Figure 10

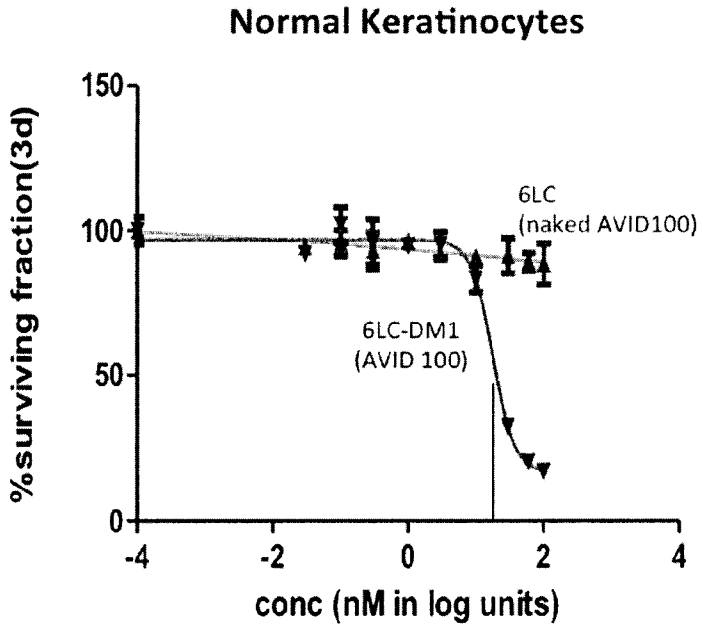


Figure 11

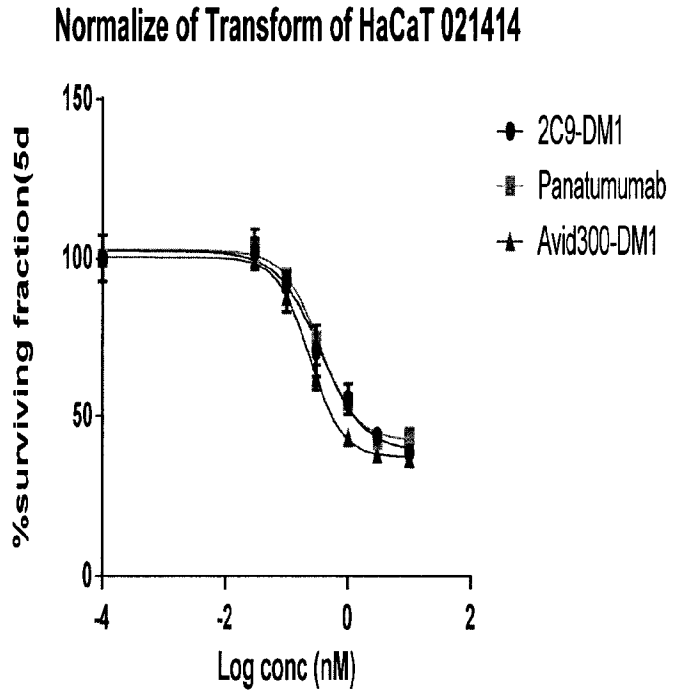


Figure 12

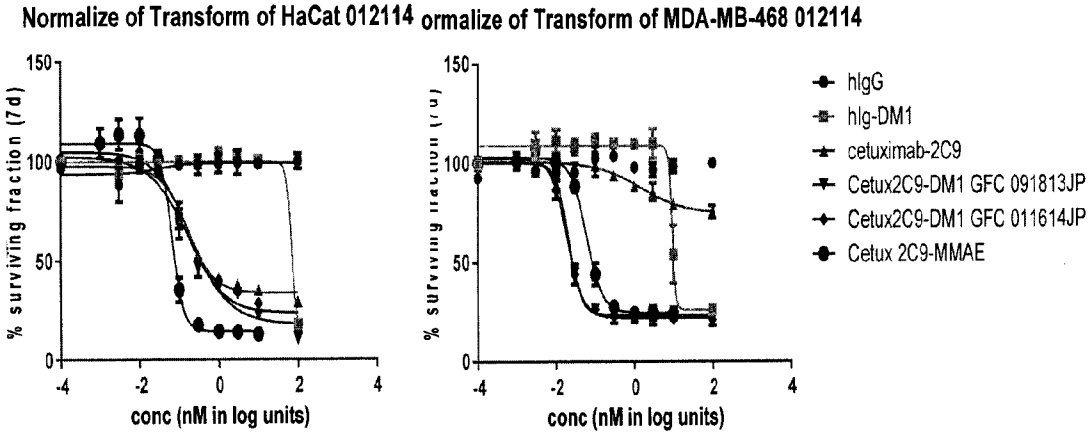

Normalize of Transform of HaCat 012114
ormalize of Transform of MDA-MB-468 012114
% surviving fraction (7d)
150
100
50
0
-4
-2
0
2
4
conc (nM in log units)
hIgG
hIg-DM1
cetuximab-2C9
Cetux2C9-DM1 GFC 091813JP
Cetux2C9-DM1 GFC 011614JP
Cetux 2C9-MMAE

Figure 13

INTERNATIONAL SEARCH REPORT

International application No.
PCT/CA2014/000543

A. CLASSIFICATION OF SUBJECT MATTER
IPC: ***C07K 16/28*** (2006.01), ***A61K 47/48*** (2006.01), ***A61P 35/00*** (2006.01)

According to International Patent Classification (IPC) or to both national classification and IPC

B. FIELDS SEARCHED

Minimum documentation searched (classification system followed by classification symbols)
IPC (2006.01): ***C07K, A61K, A61P***

Documentation searched other than minimum documentation to the extent that such documents are included in the fields searched

Electronic database(s) consulted during the international search (name of database(s) and, where practicable, search terms used)
TotalPatent, Scopus

Keywords: EGFR, antibody, cetuximab, maytansinoid, DM1, immunoconjugate, conjugate, antagonist, ErbB1, Her1

C. DOCUMENTS CONSIDERED TO BE RELEVANT

Category*	Citation of document, with indication, where appropriate, of the relevant passages	Relevant to claim No.
X Y	US2013/0156796 A1 (SETIADY, J. et al.) 20 June 2013 (20-06-2013) *paragraphs 0012-0016*	5-17 and 19 2
X Y	US2012/0156217 A1 (SETIADY, J. et al.) 21 June 2012 (21-06-2012) *Figures 2, 3 and 23, Examples 15-17, claims*	1, 3-5, 8-10 and 13-19 2, 6, 7, 11, 12

☐ Further documents are listed in the continuation of Box C. ☑ See patent family annex.

*	Special categories of cited documents:	"T"	later document published after the international filing date or priority date and not in conflict with the application but cited to understand the principle or theory underlying the invention
"A"	document defining the general state of the art which is not considered to be of particular relevance	"X"	document of particular relevance; the claimed invention cannot be considered novel or cannot be considered to involve an inventive step when the document is taken alone
"E"	earlier application or patent but published on or after the international filing date	"Y"	document of particular relevance; the claimed invention cannot be considered to involve an inventive step when the document is combined with one or more other such documents, such combination being obvious to a person skilled in the art
"L"	document which may throw doubts on priority claim(s) or which is cited to establish the publication date of another citation or other special reason (as specified)	"&"	document member of the same patent family
"O"	document referring to an oral disclosure, use, exhibition or other means		
"P"	document published prior to the international filing date but later than the priority date claimed		

Date of the actual completion of the international search 30 July 2014 (30-07-2014)	Date of mailing of the international search report 11 August 2014 (11-08-2014)
Name and mailing address of the ISA/CA Canadian Intellectual Property Office Place du Portage I, C114 - 1st Floor, Box PCT 50 Victoria Street Gatineau, Quebec K1A 0C9 Facsimile No.: 001-819-953-2476	Authorized officer Kerry Ferguson (819) 994-9451

Box No. I **Nucleotide and/or amino acid sequence(s) (Continuation of item 1.c of the first sheet)**

1. With regard to any nucleotide and/or amino acid sequence disclosed in the international application, the international search was carried out on the basis of a sequence listing filed or furnished:

a. (means)

- [x] on paper
- [ ] in electronic form

b. (time)

- [x] in the international application as filed
- [ ] together with the international application in electronic form
- [ ] subsequently to this Authority for the purposes of search

2. [ ] In addition, in the case that more than one version or copy of a sequence listing has been filed or furnished, the required statements that the information in the subsequent or additional copies is identical to that in the application as filed or does not go beyond the application as filed, as appropriate, were furnished.

3. Additional comments:

Box No. II **Observations where certain claims were found unsearchable (Continuation of item 2 of the first sheet)**

This international search report has not been established in respect of certain claims under Article 17(2)(a) for the following reasons:

1. ☑ Claim Nos.: 16, 17 and 19
because they relate to subject matter not required to be searched by this Authority, namely:

Claims 16, 17 and 19 are directed to a method for treatment of the human or animal body by surgery or therapy, which the International Searching Authority is not required to search under Rule 39.1(iv) of the PCT. However, this Authority has carried out a search based on the use of the an immunoconjugate comprising a full antagonist EGFR antibody that binds to an EGFR epitope to which cetuximab binds, or an EGFR binding fragment of said antibody or single chain polypeptide based on said antibody, conjugated to an anti-microtubule toxin by a linker for treating a subject presenting with an EGFR+ disease cell or a tumor that responds to treatment with a full antagonist EGFR antibody.

2. ☐ Claim Nos.:
because they relate to parts of the international application that do not comply with the prescribed requirements to such an extent that no meaningful international search can be carried out, specifically:

3. ☐ Claim Nos.:
because they are dependent claims and are not drafted in accordance with the second and third sentences of Rule 6.4(a).

Box No. III **Observations where unity of invention is lacking (Continuation of item 3 of first sheet)**

This International Searching Authority found multiple inventions in this international application, as follows:

1. ☐ As all required additional search fees were timely paid by the applicant, this international search report covers all searchable claims.

2. ☐ As all searchable claims could be searched without effort justifying additional fees, this Authority did not invite payment of additional fees.

3. ☐ As only some of the required additional search fees were timely paid by the applicant, this international search report covers only those claims for which fees were paid, specifically claim Nos.:

4. ☐ No required additional search fees were timely paid by the applicant. Consequently, this international search report is restricted to the invention first mentioned in the claims; it is covered by claim Nos.:

Remark on Protest

☐ The additional search fees were accompanied by the applicant=s protest and, where applicable, the payment of a protest fee.

☐ The additional search fees were accompanied by the applicant's protest but the applicable protest fee was not paid within the time limit specified in the invitation.

☐ No protest accompanied the payment of additional search fees.

INTERNATIONAL SEARCH REPORT
Information on patent family members

International application No.
PCT/CA2014/000543

Patent Document Cited in Search Report	Publication Date	Patent Family Member(s)	Publication Date
US2013/0156796 A1	20 June 2013 (20-06-2013)	WO2013078271A1	30 May 2013 (30-05-2013)
		AU2012340686A1	19 June 2014 (19-06-2014)
US2012/0156217 A1	21 June 2012 (21-06-2012)	WO2012158588A2	03 May 2012 (03-05-2012)
		WO2012158588A3	18 October 2012 (18-10-2012)
		WO2012158588A4	06 December 2012 (06-12-2012)
		AU2011320314A1	11 April 2013 (11-04-2013)
		CA2815277A1	03 May 2012 (03-05-2012)
		CN103298489A	11 September 2013 (11-09-2013)
		EA201390472A1	28 February 2014 (28-02-2014)
		JP2014500711A	16 January 2014 (16-01-2014)
		KR20140008308A	21 January 2014 (21-01-2014)
		MX2013004761A	27 August 2013 (27-08-2013)
		SG189929A1	28 June 2013 (28-06-2013)
		US2014099308A1	10 April 2014 (10-04-2014)
		US8790649B2	29 July 2014 (29-07-2014)

PTO/SB/08a (03-15)
Approved for use through 07/31/2016. OMB 0651-0031
U.S. Patent and Trademark Office; U.S. DEPARTMENT OF COMMERCE
Under the Paperwork Reduction Act of 1995, no persons are required to respond to a collection of information unless it contains a valid OMB control number.

INFORMATION DISCLOSURE STATEMENT BY APPLICANT

(Not for submission under 37 CFR 1.99)

Application Number	
Filing Date	
First Named Inventor	Hu, Chaohong
Art Unit	
Examiner Name	
Attorney Docket Number	CCPIT-002

U.S.PATENTS Remove

Examiner Initial*	Cite No	Patent Number	Kind Code[1]	Issue Date	Name of Patentee or Applicant of cited Document	Pages,Columns,Lines where Relevant Passages or Relevant Figures Appear
	1					

If you wish to add additional U.S. Patent citation information please click the Add button. Add

U.S.PATENT APPLICATION PUBLICATIONS Remove

Examiner Initial*	Cite No	Publication Number	Kind Code[1]	Publication Date	Name of Patentee or Applicant of cited Document	Pages,Columns,Lines where Relevant Passages or Relevant Figures Appear
	1					

If you wish to add additional U.S. Published Application citation information please click the Add button. Add

FOREIGN PATENT DOCUMENTS Remove

Examiner Initial*	Cite No	Foreign Document Number[3]	Country Code[2] i	Kind Code[4]	Publication Date	Name of Patentee or Applicant of cited Document	Pages,Columns,Lines where Relevant Passages or Relevant Figures Appear	T[5]
/KAC/	1	WO 2014152199	WO		2014-09-25	ABBVIE INC		
/KAC/	2	CN 103772504	CN		2014-05-07	SHANGHAI JMT BIOTECHNOLOGY CO LTD		

If you wish to add additional Foreign Patent Document citation information please click the Add button Add

NON-PATENT LITERATURE DOCUMENTS Remove

INFORMATION DISCLOSURE STATEMENT BY APPLICANT (Not for submission under 37 CFR 1.99)		
	Application Number	
	Filing Date	
	First Named Inventor	Hu, Chaohong
	Art Unit	
	Examiner Name	
	Attorney Docket Number	CCPIT-002

Examiner Initials*	Cite No	Include name of the author (in CAPITAL LETTERS), title of the article (when appropriate), title of the item (book, magazine, journal, serial, symposium, catalog, etc), date, pages(s), volume-issue number(s), publisher, city and/or country where published.	T[5]
	1		

If you wish to add additional non-patent literature document citation information please click the Add button Add

EXAMINER SIGNATURE

Examiner Signature	/Karen A. Canella/	Date Considered	03/31/2019

*EXAMINER: Initial if reference considered, whether or not citation is in conformance with MPEP 609. Draw line through a citation if not in conformance and not considered. Include copy of this form with next communication to applicant.

[1] See Kind Codes of USPTO Patent Documents at www.USPTO.GOV or MPEP 901.04. [2] Enter office that issued the document, by the two-letter code (WIPO Standard ST.3). [3] For Japanese patent documents, the indication of the year of the reign of the Emperor must precede the serial number of the patent document. [4] Kind of document by the appropriate symbols as indicated on the document under WIPO Standard ST.16 if possible. [5] Applicant is to place a check mark here if English language translation is attached.

INFORMATION DISCLOSURE STATEMENT BY APPLICANT (Not for submission under 37 CFR 1.99)		
	Application Number	
	Filing Date	
	First Named Inventor	Hu, Chaohong
	Art Unit	
	Examiner Name	
	Attorney Docket Number	CCPIT-002

CERTIFICATION STATEMENT

Please see 37 CFR 1.97 and 1.98 to make the appropriate selection(s):

That each item of information contained in the information disclosure statement was first cited in any communication from a foreign patent office in a counterpart foreign application not more than three months prior to the filing of the information disclosure statement. See 37 CFR 1.97(e)(1).

OR

☐ That no item of information contained in the information disclosure statement was cited in a communication from a foreign patent office in a counterpart foreign application, and, to the knowledge of the person signing the certification after making reasonable inquiry, no item of information contained in the information disclosure statement was known to any individual designated in 37 CFR 1.56(c) more than three months prior to the filing of the information disclosure statement. See 37 CFR 1.97(e)(2).

See attached certification statement.

The fee set forth in 37 CFR 1.17 (p) has been submitted herewith.

☒ A certification statement is not submitted herewith.

SIGNATURE

A signature of the applicant or representative is required in accordance with CFR 1.33, 10.18. Please see CFR 1.4(d) for the form of the signature.

Signature	/James S. Keddie/	Date (YYYY-MM-DD)	2017-08-14
Name/Print	James S. Keddie	Registration Number	48920

This collection of information is required by 37 CFR 1.97 and 1.98. The information is required to obtain or retain a benefit by the public which is to file (and by the USPTO to process) an application. Confidentiality is governed by 35 U.S.C. 122 and 37 CFR 1.14. This collection is estimated to take 1 hour to complete, including gathering, preparing and submitting the completed application form to the USPTO. Time will vary depending upon the individual case. Any comments on the amount of time you require to complete this form and/or suggestions for reducing this burden, should be sent to the Chief Information Officer, U.S. Patent and Trademark Office, U.S. Department of Commerce, P.O. Box 1450, Alexandria, VA 22313-1450. DO NOT SEND FEES OR COMPLETED FORMS TO THIS ADDRESS. **SEND TO: Commissioner for Patents, P.O. Box 1450, Alexandria, VA 22313-1450.**

Privacy Act Statement

The Privacy Act of 1974 (P.L. 93-579) requires that you be given certain information in connection with your submission of the attached form related to a patent application or patent. Accordingly, pursuant to the requirements of the Act, please be advised that: (1) the general authority for the collection of this information is 35 U.S.C. 2(b)(2); (2) furnishing of the information solicited is voluntary; and (3) the principal purpose for which the information is used by the U.S. Patent and Trademark Office is to process and/or examine your submission related to a patent application or patent. If you do not furnish the requested information, the U.S. Patent and Trademark Office may not be able to process and/or examine your submission, which may result in termination of proceedings or abandonment of the application or expiration of the patent.

The information provided by you in this form will be subject to the following routine uses:

1. The information on this form will be treated confidentially to the extent allowed under the Freedom of Information Act (5 U.S.C. 552) and the Privacy Act (5 U.S.C. 552a). Records from this system of records may be disclosed to the Department of Justice to determine whether the Freedom of Information Act requires disclosure of these record s.

2. A record from this system of records may be disclosed, as a routine use, in the course of presenting evidence to a court, magistrate, or administrative tribunal, including disclosures to opposing counsel in the course of settlement negotiations.

3. A record in this system of records may be disclosed, as a routine use, to a Member of Congress submitting a request involving an individual, to whom the record pertains, when the individual has requested assistance from the Member with respect to the subject matter of the record.

4. A record in this system of records may be disclosed, as a routine use, to a contractor of the Agency having need for the information in order to perform a contract. Recipients of information shall be required to comply with the requirements of the Privacy Act of 1974, as amended, pursuant to 5 U.S.C. 552a(m).

5. A record related to an International Application filed under the Patent Cooperation Treaty in this system of records may be disclosed, as a routine use, to the International Bureau of the World Intellectual Property Organization, pursuant to the Patent Cooperation Treaty.

6. A record in this system of records may be disclosed, as a routine use, to another federal agency for purposes of National Security review (35 U.S.C. 181) and for review pursuant to the Atomic Energy Act (42 U.S.C. 218(c)).

7. A record from this system of records may be disclosed, as a routine use, to the Administrator, General Services, or his/her designee, during an inspection of records conducted by GSA as part of that agency's responsibility to recommend improvements in records management practices and programs, under authority of 44 U.S.C. 2904 and 2906. Such disclosure shall be made in accordance with the GSA regulations governing inspection of records for this purpose, and any other relevant (i.e., GSA or Commerce) directive. Such disclosure shall not be used to make determinations about individuals.

8. A record from this system of records may be disclosed, as a routine use, to the public after either publication of the application pursuant to 35 U.S.C. 122(b) or issuance of a patent pursuant to 35 U.S.C. 151. Further, a record may be disclosed, subject to the limitations of 37 CFR 1.14, as a routine use, to the public if the record was filed in an application which became abandoned or in which the proceedings were terminated and which application is referenced by either a published application, an application open to public inspections or an issued patent.

9. A record from this system of records may be disclosed, as a routine use, to a Federal, State, or local law enforcement agency, if the USPTO becomes aware of a violation or potential violation of law or regulation.

Cancer Biology & Therapy

ISSN: 1538-4047 (Print) 1555-8576 (Online) Journal homepage: https://www.tandfonline.com/loi/kcbt20

Molecular mechanisms of resistance to the EGFR monoclonal antibody cetuximab

Toni M. Brand, Mari Iida & Deric L. Wheeler

To cite this article: Toni M. Brand, Mari Iida & Deric L. Wheeler (2011) Molecular mechanisms of resistance to the EGFR monoclonal antibody cetuximab, Cancer Biology & Therapy, 11:9, 777-792, DOI: 10.4161/cbt.11.9.15050

To link to this article: https://doi.org/10.4161/cbt.11.9.15050

Published online: 01 May 2011.

Submit your article to this journal

Article views: 855

Citing articles: 91 View citing articles

Full Terms & Conditions of access and use can be found at
https://www.tandfonline.com/action/journalInformation?journalCode=kcbt20

CSPC Exhibit 1004
Page 105 of 336

Cancer Biology & Therapy 11:9, 777-792; May 1, 2011; © 2011 Landes Bioscience

Molecular mechanisms of resistance to the EGFR monoclonal antibody cetuximab

Toni M. Brand, Mari Iida and Deric L. Wheeler*

Department of Human Oncology; University of Wisconsin School of Medicine and Public Health; Madison, WI USA

Key words: EGFR, cetuximab, resistance

Abbreviations: AR, amphiregulin; BTC, betacellulin; Cbl, casitas B-lineage lymphoma; CRC, colorectal cancer; DAG, diacyglycerol; EGF, epidermal growth factor; EGFR, epidermal growth factor receptor; EMT, epithelial to mesenchymal transition; ER, endoplasmic reticulum; EPR, epiregulin; ERK, extracellular signal-regulated kinase; FACS, fluorescence-activated cell sorting; FDA, food and drug administration; FGFR, fibroblast growth factor receptor; GAPs, GTPase activating proteins; GSKα/β, glycogen synthase kinase alpha and beta; HAMA, human anti-mouse antibody; HB-EGF, heparin-binding epidermal growth factor; HER2, human epidermal growth factor receptor 2; HER3, human epidermal growth factor receptor 3; HNSCC, head and neck squamous cell carcinoma; IF, immunoflourescence; IGF1R, insulin-like growth factor receptor 1; IgG, immunoglobulin G; IHC, immunohistochemistry; ILK, integrin linked kinase; IP_3, inositol triphosphate; mAb, monoclonal antibody; mCRC, metastatic colorectal cancer; MAPK, mitogen-activated protein kinase; MDGI, mammary-derived growth inhibitor; MEK, MAPK kinase; miRs, microRNAs; mTORC, mammalian target for rapamycin; MSK, mitogen and stress-activated protein kinase; nRTK, non-receptor tyrosine kinase; NLS, nuclear localization signal; NRG, neuregulins; NSCLC, non-small cell lung cancer; PI3K, phosphatidylinositol 3-kinase; PDGFR, platelet derived growth factor receptor; PDK1, phosphoinositide-dependent kinase 1; PFS, progression-free survival; PH, pleckstrin homology; PIP_2, phosphatidylinositol-4,5-bisphosphate; PIP_3, phosphatidylinositol (3,4,5)-trisphosphate; PLCγ, phospholipase C-gamma; PKC, protein kinase C; PPARγ, peroxisome-proliferator-activated receptor γ; PTEN, phosphatase and tensin homologue deleted in chromosome 10; RSK, ribosomal s6 kinase; RTK, receptor tyrosine kinase; SFKs, Src-family kinases; SH2, src homology; STAT, signal transducer and activator of transcription; TGFα, transforming growth factor receptor alpha; TUNEL, terminal deoxynucleotidyl transferase-mediated dUTP nick end labeling; TKD, tyrosine kinase domain; TKIs, tyrosine kinase inhibitors; TSC2, tuberous sclerosis protein complex 2; VEGF, vascular endothelial growth factor; VEGFR, vascular endothelial growth factor receptor 2

The epidermal growth factor receptor (EGFR) is a receptor tyrosine kinase belonging to the HER family of receptor tyrosine kinases. Receptor activation upon ligand binding leads to down stream activation of the PI3K/AKT, RAS/RAF/MEK/ERK and PLCγ/PKC pathways that influence cell proliferation, survival and the metastatic potential of tumor cells. Increased activation by gene amplification, protein overexpression or mutations of the EGFR has been identified as an etiological factor in a number of human epithelial cancers (e.g., NSCLC, CRC, glioblastoma and breast cancer). Therefore, targeting the EGFR has been intensely pursued as a cancer treatment strategy over the last two decades. To date, five EGFR inhibitors, including three small molecule tyrosine kinase inhibitors (TKIs) and two monoclonal antibodies have gained FDA approval for use in oncology. Both approaches to targeting the EGFR have shown clinical promise and the anti-EGFR antibody cetuximab is used to treat HNSCC and CRC. Despite clinical gains arising from use of cetuximab, both intrinsic resistance and the development of acquired resistance are now well recognized. In this review we focus on the biology of the EGFR, the role of EGFR in human cancer, the development of antibody-based anti-EGFR therapies and a summary of their clinical successes. Further, we provide an in depth discussion of described molecular mechanisms of resistance to cetuximab and potential strategies to circumvent this resistance.

*Correspondence to: Deric L. Wheeler; Email: dlwheeler@wisc.edu
Submitted: 11/17/10; Accepted: 11/22/10
DOI: 10.4161/cbt.11.9.15050

Introduction

Approximately 40 years ago, Graham Carpenter performed experiments identifying the presence of specific binding receptors for EGF on human fibroblast cells.[1] In 1975, Carpenter and coworkers identified the epidermal growth factor receptor (EGFR) as a 170 KDa membrane protein that increased ^{32}P incorporation in response to EGF treatment of A431 epidermoid carcinoma cells.[2] In 1984, a group of collaborators isolated, cloned and sequenced the human EGFR from normal placental cells and A431 tumor cells.[3] During this same time frame, it was discovered that modification of proteins by phosphorylation on tyrosine residues might be a critical step in tumorigenesis.[4,5] Shortly after these discoveries EGFR was recognized as a receptor protein tyrosine kinase. This two-decade effort led to the identification of the prototypical receptor tyrosine kinase (RTK) and its ligand. The identification of EGFR as a RTK contributed to pivotal studies advancing our understanding of RTK activation[6,7]

CSPC Exhibit 1004
Page 106 of 336

and phosphorylation. Elucidation of EGFR regulation of downstream signaling also contributed to understanding critical pathways involved in cell proliferation and survival.

During the 1980s, several reports described the overexpression of EGFR in a variety of epithelial tumors supporting the hypothesis that dysregulated EGFR expression and signaling play a critical role in the etiology of human cancers. These findings led to hallmark studies designed to target EGFR via two fundamental approaches. The first approach was the development of an antibody directed against the EGFR extracellular domain. The second approach focused on the rational design of anti-EGFR small-molecule tyrosine kinase inhibitors. Both targeting approaches have proved clinically useful, however, resistance (intrinsic and acquired) to both modalities is a serious treatment issue. Understanding the molecular mechanisms of resistance to EGFR inhibitors is vitally important and will lead to improvement of these promising molecular targeting agents and increased benefit to patients. In this review, we focus on the biology of EGFR, the role of EGFR in human cancer, the development of antibody-based anti-EGFR therapies, and a summary of their clinical successes. Further, we provide an in depth discussion of known molecular mechanisms of resistance to the EGFR antibody cetuximab and potential strategies to overcome resistance to antibody therapy.

EGFR Biology

Aberrant expression or activity of the EGFR has been identified as an important biological factor in many human epithelial cancers including head and neck squamous cell carcinoma (HNSCC), non-small cell lung cancer (NSCLC), colorectal cancer (CRC), breast, pancreatic and brain cancer. EGFR is a member of the EGF receptor tyrosine kinase family, which consists of the EGFR (ErbB1/HER1), HER2/neu (ErbB2), HER3 (ErbB3) and HER4 (ErbB4). These receptors contain an extracellular ligand-binding domain (domains I–IV), a single membrane-spanning region, a juxtamembrane nuclear localization signal (NLS), a cytoplasmic tyrosine kinase domain (TKD) and a C-terminal tail housing several tyrosine residues for propagating down stream signaling.

HER receptors are ubiquitously expressed in various cell types, but primarily include those of epithelial, mesenchymal and neuronal origin. Under homeostatic conditions, receptor activation is tightly regulated by the availability of ligands, which collectively form the EGF growth factor family. This family is divided into three distinct groups. The first includes EGF, transforming growth factor alpha (TGFα) and amphiregulin (AR), which all bind specifically to EGFR. The second group includes betacellulin (BTC), heparin-binding EGF (HB-EGF) and epiregulin (EPR), which bind to both EGFR and HER4. The third group is composed of the neuregulins (NRG1-4) and is further subdivided based on their ability to bind both HER3 and HER4 (NRG1 and NRG2) or only HER4 (NRG3 and NRG4) (reviewed in ref. 8 and 9). HER2 has no known ligand.[10]

Ligand precursors are cleaved by ADAM proteases at the cell surface and are subsequently secreted. EGFR ligands can participate in autocrine, paracrine, juxtacrine and/or endocrine activation of EGFR.[11] Ligand binding to the leucine-rich repeats in domains I and III of the EGFR extracellular domain triggers a conformational change in the receptor that exposes the dimerization loop (domain II) to other receptors on the cell surface (reviewed in ref. 12). Exposure of domain II allows for homo- or heterodimerization with other HER family members, activating EGFR kinase function. This induces both autophosphorylation and transphosphorylation of the C-terminal cytoplasmic tails of the receptor pairs. HER3 is the only family member that lacks intrinsic kinase activity,[13] however, downstream signaling is readily achieved through heterodimerization.[14]

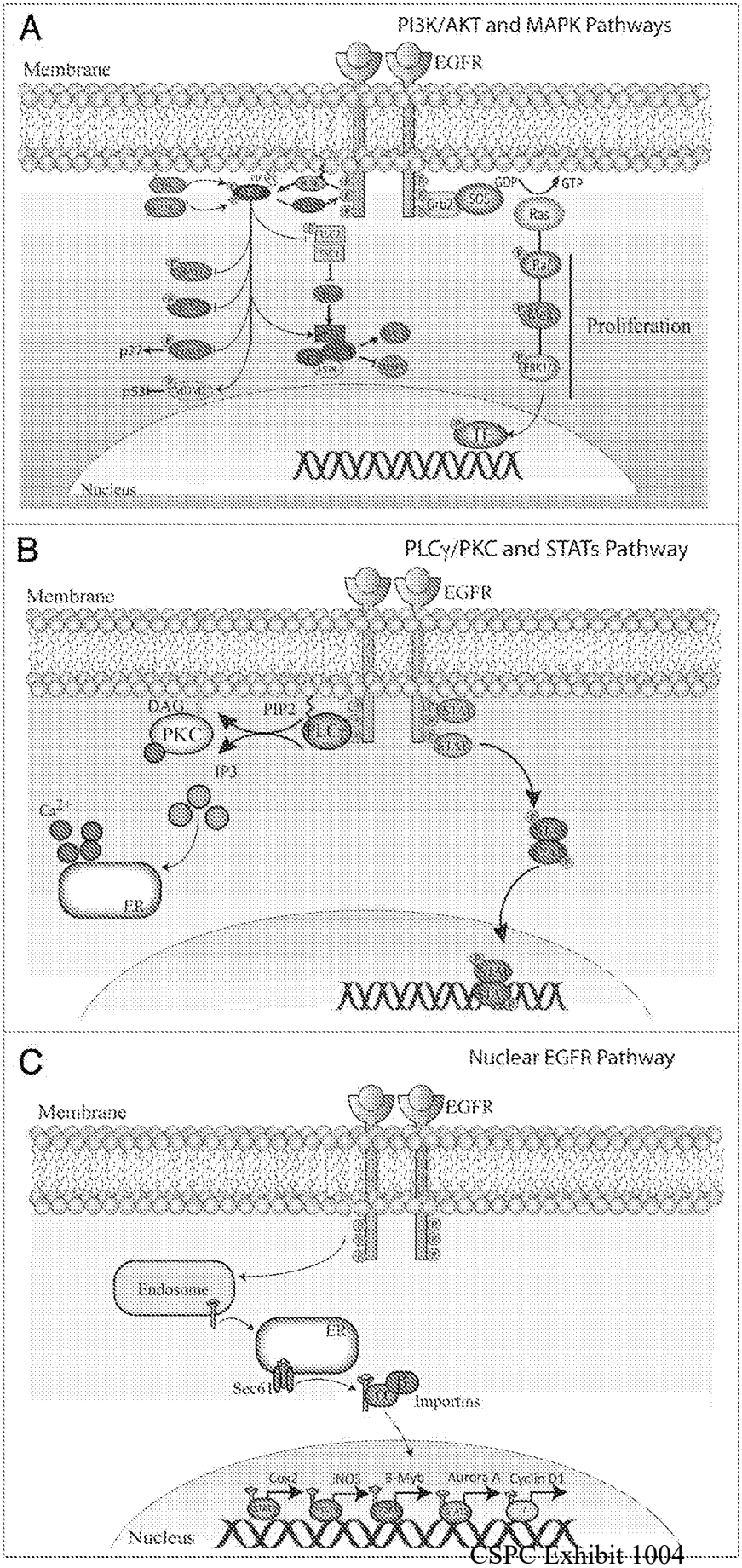
Phosphorylated cytoplasmic tails serve as docking sites for numerous proteins that contain Src Homology 2 (SH2) and phosphotyrosine binding domains. EGFR activation stimulates many complex intracellular signaling pathways tightly regulated by the presence and identity of ligand, heterodimer composition and availability of phosphotyrosine-binding proteins. The three primary signaling pathways activated by EGFR include the RAS/RAF/MEK/ERK, PI3K/AKT and PLCγ/PKC axes; however, SRC tyrosine kinases and STAT activation have also been well documented. The intersections of those pathways are shown in **Figure 1.**

Figure 1A (right) illustrates the RAS/RAF/MEK/ERK pathway, which leads to cell proliferation and is a central element in many human tumors (reviewed in ref. 15). After activation and subsequent autophosphorylation, C-terminal phospho-tyrosine residues on RTKs including PDGFR, VEGFR, HER and FGFR act as binding sites for the SH2-domain-containing protein Grb2. Grb2 recruits the guanine nucleotide exchange factor SOS via its SH3 domain, and promotes binding of GTP to Ras, a small G-protein responsible for activation of the MAPK cascade. Ras-GTP initiates this cascade by binding to and activating the RAF kinase (MAPKKK). Activated RAF in turn binds to and phosphorylates MEK (MAPKK), which then phosphorylates ERK1/2 (MAPK). Upon activation, ERK kinases can translocate to the nucleus and activate several other kinases including MNK1 and MNK2, MSK1 and MSK2, and RSK. MAPK can also phosphorylate several transcription factors including Elk-1, peroxisome-proliferator-activated receptor γ (PPARγ), signal transducer and activator of transcription 1 and 3 (STAT1 and STAT3), C-myc and AP-1. Activation of transcription factors leads to an increased transcription of genes involved in cellular proliferation, most notably cyclin D1.

Growth factor binding to RTKs also initiates the PI3K/AKT/mTOR pathway (**Fig. 1A**, left) (reviewed in ref. 16). Activated RTKs can recruit PI3K to the cell membrane. PI3K phosphorylation of phosphatidylinositol-4,5-bisphosphate (PIP_2) yields the second messenger phosphatidylinositol (3,4,5)-trisphosphate (PIP_3). PIP_3 serves as a membrane-docking site for the serine/threonine protein kinase AKT, which binds to PIP_3 with high affinity through its pleckstrin homology (PH) domain. Once positioned on the plasma membrane, AKT is phosphorylated by two kinases, phosphoinositide dependent kinase 1 (PDK1) and the mammalian target of rapamycin complex 2 (mTORC2), leading to its full activation. Phosphorylated AKT regulates a variety of different substrates, influencing cell survival, proliferation

CSPC Exhibit 1004
Page 107 of 336

Figure 1. EGFR biology. Ligand binding to domains I and III of the EGFR expose the dimerization loop in domain II and induce receptor homo- or hetero-dimerization. This process activates the intrinsic tyrosine kinase activity of the EGFR and leads to the phosphorylation of specific tyrosines on the cytoplasmic tails of the receptor pair. These phospho-tyrosines serve to recruit specific effector molecules containing SH2 or PTB domains. These effector molecules recruit and induce various signaling pathways including the PI3K/AKT (A), RAS/MAPK (A), PLCγ/PKC (B) and STAT (B) pathways. In addition, a less appreciated pathway, the nuclear EGFR signaling pathway (C), is initiated upon ligand binding and induces EGFR translocation to the nucleus where it behaves as a co-transcriptional activator regulating key genes such as Cox2, iNOS, B-myb, Aurora kinase A and Cyclin D1.



and cellular metabolism. One main effector of AKT activation is the mammalian target for rapamycin complex 1 (mTORC1). The activation of mTORC1 is regulated by AKT via the tuberous sclerosis protein complex 2 (TSC2). Phosphorylation of TSC2 by AKT cancels inhibition of the small G-protein, Ras homolog enriched in brain (RHEB), allowing binding to the mTOR catalytic domain, activating the intrinsic kinase function of mTOR. mTOR is a serine/threonine kinase having two well studied substrates, p70-S6 kinase 1 and 4E-BP1. Phosphorylation of p70-S6 kinase 1 by mTOR leads to activation and initiation of protein synthesis via the S6 ribosomal subunit. Additionally, phosphorylation of 4E-BP1 cancels inhibition of the translation initiation factor eIF4E. Overall, the activation of protein synthesis is pivotal to cancer cell growth and survival, consistent with the anticancer effects of the mTOR inhibitor rapamycin. PIP_3 is dephosphorylated to yield PIP_2 by the tumor suppressor protein PTEN (phosphatase and tensin homologue deleted in chromosome 10), which attenuates AKT signaling.

The protein kinase C (PKC) pathway (**Fig. 1B**, left) also plays an important role in mediating the effects of activated growth factor receptors including EGFR (reviewed in ref. 17–20). After EGFR activation, phospholipase C (PLC) interacts with phospho-tyrosine sites on EGFR via its SH2 domain. This leads to the specific phosphorylation of PLC by EGFR and dissociation from EGFR. Activated PLC in turn interacts with the plasma membrane, most likely mediated by PIP_3 via a PH domain, where it cleaves PIP_2 to inositol triphosphate (IP_3) and diacyglycerol (DAG). IP_3 can diffuse into the cytosol and bind IP_3 receptors on the

CSPC Exhibit 1004
Page 108 of 336

endoplasmic reticulum (ER) to induce calcium influx into the cell from the ER. DAG remains in the membrane where it can activate PKC via a conformational change that removes the pseudosubstrate region from the catalytic active site. Activated PKC is a potent serine/threonine kinase second messenger, capable of phosphorylating a plethora of substrates ultimately leading to complex cellular process including proliferation, apoptosis, cell survival and cell migration.

A new and less well-characterized EGFR signaling network, the nuclear EGFR signaling network (**Fig. 1C**), has emerged over the last decade and been implicated in both cancer progression and response to molecular targeting agents. EGFR is consistently detected in the nuclei of cancer cells, primary tumor specimens, and other highly proliferative tissues.[21-25] Increased nuclear EGFR localization correlates with poor clinical outcome in patients with breast cancer,[26] oropharyngeal SCC[27] and ovarian cancer.[28] Recent reports have characterized a novel nuclear localization sequence in EGFR and its family members.[29-31] Furthermore, transport mechanisms for EGFR to the nucleus have been described previously.[32] These mechanisms involve ligand binding, dimerization, activation and internalization. Endosomal sorting to the ER allows EGFR to associate with the Sec61 translocon for transport from the ER to the cytoplasm.[33] Here, EGFR binds importin β, which facilitates movement into the nucleus.[32] Nuclear EGFR is known to regulate the promoters of several target genes including, Cyclin D1,[23] iNOS,[29] B-myb,[34] Aurora Kinase A[35] and COX2.[31] Mechanisms of EGFR-mediated gene regulation involve direct interaction of EGFR with STAT3 to regulate iNOS[29] and COX2,[31] promoters, with STAT5 for regulation of the Aurora Kinase A promoter,[35] and with E2F1 transcription factors for regulation of the B-Myb promoter.[34] Nuclear EGFR has also recently been shown to function as a tyrosine kinase in the nucleus, phosphorylating and stabilizing PCNA and thus enhancing the proliferative potential of cancer cells.[36] In addition to ligand induced translocation of the EGFR to the nucleus, radiation induces EGFR transport to the nucleus mediated by the Src family kinases (SFKs).[37] Cetuximab, a monoclonal antibody targeting EGFR, also leads to EGFR translocation to the nucleus.[38] Collectively, these findings suggest that EGF ligand, radiation and cetuximab enhance the nuclear accumulation of EGFR. As data accrues suggesting a functional impact of nuclear EGFR, it becomes important to understand the extent to which nuclear EGFR may contribute to cancer growth and progression, as well as its effect on the therapeutic response to EGFR targeted therapies.

Attenuation of EGFR signaling is as crucial to the biology of EGFR as activation. The attenuation of the EGFR involves numerous processes including receptor ubiquitinylation, dephosphorylation, depletion of ligand access, receptor trafficking to the lysosome and subsequent destruction.[39] Clathrin-mediated endocytosis represents the major pathway by which activated surface associated EGFR is quickly internalized and degraded.[40-44] This process is well characterized and involves numerous steps.

Ligand binding and dimerization of EGFR results in phosphorylation of tyrosine residues on EGFR's C-terminal domain. Two of these residues, Y1068 and Y1086, serve as the major binding site for the Grb2 adaptor protein (**Fig. 1A**). The SH2 domain of Grb2 binds to phospho-tyrosines on EGFR, while SH3 domains of Grb2 bind other proteins coupling them to EGFR. One of the most recognized Grb2-interacting proteins is casitas B-lineage lymphoma (Cbl), a ring finger-containing E3 ubiquitin ligase. Cbl can directly bind to EGFR Y1045 and recruit E2 enzymes (UbcH4/5) to its ring domain to promote EGFR ubiquitination. Ubiquitinated EGFR is quickly recognized by the ubiquitin-binding domains of epsin, Eps15, Eps15R and Hrs/Hgs,[45,46] proteins strongly associated with clathrin. Clathrin-coated vesicles containing ubiquitinated EGFR fuse with early endosomes and interact with the endosomal sorting complex required for transport (ESCRT), which directs the ubiquitinated EGF:EGFR complex to the lysosome for degradation.

Endocytosis of EGFR doesn't always lead to its destruction; EGFR can be recycled back to the cell surface, remain active in intracellular compartments, or completely circumvent endocytosis.[39] Modulation of EGFR trafficking arises both from mutations and from overexpression and/or dimerization with other HER family members.[47-53] Recently, HER2 overexpression was shown to alter EGFR degradation by competitively binding endosomal retention components preventing their binding to EGFR.[54]

The Role of EGFR in Human Cancers

Over the past three decades, numerous reports described overexpression, increased activity or mutations of EGFR in various human epithelial tumors, strengthening the view that deregulated EGFR activity may be a causative factor in the etiology of human epithelial cancers. Most notably, deregulated EGFR activity has been linked to the development, progression and metastatic spread of HNSCC, NSCLC, CRC, breast, ovarian, cervical, bladder, pancreatic, gastric, endometrial and brain cancer.[3,55-71] In many of these cancers, EGFR expression is associated with decreased overall survival rates.[72] Modes of deregulated EGFR activity have included increased stimulation of the EGFR through ligand binding,[73] point mutations within the receptor,[74] deletion mutants of exons 2–7 of the EGFR (EGFRvIII),[75] impaired downregulation of the EGFR,[76] and gene amplification of the EGFR loci.[75] Collectively, these findings demonstrate the importance of EGFR in human cancers and the need to develop inhibitors that effectively target the activity of this RTK.

EGFR Targeted Antibodies: Discovery and Function

Targeting EGFR has been intensely pursued over the last three decades as a treatment strategy for cancer. From these efforts two fundamental approaches have proven useful. One approach involves the use of small molecule tyrosine kinase inhibitors (TKIs) that bind to the ATP-binding site in the tyrosine kinase domain (TKD) of EGFR. To date, three anti-EGFR TKIs, erlotinib (OSI-774, Tarceva), gefitinib (ZD1839, Iressa) and lapatinib (GW572016, Tykerb) are FDA-approved for use in oncology.

CSPC Exhibit 1004
Page 109 of 336

A second approach uses monoclonal antibodies (mAbs) to target the extracellular domain of EGFR to block natural ligand binding. In 1983, Sato et al. isolated four mouse (M) hybridomas secreting immunoglobulin G (IgG) against the EGFR on A431 cells. Three of the antibodies, M225 IgG, M528 IgG and M579 IgG blocked 95% of EGF binding to human A431 cells as well as competing with each other in binding assays. These three antibodies could also bind HeLa cells and foreskin fibroblasts. Further, each antibody could immunoprecipitate EGFR from A431 cells, but not from three rodent lines tested demonstrating their specificity. Finally, each antibody effectively blocked EGF-induced phosphorylation of the receptor resulting in reduced proliferative potential of the cell lines examined.[77-80]

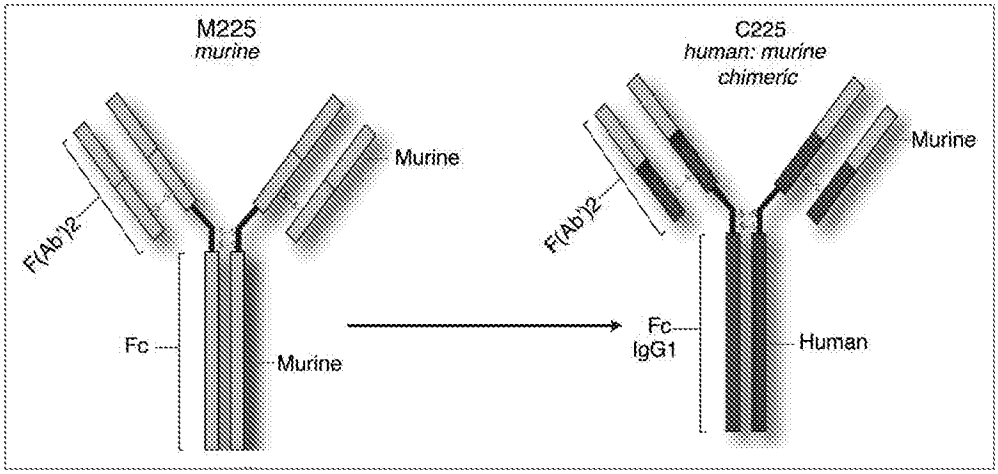


Figure 2. Structure and development of cetuximab. Three murine antibodies designated M225 IgG, M528 IgG and M579 IgG with activity against the EGFR were developed. Further testing identified M225 as being the most efficacious for anti-EGFR activity and was moved into Phase I clinical trials. Although successful, patients developed human-anti-mouse antibodies (HAMA) and therefore M225 was converted to a human:murine chimera, C225, with an IgG1 FC isotype.

M225 has slightly more effective anti-EGFR activity than M528, which is in turn more effective than M579. The phase I trial with M225 was successful, but all patients produced human-anti-mouse antibodies (HAMA). Therefore, M225 was converted to a human:murine chimera, C225, with an IgG1 Fc isotype (**Fig. 2**). The IgG1 Fc isotype was chosen for its potential to enhance the immune contribution to C225 antitumor effects (Dr. John Mendelsohn, MD Anderson Cancer Center, personal communication).

Subsequently, the anti-EGFR antibody C225 IgG1 was developed for clinical use. Cetuximab (ICM-225, Erbitux™) is a human/murine chimeric monoclonal antibody that works by binding to the extracellular domain III of EGFR. This interaction partially blocks the ligand-binding domain and sterically hinders the correct extended conformation of the dimerization arm on domain II.[81] Thus, cetuximab prevents both ligand binding and the proper exposure of the EGFR dimerization domain, preventing dimerization with other HER family members. In 2006, another monoclonal antibody directed against EGFR and having a similar mode of action was made; panitumumab (Vectibix) differs from cetuximab in that it is a fully humanized antibody.[82]

In addition to blocking ligand binding and dimerization, cetuximab effectively blocks EGFR phosphorylation, promotes EGFR internalization[83] and reduces cellular proliferation in a variety of cancer models (**Fig. 3A–C**).[84,85] Cetuximab induces arrest in the G_1 phase of the cell cycle by increasing levels of $p27^{kip1}$ (**Fig. 3D**). This in turn results in an increase in the dimerization of $p27^{Kip1}$-Cdk2 complexes, which ultimately prevents exit from G_1.[86-88]

In vivo experiments corroborated the $p27^{Kip1}$ findings as well as a reduction in PCNA in human tumor xenografts.[89] Furthermore, cetuximab decreases cancer cell metastasis in various studies via downregulation of pro-angiogenic factors and matrix metalloproteinases responsible for cell adhesion (**Fig. 3E**).[90-93] Cetuximab can induce the upregulation of various pro-apoptotic factors such as Bax, in addition to the downregulation of Bcl2, leading to the activation of caspases (**Fig. 3F**).[94-97] Cetuximab can also induce antibody-dependent cellular cytotoxicity in vivo by recruiting immune cells to tumor cells decorated by cetuximab (**Fig. 3G**).[98,99] Collectively, cetuximab results in several biological effects that have impact on the growth and spread of multiple human tumors.

Cetuximab in the Clinic

Cetuximab has exhibited promising antitumor activity in clinical trials as either monotherapy or in combination with chemotherapy and/or radiation, particularly in the settings of metastatic CRC (mCRC)[100-105] and HNSCC (**Table 1**).[106-110] In 2004, the FDA approved cetuximab for use in patients with EGFR-expressing mCRC refractory to irinotecan-based chemotherapy.[111] Since this approval, several extensive clinical trials have supported the use of cetuximab in the setting of mCRC.

In 1997–98, a phase I trial of HNSCC enrolled 16 patients with locoregionally advanced tumors and provided the first clinical demonstration that adding cetuximab to radiation may improve tumor response and disease control.[112] Despite the absence of true phase II data, a phase III trial that enrolled 424 patients was carried out between 1999–2002 that confirmed a 10% overall survival advantage for patients receiving cetuximab in combination with curative radiation for advanced HNSCC compared with radiotherapy alone.[107]

Although not yet approved by the FDA for use in advanced NSCLC, cetuximab has undergone clinical evaluation in this setting. A series of phase II trials suggested the benefit of cetuximab in combination with platinum doubles in the first-line treatment setting.[113-117] Two phase III trials have been reported, including the FLEX and BMS099 trials.[118,119] The FLEX trial demonstrated

CSPC Exhibit 1004
Page 110 of 336

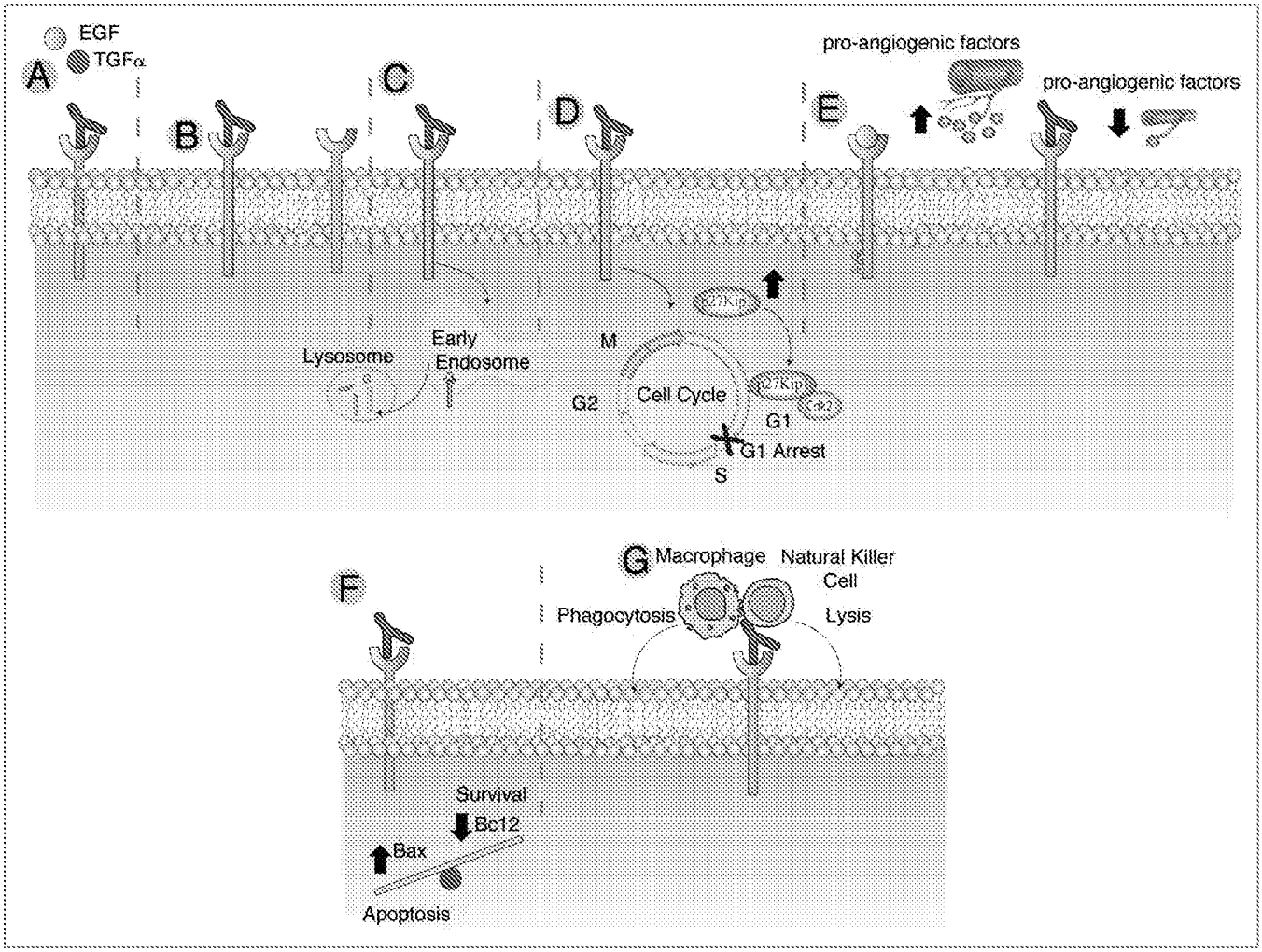


Figure 3. Mechanisms of action of cetuximab. (A) Cetuximab has a higher affinity for the EGFR than either TGFα or EGF and effectively blocks ligand binding and ligand induced EGFR phosphorylation.[77-80] (B) Cetuximab has been noted to sterically hinder the binding of EGFR to other HER family members.[5] (C) Cetuximab promotes the internalization and degradation of the EGFR, abrogating its downstream signaling cascades.[83] (D) Cetuximab treatment of cancer cell lines and human tumor xenografts have shown a dramatic cell cycle arrest in the G_1 phase of the cell cycle. Further investigations indicated that this was due to an increased expression of the cell cycle inhibitor $p27^{Kip1}$. This increased expression led to the formation of $p27^{Kip1}$-Cdk2 complexes and the prevention of cells from exiting the G_1 phase of the cell cycle.[86-88] (E) It has been noted that EGFR expressing tumor lines display a significant increase in pro-angiogenic factors leading to increased angiogenesis to the tumor. Treatment with cetuximab has been shown to dramatically decrease the expression of pro-angiogenic factors. In addition to decreased angiogenesis, there is evidence that cetuximab therapy may lead to decreased invasion and metastatic spread of tumor cell.[86,94-97] (F) Cetuximab treatment has also been noted to influence the balance of apoptosis and cell survival through modulation of the expression of Bax, which promotes apoptosis and Bcl2, which promotes survival. Treatment with cetuximab increased expression of Bax and decreased Bcl2.[95-97] (G) Antibody-dependent cellular cytotoxicity mediated by cetuximab has also been noted in several studies.[98,99]

an improvement in overall survival with the addition of cetuximab to first-line cisplatin and vinorelbine. The BMS099 trial evaluated the addition of cetuximab to carboplatin/taxane in the first-line setting and identified an improvement of overall response rate, but not a statistically significant improvement in progression-free survival (PFS).

Predictive Biomarkers of Cetuximab Response

Since the FDA approval of cetuximab and its associated clinical successes, intense investigations have been made to find markers in patient tumors that could predict individual responses to cetuximab therapy and positive clinical benefit. It was believed that expression levels of EGFR would serve as a simple predictive biomarker for the likelihood of response to cetuximab therapy. This would be akin to women with breast cancer who have high HER2 expression and are more likely to respond to trastuzumab anti-HER2 therapy. However, early clinical studies did not confirm a correlation between EGFR expression level by immunohistochemistry (IHC) and clinical response to EGFR inhibitor therapy.[100] Chung et al. confirmed that several CRC patients who received cetuximab exhibited a major objective response despite the absence of measureable EGFR. These studies suggested that IHC-based assays measuring EGFR expression do not serve as

CSPC Exhibit 1004
Page 111 of 336

Table 1. Selected clinical trials of cetuximab

Trial	Authors	Year	Cancer	Clinical design	Median over survival		Response rate		Median progression-free survival	
					Month	p value	%	p value	Month	p value
EPIC	Sobrero et al.[102]	2008	mCRC	Irinotecan	10.0	0.71	4.2	<0.001	2.6	<0.001
				Irinotecan + CTX	10.7		16.4		4.0	
OUPS	Bokemeyer et al.[104]	2009	mCRC	FOLFOX	NR	NR	36	NR	7.2	NR
				FOLFOX + CTX	NR		46		7.2	
SAKK	Borner et al.[103]	2008	mCRC	CAPOX	16.5	NR	14	NR	5.8	NR
				CAPOX + CTX	20.5		41		7.2	
CRYSTAL	Van Cutsem et al.[105]	2009	mCRC	FOLFIRI	18.6	0.31	38.7	0.004	8.0	0.048
				FOLFIRI + CTX	19.9		46.9		8.9	
NCT00004227	Bonner et al.[107]	2006	HNSCC	Radiotherapy	29.3	0.03	64	0.02	12.4	0.006
				Radiotherapy + CTX	49.0		74		17.1	
EXTREME	Vermorken et al.[106]	2008	HNSCC	Platinum CT + FU	7.4	0.04	20	<0.001	3.3	<0.001
				Platinum CT + FU + CTX	10.1		36		5.6	
BMS099	Lynch et al.[119]	2010	Lung	Taxane + Carboplatin	8.4	0.17	17.2	0.0066	4.2	0.24
				Taxane + Carboplatin + CTX	9.7		25.7		4.4	
FLEX	Pirker et al.[118]	2009	Lung	Cisplatin + vinorelbine	10.1	NR	29	0.01	4.8	NR
				Cisplatin + vinorelbine + CTX	11.3		36		4.8	

robust predictors for response to cetuximab therapy and that expression levels of the EGFR alone are not a reliable predictor of response to cetuximab therapy.

EGFR mutations as a predictor of response. In 2004, a series of landmark papers identified EGFR mutations in the tyrosine kinase domain in NSCLC patients, which predicted response to the TKIs erlotinib and gefitinib.[120-122] These gain-of-function mutations conferred dependence of tumor cells on the mutated EGFR kinase and rendered them more sensitive to erlotinib and gefitinib than tumors without these mutations. Soon after this finding it was reported that following initial sensitive response, patients harboring these mutations in the catalytic domain acquired resistance within 6–12 months of TKI therapy. Pao et al. reported that NSCLC patients with acquired resistance to gefitinib or erlotinib contain a secondary mutation in exon 20 of EGFR, which leads to substitution of methionine for threonine at position 790 (T790M) in the kinase domain.[123,124] Despite these findings for EGFR TKIs and NSCLC, no EGFR mutations have yet been identified that reliably predict response to antibody-based EGFR therapies.[125,126]

EGFR gene copy number as a predictor of response. Although mutations within the EGFR do not predict response to cetuximab therapy, increased copy number of the EGFR gene is associated with response in CRC.[127] Large CRC clinical cohorts confirmed the relationship between EGFR gene amplification and clinical response to cetuximab.[128-131] However, increased copy number of the EGFR gene does not lead to increased expression of EGFR in these patients,[127,130] and how EGFR gene copy number correlates with improved response is unknown. In lung cancer, 30–60% of patients with advanced NSCLC have increased EGFR gene copy number according to FISH analysis and respond to cetuximab plus chemotherapy.[132] However, the BMS-099 trial concluded that patient response rate to cetuximab was not dependent on EGFR gene copy number.[133] Thus, predictive response to cetuximab based on EGFR gene copy number remains controversial at this time.

EGFR ligand status as a predictor of response. Increased expression levels of the EGFR ligands AR and EPR in CRC tumors are positively associated with response to cetuximab.[134] These findings centered on the mRNA levels within the tumor itself, versus circulating serum levels. Increased mRNA expression correlates with improved disease control and PFS. These findings suggest that EGFR ligands may drive tumor proliferation in an autocrine/paracrine fashion and that cetuximab may be able to block ligand binding to the receptor.

KRAS mutations as a predictor of response. One of the most notable predictive biomarkers of response to cetuximab is the mutational status of the KRAS gene. KRAS is a small GTPase responsible for coupling EGFR to the RAF/MEK/ERK pathway. KRAS binding to GTP leads to conformational changes in RAF and activation of the down stream-signaling pathway. Although KRAS is a GTPase, its catalytic activity is slow and dramatically enhanced by accessory proteins called GTPase activating proteins (GAPs) that convert KRAS-GTP to KRAS-GDP and thus turn off RAF-mediated signaling. Mutations in codon 12 or 13 of KRAS impair the intrinsic GTPase activity and confer resistance to GAPs, thereby causing cancer-associated mutant Ras proteins to accumulate in the active, GTP-bound conformation.[135,136] Lievre et al. reported that KRAS with mutations at codon 12 or 13 might be predictive of resistance to cetuximab therapy. In this report, they analyzed 30 patients with metastatic CRC treated with cetuximab for the

CSPC Exhibit 1004
Page 112 of 336

presence of KRAS, BRAF and PIK3CA mutations. KRAS mutations were found in 43% of tumors (13 tumors), and were significantly associated with resistance to cetuximab therapy ($p = 0.002$).[137] Further, Di Fiore et al.[97] studied 59 patients with chemorefractory mCRC treated with cetuximab plus chemotherapy and found that KRAS mutations were highly predictive of resistance to cetuximab plus chemotherapy.[138] A larger study was performed to measure the KRAS mutation status in 113 patients with irinotecan-refractory mCRC treated with cetuximab. The authors reported that wild-type KRAS is a strong predictor of significant increase in overall survival ($p < 0.001$) in this cohort of patients.[139] Following this work, Van Cutsem et al. investigated the efficacy of cetuximab plus irinotecan, fluorouracil and leucovorin (FOLFIRI) as first-line treatment for mCRC and looked for associations between the mutation status of KRAS and clinical response to cetuximab. In this study, 599 patients received cetuximab plus FOLFIRI, and 599 received FOLFIRI alone. First-line treatment with cetuximab plus FOLFIRI reduced the risk of disease progression compared with FOLFIRI alone, and the benefit of cetuximab was limited to patients with KRAS wild-type tumors.[105] Since the publication of these studies, several additional clinical trials have further strengthened these findings.[140-144] This collective body of work has led to a Provisional Clinical Opinion from ASCO in 2009 stating that all patients with mCRC who are candidates for anti-EGFR antibody therapy should have their tumor tested for KRAS mutations in a clinical laboratory improvement amendments (CLIA)-accredited laboratory. If codons 12 or 13 of KRAS are mutated, patients with mCRC should not receive anti-EGFR antibody therapy as part of their treatment.[145] However, some patients carrying KRAS mutant tumors have been reported to respond to EGFR antibodies.[128,143,146,147] How to distinguish these individuals from other KRAS mutant patients is worthy of clinical investigation.

BRAF mutations as a predictor of response. BRAF is a serine-threonine kinase belonging to the RAF family of protein kinases. GTP bound KRAS activates BRAF,[148] which in turn activates the MEK pathway.[149,150] Initial work indicated that BRAF mutations impair response to EGFR antibodies in CRC.[151] This investigation indicated that clinically responsive tumors had wild-type BRAF, whereas approximately 14% of non-responders had a mutation at valine 600 (V600E). Several reports revealed that BRAF gene mutations are relatively rare events in lung cancer and HNSCC.[152-157]

IGF1R gene expression status in response to cetuximab. Fei et al. investigated the correlation between gene expression levels of IGF pathway components in 70 pre-treatment mCRC patients and the subsequent clinical benefit from cetuximab. In this cohort, patients with tumors expressing high level of IGF1R had longer PFS with cetuximab than patients with low expression levels of these genes. Additionally, patients with KRAS wild-type tumors with high expression of IGF1R had a significantly higher rate of disease control (62.5%) and longer PFS than patients with low expression (26.3% disease control).[158] These data suggested that IGF pathway activation might play an important role in predicting positive responders to cetuximab therapy.

Mechanisms of Resistance to EGFR Targeted Antibodies

Angiogenesis. Several lines of investigation have identified inhibition of angiogenesis as part of the antitumor effect of cetuximab (**Table 2**).[159-161] Thus, cetuximab resistance is partly due to the ability of cells to re-activate pro-angiogenic factors via alternate pathways. In 2001, Viloria-Petit et al. demonstrated that tumors resistant to EGFR blocking antibodies have increased VEGF production,[162] a potent stimulator of neovascularization.[163,164] Researchers established A431 squamous cell carcinoma xenografts in mice and subsequently treated them with three EGFR blocking antibodies: cetuximab, hR3 or mR3. Complete regression for each of these three antibodies was obtained after eight treatments, at which point treatment was terminated. Tumor recurrence was observed as soon as 18 days, and up to 4.5 months post treatment. Twenty percent of cetuximab-treated mice suffered tumor recurrence, while 40% of hR2 and 80% of mR3 treated mice suffered recurrence. All mice with recurrent tumors were subsequently treated with a second round of therapy. Six anti-EGFR antibody resistant variant cell lines were established from resistant recurrent tumors to hR2 and mR3 antibodies (cetuximab resistant cell lines were not established). When these cell lines were tested for response to hR2 and mR3 in vivo, they demonstrated increased growth, and decreased response rates compared to A431 parental tumors. Immunoblot analysis of the variant cells demonstrated that EGFR levels remained similar to those of parental cell lines, arguing against the possibility that changes in EGFR expression influence the resistant phenotype. Notably, resistant variant cells expressed two-fold more VEGF mRNA and protein than parental cells. When the A431 parental cell line was engineered to overexpress VEGF and injected into mice, the resulting tumors were resistant to all three anti-EGFR antibodies and demonstrated increased vascularization within the tumor itself. In support of these findings, another study used the VEGF inhibitor (DC101) combined with cetuximab and demonstrated that it had greater efficacy in treatment of gastric cancer xenografts than either agent alone, both in the inhibition of tumor growth and the induction of apoptosis.[165] Overall, these studies provide evidence for the role of VEGF and angiogenesis in resistance to EGFR targeted antibodies.

Further studies focused on angiogenesis have been reported. A study by Ciardiello et al. demonstrated the importance of VEGF signaling in resistance to EGFR targeted antibodies.[166] Researchers treated human GEO colon tumor xenografts with either cetuximab or ZD1839 (gefitinib) for four weeks, at which time complete regression of all tumors was noted. Mice taken off therapy after complete regression grew recurrent tumors within 3–5 weeks, while mice kept on therapy had prolonged tumor inhibition with recurrent tumor growth after 11–12 weeks; all recurrent tumors reached the growth rate of untreated controls. EGFR inhibitor resistant recurrent tumors were excised, and two cell lines were established in vitro. Immunoblot analysis of these resistant variants showed a 5–10 fold increase in the expression of COX-2, phosphorylated MAPK and VEGF, while EGFR expression levels remained constant. In addition, resistant variants

CSPC Exhibit 1004
Page 113 of 336

Table 2. Mechanisms of resistance to EGFR-targeted antibodies

Resistant mechanism	Study	Year	Cancer cell lines	Scientific approach	Mechanism for resistance to cetuximab
Angiogenesis	Viloria-Petit et al.[162]	2001	Squamous cell carcinoma	In vitro acquired resistance model and confirmation via mouse Xenograft	- Resistant tumor cells have increased VEGF production
Angiogenesis	Ciardiello et al.[166]	2004	Colon Cancer	In vivo xenograft acquired resistance model	-Resistant cells have increased Cox-2, pMAPK and VEGF protein expression levels, and increased secretion of VEGF -Dual VEGFR-EGFR tyrosine kinase inhibitor ZD6474 can overcome resistance to cetuximab
Angiogenesis	Bianco et al.[167]	2008	Breast, Colon and Prostate Cancer	In vivo xenograft acquired resistance model	- Resistant cells have increased VEGFR-1 and -2 activation resulting in increased migratory potential
Increased EGFR Degradation	Lu et al.[168]	2007	Colon Cancer	In vitro acquired resistance model	- Resistant cells have an increased rate of EGFR degradation, demonstrating the importance of alternative mechanisms for growth and survival
Dysregulation of EGFR internalization and degradation	Wheeler et al.[170]	2008	NSCLC	In vitro acquired resistance model	- Resistant cells have increased levels of EGFR due to dysregulated degradation via loss of binding to the E3 ubiquitin ligase c-Cbl
Oncogenic shift	Wheeler et al.[170]	2008	NSCLC and HNSCC	In vitro acquired resistance model	- Resistant cells have increased expression levels of EGFR, HER2, HER3 and C-Met - EGFG has increased binding to these receptors, indicating the role of heterodimerization in resistance
Subcellular localization of EGFR	Li et al.[182]	2009	NSCLC	In vitro and in vivo xenograft acquired resistance model	- Resistant cells have increased levels of ligand induced nuclear EGFR - The inhibition of SFKs with the drug dasatinib can block the nuclear localization of EGFR, and resensitize resistant cells to cetuximab
Subcellular localization of EGFR	Nevo et al.[184]	2009	Breast and Lung cancer	MDGI stably transfected cell lines grown in 3D matrigel, and in vivo	- MDGI expression can induce the intracellular localization of EGFR, preventing its ability to be affected by cetuximab treatment
Epithelial to mesenchymal shift	Fuchs et al.[196]	2008	Hepatocellular carcinoma	Analysis of cancer cell lines based on E-cadherin and vimentin levels In vitro	- Resistant cells are characterized as mesenchymal-like via increased vimentin expression, and increased activation of AKT, STAT3, and ILK
Epithelial to mesenchymal shift	Basu et al.[193]	2010	Squamous cell carcinoma	Analysis of cancer cell lines in vitro and in vivo that have sub-populations of both E-cadherin high and low expressing cells	- Tumors become resistant to cetuximab by selecting for E-cadherin low/vimentin high expressing sub-populations that have a low turn over rate, and a decrease in EGFR expression
Constitutive activation of EGFR effector molecules	Kim et al.[197]	2010	NSCLC	In vitro acquired resistant model	- PTEN is degraded in cetuximab resistant cells, leading to constitutive activation of AKT
Constitutive activation of EGFR effector molecules	Wheeler et al.[170]	2009	NSCLC	In vitro acquired resistant model	- Resistant cells have increased activity of SFKs, leading to increased activity of AKT - The SFK inhibitor Dasatinib can sensitize resistant cells to cetuximab by reducing SFK and AKT activation
Constitutive activation of EGFR effector molecules	Dunn et al.[201]	2010	CRC	In vitro and In vivo modeling of tumor cell lines with mutated KRAS	- Mutant KRAS CRC cells have increased activation of SFKs - The inhibition of SFKs can sensitize KRAS mutants to cetuximab In vitro and In vivo by decreasing signaling through MAPK, B-catenin and STAT pathways
Increased expression of HER family growth factors	Hatakeyama et al.[202]	2010	HNSCC	- Use of previously published cetuximab resistant and sensitive cell lines. - Examination of tumor specimens and patient plasma samples	-Resistant cell lines have increased expression of HB-EGF ligand due to a decrease in miR-212 - Patients with recurrent tumors have increased secretion and expression of HB-EGF ligand

CSPC Exhibit 1004
Page 114 of 336

secreted more VEGF into surrounding media compared to sensitive controls. Researchers showed that the dual VEGFR-EGFR tyrosine kinase inhibitor ZD6474 (vandetanib) was able to overcome resistance to EGFR targeted agents. Not only did mice initially treated with ZD6474 alone remain devoid of recurrent tumors through the end of the experimental period (23 weeks), but xenografts of resistant variants were also sensitive to ZD6474. Overall, these data support a role of VEGF signaling in the development of cetuximab resistance, and provide a rationale for targeting VEGF signaling pathways in cetuximab-resistant tumors.

In 2008, Bianco et al. used a variety of different cancer cell lines (breast, colon and prostate) with differing levels of EGFR expression. In vivo resistance to EGFR inhibitors was established for each cell line using a similar approach as Ciardiello et al.[166] This work confirmed the finding that EGFR resistance can be overcome with ZD6474 treatment, which reduced phosphorylation of AKT and p70-S6 kinase in resistant cells. Resistant cells also overexpressed VEGFR-1 at the mRNA and protein level. In addition, ZD6474 reduced the phosphorylation of both VEGFR-1 and VEGFR-2 significantly in resistant cell lines. To further support the role of VEGR-1 in resistance to EGFR inhibitors, siRNA directed towards VEGFR-1 re-sensitized resistant cell lines to EGFR inhibitors; siRNA towards VEGFR-2 restored sensitivity to EGFR inhibitors to a lesser degree. Overexpression of VEGFR-1 in ZD1839 sensitive lines conferred resistance to subsequent ZD1839 treatment. In wound-healing assays, resistant cells had up to 50% more migratory capability compared to parental cells, and treatment with ZD6474 reduced wound closure efficiency, and thus inhibited the migratory potential of resistant cells. Overall, this study provides further evidence for the role of VEGF and VEGFRs in a tumor's ability to increase its migratory potential, stimulate downstream signaling molecules, and induce EGFR inhibitor resistance in various types of cancers.[167]

Dysregulation of EGFR internalization and degradation. Dysregulated EGFR internalization and degradation has been shown to play a role in cetuximab resistance. In a study by Lu et al. a DiFi colorectal cancer cell line was subjected to increasing concentrations of cetuximab over time, producing a cetuximab-resistant cell line DiFi5.[168] DiFi5 cetuximab-resistant cells exhibited polyubiquitinated EGFR, decreased total and cell surface levels of EGFR and increased expression of SFKs compared to parental, cetuximab-sensitive controls. In addition, DiFi5 cetuximab-resistant cells showed high association with the ubiquitin E3 ligase Cbl, consistent with the high level of ubiquitinated EGFR. Contrary to previous work demonstrating that SFKs can downregulate Cbl to promote EGFR persistence,[169] Cbl was more associated with EGFR in cetuximab-resistant cells despite high SFK expression levels. The decrease in EGFR stability in this resistant model still needs to be further investigated, however authors postulate that alternative receptors/pathways are responsible for the observed continuation of cell growth and survival.[168]

In another model of acquired resistance to cetuximab, various cetuximab-resistant clones were established from the NSCLC cell line NCI-H226 by exposing these cells to increasing concentrations of cetuximab over a six-month time course. Using this model, Wheeler et al. showed that resistant cell lines have increased surface levels of EGFR compared to the parental cetuximab-sensitive line.[170] These findings were confirmed using immunofluorescence (IF) microscopy and flow cytometry. In contrast to the study by Lu et al.[168] this study demonstrated that EGFR does not seem to be associated with c-Cbl in cetuximab-resistant lines, while the parental cetuximab-sensitive line maintains this association. These data support a previously published mechanism for EGFR degradation via c-Cbl recruitment to tyrosine 1045.[171] Overall, these data suggest that impaired EGFR internalization and degradation may lead to increased EGFR expression and activity manifesting in cetuximab resistance.[170]

Oncogenic shift. The increased activation of various RTKs plays a role in cetuximab resistance in an NSCLC in vitro model.[170] The cetuximab-sensitive NSCLC cell line, NCI-H226, and the HNSCC cell line, UMSCC-1, were treated continuously with increasing concentrations of cetuximab to establish several cetuximab-resistant clones. Using an antibody-based RTK array, the levels of phosphorylated RTKs were compared between the cetuximab-resistant and the parental cetuximab-sensitive cell lines in both NSCLC and HNSCC models. In both cetuximab-resistant models, protein levels of the HER family members EGFR, HER2 and HER3 were upregulated, as well as the MET receptor compared to parental controls. Western blot analysis confirmed increased protein levels of these RTKs in the NSCLC model. Immunoprecipitaton of EGFR in resistant clones showed a steady-state increase in binding to HER2, HER3 and cMET in resistant lines. In addition, the monoclonal antibody 2C4 (Pertuzumab), which inhibits HER2 heterodimerization, was able to produce potent anti-proliferative effects in NSCLC cetuximab-resistant lines when treated simultaneously with cetuximab. This also corresponded with more potent knockdown of HER3 and AKT expression. Overall, these data suggest that resistant NSCLC and HNSCC cells may rely on the activation of various RTKs and their subsequent heterodimerization with EGFR to bypass cetuximab blockade.[170]

Subcellular localization of EGFR. The EGFR has been shown to be localized to subcellular compartments including the endosome, the mitochondria[172] and the nucleus. Nuclear EGFR has been detected in a variety of cancer types including brain,[173] breast,[174-177] bladder,[178] ovary,[179] NSCLC[180] and HNSCC[181] and serves as a prognostic factor in HNSCC, ovarian and breast cancers.[26-28] In 2009, Li et al. demonstrated in an in vitro model of cetuximab resistance that resistant clones had increased levels of nuclear EGFR, determinded via biochemical fractionization and IF.[182] Increased nuclear EGFR coincided with increased expression levels of genes known to be regulated by nuclear EGFR: Cyclin D1,[181] B-myb[177] and PCNA,[183] demonstrating a correlation of nuclear EGFR and increased expression of known nuclear EGFR gene targets. In addition, cetuximab-resistant cells had increased SFK expression.[184] Based on this knowledge, researchers postulated that SFKs may influence nuclear EGFR and modulate cetuximab resistance. Using the pan-SFK inhibitor, Dasatinib, a 2.7–5.5-fold decrease in nuclear EGFR was detected with a significant increase in surface associated EGFR levels measured via flow cytometry. Dasatinib was able to re-sensitize cetuximab

CSPC Exhibit 1004
Page 115 of 336

resistant clones to cetuximab; growth proliferation was only mildly affected by dasatinib treatment alone. Overall, these data suggest that SFKs are necessary for translocation of EGFR to the nucleus and protection from cetuximab. The authors concluded that SFK inhibition in combination with cetuximab may have clinical benefit in the future.

In another study, mammary-derived growth inhibitor (MDGI) was shown to confer cetuximab resistance in both breast and lung cancer cell models by stimulating the intracellular localization of EGFR.[185] MDGI is an intracellular fatty acid binding protein known to modulate fatty acid metabolism, in addition to having tumor suppressor activity in various cancer models.[186-189] It is expressed in 40% of human breast cancers and 85% of human lung cancers; however, expression is lost in cell culture models possibly by epigenetic silencing mechanisms.[185] Experiments investigating the role of MDGI and cetuximab resistance are based on the use of cell lines stably transfected with MDGI grown in three-dimensional cell culture models, or inoculated into mouse mammary fat pads. Cells transfected with MDGI exhibit a reduced level of cell surface EGFR and labeled EGF on the cell surface as measured by flow cytometric analysis. In addition, there was an increase in intracellular biotin-labeled EGFR as detected by western blot analysis. Increased intracellular trafficking of EGFR appeared to be independent of other HER family members, or increased caveolin activity. Interestingly, EGFR remained phosphorylated within intracellular compartments in MDGI-transfected cells. Lung cancer cells transfected with MDGI are resistant to cetuximab in the 3D matrigel model, while GFP-transfected control cells remain sensitive. Both GFP and MDGI transformants remain sensitive to EGFR TKIs in 3D matrigel, demonstrating the ability of TKIs to penetrate intracellular compartments containing the majority of EGFR. Researchers further demonstrate this finding in vivo by inoculating mouse mammary fat pads with a breast cancer cell line stably expressing MDGI or GFP. MDGI-expressing cells were resistant to cetuximab treatment, and grew much faster then the GFP control tumors. Overall, this study identifies MDGI as a determinant of intracellular localization of EGFR, and provides a rationale for considering MDGI expression levels as a biomarker for cetuximab sensitivity.

Epithelial to mesenchymal transition. Epithelial to mesenchymal transition (EMT) has been described as a hallmark of cancer.[190] EMT is characterized by the loss of adherens junction proteins, such as E-cadherin; gain of cytoskeletal filaments, such as vimentin; and the subsequent increase in cell motility and invasiveness.[191,192] These markers have been used by various investigators to characterize cells as either epithelial or mesenchymal; however, some researchers suggest that carcinomas do not fall into strict categories, and represent a mixed phenotype.[193,194] In a study by Fuchs et al., 12 human hepatocellular carcinoma cell lines were characterized as either epithelial or mesenchymal by western blot analysis of E-cadherin and vimentin protein levels. Based on this classification, mesenchymal cell lines were shown to be resistant to cetuximab, erlotinib and gefitinib, while epithelial cell lines remained sensitive to these EGFR inhibitors. Analysis of downstream signaling pathways in all 12 cell lines demonstrated that mesenchymal cell lines had increased activation of AKT, STAT3 and integrin linked kinase (ILK); independent of total EGFR expression. ILK, a known activator of AKT,[195] seemed to play a role in resistance to EGFR inhibitors because an ILK inactive mutant increased the expression of E-cadherin, indicating a transition of mesenchymal cells back to epithelial cells. This transition was associated with decreased AKT signaling, and restoration of cellular sensitivity to EGFR inhibitors. This was further verified in a xenograft model, where cells became resensitized to gefitinib. Overall, EMT and ILK may play a role in resistance to cetuximab.[196]

In 2010, mesenchymal-like squamous cell carcinomas were shown to be resistant to cetuximab treatment.[193] Using immunohistochemistry, flow cytometry and gene expression profiling, researchers identified SCC cell lines that were epithelial-like and mesenchymal-like based on E-cadherin and vimentin expression levels. In this system, researchers identified cell lines that had sub-populations of both high E-cadherin/low vimentin and low E-cadherin/high vimentin levles. Gene expression profiles of E-cadherin/high vs. E-cadherin/low sub-populations were compared, demonstrating that E-cadherin/low cells expressed various genes involved in EMT. Next, they compared this in vitro system to in vivo xenografts and clinical specimen tumor samples, which also demonstrated distinct E-cadherin/high and E-cadherin/low sub-populations. Using FACS, researchers separated out each sub-population and performed in vitro growth assays. E-cadherin/low cells exhibited attenuated growth compared to E-cadherin/high cells, and were also arrested in the G_0 phase of the cell cycle. Thus, E-cadherin/low cells have a lower turnover rate compared to E-cadherin/high cells. Flow cytometry, IF microscopy and western blot analysis demonstrated that E-cadherin/low cells from both in vitro and in vivo models had decreased EGFR expression levels. EGF ligand was unable to stimulate the activation of EGFR downstream signaling pathways in E-cadherin/low cells, demonstrating that EGF ligand regulation of AKT and ERK activation was uncoupled from the EGFR in these cells. E-cadherin/low sub populations also remained resistant to cetuximab treatment in vitro and in vivo xenograft models. When xenografts of E-cadherin/high and low subpopulations were treated with cetuximab for 12 days, a two-fold enrichment of vimentin expressing cells was noted. Thus, it seems that tumors may escape from cetuximab by either (1) depleting epithelial-like cell types (as demonstrated by the loss of E-cadherin expressing subpopulations) or by (2) actively differentiating into mesenchymal-like cell types (as demonstrated by the increase in vimentin expressing subpopulations).

Constitutive activation of EGFR downstream effector molecules. The constitutive activation of AKT due to the proteosomal degradation of PTEN induces resistance to cetuximab in the NSCLC cell line, NCI-HCC827.[197] Cetuximab-resistant HCC827 clones, produced via increased exposure to cetuximab over a six-month time period, demonstrated increased AKT activation, and markedly decreased protein levels of PTEN. In subsequent studies, researchers treated resistant cells with the proteosomal inhibitor MG-132, which prevented degradation of PTEN and reduced AKT activation. Western blot analysis of

CSPC Exhibit 1004
Page 116 of 336

cells treated with MG-132 demonstrated that PTEN was poly-ubiquitinated, suggesting that PTEN was targeted for destruction. The AKT inhibitor, LY294002, combined with cetuximab was also able to block AKT activation even more potently that LY294002 alone. Overall, it appears that functional PTEN is necessary for the complete knockdown of AKT activity by cetuximab and PTEN destruction yields resistance to cetuximab.[197]

The PI3K/AKT pathway is upregulated via increased activity of the intracellular kinase Src in cetuximab-resistant cells. In this study, Wheeler et al. used cetuximab-resistant clones derived from the NSCLC NCI-H226 cell line.[184] Cetuximab-resistant cells demonstrated a robust increase in SFK activity compared to sensitive parental control cells, possibly due to the steady state increase of EGFR in resistant lines. In addition, cetuximab-resistant cell lines had high AKT activity. The pan SFK inhibitor, dasatinib, decreased AKT activation along with the proliferative potential of cetuximab-resistant clones, demonstrating the importance of SFK signaling in resistance to cetuximab. When cetuximab-resistant cells were treated with both cetuximab and dasatinib simultaneously there were even more profound anti-proliferative effects, including enhanced decreases in downstream AKT signaling. Overall, dasatinib was able to re-sensitize resistant cells to cetuximab, providing a rationale for possible combinational therapies in the future.

Blockade of SFKs is also beneficial in the mutant KRAS setting of CRC. Clinical trials using cetuximab in patients with mCRC harboring a KRAS mutation demonstrated resistance to cetuximab therapy.[138,145,198] These trials have lead to the widely accepted view that KRAS mutation status is a predicative factor for response to cetuximab.[145,199,200] Since 30–40% of patients with CRC have a KRAS mutation, it is crucial that alternative treatment regimes be devised for these patients.[198] In 2010, Dunn et al. investigated whether SFK blockade could sensitize KRAS mutant CRC tumors to cetuximab. In this study, 16 CRCs lines were screened for expression of EGFR, SFKs, and the mutational status of KRAS. Nine of the 16 cell lines had mutations in KRAS at either codons 12 or 13, or BRAF mutations at codon 600. From these lines, three lines were chosen for continued studies based on their expression of EGFR and SFKs, KRAS mutational status, and ability to grow in vivo. KRAS mutated cell lines had a decreased response to cetuximab when plated on poly-d-lysine/laminin coated culture plates compared to wild-type KRAS cell lines, which demonstrated sensitivity. Importantly, the combination of cetuximab and dasatinib led to significant growth inhibition in KRAS mutant lines. These results encouraged researchers to perform a human phosphokinase array to identify potential mechanisms for growth inhibition. Unique kinase expression patterns were found for each KRAS mutant line treated with both cetuximab and dasatinib, however, all three lines demonstrated a common decreases in activity of the MAPK pathway, the β-catenin pathway, and of various STAT family transcription factors. Finally, researchers tested these findings in xenograft studies. Mice were injected with mutant KRAS cell lines, and treated with vehicle, cetuximab, dasatinib or the combination. These experiments demonstrated that the combinatorial treatment from initial tumor onset had statistically significant growth inhibitory effects in KRAS mutant xenografts. Overall the blockade of SFKs in mutant KRAS cell lines led to a decrease in key signaling pathways important for cell proliferation and survival, providing a rationale for treating KRAS mutant CRC patients with dasatinib and cetuximab in the clinic.[201]

Increased expression of HER family growth factors. In 2010, Hatakeyama et al. reported a role for microRNAs (miRs) in EGFR ligand suppression and cetuximab resistance. This study utilized cetuximab-resistant clone (1Cc8) derived from the HNSCC UMSCC-1 line after chronic, long-term exposure to cetuximab treatment. Using DNA microarray technology, differential gene expression patterns were compared between the UMSCC-1 parental line and 1Cc8. Examining differences in the EGFR signaling pathway revealed an increase in heparin-binding EGF (HB-EGF) in the cetuximab resistant line, 1Cc8. To confirm this result, HB-EGF and other growth factor ligands were measured via ELISA assay from conditioned media with or without cetuximab treatment in both UMSCC-1 and 1Cc8 cell lines. Indeed, 1Cc8 cells had increased HB-EGF in both untreated and cetuximab treated culture media. Additionally, 1Cc8 cells also had increased AR in both untreated and cetuximab treated culture media, while TGFα was only increased in cultured media treated with cetuximab. Stimulation of various cetuximab-sensitive cell lines with HB-EGF induced cetuximab resistance, as measured via in vitro MTS growth assay and colony formation assay. In addition, knocking down the expression of HB-EGF in 1Cc8 cells was able to resensitize these cells to cetuximab. These results suggested that deregulated ligand expression may play a role in cetuximab resistance, and led researchers to look at the expression levels of various miRs. Interestingly miR-212 was decreased 27-fold in 1Cc8 cells relative to the cetuximab sensitive UMSCC-1 cell line as measured by RT-PCR based array. To demonstrate direct interaction of miR-212 and HB-EGF, a mimic of miR-212 was used to downregulate expression of HB-EGF in various cell lines, assayed by luciferase reporter gene expression. Researchers also reported that the miR-212 mimic could resensitize 1Cc8 cells to cetuximab. Finally, experiments examined expression levels of HB-EGF, along with other EGFR ligands, in HNSCC tumor specimens taken at the time of diagnosis or recurrence. HB-EGF, TGFα and AR were expressed in all tumors, however HB-EGF was even more highly expressed in recurrent tumor specimens. HB-EGF levels in plasma samples from recurrent patients were five times higher than in patients with newly diagnosed tumors. Overall, the increased expression of HB-EGF along with the downregulation of specific miRs appear to play a role in cetuximab resistance.[202]

Concluding Remarks

The discovery of the EGFR, the understanding of its signaling pathways and role in the etiology of human cancers, and ultimately the design of rational drugs to inhibit EGFR activity represents an incredible story of collaboration of scientists and clinicians over the last 30 years. Although cetuximab, an antibody directed against the EGFR, has had clinical success there is substantial room for progress in improving the effectiveness of this molecular therapeutic. Several key areas exist including (1) the identification of biomarkers that will accurately predict optimum responses to

CSPC Exhibit 1004
Page 117 of 336

cetuximab, (2) the identification of other key signaling pathways that can be targeted to enhance cetuximab activity and (3) understanding the pathways involved in cetuximab resistance and how to circumvent them to increase survival of cancer patients. The lessons learned from the story of the EGFR and the development of cetuximab will pave the road for future scientific and clinical based investigations of other promising antibody-based therapies directed against RTKs in oncology.

Acknowledgements

We would like to thank Laura Hogan for her critical reading of the manuscript. This project was supported, in part, by grant P30CA014520 from the National Cancer Institute, grant 1UL1RR025011 from the Clinical and Translational Science Award program of the National Center for Research Resources, National Institutes of Health and by grant RSG-10-193-01-TBG from the American Cancer Society.

References

1. Carpenter G, Lembach KJ, Morrison MM, Cohen S. Characterization of the binding of ^{125}I-labeled epidermal growth factor to human fibroblasts. J Biol Chem 1975; 250:4297-304.
2. Carpenter G, King L Jr, Cohen S. Epidermal growth factor stimulates phosphorylation in membrane preparations in vitro. Nature 1978; 276:409-10.
3. Ullrich A, Coussens L, Hayflick JS, Dull TJ, Gray A, Tam AW, et al. Human epidermal growth factor receptor cDNA sequence and aberrant expression of the amplified gene in A431 epidermoid carcinoma cells. Nature 1984; 309:418-25.
4. Eckhart W, Hutchinson MA, Hunter T. An activity phosphorylating tyrosine in polyoma T antigen immunoprecipitates. Cell 1979; 18:925-33.
5. Hunter T, Sefton BM. Transforming gene product of Rous sarcoma virus phosphorylates tyrosine. Proc Natl Acad Sci USA 1980; 77:1311-5.
6. Riedel H, Dull TJ, Schlessinger J, Ullrich A. A chimaeric receptor allows insulin to stimulate tyrosine kinase activity of epidermal growth factor receptor. Nature 1986; 324:68-70.
7. Schlessinger J. Signal transduction by allosteric receptor oligomerization. Trends Biochem Sci 1988; 13:443-7.
8. Yarden Y, Sliwkowski MX. Untangling the ErbB signalling network. Nat Rev Mol Cell Biol 2001; 2:127-37.
9. Hynes NE, Lane HA. ERBB receptors and cancer: the complexity of targeted inhibitors. Nat Rev Cancer 2005; 5:341-54.
10. Klapper LN, Glathe S, Vaisman N, Hynes NE, Andrews GC, Sela M, et al. The ErbB-2/HER2 oncoprotein of human carcinomas may function solely as a shared coreceptor for multiple stroma-derived growth factors. Proc Natl Acad Sci USA 1999; 96:4995-5000.
11. Singh AB, Harris RC. Autocrine, paracrine and juxtacrine signaling by EGFR ligands. Cell Signal 2005; 17:1183-93.
12. Baselga J, Swain SM. Novel anticancer targets: revisiting ERBB2 and discovering ERBB3. Nat Rev Cancer 2009; 9:463-75.
13. Guy PM, Platko JV, Cantley LC, Cerione RA, Carraway KL, 3rd. Insect cell-expressed p180erbB3 possesses an impaired tyrosine kinase activity. Proc Natl Acad Sci USA 1994; 91:8132-6.
14. Wallasch C, Weiss FU, Niederfellner G, Jallal B, Issing W, Ullrich A. Heregulin-dependent regulation of HER2/neu oncogenic signaling by heterodimerization with HER3. EMBO J 1995; 14:4267-75.
15. Sebolt-Leopold JS, Herrera R. Targeting the mitogen-activated protein kinase cascade to treat cancer. Nat Rev Cancer 2004; 4:937-47.
16. Engelman JA. Targeting PI3K signalling in cancer: opportunities, challenges and limitations. Nat Rev Cancer 2009; 9:550-62.
17. Carpenter G, Ji Q. Phospholipase C-gamma as a signal-transducing element. Exp Cell Res 1999; 253:15-24.
18. Spitaler M, Cantrell DA. Protein kinase C and beyond. Nat Immunol 2004; 5:785-90.
19. Griner EM, Kazanietz MG. Protein kinase C and other diacylglycerol effectors in cancer. Nat Rev Cancer 2007; 7:281-94.
20. Mackay HJ, Twelves CJ. Targeting the protein kinase C family: are we there yet? Nat Rev Cancer 2007; 7:554-62.
21. Marti U, Burwen SJ, Wells A, Barker ME, Huling S, Feren AM, et al. Localization of epidermal growth factor receptor in hepatocyte nuclei. Hepatology 1991; 13:15-20.
22. Cao H, Lei ZM, Bian L, Rao CV. Functional nuclear epidermal growth factor receptors in human choriocarcinoma JEG-3 cells and normal human placenta. Endocrinology 1995; 136:3163-72.
23. Lin SY, Makino K, Xia W, Matin A, Wen Y, Kwong KY, et al. Nuclear localization of EGF receptor and its potential new role as a transcription factor. Nat Cell Biol 2001; 3:802-8.
24. Lo HW, Hsu SC, Hung MC. EGFR signaling pathway in breast cancers: from traditional signal transduction to direct nuclear translocalization. Breast Cancer Res Treat 2006; 95:211-8.
25. Lo HW, Hung MC. Nuclear EGFR signalling network in cancers: linking EGFR pathway to cell cycle progression, nitric oxide pathway and patient survival. Br J Cancer 2006; 94:184-8.
26. Lo HW, Xia W, Wei Y, Ali-Seyed M, Huang SF, Hung MC. Novel prognostic value of nuclear epidermal growth factor receptor in breast cancer. Cancer Res 2005; 65:338-48.
27. Psyrri A, Yu Z, Weinberger PM, Sasaki C, Haffty B, Camp R, et al. Quantitative determination of nuclear and cytoplasmic epidermal growth factor receptor expression in oropharyngeal squamous cell cancer by using automated quantitative analysis. Clin Cancer Res 2005; 11:5856-62.
28. Xia W, Wei Y, Du Y, Liu J, Chang B, Yu YL, et al. Nuclear expression of epidermal growth factor receptor is a novel prognostic value in patients with ovarian cancer. Mol Carcinog 2009; 48:610-7.
29. Lo HW, Hsu SC, Ali-Seyed M, Gunduz M, Xia W, Wei Y, et al. Nuclear interaction of EGFR and STAT3 in the activation of the iNOS/NO pathway. Cancer Cell 2005; 7:575-89.
30. Hsu SC, Hung MC. Characterization of a novel tripartite nuclear localization sequence in the EGFR family. J Biol Chem 2007; 282:10432-40.
31. Lo HW, Cao X, Zhu H, Ali-Osman F. Cyclooxygenase-2 is a novel transcriptional target of the nuclear EGFR-STAT3 and EGFRvIII-STAT3 signaling axes. Mol Cancer Res 2010; 8:232-45.
32. Lo HW, Ali-Seyed M, Wu Y, Bartholomeusz G, Hsu SC, Hung MC. Nuclear-cytoplasmic transport of EGFR involves receptor endocytosis, importin beta1 and CRM1. J Cell Biochem 2006; 98:1570-83.
33. Liao HJ, Carpenter G. Role of the Sec61 translocon in EGF receptor trafficking to the nucleus and gene expression. Mol Biol Cell 2007; 18:1064-72.
34. Hanada N, Lo HW, Day CP, Pan Y, Nakajima Y, Hung MC. Co-regulation of B-Myb expression by E2F1 and EGF receptor. Mol Carcinog 2006; 45:10-7.
35. Hung LY, Tseng JT, Lee YC, Xia W, Wang YN, Wu ML, et al. Nuclear epidermal growth factor receptor (EGFR) interacts with signal transducer and activator of transcription 5 (STAT5) in activating Aurora-A gene expression. Nucleic Acids Res 2008; 36:4337-51.
36. Wang SC, Nakajima Y, Yu YL, Xia W, Chen CT, Yang CC, et al. Tyrosine phosphorylation controls PCNA function through protein stability. Nat Cell Biol 2006; 8:1359-68.
37. Dittmann K, Mayer C, Kehlbach R, Rodemann HP. Radiation-induced caveolin-1 associated EGFR internalization is linked with nuclear EGFR transport and activation of DNA-PK. Mol Cancer 2008; 7:69.
38. Liao HJ, Carpenter G. Cetuximab/C225-induced intracellular trafficking of epidermal growth factor receptor. Cancer Res 2009; 69:6179-83.
39. Citri A, Yarden Y. EGF-ERBB signalling: towards the systems level. Nat Rev Mol Cell Bio 2006; 7:505-16.
40. Haglund K, Sigismund S, Polo S, Szymkiewicz I, Di Fiore PP, Dikic I. Multiple monoubiquitination of RTKs is sufficient for their endocytosis and degradation. Nat Cell Biol 2003; 5:461-6.
41. Mineo C, Gill GN, Anderson GW. Regulated migration of epidermal growth factor receptor from caveolae. J Biol Chem 1999; 274:30636-43.
42. Vieira AV, Lamaze C, Schmid SL. Control of EGF receptor signaling by clathrin-mediated endocytosis. Science 1996; 274:2086-9.
43. Yamabhai M, Anderson RGW. Second cysteine-rich region of epidermal growth factor receptor contains targeting information for caveolae/rafts. J Biol Chem 2002; 277:24843-6.
44. Soubeyran P, Kowanetz K, Szymkiewicz I, Langdon WY, Dikic I. Cbl-CIN85-endophilin complex mediates ligand-induced downregulation of EGF receptors. Nature 2002; 416:183-7.
45. de Melker AA, van der Horst G, Borst J. c-Cbl directs EGF receptors into an endocytic pathway that involves the ubiquitin-interacting motif of Eps15. J Cell Sci 2004; 117:5001-12.
46. Marmor MD, Yarden Y. Role of protein ubiquitylation in regulating endocytosis of receptor tyrosine kinases. Oncogene 2004; 23:2057-70.
47. Bache KG, Slagsvold T, Stenmark H. Defective downregulation of receptor tyrosine kinases in cancer. EMBO J 2004; 23:2707-12.
48. Hendriks BS, Opresko LK, Wiley HS, Lauffenburger D. Coregulation of epidermal growth factor receptor/human epidermal growth factor receptor 2 (HER2) levels and locations: Quantitative analysis of HER2 overexpression effects. Cancer Res 2003; 63:1130-7.
49. Worthylake R, Opresko LK, Wiley HS. ErbB-2 amplification inhibits downregulation and induces constitutive activation of both ErbB-2 and epidermal growth factor receptors. J Biol Chem 1999; 274:8865-74.
50. Baulida J, Kraus MH, Alimandi M, DiFiore PP, Carpenter G. All ErbB receptors other than the epidermal growth factor receptor are endocytosis impaired. J Biol Chem 1996; 271:5251-7.
51. Sorkin A, Waters CM. Endocytosis of growth-factor receptors. Bioessays 1993; 15:375-82.
52. Wang ZX, Zhang LF, Yeung TK, Chen XM. Endocytosis deficiency of epidermal growth factor (EGF) receptor-ErbB2 heterodimers in response to EGF stimulation. Mol Biol Cell 1999; 10:1621-36.
53. Chung BM, Raja SM, Clubb RJ, Tu C, George M, Band V, et al. Aberrant trafficking of NSCLC-associated EGFR mutants through the endocytic recycling pathway promotes interaction with Src@. Bmc Cell Biol 2009; In press.
54. Hendriks BS, Wiley HS, Lauffenburger D. HER2-mediated effects on EGFR endosomal sorting: Analysis of biophysical mechanisms. Biophys J 2003; 85:2732-45.

CSPC Exhibit 1004
Page 118 of 336

55. Weichselbaum RR, Dunphy EJ, Beckett MA, Tybor AG, Moran WJ, Goldman ME, et al. Epidermal growth factor receptor gene amplification and expression in head and neck cancer cell lines. Head Neck 1989; 11:437-42.
56. Veale D, Ashcroft T, Marsh C, Gibson GJ, Harris AL. Epidermal growth factor receptors in non-small cell lung cancer. Br J Cancer 1987; 55:513-6.
57. Libermann TA, Razon N, Bartal AD, Yarden Y, Schlessinger J, Soreq H. Expression of epidermal growth factor receptors in human brain tumors. Cancer Res 1984; 44:753-60.
58. Libermann TA, Nusbaum HR, Razon N, Kris R, Lax I, Soreq H, et al. Amplification, enhanced expression and possible rearrangement of EGF receptor gene in primary human brain tumours of glial origin. Nature 1985; 313:144-7.
59. Libermann TA, Nusbaum HR, Razon N, Kris R, Lax I, Soreq H, et al. Amplification and overexpression of the EGF receptor gene in primary human glioblastomas. J Cell Sci Suppl 1985; 3:161-72.
60. Maurizi M, Almadori G, Ferrandina G, Distefano M, Romanini ME, Cadoni G, et al. Prognostic significance of epidermal growth factor receptor in laryngeal squamous cell carcinoma. Br J Cancer 1996; 74:1253-7.
61. FischerColbrie J, Witt A, Heinzl H, Speiser P, Czerwenka K, Sevelda P, et al. EGFR and steroid receptors in ovarian carcinoma: Comparison with prognostic parameters and outcome of patients. Anticancer Res 1997; 17:613-9.
62. Kersemaekers AMF, Fleuren GJ, Kenter EG, Van den Broek LJCM, Uljee SM, Hermans J, et al. Oncogene alterations in carcinomas of the uterine cervix: Overexpression of the epidermal growth factor receptor is associated with poor prognosis. Clin Cancer Res 1999; 5:577-86.
63. Mellon K, Wright C, Kelly P, Horne CHW, Neal DE. Long-term outcome related to epidermal growth-factor receptor status in bladder-cancer. Journal of Urology 1995; 153:919-25.
64. Inada S, Koto T, Furami K, Arima S, Iwashita A. Evaluation of malignancy and the prognosis of esophageal cancer based on an immunohistochemical study (p53, E-cadherin, epidermal growth factor receptor). Surg Today 1999; 29:493-503.
65. Ohgaki H, Watanabe K, Tachibana O, Sato K, Kleihues P. Overexpression of the EGF receptor and p53 mutations are mutually exclusive in the evolution of primary and secondary glioblastomas. J Neuropathol Exp Neurol 1996; 55:3.
66. Nicholson RI, Gee JM, Harper ME. EGFR and cancer prognosis. Eur J Cancer 2001; 37:9-15.
67. Nielsen JS, Jakobsen E, Holund B, Berrelsen K, Jakobsen A. Prognostic significance of p53, Her-2 and EGFR overexpression in borderline and epithelial ovarian cancer. Int J Gynecol Cancer 2004; 14:1086-96.
68. Santini J, Formento JL, Francoual M, Milano G, Schneider M, Dassonville O, et al. Characterization, quantification and potential clinical-value of the epidermal growth-factor receptor in head and neck squamous-cell carcinomas. Head Neck 1991; 13:132-9.
69. Yasui W, Sumiyoshi H, Hata J, Kameda T, Ochiai A, Ito H, et al. Expression of epidermal growth-factor receptor in human gastric and colonic carcinomas. Cancer Res 1988; 48:137-41.
70. Piyathilake CJ, Frost AR, Manne U, Weiss H, Bell WC, Heimburger DC, et al. Differential expression of growth factors in squamous cell carcinoma and precancerous lesions of the lung. Clin Cancer Res 2002; 8:734-44.
71. Scambia G, Panici PB, Ferrandina G, Battaglia F, Distefano M, Dandrea G, et al. Significance of epidermal growth-factor receptor expression in primary human endometrial cancer. Int J Cancer 1994; 56:26-30.
72. Nicholson RI, Gee JMW, Harper ME. EGFR and cancer prognosis. Eur J Cancer 2001; 37:9-15.
73. Sizeland AM, Burgess AW. Anti-sense transforming growth factor alpha oligonucleotides inhibit autocrine stimulated proliferation of a colon carcinoma cell line. Mol Biol Cell 1992; 3:1235-43.
74. Humphrey PA, Wong AJ, Vogelstein B, Zalutsky MR, Fuller GN, Archer GE, et al. Anti-syntheric peptide antibody reacting at the fusion junction of deletion-mutant epidermal growth factor receptors in human glioblastoma. Proc Natl Acad Sci USA 1990; 87:4207-11.
75. Malden LT, Novak U, Kaye AH, Burgess AW. Selective amplification of the cytoplasmic domain of the epidermal growth factor receptor gene in glioblastoma multiforme. Cancer Res 1988; 48:2711-4.
76. Peschard P, Park M. Escape from Cbl-mediated downregulation: a recurrent theme for oncogenic deregulation of receptor tyrosine kinases. Cancer Cell 2003; 3:519-23.
77. Gill GN, Kawamoto T, Cochet C, Le A, Sato JD, Masui H, et al. Monoclonal anti-epidermal growth factor receptor antibodies which are inhibitors of epidermal growth factor binding and antagonists of epidermal growth factor-stimulated tyrosine protein kinase activity. J Biol Chem 1984; 259:7755-60.
78. Kawamoto T, Sato JD, Le A, Polikoff J, Sato GH, Mendelsohn J. Growth stimulation of A431 cells by epidermal growth factor: identification of high-affinity receptors for epidermal growth factor by an anti-receptor monoclonal antibody. Proc Natl Acad Sci USA 1983; 80:1337-41.
79. Sato JD, Kawamoto T, Le AD, Mendelsohn J, Polikoff J, Sato GH. Biological effects in vitro of monoclonal antibodies to human epidermal growth factor receptors. Mol Biol Med 1983; 1:511-29.
80. Masui H, Kawamoto T, Sato JD, Wolf B, Sato G, Mendelsohn J. Growth inhibition of human tumor cells in athymic mice by anti-epidermal growth factor receptor monoclonal antibodies. Cancer Res 1984; 44:1002-7.
81. Li S, Schmitz KR, Jeffrey PD, Wiltzius JJ, Kussie P, Ferguson KM. Structural basis for inhibition of the epidermal growth factor receptor by cetuximab. Cancer Cell 2005; 7:301-11.
82. Yang XD, Jia XC, Corvalan JRF, Wang P, Davis CG. Development of ABX-EGF, a fully human anti-EGF receptor monoclonal antibody, for cancer therapy. Crit Rev Oncol Hemat 2001; 38:17-23.
83. Sunada H, Magun BE, Mendelsohn J, MacLeod CL. Monoclonal antibody against epidermal growth factor receptor is internalized without stimulating receptor phosphorylation. Proc Natl Acad Sci USA 1986; 83:3825-9.
84. Goldstein NI, Prewett M, Zuklys K, Rockwell P, Mendelsohn J. Biological efficacy of a chimeric antibody to the epidermal growth factor receptor in a human tumor xenograft model. Clin Cancer Res 1995; 1:1311-8.
85. Sunada H, Magun BE, Mendelsohn J, Macleod CL. Monoclonal-antibody against epidermal growth-factor receptor is internalized without stimulating receptor phosphorylation. Proc Natl Acad Sci USA 1986; 83:3825-9.
86. Huang SM, Bock JM, Harari PM. Epidermal growth factor receptor blockade with C225 modulates proliferation, apoptosis and radiosensitivity in squamous cell carcinomas of the head and neck. Cancer Res 1999; 59:1935-40.
87. Peng D, Fan Z, Lu Y, DeBlasio T, Scher H, Mendelsohn J. Anti-epidermal growth factor receptor monoclonal antibody 225 upregulates $p27^{KIP1}$ and induces G_1 arrest in prostatic cancer cell line DU145. Cancer Res 1996; 56:3666-9.
88. Wu X, Rubin M, Fan Z, DeBlasio T, Soos T, Koff A, et al. Involvement of $p27^{KIP1}$ in G_1 arrest mediated by an anti-epidermal growth factor receptor monoclonal antibody. Oncogene 1996; 12:1397-403.
89. Baselga J. The EGFR as a target for anticancer therapy—focus on cetuximab. Eur J Cancer 2001; 37:16-22.
90. P OC, Rhys-Evans P, Modjtahedi H, Court W, Box G, Eccles S. Overexpression of epidermal growth factor receptor in human head and neck squamous carcinoma cell lines correlates with matrix metalloproteinase-9 expression and in vitro invasion. Int J Cancer 2000; 86:307-17.
91. P Oc, Rhys-Evans P, Court WJ, Box GM, Eccles SA. Differential modulation of proliferation, matrix metalloproteinase expression and invasion of human head and neck squamous carcinoma cells by c-erbB ligands. Clin Exp Metastasis 1999; 17:631-9.
92. Bruns CJ, Harbison MT, Davis DW, Portera CA, Tsan R, McConkey DJ, et al. Epidermal growth factor receptor blockade with C225 plus gemcitabine results in regression of human pancreatic carcinoma growing orthotopically in nude mice by antiangiogenic mechanisms. Clin Cancer Res 2000; 6:1936-48.
93. Perrotte P, Matsumoto T, Inoue K, Kuniyasu H, Eve BY, Hicklin DJ, et al. Anti-epidermal growth factor receptor antibody C225 inhibits angiogenesis in human transitional cell carcinoma growing orthotopically in nude mice. Clin Cancer Res 1999; 5:257-65.
94. Tortora G, Caputo R, Pomatico G, Pepe S, Bianco AR, Agrawal S, et al. Cooperative inhibitory effect of novel mixed backbone oligonucleotide targeting protein kinase A in combination with docetaxel and anti-epidermal growth factor-receptor antibody on human breast cancer cell growth. Clin Cancer Res 1999; 5:875-81.
95. Liu B, Fang M, Schmidt M, Lu Y, Mendelsohn J, Fan Z. Induction of apoptosis and activation of the caspase cascade by anti-EGF receptor monoclonal antibodies in DiFi human colon cancer cells do not involve the c-jun N-terminal kinase activity. Br J Cancer 2000; 82:1991-9.
96. Mandal M, Adam L, Mendelsohn J, Kumar R. Nuclear targeting of Bax during apoptosis in human colorectal cancer cells. Oncogene 1998; 17:999-1007.
97. Wu X, Fan Z, Masui H, Rosen N, Mendelsohn J. Apoptosis induced by an anti-epidermal growth factor receptor monoclonal antibody in a human colorectal carcinoma cell line and its delay by insulin. J Clin Invest 1995; 95:1897-905.
98. Kurai J, Chikumi H, Hashimoto K, Yamaguchi K, Yamasaki A, Sako T, et al. Antibody-dependent cellular cytotoxicity mediated by cetuximab against lung cancer cell lines. Clin Cancer Res 2007; 13:1552-61.
99. Kimura H, Sakai K, Arao T, Shimoyama T, Tamura T, Nishio K. Antibody-dependent cellular cytotoxicity of cetuximab against tumor cells with wild-type or mutant epidermal growth factor receptor. Cancer Sci 2007; 98:1275-80.
100. Chung KY, Shia J, Kemeny NE, Shah M, Schwartz GK, Tse A, et al. Cetuximab shows activity in colorectal cancer patients with tumors that do not express the epidermal growth factor receptor by immunohistochemistry. J Clin Oncol 2005; 23:1803-10.
101. Jonker DJ, O'Callaghan CJ, Karapetis CS, Zalcberg JR, Tu D, Au HJ, et al. Cetuximab for the treatment of colorectal cancer. N Engl J Med 2007; 357:2040-8.
102. Sobrero AF, Maurel J, Fehrenbacher L, Scheithauer W, Abubakr YA, Lutz MP, et al. EPIC: phase III trial of cetuximab plus irinotecan after fluoropyrimidine and oxaliplatin failure in patients with metastatic colorectal cancer. J Clin Oncol 2008; 26:2311-9.
103. Borner M, Koeberle D, Von Moos R, Saletti P, Rauch D, Hess V, et al. Adding cetuximab to capecitabine plus oxaliplatin (XELOX) in first-line treatment of metastatic colorectal cancer: a randomized phase II trial of the Swiss Group for Clinical Cancer Research SAKK. Ann Oncol 2008; 19:1288-92.
104. Bokemeyer C, Bondarenko I, Makhson A, Hartmann JT, Aparicio J, de Braud F, et al. Fluorouracil, leucovorin and oxaliplatin with and without cetuximab in the first-line treatment of metastatic colorectal cancer. J Clin Oncol 2009; 27:663-71.

CSPC Exhibit 1004
Page 119 of 336

105. Van Cutsem E, Kohne CH, Hitre E, Zaluski J, Chang Chien CR, Makhson A, et al. Cetuximab and chemotherapy as initial treatment for metastatic colorectal cancer. N Engl J Med 2009; 360:1408-17.
106. Vermorken JB, Mesia R, Rivera F, Remenar E, Kawecki A, Rottey S, et al. Platinum-based chemotherapy plus cetuximab in head and neck cancer. N Engl J Med 2008; 359:1116-27.
107. Bonner JA, Harari PM, Giralt J, Azarnia N, Shin DM, Cohen RB, et al. Radiotherapy plus cetuximab for squamous-cell carcinoma of the head and neck. N Engl J Med 2006; 354:567-78.
108. Herbst RS, Arquette M, Shin DM, Dicke K, Vokes EE, Azarnia N, et al. Phase II multicenter study of the epidermal growth factor receptor antibody cetuximab and cisplatin for recurrent and refractory squamous cell carcinoma of the head and neck. J Clin Oncol 2005; 23:5578-87.
109. Baselga J, Trigo JM, Bourhis J, Tortochaux J, Cortes-Funes H, Hitt R, et al. Phase II multicenter study of the antiepidermal growth factor receptor monoclonal antibody cetuximab in combination with platinum-based chemotherapy in patients with platinum-refractory metastatic and/or recurrent squamous cell carcinoma of the head and neck. J Clin Oncol 2005; 23:5568-77.
110. Burtness B, Goldwasser MA, Flood W, Mattar B, Forastiere AA. Phase III randomized trial of cisplatin plus placebo compared with cisplatin plus cetuximab in metastatic/recurrent head and neck cancer: an eastern Cooperative Oncology Group study. J Clin Oncol 2005; 23:8646-54.
111. Cunningham D, Humblet Y, Siena S, Khayat D, Bleiberg H, Santoro A, et al. Cetuximab monotherapy and cetuximab plus irinotecan in irinotecan-refractory metastatic colorectal cancer. N Engl J Med 2004; 351:337-45.
112. Robert F, Ezekiel MP, Spencer SA, Meredith RF, Bonner JA, Khazaeli MB, et al. Phase I study of anti-epidermal growth factor receptor antibody cetuximab in combination with radiation therapy in patients with advanced head and neck cancer. J Clin Oncol 2001; 19:3234-43.
113. Thienelt CD, Bunn PA Jr, Hanna N, Rosenberg A, Needle MN, Long ME, et al. Multicenter phase I/II study of cetuximab with paclitaxel and carboplatin in untreated patients with stage IV non-small-cell lung cancer. J Clin Oncol 2005; 23:8786-93.
114. Rosell R, Robinet G, Szczesna A, Ramlau R, Constenla M, Mennecier BC, et al. Randomized phase II study of cetuximab plus cisplatin/vinorelbine compared with cisplatin/vinorelbine alone as first-line therapy in EGFR-expressing advanced non-small-cell lung cancer. Ann Oncol 2008; 19:362-9.
115. Robert F, Blumenschein G, Herbst RS, Fossella FV, Tseng J, Saleh MN, et al. Phase I/IIa study of cetuximab with gemcitabine plus carboplatin in patients with chemotherapy-naive advanced non-small-cell lung cancer. J Clin Oncol 2005; 23:9089-96.
116. Herbst RS, Chansky K, Kelly K, Atkins JN, Davies AM, Dakhil SR, et al. phase II randomized selection trial evaluating concurrent chemotherapy plus cetuximab or chemotherapy followed by cetuximab in patients with advanced non-small cell lung cancer (NSCLC): Final report of SWOG 0342. ASCO 2007.
117. Butts CA, Bodkin D, Middleman EL, Englund CW, Ellison D, Alam Y, et al. Randomized phase II study of gemcitabine plus cisplatin or carboplatin [corrected], with or without cetuximab, as first-line therapy for patients with advanced or metastatic non small-cell lung cancer. J Clin Oncol 2007; 25:5777-84.
118. Pirker R, Pereira JR, Szczesna A, von Pawel J, Krzakowski M, Ramlau R, et al. Cetuximab plus chemotherapy in patients with advanced non-small-cell lung cancer (FLEX): an open-label randomised phase III trial. Lancet 2009; 373:1525-31.
119. Lynch TJ, Patel T, Dreisbach L, McCleod M, Heim WJ, Hermann RC, et al. Cetuximab and first-line taxane/carboplatin chemotherapy in advanced non-small-cell lung cancer: results of the randomized multicenter phase III trial BMS099. J Clin Oncol 2010; 28:911-7.
120. Pao W, Miller V, Zakowski M, Doherty J, Politi K, Sarkaria I, et al. EGF receptor gene mutations are common in lung cancers from "never smokers" and are associated with sensitivity of tumors to gefitinib and erlotinib. Proc Natl Acad Sci USA 2004; 101:13306-11.
121. Lynch TJ, Bell DW, Sordella R, Gurubhagavatula S, Okimoto RA, Brannigan BW, et al. Activating mutations in the epidermal growth factor receptor underlying responsiveness of non-small-cell lung cancer to gefitinib. N Engl J Med 2004; 350:2129-39.
122. Paez JG, Janne PA, Lee JC, Tracy S, Greulich H, Gabriel S, et al. EGFR mutations in lung cancer: correlation with clinical response to gefitinib therapy. Science 2004; 304:1497-500.
123. Pao W, Miller VA, Politi KA, Riely GJ, Somwar R, Zakowski MF, et al. Acquired resistance of lung adenocarcinomas to gefitinib or erlotinib is associated with a second mutation in the EGFR kinase domain. PLoS Med 2005; 2:73.
124. Kobayashi S, Boggon TJ, Dayaram T, Janne PA, Kocher O, Meyerson M, et al. EGFR mutation and resistance of non-small-cell lung cancer to gefitinib. N Engl J Med 2005; 352:786-92.
125. Tsuchihashi Z, Khambata-Ford S, Hanna N, Janne PA. Responsiveness to cetuximab without mutations in EGFR. N Engl J Med 2005; 353:208-9.
126. Mukohara T, Engelman JA, Hanna NH, Yeap BY, Kobayashi S, Lindeman N, et al. Differential effects of gefitinib and cetuximab on non-small-cell lung cancers bearing epidermal growth factor receptor mutations. J Natl Cancer Inst 2005; 97:1185-94.
127. Moroni M, Veronese S, Benvenuti S, Marrapese G, Sartore-Bianchi A, Di Nicolantonio F, et al. Gene copy number for epidermal growth factor receptor (EGFR) and clinical response to antiEGFR treatment in colorectal cancer: a cohort study. Lancet Oncol 2005; 6:279-86.
128. Frattini M, Saletti P, Romagnani E, Martin V, Molinari F, Ghisletta M, et al. PTEN loss of expression predicts cetuximab efficacy in metastatic colorectal cancer patients. Br J Cancer 2007; 97:1139-45.
129. Personeni N, Fieuws S, Piessevaux H, De Hertogh G, De Schutter J, Biesmans B, et al. Clinical usefulness of EGFR gene copy number as a predictive marker in colorectal cancer patients treated with cetuximab: a fluorescent in situ hybridization study. Clin Cancer Res 2008; 14:5869-76.
130. Cappuzzo F, Finocchiaro G, Rossi E, Janne PA, Carnaghi C, Calandri C, et al. EGFR FISH assay predicts for response to cetuximab in chemotherapy refractory colorectal cancer patients. Ann Oncol 2008; 19:717-23.
131. Sartore-Bianchi A, Moroni M, Veronese S, Carnaghi C, Bajetta E, Luppi G, et al. Epidermal growth factor receptor gene copy number and clinical outcome of metastatic colorectal cancer treated with panitumumab. J Clin Oncol 2007; 25:3238-45.
132. Hirsch FR, Herbst RS, Olsen C, Chansky K, Crowley J, Kelly K, et al. Increased EGFR gene copy number detected by fluorescent in situ hybridization predicts outcome in non-small-cell lung cancer patients treated with cetuximab and chemotherapy. J Clin Oncol 2008; 26:3351-7.
133. Khambata-Ford S, Harbison CT, Hart LL, Awad M, Xu LA, Horak CE, et al. Analysis of potential predictive markers of cetuximab benefit in BMS099, a phase III study of cetuximab and first-line taxane/carboplatin in advanced non-small-cell lung cancer. J Clin Oncol 2010; 28:918-27.
134. Khambata-Ford S, Garrett CR, Meropol NJ, Basik M, Harbison CT, Wu S, et al. Expression of epiregulin and amphiregulin and K-ras mutation status predict disease control in metastatic colorectal cancer patients treated with cetuximab. J Clin Oncol 2007; 25:3230-7.
135. Trahey M, McCormick F. A cytoplasmic protein stimulates normal N-ras p21 GTPase, but does not affect oncogenic mutants. Science 1987; 238:542-5.
136. Schubbert S, Shannon K, Bollag G. Hyperactive Ras in developmental disorders and cancer. Nat Rev Cancer 2007; 7:295-308.
137. Lievre A, Bachet JB, Le Corre D, Boige V, Landi B, Emile JF, et al. KRAS mutation status is predictive of response to cetuximab therapy in colorectal cancer. Cancer Res 2006; 66:3992-5.
138. Di Fiore F, Blanchard F, Charbonnier F, Le Pessot F, Lamy A, Galais MP, et al. Clinical relevance of KRAS mutation detection in metastatic colorectal cancer treated by Cetuximab plus chemotherapy. Br J Cancer 2007; 96:1166-9.
139. De Roock W, Piessevaux H, De Schutter J, Janssens M, De Hertogh G, Personeni N, et al. KRAS wild-type state predicts survival and is associated to early radiological response in metastatic colorectal cancer treated with cetuximab. Ann Oncol 2008; 19:508-15.
140. Punt CJ, Tol J, Rodenburg CJ, Cats A, Creemers GM, Schrama JG, et al. Randomized phase III study of capecitabine, oxaliplatin and bevacizumab with or without cetuximab in advanced colorectal cancer (ACC), the CAIRO2 study of the Dutch Colorectal Cancer Group (DCCG). ASCO Meeting Abstracts May 20 2008; 2008.
141. Van Cutsem E, Lang I, D'haens G, Moiseyenko V, Zaluski J, Folprecht G, et al. KRAS status and efficacy in the first-line treatment of patients with metastatic colorectal cancer (mCRC) treated with FOLFIRI with or without cetuximab: The CRYSTAL experience. ASCO Meeting Abstracts 2008; 2:2008.
142. Bokemeyer C, Bondarenko I, Hartmann J, De Braud F, Volovat C, Nippgen L, et al. KRAS status and efficacy of first-line treatment of patients with metastatic colorectal cancer (mCRC) with FOLFOX with or without cetuximab: The OPUS experience. ASCO Meeting Abstracts 2008; 4000.
143. Karaperis CS, Khambata-Ford S, Jonker DJ, O'Callaghan CJ, Tu D, Tebbutt NC, et al. K-ras mutations and benefit from cetuximab in advanced colorectal cancer. N Engl J Med 2008; 359:1757-65.
144. Amado RG, Wolf M, Peeters M, Van Cutsem E, Siena S, Freeman DJ, et al. Wild-type KRAS is required for panitumumab efficacy in patients with metastatic colorectal cancer. J Clin Oncol 2008; 26:1626-34.
145. Allegra CJ, Jessup JM, Somerfield MR, Hamilton SR, Hammond EH, Hayes DF, et al. American Society of Clinical Oncology provisional clinical opinion: testing for KRAS gene mutations in patients with metastatic colorectal carcinoma to predict response to anti-epidermal growth factor receptor monoclonal antibody therapy. J Clin Oncol 2009; 27:2091-6.
146. Loupakis F, Pollina L, Stasi I, Ruzzo A, Scartozzi M, Santini D, et al. PTEN expression and KRAS mutations on primary tumors and metastases in the prediction of benefit from cetuximab plus irinotecan for patients with metastatic colorectal cancer. J Clin Oncol 2009; 27:2622-9.
147. Benvenuti S, Sartore-Bianchi A, Di Nicolantonio F, Zanon C, Moroni M, Veronese S, et al. Oncogenic activation of the RAS/RAF signaling pathway impairs the response of metastatic colorectal cancers to anti-epidermal growth factor receptor antibody therapies. Cancer Res 2007; 67:2643-8.
148. Marais R, Light Y, Paterson HF, Marshall CJ. Ras recruits Raf-1 to the plasma membrane for activation by tyrosine phosphorylation. EMBO J 1995; 14:3136-45.

CSPC Exhibit 1004
Page 120 of 336

149. Roberts PJ, Der CJ. Targeting the Raf-MEK-ERK mitogen-activated protein kinase cascade for the treatment of cancer. Oncogene 2007; 26:3291-310.
150. Niault TS, Baccarini M. Targets of Raf in tumorigenesis. Carcinogenesis 2010; 31:1165-74.
151. Di Nicolantonio F, Martini M, Molinari F, Sartore-Bianchi A, Arena S, Saletti P, et al. Wild-type BRAF is required for response to panitumumab or cetuximab in metastatic colorectal cancer. J Clin Oncol 2008; 26:5705-12.
152. Blanco R, Iwakawa R, Tang M, Kohno T, Angulo B, Pio R, et al. A gene-alteration profile of human lung cancer cell lines. Hum Mutat 2009; 30:1199-206.
153. Pratilas CA, Taylor BS, Ye Q, Viale A, Sander C, Solit DB, et al. (V600E)BRAF is associated with disabled feedback inhibition of RAF-MEK signaling and elevated transcriptional output of the pathway. Proc Natl Acad Sci USA 2009; 106:4519-24.
154. Brose MS, Volpe P, Feldman M, Kumar M, Rishi I, Gerrero R, et al. BRAF and RAS mutations in human lung cancer and melanoma. Cancer Res 2002; 62:6997-7000.
155. Davies H, Bignell GR, Cox C, Stephens P, Edkins S, Clegg S, et al. Mutations of the BRAF gene in human cancer. Nature 2002; 417:949-54.
156. Weber A, Langhanki L, Sommerer F, Markwarth A, Wittekind C, Tannapfel A. Mutations of the BRAF gene in squamous cell carcinoma of the head and neck. Oncogene 2003; 22:4757-9.
157. Perrone F, Suardi S, Pastore E, Casieri P, Orsenigo M, Caramuta S, et al. Molecular and cytogeneric subgroups of oropharyngeal squamous cell carcinoma. Clin Cancer Res 2006; 12:6643-51.
158. Fei Huang LAX, Shirin Khambata-Ford. Analysis of the correlation between gene expression of IGF-pathway components and benefit from cetuximab (Erbitux™) in metastatic colorectal cancer patients. AACR meeting Abstracts 2010.
159. Perrotte P, Matsumoto T, Inoue K, Kuniyasu H, Eve BY, Hicklin DJ, et al. Anti-epidermal growth factor receptor antibody C225 inhibits angiogenesis in human transitional cell carcinoma growing orthotopically in nude mice. Clin Cancer Res 1999; 5:257-65.
160. Petit AMV, Rak J, Hung MC, Rockwell P, Goldstein N, Fendly B, et al. Neutralizing antibodies against epidermal growth factor and ErbB-2/neu receptor tyrosine kinases downregulate vascular endothelial growth factor production by tumor cells in vitro and in vivo—Angiogenic implications for signal transduction therapy of solid tumors. Am J Pathol 1997; 151:1523-30.
161. Ciardiello F, Bianco R, Damiano V, Fontanini G, Caputo R, Pomarico G, et al. Antiangiogenic and antitumor activity of anti-epidermal growth factor receptor C225 monoclonal antibody in combination with vascular endothelial growth factor antisense oligonucleotide in human GEO colon cancer cells. Clin Cancer Res 2000; 6:3739-47.
162. Viloria-Petit A, Crombet T, Jothy S, Hicklin D, Bohlen P, Schlaeppi JM, et al. Acquired resistance to the antitumor effect of epidermal growth factor receptor-blocking antibodies in vivo: A role for altered tumor angiogenesis. Cancer Res 2001; 61:5090-101.
163. Ferrara N. The role of vascular endothelial growth factor in pathological angiogenesis. Breast Cancer Res Treat 1995; 36:127-37.
164. Fontanini G, Vignati S, Boldrini L, Chine S, Silvestri V, Lucchi M, et al. Vascular endothelial growth factor is associated with neovascularization and influences progression of non-small cell lung carcinoma. Clin Cancer Res 1997; 3:861-5.
165. Jung YD, Mansfield PF, Akagi M, Takeda A, Liu W, Bucana CD, et al. Effects of combination anti-vascular endothelial growth factor receptor and anti-epidermal growth factor receptor therapies on the growth of gastric cancer in a nude mouse model. Eur J Cancer 2002; 38:1133-40.
166. Ciardiello F, Bianco R, Caputo R, Caputo R, Damiano V, Troiani T, et al. Antitumor activity of ZD6474, a vascular endothelial growth factor receptor tyrosine kinase inhibitor, in human cancer cells with acquired resistance to antiepidermal growth factor receptor therapy. Clin Cancer Res 2004; 10:784-93.
167. Bianco R, Rosa R, Damiano V, Daniele G, Gelardi T, Garofalo S, et al. Vascular endothelial growth factor receptor-1 contributes to resistance to anti-epidermal growth factor receptor drugs in human cancer cells. Clin Cancer Res 2008; 14:5069-80.
168. Lu Y, Li XQ, Liang K, Luwor R, Siddik ZH, Nuiis GB, et al. Epidermal growth factor receptor (EGFR) ubiquitination as a mechanism of acquired resistance escaping treatment by the Anti-EGFR monoclonal antibody cetuximab. Cancer Res 2007; 67:8240-7.
169. Bao J, Gur G, Yarden Y. Src promotes destruction of c-Cbl: Implications for oncogenic synergy between Src and growth factor receptors. Proc Natl Acad Sci USA 2003; 100:2438-43.
170. Wheeler DL, Huang S, Kruser TJ, Nechrebecki MM, Armstrong EA, Benavente S, et al. Mechanisms of acquired resistance to cetuximab: role of HER (ErbB) family members. Oncogene 2008; 27:3944-56.
171. Grovdal LM, Stang E, Sorkin A, Madshus IH. Direct interaction of Cbl with pTyr 1045 of the EGF receptor (EGFR) is required to sort the EGFR to lysosomes for degradation. Exp Cell Res 2004; 300:388-95.
172. Demory ML, Boerner JL, Davidson R, Faust W, Miyake T, Lee I, et al. Epidermal growth factor receptor translocation to the mitochondria: regulation and effect. J Biol Chem 2009; 284:36592-604.
173. Lo HW, Cao X, Zhu H, Ali-Osman F. Constitutively Activated STAT3 Frequently Coexpresses with Epidermal Growth Factor Receptor in High-Grade Gliomas and Targeting STAT3 Sensitizes Them to Iressa and Alkylators. Clin Cancer Res 2008; 14:6042-54.
174. Lo HW, Hsu SC, Hung MC. EGFR signaling pathway in breast cancers: from traditional signal transduction to direct nuclear translocalization. Breast Cancer Res Tr 2006; 95:211-8.
175. Lo HW, Hsu SC, Ali-Seyed M, Gunduz M, Xia WY, Wei YK, et al. Nuclear interaction of EGFR and STAT3 in the activation of the iNOS/NO pathway. Cancer Cell 2005; 7:575-89.
176. Lo HW, Ali-Seyed M, Wu Y, Bartholomeusz G, Hsu SC, Hung MC. Nuclear-cytoplasmic transport of EGFR involves receptor endocytosis, importin beta1 and CRM1. J Cell Biochem 2006; 98:1570-83.
177. Hanada N, Lo HW, Day CP, Pan Y, Nakajima Y, Hung MC. Co-regulation of B-Myb expression by E2F1 and EGF receptor. Mol Carcinogen 2006; 45:10-7.
178. Kim J, Jahng WJ, Di Vizio D, Lee JS, Jhaveri R, Rubin MA, et al. The phosphoinositide kinase PIKfyve mediates epidermal growth factor receptor trafficking to the nucleus. Cancer Res 2007; 67:9229-37.
179. Xia WY, Wei YK, Du Y, Liu JS, Chang B, Yu YL, et al. Nuclear expression of epidermal growth factor receptor is a novel prognostic value in patients with ovarian cancer. Mol Carcinogen 2009; 48:610-7.
180. Li C, Iida M, Dunn EF, Ghia AJ, Wheeler DL. Nuclear EGFR contributes to acquired resistance to cetuximab. Oncogene 2009; 28:3801-13.
181. Lin SY, Makino K, Xia WY, Matin A, Wen Y, Kwong KY, et al. Nuclear localization of EGF receptor and its potential new role as a transcription factor. Nat Cell Biol 2001; 3:802-8.
182. Li C, Iida M, Dunn EF, Ghia AJ, Wheeler DL. Nuclear EGFR contributes to acquired resistance to cetuximab. Oncogene 2009; 28:3801-13.
183. Bandyopadhyay D, Mandal M, Adam L, Mendelsohn J, Kumar R. Physical interaction between epidermal growth factor receptor and DNA-dependent protein kinase in mammalian cells. J Biol Chem 1998; 273:1568-73.
184. Wheeler DL, Iida M, Kruser TJ, Nechrebecki MM, Dunn EF, Armstrong EA, et al. Epidermal growth factor receptor cooperates with Src family kinases in acquired resistance to cetuximab. Cancer Biol Ther 2009; 8:696-703.
185. Nevo J, Mattila E, Pellinen T, Yamamoto DL, Sara H, Iljin K, et al. Mammary-derived growth inhibitor alters traffic of EGFR and induces a novel form of cetuximab resistance. Clin Cancer Res 2009; 15:6570-81.
186. Huynh HT, Larsson C, Narod S, Pollak M. Tumor suppressor activity of the gene encoding mammary-derived growth inhibitor. Cancer Res 1995; 55:2225-31.
187. Huynh H, Alpert L, Pollak M. Silencing of the mammary-derived growth inhibitor (MDGI) gene in breast neoplasms is associated with epigenetic changes. Cancer Res 1996; 56:4865-70.
188. Specht B, Barretzko N, Hohoff C, Kuhl H, Franke R, Borchers T, et al. Mammary derived growth inhibitor is not a distinct protein but a mix of heart-type and adipocyte-type fatty acid-binding protein. J Biol Chem 1996; 271:19943-9.
189. Spener F, Unterberg C, Borchers T, Grosse R. Characteristics of fatty acid-binding proteins and their relation to mammary-derived growth inhibitor. Mol Cell Biochem 1990; 98:57-68.
190. Hanahan D, Weinberg RA. The hallmarks of cancer. Cell 2000; 100:57-70.
191. Huber MA, Kraut N, Beug H. Molecular requirements for epithelial-mesenchymal transition during tumor progression. Curr Opin Cell Biol 2005; 17:548-58.
192. Thompson EW, Newgreen DF. Carcinoma invasion and metastasis: A role for epithelial-mesenchymal transition? Cancer Res 2005; 65:5991-5.
193. Basu D, Nguyen TTK, Montone KT, Zhang G, Wang LP, Diehl JA, et al. Evidence for mesenchymal-like sub-populations within squamous cell carcinomas possessing chemoresistance and phenotypic plasticity. Oncogene 2010; 29:4170-82.
194. Strauss R, Sova P, Liu Y, Li ZY, Tuve S, Pritchard D, et al. Epithelial phenotype confers resistance of ovarian cancer cells to oncolytic denoviruses. Cancer Res 2009; 69:5115-25.
195. Troussard AA, Mawji NM, Ong C, Mui A, St. Arnaud R, Dedhar S. Conditional knock-out of integrin-linked kinase demonstrates an essential role in protein kinase B/Akt activation. J Biol Chem 2003; 278:22374-8.
196. Fuchs BC, Fujii T, Dorfman JD, Goodwin JM, Zhu AX, Lanuti M, et al. Epithelial-to-mesenchymal transition and integrin-linked kinase mediate sensitivity to epidermal growth factor receptor inhibition in human hepatoma cells. Cancer Res 2008; 68:2391-9.
197. Kim SM, Kim JS, Kim JH, Yun CO, Kim EM, Kim HK, et al. Acquired resistance to cetuximab is mediated by increased PTEN instability and leads cross-resistance to gefitinib in HCC827 NSCLC cells. Cancer Lett 2010; 296:150-9.
198. Normanno N, Tejpar S, Morgillo F, De Luca A, Van Cutsem E, Ciardiello F. Implications for KRAS status and EGFR-targeted therapies in metastatic CRC. Nat Rev Clin Oncol 2009; 6:519-27.
199. De Roock W, Piessevaux H, De Schutter J, Janssens M, De Hertogh G, Personeni N, et al. KRAS wild-type state predicts survival and is associated to early radiological response in metastatic colorectal cancer treated with cetuximab. Ann Oncol 2008; 19:508-15.
200. Bardelli A, Siena S. Molecular mechanisms of resistance to cetuximab and panitumumab in colorectal cancer. J Clin Oncol 2010; 28:1254-61.
201. Dunn EF, Iida M, Myers RA, Campbell DA, Hintz KA, Armstrong EA, et al. Dasatinib sensitizes KRAS mutant colorectal tumors to cetuximab. Oncogene 2010; In press.
202. Hatakeyama H, Cheng HX, Wirth P, Counsell A, Marcrom SR, Wood CB, et al. Regulation of heparin-binding EGF-like growth factor by miR-212 and acquired cetuximab-resistance in head and neck squamous cell carcinoma. PLoS One 2010; 5:e12702.

CSPC Exhibit 1004
Page 121 of 336

To: docket@bozpat.com,,
From: PAIR_eOfficeAction@uspto.gov
Cc: PAIR_eOfficeAction@uspto.gov
Subject: Private PAIR Correspondence Notification for Customer Number 93726

Apr 04, 2019 04:56:58 AM

Dear PAIR Customer:

EPA - Bozicevic Field & Francis LLP
Bozicevic, Field & Francis
201 REDWOOD SHORES PARKWAY
SUITE 200
REDWOOD CITY, CA 94065
UNITED STATES

The following USPTO patent application(s) associated with your Customer Number, 93726 , have new outgoing correspondence. This correspondence is now available for viewing in Private PAIR.

The official date of notification of the outgoing correspondence will be indicated on the form PTOL-90 accompanying the correspondence.

Disclaimer:
The list of documents shown below is provided as a courtesy and is not part of the official file wrapper. The content of the images shown in PAIR is the official record.

Application	Document	Mailroom Date	Attorney Docket No.
15550995	CTNF	04/04/2019	CCPIT-002
	892	04/04/2019	CCPIT-002
	1449	04/04/2019	CCPIT-002

To view your correspondence online or update your email addresses, please visit us anytime at https://sportal.uspto.gov/secure/myportal/privatepair.

If you have any questions, please email the Electronic Business Center (EBC) at EBC@uspto.gov with 'e-Office Action' on the subject line or call 1-866-217-9197 during the following hours:

Monday - Friday 6:00 a.m. to 12:00 a.m.

Thank you for prompt attention to this notice,

UNITED STATES PATENT AND TRADEMARK OFFICE

PATENT APPLICATION INFORMATION RETRIEVAL SYSTEM

Doc Code: PA..
Document Description: Power of Attorney

PTO/AIA/82B (07-13)
Approved for use through 01/31/2018. OMB 0651-0035
U.S. Patent and Trademark Office; U.S. DEPARTMENT OF COMMERCE
Under the Paperwork Reduction Act of 1995, no persons are required to respond to a collection of information unless it displays a valid OMB control number

POWER OF ATTORNEY BY APPLICANT

I hereby revoke all previous powers of attorney given in the application identified in either the attached transmittal letter or the boxes below.

Application Number	Filing Date
15/550,995	August 14, 2017

(Note: The boxes above may be left blank if information is provided on form PTO/AIA/82A.)

☑ I hereby appoint the Patent Practitioner(s) associated with the following Customer Number as my/our attorney(s) or agent(s), and to transact all business in the United States Patent and Trademark Office connected therewith for the application referenced in the attached transmittal letter (form PTO/AIA/82A) or identified above: 00500

OR

☐ I hereby appoint Practitioner(s) named in the attached list (form PTO/AIA/82C) as my/our attorney(s) or agent(s), and to transact all business in the United States Patent and Trademark Office connected therewith for the patent application referenced in the attached transmittal letter (form PTO/AIA/82A) or identified above. (Note: Complete form PTO/AIA/82C.)

Please recognize or change the correspondence address for the application identified in the attached transmittal letter or the boxes above to:

☑ The address associated with the above-mentioned Customer Number

OR

☐ The address associated with Customer Number:

OR

☐ Firm or Individual Name					
Address					
City		State		Zip	
Country					
Telephone		Email			

I am the Applicant (if the Applicant is a juristic entity, list the Applicant name in the box):

SHANGHAI MIRACOGEN INC.

☐ Inventor or Joint Inventor (title not required below)

☐ Legal Representative of a Deceased or Legally Incapacitated Inventor (title not required below)

☑ Assignee or Person to Whom the Inventor is Under an Obligation to Assign (provide signer's title if applicant is a juristic entity)

☐ Person Who Otherwise Shows Sufficient Proprietary Interest (e.g., a petition under 37 CFR 1.46(b)(2) was granted in the application or is concurrently being filed with this document) (provide signer's title if applicant is a juristic entity)

SIGNATURE of Applicant for Patent

The undersigned (whose title is supplied below) is authorized to act on behalf of the applicant (e.g., where the applicant is a juristic entity).

Signature	Chaohong Hu	Date (Optional)	May 31, 2019
Name	CHAOHONG HU		
Title	CEO		

NOTE: Signature - This form must be signed by the applicant in accordance with 37 CFR 1.33. See 37 CFR 1.4 for signature requirements and certifications. If more than one applicant, use multiple forms.

☐ Total of forms are submitted.

This collection of information is required by 37 CFR 1.131, 1.32, and 1.33. The information is required to obtain or retain a benefit by the public which is to file (and by the USPTO to process) an application. Confidentiality is governed by 35 U.S.C. 122 and 37 CFR 1.11 and 1.14. This collection is estimated to take 3 minutes to complete, including gathering, preparing, and submitting the completed application form to the USPTO. Time will vary depending upon the individual case. Any comments on the amount of time you require to complete this form and/or suggestions for reducing this burden, should be sent to the Chief Information Officer, U.S. Patent and Trademark Office, U.S. Department of Commerce, P.O. Box 1450, Alexandria, VA 22313-1450. DO NOT SEND FEES OR COMPLETED FORMS TO THIS ADDRESS. **SEND TO: Commissioner for Patents, P.O. Box 1450, Alexandria, VA 22313-1450.**

If you need assistance in completing the form, call 1-800-PTO-9199 and select option 2.

Electronic Acknowledgement Receipt

EFS ID:	36199969
Application Number:	15550995
International Application Number:	
Confirmation Number:	1813
Title of Invention:	Antibody-Drug Conjugate
First Named Inventor/Applicant Name:	Chaohong Hu
Customer Number:	93726
Filer:	Qing Lin/Barbara Hannon
Filer Authorized By:	Qing Lin
Attorney Docket Number:	CCPIT-002
Receipt Date:	04-JUN-2019
Filing Date:	14-AUG-2017
Time Stamp:	16:28:24
Application Type:	U.S. National Stage under 35 USC 371

Payment information:

Submitted with Payment	no

File Listing:

Document Number	Document Description	File Name	File Size(Bytes)/ Message Digest	Multi Part /.zip	Pages (if appl.)
1	Power of Attorney	401USPC_POA-Executed.pdf	970180 47bce6d76bea69b56ac5ce6dc6b5028cfe47e6dd	no	1

Warnings:

Information:	
Total Files Size (in bytes):	970180

This Acknowledgement Receipt evidences receipt on the noted date by the USPTO of the indicated documents, characterized by the applicant, and including page counts, where applicable. It serves as evidence of receipt similar to a Post Card, as described in MPEP 503.

New Applications Under 35 U.S.C. 111

If a new application is being filed and the application includes the necessary components for a filing date (see 37 CFR 1.53(b)-(d) and MPEP 506), a Filing Receipt (37 CFR 1.54) will be issued in due course and the date shown on this Acknowledgement Receipt will establish the filing date of the application.

National Stage of an International Application under 35 U.S.C. 371

If a timely submission to enter the national stage of an international application is compliant with the conditions of 35 U.S.C. 371 and other applicable requirements a Form PCT/DO/EO/903 indicating acceptance of the application as a national stage submission under 35 U.S.C. 371 will be issued in addition to the Filing Receipt, in due course.

New International Application Filed with the USPTO as a Receiving Office

If a new international application is being filed and the international application includes the necessary components for an international filing date (see PCT Article 11 and MPEP 1810), a Notification of the International Application Number and of the International Filing Date (Form PCT/RO/105) will be issued in due course, subject to prescriptions concerning national security, and the date shown on this Acknowledgement Receipt will establish the international filing date of the application.

UNITED STATES PATENT AND TRADEMARK OFFICE

UNITED STATES DEPARTMENT OF COMMERCE
United States Patent and Trademark Office
Address: COMMISSIONER FOR PATENTS
P.O. Box 1450
Alexandria, Virginia 22313-1450
www.uspto.gov

APPLICATION NUMBER	FILING OR 371(C) DATE	FIRST NAMED APPLICANT	ATTY. DOCKET NO./TITLE
15/550,995	08/14/2017	Chaohong Hu	CCPIT-002

CONFIRMATION NO. 1813

500
SEED INTELLECTUAL PROPERTY LAW GROUP LLP
701 FIFTH AVE
SUITE 5400
SEATTLE, WA 98104

POA ACCEPTANCE LETTER

OC000000108698208

Date Mailed: 06/06/2019

NOTICE OF ACCEPTANCE OF POWER OF ATTORNEY

This is in response to the Power of Attorney filed 06/04/2019.

The Power of Attorney in this application is accepted. Correspondence in this application will be mailed to the above address as provided by 37 CFR 1.33.

Questions about the contents of this notice and the requirements it sets forth should be directed to the Office of Data Management, Application Assistance Unit, at **(571) 272-4000** or **(571) 272-4200** or **1-888-786-0101**.

/yteferra/

To: USPTOeAction@SeedIP.com,pairlinkdktg@seedip.com,
From: PAIR_eOfficeAction@uspto.gov
Cc: PAIR_eOfficeAction@uspto.gov
Subject: Private PAIR Correspondence Notification for Customer Number 500

Jun 06, 2019 03:36:46 AM

Dear PAIR Customer:

SEED INTELLECTUAL PROPERTY LAW GROUP LLP
701 FIFTH AVE
SUITE 5400
SEATTLE, WA 98104
UNITED STATES

The following USPTO patent application(s) associated with your Customer Number, 500 , have new outgoing correspondence. This correspondence is now available for viewing in Private PAIR.

The official date of notification of the outgoing correspondence will be indicated on the form PTOL-90 accompanying the correspondence.

Disclaimer:
The list of documents shown below is provided as a courtesy and is not part of the official file wrapper. The content of the images shown in PAIR is the official record.

Application	Document	Mailroom Date	Attorney Docket No.
15550995	N570	06/06/2019	CCPIT-002

To view your correspondence online or update your email addresses, please visit us anytime at https://sportal.uspto.gov/secure/myportal/privatepair.

If you have any questions, please email the Electronic Business Center (EBC) at EBC@uspto.gov with 'e-Office Action' on the subject line or call 1-866-217-9197 during the following hours:

Monday - Friday 6:00 a.m. to 12:00 a.m.

Thank you for prompt attention to this notice,

UNITED STATES PATENT AND TRADEMARK OFFICE

PATENT APPLICATION INFORMATION RETRIEVAL SYSTEM

PATENT

IN THE UNITED STATES PATENT AND TRADEMARK OFFICE

Inventor(s)	:	Chaohong Hu
Application No.	:	15/550,995
Filed	:	August 14, 2017
For	:	ANTIBODY-DRUG CONJUGATE
Examiner	:	Karen A Canella
Art Unit	:	1643
Docket No.	:	850231.401USPC
Date	:	July 1, 2019

Commissioner for Patents
P.O. Box 1450
Alexandria, VA 22313-1450

AMENDMENT

Commissioner for Patents:

In response to the Office Action dated April 4, 2019, please amend the application as follows:

Amendments to the Claims are reflected in the listing of claims which begins on page 2 of this paper.

Remarks begin on page 8 of this paper.

Amendments to the Claims:

This listing of claims will replace all prior versions, and listings, of claims in the application:

Listing of Claims:

1. (Canceled)

2. (Currently Amended) An antibody-drug conjugate, a pharmaceutically acceptable salt thereof, ~~a solvate thereof~~ or a solvate of the salt, comprising an anti-epidermal growth factor receptor antibody covalently linked to a cytotoxic agent via a cleavable linker, wherein the anti-epidermal growth factor receptor antibody comprises a heavy chain and a light chain, wherein the heavy chain has a variable region comprising CDR1, CDR2 and CDR3 having sequences as shown in SEQ ID NOs: 5 to 7 ~~or mutants thereof~~, and the light chain has a variable region comprising CDR1, CDR2 and CDR3 having sequences as shown in SEQ ID NOs: 12 to 14 ~~or mutants thereof~~.

3. (Currently Amended) The antibody-drug conjugate, the pharmaceutically acceptable salt thereof, ~~the solvate thereof~~ or the solvate of the salt according to claim 2, wherein FR1, FR2, FR3, FR4 of the variable region of the heavy chain of the anti-epidermal growth factor receptor antibody respectively comprise sequences as shown in SEQ ID NOs: 8 to 11 ~~or mutants thereof~~.

4. (Currently Amended) The antibody-drug conjugate, the pharmaceutically acceptable salt thereof, ~~the solvate thereof~~ or the solvate of the salt according to claim 2, wherein FR1, FR2, FR3, FR4 of the variable region of the light chain of the anti-epidermal growth factor receptor antibody respectively comprise sequences as shown in SEQ ID NOs: 15 to 18, ~~or mutants thereof~~.

5. (Currently Amended) The antibody-drug conjugate, the pharmaceutically acceptable salt thereof, ~~the solvate thereof~~ or the solvate of the salt according to claim 2, wherein the heavy chain of the anti-epidermal growth factor receptor antibody has a constant region selected from the group consisting of a human IgG constant region, a human IgM constant region, a human IgA constant region, and a human IgD constant region ~~and a mutant thereof~~.

6. (Currently Amended) The antibody-drug conjugate, the pharmaceutically acceptable salt thereof, ~~the solvate thereof~~ or the solvate of the salt according to claim 5, wherein the IgG is selected from the group consisting of IgG1, IgG2, IgG3 and IgG4.

7. (Currently Amended) The antibody-drug conjugate, the pharmaceutically acceptable salt thereof, ~~the solvate thereof~~ or the solvate of the salt according to claim 5, wherein the constant region of the heavy chain of the anti-epidermal growth factor receptor antibody comprises an amino acid sequence as shown in SEQ ID NO: 3, or comprises a sequence with an identity of greater than 70%, or greater than 75%, 80%, 85%, 90%, 95%, or 99% to the sequence as shown in SEQ ID NO: 3.

8. (Currently Amended) The antibody-drug conjugate, the pharmaceutically acceptable salt thereof, ~~the solvate thereof~~ or the solvate of the salt according to claim 2, wherein the light chain of the anti-epidermal growth factor receptor antibody has a constant region selected from the group consisting of a human lambda constant region, and a human kappa constant region ~~and a mutant thereof~~.

9. (Currently Amended) The antibody-drug conjugate, the pharmaceutically acceptable salt thereof, ~~the solvate thereof~~ or the solvate of the salt according to claim 8, wherein the constant region of the light chain of the anti-epidermal growth factor receptor antibody comprises an amino acid sequence as shown in SEQ ID NO: 4, or comprises a sequence with an identity of greater than 70%, or greater than 75%, 80%, 85%, 90%, 95%, or 99% to the sequence as shown in SEQ ID NO: 4.

10. (Currently Amended) The antibody-drug conjugate, the pharmaceutically acceptable salt thereof, ~~the solvate thereof~~ or the solvate of the salt according to claim 2, which has a structure as shown in Formula I,

$$Ab\text{-}(L\text{-}D)_p$$

Formula I

wherein:

Ab represents the anti-epidermal growth factor receptor antibody;

L represents a cleavable linker;

D represents the cytotoxic agent;

p represents 1-9.

11. (Currently Amended) The antibody-drug conjugate, the pharmaceutically acceptable salt thereof, ~~the solvate thereof~~ or the solvate of the salt according to claim 10, wherein the cytotoxic agent is selected from the group consisting of chemotherapeutic agents, ~~toxins,~~ radioisotopes, ~~cytokines~~, antibiotics, enzymes, ~~nanoparticles~~ and biologically active peptides.

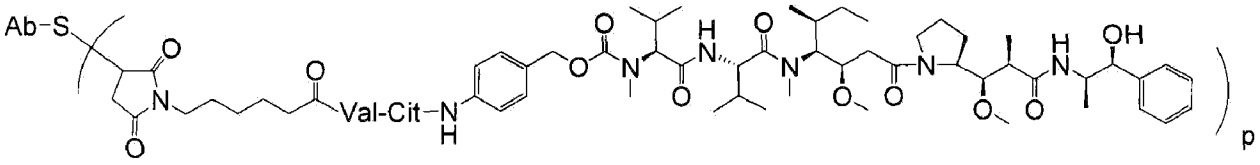
12. (Currently Amended) The antibody-drug conjugate, the pharmaceutically acceptable salt thereof, ~~the solvate thereof~~ or the solvate of the salt according to claim 11, wherein the cytotoxic agent is selected from the group consisting of Monomethyl auristatin E (MMAE), Monomethyl auristatin F (MMAF), maytansinoid alkaloids, Calicheamicin, duocarmycin MGBA, doxorubicin, ricin, diphtheria toxin ~~and other toxins~~, I131, ~~interleukins,~~ and tumor necrosis factors~~, chemokines and nanoparticles~~.

13. (Canceled)

14. (Currently Amended) The antibody-drug conjugate, the pharmaceutically acceptable salt thereof, ~~the solvate thereof~~ or the solvate of the salt according to claim ~~13~~10, wherein the linker is selected from the group consisting of ~~6-maleimidocaproyl (MC),~~

~~maleimidopropionyl (MP),~~ valine-citrulline (val-cit), alanine-phenylalanine (ala-phe), ~~p-aminobenzyloxycarbonyl (PAB),~~ N-succinimidyl 4-(2-pyridylthio)valerate (SPP), ~~N-succinimidyl 4-(N-maleimidomethyl) cyclohexane-1-carboxylate (SMCC), N-succinimidyl (4-iodo-acetyl) aminobenzoate (SIAB),~~ and 6-maleimidocaproyl-valine-citrulline-p-aminobenzyloxycarbonyl (MC-vc-PAB)~~, preferably 6-maleimidocaproyl-valine-citrulline-p-aminobenzyloxycarbonyl (MC-vc-PAB)~~.

15. (Currently Amended) The antibody-drug conjugate, the pharmaceutically acceptable salt thereof, ~~the solvate thereof~~ or the solvate of the salt according to claim 10, which is:



wherein, Ab represents the anti-epidermal growth factor receptor antibody, p is 1-8.

16. (Currently Amended) A composition, which comprises the antibody-drug conjugate, the pharmaceutically acceptable salt thereof, ~~the solvate thereof~~ or the solvate of the salt according to claim 2, optionally, further comprises at least one pharmaceutically acceptable carrier, diluent or excipient.

17.-22. (Canceled)

23. (Currently Amended) A method for ~~prophylaxis and/or~~ treatment of a disease associated with epidermal growth factor receptor (EGFR), ~~wherein the method comprises a step of~~ comprising: administering to a subject in need a ~~prophylactically and/or~~ therapeutically effective amount of the antibody-drug conjugate, the pharmaceutically acceptable salt thereof, ~~the solvate thereof~~ or the solvate of the salt according to claim 2.

24. (Previously presented) The method according to claim 23, wherein the disease associated with epidermal growth factor receptor (EGFR) is a tumor associated with overexpression of EGFR.

25. (Currently Amended) A method for inhibiting tumor angiogenesis, delaying tumor progression, inhibiting tumor growth, or inhibiting tumor cell proliferation, ~~wherein the method comprises a step of~~ comprising: administering to a subject in need a ~~prophylactically and/or~~ therapeutically effective amount of the antibody-drug conjugate, the pharmaceutically acceptable salt thereof, ~~the solvate thereof~~ or the solvate of the salt according to claim 2.

26. (Original) The method according to claim 25, wherein the tumor is selected from colon cancer, rectal cancer, head and neck cancer, lung cancer, ovarian cancer, cervical cancer, bladder cancer, esophageal cancer, breast cancer, renal cancer, prostate cancer, gastric cancer, pancreatic cancer and brain glioma.

27. (Previously presented) The method according to claim 24, wherein the tumor is a tumor with KRAS gene mutation.

28. (Previously presented) The method according to claim 24, wherein the tumor is a tumor with BRAF gene mutation.

29.-34. (Canceled)

35. (Previously presented) The method according to claim 26, wherein the tumor is a tumor with KRAS gene mutation.

36. (Previously presented) The method according to claim 26, wherein the tumor is a tumor with BRAF gene mutation.

37. (New) The antibody-drug conjugate or the pharmaceutically acceptable salt thereof according to claim 10, wherein the linker is 6-maleimidocaproyl-valine-citrulline-p-aminobenzyloxycarbonyl (MC-vc-PAB).

REMARKS

Reconsideration of the present application in view of the above amendments and the following remarks are respectfully requested.

Claims 2-16, 23-28, 35 and 36 were pending. Claim 13 has been canceled. New claim 37 has been added. Accordingly, claims 2-12, 14-16, 23-28, and 35-37 are pending. Support for new claim 37 may be found, for example, in original claim 14.

Claims 2-12, 14-16, 23 and 25 have been amended to focus on certain embodiments of the present application and/or enter minor changes. Support for the amendments to claim 2 may be found, for example, in original claim 13. No new matter has been added.

The amendments to the claims have been made to facilitate allowance without acquiescing to the rejections or disclaimers.

Rejections Under 35 U.S.C. 112(d)

Claims 11 and 12 are rejected under 35 U.S.C. 112(d) as being of improper dependent form. The Examiner contends that claims 11 and 12 are not clear because of the phrases "toxins" in claim 11 and "other toxins" in claim 12.

Applicant has amended claims 11 and 12 to delete the above-noted phrases. The objection is thus moot.

Rejections Under 35 U.S.C. 112(b)

Claims 11, 12 and 14 are rejected under 35 U.S.C. 112(b) as indefinite due to the recitations of "cytokines" and "nanoparticles" in claim 11, "interleukins," "chemokines," "nanoparticles," and "and other toxins" in claim 12, and "preferably 6-maleimidocaproyl-valine-citrulline-p-aminobenzyloxycarbonyl (MC-vc-PAB)" in claim 14.

To facilitate allowance and without acquiescing to the rejection, Applicant has amended claims 11, 12 and 14 to delete the above-noted recitations. The objection is thus moot.

Rejections Under 35 U.S.C. 112(a) (Enablement)

Claims 2-16, 23-28, 35 and 36 are rejected under 35 U.S.C. 112(a) as not enabled due to the recitations of "nanoparticles," "cytokines," "interleukins," "chemokines," in claims 11 and 12, "solvate" of the antibody conjugates in claims 2-16, 23-28, 35 and 36, "prophylaxis" in claim 23, and "prophylactically … effective amount" in claims 23 and 25.

To facilitate allowance and without acquiescing to the rejection, Applicant has amended the claims to delete the above-noted recitations. Thus, this rejection is moot.

Rejections Under 35 U.S.C. 112(a) (Written Description)

Claims 2-16, 23-28, 35 and 36 are rejected under 35 U.S.C. 112(a) as failing to comply with the written description requirement due to the recitations of "mutants thereof" in claims 2-6 and 8, "greater than 70%, … or 99% to the sequence" in claims 7 and 9, and "solvate" of the antibody conjugate recited in claims 2-16, 23, and 25.

To facilitate allowance and without acquiescing to the rejection, Applicant has amended the claims to delete the recitations of "mutants thereof" and "solvate" of the antibody conjugate. As to the recitations related to percentage sequence identity in claims 7 and 9, Applicant respectfully disagrees with the assertion in the Office Action that the alteration in sequence that contributes to less than 100% sequence identity can be alterations in the CDR regions of the antibody (*see* the sentence bridging pages 6 and 7 of the Office Action). Claims 7 and 9 specify the sequence of the constant regions, not the variable regions, of the heavy chain and the light chain of the anti-epidermal growth factor receptor antibody. An alteration in sequence that contributes to less than 100% sequence identity as recited in claims 7 and 9 does not affect the CDR regions of the antibody and therefore would not materially affect the binding affinity of the antibody.

In view of the above remarks, Applicant submits that this rejection has been overcome. Withdrawal of this rejection is respectfully requested.

Rejections Under §103

(1) Claims 2-14, 16, and 23-26 are rejected under 35 U.S.C 103 as unpatentable over Tikhomirov (WO2015/000062, D1) in view of Liu (CN103772504, D2), Brand et al. (Cancer Biology & Therapy 11:777-92, 2011, D3), and Chung et al. (New England Journal of Medicine 358:1109-17, 2008, D4).

As indicated above, to facilitate allowance and without acquiescing to the rejection, Applicant has amended claim 2 to be directed to an antibody-drug conjugate, a pharmaceutically acceptable salt thereof, or a solvate of the salt, comprising an anti-epidermal growth factor receptor antibody covalently linked to a cytotoxic agent via a cleavable linker, wherein the anti-epidermal growth factor receptor antibody comprises a heavy chain and a light chain, wherein the heavy chain has a variable region comprising CDR1, CDR2 and CDR3 having sequences as shown in SEQ ID NOs: 5 to 7, and the light chain has a variable region comprising CDR1, CDR2 and CDR3 having sequences as shown in SEQ ID NOs: 12 to 14. Applicant submits that the claims as currently amended in the present application are not obvious in view of the cited references.

First, one of ordinary skill in the art would not have been motivated by the cited references to use a cleavable linker to arrive at the antibody-drug conjugate (ADC), a pharmaceutically acceptable salt thereof, or a solvate of the salt as claimed in the present application. Among the cited references, only D1 discloses a linker used in forming an anti-EGFR ADC; the other three references relate to anti-EGFR antibodies only. However, one of ordinary skill in the art would not have been motivated to use a cleavable linker in generating an anti-EGFR ADC in view of D1 as a whole.

Specifically, D1 almost exclusively focuses on non-cleavable linkers. A few examples of the disclosures related to non-cleavable linkers in D1 are reproduced below (emphasis added):

> A maytansinoid is covalently linked through a <u>non-cleavable linker</u> to an EGFR antibody that is a full EGFR antagonist, such as cetuximab or panitumumab. The result is an anti-cancer agent having cytotoxicity that is potentiated in cancer cells

> but not normal cells. This benefit is not seen with EGFR antibodies that are partial antagonists, or with toxins that are not processed by lysosomes.[1] (*See* Abstract)
>
> The present invention draws from the unexpected initial finding that conjugation of the anti-EGFR antibody cetuximab to a toxic maytansinoid through a non-cleavable linker yields an immunoconjugate that displays enhanced cytotoxicity against cancer cells without a corresponding increase in cytotoxicity against skin cells.... (*See* the 1st sentence in the Summary of the Invention on page 3)
>
> On the basis of these and other findings herein disclosed, the present invention enables the selection of components essential to yield an immunoconjugate that comprises an EGFR antibody and a toxic payload that potentiates antibody activity toward cancer cells but not toward normal cells such as keratinocytes. Immunoconjugates having this property require the selection of an EGFR antibody that is a full antagonist, a toxin that is an anti-microtubule agent, and a linker that most desirably is not cleavable.... (*See* the paragraph bridging pages 3 and 4).
>
> Accordingly, in a general aspect, there is provided an immunoconjugate comprising an antibody having full antagonist activity at EGFR, and a toxin conjugated therewith through a non-cleavable linker, the immunoconjugate having a cytotoxic effect relative to a naked form of the antibody that is essentially not potentiated with respect to EGFR+ keratinocytes.... (*See* the 1st full paragraph on page 4).

In addition, D1 provides extensive disclosures and numerous examples of non-cleavable linkers (*see* pages 6, 13 and 14). To the contrary, the only disclosure of cleavable linkers in D1 is at page 6, lines 3-5 as optional, less desirable embodiments. Furthermore, all the ADCs disclosed with experimental data in D1 uses a non-cleavable linker, SMCC, except that Cetux2C9-MMAE uses a cleavable linker, valine-citrulline (*see* Examples 1 to 4).

Moreover, Example 4 of D1 shows that a cleavable linker is not favorable compared to a non-cleavable linker due to the fact that the resulting ADC had potentiated toxicity against normal cells (*see* Figure 13 and its description at the end of page 9). The relevant sections of Example 4 of D1 are reproduced below (emphasis added):

[1] Toxins that are not processed by lysosomes are likely those linked with an antibody via a cleavable linker in view of the disclosure in D1 that "non-cleavable linkers result in ADC constructs for which release of the cytotoxic payload is achieved by destruction of the antibody by intracellular lysosomes" (*see* page 13, the end of the 4th paragraph).

> … Figure 13 shows that conjugation of cetuximab to MMAE by a cleavable linker (valine-citrulline) potentiates its toxicity against normal cells and MDA-MB-468 cancer cells, whereas conjugation via non-cleavable linker (SMCC) potentiates anti-cancer activity.
>
> … Moreover, we subsequently tested the effect on this activity profile of the cleavable vs. non-cleavable linkers, while maintaining payload mechanism of action the same (i.e. anti-microtubule agent). The antibodies were conjugated via cleavable linker to anti-microtubule payload, MMAE as described by Doronina et al, Nature Biotechnology Nov 7, 2003, Vol 21: pp 778-784. Cleavable linker data demonstrate that when the fully antagonistic antibodies are conjugated to their payloads via cleavable linkers, their toxicity against normal cells is potentiated. Thus, a safe anti-EGFR ADC **should** incorporate a strongly antagonistic anti-EGFR antibody linked to an anti-microtubule payload by a **non-cleavable linker**.

In view of the disclosures of D1 as a whole, one of ordinary skill in the art would be discouraged from using a cleavable linker in generating anti-EGFR ADCs due to potentiated toxicity against normal cells of such ADCs. Using a cleavable linker in generating anti-EGFR ADCs would eliminate or at least reduce the primary benefit of the invention disclosed in D1, that is, potentiating anti-cancer activities of ADCs without increasing their cytotoxicity against normal cells.

Second, the ADC currently claimed in the present application is not obvious due to its unexpectedly superior property as demonstrated in Example 6 of the present application. Example 6 compares the inhibition activities on cancer cells *in vitro* between MYK-3 (containing a cleavable linker) and BA03-MC-MMAE and BA03-MCC-MMAE (both containing a non-cleavable linker). Figure 12 shows that the EC50 values of MYK-3, BA03-MC-MMAE and BA03-MCC-MMAE were 9.8 ng/mL, 72.6 ng/mL, and 71.6 ng/mL, respectively. Thus, the cell proliferation inhibitory activity of MYK-3 was significantly higher than those of BA03-MC-MMAE and BA03-MCC-MMAE. Accordingly, MYK-3 (an ADC with a cleavable linker) is superior to BA03-MC-MMAE and BA03-MCC-MMAE (ADCs with two different non-cleavable linkers).

The superiority of an anti-EGFR ADC having a cleavable linker over anti-EGFR ADCs having non-cleavable linkers was unexpected. Such superiority was not taught or suggested by

any of the cited references teach or suggest such superiority. As discussed above, to the contrary, D1 discourages the use of cleavable linkers in generating anti-EGFR ADCs.

In view of the above-remarks, Applicant submits that this ground of rejection has been overcome. Withdrawal of this rejection is respectfully requested.

(2) Claims 2-16 and 23-26 are rejected under 35 U.S.C. 103 as unpatentable over Tikhomirov (WO2015/000062, D1), Liu (CN103772504, D2), and Chung et al. (New England Journal of Medicine 358:1109-17, 2008, D4) and further in view of Chari et al. (Angewandte Chemie 53: 3796-827, 2014, D5).

Applicant submits that the claims as currently pending in the present application are not obvious in view of the cited references. As discussed above, D1, D2 and D4 do not render the currently pending claims obvious. Specifically, one of ordinary skill in the art would not have been motivated to use a cleavable linker to generate an anti-EGFR ADC in view of D1, D2 and D4. Such a deficiency has not been remedied by D5. D5 is cited in the Office Action as disclosing the cleavable linker Mal-caproyl-val-cit-PAB-MMAE linkable derivate of MMAE. This reference does not disclose generating an anti-EGFR ADC using a cleavable linker or the superior property of the currently claimed anti-EGFR ADC.

In view of the above-remarks, Applicant submits that this ground of rejection has been overcome. Withdrawal of this rejection is respectfully requested.

(3) Claims 2-14, 16, 23-27 and 35 are rejected under 35 U.S.C. 103 as unpatentable over Tikhomirov (WO2015/000062, D1), Liu (CN103772504, D2), and Chung et al. (New England Journal of Medicine 358:1109-17, 2008, D4) and further in view of Lievre et al. (Cancer Research 66: 3992-5, 2006, D6).

Applicant submits that the claims as currently pending in the present application are not obvious in view of the cited references. As discussed above, D1, D2 and D4 do not render the currently pending claims obvious. Specifically, one of ordinary skill in the art would not have been motivated to use a cleavable linker to generate an anti-EGFR ADC in view of D1, D2 and D4. Such a deficiency has not been remedied by D6. D6 is cited in the Office Action in connection with KRAS gene mutations in an EGFR positive tumor. This reference does not

disclose generating an anti-EGFR ADC using a cleavable linker or the superior property of the currently claimed anti-EGFR ADC.

In view of the above-remarks, Applicant submits that this ground of rejection has been overcome. Withdrawal of this rejection is respectfully requested.

(4) Claims 2-14, 16, 23-26, 28, and 36 are rejected under 35 U.S.C. 103 as unpatentable over Tikhomirov (WO2015/000062, D1), Liu (CN103772504, D2), and Chung et al. (New England Journal of Medicine 358:1109-17, 2008, D4) and further in view of DiNicolantonio et al. (Journal of Clinical Oncology 26: 5705-12, 2008, D7).

Applicant submits that the claims as currently pending in the present application are not obvious in view of the cited references. As discussed above, D1, D2 and D4 do not render the currently pending claims obvious. Specifically, one of ordinary skill in the art would not have been motivated to use a cleavable linker to generate an anti-EGFR ADC in view of D1, D2 and D4. Such a deficiency has not been remedied by D7. D7 is cited in the Office Action in connection with BRAF gene mutations in an EGFR positive tumor. This reference does not disclose generating an anti-EGFR ADC using a cleavable linker or the superior property of the currently claimed anti-EGFR ADC.

In view of the above-remarks, Applicant submits that this ground of rejection has been overcome. Withdrawal of this rejection is respectfully requested.

The Director is authorized to charge any additional fees due by way of this Amendment, or credit any overpayment, to our Deposit Account No. 19-1090.

Respectfully submitted,

SEED Intellectual Property Law Group LLP

/Qing Lin/
Qing Lin, Ph.D.
Registration No. 53,937

QXL:bgh

701 Fifth Avenue, Suite 5400
Seattle, Washington 98104-7092
Phone: (206) 622-4900
Fax: (206) 682-6031

Electronic Acknowledgement Receipt

EFS ID:	36464651
Application Number:	15550995
International Application Number:	
Confirmation Number:	1813
Title of Invention:	Antibody-Drug Conjugate
First Named Inventor/Applicant Name:	Chaohong Hu
Customer Number:	500
Filer:	Qing Lin/Barbara Hannon
Filer Authorized By:	Qing Lin
Attorney Docket Number:	850231.401USPC
Receipt Date:	01-JUL-2019
Filing Date:	14-AUG-2017
Time Stamp:	16:24:21
Application Type:	U.S. National Stage under 35 USC 371

Payment information:

Submitted with Payment	no

File Listing:

Document Number	Document Description	File Name	File Size(Bytes)/ Message Digest	Multi Part /.zip	Pages (if appl.)
1		401USPC_RESP.pdf	231029 bf2b949cedead3ee6092ad784fc02706e68243a7	yes	15

	Multipart Description/PDF files in .zip description		
	Document Description	**Start**	**End**
	Amendment/Req. Reconsideration-After Non-Final Reject	1	1
	Claims	2	7
	Applicant Arguments/Remarks Made in an Amendment	8	15
Warnings:			
Information:			
	Total Files Size (in bytes):	231029	

This Acknowledgement Receipt evidences receipt on the noted date by the USPTO of the indicated documents, characterized by the applicant, and including page counts, where applicable. It serves as evidence of receipt similar to a Post Card, as described in MPEP 503.

New Applications Under 35 U.S.C. 111

If a new application is being filed and the application includes the necessary components for a filing date (see 37 CFR 1.53(b)-(d) and MPEP 506), a Filing Receipt (37 CFR 1.54) will be issued in due course and the date shown on this Acknowledgement Receipt will establish the filing date of the application.

National Stage of an International Application under 35 U.S.C. 371

If a timely submission to enter the national stage of an international application is compliant with the conditions of 35 U.S.C. 371 and other applicable requirements a Form PCT/DO/EO/903 indicating acceptance of the application as a national stage submission under 35 U.S.C. 371 will be issued in addition to the Filing Receipt, in due course.

New International Application Filed with the USPTO as a Receiving Office

If a new international application is being filed and the international application includes the necessary components for an international filing date (see PCT Article 11 and MPEP 1810), a Notification of the International Application Number and of the International Filing Date (Form PCT/RO/105) will be issued in due course, subject to prescriptions concerning national security, and the date shown on this Acknowledgement Receipt will establish the international filing date of the application.

PTO/SB/06 (09-11)
Approved for use through 1/31/2014. OMB 0651-0032
U.S. Patent and Trademark Office; U.S. DEPARTMENT OF COMMERCE
Under the Paperwork Reduction Act of 1995, no persons are required to respond to a collection of information unless it displays a valid OMB control number.

PATENT APPLICATION FEE DETERMINATION RECORD Substitute for Form PTO-875	Application or Docket Number 15/550,995	Filing Date 08/14/2017	☐ To be Mailed

ENTITY: ☐ LARGE ☑ SMALL ☐ MICRO

APPLICATION AS FILED - PART I

FOR	(Column 1) NUMBER FILED	(Column 2) NUMBER EXTRA		RATE ($)	FEE ($)
☐ BASIC FEE (37 CFR 1.16(a), (b), or (c))	N/A	N/A		N/A	
☐ SEARCH FEE (37 CFR 1.16(k), (i), or (m))	N/A	N/A		N/A	
☐ EXAMINATION FEE (37 CFR 1.16(o), (p), or (q))	N/A	N/A		N/A	
TOTAL CLAIMS (37 CFR 1.16(i))	minus 20 =	*		x $40 =	
INDEPENDENT CLAIMS (37 CFR 1.16(h))	minus 3 =	*		x $210 =	
☐ APPLICATION SIZE FEE (37 CFR 1.16(s))	If the specification and drawings exceed 100 sheets of paper, the application size fee due is $310 ($155 for small entity) for each additional 50 sheets or fraction thereof. See 35 U.S.C. 41(a)(1)(G) and 37 CFR 1.16(s).				
☐ MULTIPLE DEPENDENT CLAIM PRESENT (37 CFR 1.16(j))					
* If the difference in column 1 is less than zero, enter "0" in column 2.				TOTAL	

APPLICATION AS AMENDED - PART II

		(Column 1)		(Column 2)	(Column 3)			
AMENDMENT	07/01/2019	CLAIMS REMAINING AFTER AMENDMENT		HIGHEST NUMBER PREVIOUSLY PAID FOR	PRESENT EXTRA		RATE ($)	ADDITIONAL FEE ($)
	Total (37 CFR 1.16(i))	* 23	Minus	** 23	= 0		x $50 =	0
	Independent (37 CFR 1.16(h))	* 1	Minus	*** 3	= 0		x $230 =	0
	☐ Application Size Fee (37 CFR 1.16(s))							
	☐ FIRST PRESENTATION OF MULTIPLE DEPENDENT CLAIM (37 CFR 1.16(j))							
							TOTAL ADD'L FEE	0

		(Column 1)		(Column 2)	(Column 3)			
AMENDMENT		CLAIMS REMAINING AFTER AMENDMENT		HIGHEST NUMBER PREVIOUSLY PAID FOR	PRESENT EXTRA		RATE ($)	ADDITIONAL FEE ($)
	Total (37 CFR 1.16(i))	*	Minus	**	=		x $0 =	
	Independent (37 CFR 1.16(h))	*	Minus	***	=		x $0 =	
	☐ Application Size Fee (37 CFR 1.16(s))							
	☐ FIRST PRESENTATION OF MULTIPLE DEPENDENT CLAIM (37 CFR 1.16(j))							
							TOTAL ADD'L FEE	

* If the entry in column 1 is less than the entry in column 2, write "0" in column 3.	SLIE
** If the "Highest Number Previously Paid For" IN THIS SPACE is less than 20, enter "20".	/RANELL D GRAY/
*** If the "Highest Number Previously Paid For" IN THIS SPACE is less than 3, enter "3".	
The "Highest Number Previously Paid For" (Total or Independent) is the highest number found in the appropriate box in column 1.	

This collection of information is required by 37 CFR 1.16. The information is required to obtain or retain a benefit by the public which is to file (and by the USPTO to process) an application. Confidentiality is governed by 35 U.S.C. 122 and 37 CFR 1.14. This collection is estimated to take 12 minutes to complete, including gathering, preparing, and submitting the completed application form to the USPTO. Time will vary depending upon the individual case. Any comments on the amount of time you require to complete this form and/or suggestions for reducing this burden, should be sent to the Chief Information Officer, U.S. Patent and Trademark Office, U.S. Department of Commerce, P.O. Box 1450, Alexandria, VA 22313-1450. DO NOT SEND FEES OR COMPLETED FORMS TO THIS ADDRESS. **SEND TO: Commissioner for Patents, P.O. Box 1450, Alexandria, VA 22313-1450.**

If you need assistance in completing the form, call 1-800-PTO-9199 and select option 2.

UNITED STATES PATENT AND TRADEMARK OFFICE

UNITED STATES DEPARTMENT OF COMMERCE
United States Patent and Trademark Office
Address: COMMISSIONER FOR PATENTS
P.O. Box 1450
Alexandria, Virginia 22313-1450
www.uspto.gov

APPLICATION NO.	FILING DATE	FIRST NAMED INVENTOR	ATTORNEY DOCKET NO.	CONFIRMATION NO.
15/550,995	08/14/2017	Chaohong Hu	850231.401USPC	1813

500 7590 10/18/2019

SEED INTELLECTUAL PROPERTY LAW GROUP LLP
701 FIFTH AVE
SUITE 5400
SEATTLE, WA 98104

EXAMINER	
CANELLA, KAREN A	

ART UNIT	PAPER NUMBER
1643	

NOTIFICATION DATE	DELIVERY MODE
10/18/2019	ELECTRONIC

Please find below and/or attached an Office communication concerning this application or proceeding.

The time period for reply, if any, is set in the attached communication.

Notice of the Office communication was sent electronically on above-indicated "Notification Date" to the following e-mail address(es):

USPTOeAction@SeedIP.com
pairlinkdktg@seedip.com

Office Action Summary	Application No. 15/550,995	Applicant(s) Hu, Chaohong	
	Examiner KAREN A CANELLA	Art Unit 1643	AIA (FITF) Status Yes

-- The MAILING DATE of this communication appears on the cover sheet with the correspondence address --

Period for Reply

A SHORTENED STATUTORY PERIOD FOR REPLY IS SET TO EXPIRE 3 MONTHS FROM THE MAILING DATE OF THIS COMMUNICATION.

- Extensions of time may be available under the provisions of 37 CFR 1.136(a). In no event, however, may a reply be timely filed after SIX (6) MONTHS from the mailing date of this communication.
- If NO period for reply is specified above, the maximum statutory period will apply and will expire SIX (6) MONTHS from the mailing date of this communication.
- Failure to reply within the set or extended period for reply will, by statute, cause the application to become ABANDONED (35 U.S.C. § 133). Any reply received by the Office later than three months after the mailing date of this communication, even if timely filed, may reduce any earned patent term adjustment. See 37 CFR 1.704(b).

Status

1)☑ Responsive to communication(s) filed on 7/1/2019.

☐ A declaration(s)/affidavit(s) under **37 CFR 1.130(b)** was/were filed on _____.

2a)☑ This action is **FINAL.** 2b) ☐ This action is non-final.

3)☐ An election was made by the applicant in response to a restriction requirement set forth during the interview on _____; the restriction requirement and election have been incorporated into this action.

4)☐ Since this application is in condition for allowance except for formal matters, prosecution as to the merits is closed in accordance with the practice under *Ex parte Quayle*, 1935 C.D. 11, 453 O.G. 213.

Disposition of Claims*

5) ☑ Claim(s) 2-12,14-16,23-28 and 35-37 is/are pending in the application.

5a) Of the above claim(s) _____ is/are withdrawn from consideration.

6) ☐ Claim(s) _____ is/are allowed.

7) ☑ Claim(s) 2-12,14-16,23-28 and 35-37 is/are rejected.

8) ☐ Claim(s) _____ is/are objected to.

9) ☐ Claim(s) _____ are subject to restriction and/or election requirement

* If any claims have been determined allowable, you may be eligible to benefit from the **Patent Prosecution Highway** program at a participating intellectual property office for the corresponding application. For more information, please see http://www.uspto.gov/patents/init_events/pph/index.jsp or send an inquiry to **PPHfeedback@uspto.gov.**

Application Papers

10)☐ The specification is objected to by the Examiner.

11)☐ The drawing(s) filed on _____ is/are: a)☐ accepted or b)☐ objected to by the Examiner.

Applicant may not request that any objection to the drawing(s) be held in abeyance. See 37 CFR 1.85(a).

Replacement drawing sheet(s) including the correction is required if the drawing(s) is objected to. See 37 CFR 1.121(d).

Priority under 35 U.S.C. § 119

12)☐ Acknowledgment is made of a claim for foreign priority under 35 U.S.C. § 119(a)-(d) or (f).

Certified copies:

a)☐ All b)☐ Some** c)☐ None of the:

1.☐ Certified copies of the priority documents have been received.

2.☐ Certified copies of the priority documents have been received in Application No. _____.

3.☐ Copies of the certified copies of the priority documents have been received in this National Stage application from the International Bureau (PCT Rule 17.2(a)).

** See the attached detailed Office action for a list of the certified copies not received.

Attachment(s)

1) ☑ Notice of References Cited (PTO-892)

2) ☐ Information Disclosure Statement(s) (PTO/SB/08a and/or PTO/SB/08b) Paper No(s)/Mail Date _____.

3) ☐ Interview Summary (PTO-413) Paper No(s)/Mail Date _____.

4) ☐ Other: _____.

DETAILED ACTION

Notice of Pre-AIA or AIA Status

The present application, filed on or after March 16, 2013, is being examined under the first inventor to file provisions of the AIA.

Claim 13 has been canceled. Claims 2-12, 14-16, 23-25 have been amended. Claim 37 has been added. Claims 2-12, 14-16, 23-28 and 35-37 are pending and under consideration.

The rejection of claims 11 and 12 under 35 U.S.C. 112(d) or pre-AIA 35 U.S.C. 112, 4th paragraph, as being of improper dependent form for failing to further limit the subject matter of the claim upon which it depends, or for failing to include all the limitations of the claim upon which it depends is withdrawn in light of applicant's amendments.

The rejection of claims 11, 12 and 14 under 35 U.S.C. 112(b) or 35 U.S.C. 112 (pre-AIA), second paragraph, as being indefinite for failing to particularly point out and distinctly claim the subject matter which the inventor or a joint inventor, or for pre-AIA the applicant regards as the invention is withdrawn in light of applicant's amendments.

The following is a quotation of the first paragraph of 35 U.S.C. 112(a):

> (a) IN GENERAL.—The specification shall contain a written description of the invention, and of the manner and process of making and using it, in such full, clear, concise, and exact terms as to enable any person skilled in the art to which it pertains, or with which it is most nearly connected, to make and use the same, and shall set forth the best mode contemplated by the inventor or joint inventor of carrying out the invention.

The following is a quotation of the first paragraph of pre-AIA 35 U.S.C. 112:

> The specification shall contain a written description of the invention, and of the manner and process of making and using it, in such full, clear, concise, and exact terms as to enable any person skilled in the art to which it pertains, or with which it is most nearly connected, to make and use the same, and shall set forth the best mode contemplated by the inventor of carrying out his invention.

The rejection of claims 2-12, 14-16, 23-28, 35 and 36 under 35 U.S.C. 112(a) or 35 U.S.C. 112 (pre-AIA), first paragraph, as failing to comply with the enablement requirement is maintained for partial reasons of record. Claim 37 is also rejected for the same reasons of record. The claim(s) contains subject matter which was not described in the specification in such

a way as to enable one skilled in the art to which it pertains, or with which it is most nearly connected, to make and/or use the invention.

The factors considered when determining if the disclosure satisfies the enablement requirement and whether any necessary experimentation is undue include, but are not limited to: 1) nature of the invention, 2) state of the prior art, 3) relative skill of those in the art, 4) level of predictability in the art, 5) existence of working examples, 6) breadth of claims, 7) amount of direction or guidance by the inventor, and 8) quantity of experimentation needed to make or use the invention. In re wands, 858 F.2d 731, 737.8 USPQ2d 1400, 1404 (Fed. Cir. 1988).

(C) The instant claims all require in part, a solvate of the salt of an antibody conjugate. The specification fails to provide any teachings for how to make the solvate of the instant antibody conjugates or salt thereof. A "salt" does not imply a solid format for the conjugate, only that an ion and counter ion are associated with the antibody conjugate in place of H+ and OH- to neutralize charge of particular moieties, for example, a quaternary ammonium moiety having a positive charge and a carboxylic moiety having a negative charge.

Matheus et al (U.S. 7,960,516) teach that the term solvates is taken to mean adductions of inert solvent molecules onto a solid form which adductions form owning to their mutual attractive force, and that solvates include hydrates such as monohydrates or dihydrates or alcoholates (column 10, lines 37-43). Matheus et al teach the unexpected result that stable pharmaceuticals can be prepared with solid forms of anti-EGFR antibodies such as cetuximab (column 4, lines 56-59) and that the antibodies are biologically active after re-dissolution (column 10, lines 51-59). Matheus et al teach that the difficulties in crystallizing intact glycosylated antibodies is extremely difficult due to the size of the protein, the different glycosylation patterns of the individual molecules and associated micro-heterogeneities as well as the structural flexibility of the immunoglobulin make an ordered incorporation into a crystal lattice more difficult or even impossible (column 2, lines 50-56) and that there is a risk of denaturing antibodies during the crystallization process (column 2, lines 63-66). The instant claims require a solvate of an anti-EGFR cytotoxin conjugate. The various cytotoxins and linker required in the conjugate would vastly increase the size of the molecule, the flexibility and the micro-heterogeneity, especially since the number of linkers attached to a single antibody are variable. Further some of the cytotoxins only moderately soluble in water, such as doxorubicin (Yoo and Park, Journal of Controlled Release, 2001, Vol. 70, pp. 63-70, see page 67, second

column, line 30), and the influence of a group that is less hydrophilic than an antibody on the ability of the antibody to go into a crystal lattice is unknown. The specification has not provided the conditions for the formation of a single solvate of the large genus of EGFR-conjugate as salts encompassed by the claims. It would not be expected that the conditions disclosed for the formation of hydrates of unconjugated cetuximab would be the same conditions for the formation of hydrates or solvates for the instant genus of anti-EGFR-conjugates as salts claimed. Thus one of skill in the art would be subject to undue experimentation in order to make the solvates of the large genus of anti-EGFR conjugates claimed.

The rejection of claims 2-16, 23-28, 35 and 36 under 35 U.S.C. 112(a) or 35 U.S.C. 112 (pre-AIA), first paragraph, as failing to comply with the written description requirement is maitnained for reasons of record. Claim 37 is also rejected for the same reasons of record. The claim(s) contains subject matter which was not described in the specification in such a way as to reasonably convey to one skilled in the relevant art that the inventor or a joint inventor, or for pre-AIA the inventor(s), at the time the application was filed, had possession of the claimed invention.

(A) Claims 7 and 9 encompass sequences having greater than 70% or greater than 75%, 80%, 85%, 90%, 95% or 99% identity to SEQ ID NO:3 or 4. The disclsoure of the single constant regions of SEQ ID NO:3 and 4 does not provide an adequate written description of the genus of constant regions encompassed in the claimed antibody conjugates. The specification fails to teach the correlation between antibody constant region sequences and any particular function attributed to the antibody constant regions. The genus of antibody heavy chain constant regions encompassing sequences deviating by as much as 25% from the sequences of SEQ ID NO:3 and 4 would not be expected to retain all the same functional activities as SEQ ID NO:3 and 4. Thus, the disclosed sequence of SEQ ID NO: 3 fails to adequately describe the genus of SEQ ID NO:3 heavy chain variants, and the disclosed sequence of SEQ ID NO: 4 fails to adequately describe the genus of SEQ ID NO:4 variants because the broadly claimed genus includes members which differ in function from that of SEQ ID NO:4 or SEQ ID NO:3 and the specification has not taught the portions of the sequences of SEQ ID NO: 3 and 4 which are necessary for a particular function of the constant regions. One of skill in the art would

reasonably conclude that applicant was not in possession of the claimed genus at the time of filing.

(B) The instant claims all require in part, a solvate of the salt of an antibody conjugate. The specification fails to provide any teachings for how to make the solvate of the instant antibody conjugates or salt thereof. A "salt" does not imply a solid format for the conjugate, only that an ion and counter ion are associated with the antibody conjugate in place of H+ and OH- to neutralize charge of particular moieties such as a quaternary ammonium moiety and a carboxylic moiety.

Matheus et al (U.S. 7,960,516) teach that the term solvates is taken to mean adductions of inert solvent molecules onto a solid form which adductions form owning to their mutual attractive force, and that solvates include hydrates such as monohydrates or dihydrates or alcoholates (column 10, lines 37-43). Matheus et al teach the unexpected result that stable pharmaceuticals can be prepared with solid forms of anti-EGFR antibodies such as cetuximab (column 4, lines 56-59) and that the antibodies are biologically active after re-dissolution (column 10, lines 51-59). Matheus et al teach that the difficulties in crystallizing intact glycosylated antibodies is extremely difficult due to the size of the protein, the different glycosylation patterns of the individual molecules and associated micro-heterogeneities as well as the structural flexibility of the immunoglobulin make an ordered incorporation into a crystal lattice more difficult or even impossible (column 2, lines 50-56) and that there is a risk of denaturing antibodies during the crystallization process (column 2, lines 63-66). The instant claims require a solvate of an anti-EGFR cytotoxin conjugate. The various cytotoxins and linker required in the conjugate would vastly increase the size of the molecule, the flexibility and the micro-heterogeneity, especially since the number of linkers attached to a single antibody are variable. Further some of the cytotoxins only moderately soluble in water, such as doxorubicin (Yoo and Park, Journal of Controlled Release, 2001, Vol. 70, pp. 63-70, see page 67, second column, line 30), and the influence of a group that is less hydrophilic than an antibody on the ability of the antibody to go into a crystal lattice is unknown. The specification has not provided the conditions for the formation of a single solvate of the large genus of EGFR-conjugate as salts encompassed by the claims. It would not be expected that the conditions disclosed for the formation of hydrates of unconjugated cetuximab would be the same conditions for the formation of hydrates or solvates for the instant genus of anti-EGFR-conjugates as salts claimed.

One of skill in the art would reasonably conclude that applicant was not in possession of the claimed invention at the time of filing.

In the event the determination of the status of the application as subject to AIA 35 U.S.C. 102 and 103 (or as subject to pre-AIA 35 U.S.C. 102 and 103) is incorrect, any correction of the statutory basis for the rejection will not be considered a new ground of rejection if the prior art relied upon, and the rationale supporting the rejection, would be the same under either status.

This application currently names joint inventors. In considering patentability of the claims the examiner presumes that the subject matter of the various claims was commonly owned as of the effective filing date of the claimed invention(s) absent any evidence to the contrary. Applicant is advised of the obligation under 37 CFR 1.56 to point out the inventor and effective filing dates of each claim that was not commonly owned as of the effective filing date of the later invention in order for the examiner to consider the applicability of 35 U.S.C. 102(b)(2)(C) for any potential 35 U.S.C. 102(a)(2) prior art against the later invention.

The following is a quotation of 35 U.S.C. 103 which forms the basis for all obviousness rejections set forth in this Office action:

> A patent for a claimed invention may not be obtained, notwithstanding that the claimed invention is not identically disclosed as set forth in section 102, if the differences between the claimed invention and the prior art are such that the claimed invention as a whole would have been obvious before the effective filing date of the claimed invention to a person having ordinary skill in the art to which the claimed invention pertains. Patentability shall not be negated by the manner in which the invention was made.

The rejection of claims 2-12, 14, 16, 23-26 under 35 U.S.C. 103 as being unpatentable over Tikhomirov (WO2015/000062) in view of Liu (CN103772504 reference of the IDS filed 8/14/2017), Brand et al (Cancer Biology & Therapy, 2011, Vol. 11, pp. 777-792) and Chung et al (New England Journal of Medicine, 2008, Vol. 358, pp. 1109-1117) is maintained for reasons of record.

Claim 2 is drawn in part to an antibody-drug conjugate comprising an anti-EGFR antibody covalently linked to a cytotoxic agent with a cleavable linker, wherein the anti-EGFR antibody comprises the a heavy chain and a light chain, wherein the heavy chain variable region comprises SEQ ID NO:5-7 as the heavy chain CDR1-3, and the light chain variable region comprises SEQ ID NO:12-14 as the light chain CDR1-3 Claim 3 embodies the antibody conjugate of claim 1 wherein the FR1-4 of the variable regions of the heavy chain comprises SEQ ID NO:8-11, respectively. Claim 4 embodies the antibody conjugate of claim 1 wherein the

FR1-4 of the variable regions of the light chain comprises SEQ ID NO:15-18, respectively. Claim 5 requires that the antibody conjugate of claim 2has a constant region selected from a group including the constant region of human IgG. Claim 6 specifies that the IgG constant region of claim 5 is selected from a group including IgG1. Claim 7 requires, in part, that the antibody conjugate of claim 5 has a constant region comprising SEQ ID NO:3. Claim 8 requires in part that the light chain of claim 2 has a constant region selected from a group including human kappa constant region. Claim 9 requires in part that the light chain constant region of claim 7 comprises SEQ ID NO:4. Claim 10 specifies that the antibody conjugate of claim 2 has the structure of Formula I wherein Ab is the antibody, L is the linker, D is the cytotoxic agent and p is 1-9. Claim 11 requires that the antibody conjugate of claim 10 comprises a toxin or a biological active peptide as the cytotoxin; claim 12 requires, in part, that the cytotoxic agent of claim 11 is MMAE. Claim 14 requires that the linker of claim 13 is selected from a group including 6-maleimidocaproyl (MC).

Claim 16 is drawn to a composition comprising the antibody conjugate of claim 2 optionally comprising at least one pharmaceutically acceptable carrier, diluent or excipient.

Claim 23 is drawn in part to a method for the treatment of a disease associated with EGFR comprising administering to a subject in need thereof, a therapeutically effective amount of the antibody conjugate of claim 2. Claim 24 requires that the disease associated with EGFR is a tumor with overexpression of EGFR.

Claim 25 is drawn to a method for inhibiting tumor angiogenesis, delaying tumor progression, inhibiting tumor growth or inhibiting tumor cell proliferation comprising administering to a subject in need thereof a therapeutically effective amount of the antibody conjugate of claim 2. Claim 26 embodies the method of claim 25 wherein the tumor is selected from colon cancer, rectal cancer, head and neck cancer, lung cancer, ovarian cancer, cervical cancer, bladder cancer, esophageal cancer, breast cancer, renal cancer, prostate cancer, gastric cancer, pancreatic cancer and brain glioma.

Tikhomirov et al teach method for treating a subject presenting with a tumor that responds to treatment with a full antagonist EGFR antibody, wherein treatment therewith elicits an EGFR antibody-mediated adverse response by keratinocytes, the improvement comprising treating said subject with the full antagonist EGFR antibody in a form conjugated with an anti-microtubule toxin, whereby the tumor response to treatment with conjugated antibody is

enhanced essentially without enhancing the adverse keratinocyte response to treatment, relative to treatment with naked antibody alone (claim 19 of '062) thus teaching the embodiments of instant clams 23 and 25. Tikhomirov et al teach that a preferred embodiment of the full antagonist EGFR antibody is cetuximab, but that the invention includes other antibodies which are not cetuximab; the preferred anti-microtubulin toxin is preferably an auristatin (page 15, lines 14-16) and the linker is preferably a non-cleavable linker and preferably non-cleavable malimidocaproyl linkers for linking auristatins as the anti-microtubule toxin (page 14, lines 5-7) and that conjugation of cetuximab to MMAE anti-microtubule payload by a cleavable linker potentiates its toxicity against both normal cells and MDA-MB-468 cancer cells, whereas conjugation via non-cleavable linker only potentiates anti-cancer activity, thus demonstrating a favorable therapeutic selectivity (page 9, line 24 to page 10, line 3) thus teaching the embodiments of claims 10-12 wherein the cytotoxin is MMAE, the linker linking the MMAE to the antibody is non-cleavable and maleimidocaproyl (MC). Tikhomirov et al teach pharmaceutical compositions comprising the EGFR immunoconjugates in a pharmaceutically acceptable carrier, thus teaching the limitation of claim 16.

Tikhomirov et al also teach a less preferred embodiment of a cleavable linker (page 6, lines 3-5) such as a linker incorporating valine-citrulline such as cetux-2C9-MMAE in Figure 13, which meets the specific embodiment of cleavable linker in instant claim 13.

Tikhomirov et al teach the that the subject presenting with EGFR+ cancer cells are particularly EGFR+ cells having on their surface an abnormally high density of EGFR molecules (page 18, lines 1-2) which meets the limitation of instant claim 24 requiring EGFR overexpression. Tikhomirov et al teach the that cancers treatable by the invention include $EGFR^+$ colo-rectal cancer, head and neck cancer, lung cancer, ovarian cancer, cervical cancer, bladder cancer, esophageal cancer, breast cancer, renal cancer, prostate cancer, gastric cancer, pancreatic cancer and glioblastoma (page 18, lines 10-25) which meets the limitation of claim 26.

As noted above, Tikhomirov et al teach the preferred embodiment of cetuximab as the anti-EGFR antibody of the invention. Tikhomirov et al do not teach an anti-EGFR having the required CDRs, variable regions, and constant regions set forth in claims 2-8.

Brand et al teach that cetuximab, also known as C225, is the chimeric version of the murine antibody M225 (page 781, Figure 2).

Chung et al (NEJM, 2008, Vol. 358, pp. 1109-1117) teach that among 76 cetuximab treated subjects, 25 had hypersensitivity reactions to the drug, and that most of the subjects having hypersensitivity reactions had pre-existing IgE antibodies to galactose-α-1,3-galactose which is present on the Fab portion of the cetuximab heavy chain (page 1109, under the heading of "Results"). Chung et al teach that such IgE antibodies are prevalent in the population in areas where anaphylactic reactions to cetuximab occur (page 1110, first column, last sentence before "Methods"). Chung et al teach that the Fab portion of the cetuximab heavy chain is glycosylated at residue N88 with a range of sugars including galactose-α-1,3-galactose (page 1114, second column, lines 11-15).

Liu et al teach four humanized versions of the murine M225 antibody (Translation, page10, line 20 to the end of page 11) comprising a human IgG1 Fc fragment and a kappa light chain, wherein the antibodies are termed BA03, BB03, BC03 and BD03 (translation, page 12, lines 1-6). Liu et al teach the sequence of the heavy chain variable region, wherein the N88 residue is in the FR3 domain of SEQ ID NO:17 (Translation, page 15, last paragraph, CN103772504, page 11, paragraph [0083], the "N" in QSNDT) Liu et al teach the heavy chain variable regions of BA03, BB03, BC03 and BD03, wherein SEQ ID NO:5 of the BA03 heavy chain(translation page 16, SEQ ID NO:5) comprises SEQ ID NO: 5-7 of the instant heavy chain CDRs in addition to the framework domains FR1, FR2, FR3 and FR4 comprising SEQ ID NO:8-11; SEQ ID NO: 13 of the light chain of BA03 (page 19 of the translation, SEQ ID NO:13) comprises the instant CDRs of SEQ ID NO:12-14 and the light chain framework sequences of the instant SEQ ID NO: 15-18.

The kappa light chain of the constant region (Translation, page 21, SEQ ID NO:43) is identical to the instant SEQ ID NO:4:

unnamed protein product
Sequence ID: Query_215689Length: 107Number of Matches: 1

```
Query  1    RTVAAPSVFIFPPSDEQLKSGTASVVCLLNNFYPREAKVQWKVDNALQSGNSQESVTEQD  60
            RTVAAPSVFIFPPSDEQLKSGTASVVCLLNNFYPREAKVQWKVDNALQSGNSQESVTEQD
Sbjct  1    RTVAAPSVFIFPPSDEQLKSGTASVVCLLNNFYPREAKVQWKVDNALQSGNSQESVTEQD  60

Query  61   SKDSTYSLSSTLTLSKADYEKHKVYACEVTHQGLSSPVTKSFNRGEC  107
            SKDSTYSLSSTLTLSKADYEKHKVYACEVTHQGLSSPVTKSFNRGEC
Sbjct  61   SKDSTYSLSSTLTLSKADYEKHKVYACEVTHQGLSSPVTKSFNRGEC  107
```

The IgG1 Fc fragment (Translation, page 21, SEQ ID NO: 42) is identical to the instant SEQ ID NO:3

unnamed protein product
Sequence ID: Query_227965Length: 330Number of Matches: 1

```
Query  1    ASTKGPSVFPLAPSSKSTSGGTAALGCLVKDYFPEPVTVSWNSGALTSGVHTFPAVLQSS  60
            ASTKGPSVFPLAPSSKSTSGGTAALGCLVKDYFPEPVTVSWNSGALTSGVHTFPAVLQSS
Sbjct  1    ASTKGPSVFPLAPSSKSTSGGTAALGCLVKDYFPEPVTVSWNSGALTSGVHTFPAVLQSS  60

Query  61   GLYSLSSVVTVPSSSLGTQTYICNVNHKPSNTKVDKRVEPKSCDKTHTCPPCPAPELLGG  120
            GLYSLSSVVTVPSSSLGTQTYICNVNHKPSNTKVDKRVEPKSCDKTHTCPPCPAPELLGG
Sbjct  61   GLYSLSSVVTVPSSSLGTQTYICNVNHKPSNTKVDKRVEPKSCDKTHTCPPCPAPELLGG  120

Query  121  PSVFLFPPKPKDTLMISRTPEVTCVVVDVSHEDPEVKFNWYVDGVEVHNAKTKPREEQYN  180
            PSVFLFPPKPKDTLMISRTPEVTCVVVDVSHEDPEVKFNWYVDGVEVHNAKTKPREEQYN
Sbjct  121  PSVFLFPPKPKDTLMISRTPEVTCVVVDVSHEDPEVKFNWYVDGVEVHNAKTKPREEQYN  180

Query  181  STYRVVSVITVLHQDWLNGKEYKCKVSNKALPAPIEKTISKAKGQPREPQVYTLPPSREE  240
            STYRVVSV+TVLHQDWLNGKEYKCKVSNKALPAPIEKTISKAKGQPREPQVYTLPPSREE
Sbjct  181  STYRVVSVLTVLHQDWLNGKEYKCKVSNKALPAPIEKTISKAKGQPREPQVYTLPPSREE  240

Query  241  MTKNQVSLTCLVKGFYPSDIAVEWESNGQPENNYKTTPPVLDSDGSFFLYSKLTVDKSRW  300
            MTKNQVSLTCLVKGFYPSDIAVEWESNGQPENNYKTTPPVLDSDGSFFLYSKLTVDKSRW
Sbjct  241  MTKNQVSLTCLVKGFYPSDIAVEWESNGQPENNYKTTPPVLDSDGSFFLYSKLTVDKSRW  300

Query  301  QQGNVFSCSVMHEALHNHYTQKSLSLSPGK  330
            QQGNVFSCSVMHEALHNHYTQKSLSLSPGK
Sbjct  301  QQGNVFSCSVMHEALHNHYTQKSLSLSPGK  330
```

Liu teaches that the BA03 and BD03 antibodies have higher binding affinity, stronger ligand blocking ability and stronger inhibitory activity against surface EGFR than Erbitux/cetuximab, and that BB03 and BC03 have binding affinity and ligand blocking abilities that are similar to that of Erbitux.

It would have been prima facie obvious as of the effective filing date to use the BA03 antibody in place of cetuximab in the conjugates and methods of using the conjugates of Tikhomirov et al. One of skill in the art would have been motivated to do so because the BA03 antibody is a full length antibody that is an antagonist of EGFR as demonstrated by Liu and has higher binding affinity and ligand blocking abilities than cetuximab. One of skill in the art would also be motivated to use the humanized BA03 antibody in place of cetuximab because the BA03 has humanized framework regions, and because the N88 amino acid in the chimeric 225 antibody is no longer present. Thus, one of skill in the art would know that the humanized 225 antibody of Liu BA03 would not carry galactose-α-1,3-galactose on N88 within FR3, and the

antibody would not cause hypersensitivity reactions in subjects having pre-existing IgE antibodies to galactose-α-1,3-galactose.

The rejection of claims 2-12, 14-16, and 23-26 under 35 U.S.C. 103 as being unpatentable over Tikhomirov et al , Liu and Chung et al as applied to claims 2-12, 14, 16, and 23-26 above, and further in view of Chari et al (Angewandte Chemie, 2014, Vol. 53, pp. 3796-3827, see page 3811) is maintained for reasons of record. Claim 37 is also rejected for the same reasons of record..

Claim 15 requires the antibody linked by means of a sulfonyl group to 6-malimidocaprolyl-valine-citrulline-p-aminobenzyloxycarbonyl to MMAE, wherein p is 1-8. Claim 37 requires the linker of 6-malimidocaprolyl-valine-citrulline-p-aminobenzyloxycarbonyl in the antibody-conjugate of claim 10.

Tikhomirov et al teach the linkage of MMAE to auristatins by means of maleimidocaprolyl linkers (page 14, lines 5-7) and cleavable linkers comprising valine- citrulline as less preferred embodiments (page 6, lines 3-5). Tikhomirov et al do not specifically teach the structure of claim 15.

Chari et al teach a Mal-caproyl-val-cit-PAB-MMAE linkable derivate of MMAE (middle of page 3811), and the linkage to a mAb, wherein cleavage at the cittrulene induces the self-immolation of the p-amino benzoate to release free MMAE (page 3812, top of page). Chari et al teach that the interchain disulfides can be fully or partially reduced by a mild reducing agent to give a distribution of antibody species with two to eight free thiol groups which react with a maleimide comprising auristatin derivative to give conjugates with an average of four auristatins linked per antibody (page 3811, second column, line 3 to page 3812, first column, line 7). Chari et al teach that with the auristatin MMAF, the val-cit linked MMAF can be up to 10 times more potent on some cell types versus the MMAF with a non-cleavable linker (page 3812, first column, lines 14-17).

It would have been prima facie obvious at the time of the effective filing date to make the antibody maleimidocarpoly-val-cit-PAB-MMAE of Chari et al. One of skill in the art would have been motivated to do so because Tikhomirov et al teach the linkage of MMAE to auristatins by means of maleimidocaprolyl linkers (page 14, lines 5-7) and cleavable linkers comprising

valine-citrulline and because Chari et al teach in some cases, a val-cit linked carrying an auristatin is more potent than a auristatin antibody conjugate with a non-cleavable linker.

The rejection of claims 2-12, 14, 16, 23-27 and 35 under 35 U.S.C. 103 as being unpatentable over Tikhomirov et al, Liu and Chung et al as applied to claims 2-12, 14, 16, 23-26 above, and further in view of Lievre et al (Cancer Research, 2006, Vol. 66, pp. 3992-3995) is maintained for reasons of record.

Claims 27 and 35 embody the methods of claims 24 and 26, respectively, wherein the tumor is a tumor with a KRAS mutation.

The combination of Tikhomirov et al, Liu and Chung et al render obvious claims 2-12,14, 16, 23-26 for the reasons set forth above. None of Tikhomirov et al, Liu or Chung et al teach the treatment of subject having an EGFR positive tumor with a KRAS gene mutation.

Lievre et al teach that patients with KRAS tumors are resistant to cetuximab (abstract, penultimate sentence). Lievre et al teach that the whatever the expression level of EGFR is, the presence of the KRAS mutation is associated with a downstream activation of the Ras/MAPK pathway leading to cell proliferation that cannot be significantly inhibited by cetuximab, because cetuximab acts upstream of the K-ras protein (page 3995, second column, lines 10-14).

It would have been prima facie obvious at the time of the effective filing date to treat patients with EGFR expressing tumors and KRAS mutations with the antibody conjugate rendered obvious by the combination of Tikhomirov et al, Liu and Chung et al. One of skill in the art would have been motivated to do so because one of skill in the art would know that the conjugate would have a mechanism of action that differed from the administration of the unconjugated cetuximab. One of skill in the art would understand that the conjugate would be internalized and the cytotoxic moiety would escape from the lysosomal compartment to deliver the cytotoxin intracellularly and that this cytotoxin would be toxic to cells harboring the KRAS mutation even in the event that the Ras/MAPK pathway would be potentially activated by binding of the conjugated BA03 antibody.

The rejection of claims 2-12, 14, 16, 23-26, 28 and 36 under 35 U.S.C. 103 as being unpatentable over Tikhomirov et al , Liu and Chung et al as applied to claims 2-12, 14, 16, 23-26

above, and further in view of DiNicolantonio et al (Journal of Clinical Oncology, 2008, Vol. 26, pp. 5705-5712) is maintained for reasons of record.

Claims 28 and 36 embody the methods of claims 24 and 26, respectively, wherein the tumor is a tumor with a BRAF mutation.

The combination of Tikhomirov et al, Liu and Chung et al render obvious claims 2-12, 14, 16, 23-26 for the reasons set forth above. None of Tikhomirov et al, Liu or Chung et al teach the treatment of subject having an EGFR positive tumor with a BRAF mutation.

DiNicolantonio et al teach that patients with BRAF mutated EGFR expressing tumors did not respond to cetuximab (page 5705 under "Results" and page 5706, second column, lines 6-8). DiNicolantonio et al teach that the therapeutic effect of cetuximab could be restored if administered with a BRAF inhibitor such as sorafenib or other compounds targeting BRAF or its downstream effectors.

It would have been prima facie obvious at the time of the effective filing date to treat patients with EGFR expressing tumors and BRAF mutations with the antibody conjugate rendered obvious by the combination of Tikhomirov et al, Liu and Chung et al. One of skill in the art would have been motivated to do so because one of skill in the art would know that the conjugate would have a mechanism of action that differed from the administering of the unconjugated cetuximab. One of skill in the art would understand that the conjugate would be internalized and the cytotoxic moiety would escape from the lysosomal compartment to deliver the cytotoxin intracellularly and that this cytotoxin would be toxic to cells harboring the BRAF mutation even in the event that the downstream effectors of BRAF would be activated.

Applicant argues that Tikhomirov et al teaches against the instant claims in that the cleavable linker was disclosed as being a non-preferred embodiment of the antibody conjugates. Applicant argues that there is no motivation to substitute the instant anti-EGFR antibody for the anti-EGFR antibodies of Tikhomirov et al based on the "unexpected result" demonstrated with the combination of the anti-EGFR antibodies of Tikhomirov et al with the auristatin by means of a non-cleavable liker that is not significantly more cytotoxic against normal keratinocytes that the non-conjugated antibody. This has been considered but not found persuasive. Regarding a non-preferred embodiment, section 2123 II of the M.P.E.P. states:

Disclosed examples and preferred embodiments do not constitute a teaching away from a broader disclosure or nonpreferred embodiments. In re Susi, 440 F.2d 442, 169 USPQ 423 (CCPA 1971). "A known or obvious composition does not become patentable simply because it has been described as somewhat inferior to some other product for the same use." In re Gurley, 27 F.3d 551, 554, 31 USPQ2d 1130, 1132 (Fed. Cir. 1994).

Furthermore, "[t]he prior art's mere disclosure of more than one alternative does not constitute a teaching away from any of these alternatives because such disclosure does not criticize, discredit, or otherwise discourage the solution claimed...." In re Fulton, 391 F.3d 1195, 1201, 73 USPQ2d 1141, 1146 (Fed. Cir. 2004).

Regarding cytotoxicity towards normal keratinocytes, Goldmacher and Kovtun (Therapeutic Delivery, 2011, Vol. 2, pp. 397-416) teach that expression of an antigen of interest on normal tissue does not necessarily preclude the development of an ADC targeting the antigen (page 397, second column, lines 6-8 under the heading "Target antigen selection"). Goldmacher and Kovtun teach that the normal non-proliferating cells would be relatively insensitive to the action of anti-mitotic drugs such as the auristatins (page 397, second column, lines 9-12 under the heading "Target antigen selection"). Regarding the unexpected result of Tikhomirov et al wherein the antibody-MMAE conjugate utilizing a non-cleavable linker was not significantly more cytotoxic to keratinocytes than the unconjugated antibody, and the superiority of the of the MYK3 conjugate of the instant invention having a cleavable valine-citrullene linker versus the antibody conjugates having the non-cleavable "MC" or "MCC" linkers, Polson et al (Cancer Research, 2009, Vol. 69, pp. 2358-2364) teach that antibody drug conjugates with cleavable linkers have broad efficacy and are relatively insensitive to target biology compare to ADCs with a non-cleavable "MCC" linker (pages 2359-2360, bridging sentence). Thus it was not unexpected that the antibody conjugates of Tikhomirov et al having non-cleavable linkers were not that much more cytotoxic to keratinocytes than the free antibody. Further, it was not unexpected that the antibody-MMAE conjugate with a valine-citrullene linker of the instant invention was more cytotoxic against cells bearing the target antigen that the corresponding antibody conjugates having a non-cleavable linker.

Applicant argues that the other cited references of Chari et al, Lievre et al and DiNicolantonio et al do not make up for the deficiencies of the rejection based on Tikhomirov et al, Liu and Chung et al. This has been considered but not found persuasive because Chari et al,

Lievre et al and DiNicolantonio et al are relied upon for teachings regarding the limitations of dependent claims 15, 27, 28 and 36.

All claims are rejected.

All other rejections and/or objections are withdrawn.

Applicant's amendment necessitated the new ground(s) of rejection presented in this Office action. Accordingly, **THIS ACTION IS MADE FINAL**. See MPEP § 706.07(a). Applicant is reminded of the extension of time policy as set forth in 37 CFR 1.136(a).

A shortened statutory period for reply to this final action is set to expire THREE MONTHS from the mailing date of this action. In the event a first reply is filed within TWO MONTHS of the mailing date of this final action and the advisory action is not mailed until after the end of the THREE-MONTH shortened statutory period, then the shortened statutory period will expire on the date the advisory action is mailed, and any extension fee pursuant to 37 CFR 1.136(a) will be calculated from the mailing date of the advisory action. In no event, however, will the statutory period for reply expire later than SIX MONTHS from the date of this final action.

Any inquiry concerning this communication or earlier communications from the examiner should be directed to KAREN A CANELLA whose telephone number is (571)272-0828. The examiner can normally be reached on M-F 10-6:30.

Examiner interviews are available via telephone, in-person, and video conferencing using a USPTO supplied web-based collaboration tool. To schedule an interview, applicant is encouraged to use the USPTO Automated Interview Request (AIR) at http://www.uspto.gov/interviewpractice.

If attempts to reach the examiner by telephone are unsuccessful, the examiner's supervisor, Misook Yu can be reached on 571-272-0839. The fax phone number for the organization where this application or proceeding is assigned is 571-273-8300.

Information regarding the status of an application may be obtained from the Patent Application Information Retrieval (PAIR) system. Status information for published applications may be obtained from either Private PAIR or Public PAIR. Status information for unpublished

applications is available through Private PAIR only. For more information about the PAIR system, see http://pair-direct.uspto.gov. Should you have questions on access to the Private PAIR system, contact the Electronic Business Center (EBC) at 866-217-9197 (toll-free). If you would like assistance from a USPTO Customer Service Representative or access to the automated information system, call 800-786-9199 (IN USA OR CANADA) or 571-272-1000.

KAREN A. CANELLA
Examiner
Art Unit 1643

/Karen A. Canella/
Primary Examiner, Art Unit 1643

Notice of References Cited	Application/Control No. 15/550,995	Applicant(s)/Patent Under Reexamination Hu, Chaohong	
	Examiner KAREN A CANELLA	Art Unit 1643	Page 1 of 1

U.S. PATENT DOCUMENTS

*		Document Number Country Code-Number-Kind Code	Date MM-YYYY	Name	CPC Classification	US Classification
	A					
	B					
	C					
	D					
	E					
	F					
	G					
	H					
	I					
	J					
	K					
	L					
	M					

FOREIGN PATENT DOCUMENTS

*		Document Number Country Code-Number-Kind Code	Date MM-YYYY	Country	Name	CPC Classification
	N					
	O					
	P					
	Q					
	R					
	S					
	T					

NON-PATENT DOCUMENTS

*		Include as applicable: Author, Title Date, Publisher, Edition or Volume, Pertinent Pages)
	U	Goldmacher and Kovtun (Therapeutic Delivery, 2011, Vol. 2, pp. 397-416) (Year: 2011)
	V	Polson et al (Cancer Research, 2009, Vol. 69, pp. 2358-2364) (Year: 2009)
	W	
	X	

*A copy of this reference is not being furnished with this Office action. (See MPEP § 707.05(a).)
Dates in MM-YYYY format are publication dates. Classifications may be US or foreign.

Search Notes	Application/Control No.	Applicant(s)/Patent Under Reexamination
	15/550,995	Hu, Chaohong
	Examiner	Art Unit
	KAREN A CANELLA	1643

CPC - Searched*		
Symbol	Date	Examiner

CPC Combination Sets - Searched*		
Symbol	Date	Examiner

US Classification - Searched*			
Class	Subclass	Date	Examiner

* See search history printout included with this form or the SEARCH NOTES box below to determine the scope of the search.

Search Notes		
Search Notes	Date	Examiner
STN	03/16/2019	kac
West	03/31/2019	kac
inventor [DAV]	03/31/2019	kac
West	10/13/2019	kac
inventor [DAV]	10/13/2019	kac

Interference Search			
US Class/CPC Symbol	US Subclass/CPC Group	Date	Examiner

/Karen A. Canella/ Primary Examiner, Art Unit 1643	

CSPC Exhibit 1004
Page 164 of 336

Published OnlineFirst March 3, 2009; DOI: 10.1158/0008-5472.CAN-08-2250

Research Article

Antibody-Drug Conjugates for the Treatment of Non–Hodgkin's Lymphoma: Target and Linker-Drug Selection

Andrew G. Polson, Jill Calemine-Fenaux, Pamela Chan, Wesley Chang, Erin Christensen, Suzanna Clark, Frederic J. de Sauvage, Dan Eaton, Kristi Elkins, J. Michael Elliott, Gretchen Frantz, Reina N. Fuji, Alane Gray, Kristin Harden, Gladys S. Ingle, Noelyn M. Kljavin, Hartmut Koeppen, Christopher Nelson, Saileta Prabhu, Helga Raab, Sarajane Ross, Dion S. Slaga, Jean-Philippe Stephan, Suzie J. Scales, Susan D. Spencer, Richard Vandlen, Bernd Wranik, Shang-Fan Yu, Bing Zheng, and Allen Ebens

Genentech, Inc., South San Francisco, California

Abstract

Antibody-drug conjugates (ADC), potent cytotoxic drugs covalently linked to antibodies via chemical linkers, provide a means to increase the effectiveness of chemotherapy by targeting the drug to neoplastic cells while reducing side effects. Here, we systematically examine the potential targets and linker-drug combinations that could provide an optimal ADC for the treatment for non–Hodgkin's lymphoma. We identified seven antigens (CD19, CD20, CD21, CD22, CD72, CD79b, and CD180) for potential treatment of non–Hodgkin's lymphoma with ADCs. ADCs with cleavable linkers mediated *in vivo* efficacy via all these targets; ADCs with uncleavable linkers were only effective when targeted to CD22 and CD79b. In target-independent safety studies in rats, the uncleavable linker ADCs showed reduced toxicity, presumably due to the reduced release of free drug or other toxic metabolites into the circulation. Thus, our data suggest that ADCs with cleavable linkers work on a broad range of targets, and for specific targets, ADCs with uncleavable linkers provide a promising opportunity to improve the therapeutic window for ADCs in humans. [Cancer Res 2009;69(6):2358–64]

Introduction

Antibody-drug conjugates (ADCs), cytotoxic drugs linked to antibodies through specialized chemical linkers, provide a method to target cytotoxic drugs to a tumor and minimize normal tissue damage, thereby increasing the effectiveness and reducing the toxicity of chemotherapy. The design of an ideal ADC is a dichotomy requiring tight linkage between the cytotoxic drug and the antibody to prevent nonspecific drug release while the agent is in circulation, yet appropriate release of the drug when the ADC reaches the tumor. The specific release of the cytotoxic drug is critical to the safety of the ADCs because the cytotoxic drug must be hundreds-fold more potent than the drugs used in typical systemic chemotherapy to be effective in the context of an ADC (1–3). To accomplish this specificity, specialized linkers between the antibody and drug have been designed that are cleaved only in a specific microenvironment found in or on the target tumor cell. Examples include linkers that are cleaved by acidic conditions, reducing conditions, or proteases (4–6). Another option is to have stable linkers that are not cleaved, but rather, coupled to antibodies against tumor antigens that are internalized and then degraded, releasing the drug attached to the conjugating amino acid within cells (7, 8). Thus, the active metabolite(s) and amounts of active drug released should be substantially different for the cleavable linker ADC and this could affect the safety and efficacy of the ADCs.

Another factor that has been less explored is the interaction of the linker type and the target. *In vitro* data suggest that the biology of the target, in particular, the extent of trafficking to the lysosomal compartment, will influence the effectiveness of the ADC (7–10). *In vivo*, the situation is even more complex; the extracellular microenvironment, and the intracellular trafficking of the target, the longer exposure times (weeks instead of days), in combination with the linker-drug used, will determine where, to what extent, and in what form the cytotoxic drug is released and thus which linker-drug combinations are both effective and safe.

This work focuses on four linker-drug combinations that all result in the release of cytotoxic metabolites that inhibit microtubule polymerization. We used two maytansinoid linker-drugs consisting of *N*(2′)-deacetyl-*N*(2′)-(3-mercapto-1-oxopropyl)-maytansine (DM1) with one of two different linkers that are conjugated to the antibody through lysines; the disulfide linker *N*-succinimydyl 4-(2-pyridyldithio)-pentanoate (SPP), which releases drug through the reduction of a disulfide bond (11); or the thioether linker succinimidyl-4-(*N*-maleimidomethyl)cyclohexane-1-carboxylate (MCC), which is uncleavable such that the antibody must be degraded to release the active drug lysine-MCC-DM1 (8). The other two ADCs are based on auristatins, which are mitotic inhibitors derived from dolastatin 10: monomethylauristatin E, linked to antibody cysteines by maleimidocaproyl-valine-citrulline-*p*-aminobenzyloxycarbonyl (MC-vc-PAB-MMAE); and monomethylauristatin F, linked to antibody cysteines by maleimidocaproyl (MC-MMAF). MC-vc-PAB-MMAE ADCs release free, membrane-permeable MMAE when cleaved by proteases such as cathepsin B (12). In contrast, MC-MMAF ADCs are uncleavable, like MCC-DM1, and must be internalized and degraded within a cell, releasing cysteine-MC-MMAF as the active drug (7).

The development of ADCs for the treatment of non–Hodgkin's lymphoma (NHL) provides a unique opportunity to develop ADC treatments for an important unmet medical need and as a model system to understand ADCs. NHL is responsive to chemotherapy, unconjugated antibody therapies, and radioconjugate therapies,

Note: Supplementary data for this article are available at Cancer Research Online (http://cancerres.aacrjournals.org/).

Requests for reprints: Andrew G. Polson, Genentech, Inc., 1 DNA Way, South San Francisco, CA 94080. Phone: 650-225-5134; Fax: 650-225-6240; E-mail: polson@gene.com.

©2009 American Association for Cancer Research.

doi:10.1158/0008-5472.CAN-08-2250

CSPC Exhibit 1004

Downloaded from cancerres.aacrjournals.org on October 12, 2019. © 2009 American Association for Cancer Research.

Published OnlineFirst March 3, 2009; DOI: 10.1158/0008-5472.CAN-08-2250

suggesting that these tumors are accessible by antibody-based therapies and would be responsive to cytotoxics delivered by an ADC. Furthermore, clinical experience with rituximab (chimeric IgG_1 anti-CD20), which greatly reduces the number of normal as well as malignant B cells without serious side effects, suggests that expression of an ADC target on normal B-cells and the consequent elimination of normal B cells is not a major safety concern (13). There are a number of potential ADC targets whose expression is limited to the B-cell compartment and that are expressed on NHLs. This abundance of targets with appropriate expression patterns allow for a unique opportunity to study the effect of the target on ADCs. We identified seven potential antigens with the appropriate B cell–specific expression patterns and tested the efficacy and safety of four different linker-drug formats. This combinatorial approach allowed us to elucidate some general principles for the development of ADCs, as well as identifying two targets that are responsive to ADCs with a wide range of linker-drugs and therefore hold the most promise for the treatment of NHL with ADCs.

Materials and Methods

Antibodies and ADCs. Anti-CD19 (B496, $mIgG_1$; Biomeda), anti-CD22 (RFB4; Leinco), and anti-CD180 (MHR73-11, $mIgG_1$; from eBioscience) were purchased and further purified on protein A-Sepharose and MonoQ resins to reduce endotoxin levels. The anti-CD21 (THB-5, $mIgG_{2a}$) hybridoma was obtained from American Type Culture Collection and anti-CD79b (SN8, $mIgG_1$) hybridoma was obtained from Ben Seon (Roswell Park Cancer Institute), and the antibodies from these were produced and purified as described below. Anti-CD22 (10F4v3, $huIgG_1$), anti-CD72 (10D6.8.1, $mIgG_1$), anti-gp120 ($mIgG_1$), and trastuzumab ($huIgG_1$) were generated at Genentech, Inc., using previously described methods (14–16). Hybridoma supernatants were harvested and purified by affinity chromatography (fast protein liquid chromatography; Pharmacia) as previously described (17). Purified antibodies were sterile-filtered (0.2 μm pore size; Nalgene) and stored at 4°C in PBS. MCC-DM1, MC-MMAF, and MC-vc-PAB-MMAE ADCs were made as previously described (12, 18). The SPP conjugates were prepared the same as the previously described for the MCC conjugates except that the purified antibody was buffer-exchanged into a solution containing 50 mmol/L of potassium phosphate and 2 mmol/L of EDTA (pH 6.0). SPP was dissolved in 100% ethanol and added to the antibody solution to make a final SPP/antibody molar ratio of 8:1, resulting in final DM1:antibody ratios of 3:1 to 4:1.

Xenograft models. All animal studies were performed in compliance with NIH guidelines for the care and use of laboratory animals and were approved by the Institutional Animal Care and Use Committee at Genentech. Cells for implantation were washed and suspended in HBSS (Hyclone) and inoculated subcutaneously into the flanks of female CB17 ICR severe combined immunodeficiency mice (7–16 weeks of age from Charles Rivers Laboratories), in a volume of 0.2 mL/mouse. When mean tumor size reached the desired volume, the mice were divided into groups of 8 to 10 mice with the same mean tumor size and dosed intravenously via the tail vein with ADCs or antibodies. ADC doses were either measured as the mass of the conjugated cytotoxic small molecule drug per surface area of the mouse (e.g., 300 μg antibody-linked DM1/m^2 of mouse), or as a constant mass of ADC per mass of the mouse (e.g., 5 mg of ADC/kg mouse). In general, the drug loads on the antibodies in any given experiment were similar (three to four drug molecules per antibody), so these two measures could be considered equivalent.

Antibody internalization studies. B-cell lines were incubated for 3 or 20 h at 37°C with 1 μg/mL test antibody, along with FcR block (Miltenyi), and 25 μg/mL of Alexa 647-transferrin (Invitrogen), the latter to label the recycling compartment and confirm cell viability. The incubations were carried out in RPMI culture medium, 10% heat-inactivated fetal bovine serum (Hyclone), 1% L-glutamine (Invitrogen) in the presence of 10 μg/mL leupeptin (Roche), and 5 μmol/L of pepstatin (Roche) to inhibit lysosomal degradation. Primary antibodies were then detected postfixation using Cy3 anti-mouse secondary antibodies (Jackson), and processed and photographed as previously described (18).

Rat safety and pharmacokinetic studies. Rat studies were conducted at Genentech in compliance with NIH guidelines for the care and use of laboratory animals and were approved by the Institutional Animal Care and Use Committee. Female Sprague-Dawley rats weighing 75 to 80 g were randomized on the basis of weight into groups of six animals each. On study day 1, animals were given a single intravenous dose of vehicle or anti–CD22-MC-vc-PAB-MMAE, anti–CD22-SPP-DM1, anti–CD22-MCC-DM1, or anti–CD22-MC-MMAF at 2,000 μg/m^2 conjugated cytotoxin (~20 mg/kg ADC), which was the highest tolerated dose for anti–CD22-SPP-DM1. This dose was chosen for all compounds in order to assess relative toxicities. The dose of the cytotoxin, 2,000 μg/m^2, based on body surface area was about 7-fold higher than the dose used in the efficacy studies in mice. Serum chemistry and hematology variables were measured pre-dose, on day 5, and on day 12, and included alanine aminotransferase (ALT), amylase, alkaline phosphatase (ALP), aspartate aminotransferase (AST), creatine kinase (CK), γ-glutamyl transferase, lactate dehydrogenase, sodium, potassium, chloride, calcium, inorganic phosphorous, blood urea nitrogen, creatinine, glucose, total protein, albumin, cholesterol, triglycerides, total bilirubin, WBC count, RBC count, hemoglobin, mean corpuscular volume, hematocrit, mean corpuscular hemoglobin, mean corpuscular hemoglobin concentration, RBC distribution width, mean platelet volume, platelet count (PLT), absolute segmented neutrophils (NEUT), absolute lymphocytes, absolute monocytes, absolute eosinophils, and absolute basophils. Clinical observations and body weights were also monitored throughout the study.

For pharmacokinetic studies, Sprague-Dawley rats weighing 225 to 250 g were randomized into groups of four animals each. Rats were dosed with 10 mg/kg of anti–CD22-SPP-DM1 or anti–CD22-MCC-DM1 via the jugular vein catheter. Blood samples (300 μL) were collected for pharmacokinetic analysis at 0 (pre-dose) and 3 min; 1, 6, and 24 h; and 2, 3, 4, 7, 10, 15, 21, 28, and 35 days post-dose. Serum samples were analyzed for total antibody and ADC concentration via ELISA. Pharmacokinetic variables were calculated with WinNonlin (version 5.0.1, Pharsight Corporation).

Results

Efficacy of uncleavable linker ADCs shows more target dependence than cleavable linker ADCs. We identified seven antigens, CD19, CD20, CD21, CD22, CD72, CD79b, and CD180 the expression of which is largely restricted to the B-cell compartment and are expressed in the majority of NHLs (Table 1; data not shown; refs. 19–24). Antibodies were identified that were reported, or found by ourselves (data not shown), to bind cognate antigen in flow cytometry assays. Using these antibodies, we identified cell lines that expressed each target and grew reliably with high take rates in mouse xenograft models. The models shown were not selected to be responsive to the test agents.

We made SPP-DM1 and MCC-DM1 conjugates of all the antibodies and tested their efficacy *in vivo*. We found that all of the SPP-DM1 (cleavable linker) conjugates (*red lines*, Figs. 1 and 2) were effective in the relevant xenograft models as compared with a control ADC (trastuzumab or anti–gp-120, *black lines*) that did not bind the cell line of interest (Figs. 1 and 2). The absence of activity with control conjugates indicates that the activity seen with the targeted conjugates is specific, for example, it is not due to systemic release of free drug. In several cases, tumors were not only inhibited, but also completely regressed by certain ADCs. These data indicate that all of these surface antigens are potentially effective targets for ADCs. The cleavable SPP-DM1 conjugates worked even with antibodies against targets that are very poorly internalized such as CD20, CD21, and CD72 (Fig. 3), suggesting that SPP-DM1 ADCs have broad efficacy and are relatively

CSPC Exhibit 1004

Downloaded from cancerres.aacrjournals.org on October 12, 2019. © 2009 American Association for Cancer Research.

Published OnlineFirst March 3, 2009; DOI: 10.1158/0008-5472.CAN-08-2250

Table 1. Potential antibody-drug conjugate targets for the treatment of non-Hodgkin's lymphoma

Target	Normal expression pattern	Function
CD19	B cells, FDCs	Positive regulator of BCR signaling
CD20	B cells	Unknown
CD21	B cells, FDCs	Complement receptor
CD22	B cells	Negative regulator of BCR signaling
CD72	B cells	Negative regulator of BCR signaling
CD79	B cells	Signaling component of the BCR
CD180	B cells, monocytes, DC	Inhibitor of endotoxin induced TLR4 signaling

Abbreviation: BCR, B-cell receptor.

insensitive to the target biology compared with MCC-DM1 ADCs. By contrast, only the ADCs targeted to CD79b and CD22 were effective with the uncleavable linker MCC-DM1 conjugates (*blue lines*, Figs. 1*D* and 2*B*).

In light of the relative specificity for the MCC-DM1 ADCs observed for CD22 and CD79, we decided to further explore these two antigens as targets. We tested anti-CD22 and anti-CD79b MC-vc-PAB-MMAE and MC-MMAF conjugates in relevant xenograft

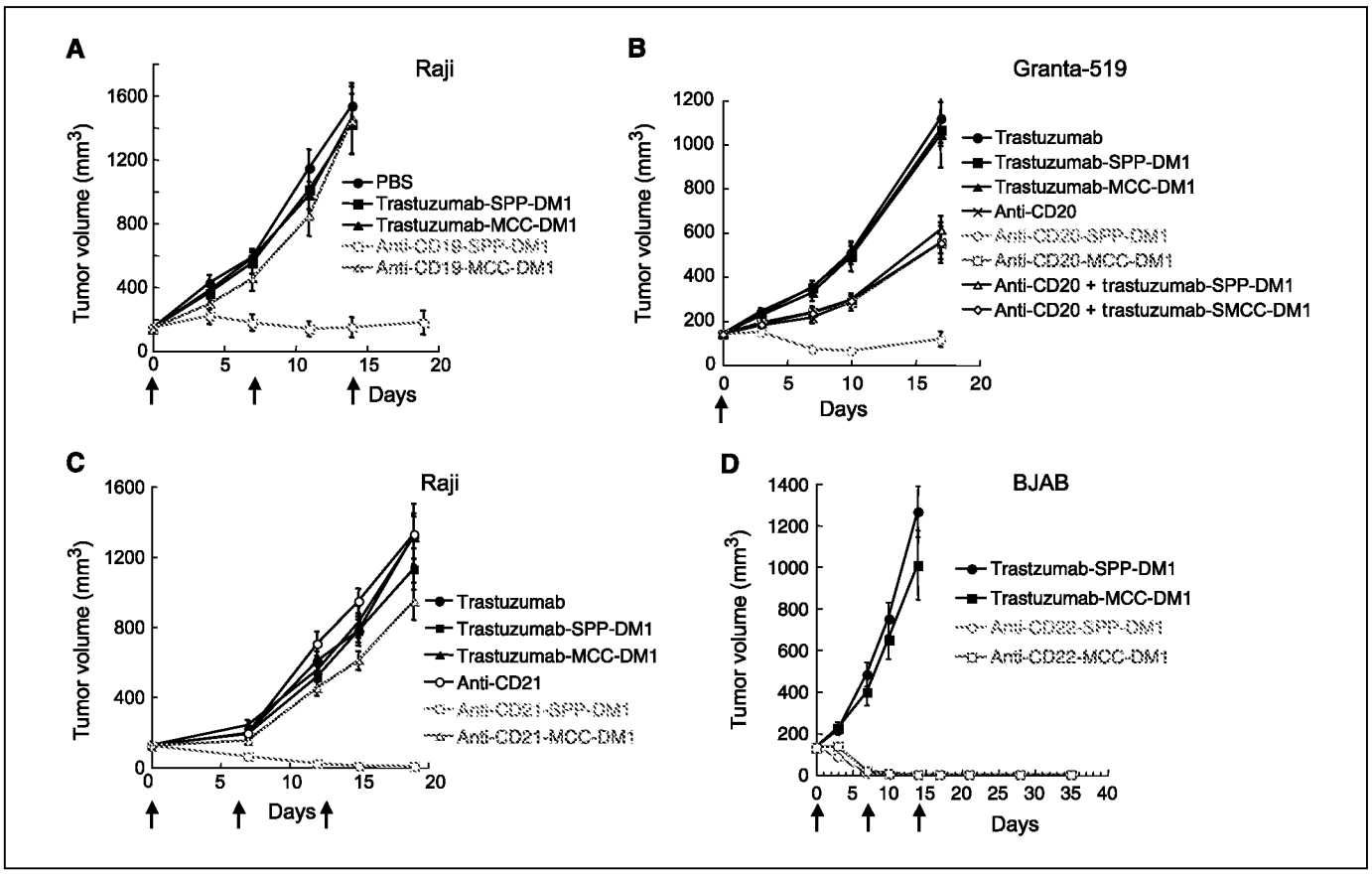


Figure 1. *In vivo* efficacy of SPP-DM1 (*red*) and MCC-DM1 (*blue*) ADCs targeted to CD19, CD20, CD21, and CD22. ADCs were tested for efficacy in various subcutaneous xenograft models of NHL. *Arrows,* the day(s) on which intravenous dosing was carried out. *A,* efficacy of anti-CD19 DM1 conjugates in RAJI cells (5×10^6 implanted) at an average starting tumor volume of 140 mm^3. Groups of eight mice were treated with 5 mg ADC/kg mouse (220–370 μg of antibody-conjugated drug/m^2 mouse) as indicated (only anti–CD19-spp-DM1–treated mice received the third dose; other groups were euthanized due to large tumor size). *B,* efficacy of anti-CD20 DM1 conjugates in Granta-519 cells (2×10^7) at an average starting tumor volume of 140 mm^3. Groups of 10 mice were treated with 5 mg ADC/kg mouse for each conjugate indicated (220–250 μg of antibody-conjugated drug/m^2 mouse). *C,* efficacy of anti-CD21 DM1 conjugates in RAJI cells (5×10^6) at an average starting tumor volume of 125 mm^3. Groups of eight mice were treated with 5 mg ADC/kg mouse (~250 μg of antibody-conjugated drug/m^2 mouse) as indicated. *D,* efficacy of anti-CD22 DM1 conjugates in BJAB-luc cells (2×10^7) at an average starting tumor volume of 130 mm^3. Groups of eight mice were treated with 214 μg of antibody-conjugated drug/m^2 mouse (~5 mg ADC/kg mouse) for the SPP-DM1 conjugates and with 405 μg of antibody-conjugated drug/m^2 mouse (~10 mg ADC/kg mouse) for the MCC-DM1 conjugates as indicated (only anti-CD22 ADC–treated mice received the third dose; control groups were euthanized due to large tumor size). The anti-CD22 antibody was RFB4. *Black symbols,* negative controls (PBS vehicle, nonbinding trastuzumab anti-HER2, and unconjugated antibodies).

CSPC Exhibit 1004

Page 167 of 336

Downloaded from cancerres.aacrjournals.org on October 12, 2019. © 2009 American Association for Cancer Research.

Published OnlineFirst March 3, 2009; DOI: 10.1158/0008-5472.CAN-08-2250

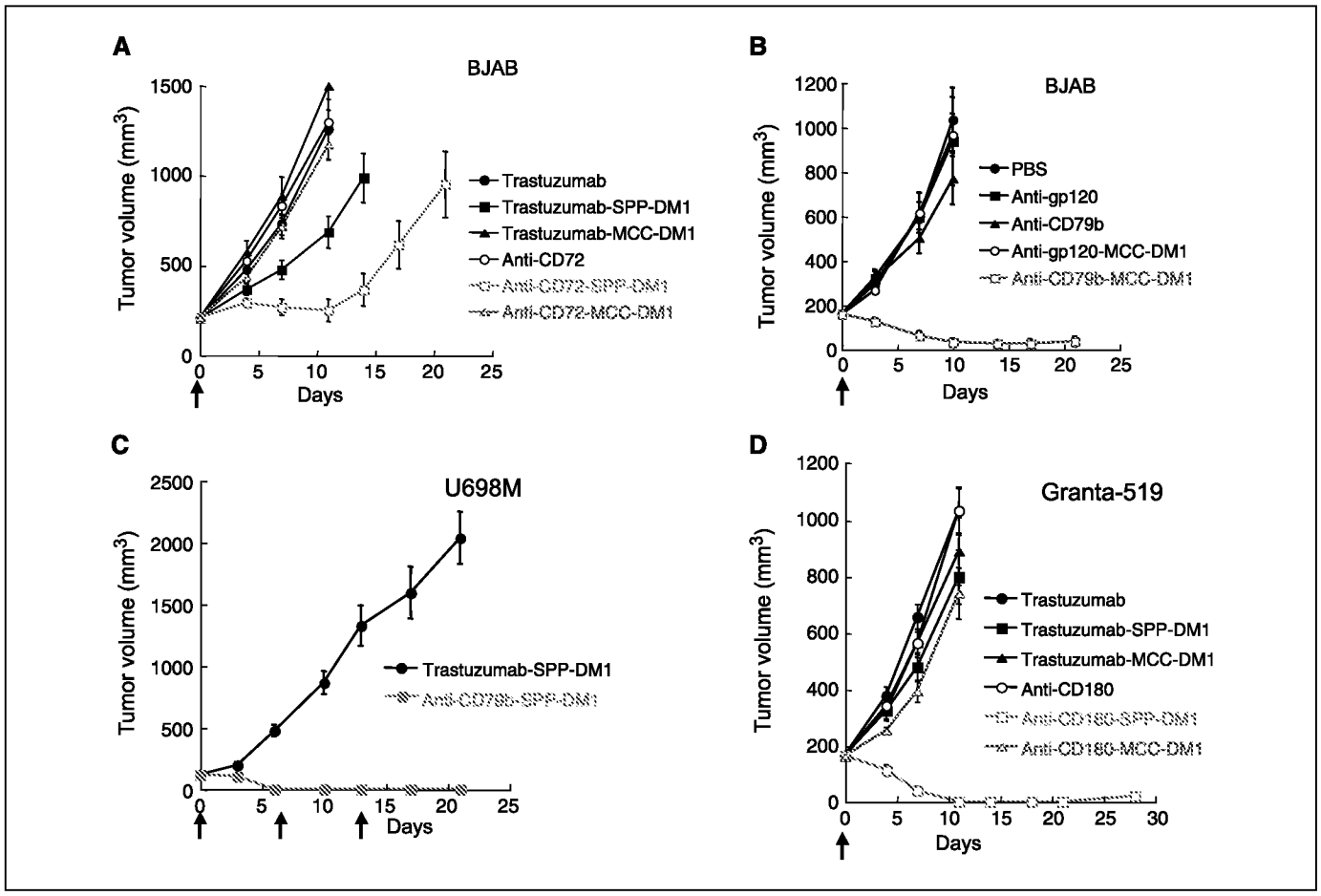


Figure 2. *In vivo* efficacy of SPP-DM1 (*red*) and MCC-DM1 (*blue*) ADCs targeted to CD72, CD79b, and CD180. ADCs were tested for efficacy in various subcutaneous xenograft models of NHL. *Arrows,* the day(s) on which intravenous dosing was carried out. *A,* efficacy of anti-CD72 DM1 conjugates in BJAB-luc cells (2×10^7) at an average starting tumor volume of 210 mm^3. Groups of 10 mice were treated with 400 μg of antibody-conjugated drug/m^2 mouse (~10 mg ADC/kg mouse) as indicated. *B,* efficacy of anti–CD79b-MCC-DM1 in BJAB-luc cells (2×10^7) at an average starting tumor volume of 159 mm^3. Groups of eight mice were treated with 200 μg of antibody-conjugated drug/m^2 mouse (~3 mg ADC/kg mouse) as indicated. *C,* efficacy of anti–CD79b-SPP-DM1 in U698M cells (5×10^6) at an average starting tumor volume of 158 mm^3. Groups of 10 mice were treated with 243 μg of antibody-conjugated drug/m^2 mouse (~5 mg ADC/kg mouse) as indicated. *D,* efficacy of anti-CD180 DM1 conjugates in Granta-519 cells (2×10^7) at an average starting tumor volume of 165 mm^3. Groups of nine mice were treated with 400 μg of antibody-conjugated drug/m^2 mouse (~7 mg ADC/kg mouse) as indicated. *Black symbols,* relevant negative controls.

models and found that all four ADCs were able to regress or eliminate the tumors (Fig. 4).

CD79b and CD22 are expressed only in the B-cell compartment and are both expressed on the surface of most NHL cells (21, 23). Furthermore, ADCs targeted against CD22 or CD79b worked with all linker-drug combinations tested, suggesting that these two antigens are particularly robust and attractive targets.

ADCs with uncleavable linkers exhibit reduced toxicity in rats when compared with cleavable linkers. ADCs with uncleavable linkers might be expected to be better tolerated than ADCs with cleavable linkers, as they should release less drug into systemic circulation, reducing the risk of toxicity (7, 8). However, this may not necessarily be the case, as even uncleavable linker ADCs are metabolized and may result in bioconcentration of the cytotoxin or its metabolites. We therefore evaluated the toxicity of ADCs with uncleavable and cleavable linker-drug combinations in rats. We used anti-CD22 conjugated to the maytansinoids, SPP-DM1 (cleavable) and MCC-DM1 (uncleavable); and the auristatins, MC-vc-PAB-MMAE (cleavable) and MC-MMAF (uncleavable), as these linker-drug combinations are already in or likely to soon enter the clinic for indications other than NHL (25). The anti-CD22 antibody does not bind rat CD22 (data not shown), so the results should reflect the systemic toxicity of ADCs in general, rather than the effects of targeting the ADC to specific tissues. Rats were chosen for these safety studies instead of mice, as it has been shown that mice are unusually tolerant of some small molecule tubulin inhibitors (26), and indeed, we observed no weight loss or other adverse effects of ADC dosing in our mouse models. Rats were given a single intravenous dose of each ADC at 2,000 μg conjugated cytotoxic drug/m^2 (~20 mg ADC/kg) and were observed for 12 days. Only anti–CD22-SPP-DM1 had a negative effect on body weights (Fig. 5*A*), indicative of toxicity. Hematology and serum chemistry, evaluated 5 and 12 days post-dosing, identified hepatic and hematologic toxicities in the two cleavable linker groups, anti–CD22-SPP-DM1 and anti–CD22-MC-vc-PAB-MMAE. Specifically, serum liver enzymes, ALT and AST, and cholesterol (data not shown) levels were mildly and transiently increased 5 days post-dosing in these cleavable linker groups. By contrast, no elevations were seen over baseline or over historical reference ranges for the groups given anti–CD22-MCC-DM1 and anti–CD22-MC-MMAF (Fig. 5*B*; Table S1). In addition, γ-glutamyl transferase and total bilirubin were elevated in the group given

CSPC Exhibit 1004

Page 168 of 336

Downloaded from cancerres.aacrjournals.org on October 12, 2019. © 2009 American Association for Cancer Research.

Published OnlineFirst March 3, 2009; DOI: 10.1158/0008-5472.CAN-08-2250

anti–CD22-SPP-DM1 (data not shown). The two groups given the cleavable linkers also developed decreases in WBC and absolute neutrophil counts on day 5 (Fig. 5*B*; Table S1) and decreases in RBC mass, hemoglobin, and hematocrit on day 12 (data not shown). Decreases in platelet counts were observed 5 days post-dosing in the group given anti–CD22-SPP-DM1 and 12 days post-dosing in the group given anti–CD22-MC-vc-PAB-MMAE (Fig. 5*B*; Table S1). In contrast, the ADCs with uncleavable linkers, MCC-DM1 and MC-MMAF, caused no significant hematologic effects compared with the control group, suggesting that they are much better tolerated than ADCs with cleavable linkers. All other clinical pathology variables (see Materials and Methods) in the ADC-dosed groups were no different from the vehicle-dosed control group.

Pharmacokinetics of cleavable and uncleavable linker ADCs. We hypothesized that the ADCs with uncleavable linkers, anti–CD22-MCC-DM1 and anti–CD22-MC-MMAF, were better tolerated because they released smaller amounts of free drug or small molecule metabolites. Another possible reason is that the uncleavable linker ADCs were cleared faster resulting in less exposure to the ADC and metabolites. To test these ideas, we performed pharmacokinetic assays on the four ADCs, measuring total antibody (which includes both the ADC and the unconjugated antibody) and drug-conjugated antibody. We found that the total antibody clearance was similar for both cleavable and uncleavable conjugates, suggesting that the type of linker has a minimal effect on the metabolism of the antibody (Fig. 5*C* and *D*). However, whereas the (drug-loaded) uncleavable linker conjugates cleared with similar kinetics as the total antibody, the cleavable linker conjugates lost drug more quickly, particularly SPP-DM1. This suggests that the cleavable linker ADCs release more free cytotoxic drug (or metabolites thereof) into the circulation. The correlation of drug loss from the antibody to hepatic and hematologic toxicities with the cleavable linker ADCs suggests that the reason that the uncleavable linkers are better tolerated than their cleavable counterparts is their decreased systemic release of free drug.

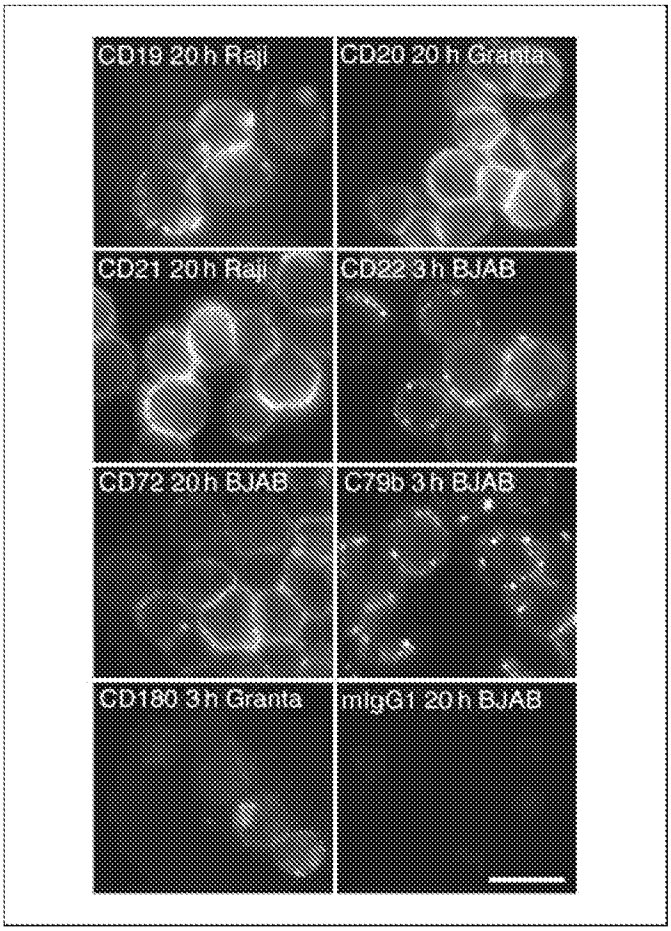


Figure 3. Different B-cell antibodies vary in the extent to which each is internalized. The same B-cell lines, as indicated, were incubated with lysosomal protease inhibitors for 3 h (for antibodies readily internalized) or 20 h (for poorly internalized antibodies) with each of the murine antibodies used in Figs. 1 and 2 as indicated. After the indicated incubation interval, cells were fixed, permeabilized, and the antibody of interest detected with Cy3 anti-mouse secondary antibody. *Bar,* 20 μm. Equivalent photographic exposures are shown.

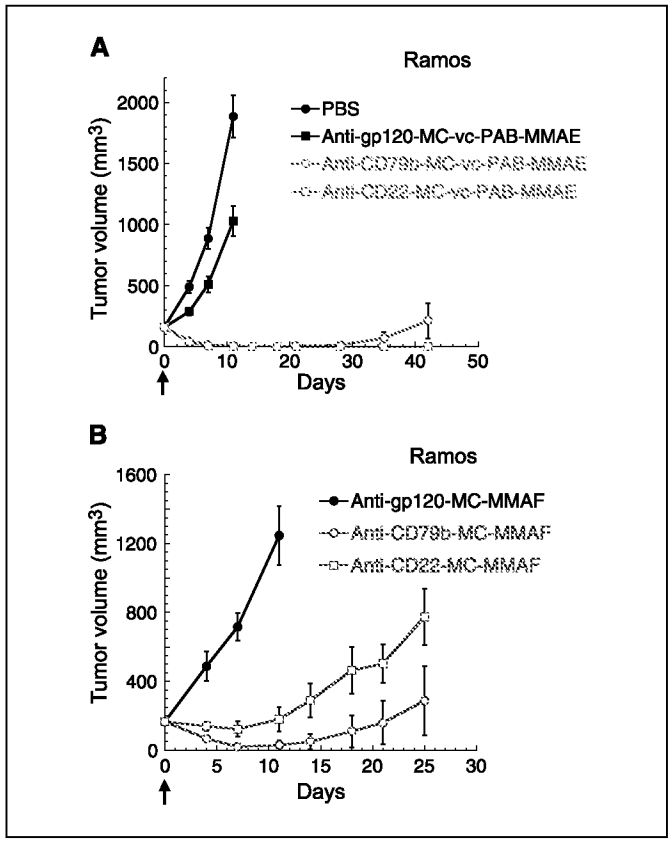


Figure 4. *In vivo* efficacy of MC-vc-PAB-MMAE and MC-MMAF ADCs targeted to CD22 or CD79b tested in a Ramos xenograft model of NHL. *Arrows,* the day(s) on which intravenous dosing was carried out. *A,* efficacy of anti–CD22-MC-vc-PAB-MMAE and anti–CD79b-MC-vc-PAB-MMAE conjugates in Ramos cells (5×10^6) at an average starting tumor volume of 160 mm^3. Groups of eight mice were treated as indicated with 405 μg of antibody-conjugated drug/m^2 mouse (~6.5 mg ADC/kg mouse) of anti–CD22-MC-vc-PAB-MMAE or 200 μg of antibody-conjugated drug/m^2 mouse (~2.5 mg ADC/kg mouse) of anti–CD79b-MC-vc-PAB-MMAE. *B,* efficacy of anti–CD22 MC-MMAF and anti–CD79b-MC-MMAF conjugates in Ramos cells (5×10^6) at an average starting tumor volume of 165 mm^3. Groups of eight mice were treated as indicated with 405 μg of antibody-conjugated drug/m^2 mouse (~7 mg ADC/kg mouse) of anti–CD22-MC-MMAF or 200 μg of antibody-conjugated drug/m^2 mouse (~2.5 mg ADC/kg mouse) of anti–CD79b-MC-MMAF.

Discussion

We examined seven potential ADC targets for the treatment of NHL, and in all cases, the cleavable-linker ADC SPP-DM1 was

CSPC Exhibit 1004
Page 169 of 336

Downloaded from cancerres.aacrjournals.org on October 12, 2019. © 2009 American Association for Cancer Research.

Published OnlineFirst March 3, 2009; DOI: 10.1158/0008-5472.CAN-08-2250

effective in xenograft models. Our observation that SPP-DM1 ADCs have activity even when the antibodies to the targets are poorly internalized seems to be a general characteristic of cleavable-linker ADCs with membrane-permeable drugs. For example, CD21 is poorly internalized (Supplemental Fig. S1; Fig. 3), yet anti–CD21-MC-vc-PAB-MMAE was effective in our model. Similarly, others have shown an anti–CD20-AcBut-calicheamicin, which also recognizes a poorly internalized target (Fig. 3) and uses an acid-cleavable linker, is effective in a xenograft model, whereas anti–CD20-amide-calicheamicin with an uncleavable linker is not (27). A likely mechanism that would explain why cleavable linkers are broadly effective and less sensitive to the biology, particularly the trafficking, of the target, is that following antibody binding, the linker is cleaved in the extracellular space and free drug subsequently permeates the cell to reach it's target. One line of evidence for this mechanism is shown in Supplemental Fig. S1; anti–CD21-MC-vc-PAB-MMAE is efficacious, but substitution of MMAF for MMAE on this conjugate results in an inactive ADC. MMAF is a more potent drug than MMAE, but is charged and relatively membrane-impermeable (7); thus, the efficacy of the MMAE conjugate in this experiment must be due to extracellular cleavage of the linker followed by cell permeation of the liberated drug. Although the data presented suggest that cleavable linkers are broadly active, our data also show that the cleavable linkers are a double-edged sword; such ADCs are more toxic in an acute setting. Still, cleavable-linker ADCs are likely to be the format of choice for many targets, particularly those with less internalization, lower copy number, or heterogeneous tumor expression (5). Indeed, the only marketed ADC, gemtuzumab ozogamicin, has an acid-cleavable linker (28).

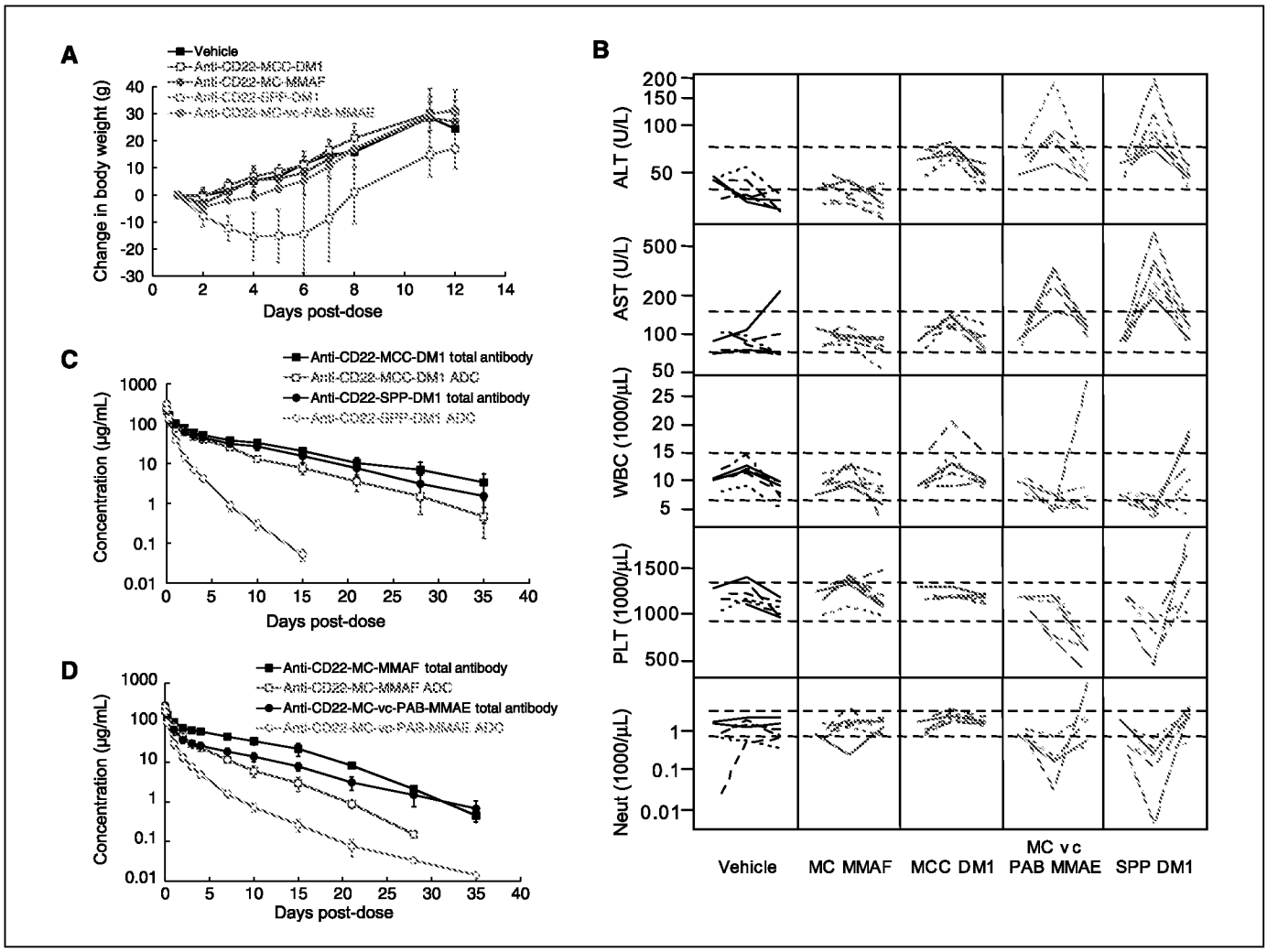


Figure 5. Safety assessment of uncleavable linker (*blue*) and cleavable-linker (*red*) ADCs in rats. Rats were dosed on day 1 with a single dose of anti–CD22-MC-MMAF, anti–CD22-MCC-DM1, anti–CD22-MC-vc-PAB-MMAE, or anti–CD22-SPP-DM1, at 0 (vehicle) or 2,000 μg/m^2 conjugated cytotoxin (n = 6 animals/group). Body weight was monitored daily (*A*) and clinical chemistry and hematology variables were measured pre-dose, on day 5, and on day 12 (*B*). The data points of the individual animals for these times are shown by lines connecting them. *ALT,* alanine aminotransferase; *AST,* aspartate aminotransferase; *PLT,* platelets; and *Neut,* neutrophils. Neutrophils, AST, and ALT are on log scale; WBC and PLT are on their original scale. *Dotted lines,* historical levels (mean ± 3 SDs) from many toxicology experiments. Median percent change of day 5 from day 0, median [100% × ($X_{day\ 5} - X_{day\ 0}$) / $X_{day\ 0}$]. Statistical analysis in Table S1. *C,* pharmacokinetic comparison of anti–CD22-MCC-DM1 and anti–CD22-SPP-DM1 in rats. The cleavable linker ADC anti–CD22-SPP-DM1 cleared faster than the uncleavable linker ADC anti–CD22-MCC-DM1 (ADC, 66.5 mL/d/kg; total antibody, 13.2 mL/d/kg anti–CD22-SPP-DM1 vs. ADC, 18.0 mL/d/kg; total antibody, 11 mL/d/kg for anti–CD22-MCC-DM1). *D,* pharmacokinetic comparison of anti–CD22-MC-MMAF and anti–CD22-MC-vc-PAB-MMAE in rats. The cleavable linker ADC anti–CD22-MC-vc-PAB-MMAE cleared faster than the uncleavable linker anti–CD22-MC-MMAF (ADC, 89.6 mL/d/kg; total antibody, 23.9 mL/d/kg for anti–CD22-MC-vc-PAB-MMAE vs. ADC, 29 mL/d/kg; total antibody, 11 mL/d/kg for anti–CD22-MC-MMAF).

CSPC Exhibit 1004

Page 16 of 336

Downloaded from cancerres.aacrjournals.org on October 12, 2019. © 2009 American Association for Cancer Research.

Published OnlineFirst March 3, 2009; DOI: 10.1158/0008-5472.CAN-08-2250

We and others (7) have hypothesized that uncleavable linker ADCs would be safer than ADCs with cleavable linkers. We tested this in a general way by using a rat model system in which the antibody was not targeted to any rat antigen, and found that, indeed, the uncleavable linker ADCs showed reduced toxicity compared with their cleavable counterparts. The faster decrease in the amount of cleavable linker ADC compared with the total antibody suggests that this is due to the release of free drug or linker-drug metabolite(s). In the context of safety, it is also important to note that there are differences in the metabolites that arise from cleavable and uncleavable linkers. For example, the reported metabolite of Ab-MCC-DM1 is lysine-MCC-DM1, a charged molecule that is relatively impermeant to cells (8). If released into the circulation, this molecule would presumably permeate normal tissues to a lesser extent than free DM1, for example. Thus, the increased safety of uncleavable linkers observed in this study could be a combination of both reduced drug release as well as differing properties of the metabolites.

Although cleavable SPP-DM1 resulted in efficacy *in vivo* when conjugated to antibodies to all seven NHL targets, uncleavable linker MCC-DM1 ADCs were only effective when targeted to two of them, CD22 and CD79b. These data suggest that ADCs targeted to CD22 and CD79b would be effective with a wide range of linker-drugs. However, it remains possible that the other antigens we tested could also be effective targets for uncleavable linker ADCs because different antibodies to the same target can sometimes lead to different efficacies (18), and other linker-drug combinations could result in greater efficacies than MCC-DM1. Thus, the right combination of antibody, linker, and drug could lead to an efficacious uncleavable ADC directed to one of the other antigens. CD19 and CD180, which are highly internalized, would seem to be the most promising antigens in this regard.

The work presented here suggests that anti–CD22-MCC-DM1, anti–CD22-MC-MMAF, anti–CD79b-MCC-DM1, and anti–CD79b-MC-MMAF are excellent candidates for the treatment for NHL. We have recently detailed the efficacy of anti–CD79b-MCC-DM1 and anti–CD79b-MC-MMAF (18) and found that these ADCs have significant efficacy in xenograft models of NHL. Our data also show that anti-CD22 and anti-CD79b ADCs with uncleavable linkers have potent efficacy and acceptable safety profiles in animal studies, and suggest that for specific targets, uncleavable linkers provide an opportunity to improve the therapeutic index of ADCs. It will be important to assess if the differences reported here are supported by additional future toxicology studies in a binding species and for extended dosing periods as anticipated for clinical use.

Disclosure of Potential Conflicts of Interest

All authors are employees of and have ownership interest in Genentech.

Acknowledgments

Received 6/13/2008; revised 12/24/2008; accepted 12/30/2008; published OnlineFirst 3/3/09.

The costs of publication of this article were defrayed in part by the payment of page charges. This article must therefore be hereby marked *advertisement* in accordance with 18 U.S.C. Section 1734 solely to indicate this fact.

We thank Ben Seon (Roswell Park Cancer Institute, Buffalo, NY) for the SN8 hybridoma, Peter Senter and Damon Meyer (Seattle Genetics, Inc., Bothell, WA) for auristatin antibody conjugations, David Xie and Rong Deng for help with the pharmacokinetic analysis, Klara Totpal and Lynne Giere for cell line production, Craig Crowley and Victoria Smith for helpful advice, Archana Uphady and Elmer Wu for project or study management and reagent inventories, Daniel Coleman for help with the statistical analysis, and Vanitha Ramakrishnan for helpful comments on the manuscript.

References

1. Garnett MC. Targeted drug conjugates: principles and progress. Adv Drug Deliv Rev 2001;53:171–216.
2. Lambert JM. Drug-conjugated monoclonal antibodies for the treatment of cancer. Curr Opin Pharmacol 2005; 5:543–9.
3. Polakis P. Arming antibodies for cancer therapy. Curr Opin Pharmacol 2005;5:382–7.
4. Hamann PR, Hinman LM, Beyer CF, et al. An anti-CD33 antibody-calicheamicin conjugate for treatment of acute myeloid leukemia. Choice of linker. Bioconjug Chem 2002;13:40–6.
5. Kovtun YV, Audette CA, Ye Y, et al. Antibody-drug conjugates designed to eradicate tumors with homogeneous and heterogeneous expression of the target antigen. Cancer Res 2006;66:3214–21.
6. Sanderson RJ, Hering MA, James SF, et al. *In vivo* drug-linker stability of an anti-CD30 dipeptide-linked auristatin immunoconjugate. Clin Cancer Res 2005;11: 843–52.
7. Doronina SO, Mendelsohn BA, Bovee TD, et al. Enhanced activity of monomethylauristatin F through monoclonal antibody delivery: effects of linker technology on efficacy and toxicity. Bioconjug Chem 2006;17: 114–24.
8. Erickson HK, Park PU, Widdison WC, et al. Antibody-maytansinoid conjugates are activated in targeted cancer cells by lysosomal degradation and linker-dependent intracellular processing. Cancer Res 2006;66:4426–33.
9. Klussman K, Mixan BJ, Cerveny CG, Meyer DL, Senter PD, Wahl AF. Secondary mAb-vcMMAE conjugates are highly sensitive reporters of antibody internalization via the lysosome pathway. Bioconjug Chem 2004;15:765–73.
10. Sutherland MS, Sanderson RJ, Gordon KA, et al. Lysosomal trafficking and cysteine protease metabolism confer target-specific cytotoxicity by peptide-linked anti-CD30-auristatin conjugates. J Biol Chem 2006;281: 10540–7.
11. Liu C, Tadayoni BM, Bourret LA, et al. Eradication of large colon tumor xenografts by targeted delivery of maytansinoids. Proc Natl Acad Sci U S A 1996;93:8618–23.
12. Doronina SO, Toki BE, Torgov MY, et al. Development of potent monoclonal antibody auristatin conjugates for cancer therapy. Nat Biotechnol 2003;21:778–84.
13. Solal-Celigny P. Safety of rituximab maintenance therapy in follicular lymphomas. Leuk Res 2006;30 Suppl 1:S16–21.
14. Foote J, Winter G. Antibody framework residues affecting the conformation of the hypervariable loops. J Mol Biol 1992;224:487–99.
15. Hongo JA, Mora-Worms M, Lucas C, Fendly BM. Development and characterization of murine monoclonal antibodies to the latency-associated peptide of transforming growth factor β 1. Hybridoma 1995;14:253–60.
16. Riechmann L, Clark M, Waldmann H, Winter G. Reshaping human antibodies for therapy. Nature 1988; 332:323–7.
17. Polson AG, Zheng B, Elkins K, et al. Expression pattern of the human FcRH/IRTA receptors in normal tissue and in B-chronic lymphocytic leukemia. Int Immunol 2006;18:1363–73.
18. Polson AG, Yu SF, Elkins K, et al. Antibody-drug conjugates targeted to CD79 for the treatment of non-Hodgkin's lymphoma. Blood 2007;1102:616–23.
19. Barclay AN, Brown M, Law SKA, McKinght AJ, Tomlinson MG, Merwe PAvd. The Leucocyte Antigen Facts Book. San Diego (CA): Academic Press; 1997.
20. Cabezudo E, Carrara P, Morilla R, Matutes E. Quantitative analysis of CD79b, CD5 and CD19 in mature B-cell lymphoproliferative disorders. Haematologica 1999;84:413–8.
21. D'Arena G, Musto P, Cascavilla N, Dell'Olio M, Di Renzo N, Carotenuto M. Quantitative flow cytometry for the differential diagnosis of leukemic B-cell chronic lymphoproliferative disorders. Am J Hematol 2000;64: 275–81.
22. Miura Y, Shimazu R, Miyake K, et al. RP105 is associated with MD-1 and transmits an activation signal in human B cells. Blood 1998;92:2815–22.
23. Olejniczak SH, Stewart CC, Donohue K, Czuczman MS. A quantitative exploration of surface antigen expression in common B-cell malignancies using flow cytometry. Immunol Invest 2006;35:93–114.
24. Schwarting R, Castello R, Moldenhauer G, et al. Human Lyb-2 homolog CD72 is a marker for progenitor B-cell leukemias. Am J Hematol 1992;41:151–8.
25. Ricart AD, Tolcher AW. Technology insight: cytotoxic drug immunoconjugates for cancer therapy. Nat Clin Pract 2007;4:245–55.
26. Mirsalis JC, Schindler-Horvat J, Hill JR, Tomaszewski JE, Donohue SJ, Tyson CA. Toxicity of dolastatin 10 in mice, rats and dogs and its clinical relevance. Cancer Chemother Pharmacol 1999;44:395–402.
27. Dijoseph JF, Dougher MM, Armellino DC, et al. CD20-specific antibody-targeted chemotherapy of non-Hodgkin's B-cell lymphoma using calicheamicin-conjugated rituximab. Cancer Immunol Immunother 2007; 56:1107–17.
28. Bross PF, Beitz J, Chen G, et al. Approval summary: gemtuzumab ozogamicin in relapsed acute myeloid leukemia. Clin Cancer Res 2001;7:1490–6.

CSPC Exhibit 1004
Page 17 of 336

Downloaded from cancerres.aacrjournals.org on October 12, 2019. © 2009 American Association for Cancer Research.

Cancer Research

Correction: Antibody-Drug Conjugates for the Treatment of Non-Hodgkin's Lymphoma: Target and Linker-Drug Selection

In this article (Cancer Res 2009;69:2358–64), which was published in the March 15, 2009 issue of *Cancer Research* (1), Dion S. Slaga should have been included as the 22nd author. The online article has been changed to reflect this correction and no longer matches the print.

Reference

1. Polson AG, Calemine-Fenaux J, Chan P, Chang W, Christensen E, Clark S, de Sauvage FJ, Eaton D, Elkins K, Elliott JM, Frantz G, Fuji RN, Gray A, Harden K, Ingle GS, Kljavin NM, Koeppen H, Nelson C, Prabhu S, Raab H, Ross S, Slaga DS, Stephan J-P, Scales SJ, Spencer SD, Vandlen R, Wranik B, Yu S-F, Zheng B, Ebens A. Antibody-drug conjugates for the treatment of non-Hodgkin's lymphoma: target and linker-drug selection. Cancer Res 2009;69:2358–64.

Published OnlineFirst 1/26/10.
©2010 American Association for Cancer Research.
doi: 10.1158/0008-5472.CAN-09-4551

CSPC Exhibit 1004
Page 172 of 336

Published OnlineFirst March 3, 2009; DOI: 10.1158/0008-5472.CAN-08-2250

AACR American Association for Cancer Research

Cancer Research

The Journal of Cancer Research (1916–1930) | The American Journal of Cancer (1931–1940)

Antibody-Drug Conjugates for the Treatment of Non–Hodgkin's Lymphoma: Target and Linker-Drug Selection

Andrew G. Polson, Jill Calemine-Fenaux, Pamela Chan, et al.

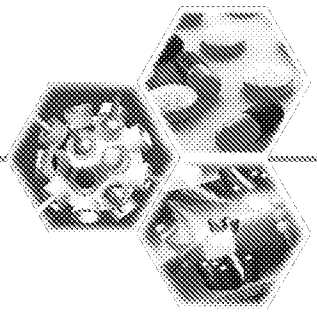
Cancer Res 2009;69:2358-2364. Published OnlineFirst March 3, 2009.

Updated version	Access the most recent version of this article at: doi:10.1158/0008-5472.CAN-08-2250
Supplementary Material	Access the most recent supplemental material at: http://cancerres.aacrjournals.org/content/suppl/2009/03/02/0008-5472.CAN-08-2250.DC1

Cited articles	This article cites 27 articles, 8 of which you can access for free at: http://cancerres.aacrjournals.org/content/69/6/2358.full#ref-list-1
Citing articles	This article has been cited by 26 HighWire-hosted articles. Access the articles at: http://cancerres.aacrjournals.org/content/69/6/2358.full#related-urls

E-mail alerts	Sign up to receive free email-alerts related to this article or journal.
Reprints and Subscriptions	To order reprints of this article or to subscribe to the journal, contact the AACR Publications Department at pubs@aacr.org.
Permissions	To request permission to re-use all or part of this article, use this link http://cancerres.aacrjournals.org/content/69/6/2358. Click on "Request Permissions" which will take you to the Copyright Clearance Center's (CCC) Rightslink site.

Downloaded from cancerres.aacrjournals.org on October 12, 2019. © 2009 American Association for Cancer Research.



For reprint orders, please contact reprints@future-science.com

Antibody–drug conjugates: using monoclonal antibodies for delivery of cytotoxic payloads to cancer cells

One approach to improving activity of anticancer drugs is to conjugate them to antibodies that recognize tumor-associated, cell-surface antigens. The antibody–drug conjugate concept evolved following major advances, first, in the development of humanized and fully human antibodies; second, in the discoveries of highly cytotoxic compounds ('drugs') linkable to antibodies; and finally, in the optimization of linkers that couple the drug to the antibody and provide sufficient stability of the antibody–drug conjugate in the circulation, optimal activation of the drug in the tumor, and the ability of the activated drug to overcome multidrug resistance. In this article, we will review the considerations for selecting a target antigen, the design of the conjugate, and the pre-clinical and clinical experiences with the current generation of antibody–drug conjugates.

Victor S Goldmacher[†1] & Yelena V Kovtun[1]

[1]ImmunoGen, Inc., 830 Winter Street, Waltham, MA 02451-1477, USA
[†]Author for correspondence:
Tel.: +1 781 895 0600
Fax: +1 781 895 0610
E-mail: victor.goldmacher@immunogen.com

Rationale for delivery of cytotoxic drugs with monoclonal antibodies

Cytotoxic chemotherapeutic drugs and therapeutic monoclonal antibodies (mAbs) represent two major classes of agents currently used for cancer treatment. The therapeutic activity of cytotoxic chemotherapeutic drugs is, in general, limited by their narrow therapeutic window, which may be attributed to their indiscriminate cytotoxicity, and/or poor pharmacokinetics and organ distribution [1]. Historically, most of the tested cytotoxic compounds have failed in clinical trials due to their excessive toxicity, and, accordingly, lack of sufficient therapeutic activity at the maximal tolerated dose (MTD).

Therapeutic mAbs display better pharmacokinetics than small-molecule drugs (longer circulation times: days vs minutes), various degrees of antigen-selective tumor accumulation, and often only moderate or no systemic toxicity [2]. Yet only a few of the large number of tested antibodies against various tumor-associated antigens, such as rituximab, trastuzumab, cetuximab and panitumumab, have made it into clinical practice [3], while the majority of the antibodies were found to lack sufficient therapeutic activity in clinical trials [4] or in preclinical studies.

The rationale for the development of **antibody–drug conjugates** (ADCs), as defined in a number of previous reviews [5–12], is to combine the selectivity, favorable pharmacokinetics, biodistribution and, when present, functional activity of antibodies with the high cytotoxic potency of a drug. An ideal ADC should: retain the favorable pharmacokinetic and functional properties of antibodies; remain intact and nontoxic in the compartment of its systemic delivery (typically blood); become active in the tumor compartment, with the active form of drug released in a sufficient amount to kill tumor cells; and combine the cytotoxic activity of the payload with the intrinsic anti-tumor activities of the antibody, including natural humoral immune responses such as the **antibody-dependent cellular cytotoxicity** (ADCC), **complement-dependent cytotoxicity** (CDC), antibody-dependent cellular phagocytosis and any direct functional activities of the antibody, such as blocking of a receptor signal transduction or engaging pro-apoptotic pathways.

Target antigen selection

The vast majority of antigens that are expressed on cancer cells have also been found to some degree on at least some normal tissues, and for this reason the term 'tumor-associated antigen' is more accurate than 'tumor-specific antigen'. The expression of an antigen of interest in some normal tissues does not necessarily preclude the development of an ADC targeting this antigen, if the normal tissue is either nonessential, or insensitive to the action of the drug (e.g., non-proliferating cells towards antimitotic agents such as **maytansinoids** or **auristatin**). Prostate-specific membrane antigen (PSMA) and HER2 are two examples of such target antigens. PSMA is expressed on normal prostate as well as on prostate cancer cells and has been the focus of

FUTURE SCIENCE

CSPC Exhibit 1004
Page 174 of 336

Key Terms

Antibody–drug conjugate: A cytotoxic drug covalently linked to a monoclonal antibody that recognizes a tumor-associated antigen.

Antibody-dependent cellular cytotoxicity: Natural killer cells and neutrophils bind to the antibody Fc portion, thus making a contact with the antigen-expressing target cell. The effector cells then use the perforin-granzyme pathway and Fas ligand to kill the target cells. In addition to antibody-dependent cellular cytotoxicity, antibody-dependent cellular phagocytosis may also contribute to the target cell eradication. Phagocytes such as monocytes/macrophages and dendritic cells take up and eliminate IgG-coated target cells.

Complement-dependent cytotoxicity: Some (but not all) human or humanized monoclonal antibodies of IgG1, IgG3, and (to a lesser degree) IgG2 isotypes trigger activation of complement pathways, which may lead to the destruction of the target cells.

Maytansinoids: Derivatives of the semi-synthetic microtubule-targeting agent maytansine.

Auristatin: Synthetic derivative of the microtubule-targeting agent dolastatin 10.

Human antimouse antibodies: Polyclonal antibodies that are produced by the human immune system against therapeutic murine monoclonal antibodies.

several ADC programs [13–16]. Targeting of normal prostate tissue may be of no safety concern and, in fact, most patients may have had their prostate surgically removed prior to ADC therapy. Trastuzumab emtansine (T–DM1) is an ADC consisting of the anti-HER2 mAb trastuzumab (Herceptin®) and the maytansinoid DM1, and has been administered safely at therapeutically effective doses, despite HER2 being expressed on some normal tissues [17–20]. Properties of a target antigen that are generally assumed to be favorable for an ADC approach include: strong expression on the surface of tumor cells; either good penetrance (percentage of tumor samples that are positive), or expression on tumors of cancer patients with high unmet medical need (a life-threatening disease with limited treatment choices); and, at the same time, little or no expression on essential normal tissues [8,11,21–23]. A requirement for the antigen of interest to be expressed homogeneously throughout a tumor tissue is probably not absolute, due to the ability of some ADCs to mediate bystander cell killing [24,25].

Accumulating, albeit still fragmentary, evidence suggests that a combination of several antigen-related factors determines the cytotoxic and anti-tumor activities of ADCs. These include, but are probably not limited to, the following parameters: the degree of the cell surface expression of the antigen; the rate of internalization of antigen–ADC complexes, and the rate and direction of their intracellular trafficking; the rate and/or degree of antigen–ADC complex processing leading to the release of the drug in its active form (proteolytic degradation of the antibody and/or cleavage of the linker). For some targets, the dynamics or efficiency of ADC internalization/trafficking may vary depending on the specific epitope on the antigen that is bound by a particular antibody. In addition, phosphorylation or other post-translational modification of the target protein or expression of cellular proteins that physically or functionally interact with the antigen may affect ADC internalization and/or its intracellular trafficking [10,11,26–31]. Available experimental evidence suggests that correlation between antigen expression and potency of an ADC is not a general phenomenon and is evident only for some antigens [12]. In one example, in an experiment evaluating the *in vitro* sensitivity of 18 non-Hodgkin lymphoma cell lines to an anti-CD22–DM1 conjugate, it was found that sensitivity to the maytansinoid component of the ADC was a more predictive indicator of sensitivity than was either the level of CD22 expression or the amount of internalized DM1 [32,33]. Therefore, selection of patients based solely on high tumor antigen expression may not guarantee clinical efficacy.

A potentially attractive property for a prospective ADC target antigen is a biological role in a pathway essential for tumor growth or survival. In principle, the intrinsic anti-tumor activity of the antibody that blocks such a pathway and the cytotoxic payload provided by the ADC format may produce a potent combined anti-tumor activity. T–DM1 [17–19] and SGN-35 [34] are examples where ADC clinical evaluation was preceded by clinical experience with the respective naked antibodies, trastuzumab and SGN-30. Trastuzumab (Herceptin) targets the HER2-receptor tyrosine kinase and suppresses the oncogenic function of this receptor, which is overexpressed on tumor cells. Trastuzumab was approved for the treatment of HER2-positive metastatic breast cancer [35]. Genentech/Roche are currently developing the ADC T–DM1 for patients with advanced HER2-positive breast cancer who have previously received multiple HER2-targeted medicines and chemotherapies [36]. Phase III studies are underway that could lead to approval of this agent in second-line and first-line therapy of HER2-positive metastatic breast cancer. Results of a Phase II study showed that T–DM1 has impressive anti-tumor activity in patients who have progressed on prior HER2-targeted therapies (including trastuzumab) [37]. The chimeric antibody SGN-30 targets CD30, a member of the TNF-R superfamily of immunoregulatory molecules, and was found to promote growth arrest and DNA fragmentation in cultured CD30-positive cells, and to have activity against Hodgkin lymphoma xenografts in immunodeficient mice [38]. Evidence of clinical activity has been reported for both SGN-30 and its conjugate with auristatin, brentuximab vedotin (SGN-35), and advanced trials are underway [34,39,40].

Apart from the biological role of the target antigen, there are two additional key considerations when developing an ADC that potentially combines anti-tumor activities provided by the cytotoxic payload with the intrinsic anti-tumor activity of its antibody component. First, the modification, conjugation, linker and payload chemistries employed must yield an ADC that retains the full biological properties of the functional antibody. T–DM1, an ADC created by conjugation of maytansinoids to trastuzumab through lysine residues, retains

CSPC Exhibit 1004
Page 175 of 33

all of trastuzumab's anti-tumor mechanisms of action, including HER2 binding affinity, inhibition of HER2 signaling and Fc-mediated immune-effector activities, such as ADCC [41]. Similar combination of the antibody functional activity and the effector drug cytotoxicity may be expected for the anti-tumor activity of the SGN-30–auristatin conjugate SGN-35.

Second, to achieve the combined effect, such ADCs may have to be administered at high enough doses, since optimal anti-tumor activity of functional antibodies in cancer patients requires relatively high doses, typically several mg/kg or greater every 3 weeks (e.g., rastuzumab, cetuximab, rituximab or panitumumab). ADCs that employ calicheamicin as a payload, a highly cytoxic DNA minor groove-binding agent, achieve an MTD of only 9 mg/m^2 or lower [42–44], doses wherein the antibody component (<0.3 mg/kg) would be unlikely to contribute to the efficacy of the ADC. By contrast, maytansinoid conjugates incorporating multiple linker formats (both cleavable and noncleavable) can achieve MTDs greater than 3 mg/kg in clinical testing [5]. In Phase I studies, the reported MTD for T–DM1 is 3.6 mg/kg when given every 3 weeks, and 2.4 mg/kg when administered weekly [19,45], which is similar to the trastuzumab dose adminstered to patients with metastatic breast cancer (e.g., 2 mg/kg weekly, after the first dose of 4 mg/kg). Therefore, maytansinoid ADC formats can produce compounds that have the prospect of retaining anti-tumor activities of the antibody component, with the added cytotoxic potency provided by the maytansinoid payload.

A wide variety of tumor-associated antigens have been explored to date as potential targets for ADCs, including various cell-surface proteins and glycoproteins, gangliosides and extracellular proteins [12,46]. In addition, in recent years, there has been increasing interest in antibody-based targeting of the tumor vasculature and stromal tissue that often play a supporting role in tumor growth [3,47–51]. ADCs that target neovasculature may act by destroying the architecture of the tumor blood supply, leading to hypoxia and nutrient deprivation [47,52], while ADCs that target the tumor stroma may reduce the level of tumor growth-supporting factors [53,54]. IMGN388 is an ADC that consists of the maytansinoid DM4 attached to an antibody against αV integrin, which is expressed on the cells of many solid tumors and also on endothelial cells during angiogenesis [55]. IMGN388 is currently in a Phase I clinical trial, and has demonstrated favorable tolerability at the dose levels evaluated to date, and evidence of activity [56]. Since it targets both tumor cells and cells that form new blood vessels that support tumor growth, its activity may exceed the clinical benefit achievable by targeting either component separately, especially with well-vascularized tumors. FAP5–DM1 is an ADC that targets fibroblast activation protein-α, an antigen found on the surface of tumor stromal fibroblasts, and it was shown to have anti-tumor activity in tumor xenografts and models of lung, pancreas, head and neck cancers in immunodeficient mice [57]. Another potential ADC stromal target is Ptk7, a pseudokinase that is highly expressed on many cancer types either in the cancer cells themselves or in the tumor stroma [58].

Targeting cancer stem cell (CSC)-specific antigens with ADCs has also been explored recently [59,60]. If the CSC hypothesis is correct then, following the elimination of the majority of cancer cells, the tumor may regrow if the CSCs are not also eradicated [61–64]. In addition to being implicated in initiating and propagating tumors, CSCs may also contribute to angiogenesis and drug resistance [65–68]. Several CSC-associated antigens are potential targets of ADC therapeutics [29,69,70]. Targeting stromal cells surrounding tumors may eliminate a source of inhibitors of bone morphogenic proteins, allowing bone morphogenic proteins to induce differentiation and inhibition of CSC proliferation [71–74].

Antibody selection

The first mAbs to be examined in the clinic were murine. In most instances, even a single injection of a murine mAbs elicits the generation of **human antimouse antibodies** within 2 weeks of antibody administration, limiting the therapeutic efficacy of murine mAbs to the first and at most, the second dose administration [2]. To date, most antibodies for use in ADCs were generated as mouse mAbs that were subsequently converted to human IgGs [3,75,76]. The initial goal for antibody chimerization (substitution of human sequences into the Fc regions) and humanization (retention of the murine complementarity-determining regions only) was to minimize the immunogenicity of antibodies when administered to human patients [76–80], and both approaches have achieved this goal [80]. Beyond reduced immunogenicity, human IgGs have two other

advantages over murine IgGs, first, they are retained longer in human circulation (because of their recognition by the human Fc neonatal receptor [FcRn], which regulates IgG circulation half-life [81]); and second, they are more effective than murine antibodies in eliciting ADCC with human effector cells [2]. Other approaches to generating human IgGs are to either directly raise human mAbs in transgenic mice in which the murine antibody-producing genes have been inactivated and replaced with human antibody-producing genes [82], or to select antibodies from large recombinant antibody libraries, such as those generated by phage display [76,83–87].

In general, desirable properties of antibodies for use in ADCs include: specificity; high binding affinity; long-circulation times; immune effector functions such as CDC, ADCC and antibody-dependent cellular phagocytosis; tumor-suppressing modulation of antigen's biological activity when possible; and minimal loss of the above-listed properties upon its conjugation to the drug of choice. To date, there are no clinical data available that would compare the anti-tumor activities of ADCs differing in one or more of these antibody-dependent properties (but made with the same drug, targeting the same antigen), and it remains unknown how much any of these properties contribute to (or interfere with) the anti-tumor efficacy of ADCs. Thus, the above-mentioned criteria are assumptions based largely on the available clinical and preclinical results obtained with naked therapeutic antibodies, and on preclinical results with ADCs in animal models, mostly immunodeficient mice. Significant differences exist between the human and murine immune systems [88,89], and between human patients' tumors and xenografts of human tumor cell lines in immunodeficient mice, and thus these criteria need further validation.

One of these factors, affinity, deserves a more detailed consideration. Typically, antibodies with the highest affinity are selected for use in ADCs on the tacit assumption that the higher affinity of an antibody will lead to the higher anti-tumor activity of its ADC. Apart from well documented *in vitro* correlation between ADC affinity and its cytotoxicity, there is no conclusive evidence of any *in vivo* correlation between affinity of an ADC and its efficacy in either preclinical models [32] or in the clinic, and it may well be that there is no such correlation because of the following considerations:

- ADCs are administered intravenously, at doses that can translate into an initial blood concentration of 0.1 μM or higher, which is much higher than the typical K_d values for antibodies used in ADCs (nM range or lower). If the ADC concentration at the tumor sites is as high as that in the blood, the ADC would be expected to saturate the antigen irrespective of its K_d;
- An exceedingly high affinity of an ADC may lead to its fast binding to the perivascular regions of the tumor, thus limiting its diffusion inside the tumor [90,91];
- A recently developed computational model of tumor targeting predicts that similar amounts of antibodies (and, by extention, ADCs) with affinities of 10^{-8} M or higher would be retained at the antigen-expressing tumor site [92].

Similarly, there are varying views on the desirability of the immune-effector functions in mAbs used in ADCs. The ADCC and CDC activities of antibodies are dependent on the antibody isotype. Human IgG1 and IgG3 isotypes elicit strong ADCC and CDC immune-effector responses, while IgG4 and IgG2 antibodies typically induce weak immune-effector responses [89,93,94]. It is generally assumed that CDC and ADCC may contribute to the anti-tumor activity of ADCs [93,94]. On the other hand, effector functions may interfere with target-cell localization or internalization of the ADC, and therefore, antibody isotypes with reduced effector functions, IgG2 and IgG4, were chosen for some ADCs [94–98].

Humanized IgG1 has been the most common isotype chosen for ADC antibodies in clinical development, with few instances of humanized IgG4 and IgG2 being selected to date (**Table 1**). The circulation half-life of human IgG3 antibodies is shorter than that of IgG1, IgG2 and IgG4 isotypes, making them less desirable for therapeutic use [89,93]. One potential disadvantage of the IgG4 subclass is the propensity of IgG4 antibodies to exchange half-molecules with other IgG4 molecules *in vivo* and hence to become bi-specific, but this can be overcome by replacing the third constant domain of the IgG4 molecule with that of human IgG1 [99]. Only one ADC that underwent clinical testing, CRO11–valine–citrilline monomethylauristatin E (vcMMAE), was of an IgG2 type [100]. IgG2 antibodies are capable of forming covalent dimers [101], which conceivably may enhance solid-phase homotypic antibody–antibody

CSPC Exhibit 1004

Table 1. Antibody–cytotoxic compound conjugates in clinical development.

Antibody–cytotoxic compound	Target antigen	Linker–cytotoxic compound, class	Antibody	Tumor type(s)	Developer	Status
Gemtuzumab ozogamicin (Mylotarg®)	CD33 (Siglec-3)	Hydrazone, AcBu, *N*-acetyl-γ calicheamicin, calicheamicin	hP67.6 humanized IgG4	Acute myeloid leukaemia	Pfizer	US FDA conditionally approved, recently withdrawn
Inotuzumab ozogamicin (CMC–544)	CD22 (Siglec-2)	Hydrazone, AcBu, *N*-acetyl-γ calicheamicin, calicheamicin	G5/44 humanized IgG4	B-cell lymphomas	Pfizer	Phase I and I/II Phase III combination
Trastuzumab–DM1 (T–DM1)	HER2 (ErbB2)	Thioether, SMCC–DM1, maytansinoid	Transtuzumab humanized IgG1	Metastatic breast cancer	Roche	Phase II and III
Lorvotuzumab mertansine (IMGN901, huN901–DM1, BB10901)	CD56 (NCAM)	Hindered disulfide, SPP–DM1, maytansinoid	huN901 humanized IgG1	Solid tumors, multiple myeloma	ImmunoGen	Phase I and II
IMGN388 (CNTO365)	Integrin	Highly hindered disulfide, SPDB–DM4, maytansinoid	Anti-integrin human IgG1	Solid tumors	ImmunoGen	Phase I
SAR3419 (huB4–DM4)	CD19	Highly hindered disulfide, SPDB–DM4, maytansinoid	huB4 humanized IgG1	Non-Hodgkin lymphoma	Sanofi–Aventis	Phase I
BIIB015	Cripto	Highly hindered disulfide SPDB–DM4, maytansinoid	Anti-Cripto humanized IgG1	Cripto-positive solid tumors	Biogen Idec	Phase I
BT062	CD138	Highly hindered disulfide SPDB–DM4, maytansinoid	Anti-CD138 chimeric IgG4	Multiple myeloma	Biotest	Phase I
Brentuximab vedotin (SGN-35)	CD30	Dipeptide, vc-MMAE, auristatin	SGN-30 chimeric IgG1	Relapsed/refractory Hodgkin lymphoma, systemic anaplastic large-cell lymphoma	Seattle Genetics, Millenium	Phase II and III
Glembatumumab vedotin (CR011–vcMMAE, CDX-011)	Glycoprotein NMB (osteoactivin)	Dipeptide, vc-MMAE, auristatin	CRO11 fully human IgG2	Metastatic breast cancer and melanoma	Celldex Therapeutics	Phase I/II
SGN-75 (h1F6–mcMMAF)	CD70	Noncleavable, mc-MMAF, auristatin	SGN-70 humanized IgG1	Non-Hodgkin lymphoma and renal carcinoma	Seattle Genetics	Phase I
PSMA ADC	Prostate-specific membrane antigen	Dipeptide, vc-MMAE, auristatin	Anti-PSMA	Progressive, metastatic, hormone-refractory prostate cancer following prior taxane chemotherapy	Progenics Pharmaceuticals	Phase I
ASG–5ME	SLC44A4 (AGS-5)	Dipeptide, vc-MMAE, auristatin	Anti-AGS-5 human IgG2	Pancreatic cancer	Agensys, Seattle Genetics	Phase I
MDX–1203	CD70	Dipeptide, MGBA	Anti-CD-70 human	Non-Hodgkin lymphoma and advanced/recurrent clear-cell renal cell carcinoma	Bristol–Myers Squibb	Phase I

MMAE: Monomethylauristatin E; MMAF: Monomethylauristatin F; NCAM: Neural cell-adhesion molecule; PSMA: Prostate-specific membrane antigen; SPDB: N*-succinimidyl-3-(2-pyridyldithio)butanoate; SPP:* N*-succinimidyl 4-(2-pyridyldithio)pentanoate.*

CSPC Exhibit 1004
Page 178 of 336

associations to boost affinity and/or internalization, but may also contribute to aggregation issues. Antibody engineering can enhance the immune-effector functions and extend the circulation half-life of antibodies [85,102], with current technologies focusing on modifying the antibody amino acid sequence or on its defucosylation to enhance affinity for IgG Fc-γ receptor IIIa (FcγRIIIa) [103–107]. The effect of isotype and FcγR binding on the properties of monomethylauristatin F (MMAF) conjugates of an anti-CD70 antibody have been recently reported [88]. Conjugates were prepared from variant antibodies of the parental anti-CD70 IgG1, which included an IgG2, an IgG4 and an IgG1v1, the latter engineered for impaired binding to huFcγ receptors, but having only modest impairment of binding to FcRn, which regulates retention of IgG in circulation. All the conjugates bound well to antigen, had good cytotoxicity activity *in vitro* and were well-tolerated *in vivo* in mice. The IgG1v1 conjugate was found to have an increased anti-tumor activity in xenograft models, and a longer circulation half-life than the parental IgG1 conjugate. Interpretation of these results and their implications for ADC clinical therapy is difficult, however, because of the above-mentioned differences between the human and murine systems, it remains to be seen how much ADCC and CDC contribute to the overall activity of ADCs.

Cytotoxic drugs used in ADCs

Considerations for ADC drugs

One important requirement for a drug to be considered as an ADC effector is that this drug should be sufficiently cytotoxic at concentrations that can be achieved by antibody delivery. Early immunoconjugates developed for oncology incorporated the standard anticancer drugs in use at the time, such as methotrexate, doxorubicin or the vinca alkaloids, and yielded disappointing results, with little or no anti-tumor activity observed in clinical trials [7,8,108,109]. Delivery of the cytotoxic agent to a tumor cell via an ADC is limited by the amount of the target antigen on the cell surface, and by the access of the ADC to the cell within the tumor. It was later proposed that one of the reasons these early ADCs failed, and had a narrow (if any) therapeutic window, was insufficient potency of the conjugated drugs [7,25,108,110,111]. Cytotoxic drugs used in the current generation of ADCs are at least 100-fold more potent than those used in the early conjugates [7]. On the other hand, more potent ADCs may be more systemically toxic, which may narrow their therapeutic window. Another common feature of effectors utilized in the current generation of ADCs is their selectivity towards killing proliferating cells. An effector that preferentially kills proliferating cells may, in principle, improve the selectivity of the ADC since the incidence of proliferating cancer cells in tumors is higher than that in most normal tissues. Other preferable characteristics for a drug include low molecular weight, and the related lack of immunogenicity, a reasonably low cost of production, availability in a linkable form and sufficient solubility and stability in water to facilitate preparation and storage of the antibody conjugates [112].

Types of ADC drugs

The drugs used in ADCs currently in the clinic or preclinical testing can be divided into two categories, those that target DNA, and those that target microtubules. In addition, several potent ADC drugs have also been reported that have not yet reached the clinic. These include the microtubule-targeting taxol derivatives (taxanes) [7,8,113–116], the DNA-targeting streptonigrin, the HSP90-targeting geldanamycin and the topoisomerase-inhibiting camptothecin analogs [117,118]. These preclinical-stage ADCs will not be discussed here further.

DNA-damaging drugs

N-acetyl-γ-calicheamicin dimethyl hydrazide, a derivative of calicheamicin, is the cytotoxic component of Mylotarg® gemtuzumab ozogamicin, which targets CD33 [96,119], and was conditionally approved in May 2000 under the US FDA's accelerated-approval program, but was recently withdrawn from the USA market by Pfizer due to its failing to show inproved efficacy in a Phase III combination trial. Calicheamicin is a highly cytotoxic enediyne antibiotic that binds to the minor groove of DNA and induces double-strand DNA breaks that result in cell death [98,120]. The ADC showed higher *in vitro* potency than unconjugated calicheamicin against CD33-positive cells, and eradicated CD33-positive HL-60 xenografts in nude mouse models [96]. Several other ADCs comprised of antibodies linked to calicheamicin are being evaluated, including inotuzumab ozogamicin (CMC-544), which targets CD22 and is in Phase III clinical testing against non-Hodgkin lymphoma [98,121,122]. Calicheamicin conjugates of several other antibodies, the anti-CD20 antibody rituximab [123], the H8 antibody directed against

CSPC Exhibit 1004
Page 179 of 331

the oncofetal antigen 5T4 expressed on various carcinomas [124], and an anti-MUC1 antibody targeting various solid tumors [125], are currently in preclinical evaluation.

Analogs of CC-1065 and the duocarmycins are highly cytotoxic DNA minor-groove binding alkylating agents (MGBA) [126]. The first MGBA-based ADCs were made with the CC-1065 analog DC1 [127], which turned out to be nearly insoluble, making conjugation reactions inefficient, and with DC4, a water-soluble phosphate prodrug of DC1 [8]. Several other conjugates have been reported more recently [16,128–132]. MDX-1203, a conjugate of the fully human anti-CD70 antibody and a duocarmycin analog has been developed at Medarex (now Bristol–Myers Squibb). In this conjugate, the cytotoxic effector is attached to the antibody in prodrug form, linked to it via a protease-cleavable dipeptide linker, and a maleimide attachment site, requiring not only release from the antibody but also esterase/protease cleavage to release the active cytotoxic drug [131]. MDX-1203 showed efficacy in renal cancer xenograft models, was well tolerated in cynomolgus monkey safety studies [131,132] and is currently in a Phase I clinical study in patients with advanced/recurrent clear-cell renal-cell carcinoma or relapsed/refractory B-cell non-Hodgkin lymphoma. Two other MGBA-based ADCs are being explored as potential prostate cancer therapeutics, one targeting PSMA, which is found on the surface of the prostate tumor cells, and another directed against the extracellular protein mindin/RG-1 which is thought to be retained in the extracellular matrix of human prostate tumors [16].

Microtubule-targeting drugs

Among ADCs based on microtubule-targeting cytotoxic drugs, two categories have reached the stage of clinical development, those utilizing derivatives of maytansine (maytansinoids), and those utilizing auristatins [5,6,8,9,110,133]. Maytansine, with IC_{50} values in the range of 10 to 100 pM depending upon the cell type [110,133], is significantly more cytotoxic against cell lines *in vitro* than clinically used microtubule-targeting drugs such as vinca alkaloids or taxol. Maytansine and maytansinoids appear to act by interfering with microtubule dynamics [134–136], thereby inducing cell-cycle arrest at G2/M, which eventually leads to cell death. This mode of cytotoxic action may explain why proliferating cells are more sensitive to maytansine than are nonproliferating cells [137]. Two maytansinoids are being used in ADCs currently in clinical development, DM1 and DM4, which differ in the degree of hindrance of the disulfide bond they afford in the linker between the drug and the antibody. The first antibody–maytansinoid conjugate to undergo clinical testing was cantuzumab mertansine [25,110], which was comprised of the cytotoxic maytansinoid compound DM1 conjugated by a disulfide linkage to the huC242 antibody, a humanized IgG1 antibody that targets the extracellular domain of the tumor-associated carbohydrate antigen CanAg, expressed on most colorectal, biliary and pancreatic cancers, as well as on many non-small-cell lung, gastric, uterine and bladder cancers [138–140]. Cantuzumab mertansine was shown to have specific and highly efficacious anti-tumor activity in preclinical xenograft models [25]. It was well-tolerated in Phase I clinical studies of CanAg-expressing solid tumors and showed evidence of biological activity in terms of tumor shrinkage and stable disease [139,141]. The development of this conjugate was stopped because its activity was considered insufficient. The evaluation of this initial antibody–maytansinoid conjugate has been followed by the development of an expanding number of antibody–maytansinoid conjugates that incorporate a growing portfolio of maytansinoid compounds and linker technologies [8,133]. At this time, six of these conjugates are undergoing clinical evaluation in a variety of tumor indications (discussed below), and many more are undergoing preclinical evaluation, including an ADC that targets CD79 on non-Hodgkin lymphoma [142]; an ADC that targets CD22, another B-cell antigen [143]; and SAR566658 (huDS6-DM4), which targets a Muc1 sialoglycotope on solid tumors [144,145]. Antibody–maytansinoid conjugates are discussed in greater detail in a recent review [5].

The auristatins, another group of antimicrotubule agents with potent cell-killing activity, are fully synthetic analogs of the pentapeptide natural product dolastatin 10 [146,147]. Auristatin E and MMAE are 50- to 200-fold more potent than the vinca alkaloids against a diverse panel of tumor cell lines, and ADCs prepared with these compounds were highly effective in preclinical studies [147]. An auristatin derivative with a negatively charged C-terminal phenylalanine residue, MMAF, was shown to have much lower cytotoxic activity as an unconjugated compound than MMAE, probably due to its reduced plasma membrane permeability

and intracellular access [148]. Nonetheless, antibody–MMAF conjugates were found to be comparable with antibody–MMAE conjugates in their cytotoxic potency towards target antigen-positive cell lines, and over three orders of magnitude more potent than free MMAF, presumably because of the different route of drug delivery by ADCs, traversing the plasma membrane [148]. It is still an open question if the low cytotoxicity of the unconjugated MMAF will result in lower toxic side-effects of its respective ADCs compared with similar MMAE conjugates. Currently, five antibody–auristatin conjugates are undergoing clinical evaluation (TABLE 1). Pre-clinical studies have been reported for several other antibody–auristatin conjugates, such as ADCs that target the B-cell antigens CD22 [143], CD19 [149,150] and CD79 [151], as well as EphA2, an antigen that is overexpressed in many solid tumors [152,153].

Linkers used in ADCs

The third ADC component is the linker used to covalently attach the drug to the antibody. Several recent reviews have focused on emerging linker technologies [8,9,11,112,154,155]. There are several important considerations regarding the linker component, including: the site of attachment on the antibody; the average number of attachment sites per antibody molecule; the cleavability of the linker, that is, its ability to chemically disintegrate releasing the drug; and the polarity of the linker.

Most drugs have been linked to antibodies at the amino groups of lysine residues or thiol groups of cysteine residues [11,112,156]. New approaches to engineer specific sites of modification are also being evaluated [157]. The relative benefit of the different approaches to the function of the resulting ADC is still largely unknown.

The number of cytotoxic molecules attached to the antibody is an important consideration. A low drug per antibody ratio (DAR) may result in low potency of the ADC, while a too-high degree of antibody modification may adversely affect its affinity towards the target antigen, FcγR, or FcRn, and may also result in aggregation and precipitation of the antibody and/or a decrease in its stability. The optimal DAR is determined empirically for each antibody on the basis of a variety of tests such as the feasibility of conjugate synthesis and solubility of the resulting conjugate, impact on antigen-binding affinity, antigen-specific as well as nontargeted cytotoxicity of the ADC, and its behavior in animal models such as anti-tumor activity, pharmacokinetics and systemic toxicity. Most of the conjugates currently in clinical testing (regardless of which cytotoxic compound, antibody or linker was used) have three to four cytotoxic molecules per antibody molecule. Gemtuzumab ozogamicin, prepared with a strategy designed to minimize aggregation, consists of an approximate 1:1 mixture of unconjugated antibody and conjugated antibody having four to six calicheamicin molecules per antibody [96,119], and inotuzumab ozogamicin has an average calicheamicin:antibody loading of five:seven per antibody [98].

The anti-tumor activity of antibody–auristatin conjugates with different molar ratios of auristatin to antibody was evaluated by Hamblett *et al.*, who separated a sample of an anti-CD30 antibody–MMAE conjugate into fractions having approximately two, four or eight MMAE molecules per antibody [158]. Although the potency of the resulting conjugates was found to correlate with auristatin load when tested *in vitro*, the therapeutic index in xenograft tumor models in mice did not improve with increasing DAR. The discrepancy between the *in vitro* and *in vivo* results was consistent with the observations that higher MMAE load resulted in faster clearance of the conjugate from circulation and increased toxicity in mice [158]. Whether the enhanced clearance is a direct effect of the increased load of MMAE on the antibody, or an effect on the antibody of progressively decreasing the number of inter-chain disulfide bonds that are used in linking MMAE, is unknown. Subsequently, the anti-CD30 antibody was engineered to generate conjugates with defined stoichiometries of either two or four auristatin molecules per antibody [159].

Since a key advantage of antibody-based therapeutics over most chemotherapeutic drugs is their long retention in circulation, an optimal conjugate linkage must be stable during circulation in the patient yet allow for efficient release of the cytotoxic compound in active form upon internalization into the tumor cell. A variety of linkers have been designed to take advantage of differences between the extracellular and intracellular environments to allow release of an active cytotoxic molecule only after antigen-specific, antibody-mediated internalization of the ADC into tumor cells has occurred. Linkers containing disulfide bonds were used to take advantage of the different concentrations of free thiols (free thiols are the main physiological substances

CSPC Exhibit 1004
Page 181 of 33

that can cleave these bonds) in the intracellular and extracellular space. The most abundant intracellular thiol, reduced glutathione, is present in cells in the concentration range of 0.5 to 10 mM [160] compared with a significantly lower concentration of the most abundant low-molecular-weight thiol in circulation, cysteine, approximately 5 μM [161]. In addition, the intracellular enzyme protein disulfide isomerase, or similar enzymes that are also capable of cleaving disulfide bonds [162], may also contribute to the preferential cleavage of disulfide bonds inside cells. Acid-labile linkers were used because of the low pH in the late endosomes and lysosomes, compared with near-neutral pH in circulation and other extracellular environments. Peptide-based linkers were used because such linkers could be cleaved by lysosomal and endosomal proteolytic enzymes. In principle, these linkers may also be cleaved by cytoplasmic proteases as well [163].

Most ADCs currently undergoing clinical evaluation contain linkers that fall into two broad categories: 'cleavable', that is, those that can disintegrate inside the cell, such as hydrazone, disulfide or protease-sensitive peptide linkers; and 'noncleavable', which require proteolytic cleavage of the antibody portion of the ADC for release of the cytotoxic molecule, still attached to the linker and the single remaining amino acid derived from the antibody. For more details the reader can refer to the recent review by Singh and Erickson [112].

Calicheamicin-containing ADCs utilize a hydrazide functionality introduced into calicheamicin γ1 to enable its linkage to an antibody via an acid-hydrolizable bond [164]. In gemtuzumab ozogamicin, *N*-acetyl-γ-calicheamicin dimethyl hydrazide is conjugated to lysines in the antibody using a 4-(4'-acetylphenoxy) butanoic acid linker, which is stable in physiological buffers (pH 7.4), but hydrolyses at the pH of lysosomes (pH ~4) [164]. Gemtuzumab ozogamicin was found to be reasonably stable in blood in animal studies [95,165] and in acute myeloid leukaemia patients [166]. In mouse circulation, the amount of calicheamicin conjugated to the hP67.6 decreased twofold in approximately a 2-day period, and the presence of a CD33-expressing xenograft did not influence the rate of this apparent decomposition, although the method used in the study could not distinguish between cleavage of calicheamicin on all the conjugate molecules and the generation of a fraction of unconjugated antibody, and between conjugate decomposition and preferential clearance of a fraction of the conjugate with a higher DAR [165].

Antibody–maytansinoid conjugates currently in clinical testing utilize either cleavable disulfide or noncleavable thioether linkages. Both are formed from a heterobifunctional crosslinking reagent that reacts with a lysine residue on an antibody, and then maytansine derivatives containing thiol groups are reacted with the other end of the heterobifunctional reagent [110,133,167]. This method of conjugation results in a random distribution of the maytansinoid molecules randomly linked to a small subset of approximately 40 different sites [156]. Newer thiol-containing maytansinoids have been synthesized with one or more methyl groups (substituting hydrogen) on the carbon atoms adjacent to the disulfide linkage, to create linkers having varying degrees of steric hindrance around the disulfide bond [8,133]. These hindering modifications were designed to minimize cleavage of the conjugates during circulation in the blood, without interfering with efficient release of the cytotoxic agents once internalized into tumor cells. Preclinical studies comparing huC242–DM4 (IMGN242), a conjugate utilizing a more-hindered maytansinoid, with huC242–DM1 (cantuzumab mertansine), a conjugate having a less-hindered maytansinoid, revealed decreased plasma clearance for huC242–DM4 and also greater anti-tumor activity in xenograft models [133,168]. Several maytansinoid conjugates currently undergoing clinical testing, IMGN388, SAR3419, BIIB015 and BT062, utilize this more-hindered disulfide linkage. One ADC in clinical testing, T–DM1, utilizes a noncleavable thioether linkage to attach the maytansinoid molecule to the antibody [18].

The intracellular processing of disulfide- or thioether-linked maytansinoid conjugates has been examined [169,170]. Both types of maytansinoid conjugates were found to degrade in lysosomes to yield metabolites consisting of a lysine adduct of the maytansinoid and linker, and this lysosomal processing was required for their cytotoxic activity. The disulfide-containing metabolites were processed further via reduction of the disulfide bond and subsequent *S*-methylation, to produce *S*-methyl-maytansinoids. These lipophilic *S*-methyl-maytansinoid metabolites were highly cytotoxic towards cell lines when added exogenously (comparable to maytansine), whereas the more hydrophilic lysine-containing

Key Term

P-glycoprotein: A transmembrane ATP-dependent drug transporter. Overexpression of P-glycoprotein often contributes to the emergence of multidrug resistance in tumors following chemotherapy.

maytansinoid metabolites were much less active. These observations may help explain both the phenomenon of target-cell-activated killing of bystander cells and the superior efficacy of disulfide-linked conjugates over noncleavable conjugates seen in some xenograft models [10,24,169,170]. Antigen-positive cells treated with a disulfide-linked conjugate, but not those treated with a thioether-linked conjugate, release the highly cytotoxic *S*-methyl-maytansinoid capable of killing nearby antigen-negative cells [24]. This additional indirect killing of adjacent tumor cells expressing little or no surface antigen may contribute to the activity of disulfide-linked antibody–maytansinoid conjugates against tumors having heterogeneous antigen expression. In addition, such bystander killing could potentially impact tumor-supporting neovasculature and proliferating stromal cells while causing minimal collateral toxicity to adjacent normal cells, as proliferating cells are much more sensitive to the cytotoxic effects of maytansine and its derivatives than are nonproliferating cells [10,24].

To prepare the auristatin conjugates, antibody disulfide bonds are reduced to generate two to eight cysteine residues that are subsequently linked to an auristatin derivative, either maleimide–MMAE or maleimide–MMAF, via a dipeptide linker [147,148,158,171]. One of the dipeptide linkers used, valine–citrulline, was designed to be cleaved by cathepsin B upon intracellular delivery of the conjugates into the lysosomal compartment [147,148]. Intracellular processing of brentuximab vedotin (anti-CD30–MMAE containing this dipeptide linker) was examined in detail [172]. Exposure of CD30-expressing cells to this conjugate resulted in its lysosomal degradation and intracellular release of chemically unmodified MMAE. Efflux of MMAE led to killing of cocultivated CD30-negative cells, a bystander killing effect similar to that observed with disulfide-linked maytansinoid ADCs.

In pre-clinical studies, the valine–citrulline peptide linkage appeared to be quite stable in circulation, with a half-life of auristatin release of 6 days in mice and 9.6 days in cynomolgus macaques [173], similar to that of *N*-succinimidyl 3-[2-pyridyldithio]-propionate (SPDB)-linked maytansinoid conjugates. New auristatin ADC linkers have been generated by replacing the maleimide with a halo-acetamide and have demonstrated improved *in vivo* stability in preclinical studies [154]. In another recent development, anti-CD70–auristatin conjugates have been synthesized utilizing novel dipeptide linkers and new auristatins linked through the C-terminus, and some of these new conjugates showed improved therapeutic windows over the original 1F6-Val-Cit-PABC–MMAF conjugate [155].

A method for site-specific antibody conjugation has been developed to reduce the heterogeneity of ADCs [157]. The 'ThiomAb' technology involves the engineering of reactive cysteine residues into specific sites of the antibody, to allow drug conjugation with defined stoichiometry and without disruption of interchain disulfide bonds [157]. A ThiomAb–drug conjugate comprised of MMAE conjugated to an anti-MUC16 antibody was found to be as efficacious as a conventional MMAE conjugate in mouse xenograft models and was better tolerated in rat and cynomolgus monkeys, possibly due to the absence of species carrying overly high MMAE loads [157].

Multidrug resistance (MDR) is a major obstacle to successful cancer chemotherapy and potentially to ADC therapy as well [27,57,133,174,175]. MDR1 (also known as **P-glycoprotein** or ABCB1), the best-characterized member of the ABC family of transporters, is expressed in a variety of cancers with evidence of increased incidence following chemotherapy, and its expression has been found to correlate with poor responses to chemotherapeutic compounds [176–178]. The majority of drugs used in ADCs are MDR1 substrates [167], and it is expected that improved intracellular retention of ADC's active metabolites would result in increased anti-tumor efficacy in cancers expressing MDR1. Efforts to evaluate cytotoxic compounds as substrates of the various MDR efflux pumps and to develop strategies to circumvent resistance mechanisms have become a priority in ADC research [125,167,179–181]. We have recently developed a new generation of hydrophilic linkers that enable antibody–maytansinoid conjugates to overcome MDR1-mediated resistance. Maytansinoid conjugates prepared with one of these linkers, maleimidyl-based PEG_4Mal, were processed by target cells to a yield a polar cytotoxic metabolite that appears to be a poor MDR substrate. The increased retention of this metabolite correlated with greater antimitotic and cytotoxic potency of the conjugates toward MDR1-expressing cells *in vitro* and with increased efficacy against MDR1-positive xenograft tumors [167,181].

CSPC Exhibit 1004
Page 183 of 33

Clinical experience with ADCs

ADCs in clinical development

A list of ADCs in clinical development at the time of preparation of this review is presented in Table 1.

Gemtuzumab ozogamicin (Mylotarg) was conditionally approved by the FDA (accelerated approval) for treatment of acute myeloid leukemia, but was recently withdrawn from the US market. A confirmatory, postapproval trial was stopped early when no improvement in clinical benefit was observed, combined with serious drug-related toxicities. A second calicheamicin conjugate, inotuzumab ozogamicin (CMC-544), targets CD22 and is undergoing clinical testing against B-cell lymphomas [98,121,182].

Maytansinoid-containing conjugates are undergoing clinical testing in a variety of tumor indications. T–DM1, comprised of Roche's anti-HER2 antibody trastuzumab linked by a noncleavable thioether linkage to the maytansinoid DM1, is in broad clinical development for HER2-positive breast cancer. Results of a Phase II study, showed that T–DM1 has impressive anti-tumor activity in patients who have progressed on prior HER2-targeted therapies (including trastuzumab) [37]. One could speculate that residual intrinsic activity of trastuzumab, insufficient to suppress tumor growth on its own in these patients, may be contributing to the efficacy observed with T–DM1. Alternatively, the efficacy of T–DM1 observed in clinical trials could be a result of the high expression of HER2 and the ability of Herceptin to stimulate endocytosis of the T–DM1 complex with HER2 and deliver the maytansinoid into the cancer cells [183]. The FDA denied accelerated approval of T–DM1 Biologics License Application (BLA) for metastatic breast cancer. The BLA was submitted in July 2010 on the basis of the results of a single-arm, Phase II study, which showed that T–DM1 shrank tumors in one-third of women with advanced HER2-positive breast cancer who had received, on average, seven prior medicines, including two HER2-targeted medicines. In its review of the BLA, the FDA stated the T–DM1 trials did not meet the standard for accelerated approval because all available treatment choices approved for metastatic breast cancer, regardless of HER2 status, had not been exhausted in the study population. Roche stated that it will submit data from the amended Phase III randomized study to the FDA to support a new T–DM1 BLA in mid 2012. This study compares T–DM1 to lapatinib in combination with capecitabine in people with advanced HER2-positive breast cancer whose disease has worsened after receiving initial treatment.

Lorvotuzumab mertansine (IMGN901, BB-10901 or huN901-DM1) [184], which targets CD56 (neural cell adhesion molecule 1) comprises a humanized version of the N901 antibody [78] conjugated to DM1 via a hindered disulfide linker. CD56 is found on a variety of tumor types of hematopoietic and neuroendocrine origin, including multiple myeloma, certain types of leukemia, neuroblastoma, astrocytoma, glioma, most cases of small-cell lung cancer and many cases of ovarian cancer [184–186]. Its normal tissue expression is restricted to natural killer cells and a subset of T cells, as well as in nerve tissue and heart muscle [187]. Encouraging anti-tumor activity of lorvotuzumab mertansine was reported in clinical studies in multiple myeloma and Merkel-cell carcinoma [188,189] (see [5] for more detail). Its clinical evaluation in patients with solid tumors, in particular small-cell lung cancer and Merkel-cell carcinoma, and multiple myeloma is continuing.

IMGN388 is a maytansinoid ADC comprised of a humanized anti-integrin antibody conjugated to DM4 [55]. The target antigen is strongly expressed on a wide variety of solid tumors, including melanomas, sarcomas and a large number of carcinomas, as well as on endothelial cells in the process of forming new blood vessels. The targeting of neovasculature and/or stromal components supporting tumor growth, in addition to the tumor cells themselves, may afford greater efficacy than targeting the tumor cells alone. The initial clinical testing of IMGN388 showed favorable tolerability and evidence of activity [190]. Several other antibody–maytansinoid conjugates (utilizing conjugate technology from ImmunoGen) are in clinical development. SAR3419 (sanofi-aventis) targets the CD19 antigen and is in clinical testing in patients with relapsed or refractory B-cell non-Hodgkin lymphoma [191]. BIIB015 (Biogen Idec), a humanized IgG1 anti-Cripto antibody conjugated to DM4, is in clinical testing for treatment of relapsed or refractory Cripto-positive solid tumors. BT062 (Biotest AG), comprised of a chimerized anti-CD138 antibody and DM4 [192], is in Phase I clinical testing for multiple myeloma [193].

A total of five auristatin conjugates are in clinical evaluation; promising Phase I/II results have been reported for two

of these conjugates (TABLE 1). SGN-35, which consists of a CD30-targeting antibody conjugated to MMAE [171,194] is undergoing clinical evaluation in Phase II and Phase III trials in patients with Hodgkin lymphoma and systemic anaplastic large-cell lymphoma. CD30 is a member of the tumor necrosis factor receptor superfamily, a transmembrane glycoprotein receptor that is highly expressed on Hodgkin lymphoma, anaplastic large cell lymphoma, and some other T-cell lymphoproliferative disorders, but is restricted on normal tissues primarily to expression on activated leukocytes [39,158]. Seattle Genetics expects to file a BLA submission to the FDA in the first half of 2011. CR011–vcMMAE is being developed by Celldex Therapeutics for the treatment of metastatic breast cancer and advanced melanoma [100,195,196]. The targeted antigen is the glycoprotein NMB (GPNMB), which is highly expressed in most metastatic melanoma samples [197], and is also expressed in liver carcinomas, squamous-cell lung cancers, breast cancers, soft-tissue tumors and gliomas [11,195,197]. CR011–vcMMAE is comprised of a fully human IgG2 antibody conjugated to MMAE via a valine–citrulline dipeptide linker, and is currently being evaluated in two Phase I/II clinical trials, for unresectable stage III or IV melanoma and for locally advanced or metastatic breast cancer, and in Phase IIb for GPNMB-expressing breast cancers.

Several auristatin conjugates have recently entered clinics. SGN-75, a conjugate of a humanized anti-CD70 mAb with MMAF, is being developed by Seattle Genetics and is currently in a Phase I clinical trial for relapsed or refractory non-Hodgkin lymphoma or metastatic renal cell carcinoma. CD70 is expressed on several types of non-Hodgkin lymphoma, multiple myeloma, renal-cell carcinoma, pancreatic, ovarian and lung cancer, while having limited expression in normal tissues. In preclinical studies, SGN-75 demonstrated potent antitumor activity in models of CD70-positive renal-cell carcinoma and hematologic malignancies. A conjugate of a fully human anti-PSMA mAb with MMAE [14] is being developed by Progenics Pharmaceuticals, and is in a Phase I trial in patients with progressive, metastatic and hormone-refractory prostate cancer [198]. PSMA is expressed on the surface of prostate cancer cells and on the neovasculature of many types of solid tumors, but has limited expression in normal tissues. PSMA expression is increased in high-grade, metastatic and hormone-refractory prostate cancer. Recently ASG–5ME, which consists of an anti-ASG-5 antibody attached via a valine–citrulline dipeptide linker to the auristatin derivative MMAE, has entered Phase I trials for pancreatic cancer patients.

Toxicity of ADCs

While ADCs retain antibody-like pharmacokinetics and biodistribution, these molecules ultimately are metabolized and eliminated *in vivo* by the same organ systems that normally metabolize circulating antibodies and/or chemotherapeutic drugs. Unlike 'naked' antibodies, ADCs will have inherent dose-limiting toxicities related to the systemic metabolism of the conjugate and its cytotoxic payload. The nature and degree of such 'nontargeted toxicity' of ADCs vary significantly depending on the cytotoxic payload and its metabolites; generally, one might expect that cytotoxic payloads with increased potency would yield ADCs with decreased MTDs. Similar to naked antibody therapeutics, ADCs also have the potential to cause toxicity in patients if they target a tumor antigen that is also expressed on normal tissues ('targeted toxicity').

Many ADCs tested to date, even those with some normal tissue crossreactivity, have been well-tolerated in patients, causing only minimal toxicities that were manageable and reversible. Examples of maytansinoid ADCs with favorable tolerability reported in clinical testing include lorvotuzumab mertansine [199–201], T–DM1 [17–19], cantuzumab mertansine (huC242–DM1) [139,141], MLN2704 [15] and AVE9633 [202]. However, sometimes significant ADC-related toxicities may only become apparent in the clinic. For example, treatment with gemtuzumab ozogamicin, which received conditional approval (accelerated approval) in 2000 based on single-arm Phase II trials [119,203] was associated with the serious, potentially fatal liver condition veno-occlusive disease [204], and the incidence of this disease increased in the confirmatory Phase III trial [301].

The clinical experience with bivatuzumab mertansine (Boehringer Ingelheim), an anti-CD44v6-directed maytansinoid ADC, provides an example of 'targeted toxicity' of an ADC. This compound showed evidence of efficacy in multiple early-stage clinical trials, but was discontinued due to skin-related adverse effects [205–208]. Since the observed toxicity was most likely due to abundant expression of the CD44v6 antigen in dividing epithelial cell layers of normal skin, as well as its high expression

CSPC Exhibit 1004
Page 185 of 33

on head and neck cancer and other epithelial cancers [209], these clinical results testify to the specificity and potency of antibody-delivered cytotoxic agents.

Soluble antigen in circulation

The presence of target antigen in patient plasma, due to cleavage of the antigen from the surface of tumor cells ('shed' antigen), or from secretion of a soluble form of the antigen, can sometimes influence the pharmacokinetics and the efficacy of an ADC. Soluble antigen can bind the circulating ADC, potentially enhancing clearance of the latter and/or interfering with targeting of the antigen on tumor cells. A correlation between high peripheral blood antigen load and decreased efficacy has been suggested for gemtuzumab ozogamicin in acute myeloid leukaemia [210] and for an anti-MUC1 (hCTM01)–calicheamicin conjugate in ovarian cancer [125,211]. For other antibodies and ADCs, such as trastuzumab and IMGN242, high peripheral blood antigen levels have been correlated with altered pharmacokinetics, but have not been predictive of clinical outcome or associated with decreased efficacy (or did not reach statistical significance with the number of patients treated) [212–214]. The half-life of trastuzumab was reported to be 2 ± 1 days for patients with circulating levels of HER2 extracellular domain ≥500 ng/ml, as compared with a half-life of 9 ± 5 days for patients with <500 ng/ml serum HER2 [212]. However, the potential for soluble antigen to influence the pharmacokinetics of trastuzumab appears not to have precluded delivery of clinical benefit in early testing of T–DM1 for metastatic breast cancer patients, where the average terminal half-life of T–DM1 was reported to be 3.5 days at the MTD of 3.6 mg/kg given every 3 weeks [17–19].

Future perspective

The field of antibody-targeted drug delivery has been fueled by the development of mAb technology in 1975 and subsequent success in identification of many tumor-associated antigens, first with the help of mAbs and later also with a variety of other methods, most notably mRNA-expression profiles. It took many years to gradually develop the current (yet

Executive summary

- Antibody–drug conjugates (ADCs) combine the selectivity, favorable pharmacokinetics, biodistribution and, when present, functional activity of antibodies with the high cytotoxic potency of a small drug.
- Factors that determine the anti-tumor activity of ADCs include antigen expression, the rate of internalization and direction of intracellular trafficking of antigen–ADC complexes, the rate and/or degree of the intracellular release of the active drug and the ability of the antibody to interfere with tumor growth or tumor cell survival.
- A wide variety of tumor-associated cell-surface antigens have been explored as targets for ADCs. Other currently explored targets for ADCs include neovasculature, tumor stroma and cancer stem cells.
- Chimerization and humanization of murine IgGs or use of fully human antibodies minimized or eliminated their immunogenicity in humans, led to their longer retention in human circulation and increased their antibody-dependent cellular cytotoxicity activity.
- At present, there is no conclusive evidence of any *in vivo* correlation between the affinity of an ADC for its target and its efficacy in either preclinical models or in the clinic. A recently developed computational model of tumor targeting predicts that antigen-selective tumor uptake of ADCs depends on the antibody affinity in the range of K_d values of 10^{-8} M to 10^{-7} M or worse, but may not improve with the higher affinity antibodies.
- The desirability of the immune-effector functions in monoclonal antibodies used in ADCs is, at present, unclear.
- The drugs currently used in ADCs in the clinic or in preclinical testing are at least 100-fold more potent than those used in the early conjugates, and can be divided into two categories, those that target DNA and those that target microtubules. Two categories of ADCs based on microtubule-targeting cytotoxic drugs have reached the clinical development stage, those utilizing derivatives of maytansine and those utilizing auristatins.
- Most ADCs currently in clinical development contain linkers that fall into two categories: 'cleavable', that is, those that can disintegrate inside the cell; and 'noncleavable', which require proteolytic cleavage of the antibody portion of the ADC for release of the cytotoxic molecule. Antibody–maytansinoid conjugates utilize either cleavable disulfide or noncleavable thioether linkages. New linkers that enable maytansinoid ADCs to overcome P-glycoprotein-mediated resistance have been developed.
- Many ADCs tested to date, even those with some normal tissue crossreactivity, have been well-tolerated in patients, causing only minimal toxicities that were manageable and reversible.
- The chances for clinical success of ADCs have increased due to the continued improvements in their design: improved understanding of target-selection criteria, advances in antibody engineering, development of more potent cytotoxic drugs, and optimization of antibody–cytotoxic agent links.

CSPC Exhibit 1004

incomplete) knowledge of how to make ADCs that are potent, well-tolerated, nonimmunogenic in the clinic and feasible to develop from both an economic and logistical perspective. The chances for clinical success have increased due to the continued improvements in the design of ADCs: improved understanding of target-selection criteria, advances in antibody engineering, development of more potent cytotoxic drugs, and optimization of antibody–cytotoxic agent linkers. Future clinical studies with ADCs and therapeutic antibodies will give us further insight into the contribution of various factors, both in ADC design (the potency of the drug, the affinity of the antibody, the cleavability, polarity and solubility of the linker, and the roles of antibody-dependent humoral responses) and in the nature of the target tumors (antigen density and heterogeneity of expression, accessibility of the tumor to the ADC, MDR status, soluble antigen levels, FcγR genotype and tumor vascularization). ADCs are poised to provide a new generation of effective oncology treatment options in the near future.

Acknowledgements

The authors thank their colleagues, Tom Chittenden and John M Lambert for the critical reading of the manuscript.

Financial & competing interests disclosure

The authors are employees of ImmunoGen, Inc. and have stock options of ImmunoGen, Inc. (Victor Goldmacher currently does not own stock of ImmunoGen). Both authors are inventors in several patents and patent applications related to their employment at ImmunoGen. The authors have no other relevant affiliations or financial involvement with any other organization or entity with a financial interest in or financial conflict with the subject matter or material discussed in the manuscript. This includes employment consultancies, honoraria, stock ownership or options, expert testimony, grants or patents received or pending, or royalties.

No writing assistance was utilized in the production of this manuscript.

Bibliography

Papers of special note have been highlighted as:
- ▪ of interest
- ▪▪ of considerable interest

1 Pratt WB, Ruddon RW, Ensminger WD *et al.* *Part 2. The Anticancer Drugs.* Oxford University Press, UK 69–198 (1994).

2 Scheinberg DA, Rosenblat TL, Jurcic JG *et al.* Antibodies. In: *Chemotherapy and Biotherapy: Principles and Practice (Fifth Edition).* Chabner BA, Longo DL (Eds). Wolters Kluwer/Lippincott Williams & Wilkins, Health, PA, USA 465–494 (2011).

3 Boyiadzis M, Foon KA. Approved monoclonal antibodies for cancer therapy. *Expert Opin. Biol. Ther.* 8(8), 1151–1158 (2008).

4 Reichert JM. Monoclonal antibodies in the clinic. *Nat. Biotechnol.* 19(9), 819–822 (2001).

5 Lambert JM. Antibody–maytansinoid conjugates: a new strategy for the treatment of cancer. *Drugs Future* 35(6), 471–480 (2010).

6 Senter PD. Potent antibody–drug conjugates for cancer therapy. *Curr. Opin. Chem. Biol.* 13 (3), 235–244 (2009).

7 Goldmacher VS, Blattler WA, Lambert JM, Chari RVJ. Immunotoxins and antibody–drug conjugates for cancer treatment. In: *Biomedical Aspects of Drug Targeting.* Torchilin V, Muzykantov V (Eds). 291–309, Kluwer Academic Publishers, MA, USA (2002).

8 Chari RV. Targeted cancer therapy: conferring specificity to cytotoxic drugs. *Acc. Chem. Res.* 41(1), 98–107 (2008).

9 Ducry L, Stump B. Antibody–drug conjugates: linking cytotoxic payloads to monoclonal antibodies. *Bioconjug. Chem.* 21(1), 5–13 (2010).

10 Kovtun YV, Goldmacher VS. Cell killing by antibody–drug conjugates. *Cancer Lett.* 255(2), 232–240 (2007).

11 Carter PJ, Senter PD. Antibody–drug conjugates for cancer therapy. *Cancer J.* 14(3), 154–169 (2008).

12 Vater AV, Goldmacher VS. Antibody–cytotoxic compound conjugates for oncology. In: *Macromolecular Anticancer Therapeutics.* Reddy LH, Couvreur P (Eds). Springer, NY, USA 331–369 (2009).

13 Henry MD, Wen S, Silva MD *et al.* A prostate-specific membrane antigen-targeted monoclonal antibody–chemotherapeutic conjugate designed for the treatment of prostate cancer. *Cancer Res.* 64(21), 7995–8001 (2004).

14 Ma D, Hopf CE, Malewicz AD *et al.* Potent antitumor activity of an auristatin-conjugated, fully human monoclonal antibody to prostate-specific membrane antigen. *Clin. Cancer Res.* 12(8), 2591–2596 (2006).

15 Galsky MD, Eisenberger M, Moore-Cooper S *et al.* Phase I trial of the prostate-specific membrane antigen-directed immunoconjugate MLN2704 in patients with progressive metastatic castration-resistant prostate cancer. *J. Clin. Oncol.* 26(13), 2147–2154 (2008).

16 Pan C, Terrett J, Rao C *et al.* Human antibody conjugates of potential utility for prostate cancer therapy: a comparison of MGBA conjugates with antibodies targeting a cell surface target (prostate-specific membrane antigen) and an extracellular matrix target (Mindin/RG-1). *AACR Annual Meeting Abstracts* 4062 (2008).

17 Beeram M, Burris HA, Modi S *et al.* A Phase I study of trastuzumab–DM1, a first-in-class HER2 antibody–drug conjugate (ADC), given every 3 weeks to patients with HER2$^+$ metastatic breast cancer. *Am. Soc. Clin. Onc. Annu. Meet. Proc.* (2008) (Abstract #1028).

18 Burris HA, Vukelja S, Rugo HS *et al.* A Phase II study of trastuzumab–DM1 (T–DM1), a HER2 antibody–drug conjugate, in patients with HER2-positive metastatic breast cancer. *ASCO Breast Cancer Symposium Proceedings* (2008) (Abstract 155).

19 Holden SN, Beeram M, Krop IE *et al.* A Phase I study of weekly dosing of trastuzumab–DM1 (T–DM1) in patients with advanced HER2$^+$ breast cancer. *Am. Soc. Clin. Onc. Annu. Meet. Proc.* (2008) (Abstract 1029).

20 Press MF, Cordon-Cardo C, Slamon DJ. Expression of the HER2/neu proto-oncogene in normal human adult and fetal tissues. *Oncogene* 5(7), 953–962 (1990).

CSPC Exhibit 1004
Page 187 of 33

21 Carter P, Smith L, Ryan M. Identification and validation of cell surface antigens for antibody targeting in oncology. *Endocr. Relat. Cancer* 11(4), 659–687 (2004).

22 Xie H, Blattler WA. *In vivo* behavior of Antibody–drug conjugates for the targeted treatment of cancer. *Expert Opin. Biol. Ther.* 6(3), 281–291 (2006).

23 Kononen J, Bubendorf L, Kallioniemi A *et al.* Tissue microarrays for high-throughput molecular profiling of tumor specimens. *Nat. Med.* 4(7), 844–847 (1998).

24 Kovtun YV, Audette CA, Ye Y *et al.* Antibody–drug conjugates designed to eradicate tumors with homogeneous and heterogeneous expression of the target antigen. *Cancer Res.* 66(6), 3214–3221 (2006).

25 Liu C, Tadayoni BM, Bourret LA *et al.* Eradication of large colon tumor xenografts by targeted delivery of maytansinoids. *Proc. Natl Acad. Sci. USA* 93 (16), 8618–8623 (1996).

26 Bhaskar V, Law DA, Ibsen E *et al.* E-selectin up-regulation allows for targeted drug delivery in prostate cancer. *Cancer Res.* 63 (19), 6387–6394 (2003).

27 Walter RB, Raden BW, Kamikura DM *et al.* Influence of CD33 expression levels and ITIM-dependent internalization on gemtuzumab ozogamicin-induced cytotoxicity. *Blood* 105 (3), 1295–1302 (2005).

28 Smith LM, Nesterova A, Alley SC *et al.* Potent cytotoxicity of an auristatin-containing antibody–drug conjugate targeting melanoma cells expressing melanotransferrin/p97. *Mol. Cancer Ther.* 5(6), 1474–1482 (2006).

29 Smith LM, Nesterova A, Ryan MC *et al.* CD133/prominin-1 is a potential therapeutic target for antibody–drug conjugates in hepatocellular and gastric cancers. *Br. J. Cancer* 99 (1), 100–109 (2008).

30 Oflazoglu E, Stone IJ, Gordon K *et al.* Potent anticarcinoma activity of the humanized anti-CD70 antibody h1F6 conjugated to the tubulin inhibitor auristatin via an uncleavable linker. *Clin. Cancer Res.* 14(19), 6171–6180 (2008).

31 Ingle GS, Chan P, Elliott JM *et al.* High CD21 expression inhibits internalization of anti-CD19 antibodies and cytotoxicity of an anti-CD19–drug conjugate. *Br. J. Haematol.* 140 (1), 46–58 (2008).

32 Polson AG, Williams M, Gray AM *et al.* Anti-CD22–MCC–DM1: an antibody–drug conjugate with a stable linker for the treatment of non-Hodgkin's lymphoma. *Leukemia* 24(9), 1566–1573 (2010).

33 Polson A. Antibody–drug conjugates for the treatment of non-Hodgkin's lymphoma. Presented at: *The Drug Discovery and Development of Innovative Therapeutics Conference.* Boston, MA, USA, 7 August 2008.

34 Younes A, Forero-Torres A, Bartlett NL *et al.* Objective responses in a Phase I dose-escalation study of SGN-35, a novel antibody–drug conjugate (ADC) targeting CD30, in patients with relapsed or refractory Hodgkin lymphoma. *Am. Soc. Clin. Onc. Annu. Meet. Proc.* 8526 (2008).

35 Harries M, Smith I. The development and clinical use of trastuzumab (Herceptin®). *Endocr. Relat. Cancer.* 9 (2), 75–85 (2002).

36 Lewis Phillips GD, Li G, Dugger DL *et al.* Targeting HER2-positive breast cancer with trastuzumab–DM1, an antibody–cytotoxic drug conjugate. *Cancer Res.* 68 (22), 9280–9290 (2008).

37 Krop I, LoRusso P, Miller KD *et al.* A Phase II study of trastuzumab–DM1 (T–DM1), a novel HER2 antibody–drug conjugate, in patients previously treated with lapatinib, trastuzumab, and chemotherapy. Presented at: *The 33rd Annual CTRC-AACR San Antonio Breast Cancer Symposium.* San Antonio, TX, USA, 12 December 2009. (Abstract 5090).

38 Wahl AF, Klussman K, Thompson JD *et al.* The anti-CD30 monoclonal antibody SGN-30 promotes growth arrest and DNA fragmentation *in vitro* and affects anti-tumor activity in models of Hodgkin's disease. *Cancer Res.* 62(13), 3736–3742 (2002).

39 Bartlett NL, Younes A, Carabasi MH *et al.* A Phase I multidose study of SGN-30 immunotherapy in patients with refractory or recurrent CD30$^+$ hematologic malignancies. *Blood* 111(4), 1848–1854 (2008).

40 Fanale M, Bartlett NL, Forero-Torres A *et al.* The antibody–drug conjugate brentuximab vedotin (SGN-35) induced multiple objective responses in patients with relapsed or refractory cd30-positive lymphomas in a Phase I weekly dosing study. Presented at: *The 51st ASH Annual Meeting.* New Orleans, LA, USA, 5–8 December 2009 (Abstract 2731).

41 Junttila TT, Li G, Parsons K *et al.* Trastuzumab–DM1 (T–DM1) retains all the mechanisms of action of trastuzumab and efficiently inhibits growth of lapatinib insensitive breast cancer. *Breast Cancer Res. Treat.* DOI: 10.1007/s10549-010-1090-x (2010) (Epub ahead of print).

42 Sievers EL, Appelbaum FR, Spielberger RT *et al.* Selective ablation of acute myeloid leukemia using antibody-targeted chemotherapy: a Phase I study of an anti-CD33 calicheamicin immunoconjugate. *Blood* 93(11), 3678–3684 (1999).

43 Arceci RJ, Sande J, Lange B *et al.* Safety and efficacy of gemtuzumab ozogamicin in pediatric patients with advanced CD33$^+$ acute myeloid leukemia. *Blood* 106(4), 1183–1188 (2005).

44 Sievers EL, Larson RA, Stadtmauer EA *et al.* Efficacy and safety of gemtuzumab ozogamicin in patients with CD33-positive acute myeloid leukemia in first relapse. *J. Clin. Oncol.* 19(13), 3244–3254 (2001).

45 Krop IE, Beeram M, Modi S *et al.* Phase I study of trastuzumab–DM1, an HER2 antibody–drug conjugate, given every 3 weeks to patients with HER2-positive metastatic breast cancer. *J. Clin. Oncol.* 28(16), 2698–2704 (2010).

▪ **Clinical study of trastuzumab–DM1 conjugate.**

46 Teicher BA. Antibody–drug conjugate targets. *Curr. Cancer Drug Targets* 9(8), 982–1004 (2009).

47 Jain RK. Normalization of tumor vasculature: an emerging concept in antiangiogenic therapy. *Science* 307(5706), 58–62 (2005).

48 Wu Y, Cain-Hom C, Choy L *et al.* Therapeutic antibody targeting of individual notch receptors. *Nature* 464(7291), 1052–1057 (2010).

49 Mukherjee S, Richardson AM, Rodriguez-Canales J *et al.* Identification of EpCAM as a molecular target of prostate cancer stroma. *Am. J. Pathol.* 175(6), 2277–2287 (2009).

50 Hofmeister V, Schrama D, Becker JC. Anti-cancer therapies targeting the tumor stroma. *Cancer Immunol. Immunother.* 57(1), 1–17 (2008).

51 Schliemann C, Neri D. Antibody-based vascular tumor targeting. *Recent Results Cancer Res.* 180, 201–216 (2010).

52 Minchinton AI, Tannock IF. Drug penetration in solid tumours. *Nat. Rev. Cancer* 6(8), 583–592 (2006).

53 Hanahan D, Weinberg RA. The hallmarks of cancer. *Cell* 100(1), 57–70 (2000).

54 Mahadevan D, Von Hoff DD. Tumor–stroma interactions in pancreatic ductal adenocarcinoma. *Mol. Cancer Ther.* 6(4), 1186–1197 (2007).

55 Vater CA, Manning C, Millar H *et al.* Anti-tumor efficacy of the integrin-targeted immunoconjugate IMGN388 in preclinical models. EORTC-NCI-AACR-2008. *Molecular Targets and Cancer therapeutics.* (2008) (Abstract #ENA-0399).

CSPC Exhibit 1004

56 Thompson DS, Patnaik A, Bendell JC *et al.* A Phase I dose-escalation study of IMGN388 in patients with solid tumors. 28(15s) *J. Clin. Oncol.* (2010) (Abstract 3058).

57 Ostermann E, Garin-Chesa P, Heider KH *et al.* Effective immunoconjugate therapy in cancer models targeting a serine protease of tumor fibroblasts. *Clin. Cancer Res.* 14(14), 4584–4592 (2008).

58 Terrett JA, Devasthali V, Pan C *et al.* Ptk7 as a direct and tumor stroma target in multiple solid malignancies. Presented at: *The 99th Annual Meeting of the American Association for Cancer Research.* Philadelphia, PA, USA, 11–15 April 2008 (Abstract #1526).

59 Boman BM, Wicha MS. Cancer stem cells: a step toward the cure. *J. Clin. Oncol.* 26(17), 2795–2799 (2008).

60 Okamoto OK, Perez JF. Targeting cancer stem cells with monoclonal antibodies: a new perspective in cancer therapy and diagnosis. *Expert. Rev. Mol. Diagn.* 8(4), 387–393 (2008).

61 Clarke MF, Dick JE, Dirks PB *et al.* Cancer stem cells – perspectives on current status and future directions: AACR Workshop on cancer stem cells. *Cancer Res.* 66(19), 9339–9344 (2006).

62 Bonnet D, Dick JE. Human acute myeloid leukemia is organized as a hierarchy that originates from a primitive hematopoietic cell. *Nat. Med.* 3(7), 730–737 (1997).

63 Gil J, Stembalska A, Pesz KA *et al.* Cancer stem cells: the theory and perspectives in cancer therapy. *J. Appl. Genet.* 49(2), 193–199 (2008).

64 Jones RJ, Matsui WH, Smith BD. Cancer stem cells: are we missing the target? *J. Natl Cancer Inst.* 96(8), 583–585 (2004).

65 Bao S, Wu Q, McLendon RE *et al.* Glioma stem cells promote radioresistance by preferential activation of the DNA damage response. *Nature* 444(7120), 756–760 (2006).

66 Bao S, Wu Q, Sathornsumetee S *et al.* Stem cell-like glioma cells promote tumor angiogenesis through vascular endothelial growth factor. *Cancer Res.* 66(16), 7843–7848 (2006).

67 Dylla SJ, Beviglia L, Park IK *et al.* Colorectal cancer stem cells are enriched in xenogeneic tumors following chemotherapy. *PLoS ONE* 3(6), E2428 (2008).

68 Eyler CE, Rich JN. Survival of the fittest: cancer stem cells in therapeutic resistance and angiogenesis. *J. Clin. Oncol.* 26(17), 2839–2845 (2008).

69 Jin L, Hope KJ, Zhai Q *et al.* Targeting of CD44 eradicates human acute myeloid leukemic stem cells. *Nat. Med.* 12(10), 1167–1174 (2006).

70 Hosen N, Park CY, Tatsumi N *et al.* CD96 is a leukemic stem cell-specific marker in human acute myeloid leukemia. *Proc. Natl Acad. Sci. USA* 104(26), 11008–11013 (2007).

71 Stabile H, Mitola S, Moroni E *et al.* Bone morphogenic protein antagonist Drm/gremlin is a novel proangiogenic factor. *Blood* 109(5), 1834–1840 (2007).

72 Sneddon JB, Zhen HH, Montgomery K *et al.* Bone morphogenetic protein antagonist gremlin 1 is widely expressed by cancer-associated stromal cells and can promote tumor cell proliferation. *Proc. Natl Acad. Sci. USA* 103(40), 14842–14847 (2006).

73 Piccirillo SG, Reynolds BA, Zanetti N *et al.* Bone morphogenetic proteins inhibit the tumorigenic potential of human brain tumour-initiating cells. *Nature* 444(7120), 761–765 (2006).

74 Namkoong H, Shin SM, Kim HK *et al.* The bone morphogenetic protein antagonist gremlin 1 is overexpressed in human cancers and interacts with YWHAH protein. *BMC Cancer* 6, 74 (2006).

75 Kohler G, Milstein C. Continuous cultures of fused cells secreting antibody of predefined specificity. *Nature* 256(5517), 495–497 (1975).

76 Almagro JC, Fransson J. Humanization of antibodies. *Front. Biosci.* 13, 1619–1633 (2008).

77 Jones PT, Dear PH, Foote J *et al.* Replacing the complementarity-determining regions in a human antibody with those from a mouse. *Nature* 321 (6069), 522–525 (1986).

78 Roguska MA, Pedersen JT, Henry AH *et al.* A comparison of two murine monoclonal antibodies humanized by CDR-grafting and variable domain resurfacing. *Protein Eng.* 9(10), 895–904 (1996).

79 Roguska MA, Pedersen JT, Keddy CA *et al.* Humanization of murine monoclonal antibodies through variable domain resurfacing. *Proc. Natl Acad. Sci. USA* 91(3), 969–973 (1994).

80 Hwang WY, Foote J. Immunogenicity of engineered antibodies. *Methods* 36(1), 3–10 (2005).

81 Roopenian DC, Akilesh S. FcRn: the neonatal Fc receptor comes of age. *Nat. Rev. Immunol.* 7(9), 715–725 (2007).

82 Lonberg N. Human antibodies from transgenic animals. *Nat. Biotechnol.* 23(9), 1117–1125 (2005).

83 Lonberg N. Fully human antibodies from transgenic mouse and phage display platforms. *Curr. Opin. Immunol.* 20(4), 450–459 (2008).

84 Hoogenboom HR. Selecting and screening recombinant antibody libraries. *Nat. Biotechnol.* 23(9), 1105–1116 (2005).

85 Kim SJ, Park Y, Hong HJ. Antibody engineering for the development of therapeutic antibodies. *Mol. Cells* 20(1), 17–29 (2005).

86 Carter PJ. Potent antibody therapeutics by design. *Nat. Rev. Immunol.* 6(5), 343–357 (2006).

87 Mascelli MA, Zhou H, Sweet R *et al.* Molecular, biologic, and pharmacokinetic properties of monoclonal antibodies: impact of these parameters on early clinical development. *J. Clin. Pharmacol.* 47(5), 553–565 (2007).

88 McDonagh CF, Kim KM, Turcott E *et al.* Engineered anti-CD70 antibody–drug conjugate with increased therapeutic index. *Mol. Cancer Ther.* 7(9), 2913–2923 (2008).

89 Strome SE, Sausville EA, Mann D. A mechanistic perspective of monoclonal antibodies in cancer therapy beyond target-related effects. *Oncologist* 12 (9), 1084–1095 (2007).

90 Fujimori K, Covell DG, Fletcher JE *et al.* A modeling analysis of monoclonal antibody percolation through tumors: a binding-site barrier. *J. Nucl. Med.* 31(7), 1191–1198 (1990).

91 Adams GP, Schier R, McCall AM *et al.* High affinity restricts the localization and tumor penetration of single-chain fv antibody molecules. *Cancer Res.* 61(12), 4750–4755 (2001).

92 Schmidt MM, Wittrup KD. A modeling analysis of the effects of molecular size and binding affinity on tumor targeting. *Mol. Cancer Ther.* 8(10), 2861–2871 (2009).

▪▪ **Model that predicts the pharmacokinetics and biodistribution of targeted drugs.**

93 Jefferis R. Antibody therapeutics: isotype and glycoform selection. *Expert Opin. Biol. Ther.* 7(9), 1401–1413 (2007).

94 Salfeld JG. Isotype selection in antibody engineering. *Nat. Biotechnol.* 25(12), 1369–1372 (2007).

▪ **Review of *in vivo* properties of various isotypes of antibodies.**

95 Stasi R. Gemtuzumab ozogamicin: an anti-CD33 immunoconjugate for the treatment of acute myeloid leukaemia. *Expert Opin. Biol. Ther.* 8(4), 527–540 (2008).

CSPC Exhibit 1004
Page 189 of 33

96 Hamann PR, Hinman LM, Hollander I *et al.* Gemtuzumab ozogamicin, a potent and selective anti-CD33 antibody–calicheamicin conjugate for treatment of acute myeloid leukemia. *Bioconjug. Chem.* 13(1), 47–58 (2002).

97 DiJoseph JF, Goad ME, Dougher MM *et al.* Potent and specific antitumor efficacy of CMC-544, a CD22-targeted immunoconjugate of calicheamicin, against systemically disseminated B-cell lymphoma. *Clin. Cancer Res.* 10(24), 8620–8629 (2004).

98 DiJoseph JF, Armellino DC, Boghaert ER *et al.* Antibody-targeted chemotherapy with CMC-544: a CD22-targeted immunoconjugate of calicheamicin for the treatment of B-lymphoid malignancies. *Blood* 103(5), 1807–1814 (2004).

99 van der Neut Kolfschoten M, Schuurman J, Losen M *et al.* Anti-inflammatory activity of human IgG4 antibodies by dynamic Fab arm exchange. *Science* 317(5844), 1554–1557 (2007).

100 Hamid O, Sznol M, Pavlick AC *et al.* Frequent dosing and GPNMB expression with CDX-011 (CR011-vcMMAE), an antibody–drug conjugate (ADC), in patients with advanced melanoma. *J. Clin. Oncol. (Meeting Abstracts)* 28(Suppl. 15), 8525 (2010).

101 Yoo EM, Wims LA, Chan LA *et al.* Human IgG2 can form covalent dimers. *J. Immunol.* 170(6), 3134–3138 (2003).

102 Ryan MC, Hering M, Peckham D *et al.* Antibody targeting of B-cell maturation antigen on malignant plasma cells. *Mol. Cancer Ther.* 6(11), 3009–3018 (2007).

103 Desjarlais JR, Lazar GA, Zhukovsky EA *et al.* Optimizing engagement of the immune system by anti-tumor antibodies: an engineer's perspective. *Drug Discov. Today* 12(21–22), 898–910 (2007).

104 Lazar GA, Dang W, Karki S *et al.* Engineered antibody Fc variants with enhanced effector function. *Proc. Natl Acad. Sci. USA* 103(11), 4005–4010 (2006).

105 Shields RL, Lai J, Keck R *et al.* Lack of fucose on human IgG1 N-linked oligosaccharide improves binding to human Fcgamma RIII and antibody-dependent cellular toxicity. *J. Biol. Chem.* 277(30), 26733–26740 (2002).

106 Shinkawa T, Nakamura K, Yamane N *et al.* The absence of fucose but not the presence of galactose or bisecting *N*-acetylglucosamine of human IgG1 complex-type oligosaccharides shows the critical role of enhancing antibody-dependent cellular cytotoxicity. *J. Biol. Chem.* 278(5), 3466–3473 (2003).

107 Schuster M, Umana P, Ferrara C *et al.* Improved effector functions of a therapeutic monoclonal Lewis Y-specific antibody by glycoform engineering. *Cancer Res.* 65(17), 7934–7941 (2005).

108 Lambert JM. Drug-conjugated monoclonal antibodies for the treatment of cancer. *Curr. Opin. Pharmacol.* 5(5), 543–549 (2005).

109 Chari RV. Targeted delivery of chemotherapeutics: tumor-activated prodrug therapy. *Adv. Drug Deliv. Rev.* 31(1–2), 89–104 (1998).

110 Chari RV, Martell BA, Gross JL *et al.* Immunoconjugates containing novel maytansinoids: promising anticancer drugs. *Cancer Res.* 52(1), 127–131 (1992).

111 Hinman LM, Hamann PR, Wallace R *et al.* Preparation and characterization of monoclonal antibody conjugates of the calicheamicins: a novel and potent family of anti-tumor antibiotics. *Cancer Res.* 53(14), 3336–3342 (1993).

112 Singh R, Erickson HK. Antibody-cytotoxic agent conjugates: preparation and characterization. In: *Methods in Molecular Biology: Therapeutic Antibodies: Methods and Protocols* 525, 445–467 (2008).

* **Typical methods of preparation of antibody–drug conjugates (ADCs).**

113 Baloglu E, Miller ML, Roller EE *et al.* Synthesis and biological evaluation of novel taxoids designed for targeted delivery to tumors. *Bioorg. Med. Chem. Lett.* 14(23), 5885–5888 (2004).

114 Miller ML, Roller EE, Wu X *et al.* Synthesis of potent taxoids for tumor-specific delivery using monoclonal antibodies. *Bioorg. Med. Chem. Lett.* 14(15), 4079–4082 (2004).

115 Miller ML, Roller EE, Zhao RY *et al.* Synthesis of taxoids with improved cytotoxicity and solubility for use in tumor-specific delivery. *J. Med. Chem.* 47(20), 4802–4805 (2004).

116 Ojima I, Geng X, Wu X *et al.* Tumor-specific novel taxoid–monoclonal antibody conjugates. *J. Med. Chem.* 45(26), 5620–5623 (2002).

117 Burke PJ, Senter PD, Meyer DW *et al.* Design, synthesis, and biological evaluation of antibody–drug conjugates comprised of potent camptothecin analogues. *Bioconjug. Chem.* 20(6), 1242–1250 (2009).

118 Burke PJ, Toki BE, Meyer DW *et al.* Novel immunoconjugates comprised of streptonigrin and 17-amino-geldanamycin attached via a dipeptide-*p*-aminobenzyl-amine linker system. *Bioorg. Med. Chem. Lett.* 19(10), 2650–2653 (2009).

119 Bross PF, Beitz J, Chen G *et al.* Approval summary: gemtuzumab ozogamicin in relapsed acute myeloid leukemia. *Clin. Cancer Res.* 7(6), 1490–1496 (2001).

120 Zein N, Sinha AM, McGahren WJ *et al.* Calicheamicin γ 1I: an antitumor antibiotic that cleaves double-stranded DNA site specifically. *Science* 240(4856), 1198–1201 (1988).

121 DiJoseph JF, Dougher MM, Kalyandrug LB *et al.* Antitumor efficacy of a combination of CMC-544 (inotuzumab ozogamicin), a CD22-targeted cytotoxic immunoconjugate of calicheamicin, and rituximab against non-Hodgkin's B-cell lymphoma. *Clin. Cancer. Res.* 12(1), 242–249 (2006).

122 DiJoseph JF, Khandke K, Dougher MM *et al.* CMC-544 (inotuzumab ozogamicin): a CD22-targeted immunoconjugate of calicheamicin. *Hematology Meeting Reports* 5(6), 74–77 (2008).

123 DiJoseph JF, Dougher MM, Armellino DC *et al.* CD20-specific antibody-targeted chemotherapy of non-Hodgkin's B-cell lymphoma using calicheamicin-conjugated rituximab. *Cancer Immunol. Immunother.* 56(7), 1107–1117 (2007).

124 Boghaert ER, Sridharan L, Khandke KM *et al.* The oncofetal protein, 5T4, is a suitable target for antibody-guided anticancer chemotherapy with calicheamicin. *Int. J. Oncol.* 32 (1), 221–234 (2008).

125 Hamann PR, Hinman LM, Beyer CF *et al.* A calicheamicin conjugate with a fully humanized anti-MUC1 antibody shows potent antitumor effects in breast and ovarian tumor xenografts. *Bioconjug. Chem.* 16(2), 354–360 (2005).

126 MacMillan KS, Boger DL. Fundamental relationships between structure, reactivity, and biological activity for the duocarmycins and CC-1065. *J. Med. Chem.* 52(19), 5771–5780 (2009).

127 Chari RV, Jackel KA, Bourret LA *et al.* Enhancement of the selectivity and antitumor efficacy of a CC-1065 analogue through immunoconjugate formation. *Cancer Res.* 55(18), 4079–4084 (1995).

128 Tietze LF, Krewer B. Antibody-directed enzyme prodrug therapy: a promising approach for a selective treatment of cancer based on prodrugs and monoclonal antibodies. *Chem. Biol. Drug Des.* 74(3), 205–211 (2009).

129 Tietze LF, Krewer B. Novel analogues of CC-1065 and the duocarmycins for the use in targeted tumour therapies. *Anticancer Agents Med. Chem.* 9(3), 304–325 (2009).

CSPC Exhibit 1004

130 Tietze LF, Panknin O, Krewer B *et al.* Synthesis and biological evaluation of a novel pentagastrin--toxin conjugate designed for a targeted prodrug monotherapy of cancer. *Int. J. Mol. Sci.* 9(5), 821–837 (2008).

131 King D, Terrett J, Cardarelli P *et al.* Mechanism of activation of a human anti-cd70 antibody-mgba conjugate and efficacy in a nude rat model of renal carcinoma. *AACR Meeting Abstracts (1 Annual Meeting 2008).* 4057 (2008).

132 Cardarelli P, King D, Terrett J *et al.* Efficacy and safety of a human anti-CD70 antibody-MGBA conjugate. *AACR Meeting Abstracts (1 Annual Meeting 2008).* 4061 (2008).

133 Widdison WC, Wilhelm SD, Cavanagh EE *et al.* Semisynthetic maytansine analogues for the targeted treatment of cancer. *J. Med. Chem.* 49(14), 4392–4408 (2006).

134 Lopus M, Oroudjev E, Wilson L *et al.* Maytansine derivatives and metabolites of antibody–maytansinoid conjugates inhibit microtubule polymerization and strongly suppress microtubule dynamics. *AACR Meeting Abstracts (1 Annual Meeting 2008).* 1406 (2008).

135 Oroudjev E, Lopus M, Wilson L *et al.* Antibody--maytansinoid conjugates affect microtubule morphology and suppress microtubule dynamics in live cells. *AACR Meeting Abstracts (1 Annual Meeting 2008).* 1403 (2008).

136 Remillard S, Rebhun LI, Howie GA *et al.* Antimitotic activity of the potent tumor inhibitor maytansine. *Science* 189(4207), 1002–1005 (1975).

137 Drewinko B, Patchen M, Yang LY *et al.* Differential killing efficacy of twenty anti-tumor drugs on proliferating and nonproliferating human tumor cells. *Cancer Res.* 41(6), 2328–2333 (1981).

138 Murphy M, Phinney S, Ab O *et al.* Immunohistochemical analysis of the glycotope targeted by huC242-DM4 indicates strong expression in several tumor types with unmet medical need. *AACR Meeting Abstracts (1 Annual Meeting 2008).* 4898 (2008).

139 Tolcher AW, Ochoa L, Hammond LA *et al.* Cantuzumab mertansine, a maytansinoid immunoconjugate directed to the CanAg antigen: a Phase I, pharmacokinetic, and biologic correlative study. *J. Clin. Oncol.* 21(2), 211–222 (2003).

140 Baeckstrom D, Hansson GC, Nilsson O *et al.* Purification and characterization of a membrane-bound and a secreted mucin-type glycoprotein carrying the carcinoma-associated sialyl-Lea epitope on distinct core proteins. *J. Biol. Chem.* 266(32), 21537--21547 (1991).

141 Helft PR, Schilsky RL, Hoke FJ *et al.* A Phase I study of cantuzumab mertansine administered as a single intravenous infusion once weekly in patients with advanced solid tumors. *Clin. Cancer Res.* 10(13), 4363–4368 (2004).

142 Polson AG, Yu SF, Elkins K *et al.* Antibody–drug conjugates targeted to CD79 for the treatment of non-Hodgkin lymphoma. *Blood* 110(2), 616–623 (2007).

143 Stephan JP, Chan P, Lee C *et al.* Anti-CD22–MCC–DM1 and MC–MMAF conjugates: impact of assay format on pharmacokinetic parameters determination. *Bioconjug. Chem.* 19(8), 1673--1683 (2008).

144 Mayo MF LA, Wang L, Wunderli P, Payne G, Xie H, Lutz RJ. *In vivo* stability in mice of SAR566658 (huDS6-DM4), an immunoconjugate targeting solid tumors. *EORTC-NCI-AACR Proceedings* (2008) (Abstract 533).

145 Carrigan C, Zuany-Amorim C, Mayo MF *et al.* Preclinical evaluation of SAR566658 (huDS6-DM4) in mice bearing human tumor xenografts of breast, ovarian, lung, cervical and pancreatic cancer. *EORTC Meeting Abstracts* Annual Meeting (2008) (Abstract 525).

146 Bai R, Petrit GR, Hamel E. Dolastatin 10, a powerful cytostatic peptide derived from a marine animal. Inhibition of tubulin polymerization mediated through the vinca alkaloid binding domain. *Biochem. Pharmacol.* 39(12), 1941--1949 (1990).

147 Doronina SO, Toki BE, Torgov MY *et al.* Development of potent monoclonal antibody auristatin conjugates for cancer therapy. *Nat. Biotechnol.* 21(7), 778–784 (2003).

148 Doronina SO, Mendelsohn BA, Bovee TD *et al.* Enhanced activity of monomethylauristatin F through monoclonal antibody delivery: effects of linker technology on efficacy and toxicity. *Bioconjug. Chem.* 17(1), 114–124 (2006).

149 Gerber H-P, Kung-Sutherland M, Stone I *et al.* Potent anti-tumor activity of the anti-CD19 auristatin antibody--drug conjugate SGN-19A in rituximab sensitive and resistant lymphomas. *EORTC Meeting Abstracts* (2008) (Abstract 507).

150 Gerber HP, Kung-Sutherland M, Stone I *et al.* Potent antitumor activity of the anti-CD19 auristatin antibody drug conjugate hBU12–vcMMAE against rituximab-sensitive and -resistant lymphomas. *Blood* 113(18), 4352–4361 (2009).

151 Dornan D, Bennett F, Chen Y *et al.* Therapeutic potential of an anti-CD79b antibody–drug conjugate, anti-CD79b–vcMMAE, for the treatment of non-Hodgkin lymphoma. *Blood* 114(13), 2721--2729 (2009).

152 Jackson D, Gooya J, Mao S *et al.* A human antibody--drug conjugate targeting EphA2 inhibits tumor growth *in vivo*. *Cancer Res.* 68(22), 9367–9374 (2008).

153 Lee JW, Han HD, Shahzad MM *et al.* EphA2 immunoconjugate as molecularly targeted chemotherapy for ovarian carcinoma. *J. Natl Cancer Inst.* 101(17), 1193–1205 (2009).

154 Alley SC, Benjamin DR, Jeffrey SC *et al.* Contribution of linker stability to the activities of anticancer immunoconjugates. *Bioconjug. Chem.* 19(3), 759--765 (2008).

155 Doronina SO, Bovee TD, Meyer DW *et al.* Novel peptide linkers for highly potent antibody-auristatin conjugate. *Bioconjug. Chem.* 19(10), 1960--1963 (2008).

156 Wang L, Amphlett G, Blattler WA *et al.* Structural characterization of the maytansinoid--monoclonal antibody immunoconjugate, huN901–DM1, by mass spectrometry. *Protein Sci.* 14(9), 2436–2446 (2005).

157 Junutula JR, Raab H, Clark S *et al.* Site-specific conjugation of a cytotoxic drug to an antibody improves the therapeutic index. *Nat. Biotechnol.* 26(8), 925–932 (2008).

- **ThiomAb technology.**

158 Hamblett KJ, Senter PD, Chace DF *et al.* Effects of drug loading on the antitumor activity of a monoclonal antibody drug conjugate. *Clin. Cancer Res.* 10(20), 7063–7070 (2004).

- **Study of the effects of drug per antibody ratio on ADC efficacy *in vivo*.**

159 McDonagh CF, Turcott E, Westendorf L *et al.* Engineered antibody–drug conjugates with defined sites and stoichiometries of drug attachment. *Protein Eng. Des. Sel.* 19(7), 299–307 (2006).

160 Wu G, Fang YZ, Yang S *et al.* Glutathione metabolism and its implications for health. *J. Nutr.* 134(3), 489–492 (2004).

161 Mills BJ, Lang CA. Differential distribution of free and bound glutathione and cyst(e)ine in human blood. *Biochem. Pharmacol.* 52(3), 401--406 (1996).

162 Appenzeller-Herzog C, Ellgaard L. The human PDI family: versatility packed into a single fold. *Biochim. Biophys. Acta* 1783(4), 535--548 (2008).

163 Ciechanover A. Intracellular protein degradation: from a vague idea thru the lysosome and the ubiquitin-proteasome system and onto human diseases and drug targeting. *Hematology Am. Soc. Hematol. Educ. Program* 1–12, 505–506 (2006).

CSPC Exhibit 1004
Page 191 of 33

164 Hamann PR, Hinman LM, Beyer CF *et al.* An anti-CD33 antibody–calicheamicin conjugate for treatment of acute myeloid leukemia. Choice of linker. *Bioconjug. Chem.* 13(1), 40–46 (2002).

165 Boghaert ER, Khandke KM, Sridharan L *et al.* Determination of pharmacokinetic values of calicheamicin–antibody conjugates in mice by plasmon resonance analysis of small (5 microl) blood samples. *Cancer Chemother. Pharmacol.* 61(6), 1027–1035 (2008).

166 Dowell JA, Korth-Bradley J, Liu H *et al.* Pharmacokinetics of gemtuzumab ozogamicin, an antibody-targeted chemotherapy agent for the treatment of patients with acute myeloid leukemia in first relapse. *J. Clin. Pharmacol.* 41(11), 1206–1214 (2001).

167 Kovtun YV, Audette CA, Mayo MF *et al.* Antibody–maytansinoid conjugates designed to bypass multidrug resistance. *Cancer Res.* 70(6), 2528–2537 (2010).

168 Lutz RJ, Xie H, Widdison WC *et al.* HuC242-DM4, an antibody–maytansinoid conjugate with superior preclinical activity in human CanAg-positive tumor xenograft models in SCID mice. *AACR Meeting Abstracts* 2005(1), 334–335 (2005).

169 Erickson HK, Park PU, Widdison WC *et al.* Antibody–maytansinoid conjugates are activated in targeted cancer cells by lysosomal degradation and linker-dependent intracellular processing. *Cancer Res.* 66(8), 4426–4433 (2006).

170 Erickson H, Wilhelm S, Widdison W *et al.* Evaluation of the cytotoxic potencies of the major maytansinoid metabolites of antibody–maytansinoid conjugates detected *in vitro* and in preclinical mouse models. *AACR Meeting Abstracts* 2008 (Annual Meeting), 2150 (2008).

171 Francisco JA, Cerveny CG, Meyer DL *et al.* cAC10-vcMMAE, an anti-CD30-monomethyl auristatin E conjugate with potent and selective antitumor activity. *Blood* 102(4), 1458–1465 (2003).

172 Okeley NM, Miyamoto JB, Zhang X *et al.* Intracellular activation of SGN-35, a potent anti-CD30 antibody–drug conjugate. *Clin. Cancer Res.* 16(3), 888–897 (2010).

173 Sanderson RJ, Hering MA, James SF *et al.* *In vivo* drug-linker stability of an anti-CD30 dipeptide-linked auristatin immunoconjugate. *Clin. Cancer Res.* 11(2 Part 1), 843–852 (2005).

174 Walter RB, Raden BW, Hong TC *et al.* Multidrug resistance protein attenuates gemtuzumab ozogamicin-induced cytotoxicity in acute myeloid leukemia cells. *Blood* 102(4), 1466–1473 (2003).

175 Linenberger ML, Hong T, Flowers D *et al.* Multidrug-resistance phenotype and clinical responses to gemtuzumab ozogamicin. *Blood* 98(4), 988–994 (2001).

176 Leonard GD, Fojo T, Bates SE. The role of ABC transporters in clinical practice. *Oncologist* 8(5), 411–424 (2003).

177 Gottesman MM, Pastan I. The multidrug transporter, a double-edged sword. *J. Biol. Chem.* 263(25), 12163–12166 (1988).

178 Takara K, Sakaeda T, Okumura K. An update on overcoming MDR1-mediated multidrug resistance in cancer chemotherapy. *Curr. Pharm. Des.* 12(3), 273–286 (2006).

179 Hamann PR, Hinman LM, Beyer CF *et al.* An anti-MUC1 antibody–calicheamicin conjugate for treatment of solid tumors. Choice of linker and overcoming drug resistance. *Bioconjug. Chem.* 16(2), 346–353 (2005).

180 Guillemard V, Uri Saragovi H. Prodrug chemotherapeutics bypass P-glycoprotein resistance and kill tumors *in vivo* with high efficacy and target-dependent selectivity. *Oncogene* 23(20), 3613–3621 (2004).

181 Kovtun Y AC, Maloney E, Mayo M *et al.* Novel antibody–maytansinoid conjugates with improved efficacy against multidrug-resistant tumors. *EORTC Proceedings* (2008) (Abstract 518).

182 DiJoseph JF, Dougher MM, Armellino DC *et al.* Therapeutic potential of CD22-specific antibody-targeted chemotherapy using inotuzumab ozogamicin (CMC-544) for the treatment of acute lymphoblastic leukemia. *Leukemia* 21(11), 2240–2245 (2007).

183 Roepstorff K, Grovdal L, Grandal M *et al.* Endocytic downregulation of ErbB receptors: mechanisms and relevance in cancer. *Histochem. Cell. Biol.* 129(5), 563–578 (2008).

184 Tassone P, Gozzini A, Goldmacher V *et al.* *In vitro* and *in vivo* activity of the maytansinoid immunoconjugate huN901-N2′-deacetyl-N2′-(3-mercapto-1-oxopropyl)-maytansine against $CD56^+$ multiple myeloma cells. *Cancer Res.* 64(13), 4629–4636 (2004).

185 Jensen M, Berthold F. Targeting the neural cell adhesion molecule in cancer. *Cancer Lett.* 258(1), 9–21 (2007).

186 Whiteman KR, Murphy M.F, Cohane KP *et al.* Preclinical evaluation of IMGN901 (huN901-DM1) as a potential therapeutic for ovarian cancer. *Am. Assoc. Clin. Res. Annu. Meet.* (2008) (Abstract 2135).

187 Roy DC, Ouellet S, Le Houillier C *et al.* Elimination of neuroblastoma and small-cell lung cancer cells with an antineural cell adhesion molecule immunotoxin. *J. Natl. Cancer Inst.* 88(16), 1136–1145 (1996).

188 Fossella F, Woll PJ, Lorigan P *et al.* Investigation of IMGN901 in $CD56^+$ solid tumors: results from a Phase I/II trial (study 001) and a Phase I trial (study 002). Presented at: *The 13th World Conference on Lung Cancer.* San Francisco, CA, USA, 31 July– 4 August 2009.

189 Woll PJ, Lorigan P, O'Brien M *et al.* Clinical experience of IMGN901 (BB-10901, huN901-DM1) in patients with Merkel-cell carcinoma (MCC). *AACR-NCI-EORTC* (2009) (Abstract B237).

190 Thompson D, Patnaik A, Bendell J *et al.* A Phase I dose-escalation study of IMGN388 in patients with solid tumors. *J. Clin. Oncol.* 28(15s) (2010) (Abstract 3058).

191 Aboukameel A, Goustin A-S, Mohammad R *et al.* Superior anti-tumor activity of the CD19-directed immunotoxin, SAR3419 to rituximab in non-Hodgkin's xenograft animal models: preclinical evaluation. *ASH Annual Meeting Abstracts* 110, (2007) (Abstract 2339).

192 Ikeda H, Hideshima T, Lutz RJ *et al.* The monoclonal antibody nBT062 conjugated to cytotoxic maytansinoids has potent and selective cytotoxicity against cd138 positive multiple myeloma cells *in vitro* and *in vivo*. *ASH Annual Meeting Abstracts.* 112(11), 1716 (2008).

193 Chanan-Khan AA, Jagannath S, Heffner LT *et al.* Phase I study of BT062 given as repeated single dose once every 3 weeks in patients with relapsed or relapsed/refractory multiple myeloma. *ASH Annual Meeting Abstracts* 114(22), 1862 (2009).

194 Oflazoglu E, Kissler KM, Sievers EL *et al.* Combination of the anti-CD30–auristatin-E antibody–drug conjugate (SGN-35) with chemotherapy improves antitumour activity in Hodgkin lymphoma. *Br. J. Haematol.* 142(1), 69–73 (2008).

195 Hwu P, Sznol M., Pavlick A. *et al.* A Phase I/II study of CRO-11–vcMMAE, an antibody–drug conjugate, in patients with unresectable stage III or stage IV melanoma. *Am. Soc. Clin. Onc. Annu. Meet. Proc.* 9029 (2008).

196 Sznol M, Hamid O, Hwu P *et al.* Pharmacokinetics (PK) of CR011–vcMMAE, an antibody–drug conjugate (ADC), in a Phase (Ph) I study of patients (pts) with advanced melanoma. *J. Clin. Oncol. (Meeting Abstracts)* 27(15S), 9063 (2009).

197 Tse KF, Jeffers M, Pollack VA *et al.* CR011, a fully human monoclonal antibody–auristatin E conjugate, for the treatment of melanoma. *Clin. Cancer Res.* 12(4), 1373–1382 (2006).

198 Kantoff P, Petrylak DP, Pomerantz M *et al.* First-in-human Phase I trial of prostate-specific membrane antigen antibody drug conjugate (PSMA ADC) in taxane-refractory prostate cancer. *J. Clin. Oncol.* 28(15S), TPS245 (2010).

CSPC Exhibit 1004

199 Tolcher AW, Forouzesh B, McCreery H *et al.* A Phase I and pharmacokinetic study of BB-10901, a maytansinoid immunoconjugate, in CD56-expressing tumors. Presented at: The *EORTC–NCI–AACR Symposium on Molecular Targets and Cancer Therapeutics* (2005).

200 Chanan-Khan AA, Jagannath S, Munshi NC *et al.* Phase I study of huN901-DM1 (BB-10901) in patients with relapsed and relapsed/refractory CD56-positive multiple myeloma. *ASH Annual Meeting Abstracts, Part 1.* 110, 1174 (2007).

201 McCann J, Fossella FV, Villalona-Calero MA *et al.* Phase II trial of huN901-DM1 in patients with relapsed small cell lung cancer (SCLC) and CD56-positive small-cell carcinoma. *Am. Soc. Clin. Onc. Annu. Meet. Proc.* 25, 18084 (2007).

202 Giles F Morariu-Zamfir R, Lambert JM, Verstovsek S *et al.* Phase I study of AVE9633, an anti-CD33–maytansinoid immunoconjugate, administered as an intravenous infusion in patients with refractory/relapsed CD33-positive acute myeloid leukemia (AML). *Am. Soc. Hematol. Annu. Meet. Proc.* (2006).

203 Larson RA, Sievers EL, Stadtmauer EA *et al.* Final report of the efficacy and safety of gemtuzumab ozogamicin (Mylotarg®) in patients with CD33-positive acute myeloid leukemia in first recurrence. *Cancer* 104(7), 1442–1452 (2005).

204 Giles FJ. Gemtuzumab ozogamicin: promise and challenge in patients with acute myeloid leukemia. *Expert Rev. Anticancer Ther.* 2(6), 630–640 (2002).

205 Sauter A, Kloft C, Gronau S *et al.* Pharmacokinetics, immunogenicity and safety of bivatuzumab mertansine, a novel CD44v6-targeting immunoconjugate, in patients with squamous cell carcinoma of the head and neck. *Int. J. Oncol.* 30(4), 927–935 (2007).

206 Rupp U, Schoendorf-Holland E, Eichbaum M *et al.* Safety and pharmacokinetics of bivatuzumab mertansine in patients with CD44v6-positive metastatic breast cancer: final results of a Phase I study. *Anticancer Drugs* 18(4), 477–485 (2007).

207 Tijink BM, Buter J, de Bree R *et al.* A Phase I dose escalation study with anti-CD44v6 bivatuzumab mertansine in patients with incurable squamous cell carcinoma of the head and neck or esophagus. *Clin. Cancer Res.* 12(20 Part 1), 6064–6072 (2006).

208 Riechelmann H, Sauter A, Golze W *et al.* Phase I trial with the CD44v6-targeting immunoconjugate bivatuzumab mertansine in head and neck squamous cell carcinoma. *Oral Oncol.* 44(9), 823–829 (2008).

209 Heider KH, Mulder JWR, Ostermann E *et al.* Splice variants of the cell surface glycoprotein CD44 associated with metastatic tumour cells are expressed in normal tissues of humans and cynomolgus monkeys. *Eur. J. Cancer* 31(13–14), 2385 (1995).

210 van der Velden VH, Boeckx N, Jedema I *et al.* High CD33-antigen loads in peripheral blood limit the efficacy of gemtuzumab ozogamicin (Mylotarg®) treatment in acute myeloid leukemia patients. *Leukemia* 18(5), 983–988 (2004).

211 Davies Q, Perkins AC, Frier M *et al.* The effect of circulating antigen on the biodistribution of the engineered human antibody hCTM01 in a nude mice model. *Eur. J. Nucl. Med.* 24(2), 206–209 (1997).

212 Baselga J, Tripathy D, Mendelsohn J *et al.* Phase II study of weekly intravenous recombinant humanized anti-p185HER2 monoclonal antibody in patients with HER2/neu-overexpressing metastatic breast cancer. *J. Clin. Oncol.* 14(3), 737–744 (1996).

213 Pegram MD, Lipton A, Hayes DF *et al.* Phase II study of receptor-enhanced chemosensitivity using recombinant humanized anti-p185HER2/neu monoclonal antibody plus cisplatin in patients with HER2/neu-overexpressing metastatic breast cancer refractory to chemotherapy treatment. *J. Clin. Oncol.* 16(8), 2659–2671 (1998).

214 Qin AW, Watermill J, Mastico RA *et al.* The pharmacokinetics and pharmacodynamics of IMGN242 (huC242-DM4) in patients with CanAg-expressing solid tumors. *Am. Soc. Clin. Onc. Annu. Meet. Proc.* 3066 (2008).

Website

301 Pfizer press release. 21 June 2010. www.pfizer.com/files/news/press_releases/2010/mylotarg_discontinuation_062110.pdf

CSPC Exhibit 1004
Page 193 of 33
future science group

WEST Search History

Hide Items | Restore | Clear | Close

DATE: Sunday, October 13, 2019

Hide?	Set Name	Query	Hit Count
DB=PGPB,USPT; PLUR=NO; OP=ADJ			
☐	L14	L13 and L6	1
☐	L13	(Hu, Chaohong)[in]	33
☐	L12	(Shanghai Miracogen)![asn]	0
☐	L11	L10 and L6	1
☐	L10	L9 or L8 or L7	6841
☐	L9	(C07K16/2863)![CPC,CPCL]	4941
☐	L8	(A61K38/1808)![CPC,CPCL]	794
☐	L7	(A61K47/6811)![CPC,CPCL]	1213
☐	L6	L1 or L2 or L3 or L4 or L5	443
☐	L5	BAO adj 3	280
☐	L4	BA adj 03	90
☐	L3	BAO3$5	8
☐	L2	BA03$5	67
☐	L1	MYK3 or (MYK adj 3)	2

END OF SEARCH HISTORY

To: USPTOeAction@SeedIP.com,pairlinkdktg@seedip.com,
From: PAIR_eOfficeAction@uspto.gov
Cc: PAIR_eOfficeAction@uspto.gov
Subject: Private PAIR Correspondence Notification for Customer Number 500

Oct 18, 2019 03:36:39 AM

Dear PAIR Customer:

SEED INTELLECTUAL PROPERTY LAW GROUP LLP
701 FIFTH AVE
SUITE 5400
SEATTLE, WA 98104
UNITED STATES

The following USPTO patent application(s) associated with your Customer Number, 500 , have new outgoing correspondence. This correspondence is now available for viewing in Private PAIR.

The official date of notification of the outgoing correspondence will be indicated on the form PTOL-90 accompanying the correspondence.

Disclaimer:
The list of documents shown below is provided as a courtesy and is not part of the official file wrapper. The content of the images shown in PAIR is the official record.

Application	Document	Mailroom Date	Attorney Docket No.
15550995	CTFR	10/18/2019	850231.401USPC
	892	10/18/2019	850231.401USPC

To view your correspondence online or update your email addresses, please visit us anytime at https://sportal.uspto.gov/secure/myportal/privatepair.

If you have any questions, please email the Electronic Business Center (EBC) at EBC@uspto.gov with 'e-Office Action' on the subject line or call 1-866-217-9197 during the following hours:

Monday - Friday 6:00 a.m. to 12:00 a.m.

Thank you for prompt attention to this notice,

UNITED STATES PATENT AND TRADEMARK OFFICE

PATENT APPLICATION INFORMATION RETRIEVAL SYSTEM

Doc Code: A.NE.AFCP
Document Description: After Final Consideration Pilot Program Request

PTO/SB/434 (05-13)

CERTIFICATION AND REQUEST FOR CONSIDERATION UNDER THE AFTER FINAL CONSIDERATION PILOT PROGRAM 2.0

Practitioner Docket No.:	Application No.:	Filing Date:
850231.401USPC	15/550,995	August 14, 2017
First Named Inventor:	**Title:**	
Chaohong HU	ANTIBODY-DRUG CONJUGATE	

APPLICANT HEREBY CERTIFIES THE FOLLOWING AND REQUESTS CONSIDERATION UNDER THE AFTER FINAL CONSIDERATION PILOT PROGRAM 2.0 (AFCP 2.0) OF THE ACCOMPANYING RESPONSE UNDER 37 CFR 1.116.

1. The above-identified application is (i) an original utility, plant, or design nonprovisional application filed under 35 U.S.C. 111(a) [a continuing application (*e.g.*, a continuation or divisional application) is filed under 35 U.S.C. 111(a) and is eligible under (i)], or (ii) an international application that has entered the national stage in compliance with 35 U.S.C. 371(c).
2. The above-identified application contains an outstanding final rejection.
3. Submitted herewith is a response under 37 CFR 1.116 to the outstanding final rejection. The response includes an amendment to at least one independent claim, and the amendment does not broaden the scope of the independent claim in any aspect.
4. This certification and request for consideration under AFCP 2.0 is the only AFCP 2.0 certification and request filed in response to the outstanding final rejection.
5. Applicant is willing and available to participate in any interview requested by the examiner concerning the present response.
6. This certification and request is being filed electronically using the Office's electronic filing system (EFS-Web).
7. Any fees that would be necessary consistent with current practice concerning responses after final rejection under 37 CFR 1.116, *e.g.*, extension of time fees, are being concurrently filed herewith. [There is no additional fee required to request consideration under AFCP 2.0.]
8. By filing this certification and request, applicant acknowledges the following:
   - Reissue applications and reexamination proceedings are not eligible to participate in AFCP 2.0.
   - The examiner will verify that the AFCP 2.0 submission is compliant, *i.e.*, that the requirements of the program have been met (see items 1 to 7 above). For compliant submissions:
     - The examiner will review the response under 37 CFR 1.116 to determine if additional search and/or consideration (i) is necessitated by the amendment and (ii) could be completed within the time allotted under AFCP 2.0. If additional search and/or consideration is required but cannot be completed within the allotted time, the examiner will process the submission consistent with current practice concerning responses after final rejection under 37 CFR 1.116, *e.g.*, by mailing an advisory action.
     - If the examiner determines that the amendment does not necessitate additional search and/or consideration, or if the examiner determines that additional search and/or consideration is required and could be completed within the allotted time, then the examiner will consider whether the amendment places the application in condition for allowance (after completing the additional search and/or consideration, if required). If the examiner determines that the amendment does not place the application in condition for allowance, then the examiner will contact the applicant and request an interview.
       - The interview will be conducted by the examiner, and if the examiner does not have negotiation authority, a primary examiner and/or supervisory patent examiner will also participate.
       - If the applicant declines the interview, or if the interview cannot be scheduled within ten (10) calendar days from the date that the examiner first contacts the applicant, then the examiner will proceed consistent with current practice concerning responses after final rejection under 37 CFR 1.116.

Signature	Date
/Qing Lin/	December 16, 2019
Name (Print/Typed) Qing Lin, Ph.D.	**Practitioner Registration No.** 53,937

***Note**: This form must be signed in accordance with 37 CFR 1.33. See 37 CFR 1.4(d) for signature requirements and certifications. Submit multiple forms if more than one signature is required, see below*.*

☐ * Total of _____ forms are submitted.

REMARKS

Reconsideration of the present application in view of the above amendments and the following remarks are respectfully requested.

Claims 2-12, 14-16, 23-28, and 35-37 were pending. Claims 2-12, 14-16, 23, and 25 have been amended to focus on certain embodiments of the present application. Such amendments have been made to facilitate allowance and without acquiescing to the rejections in the Office Action or disclaimers. No new matter has been added.

Rejections Under 35 U.S.C. 112(a) (Enablement)

Claims 2-12, 14-16, 23-28 and 35-37 are rejected under 35 U.S.C. 112(a) as failing to comply with the enablement requirement due to the recitation of "a solvate of the salt."

Without acquiescing to this rejection and to facilitate allowance, Applicant has amended the claims to delete the above-noted phrase. Accordingly, this rejection has been overcome.

Rejections Under 35 U.S.C. 112(a) (Written Description)

Claims 2-12, 14-16, 23-28 and 35-37 are rejected under 35 U.S.C. 112(a) as failing to comply with the written description requirement due to the recitations of "comprises a sequence with an identity of greater than 70%, or greater than 75%, 80%, 85%, 90%, 95%, or 99% to the sequence as shown in SEQ ID NO:3" in claim 7 and similar language in claim 9 as well as the recitation of "a solvate of the salt" in various claims.

As indicated above, to facilitate allowance, Applicant has amended the claims of the present application to delete the language "a solvate of the salt."

As to the language related to sequence identity recited in claims 7 and 9, to facilitate allowance, Applicant has amended these claim to specify that the sequence identity is greater than 90%. Applicant submits that amended claims 7 and 9 meet the written description requirement.

The written description requirement is met if the disclosure of an application relied upon reasonably conveys to those skilled in the art that the inventor had possession of the claimed subject matter as of the filing date. *Ariad Pharmaceuticals, Inc. v. Eli Lilly & Co.*, 598 F.3d 1336 (Fed. Cir. 2010) (en banc). "A claim will not be invalidated on section 112 grounds simply because the embodiments of the specification do not contain examples explicitly covering the full scope of the claim language. This is because the patent specification is written for a person of skill in the art, and such a person comes to the patent with the knowledge of what has come before. Placed in that context, it is unnecessary to spell out every detail of the invention in the specification; only enough must be included to convince a person of skill in the art that the inventor possessed the invention and to enable such a person to make and use the invention without undue experimentation." *Lizard-Tech, Inc. v. Earth Resource Mapping, PTY, Inc.*, 424 F.3d 1336, 1345; 76 USPQ2d 1724 (Fed. Cir. 2005) (emphasis added). "If a person of ordinary skill in the art would have understood the inventor to have been in possession of the claimed invention at the time of filing, even if every nuance of the claims is not explicitly described in the specification, then the adequate written description requirement is met." *In re Alton*, 76 F.3d 1168, 1175 (Fed. Cir. 1996).

In this case, one of ordinary skill in the art would have understood that the inventor had possession of the antibody-drug conjugate (ADC) or its pharmaceutically acceptable salt according to amended claims 7 and 9 at the time of filing. The present application discloses constant regions of the heavy and light chains of an anti-epidermal growth factor receptor (EGFR) antibody as shown in SEQ ID NOS:3 and 4, respectively. One skilled in the art would reasonably believe that the inventor had possession of ADC that comprises an anti-EGFR antibody having constant regions of the heavy and light chains with a sequence identity of greater than 90% to SEQ ID NOS:3 and 4, respectively, in view of the present application and the common knowledge in the art. This is because the structure-function correlation of constant regions of antibody light and heavy chains was well known in the art (*see e.g.*, Sexena and Wu, Frontiers in Immunology 7, Article 580, 2016, enclosed). For example, Figure 1 of the enclosed review shows schematics of immunoglobulin gamma overall structure and its binding regions with the immune cell receptors like Fcγ receptors (FcγRs), the complement protein C1q and the neonatal Fc receptor (FcRn). In addition, crystal structures of Fc in complex with FcγRI, Fc in

complex with FcγRII, Fc in complex with FcγRIII, Fc in complex with FcγRI, Fc in complex with FcRn, and the human C1q head have been characterized (*see* pages 2 and 4, Figure 2). Such characterization identified amino acid residues and regions of the constant regions that are important for interacting with FcγRs, C1q, and FcRn. Furthermore, other techniques, such as alanine scanning mutagenesis, also identified amino acid residues that mediate a profound effect on antibody effector functions (*see* pages 4-7, Table 1). Thus, one of ordinary skill in the art would expect that mutations in amino acid residues other than those involved in interaction with FcγRs, C1q, and FcRn or conservative mutations in the regions involved in interaction with FcγRs, C1q, and FcRn would likely result in antibodies that retain their effector functions. Accordingly, such a person would have understood that the inventor had possession of the antibody-drug conjugate (ADC) or its pharmaceutically acceptable salt according to amended claims 7 and 9 at the time of filing.

In view of the above remarks, Applicant submits that this rejection has been overcome. Withdrawal of this rejection is respectfully requested.

Rejections Under §103

(1) Claims 2-12, 14, 16, and 23-26 are rejected under 35 U.S.C 103 as unpatentable over Tikhomirov (WO2015/000062, D1) in view of Liu (CN103772504, D2), Brand et al. (Cancer Biology & Therapy 11:777-92, 2011, D3), and Chung et al. (New England Journal of Medicine 358:1109-17, 2008, D4).

Applicant respectfully traverses this rejection. Claim 2 is directed to an antibody-drug conjugate or a pharmaceutically acceptable salt thereof, comprising an anti-epidermal growth factor receptor antibody covalently linked to a cytotoxic agent via a cleavable linker, wherein the anti-epidermal growth factor receptor antibody comprises a heavy chain and a light chain, wherein the heavy chain has a variable region comprising CDR1, CDR2 and CDR3 having sequences as shown in SEQ ID NOs: 5 to 7, and the light chain has a variable region comprising CDR1, CDR2 and CDR3 having sequences as shown in SEQ ID NOs: 12 to 14. Applicant submits that the claims of the present application are not obvious in view of the cited references.

Applicant refers to its previous submission in this regard (*see* pages 10 to 13 of the Amendment filed July 1, 2019). Applicant submitted that **(1)** one of ordinary skill in the art would not have been motivated by the cited references to use a cleavable linker to arrive at the antibody-drug conjugate (ADC) or a pharmaceutically acceptable salt thereof as claimed in the present application, and **(2)** the ADC claimed in the present application is not obvious due to its unexpectedly superior property as demonstrated in Example 6 of the present application.

Briefly, as to the **first** point, Applicant noted that:

(a) the only reference cited in the office Action that discloses a linker used in forming an anti-EGFR ADC, D1, focuses almost exclusively on non-cleavable linkers (*see especially* Abstract, the first sentence in the Summary of the Invention section on page 3),

(b) D1 provides extensive disclosures and numerous examples of non-cleavable linkers (*see* pages 6, 13, and 14),

(c) all the ADCs disclosed with experimental data in D1 uses a non-cleavable linker, SMCC, except that Cetux2C9-MMAE uses a cleavable linker, valine-citrulline (*see* Examples 1 to 4),

(d) Example 4 of D1 shows that the cleavable linker, Cetux2C9-MMAE, is not favorable compared to a non-cleavable linker because this ADC with the cleavable linker had potentiated toxicity against normal cells (*see* Figure 13 and its description at the end of page 9), and

(e) D1 states that "a safe anti-EGFR ADC **should** incorporate a strongly antagonistic anti-EGFR antibody linked to an anti-microtubule payload by a **non-cleavable linker**" (*see* the last sentence of the first paragraph on page 30) (emphasis added).

Thus, in view of the disclosures of D1 as a whole, one of ordinary skill in the art would be discouraged from using a cleavable linker in generating anti-EGFR ADCs due to potentiated toxicity against normal cells of such ADCs. Using a cleavable linker in generating anti-EGFR ADCs would eliminate or at least reduce the primary benefit of the invention disclosed in D1,

that is, potentiating anti-cancer activities of ADCs without increasing their cytotoxicity against normal cells.

In response to Applicant's previous arguments, it is contended in this Office Action that disclosed examples and preferred embodiments do not constitute a teaching away from a broader disclosure or nonpreferred embodiments.

Applicant respectfully submits that although D1 mentions cleavable linkers as optional, less desirable embodiments at page 6, lines 3-5, one of ordinary skill in the art would have been motivated to use uncleavable linkers in view of D1 as a whole. For obviousness determination, prior art must be considered as a whole. "The issue with respect to obviousness is whether a challenger has carried its burden of proving, by clear and convincing evidence, facts from which it must be concluded that one skilled in the art at the time the invention was made would have found it to have been obvious, from the references as a whole, to create the claimed subject matter as a whole." *Datascope Corp. v. SMEC, Inc.*, 776 F.2d 320 (Fed. Cir. 1985) (emphasis added). "It is impermissible within the framework of 35 U.S.C. §103 to pick and choose from any one reference only so much of it will support a given position to the exclusion of other parts necessary to the full appreciation of what such reference fairly suggests to one skilled in the art." *Bausch & Lomb, Inc. v. Barnes-Hind/Hydrocurve, Inc.*, 796 F.2d 443 (Fed. Cir. 1986) (emphasis added).

In this case, D1 fairly suggests to one skilled in the art to use a non-cleavable linker in generating an anti-EGFR ADC. D1 discloses that toxicities associated with the use of EGFR-targeting antibodies demand dose reduction or warrant discontinuation of treatment in some cases, and such a concern is further amplified through conjugation to a potent cell toxin in ADCs (*see* the last paragraph of page 1 and the first paragraph of page 2). Existing approaches to solving this problems include developing conjugates based on antibodies that target a mutated but naturally occurring version of EGFR or on conformational forms of the EGFR predominating on tumor cells, not on skin cells (*see* the second paragraph on page 2). Efforts were also made to screen for anti-EGFR antibodies and ADCs for those with partial antagonistic activity against EGFR and recued activity against keratinocytes (*see* the last paragraph on page 2). D1 goes on to state that "[t]he present invention draws from the unexpected initial finding that conjugation of the anti-EGFR antibody cetuximab to a toxic maytansinoid through a **non-cleavable linker**

yields an immunoconjugate that displays enhanced cytotoxicity against cancer cells without a corresponding increase in cytotoxicity against skin cells" (*see* the first sentence in the Summary of the Invention section on page 3) (emphasis added). As discussed in detail in Applicant's previous submission and briefly summarized above, the remaining portions of D1 focuses almost exclusively on ADCs with non-cleavable linkers and their advantages over those with cleavable linkers. Viewing D1 as a whole, one of ordinary skill in the art would have been motivated to use a non-cleavable linker rather than a cleavable linker when a strongly antagonistic anti-EGFR antibody, such as an antibody comprising the CDR sequences recited in instant claim 2, is used in generating an ADC.

In response to Applicant's previous argument, it is stated in this Office Action:

> Regarding cytotoxicity towards normal keratinocytes, Goldmacher and Kovtun (Therapeutic Delivery, 2011, Vol. 2, pp. 397-416) teach that expression of an antigen of interest on normal tissue does not necessarily preclude the development of an ADC targeting the antigen (page 397, second column, lines 6-8 under the heading "Target antigen selection"). Goldmacher and Kovtun teach that the normal non-proliferating cells **would** be relatively insensitive to the action of anti-mitotic drugs such as the auristatins (page 397, second column, lines 9-12 under the heading "Target antigen selection") (*see* the third paragraph on page 14) (emphasis added).

The above-quoted statements seem to imply that toxicity associated with the use of ADCs is not a significant concern because normal cells would be relatively insensitive to the action of anti-mitotic drugs, and as such, the teaching of using a non-cleavable linker in generating anti-EGFR ADCs to reduce cytotoxicity of such ADCs as taught in D1 should be discounted.

Applicant respectfully disagrees. First, the sentence in Goldmacher and Kovtun on which the above-quoted statements in the Office Action rely is as follows: "The expression of an antigen of interest in some normal tissues does not necessarily preclude the development of an ADC targeting this antigen, **if** the normal tissue is either nonessential, or insensitive to the action of the drug (e.g., non-proliferating cells towards antimitotic agent such as maytansinoids or auristatin)" (emphasis added). The above sentence does not teach that "the normal non-proliferating cells **would** be relatively insensitive to the action of anti-mitotic drugs such as the auristatins" as asserted in the Office Action. Instead, it states that the expression of an antigen of interest in some normal tissues does not necessarily preclude the development of an ADC

targeting this antigen **if** the normal tissue is either nonessential or insensitive to the action of the drug. The two examples of the antigens used for developing ADCs in Goldmacher and Kovtun are PSMA and HER2, not EGFR as recited in the instant claims. In addition, as discussed above, D1 discloses that toxicities associated with the use of EGFR-targeting antibodies demand dose reduction or warrant discontinuation of treatment in some cases, and such a concern is further amplified through conjugation to a potent cell toxin in ADCs (*see* the last paragraph of page 1 and the first paragraph of page 2). D1 further states in the Background to the Invention section that "conjugation with a toxic maytansinoid caused severe toxicity against skin cells when delivered via a CD44v6 antibody. As a result, development of anti-EGFR immunoconjugates based on approved anti-EGFR antibodies has not been pursued because of concerns over enhanced skin toxicity of such immunoconjugates" (*see* the first paragraph on page 2). Due to such significant concerns, one of ordinary skill in the art would not discount the teaching in D1 of using a non-cleavable linker to generate an ADC that comprises a strongly antagonistic anti-EGFR antibody based on the statement in Goldmacher and Kovtun that ADCs may be developed for certain targets that are also expressed in normal tissue. This is because such a person would understand that D1, as relating to the same target antigen as the present application, is more closely related to the instantly claimed subject matter than Goldmacher and Kovtun. Accordingly, such a person would give more considerations to D1 than to Goldmacher and Kovtun.

As to the **second** point, Applicant previously argued that the ADC claimed in the present application (which comprises a cleavable linker) is unexpectedly superior to ADCs comprising non-cleavable linkers as demonstrated in Example 6 and Figure 12. Specifically, MYK-3 (an ADC with a cleavable linker) had better inhibition activities on cancer cells than BA03-MC-MMAE and BA03-MCC-MMAE (ADCs with two different non-cleavable linkers). Such superiority was unexpected because it was not taught or suggested by any of the cited references.

In response to Applicant's previous arguments, it is asserted in this Office Action that "it was not unexpected that the antibody-MMAE conjugate with a valine-citrullene linker of the instant invention was more cytotoxic against cells bearing the target antigen that [*sic*] the corresponding antibody conjugates having a non-cleavable linker" (*see* the end of the

second to last paragraph on page 14 of the Office Action). Polson *et al.* (Cancer Research 69: 2358-64, 2009) is cited in the Office Action as teaching that "antibody drug conjugates with cleavable linkers have broad efficacy and are relatively insensitive to target biology compare [*sic*] to ADCs with a non-cleavable 'MCC' linker" and as a basis for the above assertion (*see* the second to last paragraph on page 14 of the Office Action).

Applicant respectfully disagrees. Applicant submits that Polson does not show that the better inhibition activities of instantly claimed ADC on cancer cells than ADCs comprising non-cleavable linkers was expected. Polson relates to target and linker-drug selection for ADCs for treating non-Hodgkin's lymphoma (NHL). Polson identified seven antigens (CD19, CD20, CD21, CD22, CD72, CD79b, and CD180) for a potential treatment of this disease (*see* Abstract). Polson discloses that ADCs with cleavable linkers mediated *in vivo* efficacy via all these targets; ADCs with uncleavable linkers were only effective when targeted to CD22 and CD79b. *Id.* It further discloses that the uncleavable linker ADCs showed reduced toxicity. *Id.* Polson concludes that "our data suggest that ADCs with cleavable linkers work on a broad range of targets, and for specific targets, ADCs with uncleavable linkers provide a promising opportunity to improve the therapeutic window for ADCs in humans." *Id.* Thus, while disclosing that ADCs with cleavable linkers have a broader target range than those with uncleavable linkers, Polson also teaches that for antigens (*e.g.*, CD22 and CD79b) against which ADCs with cleavable and uncleavable linkers are both effective, ADCs with uncleavable linkers would likely be preferred because of their potent efficacy and acceptable safety profiles (*see also* the last paragraph in the right column on page 2364).

The assertion in the Office Action related to Applicant's unexpectedly superior property argument implies that Polson shows that ADCs with cleavable linkers were more effective in inhibiting cancer cells than those with uncleavable linkers. Such an interpretation of Polson is incorrect, at least for targets against which ADCs with cleavable and uncleavable linkers are both effective. Figure 1D of Polson shows that anti-CD22-SPP-DM1 (with the cleavable linker SPP) was similar to anti-CD22-MCC-DM1 (with the uncleavable linker MCC) in inhibiting tumor growth. Polson also describes that the interaction of the linker type and the target is complex and was not well explored (*see* the second paragraph in the right column on page 2358). Due to the

lack of understanding of such an interaction, one of ordinary skill in the art would **not** have concluded that ADCs with cleavable linkers were more effective in inhibiting cancer cells than those with uncleavable linkers regardless which targets the ADCs are directed to. Accordingly, such a person would not expect that anti-EGFR ADCs with cleavable linkers would be more effective in inhibiting cancer cells than anti-EGFR ADCs with uncleavable linkers based on the disclosure of Polson, which is silent with respect to the target antigen EGFR of the present application.

In fact, for different targets, the effect of linker type on the efficacy of ADCs is different. For example, contrary to the assertion in the Office Action that it is expected that ADCs with cleavable linkers would be more effective than those with uncleavable linkers, Phillips *et al.* (Cancer Res 68: 9280-90, 2008, enclosed) shows that trastuzuman (anti-HER2) linked to DM1 through a nonreducible thioether linkage (SMCC, non-cleavable) displayed superior activity compared with trastuzumab lined to other maytansinoids though disulfide linkers (cleavable) (*see* Abstract, Figure 3). Phillips concludes that because trastuzumab linked to DM1 through a nonreducible linker offers improved efficacy and pharmacokinetics and reduced toxicity over the reducible disulfide linkers, it was selected for clinical development (*see* Abstract, the last paragraph in the right column on page 9289).

In view of the above-remarks, Applicant submits that this ground of rejection has been overcome. Withdrawal of this rejection is respectfully requested.

(2) Claims 2-12, 14-16, 23-26 and 37 are rejected under 35 U.S.C. 103 as unpatentable over Tikhomirov (WO2015/000062, D1), Liu (CN103772504, D2), and Chung et al. (New England Journal of Medicine 358:1109-17, 2008, D4) and further in view of Chari et al. (Angewandte Chemie, 2014, vol. 53, pp. 3796-3827, D5).

Applicant submits that the claims as currently pending in the present application are not obvious in view of the cited references. As discussed above, D1, D2 and D4 do not render the currently pending claims obvious. Specifically, one of ordinary skill in the art would not have been motivated to use a cleavable linker to generate an anti-EGFR ADC in view of D1, D2

and D4. Such a deficiency has not been remedied by D5. D5 is cited in the Office Action as disclosing the cleavable linker Mal-caproyl-val-cit-PAB-MMAE linkable derivate of MMAE. This reference does not disclose generating an anti-EGFR ADC using a cleavable linker or the superior property of the currently claimed anti-EGFR ADC.

In view of the above-remarks, Applicant submits that this ground of rejection has been overcome. Withdrawal of this rejection is respectfully requested.

(3) Claims 2-12, 14, 16, 23-27 and 35 are rejected under 35 U.S.C. 103 as unpatentable over Tikhomirov (WO2015/000062, D1), Liu (CN103772504, D2), and Chung et al. (New England Journal of Medicine 358:1109-17, 2008, D4) and further in view of Lievre et al. (Cancer Research 66: 3992-5, 2006, D6).

Applicant submits that the claims as currently pending in the present application are not obvious in view of the cited references. As discussed above, D1, D2 and D4 do not render the currently pending claims obvious. Specifically, one of ordinary skill in the art would not have been motivated to use a cleavable linker to generate an anti-EGFR ADC in view of D1, D2 and D4. Such a deficiency has not been remedied by D6. D6 is cited in the Office Action in connection with KRAS gene mutations in an EGFR positive tumor. This reference does not disclose generating an anti-EGFR ADC using a cleavable linker or the superior property of the currently claimed anti-EGFR ADC.

In view of the above-remarks, Applicant submits that this ground of rejection has been overcome. Withdrawal of this rejection is respectfully requested.

(4) Claims 2-12, 14, 16, 23-26, 28, and 36 are rejected under 35 U.S.C. 103 as unpatentable over Tikhomirov (WO2015/000062, D1), Liu (CN103772504, D2), and Chung et al. (New England Journal of Medicine 358:1109-17, 2008, D4) and further in view of DiNicolantonio et al. (Journal of Clinical Oncology 26: 5705-12, 2008, D7).

Applicant submits that the claims as currently pending in the present application are not obvious in view of the cited references. As discussed above, D1, D2 and D4 do not render the

currently pending claims obvious. Specifically, one of ordinary skill in the art would not have been motivated to use a cleavable linker to generate an anti-EGFR ADC in view of D1, D2 and D4. Such a deficiency has not been remedied by D7. D7 is cited in the Office Action in connection with BRAF gene mutations in an EGFR positive tumor. This reference does not disclose generating an anti-EGFR ADC using a cleavable linker or the superior property of the currently claimed anti-EGFR ADC.

In view of the above-remarks, Applicant submits that this ground of rejection has been overcome. Withdrawal of this rejection is respectfully requested.

The Director is authorized to charge any additional fees due by way of this Amendment, or credit any overpayment, to our Deposit Account No. 19-1090.

Respectfully submitted,

SEED Intellectual Property Law Group LLP

/Qing Lin/
Qing Lin, Ph.D.
Registration No. 53,937

Enclosures:

Sexena and Wu, Frontiers in Immunology 7, Article 580, 2016
Phillips *et al.*, Cancer Res 68: 9280-90, 2008

QXL:bgh

701 Fifth Avenue, Suite 5400
Seattle, Washington 98104-7092
Phone: (206) 622-4900
Fax: (206) 682-6031

7052622.1

Targeting HER2-Positive Breast Cancer with Trastuzumab-DM1, an Antibody–Cytotoxic Drug Conjugate

Gail D. Lewis Phillips,[1] Guangmin Li,[1] Debra L. Dugger,[1] Lisa M. Crocker,[1] Kathryn L. Parsons,[1] Elaine Mai,[1] Walter A. Blättler,[2] John M. Lambert,[2] Ravi V.J. Chari,[2] Robert J. Lutz,[2] Wai Lee T. Wong,[1] Frederic S. Jacobson,[1] Hartmut Koeppen,[1] Ralph H. Schwall,[1] Sara R. Kenkare-Mitra,[1] Susan D. Spencer,[1] and Mark X. Sliwkowski[1]

[1]Genentech, Inc., South San Francisco, California and [2]ImmunoGen, Inc., Waltham, Massachusetts

Abstract

HER2 is a validated target in breast cancer therapy. Two drugs are currently approved for HER2-positive breast cancer: trastuzumab (Herceptin), introduced in 1998, and lapatinib (Tykerb), in 2007. Despite these advances, some patients progress through therapy and succumb to their disease. A variation on antibody-targeted therapy is utilization of antibodies to deliver cytotoxic agents specifically to antigen-expressing tumors. We determined *in vitro* and *in vivo* efficacy, pharmacokinetics, and toxicity of trastuzumab-maytansinoid (microtubule-depolymerizing agents) conjugates using disulfide and thioether linkers. Antiproliferative effects of trastuzumab-maytansinoid conjugates were evaluated on cultured normal and tumor cells. *In vivo* activity was determined in mouse breast cancer models, and toxicity was assessed in rats as measured by body weight loss. Surprisingly, trastuzumab linked to DM1 through a nonreducible thioether linkage (SMCC), displayed superior activity compared with unconjugated trastuzumab or trastuzumab linked to other maytansinoids through disulfide linkers. Serum concentrations of trastuzumab-MCC-DM1 remained elevated compared with other conjugates, and toxicity in rats was negligible compared with free DM1 or trastuzumab linked to DM1 through a reducible linker. Potent activity was observed on all HER2-overexpressing tumor cells, whereas nontransformed cells and tumor cell lines with normal HER2 expression were unaffected. In addition, trastuzumab-DM1 was active on HER2-overexpressing, trastuzumab-refractory tumors. In summary, trastuzumab-DM1 shows greater activity compared with nonconjugated trastuzumab while maintaining selectivity for HER2-overexpressing tumor cells. Because trastuzumab linked to DM1 through a nonreducible linker offers improved efficacy and pharmacokinetics and reduced toxicity over the reducible disulfide linkers evaluated, trastuzumab-MCC-DM1 was selected for clinical development. [Cancer Res 2008;68(22):9280–90]

Introduction

The HER2 (ErbB2) receptor tyrosine kinase is a member of the epidermal growth factor receptor family of transmembrane receptors. These receptors, which also include HER3 (ErbB3) and HER4 (ErbB4), are known to play critical roles in both development and cancer (1, 2). Importantly, amplification and overexpression of HER2 occur in 20% to 25% of human breast cancer and are predictive of poor clinical outcome (3, 4). Because of the role of HER2 in breast cancer pathogenesis and the accessibility of the extracellular portion of the receptor, HER2 was recognized as a potential candidate for targeted antibody therapy. The humanized HER2 antibody, trastuzumab (Herceptin), was approved by the Food and Drug Administration in 1998 for use in metastatic breast cancer and has subsequently shown clinical benefit when used, in combination with cytotoxic chemotherapy, as first-line or adjuvant therapy (5, 6). Importantly, trastuzumab improves overall survival in early breast cancer after chemotherapy compared with observation alone (6). Increased survival after only 2 years of follow-up is impressive in breast cancer. Tamoxifen is the only other breast cancer treatment that is reported to offer a survival benefit in this short-time period (6).

Although the mechanisms for response to trastuzumab are not completely understood, clinical benefit is attributed to interference with signal transduction pathways, impairment of extracellular domain (ECD) cleavage, inhibition of DNA repair, decreased angiogenesis; as well as induction of cell cycle arrest, and antibody-mediated cellular cytotoxicity (7, 8). Despite these diverse mechanisms of action, a significant proportion of patients treated with trastuzumab either do not respond initially or relapse after experiencing a period of clinical response (5, 9). Progression through trastuzumab-containing therapy is attributed to aberrant activation of signaling pathways, such as the phosphatidylinositol 3-kinase pathway (10–12), activation of compensatory signaling either through up-regulation of the insulin-like growth factor-I receptor (13, 14) or ErbB/HER ligands (15, 16) or generation of a constitutively active truncated form of HER2, designated p95HER2 (17, 18).

Direct covalent coupling of cytotoxic agents to monoclonal antibodies is an alternative to naked antibody-targeted therapy. To date, antitumor antibodies have been linked to cytotoxic agents, such as the calicheamicins, auristatins, maytansinoids and derivatives of CC1065 (19–22). Currently, only one such conjugate, anti-CD33 conjugated to calicheamicin (gemtuzumab ozogamicin or Mylotarg), has been granted marketing approval for the treatment of relapsed acute myeloid leukemia (23).

Maytansinoids are derivatives of the antimitotic drug maytansine. These agents bind directly to microtubules in a manner similar to the *Vinca* alkaloids (24, 25). Antibody-maytansinoid conjugates directed toward cancer antigens, such as CanAg (cantuzumab mertansine and IMGN242), prostate-specific membrane antigen (MLN2704), CD56 (IMGN901), CD33 (AVE9633), and

Note: Current address for H. Koeppen: M. D. Anderson Cancer Center, Houston, TX 77030.

Requests for reprints: Gail D. Lewis Phillips, Genentech, Inc., 1 DNA Way, South San Francisco, CA 94080. Phone: 650-225-2201; Fax: 650-225-1411; E-mail: gdl@gene.com or Mark X. Sliwkowski, Genentech, Inc., 1 DNA Way, South San Francisco, CA 94080. Phone: 650-225-1247; Fax: 650-225-5770; E-mail: marks@gene.com.

©2008 American Association for Cancer Research.

doi:10.1158/0008-5472.CAN-08-1776

CSPC Exhibit 1004
Page 208 of 336

Downloaded from cancerres.aacrjournals.org on December 6, 2019. © 2008 American Association for Cancer Research.

CD44v6 (bivatuzumab mertansine) are in early stages of clinical testing (20, 26–28). Because HER2 is highly differentially expressed on breast tumor cells (1–2 million copies per cell) compared with normal epithelial cells, HER2 represents an ideal target for antibody-drug conjugate (ADC) therapy. Numerous preclinical and clinical studies indicate that trastuzumab combines extremely well with microtubule-directed agents (29–32). Given the mechanism of action and potency of maytansine, it was deemed to be a particularly attractive cytotoxic agent to conjugate to trastuzumab. Herein, we describe the efficacy, pharmacokinetic properties, and safety of several trastuzumab-maytansinoid conjugates, with particular emphasis on the chemical nature of the linker.

Materials and Methods

Cell lines and reagents. Tumor cell lines (breast carcinoma BT-474, SK-BR-3, MCF7, MDA-MB-468, MDA-MB-361, HCC1954, lung carcinoma Calu 3, and ovarian carcinoma line SK-OV-3) and MCF 10A breast epithelial cells were obtained from American Type Culture Collection. The breast tumor line KPL-4 was obtained from Dr. J. Kurebayashi (33), and MKN7 gastric carcinoma cells were from Mitsubishi Corp. Cells were maintained in Ham's F-12; high glucose DMEM (50:50) supplemented with 10% heat-inactivated fetal bovine serum and 2 mmol/L L-glutamine (all from Invitrogen Corp.). Normal human cell lines [human mammary epithelial cells (HMEC) and normal human epidermal keratinocytes (NHEK)] and the corresponding culture medium (MEGM and KGM, respectively) were obtained from Cambrex. The BT474-EEI cell line was derived by subculturing BT-474 tumors grown *in vivo* in the absence of estrogen pellet supplementation (exogenous estrogen independent) and is resistant both *in vitro* and *in vivo* to trastuzumab treatment.

Active agents used for cell culture and animal studies were the antibody trastuzumab (Genentech, Inc.), trastuzumab-maytansinoid ADC (ImmunoGen, Inc.), and the control ADC, anti-IL-8-MCC-DM1. The maytansinoid, DM1, was conjugated to trastuzumab through SPP, SMCC, or SPDP linkers (Fig. 1; refs. 24, 34); the thiol-containing maytansinoids, DM3 and DM4, which have methyl groups adjacent to their sulfhydryl group were linked to trastuzumab with the SSNPP linker (ImmunoGen, Inc.). All trastuzumab ADCs had an average molar ratio of 3 to 3.6 maytansinoid molecules per antibody. The drug-antibody molar ratio for trastuzumab-MCC-DM1 and trastuzumab-SPP-DM1 was 3.2 for cell culture and xenograft studies, 3.6 for trastuzumab-SPP-DM1 used in the rat toxicity study, and 3.8 for anti-IL-8-MCC-DM1.

Cell viability and cell death assays. The effects of trastuzumab and trastuzumab-maytansinoid conjugates on tumor cell viability were assessed using Cell Titer-Glo (Promega Corp.). Cells were plated in black-walled 96-well plates (20,000 per well for BT-474; 10,000 cells per well for all other lines) and allowed to adhere overnight at 37°C in a humidified atmosphere of 5% CO_2. Medium was then removed and replaced by fresh culture medium containing different concentrations of trastuzumab, trastuzumab ADC, or free DM1, and the cells incubated for varying periods of time. After each time point, Cell Titer-Glo reagent was added to the wells for 10 min at room temperature and the luminescent signal was measured using a Packard/Perkin-Elmer TopCount. For measurement of apoptosis, BT-474 and SK-BR-3 were exposed to trastuzumab or trastuzumab-MCC-DM1 for 48 h. Caspase activation was assessed by adding Caspase-Glo 3/7 reagent (Promega Corp.) for 30 min at room temperature, and the luminescence was recorded using a Packard TopCount. Induction of cytotoxicity was assessed in cells treated with trastuzumab or trastuzumab-MCC-DM1 for 72 h using ToxiLight Bioassay kit (Cambrex/Lonza). This assay measures release of the intracellular enzyme adenylate kinase as a result of cell lysis.

Normal HMEC and NHEK were plated in clear 96-well plates at densities of 10,000 and 8,000 cells per well, respectively, and allowed to adhere overnight. Cells were treated with trastuzumab or trastuzumab-MCC-DM1 for 72 h. Alamar Blue reagent (Trek Diagnostics Systems) was added to all wells, plates were incubated for 3 h at 37°C, and fluorescence was measured on a SpectraMax 190 (Molecular Devices) using 530-nm excitation and 590-nm emission. Because the normal cell lines were not healthy when grown in black multiplates (which is necessary for use of Cell Titer-Glo), Alamar Blue was used as the proliferation read-out. For all cellular assays, dose-response curves were generated using Kaleidagraph 4.0 (Synergy Software) four-parameter curve fitting.

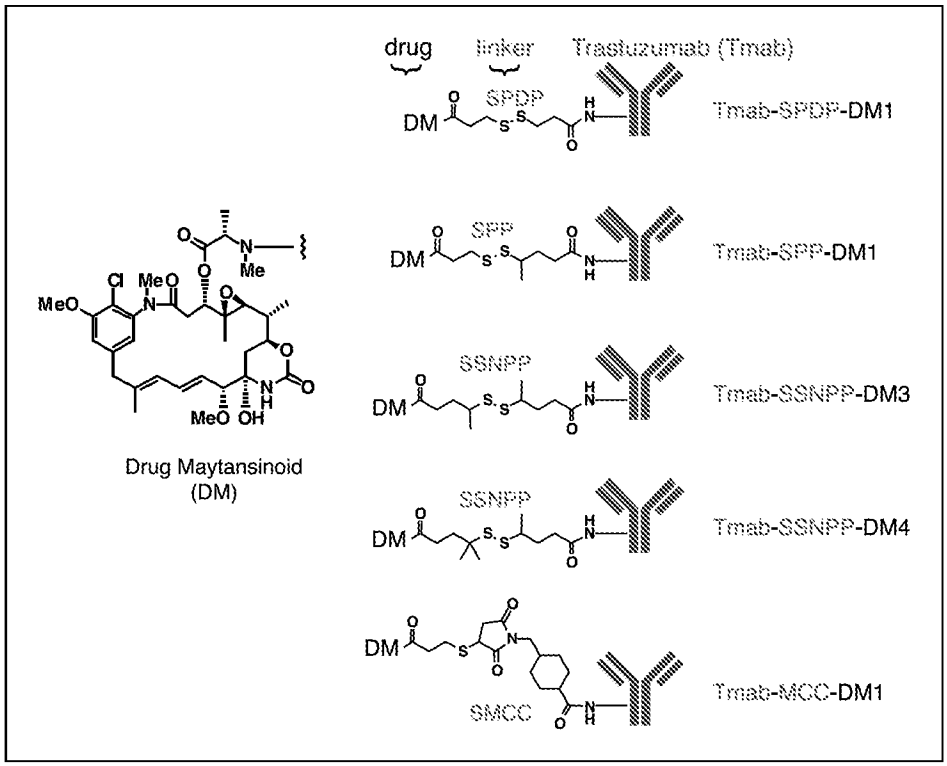


Figure 1. Structure of trastuzumab (Tmab)–maytansinoid conjugates (stability of linker, least to greatest): Tmab-SPDP-DM1, Tmab-SPP-DM1, Tmab-SSNPP-DM3, Tmab-SSNPP-DM4, and Tmab-SMCC-DM1 (nonreducible).

CSPC Exhibit 1004
Page 209 of 336

Downloaded from cancerres.aacrjournals.org on December 6, 2019. © 2008 American Association for Cancer Research.

Western immunoblot analysis. SK-BR-3 cells were seeded at a density of 1 million per dish in 100 × 15 mm dishes and allowed to adhere for 2 d. The medium was then removed and replaced with fresh medium containing either trastuzumab, free DM1, or a range of concentrations of trastuzumab-MCC-DM1. After a 48-h incubation, floating cells were collected and combined with detached adherent cells. The total cell population was then centrifuged and resuspended in lysis buffer [50 mmol/L HEPES (pH 7.5), 150 mmol/L NaCl, 1.5 mmol/L $MgCl_2$, 1.0 mmol/L EGTA, 10% glycerol, 1% Triton X-100, 10 mmol/L $Na_4P_2O_4$, 1 mmol/L Na_3VO_4, 50 mmol/L NaF, 1 μmol/L leupeptin, 0.3 μmol/L aprotinin, 1 μmol/L pepstatin A, 10 μmol/L bestatin, and 1.4 μmol/L E-64]. Lysates were cleared by centrifugation at 4°C for 15 min at 20,800 × *g* in a microcentrifuge, and protein concentrations were determined using the bicinchoninic acid (BCA) protein assay kit (Pierce). Proteins were resolved by SDS-PAGE, transferred to nitrocellulose, and immunoblotted with a polyclonal antibody against poly(ADP-ribose) polymerase (PARP), which recognizes intact 116-kDa PARP and the 23-kDa cleavage fragment (R&D Systems). Blotting was carried out in TBS containing 0.1% Triton X-100 and 5% nonfat dry milk, followed by incubation with horseradish peroxidase (HRP)–conjugated secondary antibodies (Amersham Biosciences). Proteins were visualized using enhanced chemiluminescence reagents (Amersham Biosciences).

Measurement of total and phosphorylated HER2 and p95HER2 in transgenic tumors was performed as follows. Tumors from the founder 5 (Fo5; ref. 35) and founder 2#1282 (F2#1282) lineages of MMTV-HER2 transgenic mice (Genentech, Inc.) were excised from the animals, placed in lysis buffer containing protease inhibitors, and homogenized on ice. Tumor lysates were centrifuged, and total protein levels in the supernatant were determined using a BCA protein assay kit. HER2 was immunoprecipitated overnight at 4°C using the mouse monoclonal antibody Ab-15 (Lab Vision) complexed to protein A/G sepharose, with 1 mg total protein from at least three independent tumor lysates. Complexes were pelleted by centrifugation, washed twice with lysis buffer, resuspended in SDS sample buffer, and boiled. Samples were separated on a 4% to 12% Tris-glycine gel and transferred to nitrocellulose membranes. Blots were probed with mouse monoclonal antibody Ab-18 (Lab Vision) to detect the phosphorylated forms of HER2 and p95HER2 or with Ab-15 to detect total HER2 and p95HER2.

***In vivo* efficacy and pharmacokinetic studies.** Tumor tissue from Fo5 or F2#1282 HER2 transgenic mice was collected aseptically, rinsed in HBSS, and cut into pieces of ~2 × 2 mm in size. These pieces were surgically transplanted into the mammary fat pad of female nu/nu mice (Charles River Laboratories). For efficacy studies using BT474EEI cells, naive female beige nude XID mice (Harlan Sprague-Dawley) were inoculated in the mammary fat pad with 20 million tumor cells suspended in 50% phenol red–free Matrigel (Becton Dickinson Bioscience) mixed with culture medium. All animals were randomly assigned into treatment groups, such that the mean tumor volume for each group was 100 to 200 mm^3. Trastuzumab or trastuzumab-maytansinoid conjugates were given by either a single i.v. injection or injection once every 3 wk. Vehicle control was either PBS (for pharmacokinetic studies) or ADC formulation buffer [10 mmol/L sodium succinate, 0.1% polysorbate (Tween) 20, 20 mg/mL trehalose dihydrate (pH5.0)]. Similarly, KPL-4 human breast tumor cells were inoculated (3 million cells per mouse, in Matrigel) into the mammary fat pads of SCID beige mice (Charles River Laboratories). Trastuzumab (15 mg/kg) was given i.p. once per week for 4 wk; trastuzumab-MCC-DM1 (15 mg/kg) was given i.v. (single injection on treatment day 0). All treatment groups consisted of 6 to 10 animals per group, and tumor size was monitored twice weekly using caliper measurement. Mice were housed in standard rodent microisolator cages. Environmental controls for the animal rooms were set to maintain a temperature of ~70°F, a relative humidity of 40% to 60%, and an approximate 14-h light/10-h dark cycle.

For pharmacokinetic analysis of trastuzumab-maytansinoid conjugates, female beige nude mice (age 15–20 wk; Harlan Sprague-Dawley) were injected i.v. with 2 mg/kg of different trastuzumab ADCs (four mice per group). To assess circulating levels of total and conjugated antibody, blood was collected via cardiac puncture from three animals at 5 min and 1, 6, 24, 72, and 168 h postinjection. The samples were left at room temperature for 30 min until the blood coagulated. Subsequently, serum was obtained by centrifuging the samples at 10,000 × *g* for 5 min at 4°C, after which serum samples were stored at −70°C. Total trastuzumab concentration in the serum samples was measured as follows: 96-well ELISA plates were coated with HER2 ECD in 0.05 mol/L carbonate/bicarbonate buffer (pH 9.6) at 4°C overnight. After removal of the coat solution, nonspecific binding sites were blocked by incubating with blocking solution [0.5% bovine serum albumin (BSA) in PBS] for 1 to 2 h. The plates were then washed with wash buffer (0.05% Tween in PBS), and standards or samples diluted in ELISA assay buffer [PBS containing 0.5% BSA, 0.05% Tween, 10 ppm proclin 300, 0.2% bovine γ-globulin, 0.25% CHAPS, 0.35 mol/L NaCl, 5 mmol/L EDTA (pH 7.4)] were added. After a 2-h incubation, plates were washed and HRP-conjugated goat anti-human Fc (The Jackson Laboratory) was added for an additional 2 h. Plates were then washed again, followed by the addition of tetramethyl benzidine substrate for color development. The reaction was stopped after 10 to 15 min by the addition of 1 mol/L phosphoric acid. Plates were read on a Molecular Devices microplate reader at a wavelength of 450 to 630 nm. The concentration of trastuzumab in the samples was extrapolated from a four-variable fit of the standard curve. For measurement of trastuzumab-maytansinoid concentration, wells were coated with anti-DM antibody (GNE DM1-3586) and serum samples added as above. After the 2-h sample incubation, the plates were washed, 60 ng/mL biotin-conjugated HER2 ECD was added to each well, and the plates were incubated for 1 h. Plates were then washed, and HRP-conjugated streptavidin (GE Healthcare) was added for an additional 30-min incubation. Color detection and measurement were performed as described above. Previous analyses of different preparations of trastuzumab-DM1 conjugates with drug-antibody ratios ranging from 1.9 to 3.8 showed that the conjugated antibody ELISA is not sensitive to drug load.

Circulating HER2 ECD levels from mice harboring Fo5 or F2#1282 xenograft tumors was measured, as previously described (35). Briefly, serum was diluted 1:50 with ELISA assay buffer (above) followed by 1:2 serial dilutions. HER2 ECD was captured using goat anti-HER2 polyclonal antibody (Genentech, Inc.) and detected with biotin-conjugated rabbit anti-Her2 polyclonal (Genentech, Inc.), followed by addition of streptavidin-HRP.

Rat toxicity studies. Female Sprague-Dawley rats weighing 75 to 80 g were obtained from Charles River Laboratories and allowed to acclimate for 5 d before study. Trastuzumab-SPP-DM1, trastuzumab-MCC-DM1, and free DM1 were diluted in PBS (Invitrogen Corp.) as vehicle and given as a single i.v. bolus tail-vein injection on day 1 at a dose volume of 10 mL/kg. Body weights were measured predose on day 1 and daily thereafter for 5 d.

Results

Linker optimization. Antibody-DM1 conjugates were originally designed with a disulfide-based linker for release of active drug by intracellular reduction (24). Recently, it was discovered that the endocytic pathway is oxidizing and that cleavage of the disulfide linker, SPP, is very inefficient (36). Thus, different trastuzumab ADCs were constructed to investigate the effect of disulfide linker hindrance on the biological activity of these conjugates (Fig. 1). A trastuzumab-DM1 conjugate made with the SPDP linker contains no methyl substitutions adjacent to the disulfide bond and is therefore the least hindered disulfide-containing design. Trastuzumab ADCs composed of SPP-DM1, SSNPP-DM3, or SSNPP-DM4 contain one, two, or three methyl groups, respectively, around the disulfide bridge and show increasing resistance to cleavage via thiol-disulfide exchange reactions.[3] DM3 and DM4 nomenclature

[3] ImmunoGen, Inc., unpublished data.

CSPC Exhibit 1004
Page 210 of 336

Downloaded from cancerres.aacrjournals.org on December 6, 2019. © 2008 American Association for Cancer Research.

reflects addition of methyl groups to the DM1 (drug) moiety (addition of one or two methyls, respectively). An additional ADC containing a thioether linker (SMCC, designated MCC after conjugation) was also constructed. *In vitro* potency assays were conducted for 3 days with the HER2-amplified breast cancer lines BT-474 and SK-BR-3 treated with various trastuzumab ADCs. This short treatment period was selected to minimize the effects of unconjugated trastuzumab on these trastuzumab-sensitive lines. The graphs in Fig. 2*A* show enhanced potency of trastuzumab-maytansinoid conjugates compared with trastuzumab in both cell lines, with no significant difference in activity among the various ADCs tested (IC_{50}, 0.085–0.148 μg/mL for BT-474 and 0.007–0.018 μg/mL for SK-BR-3). Because the effect of trastuzumab is cytostatic in nature, the enhanced potency of the ADC is, thus, due to exposure of the cells to the cytotoxic maytansinoid. In addition, brief exposure of SK-BR-3 cells for 10, 30, or 60 minutes to trastuzumab-MCC-DM1, followed by a 3-day incubation in culture medium, also resulted in substantial growth inhibition (data not shown). When comparing potency as molar DM1 equivalents, DM1 conjugated to trastuzumab is 5-fold more potent than free L-DM1 on SK-BR-3 and shows equal potency to free L-DM1 on BT-474 cells (Fig. 2*B*). Nontargeted effects of trastuzumab-maytansinoid conjugates were assessed on breast cancer lines expressing normal levels (MCF7) or lacking expression (MDA-MB-468) of HER2 (37). All ADCs tested showed minimal antiproliferative activity in both cell lines (Fig. 2*A*), whereas free DM1 showed potency equal to that observed on the HER2-amplified lines (Fig. 2*B*). Treatment of the four cell lines with an isotype-matched control ADC, anti-IL-8-MCC-DM1, resulted in negligible growth inhibition (data not shown). Thus, like trastuzumab, maytansinoid-conjugated trastuzumab ADCs are specific for HER2-overexpressing cells. Furthermore, the different linkers behave similarly with respect to *in vitro* antiproliferative activity.

Pharmacokinetic analyses in nude mice were performed to determine the effect of different trastuzumab ADC linkers on serum concentration. In contrast to the cell culture results, we observed a clear correlation between ADC exposure and linker hindrance. The ADC with the least hindered disulfide bond (no adjacent methyl groups), trastuzumab-SPDP-DM1, showed the fastest clearance and was undetectable by day 3. The addition of methyl groups (CH_3) on either side of the S-S bond (trastuzumab-SPP-DM1 with one CH_3 on the antibody side of the S-S; trastuzumab-SSNPP-DM3 with two CH_3, one on either side of the S-S; trastuzumab-SSNPP-DM4 with three CH_3, one on the antibody side, and two on the drug side of the S-S) resulted in increasingly sustained ADC serum concentrations (Fig. 3*A*, *left*). Trastuzumab-MCC-DM1 (nonreducible) and trastuzumab-SSNPP-DM4 (the most hindered disulfide-containing design) showed similar pharmacokinetics with the ADC concentration at 70% of the total antibody at day 7. Studies were also performed to compare clearance of DM1-conjugated trastuzumab to total trastuzumab levels (Fig. 3*A*, *right*). Serum concentrations of trastuzumab-MCC-DM1 measured for 1 week were not different from total serum trastuzumab concentration, indicating that, with the nonreducible MCC linker, the amount of maytansinoid released from the antibody was negligible over the 7 days. In contrast, only 11% of the trastuzumab-SPP-DM1, compared with total trastuzumab antibody concentration, remained in the circulation after 7 days.

In vivo efficacy studies examining the different trastuzumab-maytansinoid conjugates given as a single i.v. dose were carried out using the MMTV-HER2 Fo5 mammary tumor transplant (trastuzumab-resistant) model. This model was developed by serial transplantation of tumors derived from the HER2 transgenic mouse lineage founder 5 (35). These mouse tumors overexpress human HER2 (3+ expression) as measured by immunohistochemistry and quantitative reverse transcription–PCR. Interestingly, established tumors from this model do not respond to single-agent trastuzumab therapy. Consistent with the pharmacokinetic analysis, increased linker stability *in vivo* correlated with increased antitumor activity for trastuzumab ADCs (Fig. 3*B*). Tumor volume in both trastuzumab-MCC-DM1 and trastuzumab-SSNPP-DM3 treatment groups were statistically different from trastuzumab-SPP-DM1 (log-rank P values of 0.0165 and 0.0414, respectively). Further characterization of the HER2 transgenic models revealed the presence of high circulating levels of shed HER2 ECD in the serum of Fo5 tumor-bearing mice. Moreover, analysis of these tumors revealed increased expression of the transmembrane-containing fragment p95HER2, which is highly tyrosine-phosphorylated, indicating constitutive activation. In comparison, the trastuzumab-sensitive F2#1282 model showed 1,000-fold lower levels of circulating HER2 ECD, no detectable p95HER2, and significant tumor growth reduction after a single injection of different doses of trastuzumab-DM1 (data not shown). Thus, the trastuzumab-DM1 conjugate is efficacious in models, such as Fo5, which express reported markers of resistance to trastuzumab, i.e., high circulating HER2 ECD and activated p95HER2.

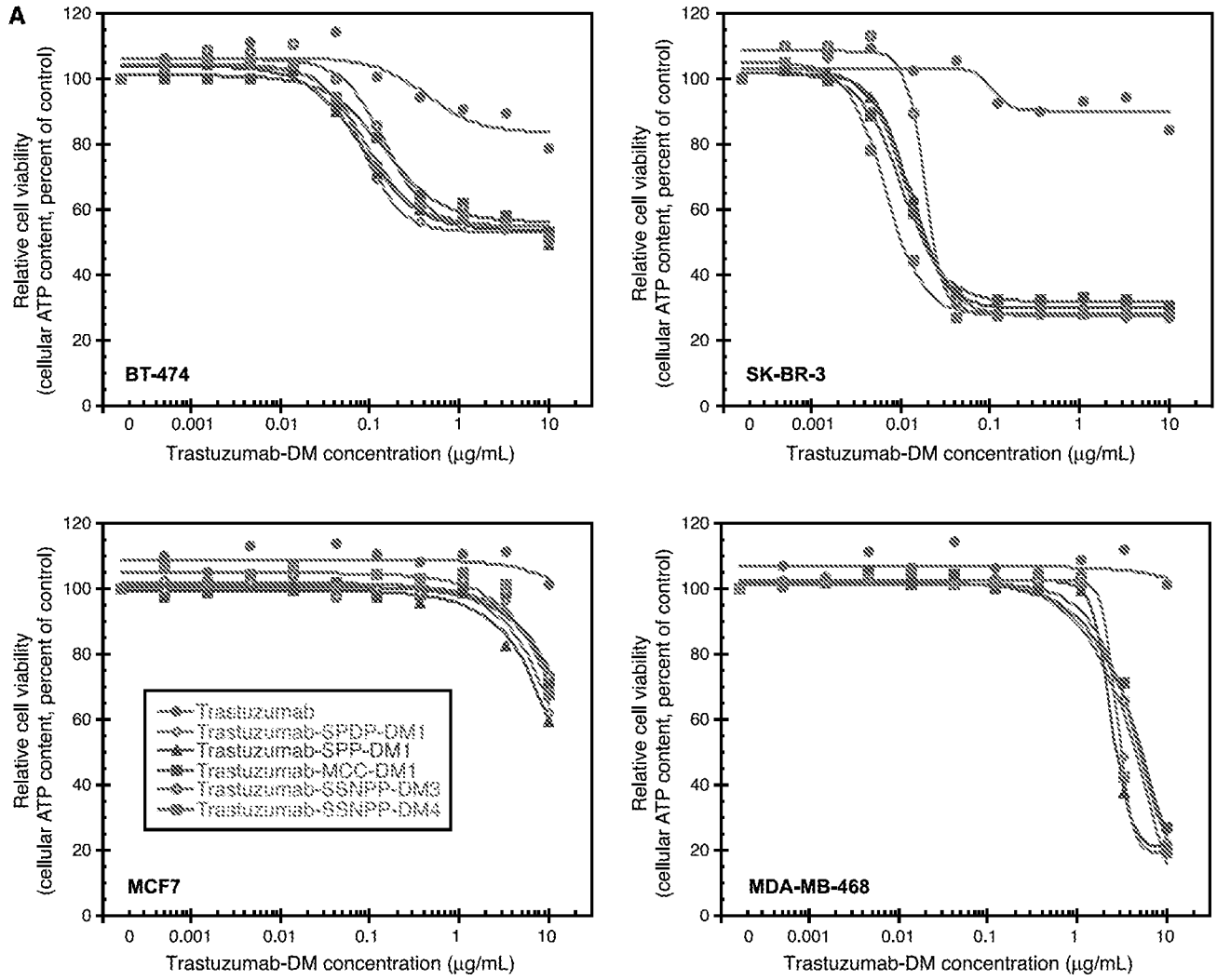
Short-term, single-dose toxicity studies were performed in female rats comparing the effects on body weight of free or conjugated (SMCC or SPP) DM1. ADCs were given as DM1 equivalents (μg/m^2). As trastuzumab does not recognize rat erbB2, this model measures antigen-independent ADC effects. Of the agents tested, trastuzumab-MCC-DM1 showed the best safety profile. Body weight gain in rats given 1,632 μg/m^2 DM1 (25 mg/kg antibody) was comparable with vehicle control animals (15.9% and 16.3%, respectively; Fig. 3*C*). In contrast, administration of trastuzumab-SPP-DM1 at an equivalent DM1 dose resulted in considerable body weight loss (−10%) by end of study. Rats treated with 3,264 μg/m^2 (50 mg/kg) trastuzumab-MCC-DM1 did not exhibit body weight loss; however, the amount of weight gained during the course of study (+6.7%) was less than in the vehicle control and the 1,632 μg/m^2 trastuzumab-MCC-DM1 groups. The change in body weight with 3,264 μg/m^2 trastuzumab-MCC-DM1 was similar to that observed with free DM1 at a dose of 653 μg/m^2 (+6.5%). In a separate study, clinical chemistry analysis of rats treated with trastuzumab-MCC-DM1 showed transient elevation of liver enzymes (aspartate aminotransferase, alanine aminotransferase, and γ-glutamyl transpeptidase) and mild, reversible thrombocytopenia at a dose of 20 mg/kg, and no clinical signs of toxicity at 6 mg/kg (data not shown). Evidently, substituting a reducible linker (SPP) with a nonreducible linker (SMCC) results in a less toxic but still efficacious trastuzumab-DM1 conjugate. Consequently, further studies focused on defining the activity of trastuzumab-MCC-DM1.

HER2-overexpressing, trastuzumab-resistant tumor cells respond to trastuzumab-MCC-DM1, whereas normal cell lines are unaffected. The effects of trastuzumab-MCC-DM1 on *in vitro* proliferation were further examined in several tumor lines shown to be resistant to trastuzumab. Additional breast cancer lines, HCC1954, KPL-4, and BT-474 EEI, all with 3+ HER2 expression, were first tested. The BT-474 EEI cell line was developed by

CSPC Exhibit 1004
Page 211 of 336

Downloaded from cancerres.aacrjournals.org on December 6, 2019. © 2008 American Association for Cancer Research.

A



B

***In vitro* activity of trastuzumab-DM1 conjugates versus free DM1 (IC_{50}, nmol/L DM1 equivalents)**

	trastuzumab-SPP-DM1	trastuzumab-MCC-DM1	free L-DM1
SK-BR-3	0.24	0.22	1.00
BT-474	2.71	4.26	4.52
MCF7	>100	>100	2.92
MDA-MB-468	18.37	41.37	0.59

Cells were treated with trastuzumab-DM1 conjugates or L-DM1 as free drug for 72 h; IC_{50} values were determined from four-parameter curve fitting.

Figure 2. Trastuzumab-maytansinoid conjugates are selective for HER2-amplified breast cancer lines, whereas free DM1 shows equivalent potency on all cell lines tested regardless of HER2 expression. *A*, trastuzumab-maytansinoid conjugates show enhanced antiproliferative activity on HER2-overexpressing breast tumor cell lines compared with trastuzumab. The nature of the linker, however, does not affect *in vitro* activity. *B*, *in vitro* potency of Tmab-SPP-DM1 and Tmab-MCC-DM1 compared with the free drug L-DM1 after 3 d of treatment (IC_{50} values, nmol/L DM1 equivalents). HER2 expression: SK-BR-3 (HER2 3+), BT-474 (HER2 3+), MCF7 (normal HER2 expression), MDA-MB-468 (HER2-negative).

CSPC Exhibit 1004
Page 212 of 336

Downloaded from cancerres.aacrjournals.org on December 6, 2019. © 2008 American Association for Cancer Research.

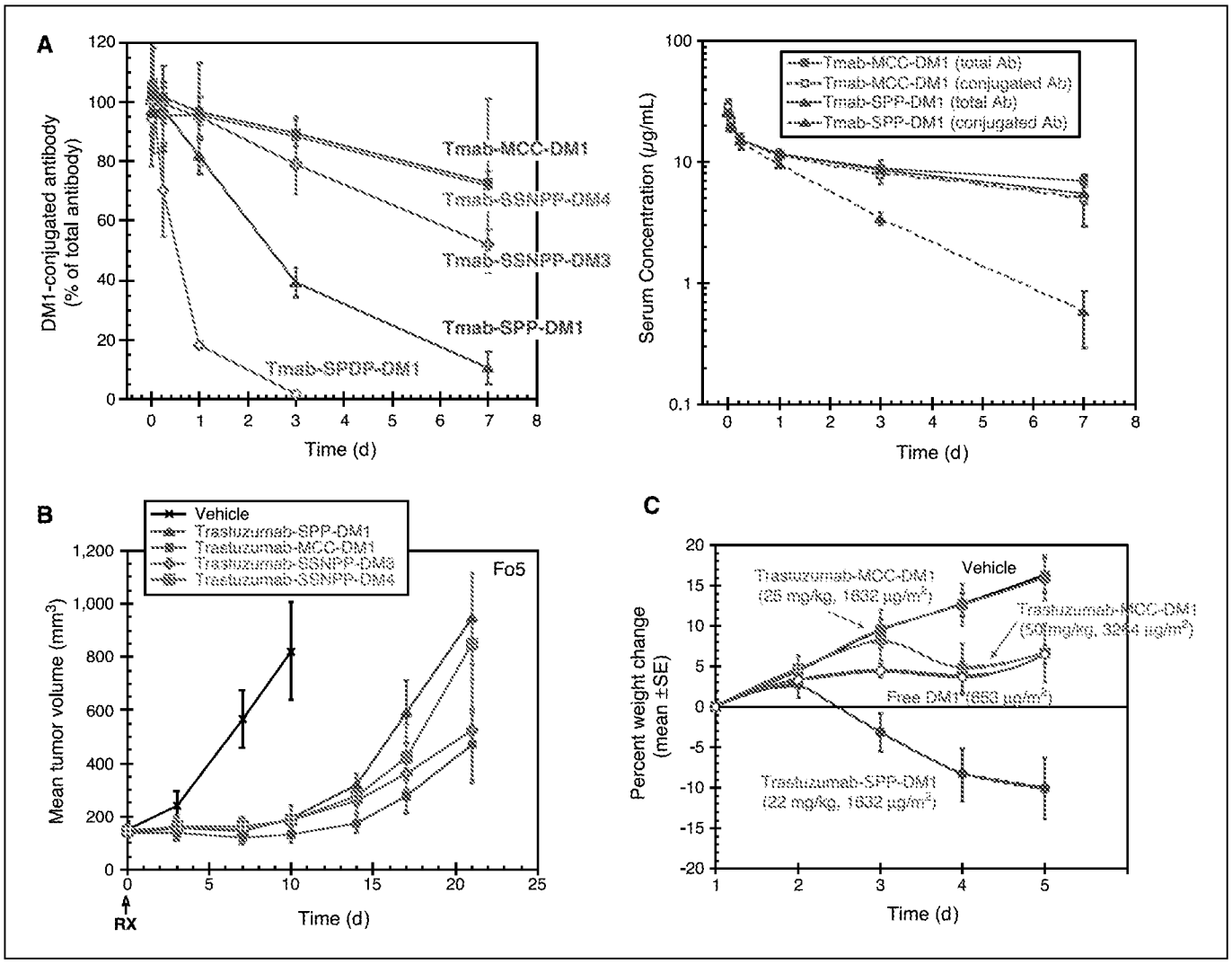


Figure 3. Trastuzumab conjugated to DM1 through the thioether SMCC linker displays better efficacy and pharmacokinetics and lower toxicity than conjugates with disulfide linkers. *A*, pharmacokinetic analysis of trastuzumab-maytansinoid conjugates shows increased serum concentrations of conjugates with more hindered disulfide linkers. Female beige nude mice were given a single i.v. injection (2 mg/kg) of different trastuzumab-maytansinoid conjugates (n = 4 mice per group). Serum samples were collected at various time points after injection for measurement of total and conjugated trastuzumab as described. *B*, increased *in vivo* linker stability results in improved efficacy *in vivo*. Mice bearing mammary tumor transplants from the MMTV-HER2 Fo5 line were given a single i.v. injection (10 mg/kg) of Tmab-SPP-DM1, Tmab-SSNPP-DM3, Tmab-SSNPP-DM4, Tmab-MCC-DM1, or vehicle (n = 7 mice per group), and tumor growth was monitored for 25 d. *C*, Tmab-MCC-DM1 displays the best safety profile, as assessed by changes in body weight, of the conjugates tested. Female Sprague-Dawley rats were given a single i.v. injection of Tmab-MCC-DM1 (1,632 or 3,264 μg/m^2, 25 or 50 mg/kg, respectively), Tmab-SPP-DM1 (1,632 μg/m^2), or free DM1 (653 μg/m^2) on day 1, and body weights were measured daily for 5 d. To give equivalent doses of DM1, animals in the Tmab-SPP-DM1 group were given 22 mg/kg due to the higher drug-antibody ratio (3.6) compared with Tmab-MCC-DM1 (3.2).

subculturing BT-474 tumors grown *in vivo* in the absence of estrogen pellet supplementation. The cell line established in this manner, while maintaining high levels of HER2 expression, had surprisingly become resistant to trastuzumab (G.P. and L.C.) and provides a useful model for determining efficacy of trastuzumab ADCs. These three breast cancer lines showed the same degree of sensitivity to trastuzumab-MCC-DM1 as the sensitive lines SK-BR-3 and BT-474 (Fig. 4*A*). Moreover, tumor lines from different tissues of origin were also responsive to treatment with trastuzumab-MCC-DM1. Calu 3 lung carcinoma (3+ HER2), SK-OV-3 ovarian carcinoma (2+ HER2), and MKN7 gastric carcinoma (2+ HER2) cells (37) displayed dose-dependent inhibition of cell growth upon treatment with the ADC while showing no response to nonconjugated trastuzumab (Fig. 4*B*). In contrast, exposure of normal human cells, HMEC and NHEK, to trastuzumab-MCC-DM1 resulted in minimal growth inhibition, similar to that observed on HER2 nonamplified MCF-7 and MDA-MB-468 breast carcinoma cells (Fig. 4*C*).

Trastuzumab-MCC-DM1 induces cell death in HER2-overexpressing breast cancer cells. Further studies were performed to address the mechanism(s) of action of trastuzumab-MCC-DM1. Cell cycle analysis of conjugate-treated cells resulted in the expected arrest in the G_2-M phase (data not shown), a known mechanism of agents that inhibit microtubule function. We examined the effects on cell death induction, as well. Trastuzumab-MCC-DM1 induced a dose-dependent increase in cell death in SK-BR-3 and BT-474 cells (Fig. 5), with EC_{50} values (in parentheses) similar to those observed in proliferation assays. Release of the

CSPC Exhibit 1004
Page 213 of 336
Downloaded from cancerres.aacrjournals.org on December 6, 2019. © 2008 American Association for Cancer Research.

intracellular enzyme adenylate kinase into the culture medium, an indicator of cellular lysis, was observed after treatment with trastuzumab-MCC-DM1 for 3 days (Fig. 5*A*). Activation of caspase-3/caspase-7 also occurred in these cell lines after a 2-day treatment with trastuzumab-MCC-DM1, indicating induction of apoptotic cell death (Fig. 5*B*). Proteolytic cleavage of 116-kDa PARP with release of the 23-kDa fragment, a known hallmark of apoptotic cell death, was also examined. PARP cleavage was observed in SK-BR-3 cells treated for 48 hours with 100 and 300 ng/mL trastuzumab-MCC-DM1, as well as with 20 nmol/L free DM1, indicating induction of

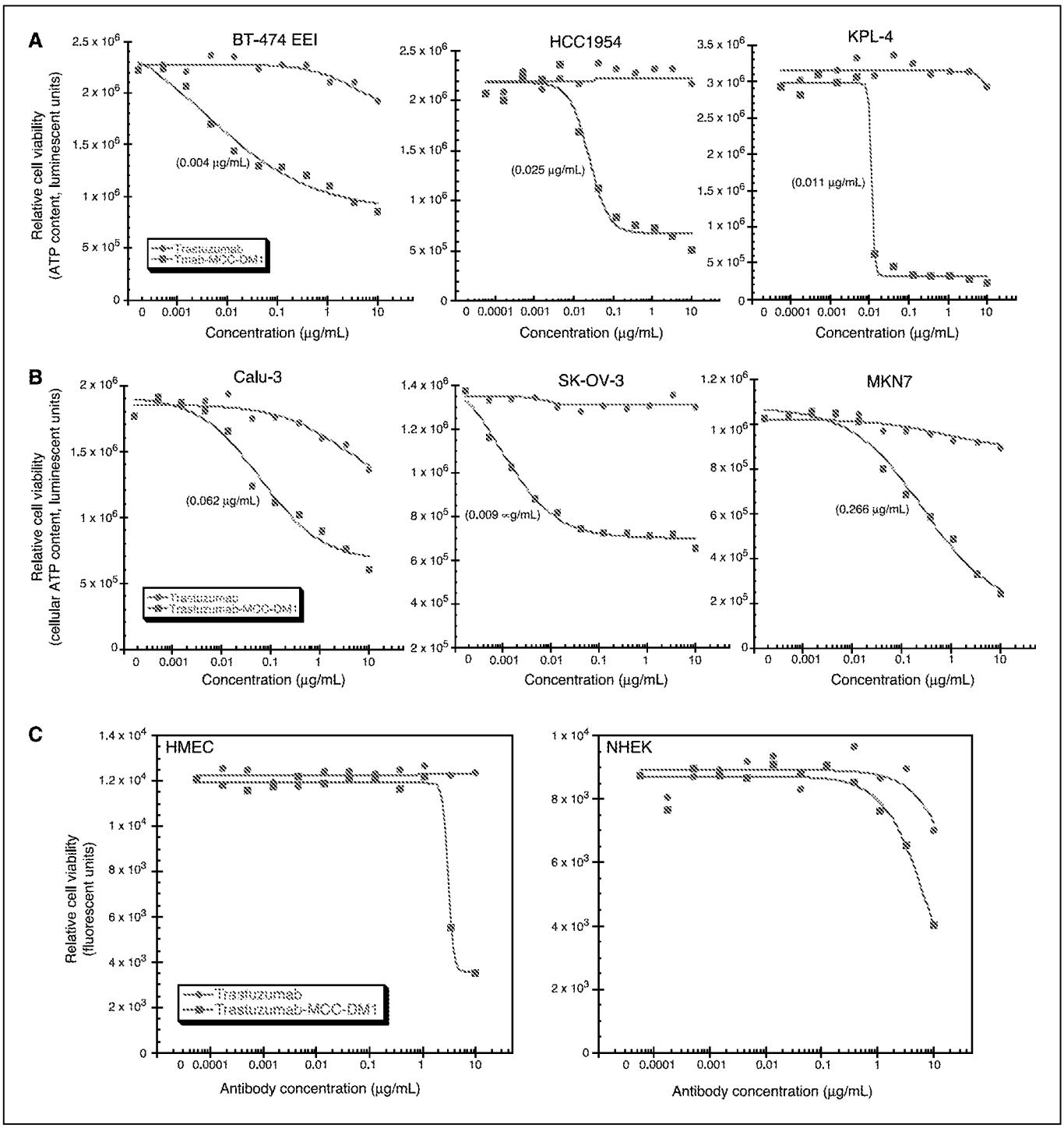


Figure 4. Trastuzumab-MCC-DM1 induces a potent antiproliferative effect in trastuzumab-resistant tumor cells but has no effect on normal human cells. *A*, breast tumor lines BT-474 EEI, HCC1954, and KPL-4 (all HER2 3+). *B*, Calu-3 lung carcinoma (HER2 3+), SK-OV-3 ovarian carcinoma, and MKN7 gastric carcinoma (both HER2 2+). *C*, normal cells HMEC and NHEK were all treated with either trastuzumab or trastuzumab-MCC-DM1 for 3 d, and relative proliferation was determined using CellTiter-Glo. IC_{50} values for each cell line are in parentheses.

CSPC Exhibit 1004
Page 214 of 336

Downloaded from cancerres.aacrjournals.org on December 6, 2019. © 2008 American Association for Cancer Research.

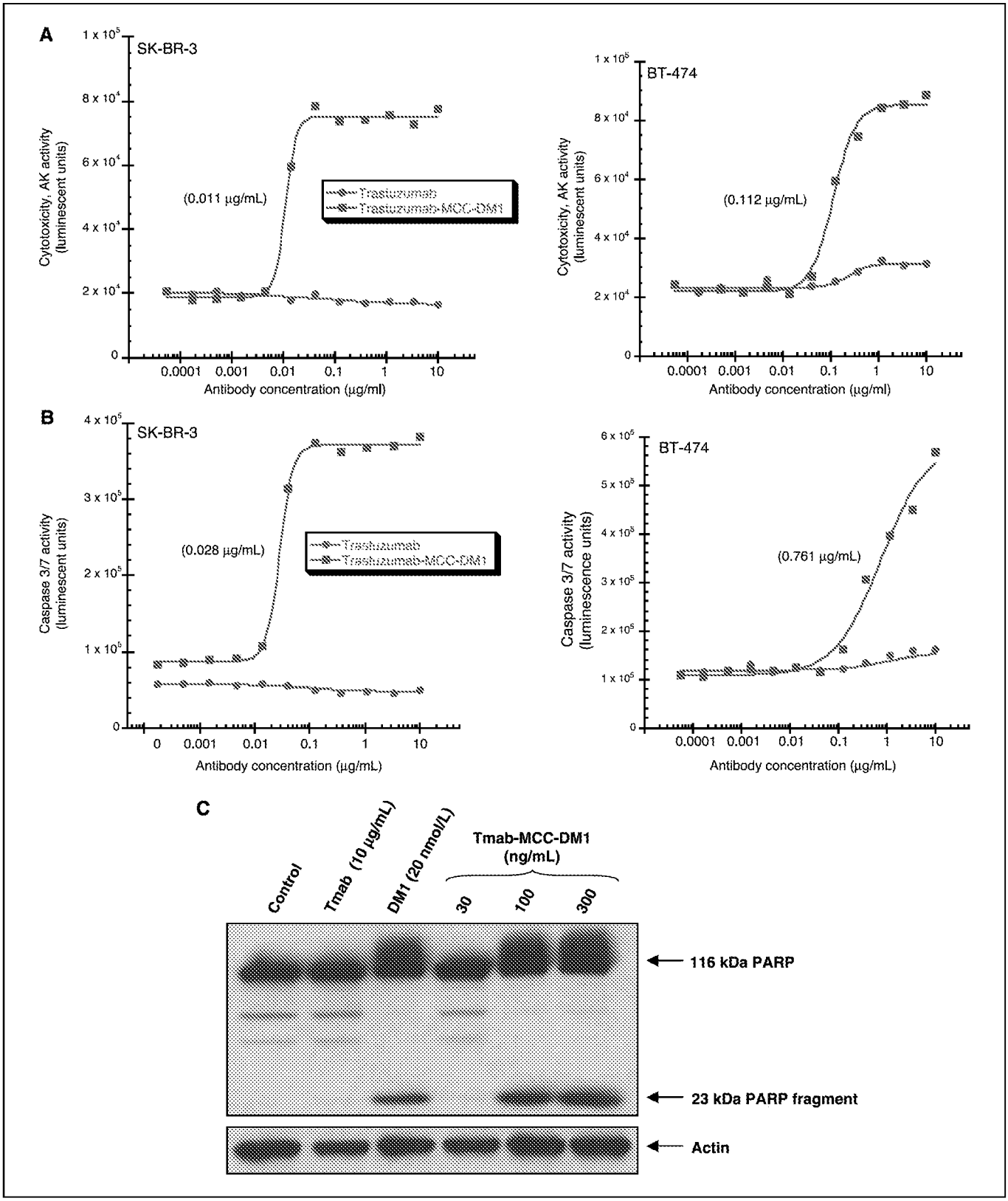


Figure 5. Trastuzumab-MCC-DM1, but not trastuzumab, induces cell lysis and apoptosis in SK-BR-3 and BT-474 breast tumor cells. Cytotoxic response (*A*), as measured by adenylate kinase release into the culture medium, and apoptosis induction (*B*), measured by activation of caspase-3/caspase-7, after treatment with trastuzumab or trastuzumab-MCC-DM1 for 3 d (cytotoxicity) or 2 d (caspase-3/caspase-7 activation). EC_{50} values are shown in parentheses. *C*, trastuzumab-MCC-DM1 and free DM1 induce PARP cleavage, whereas unconjugated trastuzumab has no effect. SK-BR-3 cells were treated with 10 μg/mL trastuzumab; 30, 100, or 300 ng/mL Tmab-MCC-DM1 (0.02, 0.67, and 2.0 nmol/L, respectively) or 20 nmol/L free DM1 for 48 h. Cells were then lysed for Western blot analysis of cleaved PARP. Appearance of the 23-kDa PARP fragment indicates apoptotic activation of PARP cleavage.

CSPC Exhibit 1004
Page 215 of 336

Downloaded from cancerres.aacrjournals.org on December 6, 2019. © 2008 American Association for Cancer Research.

apoptosis (Fig. 5C). Thus, in contrast to the cytostatic action of trastuzumab (7, 30), these data show that treatment of HER2-amplified breast tumor cells with trastuzumab-MCC-DM1 results in apoptotic cell death and cellular lysis.

Trastuzumab-MCC-DM1 inhibits growth and causes tumor regression in animal models of HER2-positive breast cancer. The *in vivo* efficacy of trastuzumab-MCC-DM1 was compared with trastuzumab in three mouse models of HER2-overexpressing breast cancer. KPL-4 human breast tumor cells were implanted into the mammary fat pads of SCID beige mice and tumors allowed to grow to an average size of 300 mm^3. Mice were then treated weekly with 15 mg/kg trastuzumab i.p. or given a single i.v. injection of 15 mg/kg trastuzumab-MCC-DM1. Complete tumor regression for the duration of the study (126 days), as determined by caliper measurement, was observed in mice receiving trastuzumab-MCC-DM1, whereas unconjugated trastuzumab induced an initial decrease in tumor size, followed by regrowth upon cessation of treatment (Fig. 6A). Although the KPL4 cell line did not respond to trastuzumab *in vitro*, we have observed with other cell lines, such as Calu 3, response to trastuzumab *in vivo*, despite lack of responsiveness *in vitro*.

The activity of trastuzumab-MCC-DM1 was further investigated in two trastuzumab-insensitive mouse xenograft models. After transplantation of MMTV-HER2 Fo5 mammary tumor explants,

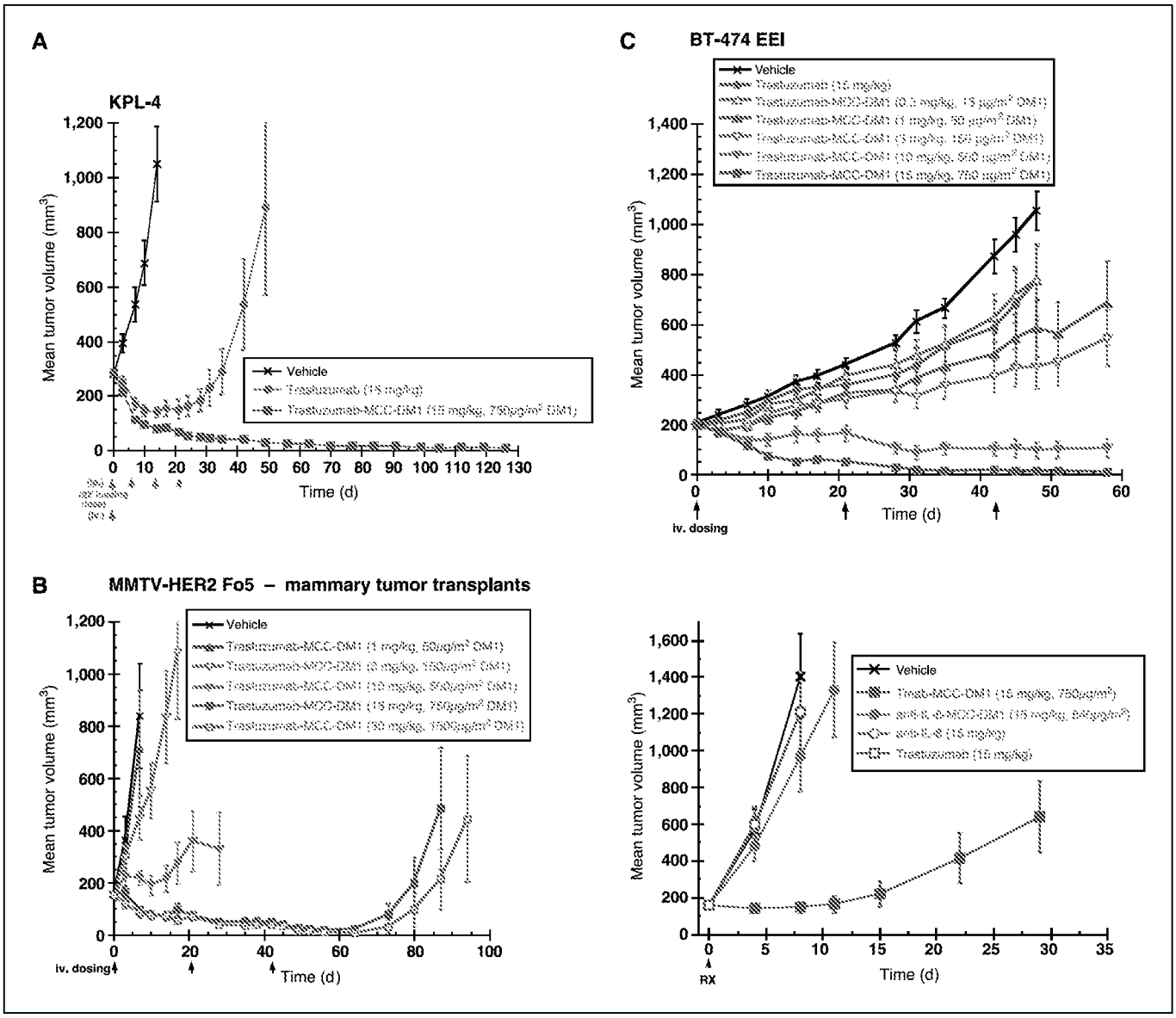


Figure 6. *In vivo* efficacy of trastuzumab-DM1 in trastuzumab-sensitive and trastuzumab-resistant breast tumor models. *A*, KPL-4 human breast cancer cells grown as tumors in SCID beige mice show complete regression after a single i.v. injection of trastuzumab-MCC-DM1 (15 mg/kg, 750 μg/m^2 DM1) compared with transient regression followed by regrowth after weekly treatment with 15 mg/kg trastuzumab ($n = 8$ mice per group). *B*, MMTV-HER2 transgenic transplants from trastuzumab-resistant line Fo5 respond to trastuzumab-MCC-DM1 in a dose-dependent manner (*left*). Injections were given once every 3 wk for three total injections at doses of 1, 3, 10, 15, and 30 mg/kg (50, 150, 500, 750, and 1,500 μg/m^2 DM1, respectively); $n = 8$ mice per group. Isotype-matched control ADC, anti–IL-8-MCC-DM1 (15 mg/kg, 840 μg/m^2 DM1; drug-antibody ratio, 3.8) showed no antitumor activity (*right*). *C*, dose-response of trastuzumab-resistant xenograft line BT-474 EEI to trastuzumab-MCC-DM1. Nude mice with established tumors were dosed i.v. with Tmab-MCC-DM1 (0.3, 1, 3, 10, or 15 mg/kg) or with 15 mg/kg trastuzumab once every 3 wk for a total of three injections, $n = 10$ mice per group.

CSPC Exhibit 1004
Page 216 of 336

Downloaded from cancerres.aacrjournals.org on December 6, 2019. © 2008 American Association for Cancer Research.

tumor-bearing nude mice were treated once every 3 weeks with 1, 3, 10, 15, or 30 mg/kg trastuzumab-MCC-DM1 (50, 150, 500, 750, and 1500 $\mu g/m^2$ of conjugated DM1, respectively; Fig. 6*B*). Doses of 1 and 3 mg/kg showed no antitumor activity, whereas administration of 10 mg/kg resulted in partial inhibition of tumor growth (this treatment group was discontinued after 30 days due to several mice having tumors in excess of 1,000 mm^3). Tumors in mice treated with either 15 or 30 mg/kg trastuzumab-MCC-DM1 regressed during the entire course of treatment. Regrowth was observed ~30 days after discontinuation of treatment. Previous studies have shown that retreatment with trastuzumab-MCC-DM1 results in a further decrease in tumor size, indicating that acquisition of resistance did not occur (data not shown). In contrast, treatment with 15 mg/kg of an irrelevant control ADC, anti-IL-8-MCC-DM1, resulted in no tumor growth inhibition (Fig. 6*B, right*).

The second trastuzumab-resistant model used the BT-474 EEI tumor-derived line. The data in Fig. 6*C* show the effects on BT-474 EEI tumor growth of different doses of trastuzumab-MCC-DM1 given once every 3 weeks for three total doses. Dose-dependent inhibition of tumor growth was observed, with 0.3, 1 and 3 mg/kg causing tumor growth delay, whereas 10 and 15 mg/kg doses resulted in tumor regression. Thus, trastuzumab-MCC-DM1 shows potent activity in trastuzumab-sensitive and trastuzumab-insensitive mouse xenograft models, with 15 mg/kg as the maximum efficacious dose.

Discussion

The anatomy of an antibody–cytotoxic drug conjugate can be divided into three general components: the antibody, the linker, and the cytotoxic drug. The efficacy of any such conjugate is dictated in part by the differential expression of the target antigen in tumor versus normal tissue. HER2 is a clinically validated target for the treatment of breast cancer. Trastuzumab (5, 35–41) and, more recently, lapatinib (42) are approved for clinical use in women whose breast cancer overexpresses HER2. To be maximally effective, both trastuzumab and lapatinib require a functional or signaling HER2 receptor, which drives key biological aspects of the tumor. It is postulated that patients whose tumors progress on these therapies may acquire alterations that activate signal transduction pathways either downstream or parallel to HER2. At present, available data indicate that cancer cells do not lose HER2 expression when they become refractory to HER2-directed therapies (14, 16). For that reason, a trastuzumab conjugate, which simply uses HER2 as an address for the delivery of a potent cytotoxic agent, may offer promise as an effective therapeutic modality.

We observed that anti-HER2 ADCs display impressive potency *in vitro* and *in vivo* and are active in trastuzumab-refractory models of HER2-amplified breast cancer. However, the tolerability of these conjugates varies considerably and is intrinsically dependent upon the chemical nature of the linker and the cytotoxic agent. In this report, we describe our characterization of several trastuzumab-maytansinoid conjugates with a special emphasis on linker chemistry. The disulfide-linked DM1-containing ADCs were designed to allow for endosomal reduction of the disulfide to result in intracellular release of the cytotoxic agent. Moreover, in antigen-expressing tumor cells, DM1 derived from ADCs designed with a disulfide linker can be released by the tumor cells and initiate a "bystander" killing effect (34). However, *in vivo*, the liberated DM1 is also rapidly cleared and, thus, may not be available for prolonged antitumor effects (43). Our results with the thioether (MCC) linker contradicted the hypothesis that selective release of DM1 by intracellular reduction of the disulfide bond in a trastuzumab-disulfide-DM1 conjugate was necessary for efficacy. Similar to huC242-MCC-DM1, a thioether-containing ADC that targets the CanAg antigen (34, 44), trastuzumab-MCC-DM1 is internalized upon binding to HER2-overexpressing tumor cells and is postulated to undergo intracellular proteolytic degradation to release active maytansinoid. As expected, the activity of trastuzumab-MCC-DM1 is blocked in the presence of protease inhibitors in cell culture experiments (data not shown). Subsequently, it has been shown that HER2 itinerary allows for lysosomal degradation of HER2-directed ADCs (45). Thus, it is likely that the trastuzumab antibody component of the trastuzumab-MCC-DM1 conjugate undergoes proteolytic degradation in the lysosome and that lysine-MCC-DM1 is a major active metabolite, as has been shown for huC242-MCC-DM1 (44). In fact, preliminary data from studies investigating the metabolism of [^{3}H]trastuzumab-MCC-DM1 in BT-474 EEI cells show lysine-N^{ε}-MCC-DM1 as the predominant metabolite (data not shown). The primary active metabolite, lysine-MCC-DM1, does not readily cross the plasma membranes of neighboring cells and, therefore, does not elicit a bystander effect (34, 44).

Non–disulfide-containing ADCs show increased pharmacokinetic exposure in both rats and cynomolgus monkeys (data not shown). This increase in conjugate exposure did not lead to an increase in either target-dependent or target-independent toxicity. As expected, trastuzumab conjugated to DM1 through the thioether MCC linker was better tolerated compared with the disulfide (SPP) linked to DM1, with regard to toxicity signals. Despite the improved pharmacokinetic profile of DM3 and DM4-containing trastuzumab conjugates, the disulfide linkage would likely render these conjugates less tolerable than the thioether-linked trastuzumab conjugate.

In summary, trastuzumab-MCC-DM1 is shown to be efficacious in trastuzumab-sensitive and trastuzumab-insensitive models of HER2-overexpressing cancer. Of equal importance, trastuzumab-MCC-DM1 has a favorable pharmacokinetic and safety profile compared with disulfide-linked trastuzumab conjugates and represents an important new approach for treating HER2-amplified human cancers. Given these promising results, early clinical studies are currently under way to assess the safety and efficacy of trastuzumab-MCC-DM1 in patients whose disease has progressed through HER2-directed therapies.

Disclosure of Potential Conflicts of Interest

G.D. Lewis Phillips, G. Li, D.L. Dugger, L.M. Crocker, K.L. Parsons, E. Mai, W. L.T. Wong, F.S. Jacobson, S.R. Kenkare-Mitra, S.D. Spencer, and M.X. Sliwkowski are employees of and shareholders in Genentech, Inc. W.A. Blättler, J.M. Lambert, R.V.J. Chari, and R.J. Lutz are employees of and shareholders in ImmunoGen, Inc. H. Koeppen is a former Genentech, Inc. employee.

Acknowledgments

Received 5/19/2008; revised 7/23/2008; accepted 9/8/2008.

The costs of publication of this article were defrayed in part by the payment of page charges. This article must therefore be hereby marked *advertisement* in accordance with 18 U.S.C. Section 1734 solely to indicate this fact.

This article is dedicated to our dear colleague, Dr. Ralph Schwall, who passed away on August 26, 2005.

We thank Drs. Vishva Dixit, Paul Polakis, Richard Scheller, and Robert Cohen for their support, interest, and valuable discussions; Allison Bruce for graphics support; and Dr. J. Kurebayashi for providing the KPL4 cell line.

CSPC Exhibit 1004
Page 217 of 336

Downloaded from cancerres.aacrjournals.org on December 6, 2019. © 2008 American Association for Cancer Research.

References

1. Yarden Y, Sliwkowski MX. Untangling the ErbB signalling network. Nat Rev Mol Cell Biol 2001;2:127–37.
2. Yarden Y. The EGFR family and its ligands in human cancer. Signaling mechanisms and therapeutic opportunities. Eur J Cancer 2001;37 Suppl 4:S3–8.
3. Slamon DJ, Clark GM, Wong SG, Levin WJ, Ullrich A, McGuire WL. Human breast cancer: correlation of relapse and survival with amplification of the HER-2/neu oncogene. Science 1987;235:177–82.
4. Slamon DJ, Godolphin W, Jones LA, et al. Studies of the HER-2/neu proto-oncogene in human breast and ovarian cancer. Science 1989;244:707–12.
5. Slamon DJ, Leyland-Jones B, Shak S, et al. Use of chemotherapy plus a monoclonal antibody against HER2 for metastatic breast cancer that overexpresses HER2. N Engl J Med 2001;344:783–92.
6. Smith I, Procter M, Gelber RD, et al. 2-year follow-up of trastuzumab after adjuvant chemotherapy in HER2-positive breast cancer: a randomised controlled trial. Lancet 2007;369:29–36.
7. Sliwkowski MX, Lofgren JA, Lewis GD, Hotaling TE, Fendly BM, Fox JA. Nonclinical studies addressing the mechanism of action of trastuzumab (Herceptin). Semin Oncol 1999;26:60–70.
8. Hudis CA. Trastuzumab-mechanism of action and use in clinical practice. N Engl J Med 2007;357:39–51.
9. Nahta R, Yu D, Hung MC, Hortobagyi GN, Esteva FJ. Mechanisms of disease: understanding resistance to HER2-targeted therapy in human breast cancer. Nat Clin Pract Oncol 2006;3:269–80.
10. Chan CT, Metz MZ, Kane SE. Differential sensitivities of trastuzumab (Herceptin)-resistant human breast cancer cells to phosphoinositide-3 kinase (PI-3K) and epidermal growth factor receptor (EGFR) kinase inhibitors. Breast Cancer Res Treat 2005;91:187–201.
11. Clark AS, West K, Streicher S, Dennis PA. Constitutive and inducible Akt activity promotes resistance to chemotherapy, trastuzumab, or tamoxifen in breast cancer cells. Mol Cancer Ther 2002;1:707–17.
12. Nagata Y, Lan KH, Zhou X, et al. PTEN activation contributes to tumor inhibition by trastuzumab, and loss of PTEN predicts trastuzumab resistance in patients. Cancer Cell 2004;6:117–27.
13. Lu Y, Zi X, Zhao Y, Mascarenhas D, Pollak M. Insulin-like growth factor-I receptor signaling and resistance to trastuzumab (Herceptin). J Natl Cancer Inst 2001;93:1852–7.
14. Nahta R, Yuan LX, Zhang B, Kobayashi R, Esteva FJ. Insulin-like growth factor-I receptor/human epidermal growth factor receptor 2 heterodimerization contributes to trastuzumab resistance of breast cancer cells. Cancer Res 2005;65:11118–28.
15. Motoyama AB, Hynes NE, Lane HA. The efficacy of ErbB receptor-targeted anticancer therapeutics is influenced by the availability of epidermal growth factor-related peptides. Cancer Res 2002;62:3151–8.
16. Ritter CA, Perez-Torres M, Rinehart C, et al. Human breast cancer cells selected for resistance to trastuzumab *in vivo* overexpress epidermal growth factor receptor and ErbB ligands and remain dependent on the ErbB receptor network. Clin Cancer Res 2007;13:4909–19.
17. Anido J, Scaltriti M, Bech Serra JJ, et al. Biosynthesis of tumorigenic HER2 C-terminal fragments by alternative initiation of translation. EMBO J 2006;25:3234–44.
18. Saez R, Molina MA, Ramsey EE, et al. p95HER-2 predicts worse outcome in patients with HER-2-positive breast cancer. Clin Cancer Res 2006;12:424–31.
19. Polakis P. Arming antibodies for cancer therapy. Curr Opin Pharmacol 2005;5:382–7.
20. Lambert JM. Drug-conjugated monoclonal antibodies for the treatment of cancer. Curr Opin Pharmacol 2005;5:543–9.
21. Payne G. Progress in immunoconjugate cancer therapeutics. Cancer Cell 2003;3:207–12.
22. Wu AM, Senter PD. Arming antibodies: prospects and challenges for immunoconjugates. Nat Biotechnol 2005;23:1137–46.
23. Bross PF, Beitz J, Chen G, et al. Approval summary: gemtuzumab ozogamicin in relapsed acute myeloid leukemia. Clin Cancer Res 2001;7:1490–6.
24. Chari RV, Martell BA, Gross JL, et al. Immunoconjugates containing novel maytansinoids: promising anticancer drugs. Cancer Res 1992;52:127–31.
25. Remillard S, Rebhun LI, Howie GA, Kupchan SM. Antimitotic activity of the potent tumor inhibitor maytansine. Science 1975;189:1002–5.
26. Helft PR, Schilsky RL, Boke FJ, et al. A phase I study of cantuzumab mertansine administered as a single intravenous infusion once weekly in patients with advanced solid tumors. Clin Cancer Res 2004;10:4363–8.
27. Tijink BM, Buter J, de Bree R, et al. A phase I dose escalation study with anti-CD44v6 bivatuzumab mertansine in patients with incurable squamous cell carcinoma of the head and neck or esophagus. Clin Cancer Res 2006;12:6064–72.
28. Tolcher AW, Ochoa L, Hammond LA, et al. Cantuzumab mertansine, a maytansinoid immunoconjugate directed to the CanAg antigen: a phase I, pharmacokinetic, and biologic correlative study. J Clin Oncol 2003;21:211–22.
29. Baselga J, Norton L, Albanell J, Kim Y-M, Mendelsohn J. Recombinant humanized anti-HER2 antibody (Herceptin™) enhances the antitumor activity of paclitaxel and doxorubicin against HER2/neu overexpressing human breast cancer xenografts. Cancer Res 1998;58:2825–31.
30. Pegram M, Hsu S, Lewis G, et al. Inhibitory effects of combinations of HER-2/neu antibody and chemotherapeutic agents used for treatment of human breast cancers. Oncogene 1999;18:2241–51.
31. Konecny GE, Thomssen C, Lück HJ, et al. HER-2/neu gene amplificaton and response to paclitaxel in patients with metastatic breast cancer. J Natl Cancer Inst 2004;96:1141–51.
32. Burstein HJ, Keshaviah A, Baron AD, et al. Trastuzumab plus vinorelbine or taxane chemotherapy for HER2-overexpressing metastatic breast cancer: the trastuzumab and vinorelbine or taxane study. Cancer 2007;110:965–72.
33. Kurebayashi J, Otsuki T, Tang CK, et al. Isolation and characterization of a new human breast cancer cell line, KPL-4, expressing the Erb B family receptors and interleukin-6. Br J Cancer 1999;79:707–17.
34. Kovtun YV, Audette CA, Ye Y, et al. Antibody-drug conjugates designed to eradicate tumors with homogeneous and heterogeneous expression of the target antigen. Cancer Res 2006;66:3214–21.
35. Finkle D, Quan ZR, Asghari V, et al. HER2-targeted therapy reduces incidence and progression of midlife mammary tumors in female murine mammary tumor virus huHER2-transgenic mice. Clin Cancer Res 2004;10:2499–511.
36. Austin CD, Wen X, Gazzard L, Nelson C, Scheller RH, Scales SJ. Oxidizing potential of endosomes and lysosomes limits intracellular cleavage of disulfide-based antibody-drug conjugates. Proc Natl Acad Sci U S A 2005;102:17987–92.
37. Lewis GD, Figari I, Fendly B, et al. Differential responses of human tumor cell lines to anti-p185HER2 monoclonal antibodies. Cancer Immunol Immunother 1993;37:255–63.
38. Vogel CL, Cobleigh MA, Tripathy D, et al. Efficacy and safety of trastuzumab as a single agent in first-line treatment of HER2-overexpressing metastatic breast cancer. J Clin Oncol 2002;20:719–26.
39. Cobleigh MA, Vogel CL, Tripathy D, et al. Multinational study of the efficacy and safety of humanized anti-HER2 monoclonal antibody in women who have HER2-overexpressing metastatic breast cancer that has progressed after chemotherapy for metastatic disease. J Clin Oncol 1999;17:2639–48.
40. Romond EH, Perez EA, Bryant J, et al. Trastuzumab plus adjuvant chemotherapy for operable HER2-positive breast cancer. N Engl J Med 2005;353:1673–84.
41. Piccart-Gebhart MJ, Procter M, Leyland-Jones B, et al. Trastuzumab after adjuvant chemotherapy in HER2-positive breast cancer. N Engl J Med 2005;353:1659–72.
42. Geyer CE, Forster J, Lindquist D, et al. Lapatinib plus capecitabine for HER2-positive advanced breast cancer. N Engl J Med 2006;355:2733–43.
43. Erickson HK, Park PU, Widdison WC, et al. Antibody-maytansinoid conjugates are activated in targeted cancer cells by lysosomal degradation and linker-dependent intracellular processing. Cancer Res 2006;66:4426–33.
44. Xie H, Audette C, Hoffee M, Lambert JM, Blättler WA. Pharmacokinetics and biodistribution of the antitumor immunoconjugate, cantuzumab mertansine (huC242-1), and its two components in mice. J Pharmacol Exp Ther 2004;308:1073–82.
45. Austin CD, De Maziere AM, Pisacane PI, et al. Endocytosis and sorting of ErbB2 and the site of action of cancer therapeutics trastuzumab and geldanamycin. Mol Biol Cell 2004;15:5268–82.

CSPC Exhibit 1004
Page 218 of 336

Downloaded from cancerres.aacrjournals.org on December 6, 2019. © 2008 American Association for Cancer Research.

AACR American Association for Cancer Research

Cancer Research

The Journal of Cancer Research (1916–1930) | The American Journal of Cancer (1931–1940)

Targeting HER2-Positive Breast Cancer with Trastuzumab-DM1, an Antibody–Cytotoxic Drug Conjugate

Gail D. Lewis Phillips, Guangmin Li, Debra L. Dugger, et al.

Cancer Res 2008;68:9280-9290.

Updated version	Access the most recent version of this article at: http://cancerres.aacrjournals.org/content/68/22/9280

Cited articles	This article cites 45 articles, 22 of which you can access for free at: http://cancerres.aacrjournals.org/content/68/22/9280.full#ref-list-1
Citing articles	This article has been cited by 100 HighWire-hosted articles. Access the articles at: http://cancerres.aacrjournals.org/content/68/22/9280.full#related-urls

E-mail alerts	Sign up to receive free email-alerts related to this article or journal.
Reprints and Subscriptions	To order reprints of this article or to subscribe to the journal, contact the AACR Publications Department at pubs@aacr.org.
Permissions	To request permission to re-use all or part of this article, use this link http://cancerres.aacrjournals.org/content/68/22/9280. Click on "Request Permissions" which will take you to the Copyright Clearance Center's (CCC) Rightslink site.

CSPC Exhibit 1004
Page 219 of 336

Downloaded from cancerres.aacrjournals.org on December 6, 2019. © 2008 American Association for Cancer Research.

frontiers in Immunology

REVIEW
published: 12 December 2016
doi: 10.3389/fimmu.2016.00580

Advances in Therapeutic Fc Engineering – Modulation of IgG-Associated Effector Functions and Serum Half-life

*Abhishek Saxena and Donghui Wu**

Laboratory of Antibody Engineering, Shanghai Institute for Advanced Immunochemical Studies, ShanghaiTech University, Shanghai, China

Today, monoclonal immunoglobulin gamma (IgG) antibodies have become a major option in cancer therapy especially for the patients with advanced or metastatic cancers. Efficacy of monoclonal antibodies (mAbs) is achieved through both its antigen-binding fragment (Fab) and crystallizable fragment (Fc). Fab can specifically recognize tumor-associated antigen (TAA) and thus modulate TAA-linked downstream signaling pathways that may lead to the inhibition of tumor growth, induction of tumor apoptosis, and differentiation. The Fc region can further improve mAbs' efficacy by mediating effector functions such as antibody-dependent cellular cytotoxicity, complement-dependent cytotoxicity, and antibody-dependent cell-mediated phagocytosis. Moreover, Fc is the region interacting with the neonatal Fc receptor in a pH-dependent manner that can slow down IgG's degradation and extend its serum half-life. Loss of the antibody Fc region dramatically shortens its serum half-life and weakens its anticancer effects. Given the essential roles that the Fc region plays in the modulation of the efficacy of mAb in cancer treatment, Fc engineering has been extensively studied in the past years. This review focuses on the recent advances in therapeutic Fc engineering that modulates its related effector functions and serum half-life. We also discuss the progress made in aglycosylated mAb development that may substantially reduce the cost of manufacture but maintain similar efficacies as conventional glycosylated mAb. Finally, we highlight several Fc engineering-based mAbs under clinical trials.

Keywords: antibody Fc region, ADCC, CDC, ADCP, serum half-life, aglycosylated antibody, FcRn, cancer therapy

OPEN ACCESS

Edited by:
Tianlei Ying,
Fudan University, China

Reviewed by:
Pierre Guermonprez,
King's College London, UK
Estrella Mariel Levy,
National Scientific and Technical Research Council, Argentina
Shane Miersch,
University of Toronto, Canada

****Correspondence:***
Donghui Wu
wudh@shanghaitech.edu.cn

Specialty section:
This article was submitted to Immunotherapies and Vaccines, a section of the journal Frontiers in Immunology

Received: *12 July 2016*
Accepted: *24 November 2016*
Published: *12 December 2016*

Citation:
Saxena A and Wu D (2016) Advances in Therapeutic Fc Engineering – Modulation of IgG-Associated Effector Functions and Serum Half-life. Front. Immunol. 7:580. doi: 10.3389/fimmu.2016.00580

INTRODUCTION

Monoclonal antibodies (mAbs) can target tumors through specific recognition of tumor-associated antigens and subsequent recruitment of effector elements including macrophages, dendritic cells, natural killer (NK) cells, T-cells, and the complement pathway components (1). Such recruitments are achieved by interactions among the immunoglobulin gamma (IgG)-crystallizable fragment (Fc) and the immune cell receptors like Fcγ receptors (FcγRs) and the complement protein C1q of the complement system (2–4). These interactions lead to the activation of immune cells for enhanced antibody-dependent cellular cytotoxicity (ADCC)/antibody-dependent cell-mediated phagocytosis (ADCP), formation of the membrane attack complex, and more efficient presentation of antigen

CSPC Exhibit 1004
Page 220 of 336

to the dendritic cells (1). Through a recycling mechanism, the neonatal Fc receptor (FcRn) prolongs the half-life of mAbs in a pH-dependent interaction with the Fc region (5). The schematic of overall IgG structure and its binding regions with FcγRs, C1q, and FcRn is depicted in **Figure 1**.

The FcγRs, consisting of FcγRI (CD64), FcγRII (CD32), and FcγRIII (CD16) classes, are heterogeneous in terms of their cellular expression and Fc binding affinities (1, 6). FcγRI binds to the Fc region with K_D ~10^{-8}–10^{-9} M and is expressed on mononuclear phagocytes, dendritic cells, and IFN-γ-activated neutrophils (1, 7, 8). FcγRII binds to the Fc region with relatively lower affinity (K_D ~10^{-7} M) and exists in five isoforms; among them, activating (FcγRIIa, harboring an immunoreceptor tyrosine-based activation motif on neutrophils) or inhibitory (FcγRIIb, harboring an immunoreceptor tyrosine-based inhibitory motif predominantly on B-lymphocytes) are critical for immune regulation (1, 7). FcγRIII, expressed in two isoforms, binds the Fc region with the lowest affinities (K_D ~10^{-6} M) (1, 7). Among these, FcγRIIIa has a moderate Fc binding allele (V158) and a low binding allele (F158), and is expressed on NK cells, macrophages, and T-cell subsets and activates NK and T cell-mediated ADCC response (1, 6, 7); FcγRIIIb is exclusively present on neutrophils and lacks signal generation capacity (1, 7).

Crystal structures of Fc in complex with FcγRI (9) (**Figure 2A**), Fc in complex with FcγRII (10) (**Figure 2B**), and Fc in complex with FcγRIII (11) (**Figure 2C**) reveal that the FcγRs' interaction sites on Fc are all located within the lower hinge-upper heavy chain constant domain 2 (CH2). Furthermore, the binding affinity of Fc region to FcγRs also varies with the IgG subclasses (12).

The C1q is a multisubunit protein of the complement system (3). It uses one of its six heads to establish a low-affinity (~10^{-6} M) interaction with the lower hinge-upper CH2 domain of the Fc region (3). Crystal structure of the human C1q head revealed that it is assembled with a heterotrimer globular architecture (14). Though the molecular basis of how the C1q head recognizes the Fc region is not known at the atomic resolution, Schneider and Zacharias (15) proposed a working model of C1q in complex with Fc based on known experimental data, docking, and molecular dynamics simulation. According to this model, upon initial weak interaction between the C1q head and the Fc region, IgGs can aggregate while recognizing "multiple epitopes" on the antigen surface and thus give many C1q molecules an opportunity to bind to their Fc regions, which enhance the "cumulative affinity" to ~10^{-9} M (3, 15). This leads to the deposition of complement component 3 (C3b) on the target cell and ultimate formation of the membrane attack complex that disrupts the lipid bilayer of the target cell, promotes cytolysis, and completes complement dependent cytotoxicity (CDC) (16, 17).

The pharmacokinetic profiles of antibodies vary among subclasses and are related to the structural features of the Fc region (18, 19). It is known that the serum half-life of IgG subclasses (IgG1, IgG2, and IgG4) is ~23 days as compared to 2–6 days for IgG3 and other Ig classes (18, 19). The Fc region spanning the interface of CH2 and CH3 domains interacts with the FcRn in the placenta, liver, mammary glands, and adult intestine to regulate IgG homeostasis and deliver maternal IgG across the placenta to the fetus (5). This interaction is favored by an acidic environment of the endosome after IgG is pinocytosed

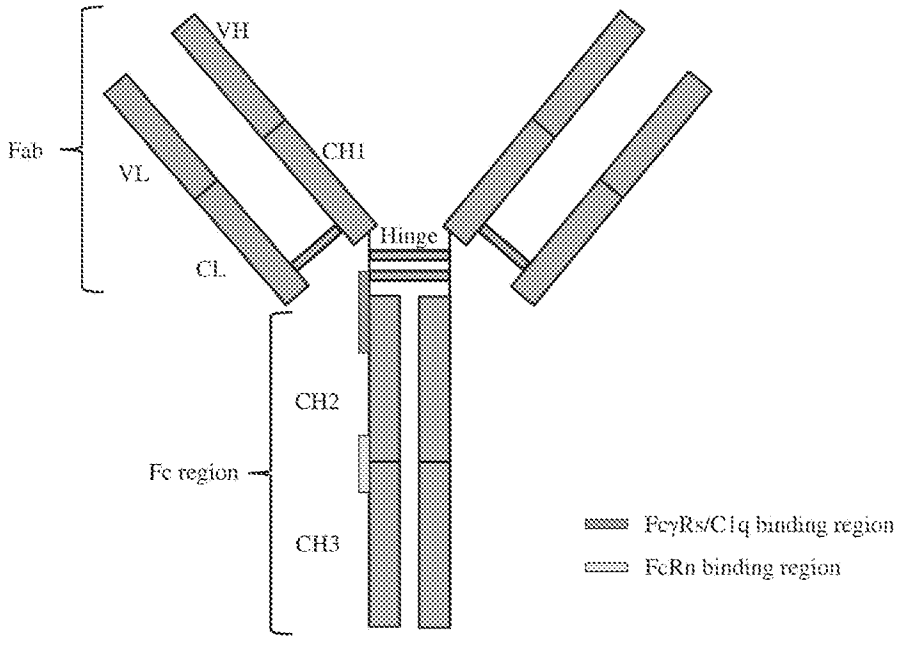


FIGURE 1 | Schematics of immunoglobulin gamma overall structure and its binding regions with FcγRs, C1q, and FcRn. The constituent heavy [VH, CH1, hinge, CH2, and CH3 (gray)] and light chains [VL and CL (gray)] linked by inter-chain disulfide bonds are shown. The site at which FcγRs/C1q interacts with the crystallizable fragment (Fc) region is located in the lower hinge-upper CH2 (green rectangle); the site at which FcRn interacts with the Fc region is located in the interface of CH2–CH3 (yellow rectangle).

CSPC Exhibit 1004
Page 221 of 336

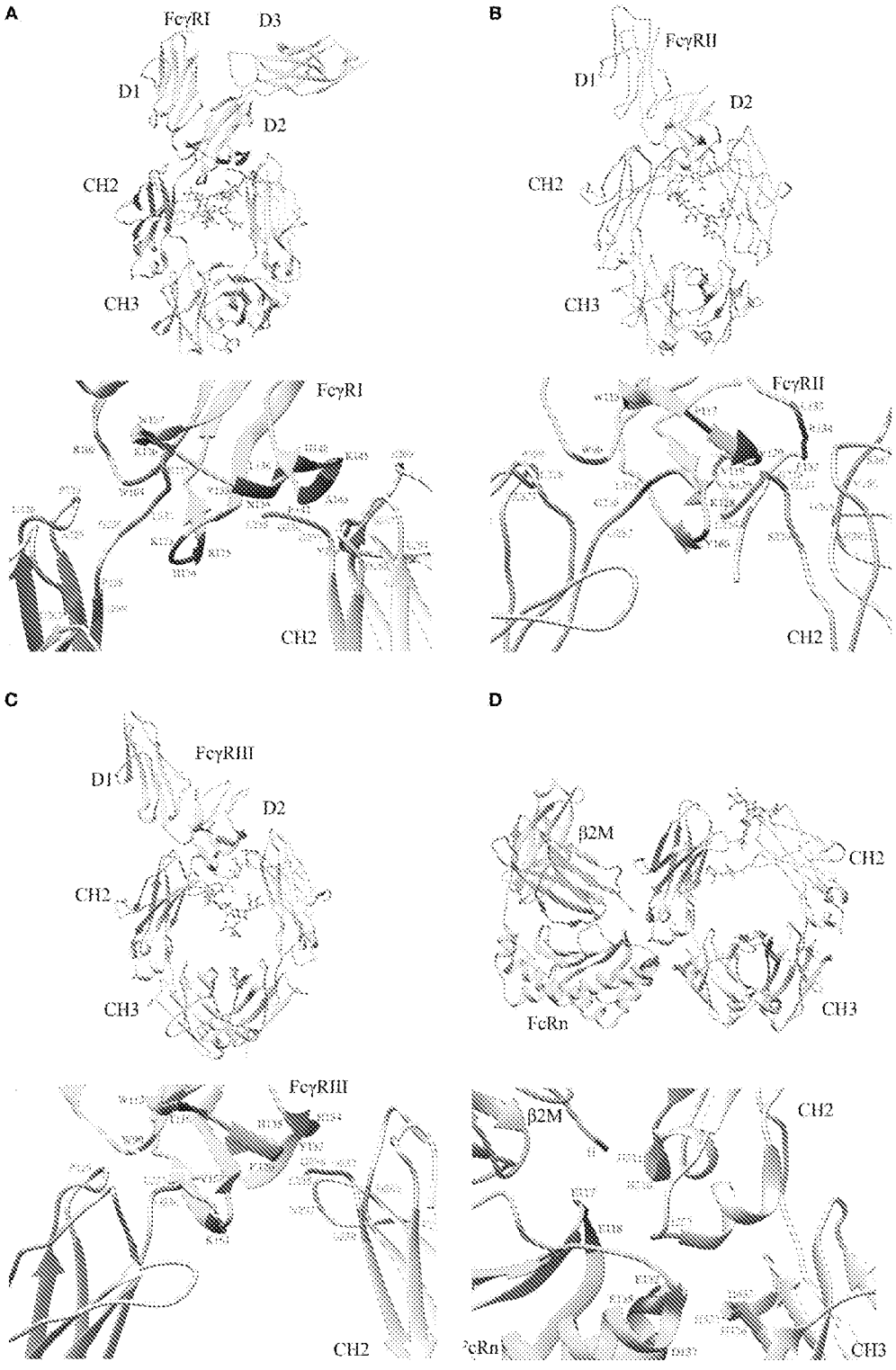


FIGURE 2 | Crystal structures illustrating crystallizable fragment (Fc) interactions with FcγRs and FcRn. Representative structures are shown for **(A)** Fc–FcγRI cocrystals [PDB: 4W4O (9)], **(B)** Fc–FcγRII cocrystals [PDB: 3RY6 (10)], **(C)** Fc–FcγRIII cocrystals [PDB: 1T89 (11)], and **(D)** Fc–FcRn cocrystals [PDB: 1I1A (12)] with β2 microglobulin (β2M) domain shown in cyan. The Fc region and FcγRs are represented by gray and yellow color, respectively **(A–D)**. N297 glycans within the CH2 domain are shown in stick model. The critical binding regions are highlighted in the upper part of each panel; region from the Fc fragment in green, region from the FcγRs, FcRn, and β2M in red. The lower part of each panel shows the detailed residues, which are involved in the interactions between Fc and its binding partners.

CSPC Exhibit 1004
Page 222 of 336

and thus IgG is protected from lysosomal degradation (20). The endocytosed IgG is then recycled to the cell surface and released into the blood stream at an alkaline pH, thereby maintaining the sufficient IgG serum half-life for proper immune functions and desired therapeutic efficacies (20). Recently, the endothelial and hematopoietic cells are identified as the major sites associated with FcRn expression and their critical role in IgG homeostasis (20–23).

Based on site-directed mutagenesis of Fc region and design of a hybrid Fc heterodimer harboring one half of Fc wild type (WT) and one half of Fc mutant, Kim and coworkers identified the key Fc residues involved in the FcRn interaction and proposed a preliminary model that one Fc hinge homodimer bound with two FcRn molecules (24, 25). Shortly thereafter, Burmeister and coworkers reported high resolution crystal structure of FcRn alone at 2.2 Å and low resolution crystal structure of Fc in complex with FcRn at 6.5 Å (26, 27). Structural analysis and biophysical data confirmed that one Fc homodimer binds with two FcRn molecules (26–29). Later, Martin and coworkers reported a high resolution crystal structure of Fc in complex with FcRn at 2.8 Å (13). This structure clearly shows the key residues involved in Fc and FcRn interactions and reveals the pH-dependent binding mechanism (13) (**Figure 2D**).

Evidence demonstrates the presence of oligosaccharides, attached to the N297 residue within the CH2 domain Asn-X-Ser/Thr glycosylation motif of Fc region, is essential in maintaining the Fc conformation and mediating its interactions with FcγRs (FcγRI, FcγRIIa, FcγRIIb, and FcγRIIIa) and C1q, but not FcRn (30–41). The glycan moiety is formed by two N-linked biantennary oligosaccharide chains consisting of a core heptasaccharide [N-acetylglucosamine (GlcNAc) and mannose (Man)] but occurrence of other residues like terminal N-acetlyneuraminic acid, galactose (Gal), bisecting N-acetylglucosamine (GlcNAc), and fucose (Fuc) have also been reported (1, 42, 43). Additionally, 5–17 and 2–7% of IgG structures could be monosialylated and disialylated, respectively (1, 44). This imparts a significant complexity and heterogeneity to therapeutic IgG molecules when expressed in mammalian cells, which can affect the therapeutic profile of IgG (30). On the other hand, the presence of bisected N-acetylglucosamine structures in rituximab, a purer glycoform with lesser heterogeneity, leads to an efficient engagement of FcγRIII and increases ADCC activity against $CD20^+$ cells by up to 20-fold (30, 45). Similarly, non-fucosylated glycoform of Herceptin produced in engineered Chinese hamster ovary (CHO) cell line (LEC13) can enhance ADCC *via* FcγRIII engagement by up to 50-fold (30, 46).

However, mAb-associated glycan heterogeneity poses several key challenges (30, 33, 48–51) including (1) difficulties in developing therapeutic mAbs with glycan composition similar to naturally occurring human IgG1, (2) difficulties in controlling glycan heterogeneity, (3) lengthier development time to construct cell lines producing glycan homogeneity, (4) lengthier IgG production time and higher manufacturing cost in mammalian cells as compared to that in *E. coli* or yeast-based expression systems, (5) dominance of particular glycoforms that can affect effector functions of IgG molecules, and (6) difficulties in separating various glycoforms generated from mammalian cells. Alternatively, development of aglycosylated mAbs with similar efficacy as glycosylated counterpart but lower manufacturing cost has attracted great efforts in the past decade.

In this review, we focus on the recent progress in therapeutic Fc engineering-associated effector functions (ADCC, ADCP, and CDC) and pharmacokinetics. The mutations known to induce profound effects on Fc interaction with FcγRs, C1q, and FcRn are summarized (see **Table 1**). We also briefly describe the advances in aglycosylated mAb development. Finally, we highlight clinical trials of several mAbs developed from relevant Fc engineering.

TABLE 1 | Tabulation of the Fc mutations known to mediate a profound effect on antibody effector functions and immunoglobulin gamma homeostasis.

Fc type	Mutation	Target	Functional	Reference
Hu-IgG2-Glyco	K326W/E333S	C1q	Yes	(52)
Mu-IgG2b-Glyco	E235L	FcγRI	Yes	(2)
Hu-IgG3-Glyco	E235Y	FcγRI	Yes	(53)
Hu-IgG1-Glyco	S239D, I332E, S239D/I332E, and S239D/I332E/A330L	FcγRIIIa	Yes	(6, 53–55)
Hu-IgG1-Glyco	G236A, G236A/I332E, S239D/I332E, and G236A/S239D/I332E	FcγRIIa > FcγRIIIa > FcγRI	Yes	(56)
Hu-IgG1-Glyco	L235V/F243L/R292P/Y300L/P396L	FcγRIIa	Yes	(57, 58)
Hu-IgG1-Glyco	P238D/L328E	FcγRIIb	NA	(59)
Hu-IgG1/IgA-Glyco	IgGA (many motifs)	FcγRs + FcαRI	Yes	(60)
Hu-IgG1-Glyco	F243L/R292P/Y300L and F243L/R292P/Y300L/P396L	FcγRIIIa/FcγRIIa	Yes	(28)
Hu-IgG1-Aglyco	S298G/T299A	FcγRIIa	NA	(61)
Hu-IgG1-(-Fuc)	F234L	FcγRIIIa	Yes	(62)
Hu-IgG1-Aglyco	E382V/M428I	FcγRI	Yes	(63)
Hu-IgG1-Aglyco	Q295R/L328W/A330V/P331V/I332Y	FcγRI	Yes	(64)
Hu-IgG1-Glyco	M428L/N434S	FcRn	Yes	(65)
Hu-IgG1-Glyco	M252Y/S254T/T256E and H433K/N434F/Y436H	FcRn	Yes	(66, 67)
Hu-IgG1-Glyco	N343A/E380A	FcRn	Yes	(68)
Hu-IgG1-Glyco	M252Y/S254T/T256E	FcRn	Yes	(69)
Hu-IgG1-Glyco	T250R/M428L	FcRn	Yes	(70)
Hu-IgG1-Aglyco	Q295R/L328W/A330V/P331V/I332Y	FcRn	Yes	(64)

Hu, Human; Mu, Murine; Glyco, Glycosylated; Aglyco, Aglycosylated; Fuc, Fucose; NA, not available.

CSPC Exhibit 1004
Page 223 of 336

MODULATION OF EFFECTOR FUNCTIONS BY Fc ENGINEERING

To develop more effective antibodies with desired ADCC, ADCP, and CDC activities, various strategies including site-directed mutagenesis, alanine scanning, structure-based computational design, and directed evolution technologies are employed.

The Fc amino acid residues that confer improved binding to FcγRs/C1q and enhanced immune response were initially characterized by site-directed mutagenesis studies. The earliest described mutations were discovered by scanning residues to isolate non-binders while focusing on the conserved residues. Fc residues (E318, K320, and L322) in the mouse IgG2b-Fc region were identified as the C1q binding site (3). However, the relevance of E318 and K320 was challenged in human Fc–C1q interaction (71). Novel residues (D270, K322, P329, and P331) were proposed for normal C1q binding on human Fc (71). This finding underscores the interspecies differences in such molecular interactions that may show a different effect in preclinical models. Furthermore, an IgG1 isotype of rituximab carrying K326W/E333S mutations was shown to have fivefold more binding to C1q (52) and the same motif, when transferred to the IgG2 isotype (poor complement activator) of rituximab, increased the cell lysis by fivefold (52). Next, a single mutation from E to L at position 235 of the mouse IgG2b-Fc region proposed it to be the "major determinant" for FcγRI binding (with ~100-fold increased affinity to human monocyte FcγRI) (2). Additionally, using a mouse–human chimeric antibody, amino acids at position 234 and 237 were shown to mainly influence the interaction with FcγRII. Based on these observations, FcγRI and FcγRII were proposed to recognize an overlapping but non-identical site on the Fc region (35).

Alanine scanning mutagenesis of selected Fc residues resulted in many variants with altered binding to specific FcγRs, which was also reflected in their ability to promote ADCC. Activating FcγRIIIa mutations improved ADCC by 100% (68). Furthermore, mutants based on the activating or suppressing effect on FcγRs were categorized into different classes. Among these, IgG1 mutations A327Q/P329A (interact with FcγRI), D265A/S267A/H268A/D270A/K326A/S337A (interact with FcγRIIa), and T256A/K290A/S298A/E333A/K334A (interact with FcγRIIIa) promoted high-affinity interactions (68).

Computational optimization of the Fc region by creating a single (S239D or I332E), double (S239D/I332E), and triple mutations (S239D/I332E/A330L) improved the affinity against human $Fc\gamma RIIIa^{V158/F158}$ allele by up to 169-fold (8). The mutations favoring Fc binding to activating (FcγRIIIa) receptor over the inhibitory (FcγRIIb) receptor are important to develop IgGs with better activating to inhibitory capacity (IIIa:IIb ratio), which was monitored using surface plasmon resonance. These mutations showed up to ninefold improvement in IIIa:IIb ratio and contributed to more than twofold enhancement in ADCC/ADCP activity, and the S239D/I332E double mutant significantly depleted $CD20^+$ B cells *in vivo* compared to WT IgG (8). The same Fc mutations also enhanced *in vitro* ADCC/ADCP activity against lymphoma cell lines and directly translated into a more effective treatment of lymphoproliferative diseases when incorporated into anti-CD19/CD40 mAbs (53, 54). Furthermore, it was shown that a change from glycine to alanine at residue 236 can shift the immune balance toward activating FcγRIIa relative to inhibitory FcγRIIb (56). The coupling of G236A to either I332E or S239D/I332E had dual beneficial effect as these mutants not only improve FcγRIIa:FcγRIIb ratio but also enhance binding to FcγRIIIa by ~6- to 31-fold (56). These mutants had significantly improved NK cell-mediated ADCC and macrophage-mediated ADCP activity (56).

In addition, "shuffled variants" of anti-CD20/CD57 antibody were constructed by grafting the CH1/hinge and CH3 carboxyl-terminal of IgG1 into the Fc of IgG3 to retain both the ADCC activity from IgG1 and the CDC activity from IgG3 (72). It is known that IgG1 is the most potent ADCC activator, while IgG3 has highest potency to recruit complement system (72). Therefore, IgG1 and IgG3 Fc regions can complement one another to maximize the immune effector response. These variants with chimeric CH regions showed ~25–60% increase in ADCC and CDC activity compared to WT of IgG1 and IgG3 molecules (72). Furthermore, the CDC activity of humanized anti-CD20 IgG1 (ocrelizumab) was increased by ~23-fold while retaining normal IgG1 ADCC by combining a triple mutant (S267E/H268F/S324T) with earlier reported G236A/I332E in the CH2 domain (73).

Multiple mutations (L235V/F243L/R292P/Y300L/P396L) in the trastuzumab Fc region (MGAH22) increased the potency against low Her2-expressing cells *via* low-affinity $Fc\gamma RIIIa^{F158}$ engagement (57). The same Fc motif was applied to the MGA271 mAb (anti-CD276), which targets $B7\text{-}H3^+$ tumor cells and resulted in an increased binding to FcγRIIIa, enhanced ADCC, and potent antitumor activity in a renal cell carcinoma/bladder cancer xenograft mouse model (58). Recently, the immune activating potential of IgA *via* FcαRI engagement was exploited by developing IgG and IgA hybrid molecules "IgGA" through substituting α1 loop residues of $CH_{\gamma}2/3$ region with $CH_{\alpha}2/3$ (60). The "IgGA" hybrid trastuzumab mediated an enhanced ADCC/ADCP activity against Her2 overexpressing cells and destroyed up to 50% SkBr3 breast cancer cells (*via* ADCC) and MDA-MB-453 cells (*via* ADCP) (60). Similarly, "IgGA" hybrid rituximab lysed ~70% of the $CD20^+$ calcein-AM-loaded Raji tumor cells when compared to the WT counterparts (60).

A negative selection strategy was applied using yeast surface display to enrich Fc mutants exhibiting selective high affinity to FcγRIIIa (29). Among these isolates, F243L was predicted to make a direct contact with the carbohydrate portion, which can "influence sialylation and affect the quaternary structure" of the Fc domain (29). Additionally, R292P partially reduced the binding to FcγRIIa, while Y300L, in combination with other mutations (F243L/R292P/V305I/P396L), showed an ~10-fold less K_D, 100-fold enhanced ADCC activity, and potency in a xenograft mouse model of ovarian and breast cancer (29). Furthermore, an Fc variant with three changes (F243L/R292P/Y300L) was also effective in increasing the rate of cytolysis by ~100-fold (29). In another report, human IgG1 Fc variants were generated by an error-prone PCR and ribosome display to select high-affinity agiycosylated binders to human FcγRIIIa using a solution phase method (62). The isolated Fc mutant (F243L) lacked Fuc residues in most oligosaccharide chains and exhibited an improved $Fc\gamma RIIIa^{V158/}$

CSPC Exhibit 1004
Page 224 of 336

^{F158} binding and enhanced ADCC as compared to WT Fc (62). Recently, an anti-EGFR antibody (S239D/I332E) was noted to elicit mononuclear cell-mediated ADCC *via* FcγRIIIa engagement and at the same time showed impaired polymorphonuclear cell (PMN)-mediated ADCC due to the engagement of FcγRIIIb, a highly homologous isoform to FcγRIIIa (55). The inability of FcγRIIIb to activate immune signaling in such a scenario can be overcome by imparting high-affinity binding to FcγRIIa, which can enhance both NK cell- and PMN mediated ADCC (55). These observations highlight that Fc engineering toward related FcγRs needs to be tailored specifically to achieve desirable immune effects.

MODULATION OF ANTIBODY PHARMACOKINETICS BY Fc ENGINEERING

Along with the efforts to engineer Fc regions for enhanced effector functions, attempts have been made to improve antibody pharmacokinetics. Clearly, enhanced Fc–FcRn interaction at acidic pH can extend IgG's serum half-life and positively regulate its homeostasis, which may benefit patients by greater therapeutic efficacy, less frequent dosing, and lower cost burden. Alanine scanning and display/directed evolution are commonly used techniques to identify favorable Fc mutants that can strengthen Fc–FcRn pH-dependent interactions.

A human Fc variant (N434A), isolated by alanine scanning of all solvent-exposed residues, showed fourfold increased binding to FcRn at pH 6.0 (68), which later, when studied in cynomolgus monkeys, showed a twofold extension of IgG serum half-life confirming the modulation of pharmacokinetics (74). Such an interaction at pH 6.0 prolongs IgG availability in serum, which correlates with the therapeutic effectiveness as demonstrated by the improved antitumor activity of IgG-Fc mutant (M428L/N434S from the CH3 domain) in a human FcRn transgenic mouse model (65).

A phage displayed antibody library approach was employed with the aim of isolating high-affinity binders against FcRn at pH 6.0. Random mutations were created at residues T252, T254, and T256, which are proximal to the IgG–FcRn interaction site, and binders were selected in a solution phase against FcRn at pH 6.0 and eluted by PBS at pH 7.4 (66). The Fc mutants generated in this manner were able to bind both human and rat FcRn with high affinity at pH 6.0; however, these variants (M252Y/S254T/T256E from the CH2 domain and H433K/N434F/Y436H from the CH3 domain) also showed tighter binding to mouse FcRn at pH 7.4 that decreased the serum IgG concentration in a mouse model (67). Yeung and coworkers (74) reported a similar observation that an Fc mutant (N434W), though possessing an ~80-fold enhanced affinity to FcRn at both acidic and neutral pH, did not stabilize serum IgG due to the loss in pH selectivity. These results suggest that high-affinity binding to the receptor at neutral pH can compromise the "beneficiary effect" of increased affinity at pH 6.0. Later, a humanized anti-respiratory syncytial virus antibody (MEDI-524) with a triple mutant Fc (M252Y/S254T/T256E from the CH2 domain) was reported to have a 10-fold increase in a pH-dependent way toward FcRn and about 4-fold improvement in serum half-life in cynomolgus monkey (69). Similarly, a high-affinity Fc variant (T250R/M428L) bound FcRn selectively at pH 6.0 and accounted for a 2.8-fold lesser degradation of serum IgG2 (70) and IgG1 (75) in rhesus monkey. Accumulating studies highlight that to prolong IgG serum half-life, pH-dependent FcRn affinity has to be maintained.

Of note, Grevys and coworkers recently analyzed known IgG-Fc mutants, which show enhanced FcRn pH-dependent affinity and extended serum half-life (M252Y/S254T/T256E from the CH2 domain and M428L/N434S from the CH3 domain), for their effects on ADCC, ADCP, and CDC (65, 69, 76). Surprisingly, they found that both mutants showed reduced effector functions with regards to ADCC, ADCP, and CDC. More interestingly, they found one previously known mutant (H433K/N434F from the CH3 domain), which showed reduced FcRn pH-dependent affinity and shortened serum half-life, displayed enhanced effector functions in ADCP, CDC, and ADCC (76, 77). These findings highlight that, though the interaction region of Fc with FcγRs and C1q (lower hinge region-CH2 domain) is distant from its interaction with FcRn (CH2–CH3 domain interface), it is still possible that these mutants can trigger a long range effect to other part of the Fc region in an unknown mechanism.

AGLYCOSYLATED Fc TO OVERCOME GLYCAN HETEROGENEITY

The demand for therapeutic antibodies is high, and it has been estimated that 8,000 kg of clinical grade mAbs were produced in 2013 (78). Currently, ~50% of the clinical grade biologics are produced in mammalian cells like CHO, mouse myeloma cell lines NSO and SP2/0 (30, 78–80).

However, the inherent glycan heterogeneity of mAbs when expressed in mammalian cell systems can cause high production cost and variations of mAb functions from batch to batch. Recently, great efforts have been invested in developing aglycosylated mAbs as an alternative. Ideally, aglycosylated mAbs would be as efficient as or even better than its glycosylated peers in mediating effector functions for antigen or target cell clearance.

To develop aglycosylated IgGs as alternatives, Sazinsky and coworkers constructed three small subsets of saturation substitutions covering the Asn-X-Ser/Thr glycan motif of the Fc C′/E loop and displayed these libraries on the yeast cell surface (61). After selection against FcγRIIa by fluorescence-activated cell sorting (FACS), a double Fc mutant isolate (S298G/T299A) in an aglycosylated form showed threefold stronger binding as compared to the WT and variants with single mutation, which indicates that the glycosylation of N297 is not a strict requirement for the interaction of Fc with FcγRIIa (61). In contrast, the indispensable role of asparagine at position 297 was demonstrated in the backdrop of N297Q, N297D, or N297A mutation, which abolished the double mutant (S298G/T299A) binding to FcγRIIa (61). Moreover, this dual mutant is functional *in vivo* in that murine platelet clearance is as efficient as that of WT mAb. Based on the modeling of Fc dual mutants in complex with FcγRIIa, the N297 residue of an aglycosylated IgG can

CSPC Exhibit 1004
Page 225 of 336

make a hydrogen bond with the S126 residue of FcγRIIa (61, 81). Furthermore, such interaction may be strengthened by a bridging water molecule present in an unbound FcγRII crystal (61, 81). However, this dual mutant showed 10-fold reduced FcγRI binding and no binding to both FcγRIII and C1q proteins. The inability of aglycosylated mAbs to bind with C1q and thus activate CDC can limit their application in treating hospital acquired microbial infections among cancer patients where complement activity plays an important role (82).

In another major breakthrough, bacterial display and FACS was used to isolate Fc variants displaying increased binding and specificity to FcγRI (63). One such aglycosylated variant called "Fc5" (E382V/M428I) was incorporated into trastuzumab. The trastuzumab-Fc5 variant bound selectively to the FcγRI with nanomolar range affinity and promoted monocyte-derived dendritic cell-dependent lysis of SkBr3 breast cancer cells that overexpress Her2. (63). The three-dimensional structure of human aglycosylated Fc domain suggests a greater "conformational flexibility of the CH2-CH3 domain interface," as compared to the glycosylated counterpart (83). Additional mutations (Q295R/L328W/A330V/P331V/I332Y) in trastuzumab-Fc5 variant (63) increased the affinity for FcγRI by ~120-fold and retained pH-dependent FcRn binding and function (84). Other mutants were also reported with specific binding to FcγRI and without compromising the pH-dependent FcRn binding (84).

It is worth mentioning that removal of appended glycans, though does not affect IgG's solubility, binding affinities to FcγRs, and *in vivo* half-life but often compromises IgG related CDC, lowers its thermostability and increases its aggregation at the low pH (85–87).

Fc ENGINEERING-BASED mAbs UNDER CLINICAL TRIALS

A number of mAbs harboring various modifications in the Fc region are being investigated in different clinical trial stages (see **Table 2** for Fc engineering-based mAbs being tested in clinics). These molecules broadly fall into three categories (1) with enhanced effector response to treat cancer and infectious diseases, (2) capable of inhibiting immune activation to treat inflammatory diseases, and (3) new class of aglycosylated mAbs with either inert or active-immune function.

The Fc variants capable of inducing enhanced ADCC are being tested in many antibody candidates. Anti-CD37 antibody (BI836826; Boehringer) against B cell malignancies is currently under phase-1 trial for the treatment of chronic lymphocytic leukemia (CLL) (6, 88, 89). This is a mouse–human chimeric antibody, which targets tetraspanin CD37 and shows high proapoptotic activity against malignant B cells *via* enhanced ADCC. Using human CD37 transgenic mice, a single dose of BI836826 was demonstrated to reduce peripheral B cells (88) and efficacious in suppressing tumor growth in Ramos mouse model of human B-cell lymphoma (88). Furthermore, therapeutic efficacy of a surrogate Fc-engineered antibody against macaque CD37 has also been demonstrated in cynomolgus monkey (88). A fully humanized anti-CD123 antibody (JNJ-56022473; Janssen R & D) targeting overexpressed interleukin-3 receptor α-chain is being tested in acute myeloid leukemia patients (89–91). The Fc fragment of JNJ-56022473 has been engineered for enhanced NK cell-mediated ADCC. The molecule efficiently reduced the growth of the patient-derived acute myelogenous leukemia xenografts in bone marrow and peripheral organs and increased the survival in animal models (91). Similarly, a humanized anti-CD30 antibody (XmAb2513; Xencor) with enhanced binding to FcγRIIIa is being evaluated in the treatment of $CD30^+$ Hodgkin's lymphoma (HL) patients who had previously received two or more therapies (89, 92, 93). It has been shown to be safely administered and biologically active in relapsed, refractory HL subjects and reduces tumor in a majority of patients (92, 93). Another interesting molecule is an anti-CD19 antibody (XmAb5774; Xencor), which induces potent NK cell-mediated ADCC/ADCP response against CLL (89, 96). The antibody is known to get internalized in primary CLL cells and induces a modest toxicity (96).

Antibodies harboring Fc mutations that can suppress the immune response are being tested for the treatment of inflammatory diseases. The immunosuppressive version of anti-CD19 antibody (XmAb5871; Xencor) binds inhibitory FcγRIIb with ~430-fold enhanced affinity and efficiently depletes $CD19^+$ B-cells in systemic lupus erythematosus (SLE) patients (90, 94). The depletion of $CD19^+$ B-cells correlates with the strong inhibition

TABLE 2 | Fc-engineered antibody candidates under clinical evaluation.

Antibody	Target	Fc modification	Disease	Clinical development	Company	Reference
BI836826	CD37	NA	CLL	Phase-1	Boehringer	(6, 88, 89)
JNJ56022473	CD123	NA	AML	Phase-2	Janssen R & D	(89–91)
XmAb2513	CD30	NA	Hodgkin/large cell lymphoma	Phase-1	Xencor, Inc.	(89, 92, 93)
XmAb5871	CD19	S267E/L328F	SLE	Phase-1	Xencor, Inc.	(90, 94)
XmAb7195	IgE	S267E/L328F	Allergic diseases	Phase-1	Xencor, Inc.	(95)
XmAb5774	CD19	S239D/I332E	CLL	Phase-1	Xencor, Inc.	(89, 96)
TRX4	CD8	N297A	Type-1 diabetes mellitus (autoimmune)	Phase-3	GSK/Tolerx	(48, 49, 97)
Onartuzumab	MET	N297A	NSCLC/gastroesophageal cancer	Phase-3	Roche	(48, 98, 99)
ALD518	IL-6	N297A	RA/NSCLC/oral mucositis	Phase-2	Alder	(48, 49, 100)
TRX518	GITR	N297A	Malignant melanoma	Phase-1	Tolerx	(48, 49, 101)

CLL, chronic lymphocytic leukemia; AML, acute myeloid leukemia; SLE, systemic lupus erythematosus; NSCLC, non-small cell lung cancer; RA, rheumatoid arthritis; NA, not available.

Source: https://clinicaltrials.gov/.

CSPC Exhibit 1004
Page 226 of 336

of B-cell receptor-induced calcium mobilization among healthy volunteers and SLE patients (94). The same Fc fragment has been engineered into a humanized anti-IgE antibody (XmAb7195; Xencor) for the treatment of allergies (95). This antibody prevents the binding of IgE to its high-affinity IgE receptor (FceRI) that is present on basophils and mast cells and is useful in the treatment of allergic asthma (95). The XmAb7195 has 5- and ~430-fold higher affinity for human IgE and FcγRIIb, respectively, and therefore is effective in inhibiting IgE production and plasma cell differentiation (95).

Finally, aglycosylated IgG molecules have recently been shown to have therapeutic properties (48, 49, 61, 63), and a few of them are undergoing clinical testing. An anti-CD3 antibody (TRX4; Tolerx) incorporating the N297A mutation suppresses pathogenic T-cells in type-1 diabetes (T1D) patients (48, 49, 97) and is being evaluated in phase-3 trials. The antibody downregulates pathogenic T-cells while restoring the normal activity of T-regulatory cells and thereby inhibits autoimmune mediated T1D (97).

It is widely accepted that hepatocyte growth factor (HGF) binding to receptor tyrosine kinase MET aggravates malignancy in a variety of cancers (98). Therefore, an aglycosylated anti-MET antibody (Onartuzumab; Roche) is being evaluated in phase-3 trials to inhibit the binding of HGF for treating lung and gastroesophageal cancers (49, 98, 99). This is an *E. coli*-derived humanized, affinity-matured antibody, which engages MET, thereby inhibiting HGF binding and receptor phosphorylation in HGF-dependent tumor models (98). Similarly, an aglycosylated mAb (ALD518; Alder) targeting IL-6 is being tested in phase-2 for a variety of diseases including rheumatoid arthritis, non-small cell lung cancer (NSCLC), and oral mucositis (48, 49, 100). The antibody was developed to inhibit proinflammatory cytokine IL-6 in oncogenic niches, which can otherwise lead to a cancer. The mAb ALD518 is reported to be well tolerated in phase-1 and -2 studies and ameliorated NSCLC-related anemia and cachexia (100). Another aglycosylated mAb (TRX518; Tolerx) is currently in phase-1 trials to treat malignant myeloma (48, 49, 101). TRX518 mAb recognizes the glucocorticoid-induced tumor necrosis factor receptor on regulatory and effector T-cells, B-cells, NK cells, and antigen-presenting cells to enhance effector T-cell response and inhibits T-regulatory cell-mediated suppression (101). Furthermore, the efficacy of TRX518 mAb in reducing tumor burden and increased survival rates has been demonstrated in mouse and non-human primate models (101).

These studies highlight that Fc engineering has played important roles in developing antibodies with desirable properties and functions, and the ongoing clinical studies can give valuable information on the efficacy of the Fc-engineered mAbs, as compared to their existing peers.

FINAL REMARKS

Crystallizable fragment engineering has made substantial progress in the identification of new mutant(s) that can enhance effector functions and improve pharmacokinetics of mAbs for cancer treatment. Two major notions have emerged during the past decades' efforts. First, the ratio of human activating FcγRs (FcγRI, FcγRIIa, and FcγRIIIa) and inhibitory FcγR (FcγRIIb) has to be taken into account during Fc engineering design. Beneficial effect can be achieved when Fc mutant(s) show higher selectivity and binding affinity toward activating FcγRs, as compared to the inhibitory FcγR. Second, the synergistic effects of improved ADCC, ADCP, and CDC of Fc region could increase the potency in cancer treatment.

Excitingly, aglycosylated mAb, expressed in bacteria and yeast, have been found to possess similar properties as glycosylated mAb with regards to FcγRs binding and serum half-life. However, efforts are still needed to improve its thermostability, solubility, and its binding affinity to C1q and CDC activity before it can really compete with its glycosylated peer for cancer therapy. On the other hand, the inability of aglycosylated mAbs to bind to C1q may have beneficial effects when CDC activity is not required such as for treatment of autoimmune diseases where CDC is chronically and pathologically activated (102). Similarly, aglycosylated mAbs may have advantages over glycosylated counterparts when only selective activation of FcγRs is desired such as activation of FcγRI (63) or FcγRIIa (84) to stimulate tumor cell killing.

AUTHOR CONTRIBUTIONS

DW conceived the topic; AS and DW wrote the manuscript; and DW revised the manuscript.

FUNDING

This work was supported by National Natural Science Foundation of China (Grant No: 81572698) to DW.

REFERENCES

1. Jefferis R, Lund J, Pound JD. IgG-Fc-mediated effector functions: molecular definition of interaction sites for effector ligands and the role of glycosylation. *Immunol Rev* (1998) 163:59–76. doi:10.1111/j.1600-065X.1998.tb01188.x
2. Duncan AR, Woof JM, Partridge LJ, Burton DR, Winter G. Localization of the binding site for the human high-affinity Fc receptor on IgG. *Nature* (1988) 332:563–4. doi:10.1038/332563a0
3. Duncan AR, Winter G. The binding site for C1q on IgG. *Nature* (1988) 332:738–40. doi:10.1038/332738a0
4. Rayner LE, Hui GK, Gor J, Heenan RK, Dalby PA, Perkins SJ. The solution structures of two human IgG1 antibodies show conformational stability and accommodate their C1q and FcgammaR ligands. *J Biol Chem* (2015) 290:8420–38. doi:10.1074/jbc.M114.631002
5. Ghetie V, Ward ES. Multiple roles for the major histocompatibility complex class I-related receptor FcRn. *Annu Rev Immunol* (2000) 18:739–66. doi:10.1146/annurev.immunol.18.1.739
6. Lazar GA, Dang W, Karki S, Vafa O, Peng JS, Hyun L, et al. Engineered antibody Fc variants with enhanced effector function. *Proc Natl Acad Sci U S A* (2006) 103:4005–10. doi:10.1073/pnas.0508123103
7. Ghirlando R, Keown MB, Mackay GA, Lewis MS, Unkeless JC, Gould HJ. Stoichiometry and thermodynamics of the interaction between the Fc fragment of human IgG1 and its low-affinity receptor Fc.gamma.RIII. *Biochemistry* (1995) 34:13320–7. doi:10.1021/bi00041a007

CSPC Exhibit 1004
Page 227 of 336

8. Ravetch JV, Bolland S. IgG Fc receptors. *Annu Rev Immunol* (2001) 19:275–90. doi:10.1146/annurev.immunol.19.1.275
9. Kiyoshi M, Caaveiro JM, Kawai T, Tashiro S, Ide T, Asaoka Y, et al. Structural basis for binding of human IgG1 to its high-affinity human receptor FcγRI. *Nat Commun* (2015) 6:6866. doi:10.1038/ncomms7866
10. Ramsland PA, Farrugia W, Bradford TM, Sardjono CT, Esparon S, Trist HM, et al. Structural basis for Fc gammaRIIa recognition of human IgG and formation of inflammatory signaling complexes. *J Immunol* (2011) 187:3208–17. doi:10.4049/jimmunol.1101467
11. Radaev S, Motyka S, Fridman WH, Sautes-Fridman C, Sun PD. The structure of a human type III Fcgamma receptor in complex with Fc. *J Biol Chem* (2001) 276:16469–77. doi:10.1074/jbc.M100350200
12. Bruhns P, Iannascoli B, England P, Mancardi DA, Fernandez N, Jorieux S, et al. Specificity and affinity of human Fcgamma receptors and their polymorphic variants for human IgG subclasses. *Blood* (2009) 113:3716–25. doi:10.1182/blood-2008-09-179754
13. Martin WL, West AP, Gan L, Bjorkman PJ. Crystal structure at 2.8 Å of an FcRn/heterodimeric Fc complex. *Mol Cell* (2001) 7:867–77. doi:10.1016/s1097-2765(01)00230-1
14. Gaboriaud C, Juanhuix J, Gruez A, Lacroix M, Darnault C, Pignol D, et al. The crystal structure of the globular head of complement protein C1q provides a basis for its versatile recognition properties. *J Biol Chem* (2003) 278:46974–82. doi:10.1074/jbc.M307764200
15. Schneider S, Zacharias M. Atomic resolution model of the antibody Fc interaction with the complement C1q component. *Mol Immunol* (2012) 51:66–72. doi:10.1016/j.molimm.2012.02.111
16. Sarma JV, Ward PA. The complement system. *Cell Tissue Res* (2011) 343:227–35. doi:10.1007/s00441-010-1034-0
17. Vidarsson G, Dekkers G, Rispens T. IgG subclasses and allotypes: from structure to effector functions. *Front Immunol* (2014) 5:520. doi:10.3389/fimmu.2014.00520
18. Firan M, Bawdon R, Radu C, Ober RJ, Eaken D, Antohe F, et al. The MHC class I-related receptor, FcRn, plays an essential role in the maternofetal transfer of gamma-globulin in humans. *Int Immunol* (2001) 13:993–1002. doi:10.1093/intimm/13.8.993
19. Medesan C, Matesoi D, Radu C, Ghetie V, Ward ES. Delineation of the amino acid residues involved in transcytosis and catabolism of mouse IgG1. *J Immunol* (1997) 158:2211–7.
20. Pyzik M, Rath T, Lencer WI, Baker K, Blumberg RS. FcRn: the architect behind the immune and nonimmune functions of IgG and albumin. *J Immunol* (2015) 194:4595–603. doi:10.4049/jimmunol.1403014
21. Akilesh S, Christianson GJ, Roopenian DC, Shaw AS. Neonatal FcR expression in bone marrow-derived cells functions to protect serum IgG from catabolism. *J Immunol* (2007) 179:4580–8. doi:10.4049/jimmunol.179.7.4580
22. Montoyo HP, Vaccaro C, Hafner M, Ober RJ, Mueller W, Ward ES. Conditional deletion of the MHC class I-related receptor FcRn reveals the sites of IgG homeostasis in mice. *Proc Natl Acad Sci U S A* (2009) 106:2788–93. doi:10.1073/pnas.0810796106
23. Zhu X, Meng G, Dickinson BL, Li X, Mizoguchi E, Miao L, et al. MHC class I-related neonatal Fc receptor for IgG is functionally expressed in monocytes, intestinal macrophages, and dendritic cells. *J Immunol* (2001) 166:3266–76. doi:10.4049/jimmunol.166.5.3266
24. Kim JK, Tsen MF, Ghetie V, Ward ES. Localization of the site of the murine IgG1 molecule that is involved in binding to the murine intestinal Fc receptor. *Eur J Immunol* (1994) 24:2429–34. doi:10.1002/eji.1830241025
25. Kim JK, Tsen MF, Ghetie V, Ward ES. Identifying amino acid residues that influence plasma clearance of murine IgG1 fragments by site-directed mutagenesis. *Eur J Immunol* (1994) 24:542–8. doi:10.1002/eji.1830240308
26. Burmeister WP, Huber AH, Bjorkman PJ. Crystal structure of the complex of rat neonatal Fc receptor with Fc. *Nature* (1994) 372:379–83. doi:10.1038/372379a0
27. Burmeister WP, Gastinel LN, Simister NE, Blum ML, Bjorkman PJ. Crystal structure at 2.2 A resolution of the MHC-related neonatal Fc receptor. *Nature* (1994) 372:336–43. doi:10.1038/372336a0
28. Huber AH, Kelley RF, Gastinel LN, Bjorkman PJ. Crystallization and stoichiometry of binding of a complex between a rat intestinal Fc receptor and Fc. *J Mol Biol* (1993) 230:1077–83. doi:10.1006/jmbi.1993.1220
29. Stavenhagen JB, Gorlatov S, Tuaillon N, Rankin CT, Li H, Burke S, et al. Fc optimization of therapeutic antibodies enhances their ability to kill tumor cells in vitro and controls tumor expansion in vivo via low-affinity activating Fcgamma receptors. *Cancer Res* (2007) 67:8882–90. doi:10.1158/0008-5472.CAN-07-0696
30. Jefferis R. Glycosylation of recombinant antibody therapeutics. *Biotechnol Prog* (2005) 21:11–6. doi:10.1021/bp040016j
31. Wright A, Morrison SL. Effect of glycosylation on antibody function: implications for genetic engineering. *Trends Biotechnol* (1997) 15:26–32. doi:10.1016/S0167-7799(96)10062-7
32. Krapp S, Mimura Y, Jefferis R, Huber R, Sondermann P. Structural analysis of human IgG-Fc glycoforms reveals a correlation between glycosylation and structural integrity. *J Mol Biol* (2003) 325:979–89. doi:10.1016/s0022-2836(02)01250-0
33. Jefferis R. Recombinant antibody therapeutics: the impact of glycosylation on mechanisms of action. *Trends Pharmacol Sci* (2009) 30:356–62. doi:10.1016/j.tips.2009.04.007
34. Jefferis R, Lund J. Interaction sites on human IgG-Fc for FcgammaR: current models. *Immunol Lett* (2002) 82:57–65. doi:10.1016/S0165-2478(02)00019-6
35. Lund J, Winter G, Jones PT, Pound JD, Tanaka T, Walker MR, et al. Human Fc gamma RI and Fc gamma RII interact with distinct but overlapping sites on human IgG. *J Immunol* (1991) 147:2657–62.
36. Lund J, Toshiyuki T, Noriko T, Sarmay G, Yoji A, Jefferis R. A protein structural change in aglycosylated IgG3 correlates with loss of huFcγRI and hufcγRIII binding and/or activation. *Mol Immunol* (1990) 27:1145–53. doi:10.1016/0161-5890(90)90103-7
37. Medesan C, Radu C, Kim JK, Ghetie V, Ward ES. Localization of the site of the IgG molecule that regulates maternofetal transmission in mice. *Eur J Immunol* (1996) 26:2533–6. doi:10.1002/eji.1830261038
38. Mimura Y, Sondermann P, Ghirlando R, Lund J, Young SP, Goodall M, et al. Role of oligosaccharide residues of IgG1-Fc in Fc gamma RIIb binding. *J Biol Chem* (2001) 276:45539–47. doi:10.1074/jbc.M107478200
39. Radaev S, Sun PD. Recognition of IgG by Fcgamma receptor. The role of Fc glycosylation and the binding of peptide inhibitors. *J Biol Chem* (2001) 276:16478–83. doi:10.1074/jbc.M100351200
40. Roopenian DC, Akilesh S. FcRn: the neonatal Fc receptor comes of age. *Nat Rev Immunol* (2007) 7:715–25. doi:10.1038/nri2155
41. Walker MR, Lund J, Thompson KM, Jefferis R. Aglycosylation of human IgG1 and IgG3 monoclonal antibodies can eliminate recognition by human cells expressing FcγRI and/or FcγRII receptors. *Biochem J* (1989) 259:347–53. doi:10.1042/bj2590347
42. Jefferis R, Lund J, Mizutani H, Nakagawa H, Kawazoe Y, Arata Y, et al. A comparative study of the N-linked oligosaccharide structures of human IgG subclass proteins. *Biochem J* (1990) 268:529–37. doi:10.1042/bj2680529
43. Raju TS. Terminal sugars of Fc glycans influence antibody effector functions of IgGs. *Curr Opin Immunol* (2008) 20:471–8. doi:10.1016/j.coi.2008.06.007
44. Routier FH, Hounsell EF, Rudd PM, Takahashi N, Bond A, Hay FC, et al. Quantitation of the oligosaccharides of human serum IgG from patients with rheumatoid arthritis: a critical evaluation of different methods. *J Immunol Methods* (1998) 213:113–30. doi:10.1016/S0022-1759(98)00032-5
45. Davies J, Jiang L, Pan LZ, LaBarre MJ, Anderson D, Reff M. Expression of GnTIII in a recombinant anti-CD20 CHO production cell line: expression of antibodies with altered glycoforms leads to an increase in ADCC through higher affinity for FC gamma RIII. *Biotechnol Bioeng* (2001) 74:288–94. doi:10.1002/bit.1119.abs
46. Shields RL, Lai J, Keck R, O'Connell LY, Hong K, Meng YG, et al. Lack of fucose on human IgG1 N-linked oligosaccharide improves binding to human Fcgamma RIII and antibody-dependent cellular toxicity. *J Biol Chem* (2002) 277:26733–40. doi:10.1074/jbc.M202069200
47. Jefferis R. Glycosylation as a strategy to improve antibody-based therapeutics. *Nat Rev Drug Discov* (2009) 8:226–34. doi:10.1038/nrd2804
48. Ju MS, Jung ST. Aglycosylated full-length IgG antibodies: steps toward next-generation immunotherapeutics. *Curr Opin Biotechnol* (2014) 30:128–39. doi:10.1016/j.copbio.2014.06.013
49. Jung ST, Kang TH, Kelton W, Georgiou G. Bypassing glycosylation: engineering aglycosylated full-length IgG antibodies for human therapy. *Curr Opin Biotechnol* (2011) 22:858–67. doi:10.1016/j.copbio.2011.03.002

CSPC Exhibit 1004
Page 228 of 336

50. Raju TS. Assessing Fc glycan heterogeneity of therapeutic recombinant monoclonal antibodies using NP-HPLC. *Methods Mol Biol* (2013) 988:169–80. doi:10.1007/978-1-62703-327-5_10
51. Kubota T, Niwa R, Satoh M, Akinaga S, Shitara K, Hanai N. Engineered therapeutic antibodies with improved effector functions. *Cancer Sci* (2009) 100:1566–72. doi:10.1111/j.1349-7006.2009.01222.x
52. Idusogie EE, Wong PY, Presta LG, Gazzano-Santoro H, Totpal K, Ultsch M, et al. Engineered antibodies with increased activity to recruit complement. *J Immunol* (2001) 166:2571–5. doi:10.4049/jimmunol.166.4.2571
53. Horton HM, Bernett MJ, Pong E, Peipp M, Karki S, Chu SY, et al. Potent in vitro and in vivo activity of an Fc-engineered anti-CD19 monoclonal antibody against lymphoma and leukemia. *Cancer Res* (2008) 68:8049–57. doi:10.1158/0008-5472.CAN-08-2268
54. Horton HM, Bernett MJ, Peipp M, Pong E, Karki S, Chu SY, et al. Fc-engineered anti-CD40 antibody enhances multiple effector functions and exhibits potent in vitro and in vivo antitumor activity against hematologic malignancies. *Blood* (2010) 116:3004–12. doi:10.1182/blood-2010-01-265280
55. Derer S, Glorius P, Schlaeth M, Lohse S, Klausz K, Muchhal U, et al. Increasing FcgammaRIIa affinity of an FcgammaRIII-optimized anti-EGFR antibody restores neutrophil-mediated cytotoxicity. *MAbs* (2014) 6:409–21. doi:10.4161/mabs.27457
56. Richards JO, Karki S, Lazar GA, Chen H, Dang W, Desjarlais JR. Optimization of antibody binding to FcgammaRIIa enhances macrophage phagocytosis of tumor cells. *Mol Cancer Ther* (2008) 7:2517–27. doi:10.1158/1535-7163.MCT-08-0201
57. Nordstrom JL, Gorlatov S, Zhang W, Yang Y, Huang L, Burke S, et al. Anti-tumor activity and toxicokinetics analysis of MGAH22, an anti-HER2 monoclonal antibody with enhanced Fcgamma receptor binding properties. *Breast Cancer Res* (2011) 13:R123. doi:10.1186/bcr3069
58. Loo D, Alderson RF, Chen FZ, Huang L, Zhang W, Gorlatov S, et al. Development of an Fc-enhanced anti-B7-H3 monoclonal antibody with potent antitumor activity. *Clin Cancer Res* (2012) 18:3834–45. doi:10.1158/1078-0432.CCR-12-0715
59. Mimoto F, Katada H, Kadono S, Igawa T, Kuramochi T, Muraoka M, et al. Engineered antibody Fc variant with selectively enhanced FcgammaRIIb binding over both FcgammaRIIa(R131) and FcgammaRIIa(H131). *Protein Eng Des Sel* (2013) 26:589–98. doi:10.1093/protein/gzt022
60. Kelton W, Mehta N, Charab W, Lee J, Lee CH, Kojima T, et al. IgGA: a "cross-isotype" engineered human Fc antibody domain that displays both IgG-like and IgA-like effector functions. *Chem Biol* (2014) 21:1603–9. doi:10.1016/j.chembiol.2014.10.017
61. Sazinsky SL, Ott RG, Silver NW, Tidor B, Ravetch JV, Wittrup KD. Aglycosylated immunoglobulin G1 variants productively engage activating Fc receptors. *Proc Natl Acad Sci U S A* (2008) 105:20167–72. doi:10.1073/pnas.0809257105
62. Stewart R, Thom G, Levens M, Guler-Gane G, Holgate R, Rudd PM, et al. A variant human IgG1-Fc mediates improved ADCC. *Protein Eng Des Sel* (2011) 24:671–8. doi:10.1093/protein/gzr015
63. Jung ST, Reddy ST, Kang TH, Borrok MJ, Sandlie I, Tucker PW, et al. Aglycosylated IgG variants expressed in bacteria that selectively bind FcgammaRI potentiate tumor cell killing by monocyte-dendritic cells. *Proc Natl Acad Sci U S A* (2010) 107:604–9. doi:10.1073/pnas.0908590107
64. Jung ST, Kang TH, Kim D-il. Engineering an aglycosylated Fc variant for enhanced FcγRI engagement and pH-dependent human FcRn binding. *Biotechnol Bioprocess Eng* (2014) 19:780–9. doi:10.1007/s12257-013-0432-z
65. Zalevsky J, Chamberlain AK, Horton HM, Karki S, Leung IW, Sproule TJ, et al. Enhanced antibody half-life improves in vivo activity. *Nat Biotechnol* (2010) 28:157–9. doi:10.1038/nbt.1601
66. Ghetie V, Popov S, Borvak J, Radu C, Matesoi D, Medesan C, et al. Increasing the serum persistence of an IgG fragment by random mutagenesis. *Nat Biotechnol* (1997) 15:637–40. doi:10.1038/nbt0797-637
67. Dall'Acqua WF, Woods RM, Ward ES, Palaszynski SR, Patel NK, Brewah YA, et al. Increasing the affinity of a human IgG1 for the neonatal Fc receptor: biological consequences. *J Immunol* (2002) 169:5171–80. doi:10.4049/jimmunol.169.9.5171
68. Shields RL, Namenuk AK, Hong K, Meng YG, Rae J, Briggs J, et al. High resolution mapping of the binding site on human IgG1 for Fc gamma RI, Fc gamma RII, Fc gamma RIII, and FcRn and design of IgG1 variants with improved binding to the Fc gamma R. *J Biol Chem* (2001) 276:6591–604. doi:10.1074/jbc.M009483200
69. Dall'Acqua WF, Kiener PA, Wu H. Properties of human IgG1s engineered for enhanced binding to the neonatal Fc receptor (FcRn). *J Biol Chem* (2006) 281:23514–24. doi:10.1074/jbc.M604292200
70. Hinton PR, Johlfs MG, Xiong JM, Hanestad K, Ong KC, Bullock C, et al. Engineered human IgG antibodies with longer serum half-lives in primates. *J Biol Chem* (2004) 279:6213–6. doi:10.1074/jbc.C300470200
71. Idusogie EE, Presta LG, Gazzano-Santoro H, Totpal K, Wong PY, Ultsch M, et al. Mapping of the C1q binding site on rituxan, a chimeric antibody with a human IgG1 Fc. *J Immunol* (2000) 164:4178–84. doi:10.4049/jimmunol.164.8.4178
72. Natsume A, In M, Takamura H, Nakagawa T, Shimizu Y, Kitajima K, et al. Engineered antibodies of IgG1/IgG3 mixed isotype with enhanced cytotoxic activities. *Cancer Res* (2008) 68:3863–72. doi:10.1158/0008-5472.CAN-07-6297
73. Moore GL, Chen H, Karki S, Lazar GA. Engineered Fc variant antibodies with enhanced ability to recruit complement and mediate effector functions. *MAbs* (2010) 2:181–9. doi:10.4161/mabs.2.2.11158
74. Yeung YA, Leabman MK, Marvin JS, Qiu J, Adams CW, Lien S, et al. Engineering human IgG1 affinity to human neonatal Fc receptor: impact of affinity improvement on pharmacokinetics in primates. *J Immunol* (2009) 182:7663–71. doi:10.4049/jimmunol.0804182
75. Hinton PR, Xiong JM, Johlfs MG, Tang MT, Keller S, Tsurushita N. An engineered human IgG1 antibody with longer serum half-life. *J Immunol* (2006) 176:346–56. doi:10.4049/jimmunol.176.1.346
76. Grevys A, Bern M, Foss S, Bratlie DB, Moen A, Gunnarsen KS, et al. Fc engineering of human IgG1 for altered binding to the neonatal Fc receptor affects Fc effector functions. *J Immunol* (2015) 194:5497–508. doi:10.4049/jimmunol.1401218
77. Vaccaro C, Bawdon R, Wanjie S, Ober RJ, Ward ES. Divergent activities of an engineered antibody in murine and human systems have implications for therapeutic antibodies. *Proc Natl Acad Sci U S A* (2006) 103:18709–14. doi:10.1073/pnas.0606304103
78. Ecker DM, Jones SD, Levine HL. The therapeutic monoclonal antibody market. *MAbs* (2015) 7:9–14. doi:10.4161/19420862.2015.989042
79. Naso MF, Tam SH, Scallon BJ, Raju TS. Engineering host cell lines to reduce terminal sialylation of secreted antibodies. *MAbs* (2010) 2:519–27. doi:10.4161/mabs.2.5.13078
80. Chu L, Robinson DK. Industrial choices for protein production by large-scale cell culture. *Curr Opin Biotechnol* (2001) 12:180–7. doi:10.1016/S0958-1669(00)00197-X
81. Maxwell KF, Powell MS, Hulett MD, Barton PA, McKenzie IF, Garrett TP, et al. Crystal structure of the human leukocyte Fc receptor, Fc gammaRIIa. *Nat Struct Biol* (1999) 6:437–42. doi:10.1038/8241
82. Steele RW. Managing infection in cancer patients and other immunocompromised children. *Ochsner J* (2012) 12:202–10.
83. Borrok MJ, Jung ST, Kang TH, Monzingo AF, Georgiou G. Revisiting the role of glycosylation in the structure of human IgG Fc. *ACS Chem Biol* (2012) 7:1596–602. doi:10.1021/cb300130k
84. Jung ST, Kelton W, Kang TH, Ng DT, Andersen JT, Sandlie I, et al. Effective phagocytosis of low Her2 tumor cell lines with engineered, aglycosylated IgG displaying high FcgammaRIIa affinity and selectivity. *ACS Chem Biol* (2013) 8:368–75. doi:10.1021/cb300455f
85. Latypov RF, Hogan S, Lau H, Gadgil H, Liu D. Elucidation of acid-induced unfolding and aggregation of human immunoglobulin IgG1 and IgG2 Fc. *J Biol Chem* (2012) 287:1381–96. doi:10.1074/jbc.M111.297697
86. Alsenaidy MA, Kim JH, Majumdar R, Weis DD, Joshi SB, Tolbert TJ, et al. High-throughput biophysical analysis and data visualization of conformational stability of an IgG1 monoclonal antibody after deglycosylation. *J Pharm Sci* (2013) 102:3942–56. doi:10.1002/jps.23730
87. Hristodorov D, Fischer R, Joerissen H, Muller-Tiemann B, Apeler H, Linden L. Generation and comparative characterization of glycosylated and aglycosylated human IgG1 antibodies. *Mol Biotechnol* (2013) 53:326–35. doi:10.1007/s12033-012-9531-x
88. Hender KH, Kiefer K, Zenz T, Volden M, Stilgenbauer S, Ostermann E, et al. A novel Fc-engineered monoclonal antibody to CD37 with enhanced ADCC

CSPC Exhibit 1004
Page 229 of 336

and high proapoptotic activity for treatment of B-cell malignancies. *Blood* (2011) 118:4159–68. doi:10.1182/blood-2011-04-351932

89. Sondermann P, Szymkowski DE. Harnessing Fc receptor biology in the design of therapeutic antibodies. *Curr Opin Immunol* (2016) 40:78–87. doi:10.1016/j.coi.2016.03.005
90. Horton HM, Chu SY, Ortiz EC, Pong E, Cemerski S, Leung IW, et al. Antibody-mediated coengagement of FcgammaRIIb and B cell receptor complex suppresses humoral immunity in systemic lupus erythematosus. *J Immunol* (2011) 186:4223–33. doi:10.4049/jimmunol.1003412
91. Lee EM, Yee D, Busfield SJ, McManus JF, Cummings N, Vairo G, et al. Efficacy of an Fc-modified anti-CD123 antibody (CSL362) combined with chemotherapy in xenograft models of acute myelogenous leukemia in immunodeficient mice. *Haematologica* (2015) 100:914–26. doi:10.3324/haematol.2014.113092
92. Blum KA, Smith M, Fung H, Zalevsky J, Combs D, Ramies DA, et al. Phase I study of an anti-CD30 Fc engineered humanized monoclonal antibody in Hodgkin lymphoma (HL) or anaplastic large cell lymphoma (ALCL) patients: safety, pharmacokinetics (PK), immunogenicity, and efficacy. *J Clin Oncol* (2009) 27:8531.
93. Kumar A, Blum KA, Fung HC, Smith MR, Foster PA, Younes A. A phase 1 dose-escalation study of XmAb(R) 2513 in patients with relapsed or refractory Hodgkin lymphoma. *Br J Haematol* (2015) 168:902–4. doi:10.1111/bjh.13152
94. Chu SY, Vostiar I, Karki S, Moore GL, Lazar GA, Pong E, et al. Inhibition of B cell receptor-mediated activation of primary human B cells by coengagement of CD19 and FcgammaRIIb with Fc-engineered antibodies. *Mol Immunol* (2008) 45:3926–33. doi:10.1016/j.molimm.2008.06.027
95. Chu SY, Horton HM, Pong E, Leung IW, Chen H, Nguyen DH, et al. Reduction of total IgE by targeted coengagement of IgE B-cell receptor and FcgammaRIIb with Fc-engineered antibody. *J Allergy Clin Immunol* (2012) 129:1102–15. doi:10.1016/j.jaci.2011.11.029
96. Awan FT, Lapalombella R, Trotta R, Butchar JP, Yu B, Benson DM Jr, et al. CD19 targeting of chronic lymphocytic leukemia with a novel Fc-domain-engineered monoclonal antibody. *Blood* (2010) 115:1204–13. doi:10.1182/blood-2009-06-229039
97. Aronson R, Gottlieb PA, Christiansen JS, Donner TW, Bosi E, Bode BW, et al. Low-dose otelixizumab anti-CD3 monoclonal antibody DEFEND-1 study: results of the randomized phase III study in recent-onset human type 1 diabetes. *Diabetes Care* (2014) 37:2746–54. doi:10.2337/dc13-0327
98. Merchant M, Ma X, Maun HR, Zheng Z, Peng J, Romero M, et al. Monovalent antibody design and mechanism of action of onartuzumab, a MET antagonist with anti-tumor activity as a therapeutic agent. *Proc Natl Acad Sci U S A* (2013) 110:E2987–96. doi:10.1073/pnas.1302725110
99. Park H, Yoon HW, Jung ST. The highly evolvable antibody Fc domain. *Trends Biotechnol* (2016) 34:895–908. doi:10.1016/j.tibtech.2016.04.005
100. Bayliss TJ, Smith JT, Schuster M, Dragnev KH, Rigas JR. A humanized anti-IL-6 antibody (ALD518) in non-small cell lung cancer. *Expert Opin Biol Ther* (2011) 11:1663–8. doi:10.1517/14712598.2011.627850
101. Rosenzweig M, Ponte J, Apostolou I, Doty D, Guild J, Slavonic M, et al. Development of TRX518, an aglycosyl humanized monoclonal antibody (Mab) agonist of huGITR. *J Clin Oncol* (2010) 28:e13028.
102. Melis JP, Strumane K, Ruuls SR, Beurskens FJ, Schuurman J, Parren PW. Complement in therapy and disease: regulating the complement system with antibody-based therapeutics. *Mol Immunol* (2015) 67:117–30. doi:10.1016/j.molimm.2015.01.028

Conflict of Interest Statement: The authors declare that the research was conducted in the absence of any commercial or financial relationships that could be construed as a potential conflict of interest.

Copyright © 2016 Saxena and Wu. This is an open-access article distributed under the terms of the Creative Commons Attribution License (CC BY). The use, distribution or reproduction in other forums is permitted, provided the original author(s) or licensor are credited and that the original publication in this journal is cited, in accordance with accepted academic practice. No use, distribution or reproduction is permitted which does not comply with these terms.

CSPC Exhibit 1004
Page 230 of 336

Amendments to the Claims:

This listing of claims will replace all prior versions, and listings, of claims in the application:

Listing of Claims:

1. (Canceled)

2. (Currently Amended) An antibody-drug conjugate~~,~~ or a pharmaceutically acceptable salt thereof, ~~or a solvate of the salt,~~ comprising an anti-epidermal growth factor receptor antibody covalently linked to a cytotoxic agent via a cleavable linker, wherein the anti-epidermal growth factor receptor antibody comprises a heavy chain and a light chain, wherein the heavy chain has a variable region comprising CDR1, CDR2 and CDR3 having sequences as shown in SEQ ID NOs: 5 to 7, and the light chain has a variable region comprising CDR1, CDR2 and CDR3 having sequences as shown in SEQ ID NOs: 12 to 14.

3. (Currently Amended) The antibody-drug conjugate~~,~~ or the pharmaceutically acceptable salt thereof~~, or the solvate of the salt~~ according to claim 2, wherein FR1, FR2, FR3, FR4 of the variable region of the heavy chain of the anti-epidermal growth factor receptor antibody respectively comprise sequences as shown in SEQ ID NOs: 8 to 11.

4. (Currently Amended) The antibody-drug conjugate~~,~~ or the pharmaceutically acceptable salt thereof~~, or the solvate of the salt~~ according to claim 2, wherein FR1, FR2, FR3, FR4 of the variable region of the light chain of the anti-epidermal growth factor receptor antibody respectively comprise sequences as shown in SEQ ID NOs: 15 to 18,.

5. (Currently Amended) The antibody-drug conjugate~~,~~ or the pharmaceutically acceptable salt thereof~~, or the solvate of the salt~~ according to claim 2, wherein the heavy chain of the anti-epidermal growth factor receptor antibody has a constant region selected

from the group consisting of a human IgG constant region, a human IgM constant region, a human IgA constant region, and a human IgD constant region.

6. (Currently Amended) The antibody-drug conjugate~~,~~ or the pharmaceutically acceptable salt thereof~~, or the solvate of the salt~~ according to claim 5, wherein the IgG is selected from the group consisting of IgG1, IgG2, IgG3 and IgG4.

7. (Currently Amended) The antibody-drug conjugate~~,~~ or the pharmaceutically acceptable salt thereof~~, or the solvate of the salt~~ according to claim 5, wherein the constant region of the heavy chain of the anti-epidermal growth factor receptor antibody comprises an amino acid sequence as shown in SEQ ID NO: 3, or comprises a sequence with an identity of greater than ~~70%, or greater than 75%, 80%, 85%,~~ 90%, 95%, or 99% to the sequence as shown in SEQ ID NO: 3.

8. (Currently Amended) The antibody-drug conjugate~~,~~ or the pharmaceutically acceptable salt thereof~~, or the solvate of the salt~~ according to claim 2, wherein the light chain of the anti-epidermal growth factor receptor antibody has a constant region selected from the group consisting of a human lambda constant region, and a human kappa constant region.

9. (Currently Amended) The antibody-drug conjugate~~,~~ or the pharmaceutically acceptable salt thereof~~, or the solvate of the salt~~ according to claim 8, wherein the constant region of the light chain of the anti-epidermal growth factor receptor antibody comprises an amino acid sequence as shown in SEQ ID NO: 4, or comprises a sequence with an identity of greater than ~~70%, or greater than 75%, 80%, 85%,~~ 90%, 95%, or 99% to the sequence as shown in SEQ ID NO: 4.

10. (Currently Amended) The antibody-drug conjugate~~,~~ or the pharmaceutically acceptable salt thereof~~, or the solvate of the salt~~ according to claim 2, which has a structure as shown in Formula I,

$Ab\text{-}(L\text{-}D)_p$

Formula I

wherein:

Ab represents the anti-epidermal growth factor receptor antibody;

L represents a cleavable linker;

D represents the cytotoxic agent;

p represents 1-9.

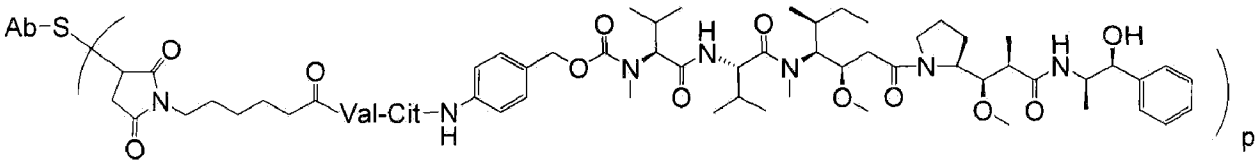
11. (Currently Amended) The antibody-drug conjugate~~,~~ or the pharmaceutically acceptable salt thereof~~, or the solvate of the salt~~ according to claim 10, wherein the cytotoxic agent is selected from the group consisting of chemotherapeutic agents, radioisotopes, ~~,~~antibiotics, enzymes, and biologically active peptides.

12. (Currently Amended) The antibody-drug conjugate~~,~~ or the pharmaceutically acceptable salt thereof~~, or the solvate of the salt~~ according to claim 11, wherein the cytotoxic agent is selected from the group consisting of Monomethyl auristatin E (MMAE), Monomethyl auristatin F (MMAF), maytansinoid alkaloids, Calicheamicin, duocarmycin MGBA, doxorubicin, ricin, diphtheria toxin, I131, and tumor necrosis factors.

13. (Canceled)

14. (Currently Amended) The antibody-drug conjugate~~,~~ or the pharmaceutically acceptable salt thereof~~, or the solvate of the salt~~ according to claim 10, wherein the linker is selected from the group consisting of valine-citrulline (val-cit), alanine-phenylalanine (ala-phe), N-succinimidyl 4-(2-pyridylthio)valerate (SPP), and 6-maleimidocaproyl-valine-citrulline-p-aminobenzyloxycarbonyl (MC-vc-PAB).

15. (Currently Amended) The antibody-drug conjugate~~,~~ or the pharmaceutically acceptable salt thereof~~, or the solvate of the salt~~ according to claim 10, which is:



wherein, Ab represents the anti-epidermal growth factor receptor antibody, p is 1-8.

16. (Currently Amended) A composition, which comprises the antibody-drug conjugate, or the pharmaceutically acceptable salt thereof, ~~or the solvate of the salt~~ according to claim 2, optionally, further comprises at least one pharmaceutically acceptable carrier, diluent or excipient.

17.-22. (Canceled)

23. (Currently Amended) A method for treatment of a disease associated with epidermal growth factor receptor (EGFR), comprising: administering to a subject in need a therapeutically effective amount of the antibody-drug conjugate, or the pharmaceutically acceptable salt thereof, ~~or the solvate of the salt~~ according to claim 2.

24. (Previously Presented) The method according to claim 23, wherein the disease associated with epidermal growth factor receptor (EGFR) is a tumor associated with overexpression of EGFR.

25. (Currently Amended) A method for inhibiting tumor angiogenesis, delaying tumor progression, inhibiting tumor growth, or inhibiting tumor cell proliferation, comprising: administering to a subject in need a therapeutically effective amount of the antibody-drug conjugate, or the pharmaceutically acceptable salt thereof, ~~or the solvate of the salt~~ according to claim 2.

26. (Original) The method according to claim 25, wherein the tumor is selected from colon cancer, rectal cancer, head and neck cancer, lung cancer, ovarian cancer, cervical cancer,

bladder cancer, esophageal cancer, breast cancer, renal cancer, prostate cancer, gastric cancer, pancreatic cancer and brain glioma.

27. (Previously presented) The method according to claim 24, wherein the tumor is a tumor with KRAS gene mutation.

28. (Previously presented) The method according to claim 24, wherein the tumor is a tumor with BRAF gene mutation.

29.-34. (Canceled)

35. (Previously presented) The method according to claim 26, wherein the tumor is a tumor with KRAS gene mutation.

36. (Previously presented) The method according to claim 26, wherein the tumor is a tumor with BRAF gene mutation.

37. (Previously Presented) The antibody-drug conjugate or the pharmaceutically acceptable salt thereof according to claim 10, wherein the linker is 6-maleimidocaproyl-valine-citrulline-p-aminobenzyloxycarbonyl (MC-vc-PAB).

PATENT

IN THE UNITED STATES PATENT AND TRADEMARK OFFICE

First Named Inventor	:	Chaohong Hu
Application No.	:	15/550,995
Filed	:	August 14, 2017
For	:	ANTIBODY-DRUG CONJUGATE
Examiner	:	Karen A Canella
Art Unit	:	1643
Docket No.	:	850231.401USPC
Date	:	December 16, 2019

Commissioner for Patents
P.O. Box 1450
Alexandria, VA 22313-1450

AMENDMENT

Commissioner for Patents:

In response to the final Office Action dated October 18, 2019, please amend the application as follows:

Amendments to the Claims are reflected in the listing of claims which begins on page 2 of this paper.

Remarks begin on page 7 of this paper.

Electronic Acknowledgement Receipt

EFS ID:	38038218
Application Number:	15550995
International Application Number:	
Confirmation Number:	1813
Title of Invention:	Antibody-Drug Conjugate
First Named Inventor/Applicant Name:	Chaohong Hu
Customer Number:	500
Filer:	Qing Lin/Barbara Hannon
Filer Authorized By:	Qing Lin
Attorney Docket Number:	850231.401USPC
Receipt Date:	16-DEC-2019
Filing Date:	14-AUG-2017
Time Stamp:	15:35:33
Application Type:	U.S. National Stage under 35 USC 371

Payment information:

Submitted with Payment	no

File Listing:

Document Number	Document Description	File Name	File Size(Bytes)/ Message Digest	Multi Part /.zip	Pages (if appl.)
1	After Final Consideration Program Request	401USPC_AFCP_REQ.pdf	308907 cfc0dab8dcd829eae4abbf7851ba549008770c18	no	1

Warnings:

Information:					
2		401USPC_RESP.pdf	13366714 7da9f8ac72b43bf91b71136657d739126611 181c	yes	40

Multipart Description/PDF files in .zip description		
Document Description	**Start**	**End**
Applicant Arguments/Remarks Made in an Amendment	7	40
Claims	2	6
Response After Final Action	1	1

Warnings:	
Information:	
Total Files Size (in bytes):	13675621

This Acknowledgement Receipt evidences receipt on the noted date by the USPTO of the indicated documents, characterized by the applicant, and including page counts, where applicable. It serves as evidence of receipt similar to a Post Card, as described in MPEP 503.

New Applications Under 35 U.S.C. 111

If a new application is being filed and the application includes the necessary components for a filing date (see 37 CFR 1.53(b)-(d) and MPEP 506), a Filing Receipt (37 CFR 1.54) will be issued in due course and the date shown on this Acknowledgement Receipt will establish the filing date of the application.

National Stage of an International Application under 35 U.S.C. 371

If a timely submission to enter the national stage of an international application is compliant with the conditions of 35 U.S.C. 371 and other applicable requirements a Form PCT/DO/EO/903 indicating acceptance of the application as a national stage submission under 35 U.S.C. 371 will be issued in addition to the Filing Receipt, in due course.

New International Application Filed with the USPTO as a Receiving Office

If a new international application is being filed and the international application includes the necessary components for an international filing date (see PCT Article 11 and MPEP 1810), a Notification of the International Application Number and of the International Filing Date (Form PCT/RO/105) will be issued in due course, subject to prescriptions concerning national security, and the date shown on this Acknowledgement Receipt will establish the international filing date of the application.

PTO/SB/06 (09-11)
Approved for use through 1/31/2014. OMB 0651-0032
U.S. Patent and Trademark Office; U.S. DEPARTMENT OF COMMERCE
Under the Paperwork Reduction Act of 1995, no persons are required to respond to a collection of information unless it displays a valid OMB control number.

PATENT APPLICATION FEE DETERMINATION RECORD Substitute for Form PTO-875	Application or Docket Number 15/550,995	Filing Date 08/14/2017	☐ To be Mailed

ENTITY: ☐ LARGE ☑ SMALL ☐ MICRO

APPLICATION AS FILED - PART I

FOR	(Column 1) NUMBER FILED	(Column 2) NUMBER EXTRA		RATE ($)	FEE ($)
☐ BASIC FEE (37 CFR 1.16(a), (b), or (c))	N/A	N/A		N/A	
☐ SEARCH FEE (37 CFR 1.16(k), (i), or (m))	N/A	N/A		N/A	
☐ EXAMINATION FEE (37 CFR 1.16(o), (p), or (q))	N/A	N/A		N/A	
TOTAL CLAIMS (37 CFR 1.16(i))	minus 20 =	*		x $40 =	
INDEPENDENT CLAIMS (37 CFR 1.16(h))	minus 3 =	*		x $210 =	
☐ APPLICATION SIZE FEE (37 CFR 1.16(s))	If the specification and drawings exceed 100 sheets of paper, the application size fee due is $310 ($155 for small entity) for each additional 50 sheets or fraction thereof. See 35 U.S.C. 41(a)(1)(G) and 37 CFR 1.16(s).				
☐ MULTIPLE DEPENDENT CLAIM PRESENT (37 CFR 1.16(j))					
* If the difference in column 1 is less than zero, enter "0" in column 2.				TOTAL	

APPLICATION AS AMENDED - PART II

		(Column 1)		(Column 2)	(Column 3)			
AMENDMENT	12/16/2019	CLAIMS REMAINING AFTER AMENDMENT		HIGHEST NUMBER PREVIOUSLY PAID FOR	PRESENT EXTRA		RATE ($)	ADDITIONAL FEE ($)
	Total (37 CFR 1.16(i))	* 23	Minus	** 23	= 0		x $50 =	0
	Independent (37 CFR 1.16(h))	* 1	Minus	*** 3	= 0		x $230 =	0
	☐ Application Size Fee (37 CFR 1.16(s))							
	☐ FIRST PRESENTATION OF MULTIPLE DEPENDENT CLAIM (37 CFR 1.16(j))							
							TOTAL ADD'L FEE	0

		(Column 1)		(Column 2)	(Column 3)			
AMENDMENT		CLAIMS REMAINING AFTER AMENDMENT		HIGHEST NUMBER PREVIOUSLY PAID FOR	PRESENT EXTRA		RATE ($)	ADDITIONAL FEE ($)
	Total (37 CFR 1.16(i))	*	Minus	**	=		x $0 =	
	Independent (37 CFR 1.16(h))	*	Minus	***	=		x $0 =	
	☐ Application Size Fee (37 CFR 1.16(s))							
	☐ FIRST PRESENTATION OF MULTIPLE DEPENDENT CLAIM (37 CFR 1.16(j))							
							TOTAL ADD'L FEE	

* If the entry in column 1 is less than the entry in column 2, write "0" in column 3.	LIE
** If the "Highest Number Previously Paid For" IN THIS SPACE is less than 20, enter "20".	/TINA J BARDEN/
*** If the "Highest Number Previously Paid For" IN THIS SPACE is less than 3, enter "3".	
The "Highest Number Previously Paid For" (Total or Independent) is the highest number found in the appropriate box in column 1.	

This collection of information is required by 37 CFR 1.16. The information is required to obtain or retain a benefit by the public which is to file (and by the USPTO to process) an application. Confidentiality is governed by 35 U.S.C. 122 and 37 CFR 1.14. This collection is estimated to take 12 minutes to complete, including gathering, preparing, and submitting the completed application form to the USPTO. Time will vary depending upon the individual case. Any comments on the amount of time you require to complete this form and/or suggestions for reducing this burden, should be sent to the Chief Information Officer, U.S. Patent and Trademark Office, U.S. Department of Commerce, P.O. Box 1450, Alexandria, VA 22313-1450. DO NOT SEND FEES OR COMPLETED FORMS TO THIS ADDRESS. **SEND TO: Commissioner for Patents, P.O. Box 1450, Alexandria, VA 22313-1450.**

If you need assistance in completing the form, call 1-800-PTO-9199 and select option 2.

UNITED STATES PATENT AND TRADEMARK OFFICE

UNITED STATES DEPARTMENT OF COMMERCE
United States Patent and Trademark Office
Address: COMMISSIONER FOR PATENTS
P.O. Box 1450
Alexandria, Virginia 22313-1450
www.uspto.gov

APPLICATION NO.	FILING DATE	FIRST NAMED INVENTOR	ATTORNEY DOCKET NO.	CONFIRMATION NO.
15/550,995	08/14/2017	Chaohong Hu	850231.401USPC	1813

500 7590 01/17/2020

SEED INTELLECTUAL PROPERTY LAW GROUP LLP
701 FIFTH AVE
SUITE 5400
SEATTLE, WA 98104

EXAMINER	
CANELLA, KAREN A	

ART UNIT	PAPER NUMBER
1643	

NOTIFICATION DATE	DELIVERY MODE
01/17/2020	ELECTRONIC

Please find below and/or attached an Office communication concerning this application or proceeding.

The time period for reply, if any, is set in the attached communication.

Notice of the Office communication was sent electronically on above-indicated "Notification Date" to the following e-mail address(es):

USPTOeAction@SeedIP.com
pairlinkdktg@seedip.com

Office Action Summary	Application No. 15/550,995	Applicant(s) Hu, Chaohong	
	Examiner KAREN A CANELLA	Art Unit 1643	AIA (FITF) Status Yes

-- The MAILING DATE of this communication appears on the cover sheet with the correspondence address --

Period for Reply

A SHORTENED STATUTORY PERIOD FOR REPLY IS SET TO EXPIRE 3 MONTHS FROM THE MAILING DATE OF THIS COMMUNICATION.

- Extensions of time may be available under the provisions of 37 CFR 1.136(a). In no event, however, may a reply be timely filed after SIX (6) MONTHS from the mailing date of this communication.
- If NO period for reply is specified above, the maximum statutory period will apply and will expire SIX (6) MONTHS from the mailing date of this communication.
- Failure to reply within the set or extended period for reply will, by statute, cause the application to become ABANDONED (35 U.S.C. § 133). Any reply received by the Office later than three months after the mailing date of this communication, even if timely filed, may reduce any earned patent term adjustment. See 37 CFR 1.704(b).

Status

1)☑ Responsive to communication(s) filed on 12-16-2019.

☐ A declaration(s)/affidavit(s) under **37 CFR 1.130(b)** was/were filed on _____.

2a)☐ This action is **FINAL.** 2b) ☑ This action is non-final.

3)☐ An election was made by the applicant in response to a restriction requirement set forth during the interview on _____; the restriction requirement and election have been incorporated into this action.

4)☐ Since this application is in condition for allowance except for formal matters, prosecution as to the merits is closed in accordance with the practice under *Ex parte Quayle*, 1935 C.D. 11, 453 O.G. 213.

Disposition of Claims*

5) ☑ Claim(s) 2-12,14-16,23-28 and 35-37 is/are pending in the application.

5a) Of the above claim(s) _____ is/are withdrawn from consideration.

6) ☐ Claim(s) _____ is/are allowed.

7) ☑ Claim(s) 2-12,14-16,23-26 and 37 is/are rejected.

8) ☑ Claim(s) 27-28 and 35-36 is/are objected to.

9) ☐ Claim(s) _____ are subject to restriction and/or election requirement

* If any claims have been determined allowable, you may be eligible to benefit from the **Patent Prosecution Highway** program at a participating intellectual property office for the corresponding application. For more information, please see http://www.uspto.gov/patents/init_events/pph/index.jsp or send an inquiry to **PPHfeedback@uspto.gov.**

Application Papers

10)☐ The specification is objected to by the Examiner.

11)☐ The drawing(s) filed on _____ is/are: a)☐ accepted or b)☐ objected to by the Examiner.

Applicant may not request that any objection to the drawing(s) be held in abeyance. See 37 CFR 1.85(a).

Replacement drawing sheet(s) including the correction is required if the drawing(s) is objected to. See 37 CFR 1.121(d).

Priority under 35 U.S.C. § 119

12)☐ Acknowledgment is made of a claim for foreign priority under 35 U.S.C. § 119(a)-(d) or (f).

Certified copies:

a)☐ All b)☐ Some** c)☐ None of the:

1.☐ Certified copies of the priority documents have been received.

2.☐ Certified copies of the priority documents have been received in Application No. _____.

3.☐ Copies of the certified copies of the priority documents have been received in this National Stage application from the International Bureau (PCT Rule 17.2(a)).

** See the attached detailed Office action for a list of the certified copies not received.

Attachment(s)

1) ☑ Notice of References Cited (PTO-892)

2) ☐ Information Disclosure Statement(s) (PTO/SB/08a and/or PTO/SB/08b) Paper No(s)/Mail Date _____.

3) ☐ Interview Summary (PTO-413) Paper No(s)/Mail Date _____.

4) ☐ Other: _____.

DETAILED ACTION

Notice of Pre-AIA or AIA Status

The present application, filed on or after March 16, 2013, is being examined under the first inventor to file provisions of the AIA.

After review and reconsideration, the finality of the last Office action is withdrawn in favor of the rejections below.

Claims 2-12, 14-16, 23 and 25 have been amended. Claims 2-12, 14-16, 23-28 and 35-37 are pending and under consideration.

In the event the determination of the status of the application as subject to AIA 35 U.S.C. 102 and 103 (or as subject to pre-AIA 35 U.S.C. 102 and 103) is incorrect, any correction of the statutory basis for the rejection will not be considered a new ground of rejection if the prior art relied upon, and the rationale supporting the rejection, would be the same under either status.

This application currently names joint inventors. In considering patentability of the claims the examiner presumes that the subject matter of the various claims was commonly owned as of the effective filing date of the claimed invention(s) absent any evidence to the contrary. Applicant is advised of the obligation under 37 CFR 1.56 to point out the inventor and effective filing dates of each claim that was not commonly owned as of the effective filing date of the later invention in order for the examiner to consider the applicability of 35 U.S.C. 102(b)(2)(C) for any potential 35 U.S.C. 102(a)(2) prior art against the later invention.

The following is a quotation of 35 U.S.C. 103 which forms the basis for all obviousness rejections set forth in this Office action:

> A patent for a claimed invention may not be obtained, notwithstanding that the claimed invention is not identically disclosed as set forth in section 102, if the differences between the claimed invention and the prior art are such that the claimed invention as a whole would have been obvious before the effective filing date of the claimed invention to a person having ordinary skill in the art to which the claimed invention pertains. Patentability shall not be negated by the manner in which the invention was made.

Claims 2-12, 14-16, 23-26 and 37 are rejected under 35 U.S.C. 103 as being unpatentable over Tikhomirov (WO2015/000062, cited in the prior action) in view of Liu (CN103772504 reference of the IDS filed 8/14/2017), Brand et al (Cancer Biology & Therapy, 2011, Vol. 11, pp. 777-792, cited in the prior action), Chung et al (New England Journal of Medicine, 2008, Vol.

358, pp. 1109-1117, cited in the prior action) and Doronina et al (Cancer Research, 2006, Vol. 17, pp. 114-124).

Claim 2 is drawn in part to an antibody-drug conjugate comprising an anti-EGFR antibody covalently linked to a cytotoxic agent with a cleavable linker, wherein the anti-EGFR antibody comprises the a heavy chain and a light chain, wherein the heavy chain variable region comprises SEQ ID NO:5-7 as the heavy chain CDR1-3, and the light chain variable region comprises SEQ ID NO:12-14 as the light chain CDR1-3 Claim 3 embodies the antibody conjugate of claim 1 wherein the FR1-4 of the variable regions of the heavy chain comprises SEQ ID NO:8-11, respectively. Claim 4 embodies the antibody conjugate of claim 1 wherein the FR1-4 of the variable regions of the light chain comprises SEQ ID NO:15-18, respectively. Claim 5 requires that the antibody conjugate of claim 2has a constant region selected from a group including the constant region of human IgG. Claim 6 specifies that the IgG constant region of claim 5 is selected from a group including IgG1. Claim 7 requires, in part, that the antibody conjugate of claim 5 has a constant region comprising SEQ ID NO:3. Claim 8 requires in part that the light chain of claim 2 has a constant region selected from a group including human kappa constant region. Claim 9 requires in part that the light chain constant region of claim 7 comprises SEQ ID NO:4. Claim 10 specifies that the antibody conjugate of claim 2 has the structure of Formula I wherein Ab is the antibody, L is the linker, D is the cytotoxic agent and p is 1-9. Claim 11 requires that the antibody conjugate of claim 10 comprises a toxin or a biological active peptide as the cytotoxin; claim 12 requires, in part, that the cytotoxic agent of claim 11 is MMAE. Claim 14 requires that the linker of claim 13 is selected from a group including 6-maleimidocaproyl (MC).

Claim 16 is drawn to a composition comprising the antibody conjugate of claim 2 optionally comprising at least one pharmaceutically acceptable carrier, diluent or excipient.

Claim 23 is drawn in part to a method for the treatment of a disease associated with EGFR comprising administering to a subject in need thereof, a therapeutically effective amount of the antibody conjugate of claim 2. Claim 24 requires that the disease associated with EGFR is a tumor with overexpression of EGFR.

Claim 25 is drawn to a method for inhibiting tumor angiogenesis, delaying tumor progression, inhibiting tumor growth or inhibiting tumor cell proliferation comprising administering to a subject in need thereof a therapeutically effective amount of the antibody

conjugate of claim 2. Claim 26 embodies the method of claim 25 wherein the tumor is selected from colon cancer, rectal cancer, head and neck cancer, lung cancer, ovarian cancer, cervical cancer, bladder cancer, esophageal cancer, breast cancer, renal cancer, prostate cancer, gastric cancer, pancreatic cancer and brain glioma.

Claim 15 requires the antibody linked by means of a sulfonyl group to 6-malimidocaprolyl-valine-citrulline-p-aminobenzyloxycarbonyl to MMAE, wherein p is 1-8. Claim 37 requires the linker of 6-malimidocaprolyl-valine-citrulline-p-aminobenzyloxycarbonyl in the antibody-conjugate of claim 10.

Tikhomirov et al teach method for treating a subject presenting with a tumor that responds to treatment with a full antagonist EGFR antibody, wherein treatment therewith elicits an EGFR antibody-mediated adverse response by keratinocytes, the improvement comprising treating said subject with the full antagonist EGFR antibody in a form conjugated with an anti-microtubule toxin, whereby the tumor response to treatment with conjugated antibody is enhanced essentially without enhancing the adverse keratinocyte response to treatment, relative to treatment with naked antibody alone (claim 19 of '062) thus teaching the embodiments of instant clams 23 and 25. Tikhomirov et al teach that a preferred embodiment of the full antagonist EGFR antibody is cetuximab, but that the invention includes other antibodies which are not cetuximab; the preferred anti-microtubulin toxin is preferably an auristatin (page 15, lines 14-16) and the linker is preferably a non-cleavable linker and preferably non-cleavable malimidocaproyl linkers for linking auristatins as the anti-microtubule toxin (page 14, lines 5-7) and that conjugation of cetuximab to MMAE anti-microtubule payload by a cleavable linker potentiates its toxicity against both normal cells and MDA-MB-468 cancer cells, whereas conjugation via non-cleavable linker only potentiates anti-cancer activity, thus demonstrating a favorable therapeutic selectivity (page 9, line 24 to page 10, line 3) thus teaching the embodiments of claims 10-12 wherein the cytotoxin is MMAE, the linker linking the MMAE to the antibody is non-cleavable and maleimidocaproyl (MC). Tikhomirov et al teach pharmaceutical compositions comprising the EGFR immunoconjugates in a pharmaceutically acceptable carrier, thus teaching the limitation of claim 16.

Tikhomirov et al also teach a less preferred embodiment of a cleavable linker (page 6, lines 3-5) such as a linker incorporating valine-citrulline such as cetux-2C9-MMAE in Figure 13, which meets the specific embodiment of cleavable linker in instant claim 13.

Tikhomirov et al teach the that the subject presenting with EGFR+ cancer cells are particularly EGFR+ cells having on their surface an abnormally high density of EGFR molecules (page 18, lines 1-2) which meets the limitation of instant claim 24 requiring EGFR overexpression. Tikhomirov et al teach the that cancers treatable by the invention include $EGFR^+$ colo-rectal cancer, head and neck cancer, lung cancer, ovarian cancer, cervical cancer, bladder cancer, esophageal cancer, breast cancer, renal cancer, prostate cancer, gastric cancer, pancreatic cancer and glioblastoma (page 18, lines 10-25) which meets the limitation of claim 26.

As noted above, Tikhomirov et al teach the preferred embodiment of cetuximab as the anti-EGFR antibody of the invention. Tikhomirov et al do not teach an anti-EGFR having the required CDRs, variable regions, and constant regions set forth in claims 2-8.

Brand et al teach that cetuximab, also known as C225, is the chimeric version of the murine antibody M225 (page 781, Figure 2).

Chung et al (NEJM, 2008, Vol. 358, pp. 1109-1117) teach that among 76 cetuximab treated subjects, 25 had hypersensitivity reactions to the drug, and that most of the subjects having hypersensitivity reactions had pre-existing IgE antibodies to galactose-α-1,3-galactose which is present on the Fab portion of the cetuximab heavy chain (page 1109, under the heading of "Results"). Chung et al teach that such IgE antibodies are prevalent in the population in areas where anaphylactic reactions to cetuximab occur (page 1110, first column, last sentence before "Methods"). Chung et al teach that the Fab portion of the cetuximab heavy chain is glycosylated at residue N88 with a range of sugars including galactose-α-1,3-galactose (page 1114, second column, lines 11-15).

Liu et al teach four humanized versions of the murine M225 antibody (Translation, page10, line 20 to the end of page 11) comprising a human IgG1 Fc fragment and a kappa light chain, wherein the antibodies are termed BA03, BB03, BC03 and BD03 (translation, page 12, lines 1-6). Liu et al teach the sequence of the heavy chain variable region, wherein the N88 residue is in the FR3 domain of SEQ ID NO:17 (Translation, page 15, last paragraph, CN103772504, page 11, paragraph [0083], the "N" in QSNDT) Liu et al teach the heavy chain variable regions of BA03, BB03, BC03 and BD03, wherein SEQ ID NO:5 of the BA03 heavy chain(translation page 16, SEQ ID NO:5) comprises SEQ ID NO: 5-7 of the instant heavy chain CDRs in addition to the framework domains FR1, FR2, FR3 and FR4 comprising SEQ ID NO:8-

11; SEQ ID NO: 13 of the light chain of BA03 (page 19 of the translation, SEQ ID NO:13) comprises the instant CDRs of SEQ ID NO:12-14 and the light chain framework sequences of the instant SEQ ID NO: 15-18.

The kappa light chain of the constant region (Translation, page 21, SEQ ID NO:43) is identical to the instant SEQ ID NO:4:

unnamed protein product
Sequence ID: Query_215689Length: 107Number of Matches: 1

```
Query  1    RTVAAPSVFIFPPSDEQLKSGTASVVCLLNNFYPREAKVQWKVDNALQSGNSQESVTEQD  60
            RTVAAPSVFIFPPSDEQLKSGTASVVCLLNNFYPREAKVQWKVDNALQSGNSQESVTEQD
Sbjct  1    RTVAAPSVFIFPPSDEQLKSGTASVVCLLNNFYPREAKVQWKVDNALQSGNSQESVTEQD  60

Query  61   SKDSTYSLSSTLTLSKADYEKHKVYACEVTHQGLSSPVTKSFNRGEC  107
            SKDSTYSLSSTLTLSKADYEKHKVYACEVTHQGLSSPVTKSFNRGEC
Sbjct  61   SKDSTYSLSSTLTLSKADYEKHKVYACEVTHQGLSSPVTKSFNRGEC  107
```

The IgG1 Fc fragment (Translation, page 21, SEQ ID NO: 42) is identical to the instant SEQ ID NO:3

unnamed protein product
Sequence ID: Query_227965Length: 330Number of Matches: 1

```
Query  1    ASTKGPSVFPLAPSSKSTSGGTAALGCLVKDYFPEPVTVSWNSGALTSGVHTFPAVLQSS  60
            ASTKGPSVFPLAPSSKSTSGGTAALGCLVKDYFPEPVTVSWNSGALTSGVHTFPAVLQSS
Sbjct  1    ASTKGPSVFPLAPSSKSTSGGTAALGCLVKDYFPEPVTVSWNSGALTSGVHTFPAVLQSS  60

Query  61   GLYSLSSVVTVPSSSLGTQTYICNVNHKPSNTKVDKRVEPKSCDKTHTCPPCPAPELLGG  120
            GLYSLSSVVTVPSSSLGTQTYICNVNHKPSNTKVDKRVEPKSCDKTHTCPPCPAPELLGG
Sbjct  61   GLYSLSSVVTVPSSSLGTQTYICNVNHKPSNTKVDKRVEPKSCDKTHTCPPCPAPELLGG  120

Query  121  PSVFLFPPKPKDTLMISRTPEVTCVVVDVSHEDPEVKFNWYVDGVEVHNAKTKPREEQYN  180
            PSVFLFPPKPKDTLMISRTPEVTCVVVDVSHEDPEVKFNWYVDGVEVHNAKTKPREEQYN
Sbjct  121  PSVFLFPPKPKDTLMISRTPEVTCVVVDVSHEDPEVKFNWYVDGVEVHNAKTKPREEQYN  180

Query  181  STYRVVSVITVLHQDWLNGKEYKCKVSNKALPAPIEKTISKAKGQPREPQVYTLPPSREE  240
            STYRVVSV+TVLHQDWLNGKEYKCKVSNKALPAPIEKTISKAKGQPREPQVYTLPPSREE
Sbjct  181  STYRVVSVLTVLHQDWLNGKEYKCKVSNKALPAPIEKTISKAKGQPREPQVYTLPPSREE  240

Query  241  MTKNQVSLTCLVKGFYPSDIAVEWESNGQPENNYKTTPPVLDSDGSFFLYSKLTVDKSRW  300
            MTKNQVSLTCLVKGFYPSDIAVEWESNGQPENNYKTTPPVLDSDGSFFLYSKLTVDKSRW
Sbjct  241  MTKNQVSLTCLVKGFYPSDIAVEWESNGQPENNYKTTPPVLDSDGSFFLYSKLTVDKSRW  300

Query  301  QQGNVFSCSVMHEALHNHYTQKSLSLSPGK  330
            QQGNVFSCSVMHEALHNHYTQKSLSLSPGK
Sbjct  301  QQGNVFSCSVMHEALHNHYTQKSLSLSPGK  330
```

Liu teaches that the BA03 and BD03 antibodies have higher binding affinity, stronger ligand blocking ability and stronger inhibitory activity against surface EGFR than Erbitux/cetuximab, and that BB03 and BC03 have binding affinity and ligand blocking abilities that are similar to that of Erbitux.

Doronina et al teach that the mechanisms of drug release from an antibody conjugate having a non-cleavable linker involves complete degradation of the antibody (pages 122-123, bridging sentence).

Doronina et al teach that drugs released from antibody drug conjugates utilizing non-cleavable linkers may be released in a modified form, and that many drugs loose activity as a result of the modification (page 123, first column, lines 3-6). Doronina et al conclude that the use of non-cleavable linkers may not be uniformly applicable for the linking of any drug to a targeting antibody because of the inability of all drugs to retain activity when released in a modified form (page 123, first column, lines 3-8). Doronina et al teach the antibody conjugate cAC10-L1-MMAE conjugate having a cleavable linker and an cAC10-L4-MMAE conjugate having a non-cleavable linker, wherein the conjugate with the cleavable linker has a potency of over 270X that of the conjugate with the non-cleavable linker when tested on target cells in vitro (page 120, Table 3). The L1-MMAE8 of Table 3 of Doronina e al meets the limitation of instant claim 15 after conjugation with an antibody and the limitation of 6-maleimidocaproyl-valine-citrulline-p-aminobenzyloxycarbonyl (MC-vc-PAB) in claim 14.

It would have been prima facie obvious as of the effective filing date to use the BA03 antibody in place of cetuximab in the conjugates and methods of using the conjugates of Tikhomirov et al. One of skill in the art would have been motivated to do so because the BA03 antibody is a full length antibody that is an antagonist of EGFR as demonstrated by Liu and has higher binding affinity and ligand blocking abilities than cetuximab. One of skill in the art would also be motivated to use the humanized BA03 antibody in place of cetuximab because the BA03 has humanized framework regions, and because the N88 amino acid in the chimeric 225 antibody is no longer present. Thus, one of skill in the art would know that the humanized 225 antibody of Liu BA03 would not carry galactose-α-1,3-galactose on N88 within FR3, and the antibody would not cause hypersensitivity reactions in subjects having pre-existing IgE antibodies to galactose-α-1,3-galactose.

It would have been prima facie obvious as of the effective filing date to use a cleavable linker rather than a non-cleavable linker in cases where the linked drug loses activity as a result of modification of the released drug such as the instant drug, MMAE, required in claim 15. . One of skill in the art would have been motivated to do so by the teachings of Doronina et al regarding loss of drug activity as a result of degradation of the antibody-drug conjugate resulting in release of a modified form of the drug which is not active. One of skill in the art would have been motivated to use the L1 linker-drug of instant claim 15 comprising the MC-vc-PAB linker of claim 14 because conjugates comprising the L1 cleavable linker versus the L2 cleavable linker appear to exert more potency against the target cells in vitro (Table 3, L1-MMAF versus L2-MMAF).

Applicant argues again that because Tikhomirov et al teach that toxicities are associated with the use of cleavable linkers in conjunction with EGFR targeting, one of skill in the art would not be motivated to use cleavable linkers, and points specifically to statement that a non-cleavable linker displays enhanced cytotoxicity against cancer cells without a corresponding increase in cytotoxicity against skin cells. This has been considered but not found persuasive. Tikhomirov et al teach that conjugation of panitumumab to the anti-microtubulin toxin, DM1, through a non-cleavable linker does not potentiate the toxicity of the antibody to keratinocytes in vitro (pages 28-29, Example 3). Tikhomirov et al teach conjugation of the fully antagonistic anti-EGFR antibodies to MMAE via a cleavable linker which potentiates toxicity agonist normal cells by the method of Doronina et al (2003) (page 30, lines 2-6). Tikhomirov et al conclude that the anti-EGFR conjugate should comprise a non-cleavable linker (page 30, lines 6-8).

Based on the teachings of Tikhomirov et al in view of Doronina et al, one of skill in the art would not pair the anti-tubulin MMAE with a non-cleavable linker because the MMAE released after degradation from the antibody is modified and the cytotoxicity of the MMAE is lost. It is noted that Erickson et al (Molecular Cancer Therapeutics, 2012, Vol. 11, pp. 1133-1142) teach two conjugates to DM1 with non-cleavable linkers wherein the targeting antibody was trastuzumab, wherein both conjugates were toxic against target positive breast cancer cell lines (pages 1135-1136 under the heading Her2-positive breast carcinoma cells display high..."). Erickson et al teach that the sole T-DM1 catabolite was lysine-Nε-MCC-DM1, and that the corresponding lysine Nε-SPP-DM1 catabolite was also observed along with a similarly abundant

DM1 catabolite (pages 1136-1137, bridging paragraph). One of skill in the art would reasonably conclude that degradation of the internalized antibody conjugated to DM1 via a non cleavable linker produced modified DM1 that retained cytotoxic activity in contrast to MMAE which does not. Thus one of skill in the art would not pick a non-cleavable linker with which to conjugate MMAE, and thus applicants unexpected results with MMAE conjugates comprising cleavable linkers versus non-cleavable linkers would have been anticipated by one of skill in the art..

With regard to toxicity against normal keratinocytes, it is noted that Tikhomirov et al teach that the in vitro assay was done in the presence of 10% FBS. Dorywalska et al (Bioconjugate Chemistry, February 2, 2015, Vol.26, pp. 650-659) teach that plasma from different sources comprise a factor, which cleaves VC-PABC resulting in drug loss from the antibody-drug conjugate (page 651, first column, lines 17-20 and page 652, second column, lines 7-10). One of skill in the art would reasonably conclude that increased toxicity observed by Tikhomirov et al against keratinocytes in vitro on exposure to the cleavable DM1 conjugate was the result of exposure to untargeted DM1 rather than targeted DM1 relying on uptake by Her2 internalization.

The rejection of claims 2-12, 14-16, 23-28 and 35-37 under 35 U.S.C. 112(a) or 35 U.S.C. 112 (pre-AIA), first paragraph, as failing to comply with the enablement requirement is withdrawn in light of applicant's amendments.

The following is a quotation of the first paragraph of 35 U.S.C. 112(a):

> (a) IN GENERAL.—The specification shall contain a written description of the invention, and of the manner and process of making and using it, in such full, clear, concise, and exact terms as to enable any person skilled in the art to which it pertains, or with which it is most nearly connected, to make and use the same, and shall set forth the best mode contemplated by the inventor or joint inventor of carrying out the invention.

The following is a quotation of the first paragraph of pre-AIA 35 U.S.C. 112:

> The specification shall contain a written description of the invention, and of the manner and process of making and using it, in such full, clear, concise, and exact terms as to enable any person skilled in the art to which it pertains, or with which it is most nearly connected, to make and use the same, and shall set forth the best mode contemplated by the inventor of carrying out his invention.

The rejection of claims 7 and 9 under 35 U.S.C. 112(a) or 35 U.S.C. 112 (pre-AIA), first paragraph, as failing to comply with the written description requirement is maintained for reasons of record.

(A) Claims 7 and 9 encompass sequences having greater than 70% or greater than 75%, 80%, 85%, 90%, 95% or 99% identity to SEQ ID NO:3 or 4. The disclsoure of the single constant regions of SEQ ID NO:3 and 4 does not provide an adequate written description of the genus of constant regions encompassed in the claimed antibody conjugates. The specification fails to teach the correlation between antibody constant region sequences and any particular function attributed to the antibody constant regions. The genus of antibody heavy chain constant regions encompassing sequences deviating by as much as 25% from the sequences of SEQ ID NO:3 and 4 would not be expected to retain all the same functional activities as SEQ ID NO:3 and 4. Thus, the disclosed sequence of SEQ ID NO: 3 fails to adequately describe the genus of SEQ ID NO:3 heavy chain variants, and the disclosed sequence of SEQ ID NO: 4 fails to adequately describe the genus of SEQ ID NO:4 variants because the broadly claimed genus includes members which differ in function from that of SEQ ID NO:4 or SEQ ID NO:3 and the specification has not taught the portions of the sequences of SEQ ID NO: 3 and 4 which are necessary for a particular function of the constant regions. One of skill in the art would reasonably conclude that applicant was not in possession of the claimed genus at the time of filing.

Applicant argues that it is not necessary to spell out every detail of the invention , and that only enough must be included to convince a person of skill in the art that the invention had possession of the invention. Applicant argues that the structure function correlation of constant regions of antibody light chain and heavy chains are well known in the art, and has enclosed the article of Sexena and Wu to demonstrate. This has been considered but not found persuasive. Claim 7 requires that the heavy chain of the instant antibody comprises the CDR sequences of claim 2 and wherein the remaining antibody sequence outside of the CDR sequences can vary by as much as 10%. Applicant has not demonstrated possession of such variants. Considering Table 1 of Sexena and Wu it is noted that the IgG1 with the greatest number of mutations is Hu-IgG1-Aglyco (last entry) having 5 substitutions in the Fc. The instant antibody heavy chain constant region of SEQ ID NO:3 has 330 residues. Substitution of 10% of these residues would

be substitution at 33 positions. The instant antibody light chain constant region of SEQ ID NO:4 has 107 residues. Substitution of 10% of these residues would be substitution at 10 positions. Thus, the art does not support applicant allegation that because the CDR residues are conserved in the variants up to 10% are within knowledge of the art such that an exact description need not be made of the antibody sequences that are encompassed by claims 7 and 9.

All other rejections as set forth or maintained in the prior Office action are withdrawn in light of applicant's amendments.

Allowable Subject Matter

Claims 27, 28, 35 and 36 are objected to as being dependent upon a rejected base claim, but would be allowable if rewritten in independent form including all of the limitations of the base claim and any intervening claims.

Any inquiry concerning this communication or earlier communications from the examiner should be directed to KAREN A CANELLA whose telephone number is (571)272-0828. The examiner can normally be reached on M-F 10-6:30.

Examiner interviews are available via telephone, in-person, and video conferencing using a USPTO supplied web-based collaboration tool. To schedule an interview, applicant is encouraged to use the USPTO Automated Interview Request (AIR) at http://www.uspto.gov/interviewpractice.

If attempts to reach the examiner by telephone are unsuccessful, the examiner's supervisor, Misook Yu can be reached on 571-272-0839. The fax phone number for the organization where this application or proceeding is assigned is 571-273-8300.

Information regarding the status of an application may be obtained from the Patent Application Information Retrieval (PAIR) system. Status information for published applications may be obtained from either Private PAIR or Public PAIR. Status information for unpublished

applications is available through Private PAIR only. For more information about the PAIR system, see https://ppair-my.uspto.gov/pair/PrivatePair. Should you have questions on access to the Private PAIR system, contact the Electronic Business Center (EBC) at 866-217-9197 (toll-free). If you would like assistance from a USPTO Customer Service Representative or access to the automated information system, call 800-786-9199 (IN USA OR CANADA) or 571-272-1000.

KAREN A. CANELLA
Examiner
Art Unit 1643

/Karen A. Canella/
Primary Examiner, Art Unit 1643

Notice of References Cited	Application/Control No. 15/550,995	Applicant(s)/Patent Under Reexamination Hu, Chaohong	
	Examiner KAREN A CANELLA	Art Unit 1643	Page 1 of 1

U.S. PATENT DOCUMENTS

*		Document Number Country Code-Number-Kind Code	Date MM-YYYY	Name	CPC Classification	US Classification
	A					
	B					
	C					
	D					
	E					
	F					
	G					
	H					
	I					
	J					
	K					
	L					
	M					

FOREIGN PATENT DOCUMENTS

*		Document Number Country Code-Number-Kind Code	Date MM-YYYY	Country	Name	CPC Classification
	N					
	O					
	P					
	Q					
	R					
	S					
	T					

NON-PATENT DOCUMENTS

*		Include as applicable: Author, Title Date, Publisher, Edition or Volume, Pertinent Pages)
	U	Doronina et al (Cancer Research, 2006, Vol. 17, pp. 114-124) (Year: 2006)
	V	Dorywalska et al (Bioconjugate Chemistry, February 2, 2015, Vol.26, pp. 650-659) (Year: 2015)
	W	Erickson et al (Molecular Cancer Therapeutics, 2012, Vol. 11, pp. 1133-1142) (Year: 2012)
	X	

*A copy of this reference is not being furnished with this Office action. (See MPEP § 707.05(a).)
Dates in MM-YYYY format are publication dates. Classifications may be US or foreign.

Search Notes	Application/Control No.	Applicant(s)/Patent Under Reexamination
	15/550,995	Hu, Chaohong
	Examiner	Art Unit
	KAREN A CANELLA	1643

CPC - Searched*		
Symbol	**Date**	**Examiner**
A61K47/6889	01/08/2020	kac
A61K47/6849	01/08/2020	kac
A61K38/1808	01/08/2020	kac

CPC Combination Sets - Searched*		
Symbol	**Date**	**Examiner**

US Classification - Searched*			
Class	**Subclass**	**Date**	**Examiner**

* See search history printout included with this form or the SEARCH NOTES box below to determine the scope of the search.

Search Notes		
Search Notes	**Date**	**Examiner**
STN	03/16/2019	kac
West	03/31/2019	kac
inventor [DAV]	03/31/2019	kac
West	10/13/2019	kac
inventor [DAV]	10/13/2019	kac
West	01/08/2020	kac
inventor [DAV]	01/08/2020	kac

/Karen A. Canella/ Primary Examiner, Art Unit 1643	

CSPC Exhibit 1004
Page 254 of 336

Search Notes	Application/Control No.	Applicant(s)/Patent Under Reexamination
	15/550,995	Hu, Chaohong
	Examiner	Art Unit
	KAREN A CANELLA	1643

Interference Search			
US Class/CPC Symbol	US Subclass/CPC Group	Date	Examiner

/Karen A. Canella/
Primary Examiner, Art Unit 1643

CSPC Exhibit 1004
Page 255 of 336

WEST Search History

Hide Items | Restore | Clear | Close

DATE: Wednesday, January 08, 2020

Hide?	Set Name	Query	Hit Count
DB=PGPB,USPT; PLUR=NO; OP=ADJ			
☐	L56	L55 and @ad<20160216	39
☐	L55	L54 and L48	52
☐	L54	L22 with L47	113
☐	L53	L52 and @ad<20160216	52
☐	L52	L51 and L48	70
☐	L51	L22 same L47	205
☐	L50	L49 and L47	620
☐	L49	L48 and L22	769
☐	L48	L2 and L7	1476
☐	L47	L43 or L44 or L45 or L46	531784
☐	L46	(succinimidyl adj propionate) or succinimidylpropionate	9397
☐	L45	SPP or SPDP or DSP	500767
☐	L44	pyridylthio adj (pentanoate or propionate)	1536
☐	L43	(valine adj citrulline) or (alanine adj phenylalanine) or (val adj cit) or (ala adj Phe) or (MC adj vc) or (vc adj PAB)	36683
☐	L22	L12 or L13 or L14 or L15 or L16 or L17 or L18 or L19 or L20 or L21	40464
☐	L21	matuzumab or EMD72000 or (EMD adj 72000)	4384
☐	L20	zalutumumab or (EGFR adj 2F8)	2554
☐	L19	nimotuzumab or theracim or theraloc	4508
☐	L18	imgatuzumab or RG7160 or (RG adj 7160) or GA201 or (GA adj 201) or RO5083945 or (RO adj 5083945)	674
☐	L17	laprituximab	35
☐	L16	modotuximab	17
☐	L15	futuximab or Sym004 or (Sym adj 004) or (992 near DS) or (mab adj (992 or 1024)) or mAb992 or mAb1024	548
☐	L14	panitumumab or vecibix or (ABX adj EGF)	16585
☐	L13	cetuximab or erbitux or IMC225 or ((IMC or mAb) adj 225) or C225	31970
☐	L12	L11 near5 (antibod$3)	20293
☐	L11	EGFR or EGFR1 or ERBB or ERBB1 or HER1 or (epidermal adj growth adj factor adj receptor) or (EGF adj (R or R1 or receptor$1)) or (her adj 1) or cerbB1 or (ERbB adj 1)	78327

☐	L10	cleavable[clm]	7366
☐	L9	L8 and L3	0
☐	L8	L7 and L2	1476
☐	L7	(a61k47/6803)![CPC,CPCL]	3014
☐	L6	L4 and cetuximab	220
☐	L5	L4 and L3	0
☐	L4	l1 AND l2	483
☐	L3	(a61k38/1808)![CPC,CPCL]	809
☐	L2	(a61k47/6849)![CPC,CPCL]	3848
☐	L1	(a61k47/6889)![CPC,CPCL]	1123

END OF SEARCH HISTORY

Published OnlineFirst March 9, 2012; DOI: 10.1158/1535-7163.MCT-11-0727

Molecular Cancer Therapeutics

Preclinical Development

The Effect of Different Linkers on Target Cell Catabolism and Pharmacokinetics/Pharmacodynamics of Trastuzumab Maytansinoid Conjugates

Hans K. Erickson[1], Gail D. Lewis Phillips[2], Douglas D. Leipold[3], Carmela A. Provenzano[1], Elaine Mai[4], Holly A. Johnson[1], Bert Gunter[5], Charlene A. Audette[1], Manish Gupta[3], Jan Pinkas[1], and Jay Tibbitts[3]

Abstract

Trastuzumab emtansine (T-DM1) is an antibody–drug conjugate consisting of the anti-HER2 antibody trastuzumab linked via a nonreducible thioether linker to the maytansinoid antitubulin agent DM1. T-DM1 has shown favorable safety and efficacy in patients with HER2-positive metastatic breast cancer. In previous animal studies, T-DM1 exhibited better pharmacokinetics (PK) and slightly more efficacy than several disulfide-linked versions. The efficacy findings are unique, as other disulfide-linked antibody–drug conjugates (ADC) have shown greater efficacy than thioether-linked designs. To explore this further, the *in vitro* and *in vivo* activity, PK, and target cell activation of T-DM1 and the disulfide-linked T-SPP-DM1 were examined. Both ADCs showed high *in vitro* potency, with T-DM1 displaying greater potency in two of four breast cancer cell lines. *In vitro* target cell processing of T-DM1 and T-SPP-DM1 produced lysine-N^{ε}-MCC-DM1, and lysine-N^{ε}-SPP-DM1 and DM1, respectively; *in vivo* studies confirmed these results. The *in vitro* processing rates for the two conjugate to their respective catabolites were similar. *In vivo*, the potencies of the conjugates were similar, and T-SPP-DM1 had a faster plasma clearance than T-DM1. Slower T-DM1 clearance translated to higher overall tumor concentrations (conjugate plus catabolites), but unexpectedly, similar levels of tumor catabolite. These results indicate that, although the ADC linker can have clear impact on the PK and the chemical nature of the catabolites formed, both linkers seem to offer the same payload delivery to the tumor. *Mol Cancer Ther; 11(5); 1133–42. ©2012 AACR.*

Introduction

An increasing number of antibody–drug conjugates (ADC) are entering clinical trials for the treatment of cancer (1). One of the most advanced and promising, trastuzumab emtansine (T-DM1) has shown favorable efficacy and safety in clinical trials for the treatment of patients with HER2-positive metastatic breast cancer (2–4). T-DM1 is an ADC that contains the humanized anti-HER2 immunoglobulin G (IgG)1 trastuzumab linked to the maytansinoid antitubulin agent DM1 via a thioether bond. T-DM1 retains the multiple mechanisms of action (MOA) described for trastuzumab, (5) and conjugation with DM1 confers the potential for additional cell killing activity via the delivery of potent antimitotic maytansinoid catabolites to targeted cancer cells. The efficacy of T-DM1 in patients who progressed on HER2-directed therapies underscores the importance of this additional activity (2–4).

T-DM1 is distinct from other clinically tested maytansinoid containing ADCs by virtue of its thioether linker. All other such ADCs in clinical testing use disulfide-based linkers (1). The thioether linker is considered more stable because it resists chemical or enzymatic cleavage in biological systems, in contrast to disulfide-based linkers that may be cleaved following thiol-disulfide exchange reactions. T-DM1 was found to be slightly more active in mouse models than T-SPP-DM1 and several other disulfide-linked ADCs (6). This contrasts with similar studies of other ADCs that led to the selection of disulfide-based linkers for clinical development (7–9).

The factors determining the efficacy of an ADC include pharmacokinetics (PK), tumor penetration and accumulation, target binding and cellular uptake, release of active catabolic products, and potency of the catabolic products. Previous studies have shown that the plasma concentrations of thioether-linked ADCs decrease more slowly than those of disulfide-linked ADCs, likely due to greater linker stability (6, 10); which may account for differences in the efficacy between T-DM1 and disulfide-linked analogues. It has also been shown that other aspects of the MOA

Authors' Affiliations: [1]ImmunoGen, Inc., Waltham, MA; and [2]Research Oncology, [3]Pharmacokinetics and Pharmacodynamics, [4]Assay and Automation Technologies, and [5]Nonclinical Biostatistics, Genentech, Inc., South San Francisco, CA.

Note: Supplementary material for this article is available at Molecular Cancer Therapeutics Online (http://mct.aacrjournals.org/).

Corresponding Author: Jay Tibbitts, Genentech, 1 DNA Way, MS463A, South San Francisco, CA 94080. Phone: 650-467-3194; Fax: 650-742-5234; E-mail: tibbitts@gene.com

doi: 10.1158/1535-7163.MCT-11-0727

©2012 American Association for Cancer Research.

CSPC Exhibit 1004
Page 258 of 336

Downloaded from mct.aacrjournals.org on January 13, 2020. © 2012 American Association for Cancer Research.

Published OnlineFirst March 9, 2012; DOI: 10.1158/1535-7163.MCT-11-0727

(i.e., target binding, cellular uptake, and release of catabolic products) may be similar for disulfide-linked and thioether-linked ADCs (11). To develop a better understanding of the MOA of trastuzumab maytansinoid conjugates and differences in the preclinical activity between these ADCs, we investigated the molecular basis for the anticancer activity in *in vitro* and *in vivo* efficacy, PK, and qualitative and quantitative tumor catabolism studies.

Materials and Methods

All experimental procedures conformed to the principles of the Guide for the Care and Use of Laboratory Animals and the American Physiological Society and were approved by the Institutional Animal Care and Use Committees of the respective laboratories.

Cell lines and reagents

The SK-BR-3 and BT-474 breast carcinoma cell lines were obtained from The American Type Culture Collection and used within 2 months of receipt. The BT-474EEI trastuzumab-resistant breast carcinoma cell line was derived at Genentech (6) by subculturing tumors derived from a BT-474 variant line (courtesy of Dr. Jose Baselga). BT-474EEI tumors express approximately 0.25×10^6 HER2 receptors per tumor cell and are insensitive to trastuzumab. MCF7-neo/HER2s are HER2-transfected cells made at Genentech. Cells were cultured in RPMI medium supplemented with 10% heat-inactivated FBS. MCF7-neo/HER2, BT-474, and BT-474 *in vivo*-selected variant (Baselga) were genotyped and authenticated using Illumina Golden Gate single-nucleotide polymorphism testing. Although the parent cells of the BT-474EEI cells (BT-474 Baselga variant) were genotyped as BT-474, the resulting cells (EEI) after *in vivo* selection have not been authenticated at this point. Porapak extraction cartridges were obtained from Waters. Ultima Gold scintillation fluid was obtained from PerkinElmer. *N*-ethylmaleimide (NEM) and all other chemicals were obtained from Sigma-Aldrich. The 10 mm C-18 column (0.46 × 25 cm; Vydak) was obtained from the Nest Group. The ULTRA-TURRAX T8 dispersing instrument with an S8N dispersing tool was obtained from IKA Works Inc. Trastuzumab and the humanized antiglycoprotein D (gD) control antibody, 5B6, were prepared at Genentech. Antibody-[^{3}H]maytansinoid conjugates were prepared at ImmunoGen, Inc., as described previously (12). The ratio of linked [^{3}H]maytansinoid per antibody molecule (MAR) for each conjugate was as follows: T-SPP-[^{3}H]DM1 (3.2), T-[^{3}H]DM1 (4.0), 5B6-SPP-[^{3}H]DM1 (3.5) [SPP = *N*-succinimidyl 4-(2-pyridyldithio)pentanoate], and hu5B6-MCC-[^{3}H]DM1 (3.6) [SMCC = *N*-succinimidyl 4-(*N*-maleimidomethyl)cyclohexane-1 carboxylate]. Unlabeled antibody–maytansinoid conjugates with similar MAR values were prepared at Genentech.

Clonogenic assays

Cells were plated at low density (100 cells per well for SK-BR-3, MCF7-neo/HER2, and BT-474EEI; 200 cells per well for BT-474) in Ham's F-12:DMEM (50:50) + 10% FBS + 2 mmol/L L-glutamine and allowed to adhere overnight. Conjugates were added the next day and the cells incubated until colony formation was determined to be maximal. The medium was removed and the colonies stained with crystal violet dye (0.5% in methanol). Colonies were quantified with a GelCount (Oxford Optronix).

In vitro catabolism studies

A stable tritium label was incorporated into the C-20 methoxy group of the DM1 used to prepare the ^{3}H-labeled conjugates as described previously (12). HER2-dependent processing of the ^{3}H-labeled conjugates was investigated in HER2-overexpressing BT-474EEI, MCF7-neo/HER2, and SK-BR-3. Cells were plated in flat bottom T-75 cell culture flasks in cell culture medium and grown to a density of approximately 10^7 cells per flask. The medium was exchanged with 10 mL of RPMI containing 10% FBS and 20 to 40 nmol/L of T-[^{3}H]DM1 or T-SPP-[^{3}H]DM1. The cells were placed on ice for 2 to 3 hours or for 30 minutes at 37°C with 6% CO_2. The treated cells were then washed 3 times with fresh medium and incubated at 37°C with 6% CO_2 with 10 mL fresh culture medium for 3 to 24 hours. The spent medium was separated and cells were harvested at selected time intervals and analyzed for catabolites following acetone extraction as described previously (11, 12). The precipitates from the acetone extractions were solubilized and analyzed for tritium by liquid scintillation counting (LSC) to assess the level of protein-bound maytansinoid associated with the cell pellet, presumed to be nonmetabolized conjugate or DM1 still linked to large protein fragments.

Maytansinoid catabolites were isolated from the medium by solid phase extraction followed by reversed-phase high-pressure liquid chromatography (HPLC). Media samples were applied to 6 mL porapak cartridges equilibrated with 3 mL acetone and then with 3 mL water. The cartridges were washed with 4 mL water and the maytansinoids eluted with 4 mL acetone. The eluates were evaporated and analyzed by reversed-phase HPLC and LSC as described for extracts containing the cell catabolites.

Cell volume measurements

Cell volumes were calculated from average cell diameters as measured by a cell viability analyzer (Beckman Coulter). Cell volumes for the SK-BR-3, BT-474EEI, and MCF7/neo-HER2 cells were 3823, 3955, and 3648 μm^3, respectively.

Animals

Female beige nude XID mice (Charles Rivers Laboratory) were used for all *in vivo* studies. Mice were housed in a clean barrier facility in standard rodent microisolator cages.

In vivo efficacy studies

To allow comparison of results obtained *in vitro* and *in vivo*, a mouse xenograft model was selected that

CSPC Exhibit 1004
Page 259 of 336

Downloaded from mct.aacrjournals.org on January 13, 2020. © 2012 American Association for Cancer Research.

Published OnlineFirst March 9, 2012; DOI: 10.1158/1535-7163.MCT-11-0727

was suitable for both systems. Previously, the founder 5 (Fo5) mouse allograft transplant model was used for *in vivo* comparisons of maytansinoid ADC efficacy (6). However, this model was not suitable for these studies as it cannot be cultured *in vitro*. Thus, the BT-474EEI xenograft model, suitable for *in vitro* and *in vivo* investigations, was chosen (13). BT-474EEI cells (2×10^7) were injected into the mammary fat pad of beige nude XID mice, and tumors were grown to approximately 250 mm^3. Animals were then randomized into 9 groups ($n = 10$ per group) and treated with a single i.v. bolus dose of 3 to 18 mg/kg (~60–360 μg/kg based on DM1 dose) of the conjugates. Tumors were measured with calipers twice weekly for 24 days following dosing, and then weekly for 120 days or until tumors reached a volume of 3,000 mm^3. Tumor volumes were determined with the formula: Tumor volume (mm^3) = (longer diameter × shorter diameter)^2 × 0.5.

In vivo catabolism studies

Mice-bearing BT-474EEI tumors (as described above) were randomized into 2 groups ($n = 15$ per group) and treated with a single 300 μg/kg i.v. bolus dose of T-[^{3}H]DM1 or T-SPP-[^{3}H]DM1 (doses based on DM1, equivalent to 10–12 mg/kg antibody). Three mice per group were sacrificed after 8 hours and 1, 2, 4, and 7 days. Immediately following sacrifice, the systemic circulation was flushed by injecting 5.0 mL PBS into the left ventricle and draining through an incision in the inferior vena cava. Whole tumor tissues were collected and frozen at −80°C. Two control groups of mice ($n = 3$ per group) were treated with matching doses of nontargeting 5B6-MCC-[^{3}H]DM1 or 5B6-SPP-[^{3}H]DM1 conjugates and sacrificed after 2 days. Tumors were homogenized and analyzed for total radioactivity by solubilization and LSC, and maytansinoid catabolites by HPLC and LSC as described previously. To determine the amount of protein-free maytansinoid catabolites present in the tumors, the tumor homogenates were extracted with organic solvent and analyzed as described previously (12).

Analytic methods

All maytansinoids were separated on an analytic C-18 column equilibrated with 20% aqueous acetonitrile (CH_3CN) containing 0.025% trifluoroacetic acid and using a linear gradient of 2% CH_3CN min^{-1} and a flow rate of 1 mL·min^{-1}. The effluent was collected in 6 mL polypropylene scintillation vials (1 mL fractions). Counts per minute (CPM) of tritium associated with each fraction were determined by mixing each vial with 4 mL Ultima Gold liquid scintillation cocktail before counting for 5 minutes in a Tri-Carb 2900T liquid scintillation counter (Packard BioScience).

The identities of the catabolites were confirmed by liquid chromatography mass spectrometry by methods similar to those described previously (11).

Pharmacokinetic studies

Animals ($n = 20$ per group) were administered a 3 mg/kg i.v. bolus dose of T-DM1 or T-SPP-DM1. At selected intervals up to 42 days following dosing, blood samples were collected on a rotational basis, with $n = 4$ animals per time point. Blood samples were processed for plasma by centrifugation and plasma decanted to polypropylene collection tubes. Samples were stored at −60°C to −80°C until analysis.

ADC plasma concentration analysis

Plasma ADC concentrations were determined with an ELISA that measured any trastuzumab antibody containing one or more conjugated DM1 molecules. An anti-DM1 monoclonal antibody was coated on ELISA plates. Captured ADC was detected with biotinylated HER2 extracellular domain (HER2 ECD) followed by streptavidin-horseradish peroxidase. The limit of quantitation (LOQ) was 1.6 ng/mL. Total trastuzumab concentrations were determined as described previously (6) using an ELISA that measured any trastuzumab antibody. In brief, HER2 ECD was coated on ELISA plates. Captured total trastuzumab was detected with goat-anti-human IgG-horseradish peroxidase. The LOQ was 1.6 ng/mL.

Pharmacokinetic analysis

The PK analysis of plasma ADC ELISA concentration–time data was conducted using a naïve pool approach with individual data from all animals. Data were fit to a 2-compartmental model with i.v. bolus input, first-order elimination, and macro rate constants (Model 8, WinNonlin Pro, v.5.2.1; Pharsight Corporation). Nominal sample collection times and dose concentrations were used in the data analysis.

Exposure response

In vivo response was assessed by calculating the mean tumor volume for each animal up to day 38 following dosing. The mean tumor volume is a sum of the measured tumor volumes in an individual animal from days 0 to 38, divided by the number of sampling times. Day 38 was chosen to allow for the observation of full ADC response without substantial tumor regrowth. Evaluation of other time points did not affect the results (data not shown). To show exposure response, the individual animal mean tumor volume value for each dose group was plotted against the estimated plasma ADC exposure [area under the curve (AUC)] for that dose group.

Results

HER2-positive breast carcinoma cells display high sensitivity to T-DM1 and T-SPP-DM1

The cytotoxic potencies of T-DM1 and T-SPP-DM1 and the matching nonbinding conjugates were compared in the trastuzumab-sensitive breast cancer cell lines SK-BR-3 and BT-474, and the trastuzumab-insensitive breast cancer cell lines BT-474EEI and MCF7-neo/HER2 using a

CSPC Exhibit 1004
Page 260 of 336

Downloaded from mct.aacrjournals.org on January 13, 2020. © 2012 American Association for Cancer Research.

Published OnlineFirst March 9, 2012; DOI: 10.1158/1535-7163.MCT-11-0727

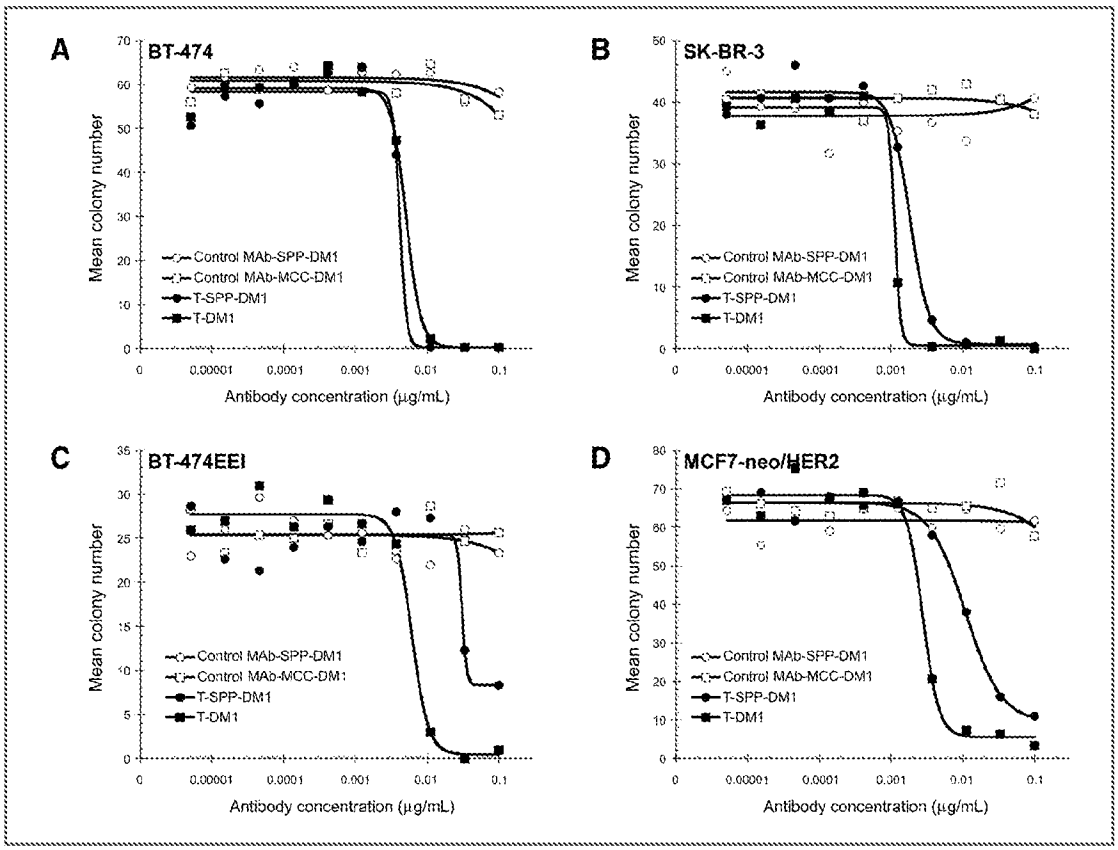


Figure 1. *In vitro* clonogenic survival assays of trastuzumab–DM1 conjugates in HER2-overepressing breast cancer cell lines [IC_{50} values (ng/mL)]. Colony number was assessed after 7 (MCF7-neo/HER2) to 21 (BT-474) days of exposure to T-DM1, T-SPP-DM1, or control ADCs. A, T-SPP-DM1 = 4.0, T-DM1 = 5.0. B, T-SPP-DM1 = 1.8, T-DM1 = 1.1. C, T-SPP-DM1 = 30.0, T-DM1 = 6.0. D, T-SPP-DM1 = 10.0, T-DM1 = 3.0.

clonogenic assay (Fig. 1). Both trastuzumab conjugates were found to be potent inhibitors of colony formation in the HER2-positive cell lines, whereas the nontargeting conjugates displayed little cytotoxicity. The chemical nature of the linker had little influence on the cytotoxicity of trastuzumab–DM1 conjugates toward BT-474 (Fig. 1A) and SK-BR-3 cells (Fig. 1B), consistent with an earlier report (6). However, the T-DM1 was more cytotoxic than T-SPP-DM1 toward BT-474EEI (Fig. 1C) and MCF7-neo/HER2 cells (Fig. 1D).

T-DM1 and T-SPP-DM1 display similar efficacy in mice bearing trastuzumab-insensitive BT-474EEI tumors

The antitumor activity associated with T-DM1 and T-SPP-DM1 in mice bearing the BT-474EEI tumors is shown in Fig. 2A. Following treatment with trastuzumab conjugates, tumor volume decreased in proportion to dose with maximum response at 18 mg/kg of either conjugate. Tumor regression reached its maximum approximately 10 to 21 days after dosing with subsequent stasis or regrowth. The exposure-response relationship for T-DM1 and T-SPP-DM1 was similar (Fig. 2B).

Pharmacokinetics of T-DM1 and T-SPP-DM1

The PK of T-DM1 and T-SPP-DM1 are shown in Fig. 3 and Supplementary Table S1. Total trastuzumab (Tab) PK were similar for both conjugates (Supplementary Table S1), indicating that conjugation with the respective linker-DM1 did not differentially affect the antibody PK behavior. T-SPP-DM1 ADC concentrations decreased more rapidly than T-DM1, with T-SPP-DM1 exhibiting a faster clearance (40.1 ± 1.87 vs. 18.9 ± 0.29 mL/d/kg) and shorter terminal half-life (2.69 ± 0.087 vs. 5.72 ± 0.150 days), consistent with a previous report (6). Central compartment volume of distribution was similar between the conjugates, as expected, based on the general similarity in their structure.

Characterization of maytansinoid catabolites following *in vitro* exposure of breast cancer cells to T-DM1 and T-SPP-DM1

The radiochromatograms in Fig. 4A show the catabolites of T-[^{3}H]DM1 and T-SPP-[^{3}H]DM1 following treatment of the BT-474EEI cells. The sole T-[^{3}H]DM1 catabolite at each time point was found to be lysine-N^{ε}-MCC-[^{3}H]DM1. The corresponding lysine-N^{ε}-SPP-

CSPC Exhibit 1004
Page 261 of 336

Downloaded from mct.aacrjournals.org on January 13, 2020. © 2012 American Association for Cancer Research.

Published OnlineFirst March 9, 2012; DOI: 10.1158/1535-7163.MCT-11-0727

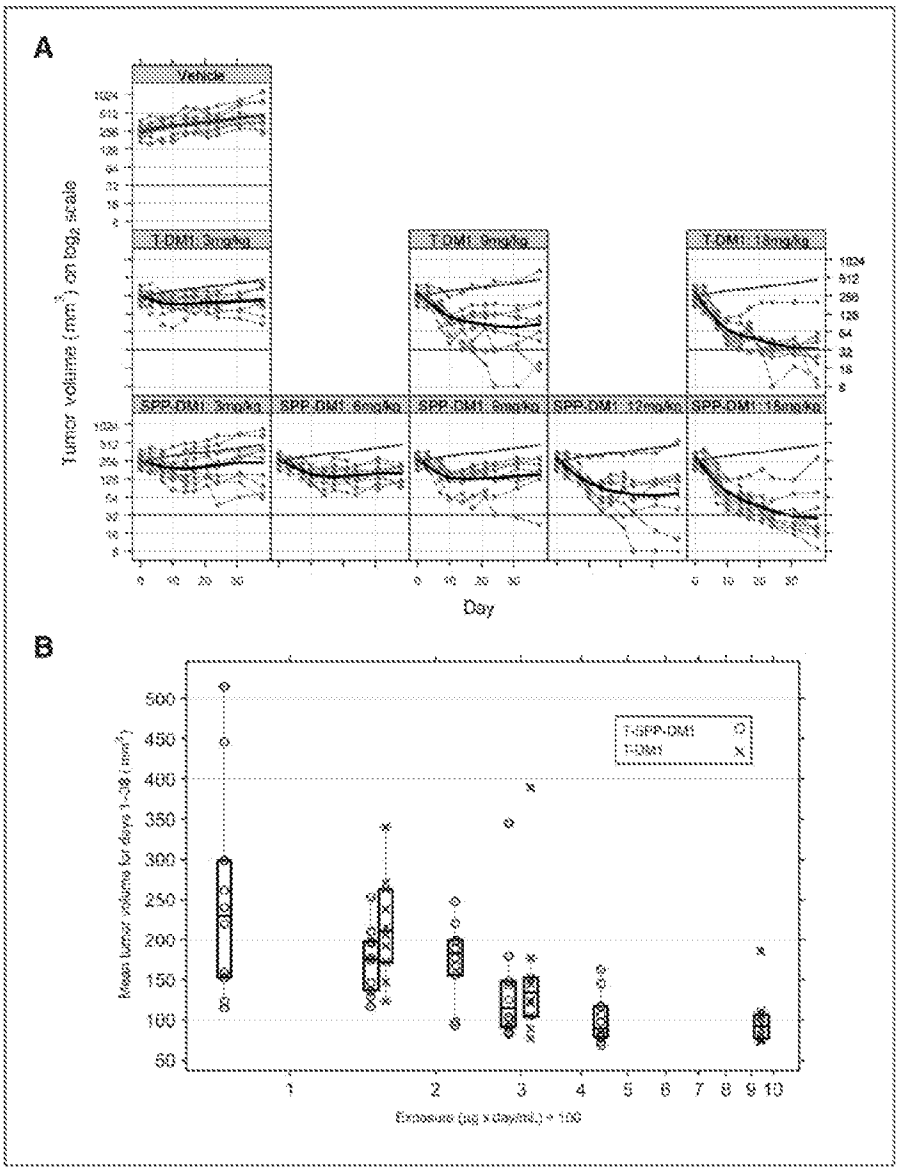


Figure 3. A, efficacy of trastuzumab–DM1 conjugates in mice-bearing BT-474EEI tumors. Individual tumor volumes versus time following a single i.v. bolus dose of trastuzumab–DM1 conjugates on day 0. Solid gray lines represent individual animal tumor volumes. The green line is lower LOQ (8 mm^3). Values below this are statistically imputed and recorded as 8 to avoid extreme negative or infinite values on log scale. The blue line is fitted control profile. B, mean tumor volume measurements for each animal through day 36 versus ADC exposure (AUC) with box plots overlaid. The horizontal line is the median of the 10 animal mean volumes in each group; the ends of the box range from the 3rd to 7th highest of the 10 means. This interquartile range (IQR) is an outlier-resistant estimate of the variability of each group of mean volumes. The dashed whiskers extend 1.5 IQR's from the ends of the box, denoting a Gaussian distribution-based estimate of statistical variability. Values beyond the whiskers are therefore considered statistically aberrant.

[^{3}H]DM1 catabolite of T-SPP-[^{3}H]DM1 was observed along with a similarly abundant DM1 catabolite. The DM1 catabolite was alkylated at its free sulfhydryl group by NEM in the suspension buffer before extraction and thus was detected as its NEM adduct in the radiograms. No maytansinoid catabolites (<0.1 pmol/10^6 cells) were detected in the acetone extracts of the spent medium samples indicating that little, if any, efflux of maytansinoids from the cells had occurred over the 24-hour assay.

The catabolism rates of trastuzumab conjugates following exposure to BT-474EEI cells are similar

The radioactivity associated with the maytansinoid catabolites in acetone extracts (Fig. 4A) and precipitates from the acetone extractions were converted to pmol/cell and nmol/L and plotted versus time (Fig. 4B). Of particular interest for understanding the antimitotic activity of T-DM1 is the concentration of its maytansinoid catabolites in the cytoplasm of the targeted cells. The molar values for the catabolites in Fig. 4B may not accurately reflect their cytoplasmic concentrations if they accumulate in subcellular compartments such as lysosomes. However, previous studies with anti-CanAg maytansioid conjugates similar to those described here suggest that maytansinoid catabolites are retained by targeted cells through binding to their cytoplasmic tubulin target (11). Therefore, the molar values in Fig. 4 likely approximate the true cytoplasmic values. The amount of maytansinoids in the precipitates (representing intact conjugates and any

CSPC Exhibit 1004
Page 262 of 336

Downloaded from mct.aacrjournals.org on January 13, 2020. © 2012 American Association for Cancer Research.

Published OnlineFirst March 9, 2012; DOI: 10.1158/1535-7163.MCT-11-0727

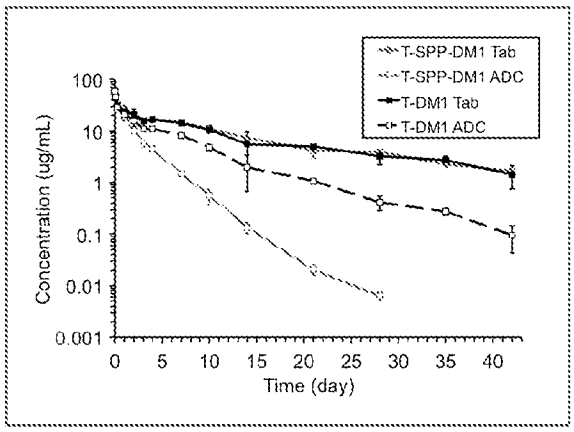


Figure 3. Plasma pharmacokinetics in nontumor-bearing mice. Mean (± SD) ADC and Tab concentrations following i.v. bolus administration of 3 mg/kg of trastuzumab–DM1 conjugates.

potential protein fragments) was found to decrease at approximately the same rate for both conjugates. This decrease was matched by a corresponding increase in the maytansinoid catabolites in the extracts, reaching maximal intracellular maytansinoid concentrations of 200 nmol/L and 300 nmol/L after 24 hours for cells treated with T-SPP-DM1 and T-DM1, respectively. In separate experiments, the total maytansinoids associated with the extract and the precipitate for each time point were equivalent to the amount of conjugate bound at $t = 0$ (data not shown) indicating that all maytansinoid catabolites had been accounted for (upper curves, Fig. 4B). Approximately 30% more T-DM1 was bound to cells after the incubation and wash steps than T-SPP-DM1. This, coupled with a higher MAR for T-DM1 compared with T-SPP-DM1 (4.0 vs. 3.2) accounts for the higher maytansinoid values associated with cells treated with T-DM1 (Fig. 4B, a and b). The catabolite levels for the conjugates were divided by the total maytansinoids in the sample (acetone pellet + extract ~ conjugate bound at $t = 0$) to determine the

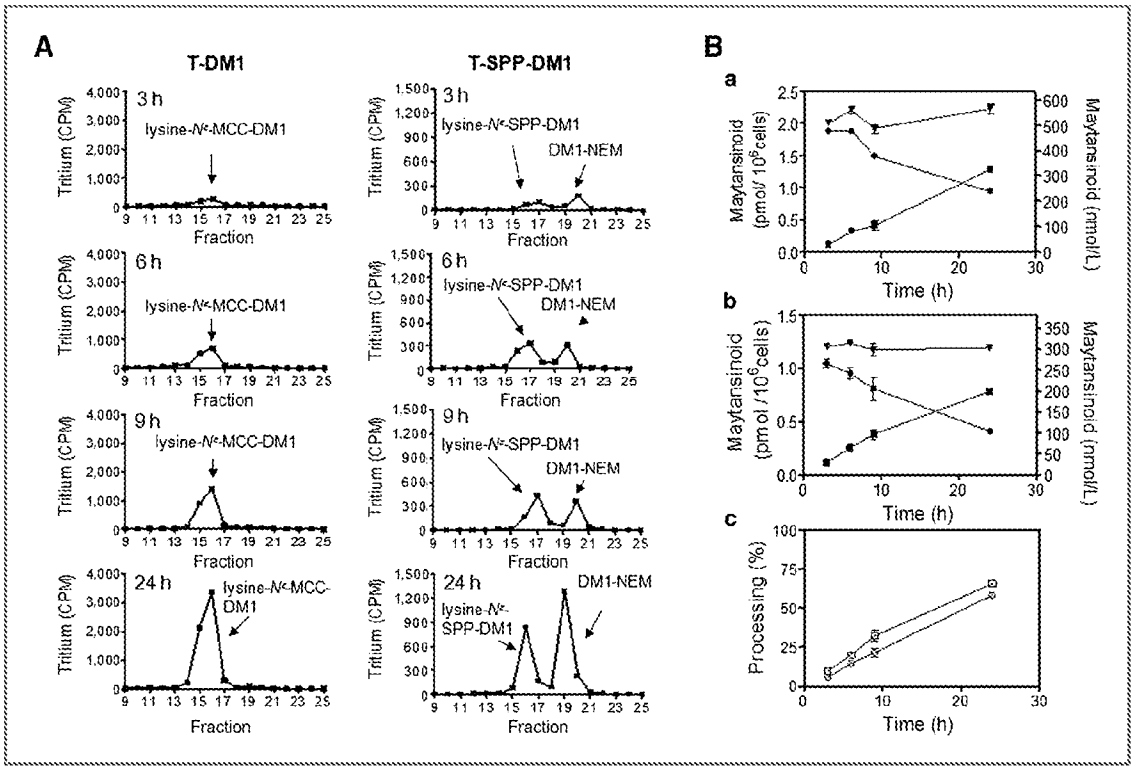


Figure 4. Activation of trastuzumab–DM1 conjugates in HER2-positive breast carcinoma cells. A, HPLC radiograms of the target cell catabolites following exposure of BT474EEI cells to T-[^{3}H]DM1 and T-SPP-[^{3}H]DM1. Cells were harvested at the indicated time points and analyzed for maytansinoids. The chromatograms show the fraction number (x-axis) and the CPM (y-axis). B, rates for the catabolism of conjugates. Panels a and b show the concentration of maytansinoid catabolites of T-DM1 (a) and T-SPP-DM1 (b) formed within cells over time. Concentrations were calculated from the radioactivities in A and plotted versus time. A total of 1 pmol/10^6 cells is equivalent to 253 nmol/L. The corresponding concentration of intact conjugate still associated with the cells (●) was determined from the radioactivity associated with the acetone precipitates. ▲, total maytansinoid levels. Panel c shows the percentage of the conjugates processed at each time. The processing of T-DM1 (□) and T-SPP-DM1(○) was calculated from a and b by dividing the catabolites of each conjugate formed at each time by the corresponding total maytansinoid levels.

CSPC Exhibit 1004
Page 263 of 336

Downloaded from mct.aacrjournals.org on January 13, 2020. © 2012 American Association for Cancer Research.

Published OnlineFirst March 9, 2012; DOI: 10.1158/1535-7163.MCT-11-0727

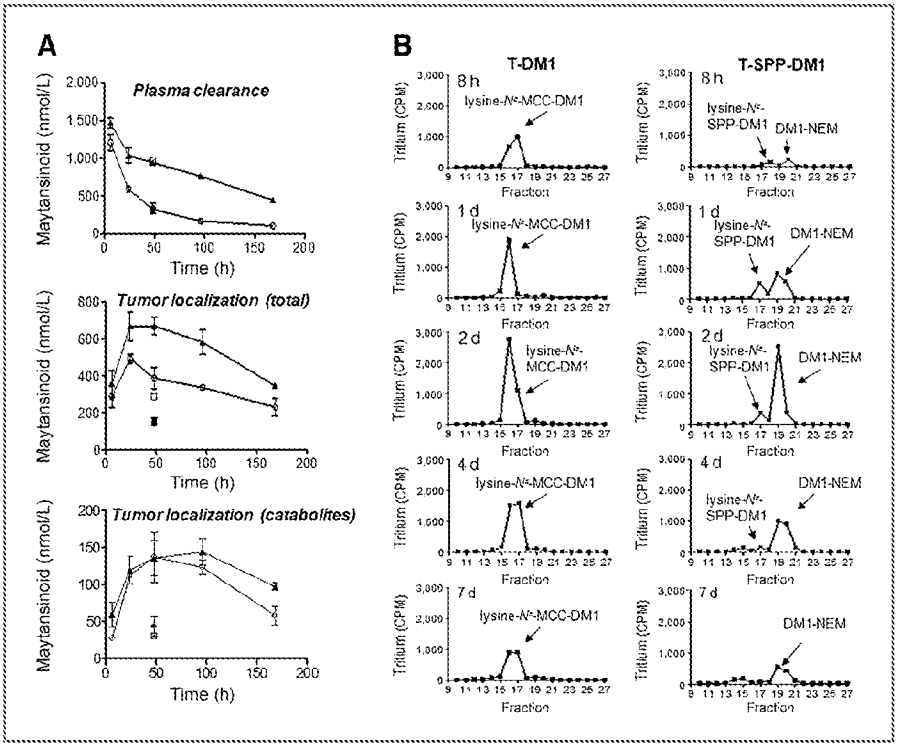


Figure 5. Tumor localization and catabolism of trastuzumab–DM1 conjugates. A, plasma clearance of conjugate (top) and accumulation of total maytansinoids (middle) and maytansinoid catabolites (bottom) in tumors following administration of a single i.v. dose of 200 μg/kg (based on DM1 concentration) of T-[^{3}H]DM1 (▲), T-SPP-[^{3}H]DM1 (○), 5B6-MCC-[^{3}H]DM1 (□), and 5B6-SPP-[^{3}H]DM1 (●) to mice. Concentrations of conjugate in plasma (DM1 concentration) and total maytansinoid (conjugate + catabolites) in tumor were calculated from the total radioactivity in plasma and tumors samples, respectively, expressed as concentration. The maytansinoid catabolite levels in the tumors were determined by the radioactivity associated with HPLC catabolites shown in B. The counts per minute (CPM) of tritium in each effluent fraction was determined by LSC. The radiograms show the fraction number on the x-axis and CPM of tritium on the y-axis.

fraction of the conjugates processed to the observed catabolites and replotted in Fig. 4B, c. The rates of formation of catabolites from the 2 conjugates are similar when so normalized. HER2-mediated processing of these conjugates is similar in other breast carcinoma lines (Supplementary Fig. S1).

Catabolism of trastuzumab conjugates within tumor tissue

The concentration of the conjugates in plasma (based on DM1) was calculated from the plasma radioactivity and shown in Fig. 5A. The concentration of T-DM1 after 7 days is about 3-fold greater than the concentration of T-SPP-DM1 (top), consistent with the ELISA PK in nontumor-bearing mice (Fig. 3). The plasma conjugate concentrations (ELISA) in nontumor-bearing mice (Fig. 3) when adjusted for dose, were approximately ×2 higher than the estimated plasma conjugate concentrations derived from the plasma radioactivity measurements in tumor bearing mice, consistent with observations from a separate study (14). The causes of these discrepancies are not known, but do not affect the interpretation of this study. The plasma concentrations of the nonbinding control conjugates after 2 days were equivalent to the matched trastuzumab conjugates, as expected.

Maytansinoid concentrations in the tumors of mice treated with trastuzumab conjugates were found to reach a maximum level at about 1 to 2 days with peak concentrations of approximately 700 nmol/L (equivalent to 9% ID/g) or 500 nmol/L, (equivalent to 7% ID/g) for T-DM1 or T-SPP-DM1, respectively, followed by a gradual decline (Fig. 5A, middle). The 7 day AUC for the total maytansinoids in the tumors treated with T-DM1 was 1.5- fold higher than T-SPP-DM1.

On the basis of HPLC radiochromatograms, the catabolites of the trastuzumab conjugates in tumor tissues were identical to those identified *in vitro*—lysine-N^{ε}-MCC-DM1 for T-DM1 and lysine-N^{ε}-SPP-DM1 and DM1 for T-SPP-DM1 (Fig. 5B). The concentrations of the maytansinoid catabolites for the 2 conjugates (Fig. 5A, bottom) were very similar despite the differences in total maytansinoid levels (Fig. 5A, middle), with maximal maytansinoid catabolite concentration for both conjugates of approximately 150 nmol/L.

The lysine-N^{ε}-MCC-DM1 catabolite observed with T-DM1 was also observed for the control 5B6-MCC-DM1 conjugate at substantially reduced levels (Fig. 6A). Similarly, the lysine-N^{ε}-SPP-DM1 and DM1 catabolites observed for T-SPP-DM1 were also observed for the 5B6-SPP-DM1 conjugate—again at reduced levels. Concentrations of maytansinoid catabolites of the nontargeting conjugates were approximately 5-fold and 3-fold lower, respectively, than the concentrations of the catabolites of T-DM1 and T-SPP-DM1 (Fig. 6B). These results show the effect of HER2 targeting on the maytansinoid delivery of trastuzumab–DM1 conjugates.

CSPC Exhibit 1004
Page 264 of 336

Downloaded from mct.aacrjournals.org on January 13, 2020. © 2012 American Association for Cancer Research.

Published OnlineFirst March 9, 2012; DOI: 10.1158/1535-7163.MCT-11-0727

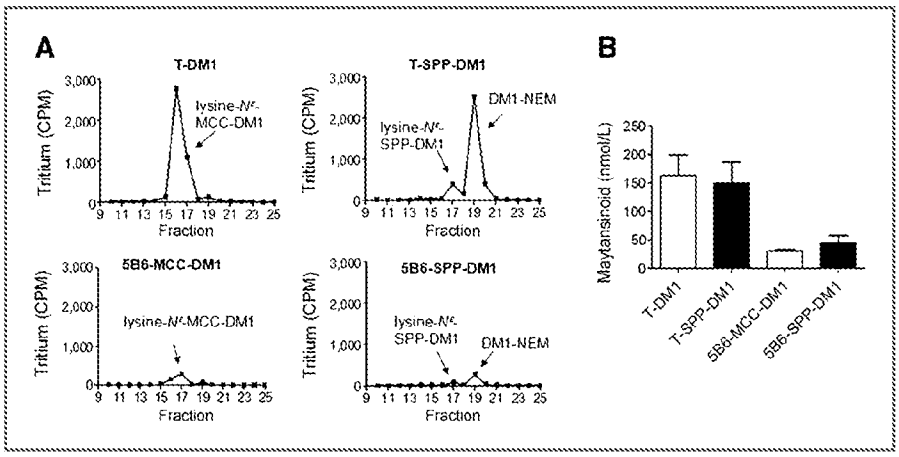


Figure 5. HER2 dependence of maytansinoid delivery to tumor. A, HPLC radiograms associated with the 2-day tumor catabolites of T-[^{3}H]DM1, T-SPP-[^{3}H]DM1, and the nontargeting 5B6-MCC-[^{3}H]DM1 and 5B6-SPP-[^{3}H]DM1 conjugate. The radiograms show the fraction number (x-axis) and CPM of tritium (y-axis). B, concentrations of the 2-day tumor catabolites were calculated from the peaks of radioactivity in the radiograms from A.

Discussion

Interest in ADCs has grown in response to the favorable safety and efficacy associated with T-DM1 and SGN-35—the latter, an antibody-auristatin conjugate targeting CD30-positive tumors (2, 15). Additional ADCs are in early clinical trials and more are expected to follow (1, 16). Efforts to understand the molecular basis for the anticancer activities of ADCs have intensified; with studies of maytansinoid and auristatin conjugates providing a mechanistic basis for their clinical activity (11, 12, 17–20).

The aims of these studies were to investigate the MOA and anticancer activity of T-DM1 and the role of the linker in these processes. To explore the underlying mechanisms determining trastuzumab–maytansinoid ADC activity, *in vitro* studies were conducted assessing ADC potency and the kinetics of ADC uptake into tumor cells, and the identity and accumulation of the catabolic products. Both trastuzumab conjugates were highly, and similarly, potent against HER2-expressing cell lines (Fig. 1; SK-BR-3, BT-474), consistent with a previous report (6). However, T-DM1 exhibited slightly greater potency in the BT474EEI and MCF7-neo/HER2 cell lines. It is not clear why these cell lines behave differently than the other cell lines tested.

In vitro tumor cell uptake and catabolism studies showed that the uptake and catabolism occurred at a comparable rate for both ADCs (Fig. 4B). This finding was expected, based on the similarity in HER2 binding affinity of the ADCs (data not shown), and the assumption that target-mediated cellular trafficking and catabolism of the ADCs are independent of linker type. The half-life of cellular catabolism of the ADCs was found to be approximately 19 hours, consistent with data reported for ^{125}I-trastuzumab; indicating that the maytansinoid conjugation does not alter catabolism rate (21). These studies also showed that lysine-N^{ε}-MCC-DM1 is the sole T-DM1 catabolite accumulating in the tumor cells tested (Fig. 4A). The high *in vitro* activation rate for T-DM1 within cancer cells is consistent with its potent cytotoxicity (Fig. 1) and is likely an important factor in its antitumor activity.

To explore the *in vitro–in vivo* correlation of these findings, PK, efficacy, *in vivo* tumor uptake, and catabolism studies were conducted with the HER2$^+$, trastuzumab insensitive, xenograft tumor BT474EEI. *In vivo* tumor catabolism data confirmed the *in vitro* data identifying lysine-N^{ε}-MCC-DM1 as the sole catabolic product (Fig. 5B).

Previous nonclinical studies reported that T-DM1 displayed slightly greater efficacy than T-SPP-DM1, when compared by dose (6). It was hypothesized that the greater efficacy of T-DM1, which uses a thioether to link DM1 to the antibody, compared with T-SPP-DM1, which contains a disulfide linker, may be related to improved PK or differences in the tumor accumulation of active catabolic products. The plasma clearance of T-DM1 is approximately 2 times slower than T-SPP-DM1 (Supplementary Table S1), likely due to greater stability of the thioether linker. This results in greater plasma exposure (AUC) per unit dose of T-DM1, but does not result in a substantive increase in efficacy (Fig. 2A). Indeed, comparing ADC efficacy as a function of plasma ADC exposure indicates similar *in vivo* potency (Fig. 2B).

The greater exposure of T-DM1 compared with T-SPP-DM1 corresponds with increased total tumor maytansinoid concentrations (Fig. 5A) for T-DM1, a logical sequela based on the similarity in the factors determining tumor uptake and binding for both ADCs. However, despite differences in total tumor maytansinoid concentrations, the tumor catabolite exposure levels for the 2 conjugates are similar (Fig. 5A). This was not expected, as the higher total maytansinoid concentrations for T-DM1, coupled with the more residualizing nature of its catabolic product predicted higher catabolite concentrations for T-DM1. The reasons for the similarity in tumor catabolite levels are unclear. One possibility is that the primary accumulation of conjugate in the tumor driving the subsequent HER2-mediated catabolism occurs within the first day or so when the plasma concentrations for the 2 conjugates are

CSPC Exhibit 1004
Page 265 of 336

Downloaded from mct.aacrjournals.org on January 13, 2020. © 2012 American Association for Cancer Research.

Published OnlineFirst March 9, 2012; DOI: 10.1158/1535-7163.MCT-11-0727

similar. Another possibility is that the *in vivo* cleavage of the disulfide-linked T-SPP-DM1 was more efficient than T-DM1 despite similar *in vitro* processing rates. For example, direct cleavage of DM1 from T-SPP-DM1 within tumor tissue via thiol-disulfide exchange reactions could increase the processing rate by complementing the lysine-N^{ε}-SPP-DM1 released via the lysosomal degradation route.

It is postulated that the cellular catabolic products of ADCs are responsible for their cytotoxic activity. The observation of similar tumor catabolite concentrations for T-DM1 and T-SPP-DM1 when both conjugates are administered at the same ADC dose coupled with the slightly greater *in vitro* potency of T-DM1 in BT474EEI cells would predict greater efficacy for T-DM1; however, no substantive difference in efficacy was observed (Fig. 2). This is a unique observation as, in studies with ADCs targeting the CanAg antigen antibody maytansioid conjugate, thioether-linked conjugates were less active than disulfide-linked conjugates, even when tumor catabolite concentrations for the thioether-linked ADC were somewhat higher than those of the disulfide-linked ADC (12), an observation attributed to bystander killing (11–13). Both the disulfide-linked and thioether-linked anti-CanAg conjugates were efficiently degraded in the lysosomes of cancer cells to yield the corresponding lysine-linker-maytansinoid catabolites. For the thioether-linked conjugate, no further catabolism was observed. However, the catabolites of the 2 disulfide-linked conjugates huC242-SPP-DM1 and huC242-SPDB-DM4 were both further processed to yield catabolites capable of diffusing throughout tumor tissue, thereby enhancing the activity of the disulfide-linked conjugates through bystander killing mechanisms. Although this may also apply to the trastuzumab ADCs in this study, the greater *in vitro* potency of T-DM1 may compensate for the bystander effect associated with T-SPP-DM1 to explain the similarity in *in vivo* efficacy.

In summary, the studies described herein provide a detailed understanding of mechanistic aspects of the PK, tumor uptake, and pharmacologic activity of T-DM1 and contrast those properties with a more labile disulfide linker. These studies confirm that T-DM1 and T-SPP-DM1 have potent antitumor activity in HER2-expressing cell lines and show that T-DM1 is rapidly activated by HER2-positive cancer cells to lysine-N^{ε}-MCC-DM1. Improved linker stability with T-DM1 leads to greater plasma ADC exposure and tumor uptake of total maytansinoid than T-SPP-DM1. Surprisingly, the increase in total tumor uptake with T-DM1 does not translate into greater tumor catabolite concentrations or improved efficacy, when compared with T-SPP-DM1. Sustained exposure of the lysine-N^{ε}-MCC-DM1 catabolite in tumors of treated mice provides a mechanistic basis for the preclinical activity of T-DM1. The efficacy and tumor-targeting characteristics of T-DM1 and T-SPP-DM1 suggest that both linker formats are effective in payload delivery and antitumor activity.

Disclosure of Potential Conflicts of Interest

C. Audette has an ownership interest in ImmunoGen, Inc. J. Pinkas held the role of Director (Pharmacology) in ImmunoGen, Inc.; also has ownership interest in ImmunoGen, Inc. J. Tibbitts has ownership interest (including patents) in Roche. No potential conflicts of interest were disclosed by the other authors.

Authors' Contributions

Conception and design: H.K. Erickson, G.D. Lewis Phillips, C.A. Provenzano, B. Gunter, J. Pinkas, J. Tibbitts
Development of methodology: H.K. Erickson, G.D. Lewis Phillips, E. Mai, M. Gupta, J. Tibbitts
Acquisition of data: H.K. Erickson, G.D. Lewis Phillips, D.D. Leipold, E. Mai, H.A. Johnson, J. Pinkas, J. Tibbitts
Analysis and interpretation of data: H.K. Erickson, G.D. Lewis Phillips, D.D. Leipold, E. Mai, C.A. Provenzano, B. Gunter, M. Gupta, J. Pinkas, J. Tibbitts
Writing, review, and/or revision of the manuscript: H.K. Erickson, G.D. Lewis Phillips, D.D. Leipold, E. Mai, B. Gunter, C.A. Audette, M. Gupta, J. Pinkas, J. Tibbitts
Administrative, technical, or material support: C.A. Audette, E. Mai, J. Tibbitts
Study supervision: H.K. Erickson, D.D. Leipold, J. Pinkas, J. Tibbitts

Acknowledgments

The authors thank John Lambert and Ravi Chari for their many helpful suggestions and careful reading of the manuscript.

The costs of publication of this article were defrayed in part by the payment of page charges. This article must therefore be hereby marked *advertisement* in accordance with 18 U.S.C. Section 1734 solely to indicate this fact.

Received October 4, 2011; revised January 24, 2012; accepted January 31, 2012; published OnlineFirst March 9, 2012.

References

1. Lambert JM. Antibody–maytansinoid conjugates: a new strategy for the treatment of cancer. Drugs Fut 2010;35:471–80.
2. Krop IE, Beeram M, Modi S, Jones SF, Holden SN, Yu W, et al. Phase I study of trastuzumab-DM1, an HER2 antibody-drug conjugate, given every 3 weeks to patients with HER2-positive metastatic breast cancer. J Clin Oncol 2010;28:2698–704.
3. Burris HA, Rugo HS, Vukelja SJ, Vogel CL, Borson RA, et al. Phase II study of the antibody drug conjugate trastuzumab-DM1 for the treatment of human epidermal growth factor receptor 2 (HER2)-positive breast cancer after prior HER2-directed therapy. J Clin Oncol 2011;29:398–405.
4. Burris HA. Trastuzumab emtansine: a novel antibody-drug conjugate for HER2-positive breast cancer. Expert Opin Biol Ther 2011;11:807–19.
5. Junttila TT, Li G, Parsons K, Phillips GL, Sliwkowski MX. Trastuzumab-DM1 (T-DM1) retains all the mechanisms of action of trastuzumab and efficiently inhibits growth of lapatinib insensitive breast cancer. Breast Cancer Res Treat 2011;128:347–56.
6. Lewis Phillips GD, Li G, Dugger DL, Crocker LM, Parsons KL, Mai E, et al. Targeting HER2-positive breast cancer with trastuzumab-DM1, an antibody-cytotoxic drug conjugate. Cancer Res 2008;68:9280–90.

CSPC Exhibit 1004
Page 266 of 336

Downloaded from mct.aacrjournals.org on January 13, 2020. © 2012 American Association for Cancer Research.

Published OnlineFirst March 9, 2012; DOI: 10.1158/1535-7163.MCT-11-0727

7. Al-Katib AM, Aboukameel A, Mohammad R, Bissery MC, Zuany-Amorim C. Superior antitumor activity of SAR3419 to rituximab in xenograft models for non-Hodgkin's lymphoma. Clin Cancer Res 2009;15:4038–45.
8. Chen Q, Millar HJ, McCabe FL, Manning CD, Steeves R, Lai K, et al. Alpha V integrin-targeted immunoconjugates regress established human tumors in xenograft models. Clin Cancer Res 2007;13:3689–95.
9. Ikeda H, Hideshima T, Fulciniti M, Lutz RJ, Yasui H, Okawa Y, et al. The monoclonal antibody nBT062 conjugated to cytotoxic maytansinoids has selective cytotoxicity against CD138-positive multiple myeloma cells *in vitro* and *in vivo*. Clin Cancer Res 2009;15:4028–37.
10. Kellogg BA, Garrett L, Kovtun Y, Lai KC, Leece B, Miller M, et al. Disulfide-linked antibody-maytansinoid conjugates: optimization of *in vivo* activity by varying the steric hindrance at carbon atoms adjacent to the disulfide linkage. Bioconjugate Chem 2011;22:717–27.
11. Erickson HK, Park PU, Widdison WC, Kovtun YV, Garrett LM, Hoffman K, et al. Antibody-maytansinoid conjugates are activated in targeted cancer cells by lysosomal degradation and linker-dependent intracellular processing. Cancer Res 2006;66:4426–33.
12. Erickson HK, Widdison WC, Mayo MF, Whiteman K, Audette C, Wilhelm SD, et al. Tumor delivery and *in vivo* processing of disulfide-linked and thioether-linked antibody-maytansinoid conjugates. Bioconjug Chem 2010;21:84–92.
13. Kovtun YV, Audette CA, Ye Y, Xie H, Ruberti MF, Phinney SJ, et al. Antibody-drug conjugates designed to eradicate tumors with homogeneous and heterogeneous expression of the target antigen. Cancer Res 2006;66:3214–21.
14. Xie H, Audette C, Hoffee M, Lambert JM, Blattler WA. Pharmacokinetics and biodistribution of the antitumor immunoconjugate, cantuzumab mertansine (huC242-DM1), and its two components in mice. J Pharmacol Exp Ther 2004;308:1073–82.
15. Younes A, Bartlett NL, Leonard JP, Kennedy DA, Lynch CM, Sievers EL, et al. Brentuximab vedotin (SGN-35) for relapsed CD30-positive lymphomas. N Engl J Med 2010;363:1812–21.
16. Senter PD. Potent antibody drug conjugates for cancer therapy. Curr Opin Chem Biol 2009;13:235–44.
17. Jumbe NL, Xin Y, Leipold DD, Crocker L, Dugger D, Mai E, et al. Modeling the efficacy of trastuzumab-DM1, an antibody drug conjugate, in mice. J Pharmacokinet Pharmacodyn 2010;37:221–42.
18. Alley SC, Zhang X, Okeley NM, Anderson M, Law CL, Senter PD, et al. The pharmacologic basis for antibody-auristatin conjugate activity. J Pharmacol Exp Ther 2009;330:932–8.
19. Doronina SO, Mendelsohn BA, Bovee TD, Cerveny CG, Alley SC, Meyer DL, et al. Enhanced activity of monomethylauristatin F through monoclonal antibody delivery: effects of linker technology on efficacy and toxicity. Bioconjug Chem 2006;17:114–24.
20. Okeley NM, Miyamoto JB, Zhang X, Sanderson RJ, Benjamin DR, Sievers EL, et al. Intracellular activation of SGN-35, a potent anti-CD30 antibody-drug conjugate. Clin Cancer Res 2010;16:888–97.
21. Austin CD, De Maziere AM, Pisacane PI, van Dijk SM, Eigenbrot C, Sliwkowski MX, et al. Endocytosis and sorting of ErbB2 and the site of action of cancer therapeutics trastuzumab and geldanamycin. Mol Biol Cell 2004;15:5268–82.

CSPC Exhibit 1004
Page 267 of 336

Downloaded from mct.aacrjournals.org on January 13, 2020. © 2012 American Association for Cancer Research.

Published OnlineFirst March 9, 2012; DOI: 10.1158/1535-7163.MCT-11-0727

AACR American Association for Cancer Research

Molecular Cancer Therapeutics

The Effect of Different Linkers on Target Cell Catabolism and Pharmacokinetics/Pharmacodynamics of Trastuzumab Maytansinoid Conjugates

Hans K. Erickson, Gail D. Lewis Phillips, Douglas D. Leipold, et al.

Mol Cancer Ther 2012;11:1133-1142. Published OnlineFirst March 9, 2012.

Updated version	Access the most recent version of this article at: doi:10.1158/1535-7163.MCT-11-0727
Supplementary Material	Access the most recent supplemental material at: http://mct.aacrjournals.org/content/suppl/2012/03/09/1535-7163.MCT-11-0727.DC1

Cited articles	This article cites 21 articles, 12 of which you can access for free at: http://mct.aacrjournals.org/content/11/5/1133.full#ref-list-1
Citing articles	This article has been cited by 22 HighWire-hosted articles. Access the articles at: http://mct.aacrjournals.org/content/11/5/1133.full#related-urls

E-mail alerts	Sign up to receive free email-alerts related to this article or journal.
Reprints and Subscriptions	To order reprints of this article or to subscribe to the journal, contact the AACR Publications Department at pubs@aacr.org.
Permissions	To request permission to re-use all or part of this article, use this link http://mct.aacrjournals.org/content/11/5/1133. Click on "Request Permissions" which will take you to the Copyright Clearance Center's (CCC) Rightslink site.

Downloaded from mct.aacrjournals.org on January 13, 2020. © 2012 American Association for Cancer Research.

OK TO ENTER: /KAC/

PATENT

IN THE UNITED STATES PATENT AND TRADEMARK OFFICE

First Named Inventor	:	Chaohong Hu
Application No.	:	15/550,995
Filed	:	August 14, 2017
For	:	ANTIBODY-DRUG CONJUGATE
Examiner	:	Karen A Canella
Art Unit	:	1643
Docket No.	:	850231.401USPC
Date	:	December 16, 2019

Commissioner for Patents
P.O. Box 1450
Alexandria, VA 22313-1450

AMENDMENT

Commissioner for Patents:

In response to the final Office Action dated October 18, 2019, please amend the application as follows:

Amendments to the Claims are reflected in the listing of claims which begins on page 2 of this paper.

Remarks begin on page 7 of this paper.

Enhanced Activity of Monomethylauristatin F through Monoclonal Antibody Delivery: Effects of Linker Technology on Efficacy and Toxicity

Svetlana O. Doronina,* Brian A. Mendelsohn, Tim D. Bovee, Charles G. Cerveny, Stephen C. Alley, Damon L. Meyer, Ezogelin Oflazoglu, Brian E. Toki, Russell J. Sanderson, Roger F. Zabinski, Alan F. Wahl, and Peter D. Senter

Seattle Genetics, Inc., 21823 30th Drive SE, Bothell, Washington 98021. Received October 4, 2005; Revised Manuscript Received October 19, 2005

We have previously shown that antibody–drug conjugates (ADCs) consisting of cAC10 (anti-CD30) linked to the antimitotic agent monomethylauristatin E (MMAE) lead to potent in vitro and in vivo activities against antigen positive tumor models. MMAF is a new antimitotic auristatin derivative with a charged C-terminal phenylalanine residue that attenuates its cytotoxic activity compared to its uncharged counterpart, MMAE, most likely due to impaired intracellular access. In vitro cytotoxicity studies indicated that mAb–maleimidocaproyl-valine-citrulline-*p*-aminobenzyloxycarbonyl–MMAF (mAb–L1–MMAF) conjugates were >2200-fold more potent than free MMAF on a large panel of CD30 positive hematologic cell lines. As with cAC10–L1–MMAE, the corresponding MMAF ADC induced cures and regressions of established xenograft tumors at well tolerated doses. To further optimize the ADC, several new linkers were generated in which various components within the L1 linker were either altered or deleted. One of the most promising linkers contained a noncleavable maleimidocaproyl (L4) spacer between the drug and the mAb. cAC10–L4–MMAF was approximately as potent in vitro as cAC10–L1–MMAF against a large panel of cell lines and was equally potent in vivo. Importantly, cAC10–L4–MMAF was tolerated at >3 times the MTD of cAC10–L1–MMAF. LCMS studies indicated that drug released from cAC10–L4–MMAF was the cysteine–L4–MMAF adduct, which likely arises from mAb degradation within the lysosomes of target cells. This new linker technology appears to be ideally suited for drugs that are both relatively cell-impermeable and tolerant of substitution with amino acids. Thus, alterations of the linker have pronounced impacts on toxicity and lead to new ADCs with greatly improved therapeutic indices.

Downloaded via US PATENT AND TRADEMARK OFFICE on January 11, 2020 at 07:43:04 (UTC).
See https://pubs.acs.org/sharingguidelines for options on how to legitimately share published articles.

INTRODUCTION

In recent years, the impact that monoclonal antibodies (mAbs)[1] have had in the clinical treatment of cancer has been pronounced. There are now several approved therapeutic antibodies, including trastuzumab (Herceptin), rituximab (Rituxan), cetuximab (Erbitux), and bevacizumab (Avastin), and many others are in late-stage development (reviewed in refs 1, 2). While these agents display significant activities through such mechanisms as antibody-dependent cellular cytotoxicity, complement-dependent cytotoxicity, and signal transduction, the activities are generally suboptimal, even when combined with conventional cancer chemotherapeutic agents. Consequently, significant attention has turned toward the use of mAb-based immunoconjugates, in which the mAb carries a toxic payload to tumor cells (reviewed in refs 3, 4). Three such agents are now clinically approved: ibritumomab tiuxetan (Zevalin), a ^{90}Y labeled anti-CD20 mAb; tositumomab (Bexxar), an ^{131}I labeled anti-CD20 mAb; and gemtuzumab ozogamicin (Mylotarg), an anti-CD33–calicheamicin conjugate. The activities of these conjugated mAbs provide validation for the concept, and a basis for developing other such agents for cancer therapy.

The goal of targeted therapy with mAb–drug conjugates is to achieve high degrees of therapeutic activity, while sparing normal tissues from chemotherapeutic damage. Toward this end, several critical parameters have been identified that must be addressed. These include the barriers to mAb extravasation, conjugate immunogenicity, widespread expression of the target antigen on normal tissue, metabolism at nontarget sites, low drug potency, and efficient release of the drug in forms that do not impair activity (*3*–*6*). Consequently, the focus in many laboratories has been to use chimeric or humanized mAbs against highly selective tumor-associated antigens, attached to potent drugs through linkers that allow for efficient drug release once the antibody–drug conjugate (ADC) has bound to the target and has undergone internalization. Examples of some advanced agents include C242-DM1 (cantuzumab mertansine), an anticarcinoma mAb linked to a derivative of maytansine (*7*), MLN2704, an anti-prostate cancer mAb attached to maytansine (*5*), and an anti-CD22–calicheamicin conjugate for the treatment of B-cell lymphomas (*8*).

In developing highly active agents that address the issues described for targeted therapy, we have focused considerable attention on the drug payload, the linker used for drug attachment, and the method by which the antibody is modified. This has led to the development of mAb–auristatin conjugates

* To whom correspondence should be addressed. E-mail: sdoronina@seagen.com

[1] Abbreviations: ADC, antibody–drug conjugate; cAC10–linker–drug$_{4 \text{ or } 8}$, cAC10 ADC with four or eight drugs/mAb; Cit, L-citrulline; Cys, L-cysteine; Dap, dolaproine; DEPC, diethyl cyanophosphonate; DIEA, *N,N*-diisopropylethylamine; Dil, dolaisoleuine; DMF, dimethylformamide; DTNB, 5,5′-dithio-bis(2-nitrobenzoic acid); DTT, dithiothreitol; Fmoc, 9-fluorenylmethoxycarbonyl; HATU, *O*-(7-azabenzotriazol-1-yl)-*N,N,N′,N′*-tetramethyluronium hexafluorophosphate; HRP, horseradish peroxidase; IC_{50}, dose that inhibits cell growth by 50%; L1–4, linkers 1–4 (Table 1); MeVal, *N*-methyl valine; mAb, monoclonal antibody; MDR, multidrug resistance; MMAE, monomethylauristatin E; MMAF, monomethylauristatin F; MMAF-OMe, monomethylauristatin F methyl ester; MTD, maximum tolerated dose; PAB, *p*-aminobenzyl; PABC, *p*-aminobenzyloxycarbonyl; PABOH, *p*-aminobenzyl alcohol; PBS, phosphate-buffered saline; Phe, L-phenylalanine; pNP, *p*-nitrophenyl; TFA, trifluoroacetic acid; Val, L-valine.

10.1021/bc0502917 CCC: $33.50 © 2006 American Chemical Society
Published on Web 12/22/2005

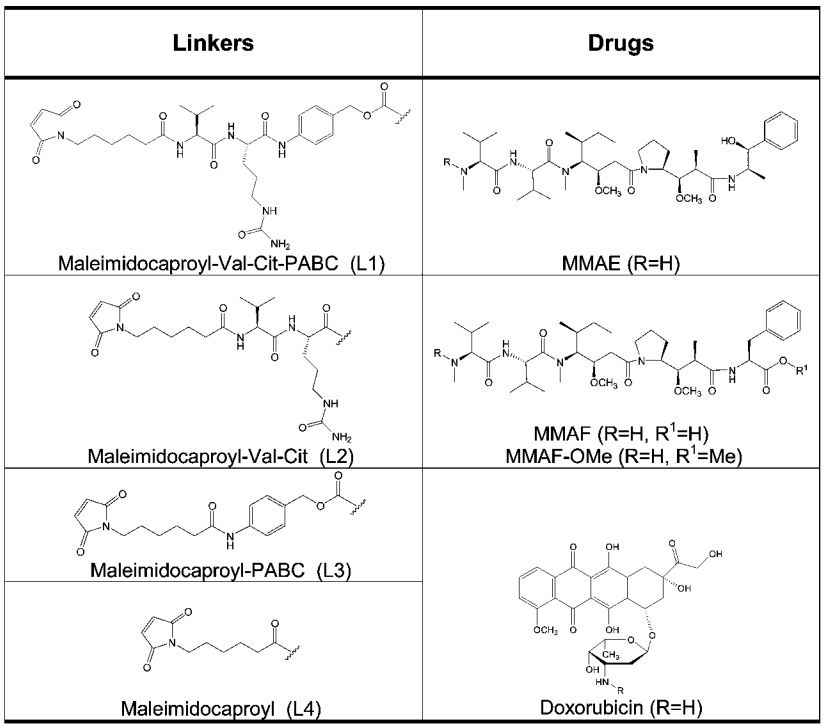


Figure 1. Structures of drugs and linkers.

that include a highly potent and totally synthetic drug attached to mAb cysteine residues through a proteolytically cleavable linker (*3*, *6*, *9*−*12*). The most advanced agent that we have described (*12*−*15*) is cAC10−maleimidocaproyl-valine-citrulline-*p*-aminobenzyloxycarbonyl-monomethylauristatin E (cAC10−maleimidocaproyl-Val-Cit-PABC−MMAE, or cAC10−L1−MMAE, shown in Figure 1). This is comprised of the highly potent antimitotic agent MMAE, attached to mAb−cysteines through the L1 linker that is cleaved by intracellular proteases such as cathepsin B. The optimal number of drugs/mAb was found to be four (*14*), where pronounced activities at well tolerated doses were obtained in CD30 positive hematologic malignancies.

Here, we describe the properties of a new auristatin, MMAF, that was designed to be much more active when actively delivered inside cells with a mAb, compared to treatment in the untargeted form. We viewed such an approach to targeted delivery as advantageous compared to that of drugs that have high potency in the untargeted form, since any drug that is systemically released would not be expected to contribute to toxic side-effects. Several linker technologies were evaluated to optimize the delivery of MMAF to target cells. In this report, we demonstrate that targeted MMAF is much more potent than the free drug, and that cAC10 conjugates of MMAF display pronounced activities, both in vitro and in vivo. In addition, conjugates of MMAF circumvent a common form of multidrug resistance (MDR). The development of this drug, together with the biological activities of ADCs derived from it, are described for the first time.

EXPERIMENTAL PROCEDURES

General. Unless otherwise noted, materials were obtained from commercial suppliers in the highest purity grade available and used without further purifications. Anhydrous DMF and CH_2Cl_2 were purchased from Aldrich. *N*-Fmoc-L-[ring-$^{13}C_6$]-Phenylalanine was obtained from Cambridge Isotope Laboratories, Inc. (Andover, MA). 2-Chlorotrityl chloride resin was purchased from Advanced ChemTech and loaded with *N*-Fmoc-L-[ring-$^{13}C_6$]-phenylalanine according to manufacturer's specifications. Phenylalanine-2-chlorotrityl resin was purchased from Novabiochem. Phenylalanine loading level of the resin was determined (0.55 mmol/gram) by extensive acylation with Fmoc-Cl followed by spectrophotometric Fmoc-quantitation assay. Solid-phase synthesis was performed in plastic syringes (National Scientific Company) fitted with a filter cut out of fritware PE medium grade porous sheet (Scienceware). Burrell wrist action shaker (Burrell Scientific, Pittsburgh, PA) was used for agitation. All solid-phase yields reported are based upon the initial phenylalanine substitution level of the resin and constitute a mass balance of isolated pure material from support, unless otherwise stated. Fmoc-Dap was custom synthesized by Albany Molecular Research, Inc. (Albany, NY).

HPLC assays were performed using C12 Phenomenex Synergy MAX-RP 4μ, 80 Å reversed-phase column, 150 × 2.0 mm. The eluent was a linear gradient of acetonitrile from 5% to 95% in 5 mM aqueous ammonium phosphate, pH 7.0, in 10 min, then 95% acetonitrile for 10 min, flow rate 1 mL/min, 215 nm detection. Preparative HPLC purifications were performed on Varian instrument equipped with C12 Phenomenex Synergy MAX-RP 4μ reversed phase column, 250 × 21.2 mm, eluting with 0.1% TFA in a water−acetonitrile gradient. Flash chromatography was carried out using Whatman 60 Å 230−400 mesh ASTM silica gel.

Low resolution mass spectra (LCMS) were recorded on a ZMD-Micromass Single Quadrupole Mass Spectrometer equipped with an electrospray ion source (45 eV) coupled with HP1100 HPLC system (reverse phase C12 Phenomenex column, 4 μ, 100 Å, 150 × 2.0 mm. The eluent was a linear gradient of acetonitrile from 5% to 95% in water in the presence of 0.1% formic acid in 10 min, then 95% acetonitrile for 5 min, flow rate 400 μL/min). High resolution (exact mass, HRMS) electrospray ionization (ESI) data were obtained at the University of Washington Medicinal Chemistry Mass Spectrometry Center on a Bruker APEXIII 47e [FT(ICR)]MS. NMR data were recorded on Varian Mercury 400 MHz Instrument. Chemical shifts (δ) are reported in ppm downfield from an internal solvent peak, and J values are in hertz.

CSPC Exhibit 1004

The chimeric IgG_1 cAC10 (*16*) and cBR96 (*17*) mAbs recognize the CD30 and Lewis Y antigens, respectively. The human lymphoma cell lines Karpas 299, SUP-M2, SU-DHL-1, SR-786, DEL, HDLM-2, L428, KMH-2, and WSU-NHL were obtained from the DSMZ (Braunschweig, Germany). 786-O and Caki-1 renal cell carcinoma and HH lymphoma cell lines were purchased from the ATCC (Manassas, VA). H3396 breast carcinoma cells were obtained as described earlier (*16*). The parent/drug resistant cell line pair NCI-H69, NCI-H69/LX4 were obtained from the ECACC (Salisbury, England), and the Hodgkin's disease cell line L540cy has been previously described (*18*). All cell lines were grown according to the manufacturers' recommendations and routinely checked for mycoplasma contamination.

Maleimidocaproyl−MMAE (L4−MMAE). To a solution of MMAE (*12*) (72 mg, 0.1 mmol) in anhydrous CH_2Cl_2 (2 mL) 6-maleimidocaproic acid (30 mg, 0.15 mmol, 1.5 equiv) was added followed by DEPC (36 μL, 0.2 mmol, 2 equiv) and DIEA (55 μL, 0.3 mmol, 3 equiv). The reaction mixture was stirred at room temperature for 2 h. CH_2Cl_2 (30 mL) was added, and the mixture was washed with 10% aqueous citric acid (2 × 20 mL), water (20 mL), and brine (20 mL) and concentrated to near dryness. Product was isolated by flash chromatography on silica gel eluting with 5% MeOH in CH_2Cl_2 to give a white solid, 32 mg (35%). Reversed-phase HPLC analysis: 98% at 9.48 min. ^{1}H NMR (DMSO-d_6): δ 0.70−0.89 (18H, m), 0.95−1.05 (6H, m), 1.19−1.34 (m), 1.44−1.55 (m), 1.66−1.84 (m), 1.88−2.02 (m), 2.06−2.16 (m), 2.22−2.46 (m), 2.81 (s), 2.86 (s), 2.90 (s), 2.93 (s), 2.97 (d), 3.01−3.08 (m), 3.12 (d), 3.17 (d), 3.20 (d), 3.23 (dd), 3.35−3.40 (m), 3.42−3.50 (m), 3.52−3.59 (m), 3.77 (d), 3.93−4.04 (m), 4.37−4.54 (m), 4.59−4.64 (m), 4.70−4.78 (m), 5.36 (d), 5.43 (d), 7.01−7.02 (2H, m), 7.14−7.31 (5H, m), 7.65 (d), 7.74 (d), 7.78 (d), 7.89−7.92 (m), 8.56−8.61 (m). HRMS (ESI) calcd for $C_{49}H_{79}N_6O_{10}$ $(MH)^+$ 911.5858; found, *m/z* 911.5839.

Fmoc-MMAF-OMe. Fmoc-MeVal-Val-Dil (*12*) (0.50 g, 0.78 mmol) and Dap-Phe-OMe·HCl (*12*) (0.30 g, 0.78 mmol) were dissolved in CH_2Cl_2 (5 mL) followed by the addition of DIEA (0.30 mL, 1.71 mmol, 2.2 equiv). DEPC (0.20 mL, 1.17 mmol, 1.5 equiv) was added next while the contents stirred under Ar. Reaction was complete according to HPLC analysis after 1 h. The mixture was concentrated and purified on silica gel eluting with a step gradient of ethyl acetate (from 50% to 100%) in hexane to provide a white foam, 0.65 g (87%). Reversed-phase HPLC analysis: 95% at 16.2 min. ^{1}H NMR (DMSO-d_6): δ 0.71−0.95 (20H, m), 1.01−1.07 (3H, dd), 1.22−1.30 (m), 1.34−1.52 (m), 1.60−1.83 (m), 1.92−2.11 (m), 2.16−2.28 (2H, m), 2.31−2.42 (m), 2.79−2.89 (m), 2.96−3.07 (m), 3.15−3.16 (m), 3.19 (s), 3.24 (s), 3.29 (d), 3.42−3.55 (m), 3.63 (1.5H, s), 3.66 (1.5H, s), 3.75 (0.5H, d), 3.96 (1H, m), 4.09−4.11 (m), 4.21−4.51 (m), 4.61−4.74 (m), 7.15−7.23 (5H, m), 7.31 (2H, t), 7.41 (3H, t), 7.62 (2H, d), 7.89 (2H, d), 8.05 (0.5H, d), 8.11 (0.5H, d), 8.29 (0.5H, d), 8.51 (0.5H, d). LCMS (ESI): *m/z* 968.35 $(MH)^+$ (eluted at 14.84 min).

MMAF-OMe. Fmoc-MMAF-OMe (140 mg, 0.14 mmol) in CH_2Cl_2 (5 mL) was treated with diethylamine (2 mL). After 2 h, the reaction was concentrated and purified by preparative HPLC to give a TFA salt of MMAF-OMe as a white solid, 126 mg (98%). Reversed-phase HPLC analysis: 94% at 11.25 min.^{1}H NMR (DMSO-d_6): δ 0.77 (3H, m), 0.87−1.07 (19H, m), 1.22−1.32 (m), 1.37−1.52 (m), 1.60−1.88 (m), 1.96−2.12 (m), 2.18−2.29 (m), 2.32−2.54 (m), 2.83−2.90 (m), 2.99 (s), 3.07 (s), 3.16−3.20 (m), 3.26 (s), 3.42−3.58 (m), 3.64 (s), 3.66 (s), 3.75 (d), 3.98 (m), 4.43−4.52 (m), 4.55−4.76 (m), 7.17−7.58 (5H, m), 8.30 (0.5H, d), 8.56 (0.5H, d), 8.83−8.93 (3H, m). HRMS (ESI) calcd for $C_{40}H_{68}N_5O_8$ $(MH)^+$ 746.5068; found, *m/z* 746.5037.

Maleimidocaproyl-Val-Cit-PABC−MMAF-OMe (L1−MMAF-OMe). MMAF-OMe·TFA (110 mg, 0.13 mmol, 1.0 equiv), maleimidocaproyl-Val-Cit-PAB-OCO-pNP (*10*) (103 mg, 0.14 mmol, 1.1 equiv), and 1-hydroxybenzotriazole (HOBt, 3.4 mg, 26 μmol, 0.2 equiv) were dissolved in pyridine (0.5 mL) and DMF (2 mL) under Ar. To this mixture was added DIEA (22.5 μL, 0.13 mmol, 1.0 equiv). The resulting solution stirred for 3 h before more DIEA (22.5 μL) was added. After stirring for 40 h total, the mixture was concentrated, taken up in DMSO (2 mL). Preparative HPLC purification followed by precipitation from CH_2Cl_2 (2 mL) with ether resulted in 90 mg (52%) of white solid. Reversed-phase HPLC analysis: 95% at 9.48 min. ^{1}H NMR (DMSO-d_6): δ 0.72−0.94 (28H, m), 1.02−1.06 (3H, dd), 1.14−1.52 (m), 1.54−1.82 (m), 1.90−2.38 (m), 2.28−2.46 (m), 2.85 (br s), 2.97 (s), 3.04 (s), 3.16 (s), 3.18 (s), 3.20 (s), 3.25 (s), 3.28−3.30 (m), 3.42−3.58 (m), 3.63 (s), 3.66 (s), 3.75 (d), 3.96 (m), 4.17−4.21 (m), 4.23−4.28 (m), 4.32−4.42 (m), 4.44−4.55 (m), 4.60−4.74 (m), 4.94−5.12 (m), 6.01 (1H, br s), 7.01 (2H, s), 7.18−7.32 (9H, m), 7.58 (2H, m), 7.81 (1H, d), 8.07−8.12 (1.5H, m), 8.29 (1H, m), 8.51 (0.5H, d), 10.0 (1H, d). HRMS (ESI) calcd for $C_{69}H_{106}N_{11}O_{16}$ $(MH)^+$ 1344.7819; found, *m/z* 1344.7776.

Maleimidocaproyl-PAB-OCO-pNP. To a suspension of 6-maleimidocaproic acid (1.0 g, 4.52 mmol) in CH_2Cl_2 (13.0 mL) was added *p*-aminobenzyl alcohol (PABOH, 1.11 g, 9.04 mmol, 2.0 equiv) and 2-ethoxy-1-ethoxycarbonyl-1,2-dihydroquinoline (EEDQ, 2.24 g, 9.04 mmol, 2.0 equiv). The reaction mixture was stirred at ambient temperature for 16 h, and then concentrated to near dryness. The residue was purified by flash chromatography on silica gel, eluting with a step gradient from 25 to100% ethyl acetate in hexane, to give 1.38 g (96%) of maleimidocaproyl-PABOH as a white solid. Maleimidocaproyl-PABOH (0.85 g, 2.69 mmol) was then activated by reaction with bis *p*-nitrophenyl carbonate (2.45 g, 8.07 mmol, 3 equiv) and DIEA (0.94 mL, 5.38 mmol, 2 equiv) in DMF (10 mL). After 1 h, HPLC analysis indicated complete consumption of starting material. Solvent was removed under reduced pressure, and the residue was triturated with diethyl ether (5 × 20 mL) resulting in 1.25 g (96%) of an off white solid. Reversed-phase HPLC analysis: 99% at 9.98 min. ^{1}H NMR ($CDCl_3$): δ 1.37 (2H, m), 1.64 (2H, m), 1.77 (2H, m), 2.37 (2H, t, J = 7.6), 3.54 (2H, t, J = 7.2), 6.68 (2H, s), 7.37 (2H, d, J = 9.2), 7.41 (2H, d, J = 8.8), 7.57 (2H, d, J = 8.8), 8.27 (2H, d, J = 9.2).

MeVal-Val-Dil-Dap-Phe-2-chlorotrityl Resin. Fmoc-Dap (450 mg, 1.1 mmol) and HATU (418 mg, 1.1 mmol, 2 equiv) were dissolved in anhydrous DMF (8 mL), and DIEA (384 μL, 2.2 mmol, 4 equiv). The resulting solution was added to the 20 mL syringe containing Phe-2-chlorotrityl resin (1 g, 0.55 mmol). Mixture was agitated for 3 h. Reaction completion was determined by LCMS analysis of material cleaved off a small amount of resin. The resin was filtered, washed with DMF (6 × 10 mL), CH_2Cl_2 (6 × 10 mL), ethyl ether (6 × 10 mL), and dried in vacuo for 2 h. A 20% piperidine in DMF solution (5 mL) was added to the syringe, and the mixture was agitated for 2 h. The resin was then filtered, rinsed with DMF (6 × 10 mL), CH_2Cl_2 (6 × 10 mL), and ethyl ether (6 × 10 mL), and dried in vacuo. In a separate flask Fmoc-MeVal-Val-Dil tripeptide (*12*) (702 mg, 1.1 mmol) and HATU (418 mg, 1.1 mmol, 2 equiv) were dissolved in anhydrous DMF (8 mL) followed by the addition of DIEA (384 μL, 2.2 mmol, 4 equiv). The solution was then transferred to the syringe containing the resin, and the mixture was agitated for 3 h. LCMC analysis of material cleaved from a small amount of resin was used to determine reaction completion. The resin was filtered, washed with DMF (6 × 10 mL), CH_2Cl_2 (6 × 10 mL), and ethyl ether (6 × 10 mL), and dried in vacuo. A 20% piperidine solution in DMF (5 mL) was added to the resin, and the mixture

CSPC Exhibit 1004
Page 272 of 336

was agitated for 2 h. The resin was then filtered, washed with DMF (6 × 10 mL), CH_2Cl_2 (6 × 10 mL), and ethyl ether (6 × 10 mL), and dried in vacuo.

MMAF (MeVal-Val-Dil-Dap-Phe). MeVal-Val-Dil-Dap-Phe-2-chlorotrityl resin (100 mg, 0.044 mmol) in a 5 mL syringe was treated with 2% TFA in CH_2Cl_2 (4 mL) for 5 min at ambient temperature. Preparative HPLC purification provided 27 mg (73%) of white solid. Reversed-phase HPLC analysis: 95% at 5.74 min. ^{1}H NMR (DMF-d_7): δ 0.78 (3H, t), 0.90−1.15 (19H, m), 1.28−1.44 (m), 1.46−1.62 (m), 1.75−2.00 (m), 2.03−2.12 (m), 2.14−2.23 (m), 2.24−2.48 (m), 2.50−2.61 (m), 2.78−2.82 (m), 2.97−3.09 (m), 3.12 (s), 3.18−3.21 (m), 3.26 (d), 3.30 (s), 3.34 (s), 3.41−3.46 (m), 3.49 (d), 3.53−3.60 (m), 3.61−3.69 (m), 3.72−3.78 (m), 3.93 (d), 4.10 (2H, br d), 4.12−4.38 (1H, br), 4.64−4.92 (3H, m), 7.21−7.35 (5H, m), 8.12 (0.5H, d), 8.40 (0.5H, d), 8.78−8.83 (1H, m), 9.03 (1H, br s), 9.63 (1H, br s). HRMS (ESI) calcd for $C_{39}H_{66}N_5O_8$ $(MH)^+$ 732.4911; found, *m/z* 732.4890.

Maleimidocaproyl-Val-Cit-PABC−MMAF (L1−MMAF). MeVal-Val-Dil-Dap-Phe-2-chlorotrityl resin (120 mg, 0.053 mmol) in a 5 mL syringe was treated with a solution of maleimidocaproyl-Val-Cit-PAB-OCOpNP (313 mg, 0.42 mmol, 8 equiv), 1-hydroxy-7-azabenzotriazole (HOAt, 2 mg, 0.015 mmol, 0.3 equiv), and DIEA (148 μL, 0.84 mmol, 16 equiv) in DMF (4 mL) for 16 h. The resin was then filtered and washed with DMF (6 × 3 mL), CH_2Cl_2 (6 × 3 mL) and ethyl ether (6 × 3 mL). Cleavage from resin by treatment with 2% TFA in CH_2Cl_2 (4 mL) for 5 min and preparative HPLC purification of the released material generated 15 mg (21%) of white solid that was 98% pure by reversed-phase HPLC analysis (retention time 7.20 min).^{1}H NMR (DMSO-d_6): δ 0.75−0.95 (28H, m), 1.05 (3H, t), 1.14 (m), 1.22−1.53 (m), 1.53−1.80 (m), 1.80−2.40 (m), 2.80 (br s), 2.96 (d), 3.11 (s), 3.13 (s), 3.20 (s), 3.62−3.70 (d), 3.83−3.94 (m), 4.08−4.24 (m), 4.28−4.5 (m), 4.50−4.68 (m), 4.90−5.10 (m), 5.35 (s), 5.96 (1H, t), 7.02 (2H, s), 7.08−7.32 (9H, m), 7.54 (2H, d), 7.80 (d), 8.04−8.12 (m), 8.16−8.33 (m), 10.0 (1H, br s). HRMS (ESI) calcd for $C_{68}H_{104}N_{11}O_{16}$ $(MH)^+$ 1330.7663; found, *m/z* 1330.7665.

Maleimidocaproyl-Val-Cit−MMAF (L2−MMAF). Fmoc-Cit (140 mg, 0.352 mmol) and Fmoc-Val (60 mg, 0.176 mmol) were coupled sequentially to MeVal-Val-Dil-Dap-Phe-2-chlorotrityl resin (200 mg, 0.088 mmol) using HATU coupling chemistry as described above for MeVal-Val-Dil-Dap-Phe-2-chlorotrityl resin. Then, to the dry Val-Cit-MeVal-Val-Dil-Dap-Phe-2-chlorotrityl resin a solution of 6-maleimidocaproic acid *N*-hydroxysuccinimide ester (54 mg, 0.176 mmol) in DMF (3 mL) was added. The mixture was shaken at room temperature for 4 h. Cleavage from resin by treatment with 2% TFA in CH_2Cl_2 (4 mL) for 5 min provided 28 mg (27%) of white solid after preparative HPLC purification. Reversed-phase HPLC analysis: 98% at 6.16 min. ^{1}H NMR (DMF-d_7): δ 0.69−0.92 (28H, m), 1.01−1.06 (3H, m), 1.17 (m), 1.42−1.53 (m), 1.53−1.68 (m), 1.70−2.28 (m), 2.28−2.46 (m), 2.74−2.88 (m), 2.89−3.00 (m), 3.04−3.06 (m), 3.15 (s), 3.18 (s), 3.24 (s), 3.40−3.47 (m), 3.48−3.58 (m), 3.59−3.68 (m), 3.71−3.76 (d), 3.96 (m), 4.14 (t), 4.23 (m), 4.38−4.52 (m), 4.58−4.76 (m), 4.89 (m), 5.95 (m), 7.01 (2H, s), 7.17−7.28 (5H, m), 7.77 (m), 7.89 (m), 7.96 (m), 8.04 (m), 8.17 (m), 8.28 (m), 8.38 (d), 8.47 (m). HRMS (ESI) calcd for $C_{60}H_{97}N_{10}O_{14}$ $(MH)^+$ 1181.7186; found, *m/z* 1181.7164.

Maleimidocaproyl-PABC−MMAF (L3−MMAF). MeVal-Val-Dil-Dap-Phe-2-chlorotrityl resin (100 mg, 0.044 mmol) was treated with a solution of maleimidocaproyl-PAB-OCO-pNP (42 mg, 0.088 mmol, 2 equiv), 1-hydroxybenzotriazole (HOBt, 1 mg, 9 μmol, 0.1 equiv), and DIEA (30 μL, 0.176 mmol, 4 equiv) in DMF (3 mL) for 16 h. The resin was then filtered and washed with DMF (6 × 3 mL), CH_2Cl_2 (6 × 3 mL), and ethyl ether (6 × 3 mL). Cleavage from resin by treatment with 2% TFA in CH_2Cl_2 (4 mL) for 5 min followed by preparative HPLC purification provided 31 mg (66%) of white solid which was 99% pure by reversed-phase HPLC analysis (retention time 7.14 min).^{1}H NMR (DMF-d_7): δ 0.76−0.98 (18H, m), 1.04 (2H, d), 1.12 (3H, m), 1.25−1.40 (m), 1.51−1.61 (m), 1.63−1.69 (m), 1.76−1.90 (m), 1.94−2.40 (m), 1.35−2.38 (m), 2.50−2.60 (m), 2.96 (s), 3.10 (s), 3.23 (s), 3.27 (s), 3.30 (s), 3.34 (s), 3.41−3.50 (m), 3.50−3.80 (m), 3.90−4.20 (m), 4.33−4.48 (m), 4.54−4.62 (m), 4.63−4.77 (m), 4.82−4.93 (m), 5.06−5.20 (m), 7.02 (2H, s), 7.36−7.21 (9H, m), 7.70 (2H, d), 8.11 (0.5H, d), 8.36 (0.5H, d), 10.00 (1H, br s). HRMS (ESI) calcd for $C_{57}H_{84}N_7O_{13}$ $(MH)^+$ 1074.6127; found, *m/z* 1074.6095.

Maleimidocaproyl−MMAF (L4−MMAF). 6-Maleimidocaproic acid (37 mg, 0.176 mmol, 2 equiv) and HATU (67 mg, 0.176 mmol, 2 equiv) were dissolved in anhydrous DMF (3 mL), followed by the addition of DIEA (62 μL, 0.35 mmol, 4 equiv). The solution was then transferred to a 5 mL syringe containing MeVal-Val-Dil-Dap-Phe-2-chlorotrityl resin (200 mg, 0.088 mmol), and the mixture was agitated for 3 h. The resin was filtered, washed with DMF (6 × 3 mL), CH_2Cl_2 (6 × 3 mL), and ethyl ether (6 × 3 mL), and dried in vacuo. Drug−linker was cleaved off the resin by treatment with 2% TFA in CH_2Cl_2 (4 mL) for 5 min and then purified by preparative HPLC to give 57 mg (70%) of white solid. Reversed-phase HPLC analysis: 98% at 6.72 min. ^{1}H NMR (DMF-d_7): δ 0.78−0.96 (18H, m), 1.04 (2H, t), 1.12 (3H, m), 1.25−1.36 (m), 1.41 (2H, d), 1.46−1.65 (m), 1.73−1.87 (m), 1.88−2.07 (m), 2.08−2.26 (m), 2.32−2.48 (m), 2.48−2.67 (m), 2.79−2.84 (m), 2.96 (d), 3.02 (d), 3.10 (d), 3.23 (d), 3.27 (s), 3.30 (s), 3.34 (s), 3.45 (t), 3.52−3.61 (m), 3.62−3.80 (m), 3.93 (d), 4.09−4.28 (m), 4.54−4.78 (m), 4.82−4.91 (2H, m), 7.03 (2H, s), 7.21−7.35- (5H, m), 7.51 (0.5H, d), 8.11 (0.5H, d), 8.36 (0.5H, d), 8.48 (0.5H, d), 13.0 (br s). HRMS (ESI) calcd for $C_{49}H_{77}N_6O_{11}$ $(MH)^+$ 925.5650; found, *m/z* 925.5636.

Maleimidocaproyl−[^{13}C]MMAF (L4−[^{13}C]MMAF) was prepared as described above starting from *N*-Fmoc-L-[ring-$^{13}C_6$]-phenylalanine-2-chlorotrityl resin. LCMS (ESI): *m/z* 931.62 $(MH)^+$.

Preparation of Antibody−Drug Conjugates. The conjugates with eight drug molecules per antibody were prepared as described previously (*12, 19*). Briefly, cBR96 or cAC10 (5−15 mg/mL) were mixed with DTT (10 mM, final) at 37 °C for 30 min, and the buffer was exchanged by elution through Sephadex G-25 resin with PBS containing 1 mmol/L diethylenetriaminepentaacetic acid. PBS containing 1 mmol/L diethylenetriaminepentaacetic acid was added to the reduced mAb bringing its final concentration to 2.5 mg/mL. The thiol concentration was ~8.4 thiols/mAb as measured by Ellman's reagent, DTNB. A 9.5-fold molar excess of linker−drug (L1−MMAF, L1−Dox (*10*), L1−MMAE (*12*), or L4−MMAE) was added to the reduced antibody at 4 °C for 1 h, and the conjugation reaction was quenched by adding a 20-fold excess of cysteine. The reaction mixture was concentrated by centrifugal ultrafiltration and buffer-exchanged through Sephadex G-25 equilibrated with PBS at 4 °C. The conjugate was then sterile filtered through a 0.2-μm filter.

cAC10 antibody−drug conjugates with four drugs per antibody were prepared by partial reduction of the mAb (*14, 20*) followed by reaction with desired linker−drug (L1−MMAF, L2−MMAF, L3−MMAF, or L4−MMAF). The antibody cAC10 (10 mg/mL) was partially reduced by addition of 3.0 molar equivalents of DTT at pH 8.0, followed by incubation at 37 °C for ~2 h. The reduction reaction was then chilled to ~10 °C and the excess DTT removed via diafiltration. The thiol concentration was determined by [illegible] and the [illegible] ratio was found to be in the range of 3.8−4.5. The linker−drug was

CSPC Exhibit 1004
Page 273 of 336

then added to a linker−drug/thiol molar ratio of ~1.15. The conjugation reaction was carried out in the presence of 15% v/v of DMSO. After conjugation, excess free cysteine (2 mol/L cysteine per mol/L linker−drug) was added to quench unreacted linker−drug to produce the cysteine−linker−drug adduct. The reaction mixture was purified and buffer-exchanged into PBS by diafiltration to obtain the partially loaded cAC10−linker−$drug_4$ conjugate. The molar ratio of drug substitution was determined according to previously published methods (*14, 20*).

Released Drug Identification. Lysosomal extracts of L540cy cells were prepared by swelling 2.4×10^8 cells in 9 mL of 0.25 M sucrose, 1 mM EDTA, and 10 mM HEPES (4-(2-hydroxyethyl)piperazine-1-ethansulfonic acid), pH 7.4. After 30 min on ice, cells were Dounce homogenized until >95% were broken as measured by Trypan Blue dye exclusion. Homogenates were centrifuged (3000*g*, 10 min, 4 °C) to pellet cellular debris, and the supernatant (4×10^7 cell equivalents per tube) was transferred to polyallomar ultracentrifuge tubes (13 × 51 mm) and centrifuged (17000*g*, 15 min, 4 °C) in a TLA100.3 rotor to isolate the lysosome-containing light mitochondrial pellet. Pellets were stored at −80 °C. The pellets were thawed and resuspended in 500 μL of 50 mM sodium acetate pH 5.0 and 2 mM DTT. cAC10−L4-[^{12}C]$MMAF_4$, cAC10−L4-[^{13}C]-$MMAF_4$, and cAC10−L4-[$^{12/13}$C]$MMAF_4$ (50 μg/mL) were independently added to one pellet. After three freeze/thaw cycles to break open lysosomes, samples were incubated for 24 h at 37 °C. Cold methanol (2 vol) was added to precipitate protein, the samples were centrifuged at 14000*g* to pellet debris, and 100 μL of supernatant was analyzed by low resolution mass spectrometry as described above. Authentic cysteine−L4−MMAF was prepared by treating 100 μM L4−MMAF with 1 mM cysteine in PBS at room temperature for 10 min.

In Vitro Growth Inhibition. Log phase cultures of cells were collected and cells plated at seeding densities ranging from 500 to 10000 cells/well according to predetermined conditions. After incubating 24 h to allow surface protein reconstitution, serial dilutions of test molecules were added and cultures incubated a further 4−6 days depending on cell line. Assessment of cellular growth and data reduction to generate IC_{50} values was done using Alamar Blue (Biosource International, Camarillo, CA) dye reduction assay as previously described, according to previously published methods (*12, 14, 15, 19*). Briefly, a 40% solution (wt/vol) of Alamar Blue was freshly prepared in complete media just before cultures were added. Ninety-two hours after drug exposure, Alamar Blue solution was added to cells to constitute 10% culture volume. Cells were incubated for 4 h, and dye reduction was measured on a Fusion HT fluorescent plate reader (Packard Instruments, Meriden, CT).

In Vivo Therapy Experiments. For the localized, subcutaneous disease model of anaplastic large cell lymphoma, 5×10^6 Karpas 299 cells were implanted into the right flanks of C.B.-17 SCID mice. Therapy was initiated when the tumor size in each group of six animals averaged approximately 100 mm^3. Treatments consisted of a single injection of solutions of the conjugates or controls in PBS intravenously (tail vein). Tumor volume was determined using the formula $(L \times W^2)/2$. For the disseminated ALCL model, 1×10^6 Karpas 299 were injected in the tail vein into C. B.-17 SCID mice. Single dose injection treatment was performed at 9 days after tumor injection. Mice that developed hind limb paralysis or other signs of significant disease were euthanized in accordance with Animal Care and Use Committee guidelines.

In Vivo Localization of Antibodies via Immunohistochemistry. When subcutaneous Karpas 299 tumor size reached 300 mm^3, three animals per group received one injection of 10 mg antibody component/kg body weight of either cAC10−L1−$MMAF_4$ or cBR96−L1−$MMAF_4$ intravenously. Tumors were then removed and placed in optimal cutting temperature (OCT) compound (Sakura Finetec, Torrence, CA), and 5 μm-thin frozen tissue sections were stained using immunohistochemistry evaluation. Briefly, frozen tissues on the slides were air-dried then fixed in 4% paraformaldehyde for 15 min at room temperature. Endogenous peroxidase activity was blocked using 0.6% H_2O_2 for 15 min. Additional blocking for endogenous biotin was done using the Avidin−Biotin Blocking kit (Vector Labs). Biotinylated-anti-human-Fc and biotinylated-anti-drug antibodies (both Seattle Genetics) were incubated on tissues at 2 μg/mL concentration for 1 h at room temperature. Following incubation of slides with avidin conjugated to HRP (Vectastatin Elite ABC kit, Vector Labs), 3,3′-diabenzidine (DAB) was used as a substrate for HRP. Tissues were counterstained using hematoxylin, slides were dehydrated, and slips were applied. Images were taken using the Zeiss Axiovert light microscope.

TUNEL Assay. Apoptosis was evaluated by TUNEL Staining (In Situ Cell Death Detection Kit, TR Red, Roche Applied Science, Germany) according to the manufacturer's instructions. TUNEL staining was carried out on sections of frozen specimens embedded in OCT. Labeling was visualized by Zeiss Axiovert fluorescence microscopy.

Table 1. In Vitro Cytotoxicity of Auristatins

cell line	type	IC_{50} (nM)[a] MMAE	MMAF	MMAF-OMe
Karpas 299	anaplastic large cell lymphoma	0.5	119	<0.001
H3396	breast carcinoma	0.1	105	<0.001
786-O	renal cell carcinoma	2.0	257	0.01
Caki-1	renal cell carcinoma	0.7	200	<0.001

[a] Cells were exposed to the drugs, and the cytotoxic activities were determined 96 h later using Alamar Blue dye conversion as a measure of cell viability.

RESULTS

Development of MMAF-Based Conjugates. The structure of the antimitotic agent MMAE is shown in Figure 1. This drug has previously displayed IC_{50} values in the range of 1−5 nM on hematologic cell lines (*12, 15*) and was designed for mAb-based targeted delivery using peptide-based linkers appended to the N-terminal methylvaline residue (*12, 19*). The synthesis of MMAE proceeded through a solution-phase route involving the coupling of the amino-protected N-terminal trimer to the C-terminal dimer. Due to the convergent nature of the process, it was possible for us to produce a large number of auristatins with varied solubilities, potencies, and pharmacokinetic properties. One molecule that emerged was MMAF-OMe (Figure 1), a C-terminal phenylalanine containing auristatin that remains one of the most potent drugs we have ever made (Table 1). We regarded MMAF-OMe as a prodrug of MMAF (Figure 1), with the potential of having facilitated intracellular uptake due to the presence of a neutral C-terminus. In addition, intracellular ester hydrolysis of MMAF-OMe should rapidly generate MMAF, a C-terminally charged molecule expected to have impaired membrane translocation capabilities. Therefore, MMAF was synthesized using solid-phase synthetic methodology and as expected was much less potent than MMAE on all cell lines tested (Table 1). In addition, the maximum tolerated dose in mice of MMAF (>16 mg/kg) was much higher than MMAE (1 mg/kg). Thus, MMAF was of great interest for targeted delivery, since the free drug had attenuated potency, lower toxicity, and much higher aqueous solubility compared to MMAE. Facilitated intracellular transport was expected to greatly enhance its activity.

Conjugates of MMAF were prepared via the maleimidocaproyl-Val-Cit-PABC linker (L1, Figure 1) as described

CSPC Exhibit 1004
Page 274 of 336

Table 2. In Vitro Cytotoxicity of cAC10−MMAF ADCs and Free MMAF on a Panel of CD30$^+$ and CD30$^-$ Cell Lines

		IC_{50} (nM)[a]		
cell line tumor	type	cAC10−L1−$MMAF_4$	cAC10−L4−$MMAF_4$	MMAF
Karpas 299	anaplastic large cell lymphoma	0.057	0.059	119
SUP-M2	anaplastic large cell lymphoma	0.023	0.024	79.7
SU-DHL-1	anaplastic large cell lymphoma	0.007	0.045	34.7
SR-786	anaplastic large cell lymphoma	0.010	0.016	38.1
DEL	anaplastic large cell lymphoma	0.038	0.046	69.0
HH	cutaneous T-cell lymphoma	0.016	0.022	30.7
L540cy	Hodgkin's disease	0.060	0.085	70.4
HDLM-2	Hodgkin's disease	0.080	0.210	66.0
L428	Hodgkin's disease	0.021	0.058	68.0
KMH-2	Hodgkin's disease	0.009	0.068	45.4
RPMI 6666	Hodgkin's disease	0.091	0.180	164
WSU-NHL	Non-Hodgkin's lymphoma, CD30$^-$	>25[b]	>25[b]	60.3
	mean (all lines)	0.034[c]	0.066[d]	70.4

[a] Cytotoxicity was measured as indicated in Table 1. Concentrations of the ADCs are represented by the drug component. [b] Represents 1000 ng/mL mAb component. [c] Represents 1.36 ng/mL mAb component. [d] Represents 2.64 ng/mL mAb component.

earlier for MMAE (*12, 19*). The mAbs used were BR96 (*17*) and AC10 (*19*), chimeric IgG1 mAbs that bind to the LewisY antigen on human carcinomas, and the CD30 antigen on hematologic malignancies, respectively. Initial studies were undertaken with conjugates that had eight drugs/mAb, but more recent data demonstrating improved pharmacokinetic and toxicologic properties of conjugates having lower drug loadings (*14*) prompted us to investigate the activities of conjugates with fewer drugs/mAb. These were obtained through carefully controlled mAb disulfide reduction with limiting amounts of DTT sufficient to produce an average of four thiol groups/mAb. Alkylation with drugs bearing thiol-reactive maleimide functionalities led to the formation of conjugates having an average of four drugs/mAb. The resulting distributions of species were as previously described (*20*). It was found that the ability of the parent unmodified mAb to bind to cell-surface receptors was maintained in conjugates (*12*), and aggregate (<5%) and free drug levels (0.5%) were very low.

In Vitro Growth Inhibition. cAC10−L1−$MMAF_4$ was tested on a panel of both CD30 positive and negative cell lines as shown in Table 2. Cells were exposed to the ADCs continuously for 96 h, and the cytotoxic effects, as determined by Alamar Blue conversion, were compared to those of free MMAF. On a molar basis, the cAC10−L1−$MMAF_4$ was an average of >2200-fold more potent than free MMAF and was active on all the CD30-positive cell lines tested. The effects were immunologically specific, since WSU-NHL cells, which do not express detectable levels of the CD30 antigen, were unaffected by the conjugate. Limited studies were also undertaken with the cAC10−L1−MMAF-OMe_4-based conjugates, and it was found that they displayed IC_{50} values on Karpas 299 (0.04 nM) and L540cy (0.11 nM) cells that were comparable to those of cAC10−L1−$MMAF_4$ (Table 2). This is consistent with the assumption stated earlier that the active form of MMAF-OMe is the free acid MMAF.

Further studies were undertaken with MMAF and the cBR96−L1−$MMAF_8$ conjugate on a LewisY positive human small cell lung carcinoma cell line (H69) and its P-glycoprotein-overexpressing counterpart H69/LX4 (*18*). The results were compared to doxorubicin and cBR96−L1−$doxorubicin_8$, a previously described conjugate with eight doxorubicin molecules/mAb (*17, 21*). H69/LX-4 cells were approximately 100-times less sensitive to doxorubicin compared to the parental cell (Figure 2A), while there was only a 3-fold difference with MMAF (Figure 2B). This trend extended to the conjugates, in that the drug resistant cell line was refractory to BR96−L1−$doxorubicin_8$ (Figure 2C), but quite sensitive to the corresponding MMAF conjugate (Figure 2D). These results have been confirmed on several MDR positive cell lines (data not shown), in which it has been found that MMAF and MMAF-based immunoconjugates circumvent common forms of the MDR phenotype.

New Linker Technologies. The linker joining the drug to the mAb carrier plays a critical role in conjugate potency (*3, 21−24*). We applied our peptide linker technology to MMAF, based on its successful application with MMAE (*12, 14, 15, 19, 20*) and other drug classes (*6, 9−11*). To expand our understanding of the role that the linker plays in drug release and cytotoxicity, we made truncated linker−MMAF derivatives lacking the *p*-aminobenzyloxycarbonyl (PABC) self-immolative group (L2, Figure 1), the peptide (L3), and both the peptide and the PABC group (L4). The resulting modified drugs were attached to cAC10, forming ADCs with approximately four drugs/mAb. As expected from earlier work with related doxorubicin ADCs (*6, 9−11*), cAC10−L2−$MMAF_4$ was devoid of activity on Karpas 299 cells (Table 3). In contrast, both cAC10−L3−$MMAF_4$ and cAC10−L4−$MMAF_4$ were highly active, and were as active as the full-length construct (cAC10−L1−$MMAF_4$). Interestingly, ADCs with truncated linkers (L2, L3, and L4) were not substrates for human cathepsin B, which was a critical design element in forming the original proteolytically cleavable linker technology for doxorubicin (*6, 9−11*). The effects of the truncated linkers were drug-dependent, in that cAC10−L4−$MMAE_8$ had no cytotoxic activity above 50 nM (1000 ng/mL) on Karpas 299 cells.

The results prompted us to test cAC10−L4−$MMAF_4$ on the broad panel of hematologic cell lines shown in Table 2. The conjugate was active against all CD30 positive cell lines tested and had approximately half the activity of cAC10−L1−$MMAF_4$. In addition, the effects were immunologically specific, as CD30 negative SU-NHL cells were not affected by cAC10−L4−$MMAF_4$. Thus, MMAF can be attached to cAC10 through linkers not designed for proteolytic cleavage, without significant loss in potency.

The high potency and broad reactivity of cAC10−L4−$MMAF_4$ conjugates raised the question of precisely what drug related molecule might be released from the conjugate, since the L4 linker would appear to be noncleavable. To elucidate this, ^{13}C-phenylalanine substituted L4−MMAF was synthesized and conjugated to cAC10. ^{12}C, ^{13}C, and a 1:1 mixture of ^{12}C and ^{13}C cAC10−L4−$MMAF_4$ were then incubated in lysosomal extracts of L540cy cells. Low molecular weight products were separated from proteins and were analyzed by LCMS. The identification of released drugs was based on the 6 mass unit shifts between the ^{12}C and ^{13}C derivatives of the drug. After inspection of mass spectra for such shifts, the only detectable drug-related molecule that was found was the [illegible] product of maleimidocaproyl−MMAF (Figure 3). To confirm this, an

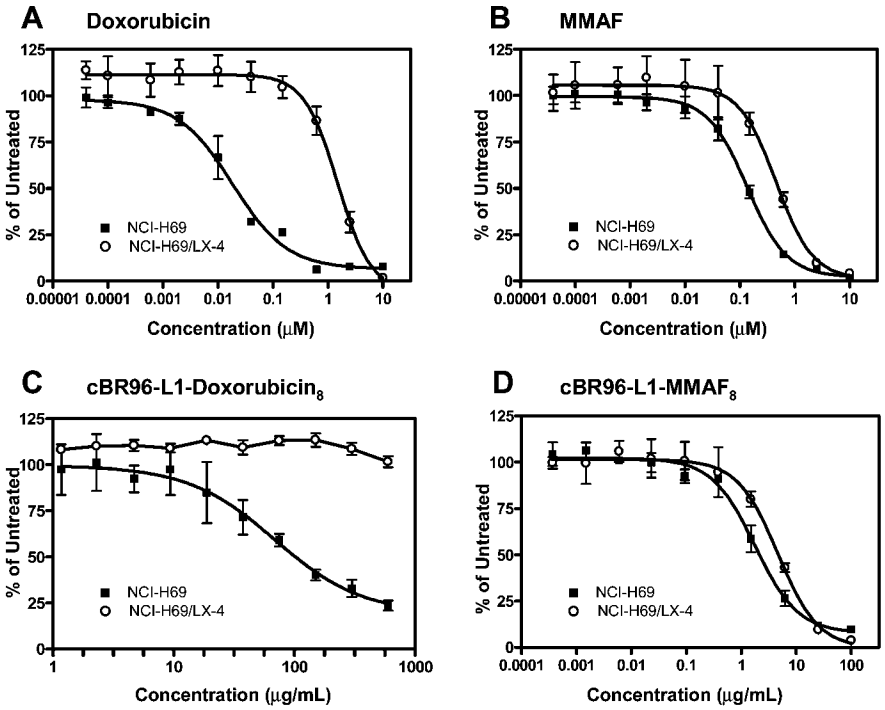


Figure 2. Cytotoxic effects of drugs (A, B) and cBR96-drug conjugates (C, D) on human small cell lung carcinoma cell line H69 (-■-) and its P-glycoprotein-overexpressing counterpart H69/LX-4 (-○-). Both cell lines are Lewis Y positive. The cells were incubated with either the drugs or the conjugates for 6 days, and the cytotoxic effects were determined by metabolism of Alamar Blue during the last 24 h of incubation.

Table 3. In Vitro Cytotoxicity of Drug−Linker Combinations

conjugate	target antigen	IC_{50} (nM) Karpas 299 cells[a]
cAC10−L1−$MMAF_4$	CD30	0.03
cAC10−L2−$MMAF_4$	CD30	>25
cAC10−L3−$MMAF_4$	CD30	0.055
cAC10−L4−$MMAF_4$	CD30	0.065
cAC10−L1−$MMAE_8$	CD30	0.18
cAC10−L4−$MMAE_8$	CD30	>50
cBR96−L1−$MMAF_4$	Lewis Y	>25
cBR96−L4−$MMAF_4$	Lewis Y	>25

[a] Karpas 299 cells are CD30 positive, Lewis Y negative. Cytotoxicity was measured as indicated in Table 1. Concentrations of the ADCs are represented by the drug component. The numbers reported are representative of at least two independent experiments.

authentic sample of cysteine−L4−MMAF was synthesized and was shown to have the same elution and LCMS profile as the drug released from the cAC10−L4−$MMAF_4$ ADC (data not shown). The mAb is the likely source for cysteine in cysteine−L4−MMAF, since this was the residue to which the drug was attached. Thus, drug release takes place through mAb degradation. Studies are currently ongoing to identify other products that might also be formed and to establish the rates and extent of drug release.

Maximum Tolerated Doses. The maximum tolerated doses (MTDs) of the cAC10−MMAF conjugates were determined in BALB/c mice and in Sprague−Dawley rats and are defined as the highest dose that did not induce >20% weight loss, distress, or overt toxicities in any of the animals. This dose was generally within 20% of doses where such events took place. cAC10−L1−$MMAF_4$ has an MTD of 50 mg/kg in mice and 15 mg/kg in rats. The corresponding cAC10−L4−$MMAF_4$ ADC was much less toxic, having MTDs in mice and rats of >150 mg/kg (the highest dose tested, which resulted in no apparent toxicity) and 90 mg/kg in rats, respectively. This clearly indicates that the method by which the drug is attached to the mAb can have a pronounced effect on ADC tolerability, and the ADC lacking the peptide spacer within the linker was much less toxic than the peptide-based ADC.

Immunohistochemical Analyses. Studies were undertaken to determine if cAC10−L1−$MMAF_4$ localized into subcutaneous Karpas 299 tumors in nude mice. Animals were injected intravenously with cAC10−L1−$MMAF_4$ or cBR96−L1−$MMAF_4$ at 10 mg antibody component/kg body weight. Tumors were removed 24 h later, and frozen sections were evaluated for the presence of the mAb and drug components using immunohistochemistry with biotinylated anti-human-Fc and anti−MMAF mAbs as secondary antibodies, respectively. Figures 4A and 4C show that cAC10−L1−$MMAF_4$ accumulated much more efficiently within Karpas 299 tumors compared to the cBR96 nonbinding control ADC (Figure 4B and 4D). Since both the mAb (Figure 4A) and drug (Figure 4C) moieties were detected throughout the tumor, we conclude that the ADC is delivered as an intact molecule.

Additional studies were undertaken to determine the effects of ADC localization on apoptosis. Figure 4E demonstrates that there were significant levels of fragmented DNA in tumors of animals that received cAC10−L1−$MMAF_4$. This was established by TUNEL analysis, which measures bromodeoxyuridine incorporation into fragmented DNA. A nonbinding control ADC (Figure 4F) did not induce nearly this level of fragmentation, which is consistent with the localization data.

In Vivo Therapy Studies. The therapeutic effects of the ADCs were determined in nude mice with subcutaneous or disseminated Karpas 299 tumors. In animals with subcutaneous tumors, significant antitumor effects were obtained with a single injection of either cAC10−L1−$MMAF_4$ or cAC10−L4−$MMAF_4$, which were indistinguishably potent and active (Figure 5A). Nearly all animals that received single ADC injections at 2 mg antibody component/kg body weight were cured. In lowering the dose to 1 mg/kg, efficacy for both ADCs, dropped off in an apparently equal manner. At this dose, there were still two of six and three of six animals cured with the cAC10−L1−$MMAF_4$ and cAC10−L4−$MMAF_4$ ADCs, respectively.

To establish disseminated tumors, Karpas 299 cells were injected intravenously and allowed to disseminate and become established before therapy was initiated 9 days later. In the

CSPC Exhibit 1004
Page 276 of 336

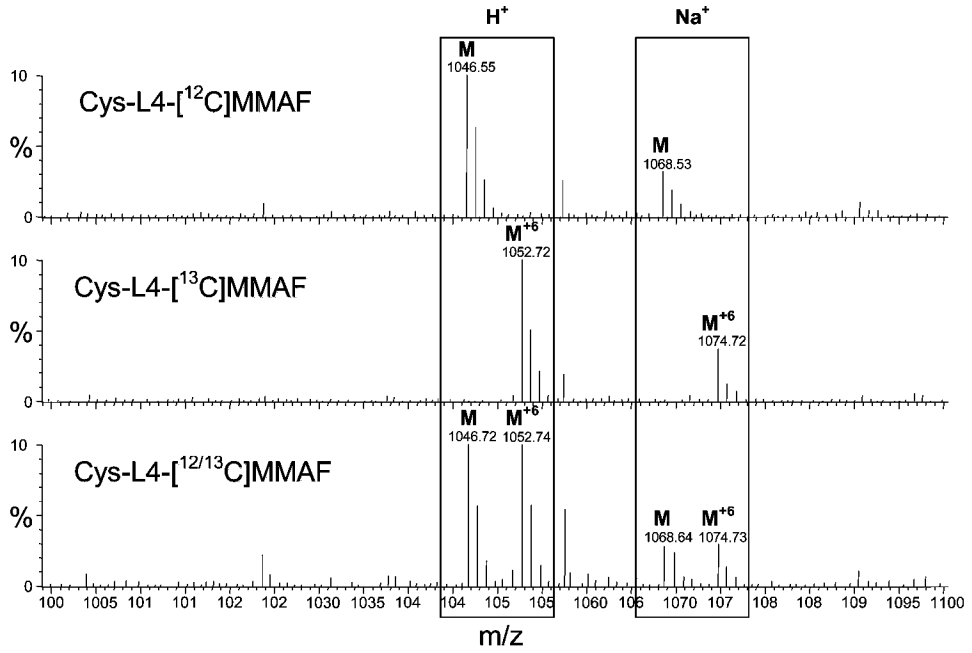


Figure 3. LCMS analysis of products released in lysosomal extracts of L540cy cells from cAC10−L4−MMAF$_4$ conjugate composed of [$^{12}C_6$-Phe]−MMAF (top), [$^{13}C_6$-Phe]−MMAF (middle), and a 1:1 mixture of these two conjugates (bottom). The fragments obtained from the co-mixture of the conjugates were analyzed for (M) and (M + 6) molecular ion clusters. Cysteine−L4−MMAF, *m/z* 1046/1052, was the only identifiable MMAF component.

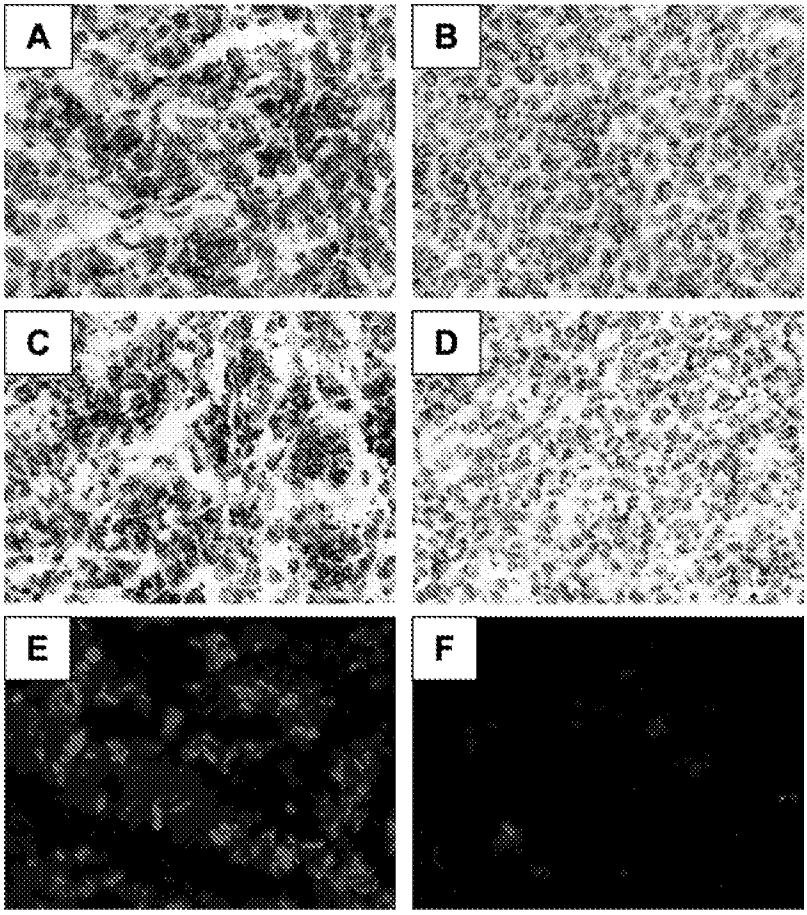


Figure 4. In vivo localization and activities of mAb−L1−MMAF$_4$ ADCs. Nude mice with subcutaneous Karpas 299 human tumors (cAC10 antigen positive, cBR96 antigen negative) were injected either with cAC10−L1−MMAF$_4$ (A, C, E) or with cBR96−L1−MMAF$_4$ (B, D, F) to investigate the localization and the induction of apoptosis on tumor xenografts. The presence of intratumoral mAb (A, B) and intratumoral MMAF (C, D) were determined by immunohistochemistry using either biotinylated anti-human-Fc or biotinylated anti-MMAF mAbs, respectively, as secondary antibodies. The tumors were excised and sectioned 24 h postconjugate administration. The apoptotic effect of ADCs (E, F) were investigated using the TUNEL assay. The images were taken using 20× objectives on a Zeiss microscope.

CSPC Exhibit 1004
Page 277 of 336

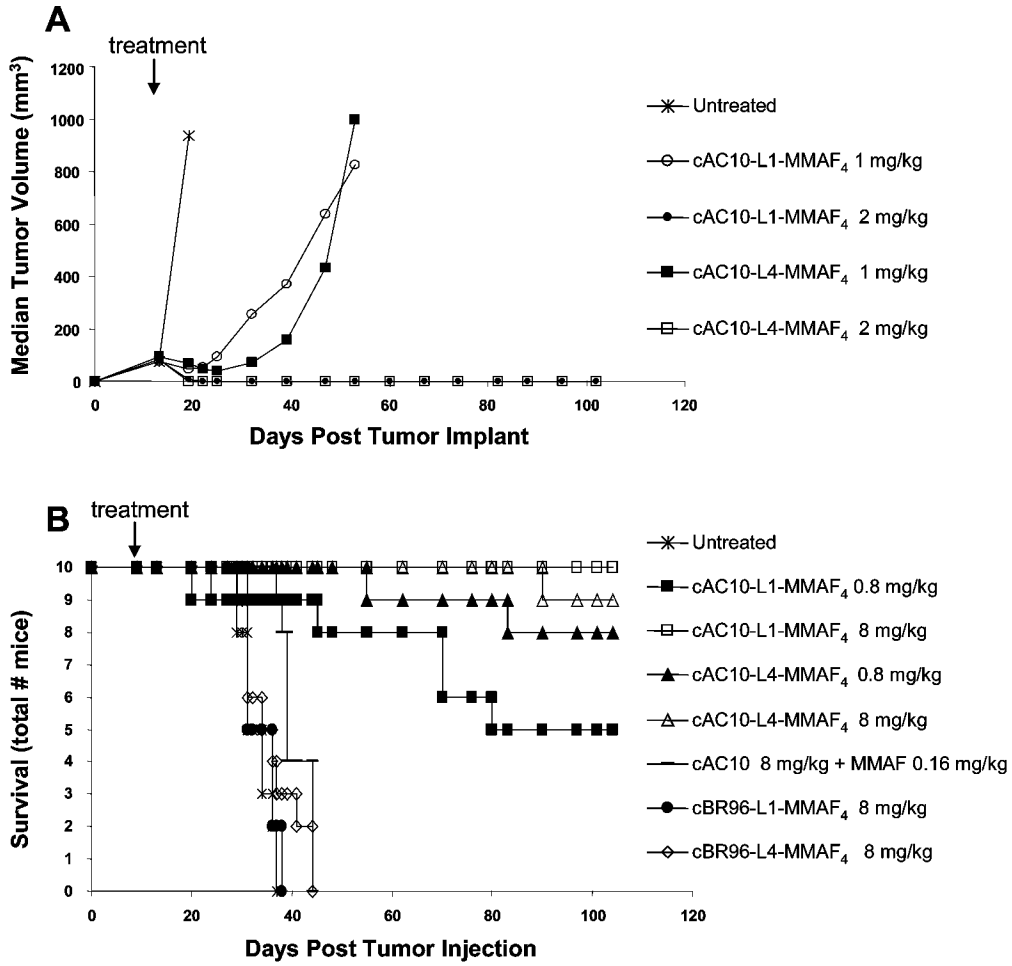


Figure 5. In vivo therapeutic efficacy of the conjugates in SCID mice. The data reported are representative of a number of independent studies. (A) Groups of mice (six/group) with subcutaneous Karpas 299 human ALCL tumors (cAC10 Ag^+) of approximately 100 mm^3 average in size were treated with cAC10−L1−$MMAF_4$ or cAC10−L4−$MMAF_4$ at 1 mg and 2 mg mAb component/kg. Cures: 1 mg/kg cAC10−L1−$MMAF_4$, two out of six; 1 mg/kg cAC10−L4−$MMAF_4$, three out of six; 2 mg/kg cAC10−L4−$MMAF_4$, five out of six; 2 mg/kg cAC10−L1−$MMAF_4$, six out of six. (B) Groups of mice (ten/group) with disseminated Karpas 299 ALCL tumor model (cAC10 Ag^+, cBR96 Ag^-) were treated on day 9 after tumor injection with cAC10−L1−$MMAF_4$, cAC10−L4−$MMAF_4$, cAC10 + unconjugated MMAF, cBR96−L1−$MMAF_4$, or cBR96−L4−$MMAF_4$ at the doses indicated.

absence of any treatment, all of the animals succumbed to disseminated disease by day 45. A single administration with either cAC10−L1−$MMAF_4$ or cAC10−L4−$MMAF_4$ was sufficient to cure most of the animals, with a slight dose response between 0.8 mg/kg and 8 mg/kg. The differences between the L1 and L4 linkers were not significant in this tumor model. One of the noteworthy findings in this experiment was the level of specificity. The nonbinding control ADCs, cBR96−L1−$MMAF_4$ and cBR96−L1−$MMAF_4$ were inactive, even at 8 mg/kg, which is 10-times the effective dose of the corresponding cAC10 ADCs. Thus, the MMAF conjugates exhibit pronounced activity at very well tolerated doses and are highly immunologically specific. Furthermore, the therapeutic window of cAC10−L4−$MMAF_4$ is measurably greater than that of cAC10−L1−$MMAF_4$, indicating that the linker technology plays a critical role in the design of effective ADCs that can be safely administered.

DISCUSSION

In this paper, we describe the synthesis and properties of MMAF, a new auristatin antimitotic agent designed for attachment to mAbs through the secondary amino terminus. MMAF has much lower cytotoxic activity than MMAE (*12, 14, 15, 19*), presumably owing to the charged C-terminal phenylalanine group that impairs intracellular access. This hypothesis is supported by the pronounced activity of MMAF-OMe, one of the most potent auristatins that we have developed. To further understand the precise cause of the attenuated activity of MMAF compared to the other drugs, studies are currently underway to measure intracellular concentrations in MDR positive and negative cell lines.

ADCs comprised of MMAF are distinct from those of other drugs, including MMAE. We show that the activities of MMAF are potentiated an average of 2200-fold when the drug is attached through the L1 linker to cAC10, a mAb that is efficiently taken up within the lysosomes of target cells (Table 2). With one exception that is likely cell line dependent (*25*), broad-scale drug potentiation through ADC formation is generally not seen, as evidenced by the in vitro results of MMAE (*12*) and other drug-containing ADCs (*23, 24, 26, 27*). The significance of this finding will become evident though detailed toxicological analyses, in which MMAE- and MMAF-based ADCs should be quite distinct if systemically released drug contributes to ADC toxicity.

One of the most striking results from this work surrounds the unexpected activity of cAC10−L4−$MMAF_4$, an ADC that has no built-in provision for drug release. Purified human enzymes that we have tested were unable to facilitate release of MMAF or any identifiable MMAF-containing fragment. cAC10−L4−$MMAF_4$ is highly potent, both in vitro and in vivo. We

CSPC Exhibit 1004
Page 278 of 336

propose that the mechanism of drug release involves complete degradation of the mAb, based on the identification of the cysteine adduct of L4−MMAF. The finding that the released drug from the L4 linker is highly modified might explain why such truncated linker technology is not uniformly applicable, since many drugs lose activity as a result of derivatization. Indeed, MMAE was not tolerant of such modification (Table 3), and corresponding doxorubicin ADCs have also proven to be inactive (data not shown). The data in Table 3 also demonstrate that the various linkers within the MMAF ADC family provide a range of cytotoxic activities. The fact that cAC10−L2−$MMAF_4$ was inactive suggests that the released agent from the L2−MMAF ADC is highly attenuated in activity. We focused on cAC10−L4−$MMAF_4$ for further work rather than cAC10−L3−$MMAF_4$, since the PABC group in the L3 linker is hydrophobic and apparently unnecessary for activity.

The objective of the investigations with various linkers was to determine if the mode of drug release could affect ADC therapeutic index. We found that cAC10−L4−$MMAF_4$ differed from cAC10−L1−$MMAF_4$ by an average of only 2-fold on a large panel of hematologic cell lines (Table 2) although L1 linker cleavage is quite facile through enzymes such as cathepsin B, while drug release through the L4 linker requires antibody degradation. This provided the basis for in vivo experiments, since we anticipated that the different pathways required for drug elimination could strongly influence the therapeutic windows of the ADCs. Indeed, it was found that cAC10−L4−$MMAF_4$ was tolerated at significantly higher doses in rodents than cAC10−L1−$MMAF_4$ but was equally efficacious in vivo. Our results suggest that the therapeutic window is increased by at least 3-fold through the L4 linker system.

We are in the process of assessing several aspects of MMAF linker technology. Current studies include the application of mAb−L4−MMAF ADCs directed against antigens on an array of tumor types. Our preliminary data suggest that such ADCs are broadly active against hematologic malignancies but are only sporadically effective in the carcinomas we have evaluated. We are gaining insight into the factors that influence activity by assessing bound and unbound drug both inside and outside target cells. In addition, we are characterizing the mechanisms of drug release in target and nontarget cells in order to further understand the principles that influence activity and toxicity.

Supporting Information Available: Synthetic schemes for all linker−drugs. This material is available free of charge via the Internet at http://pubs.acs.org/BC.

LITERATURE CITED

(1) Adams, G. P., and Weiner, L. M. (2005) Monoclonal antibody therapy of cancer. *Nat. Biotechnol. 23*, 1147−57.

(2) Baker, M. (2005) Upping the ante on antibodies. *Nat. Biotechnol. 23*, 1065−72.

(3) Wu, A. M., and Senter, P. D. (2005) Arming antibodies: prospects and challenges for immunoconjugates. *Nat. Biotechnol. 23*, 1137−46.

(4) Lambert, J. M. (2005) Drug-conjugated monoclonal antibodies for the treatment of cancer. *Curr. Opin. Pharmacol. 5*, 543−9.

(5) Payne, G. (2003) Progress in immunoconjugate cancer therapeutics. *Cancer Cell 3*, 207−12.

(6) Dubowchik, G. M., and Walker, M. A. (1999) Receptor-mediated and enzyme-dependent targeting of cytotoxic anticancer drugs. *Pharmacol. Ther. 83*, 67−123.

(7) Smith, S. V. (2004) Technology evaluation: cantuzumab mertansine, ImmunoGen. *Curr. Opin. Mol. Ther. 6*, 666−74.

(8) DiJoseph, J. F., Popplewell, A., Tickle, S., Ladyman, H., Lawson, A., Kunz, A., Khandke, K., Armellino, D. C., Boghaert, E. R., Hamann, P., Zinkewich-Peotti, K., Stephens, S., Weir, N., and Damle, N. K. (2005) Antibody-targeted chemotherapy of B-cell lymphoma using calicheamicin conjugated to murine or humanized antibody against CD22. *Cancer Immunol. Immunother. 54*, 11−24.

(9) Dubowchik, G. M., and Firestone, R. A. (1998) Cathepsin B-sensitive dipeptide prodrugs. 1. A model study of structural requirements for efficient release of doxorubicin. *Bioorg. Med. Chem. Lett. 8*, 3341−6.

(10) Dubowchik, G. M., Firestone, R. A., Padilla, L., Willner, D., Hofstead, S. J., Mosure, K., Knipe, J. O., Lasch, S. J., and Trail, P. A. (2002) Cathepsin B-labile dipeptide linkers for lysosomal release of doxorubicin from internalizing immunoconjugates: model studies of enzymatic drug release and antigen-specific in vitro anticancer activity. *Bioconjugate Chem. 13*, 855−69.

(11) Dubowchik, G. M., Mosure, K., Knipe, J. O., and Firestone, R. A. (1998) Cathepsin B-sensitive dipeptide prodrugs. 2. Models of anticancer drugs paclitaxel (Taxol), mitomycin C and doxorubicin. *Bioorg. Med. Chem. Lett. 8*, 3347−52.

(12) Doronina, S. O., Toki, B. E., Torgov, M. Y., Mendelsohn, B. A., Cerveny, C. G., Chace, D. F., DeBlanc, R. L., Gearing, R. P., Bovee, T. D., Siegall, C. B., Francisco, J. A., Wahl, A. F., Meyer, D. L., and Senter, P. D. (2003) Development of potent monoclonal antibody auristatin conjugates for cancer therapy. *Nat. Biotechnol. 21*, 778−84.

(13) Sanderson, R. J., Hering, M. A., James, S. F., Sun, M. M., Doronina, S. O., Siadak, A. W., Senter, P. D., and Wahl, A. F. (2005) In vivo drug-linker stability of an anti-CD30 dipeptide-linked auristatin immunoconjugate. *Clin. Cancer Res. 11*, 843−52.

(14) Hamblett, K. J., Senter, P. D., Chace, D. F., Sun, M. M., Lenox, J., Cerveny, C. G., Kissler, K. M., Bernhardt, S. X., Kopcha, A. K., Zabinski, R. F., Meyer, D. L., and Francisco, J. A. (2004) Effects of drug loading on the antitumor activity of a monoclonal antibody drug conjugate. *Clin. Cancer Res. 10*, 7063−70.

(15) Law, C. L., Cerveny, C. G., Gordon, K. A., Klussman, K., Mixan, B. J., Chace, D. F., Meyer, D. L., Doronina, S. O., Siegall, C. B., Francisco, J. A., Senter, P. D., and Wahl, A. F. (2004) Efficient elimination of B-lineage lymphomas by anti-CD20-auristatin conjugates. *Clin. Cancer Res. 10*, 7842−51.

(16) Wahl, A. F., Klussman, K., Thompson, J. D., Chen, J. H., Francisco, L. V., Risdon, G., Chace, D. F., Siegall, C. B., and Francisco, J. A. (2002) The anti-CD30 monoclonal antibody SGN-30 promotes growth arrest and DNA fragmentation in vitro and affects antitumor activity in models of Hodgkin's disease. *Cancer Res. 62*, 3736−42.

(17) Trail, P. A., Willner, D., Lasch, S. J., Henderson, A. J., Hofstead, S., Casazza, A. M., Firestone, R. A., Hellstrom, I., and Hellstrom, K. E. (1993) Cure of xenografted human carcinomas by BR96-doxorubicin immunoconjugates. *Science 261*, 212−5.

(18) Reeve, J. G., Rabbitts, P. H., and Twentyman, P. R. (1989) Amplification and expression of mdr1 gene in a multidrug resistant variant of small cell lung cancer cell line NCI-H69. *Br. J. Cancer 60*, 339−42.

(19) Francisco, J. A., Cerveny, C. G., Meyer, D. L., Mixan, B. J., Klussman, K., Chace, D. F., Rejniak, S. X., Gordon, K. A., DeBlanc, R., Toki, B. E., Law, C. L., Doronina, S. O., Siegall, C. B., Senter, P. D., and Wahl, A. F. (2003) cAC10-vcMMAE, an anti-CD30-monomethyl auristatin E conjugate with potent and selective antitumor activity. *Blood 102*, 1458−65.

(20) Sun, M. M., Beam, K. S., Cerveny, C. G., Hamblett, K. J., Blackmore, R. S., Torgov, M. Y., Handley, F. G., Ihle, N. C., Senter, P. D., and Alley, S. C. (2005) Reduction-alkylation strategies for the modification of specific monoclonal antibody disulfides. *Bioconjugate Chem. 16*, 1282−90.

(21) Trail, P. A., Willner, D., Knipe, J., Henderson, A. J., Lasch, S. J., Zoeckler, M. E., TrailSmith, M. D., Doyle, T. W., King, H. D., Casazza, A. M., Braslawsky, G. R., Brown, J., Hofstead, S. J., Greenfield, R. S., Firestone, R. A., Mosure, K., Kadow, K. F., Yang, M. B., Hellstrom, K. E., and Hellstrom, I. (1997) Effect of linker variation on the stability, potency, and efficacy of carcinoma-reactive BR64-doxorubicin immunoconjugates. *Cancer Res. 57*, 100−5.

(22) Chari, R. V., Martell, B. A., Gross, J. L., Cook, S. B., Shah, S. A., Blattler, W. A., McKenzie, S. J., and Goldmacher, V. S. (1992) Immunoconjugates containing novel maytansinoids: promising anticancer drugs. *Cancer Res. 52*, 127−31.

(23) Hamann, P. R., Hinman, L. M., Beyer, C. F., Greenberger, L. M., Lin, C., Lindh, D., Menendez, A. T., Wallace, R., Durr, F. E., and Upeslacis, J. (2005) An anti-MUC1 antibody-calicheamicin conjugate for treatment of solid tumors. Choice of linker and overcoming drug resistance. *Bioconjugate Chem. 16*, 346−53.

(24) Hamann, P. R., Hinman, L. M., Beyer, C. F., Lindh, D., Upeslacis, J., Shochat, D., and Mountain, A. (2005) A calicheamicin conjugate with a fully humanized anti-MUC1 antibody shows potent antitumor effects in breast and ovarian tumor xenografts. *Bioconjugate Chem. 16*, 354−60.

(25) Hamann, P. R., Hinman, L. M., Hollander, I., Beyer, C. F., Lindh, D., Holcomb, R., Hallett, W., Tsou, H. R., Upeslacis, J., Shochat, D., Mountain, A., Flowers, D. A., and Bernstein, I. (2002) Gemtuzumab ozogamicin, a potent and selective anti-CD33 antibody-calicheamicin conjugate for treatment of acute myeloid leukemia. *Bioconjugate Chem. 13*, 47−58.

(26) Miller, M. L., Roller, E. E., Wu, X., Leece, B. A., Goldmacher, V. S., Chari, R. V., and Ojima, I. (2004) Synthesis of potent taxoids for tumor-specific delivery using monoclonal antibodies. *Bioorg. Med. Chem. Lett. 14*, 4079−82.

(27) Ojima, I., Geng, X., Wu, X., Qu, C., Borella, C. P., Xie, H., Wilhelm, S. D., Leece, B. A., Bartle, L. M., Goldmacher, V. S., and Chari, R. V. (2002) Tumor-specific novel taxoid-monoclonal antibody conjugates. *J. Med. Chem. 45*, 5620−3.

BC0502917

Bioconjugate Chemistry

Article

pubs.acs.org/bc

Effect of Attachment Site on Stability of Cleavable Antibody Drug Conjugates

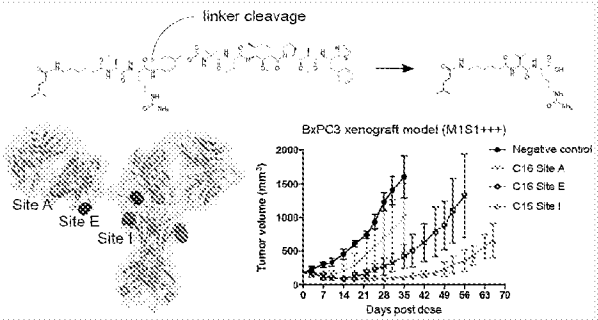
Magdalena Dorywalska,[†] Pavel Strop,*[,†] Jody A. Melton-Witt,[†] Adela Hasa-Moreno,[†] Santiago E. Farias,[†] Meritxell Galindo Casas,[†] Kathy Delaria,[†] Victor Lui,[†] Kris Poulsen,[†] Carole Loo,[†] Stellanie Krimm,[†] Gary Bolton,[†] Ludivine Moine,[‡] Russell Dushin,[‡] Thomas-Toan Tran,[†] Shu-Hui Liu,[†] Mathias Rickert,[†] Davide Foletti,[†] David L. Shelton,[†] Jaume Pons,[†] and Arvind Rajpal[†]

[†]Rinat Laboratories, Pfizer Inc., 230 East Grand Avenue, South San Francisco, California 94080, United States

[‡]Worldwide Medicinal Chemistry, Pfizer Inc., 445 Eastern Point Road, Groton, Connecticut 06340, United States

Supporting Information

ABSTRACT: The systemic stability of the antibody−drug linker is crucial for delivery of an intact antibody−drug conjugate (ADC) to target-expressing tumors. Linkers stable in circulation but readily processed in the target cell are necessary for both safety and potency of the delivered conjugate. Here, we report a range of stabilities for an auristatin-based payload site-specifically attached through a cleavable valine-citrulline-*p*-aminobenzylcarbamate (VC-PABC) linker across various sites on an antibody. We demonstrate that the conjugation site plays an important role in determining VC-PABC linker stability in mouse plasma, and that the stability of the linker positively correlates with ADC cytotoxic potency both in vitro and in vivo. Furthermore, we show that the VC-PABC cleavage in mouse plasma is not mediated by Cathepsin B, the protease thought to be primarily responsible for linker processing in the lysosomal degradation pathway. Although the VC-PABC cleavage is not detected in primate plasma in vitro, linker stabilization in the mouse is an essential prerequisite for designing successful efficacy and safety studies in rodents during preclinical stages of ADC programs. The divergence of linker metabolism in mouse plasma and its intracellular cleavage offers an opportunity for linker optimization in the circulation without compromising its efficient payload release in the target cell.



INTRODUCTION

Antibody−drug conjugates offer the advantage of delivering cytotoxic agents directly to the target-expressing cells, thus potentially improving the therapeutic efficacy and minimizing harmful side effects as compared to conventional chemotherapy.[1−3] Loss of toxin from the conjugate while in circulation can result in off-target toxicity from the released payload, and generation of an unconjugated antibody that can compete for target binding with the intact ADC, leading to loss of efficacy. Therefore, it is highly desirable that cytotoxic agents remain stably attached until the conjugate reaches the tumor, where the toxic payload may then be efficiently released into the tumor cell only after internalization.[4,5]

Previously, we described an efficient site-specific conjugation method using microbial transglutaminase to attach a wide range of cleavable and noncleavable payloads to various sites in an antibody to generate homogeneous conjugates with unique properties.[6−8] In this approach, a glutamine-containing tag (LLQG) was engineered into selected positions in an antibody sequence, and microbial transglutaminase was used to catalyze transamidation reaction between the glutamine γ-carboxamide group and a primary amine of the payload of choice, creating a covalent isopeptide bond. The selected sites were shown to be transferrable among several different antibodies. We further showed that the glutamine tag engineered into the antibody sequence, as well as the transglutaminase-catalyzed isopeptide linkage between the engineered antibody and the payload, remain intact upon exposure to rodent serum in vitro and upon administration in vivo. We did, however, detect plasma cleavage of the VC-PABC linker resulting in a loss of the payload moiety.[7] Here, we investigate the stability of a cleavable linker-payload conjugated at a wide range of positions, its dependence on the site of conjugation, and the correlation of stability with efficacy in vitro and in vivo. While the site of attachment has previously been shown to modulate stability of maleimide-based conjugates, the effect was due to chemical decoupling of the maleimide linkage[9] rather than the enzymatic processing of the VC-PABC linker during circulation. We further examine the cleavage of the VC-PABC linker resulting in the loss of an auristatin-based payload from a mechanistic perspective to gain insight into the plasma enzyme(s) responsible for this process.

Received: December 5, 2014
Revised: January 27, 2015
Published: February 2, 2015

Downloaded via US PATENT AND TRADEMARK OFFICE on January 10, 2020 at 21:31:35 (UTC).
See https://pubs.acs.org/sharingguidelines for options on how to legitimately share published articles.

 © 2015 American Chemical Society

CSPC Exhibit 1004
Page 281 of 356

DOI: 10.1021/bc5005747
Bioconjugate Chem. 2015, 26, 650−659

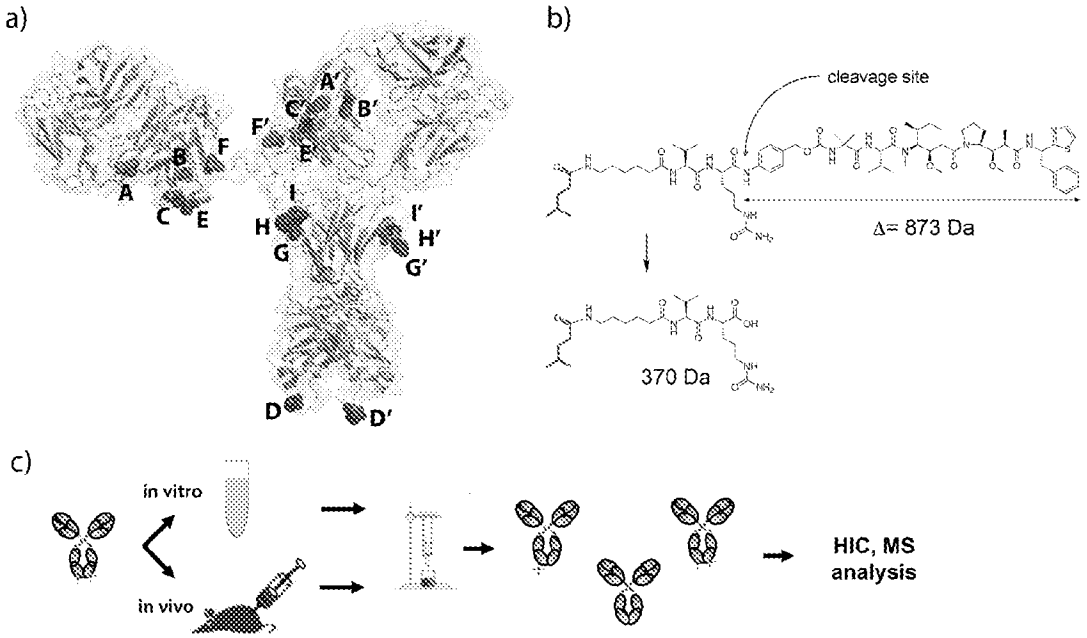


Figure 1. Stability studies of site-specific cleavable ADCs. (a) Positions of conjugation sites on an antibody. (b) Structure of the cleavable C6-VC-PABC-Aur0101 payload conjugated to the glutamine tag on the antibody, and its cleavage product. The glutamine residue is shown in blue. (c) Experimental setup for in vitro and in vivo ADC stability assays.

RESULTS

Stability and Cytotoxic Potency of Cleavable Conjugates in Vitro. Earlier studies of transglutaminase-based conjugates revealed the significant role played by the conjugation site in determining the stability and pharmacokinetic properties of ADCs.[7] To further evaluate linker-payload stability across a number of conjugation sites (Figure 1a), we generated a series of site-specific conjugates using an auristatin-based cleavable linker-payload, Aminocaproyl-VC-PABC-Aur0101 (C6-VC-PABC-Aur0101, Scheme 1)[10] conjugated to a glutamine residue (Figure 1b) that had been engineered into anti-M1S1 antibody C16 using site directed mutagenesis at selected positions (Figure 1a, Table 1). The conjugates were incubated in the blood plasma of several species, followed by purification and analysis of their drug loading using hydrophobic interaction chromatography (HIC) and mass spectrometry (Figure 1c). While the isopeptide linkage resulting from transglutaminase conjugation was intact across all sites and all species, in mouse plasma we observed cleavage of the VC-PABC linker resulting in the loss of the hydrophobic PABC-Aur0101 moiety (Figure 1b), and a shift toward lower retention time on HIC (Supporting Information Figure 1). Mass spectrometric analysis following incubation in mouse plasma reveals a corresponding 873 Da mass loss from the ADC (Figure 1b, Figure 2a,b, Supporting Information Figure 2). This cleavage appears to be at the same Cit-PABC amide bond as occurs through normal processing in lysosomal compartments that leads to payload release in target cells.[11−13] The VC-PABC linker is cleaved in this way to a varying extent at different sites on either heavy and/or light chains of the antibody when incubated in mouse plasma from either Balb/c or SCID strains, but appears to be more stable in rat, cynomolgus monkey, and human plasma (Table 1). The wide range of mouse plasma stabilities across conjugation sites suggests varied degrees of protection of the linker from proteolytic cleavage through steric hindrance by adjacent antibody domains.

Linker stability is a key determinant of ADC potency which relies on the efficient linker processing and payload release inside target cells and, at the same time, the exquisite systemic stability prior to internalization. To examine how the differential C6-VC-PABC-Aur0101 linker stability across conjugation sites correlates with the cytotoxic activity of the ADCs, we performed in vitro cytotoxicity assays using C16 conjugates before and after incubation in mouse plasma. All of the untreated C6-VC-PABC-Aur0101 conjugates showed comparable and target specific potency against the BxPC3 cell line (M1S1+++) demonstrating an efficient mechanism of intracellular payload release at all conjugation sites (Figure 3a−c, Supporting Information Figure 3a,c and Table 1). Lack of efficacy from a nonbinding, negative control conjugate NCC Site F-C6-VC-PABC-Aur0101 verified that target recognition and conjugate internalization are required for specific cell killing (Supporting Information Figure 3b). Target specificity was also demonstrated using the SW620 cell line that does not express M1S1 (Supporting Information Figure 3c). In contrast to untreated conjugates which show similar anti-BxPC3 IC_{50} values (0.6−1.2 nM), ADCs purified after a 4.5 day incubation in mouse plasma showed varying degrees of potency decrease that correlated with their VC-PABC linker instability, with the most stable Site I-C6-VC-PABC-Aur0101 conjugate showing no change in the IC_{50} value after plasma exposure (IC_{50} before and after exposure of 1.0 and 0.9 nM, respectively), and the least stable Site A-C6-VC-PABC-Aur0101 conjugate showing significantly reduced cytotoxicity (IC_{50} changed from 1.2 nM for untreated conjugate to ≥266 nM after treatment) (Figure 3a−c, Supporting Information Figure 3a and Table 1). Establishing an exact quantitative dependence between ADC potency and linker stability is not possible due to the presence of other factors that affect ADC activity (such as internalization rates, possible differential intracellular processing by lysosomal proteases), all of which are functions of time. Nevertheless, the qualitative correlation between stability and potency can be seen

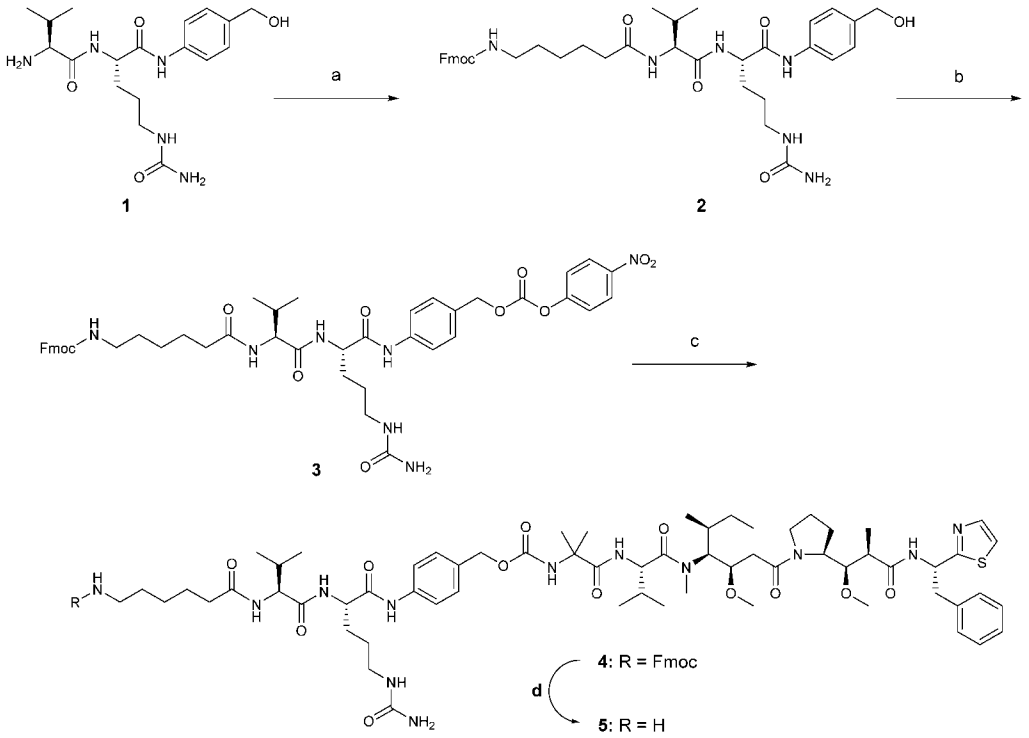
DOI: 10.1021/bc5005747
Bioconjugate Chem. 2014, 25, 651−659
CSPC Exhibit 1004
Page 282 of 336

Table 1. Stability of the Cleavable C6-VC-PABC-Aur0101 Conjugate Series under Various Conditions[a]

site	position	payload	mouse plasma stability (%)	rat plasma stability (%)	cyno plasma stability (%)	human plasma stability (%)	mouse in vivo stability (%)
A	LC 200–202	C6-VC-PABC-Aur0101	5	94	99	99	0
B	HC 160	C6-VC-PABC-Aur0101	12	99	100	100	-
C	HC 135	C6-VC-PABC-Aur0101	22	97	98	96	-
D	HC C-terminus	C6-VC-PABC-Aur0101	34	97	99	100	-
E	HC 190–192	C6-VC-PABC-Aur0101	42	97	97	100	0
F	LC C-terminus	C6-VC-PABC-Aur0101	86	99	100	98	-
G	N297A	C6-VC-PABC-Aur0101	88	100	99	100	-
H	N297Q	C6-VC-PABC-Aur0101	100	100	100	100	-
I	HC 294–297	C6-VC-PABC-Aur0101	100	100	100	100	57

[a]Stability values are calculated as the ratio of drug loading after treatment and before treatment, and expressed as a percentage. Calculations are based on DAR values obtained from HIC analysis for most conjugates, except for Site G, H, and I conjugates for which DAR values are determined by mass spec analysis. Both methods give consistent DAR values; however, HIC chromatograms of Site G, H, and I conjugates show insufficient shift between DAR 0, 1, and 2 peaks for accurate integration.

Scheme 1. [a]



[a]Reagents and conditions: (a) Fmoc-aminohexanoic acid, HATU, *i*-Pr_2NEt, DMF; (b) (*p*-NO_2-Ph)$_2$CO, *i*-Pr_2NEt, DMF; (c) Aur-0101, HOAT, 2,6-lutidine, DMF; (d) piperidine.

when stability is plotted against in vitro cytotoxicity data (Supporting Information Figure 4).

In Vivo Efficacy and Its Relation to Stability of Cleavable ADCs. To evaluate whether the in vitro VC-PABC linker stability differences observed in the mouse plasma translate into differences in antitumor efficacy, we selected three C16 conjugates for comparative in vivo efficacy study: the unstable Site A-C6-VC-PABC-Aur0101, the intermediate stability Site E-C6-VC-PABC-Aur0101, and the stable Site I-C6-VC-PABC-Aur0101. A single intravenous dose of the three conjugates given to mice implanted with BxPC3 cells resulted in varying degrees of tumor growth inhibition or tumor regression that correlated with the VC-PABC linker stability observed in vitro (Figure 3d). The NCC Site F-C6-VC-PABC-Aur0101 conjugate was used as a negative control to monitor tumor response to nontargeting conjugate present in the circulation (Figure 3d). A pharmacokinetic study in non-tumor-bearing mice verified that the observed efficacy differences among the conjugates were not a result of different whole antibody exposure as demonstrated using total antibody ELISA (Figure 3e). Instead, the efficacy differences can be attributed to differential amount of drug loss resulting in different ADC exposure (Figure 3e). These data suggest that a kinetic competition between the rate of VC-PABC cleavage in the plasma and the rate of cell killing by the ADC, even in the early days post dosing, will have a significant effect on the antitumor outcome of the treatment.

The varying extent of PABC-Aur0101 payload loss in vivo was confirmed by isolating the three conjugates from non-tumor-bearing

CSPC Exhibit 1004
Page 283 of 330

DOI: 10.1021/bc5005747
Bioconjugate Chem. 2014, 25, 652−659

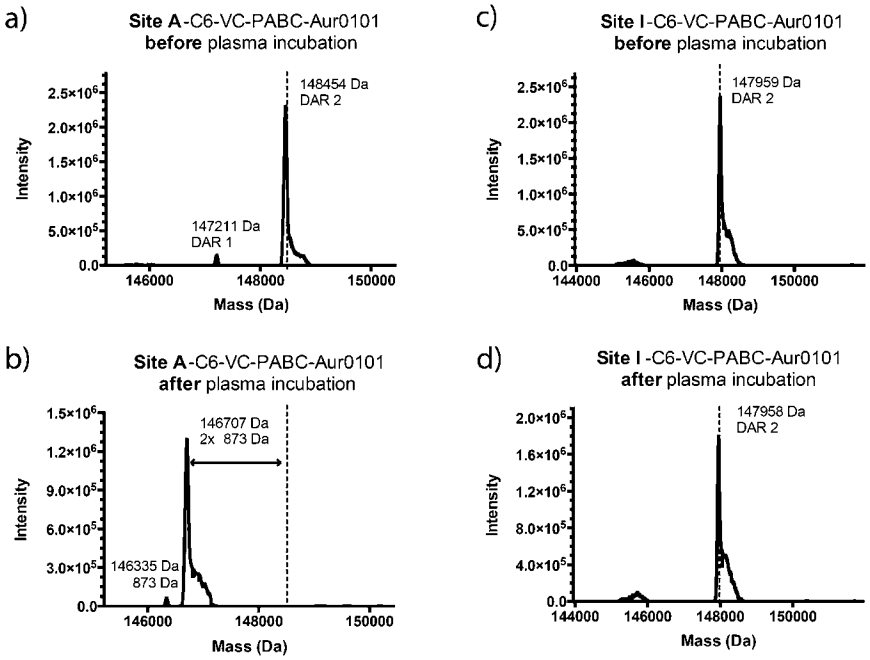


Figure 2. Mass spectrometric analysis of cleavable conjugates before (a and c) and after (b and d) incubation in mouse plasma. The figure labels represent experimentally observed masses. (a) Intact mass deconvolution of C16 Site A-C6-VC-PABC-Aur0101 conjugate before plasma incubation. The mass difference between the peak representing drug to antibody ratio of 1 (DAR 1) and DAR 2 is approximately 1243 Da which corresponds to the mass of the cytotoxic drug plus the linker (less ammonia). (b) Intact mass analysis of C16 Site A-C6-VC-PABC-Aur0101 conjugate after plasma exposure. Cleavage by a plasma protease results in a loss of 873 Da from each conjugated payload, shifting the DAR 2 peak by 2 × 873 Da, and the DAR 1 peak by 1 × 873 Da. (c) Intact mass deconvolution of C16 Site I-C6-VC-PABC-Aur0101 conjugate before plasma incubation. The observed DAR 2 peak represents the mass of the antibody conjugated to two linker-payload molecules. (d) Intact mass analysis of C16 Site I-C6-VC-PABC-Aur0101 conjugate after mouse plasma treatment. No mass difference is observed for this conjugate, indicating a high degree of stability in mouse plasma.

mice at 4.5 days after a 3 mg/kg dose, and evaluating their drug loading using HIC and mass spectrometry (Table 1). We note that in mice the VC-PABC linker appears to be cleaved more efficiently in vivo relative to the in vitro assay. This could be a result of a continuous source of putative enzyme(s) in vivo, or alternatively due to a contribution from intracellular cleavage and release of the unconjugated antibody through endocytic recycling. Target-mediated recycling is unlikely in this case, since the C16 antibody does not recognize the mouse M1S1 protein in non-tumor-bearing mice. While we detect only low levels of VC degradation in rat plasma, and practically none in monkey or human plasma in vitro assays (Table 1), the loss of payload due to VC-PABC cleavage from a related C16 Site D-C6-VC-PABC-MMAD conjugate was observed in pharmacokinetic studies in both rat and cynomolgus monkey (Supporting Information Figure 5).

Mechanistic Comparison of VC-PABC Cleavage in Mouse Plasma to Cathepsin B Activity. To determine whether an enzymatic mechanism is responsible for the hydrolysis of the VC-PABC linker in the mouse plasma, we conducted thermal inactivation, protease inhibitor, and pH dependence studies. Preincubation of mouse plasma at 65 °C for 1 h completely abolished its VC-PABC cleavage activity (data not shown), suggesting that the VC metabolism in plasma is a result of a thermo-labile enzymatic process. Next, we investigated whether the cleavage of the VC-PABC linker in the plasma occurs through the activity of Cathepsin B, one of the key endosomal/lysosomal cysteine proteases believed to be responsible for intracellular VC-PABC cleavage and toxin release.[11,14,15] While Cathepsin B is not thought to be prevalent in the plasma of healthy individuals, increased extracellular levels of the enzyme and other cysteine cathepsins have been described in various pathological states such as neurodegenerative disease, arthritis, and tumorigenic and metastatic pathways.[16−22]

All of the described cleavable C6-VC-PABC-Aur0101 C16 conjugates displayed comparable in vitro efficacy profiles against target positive BxPC3 cells (Figure 3a−c, Supporting Information Figure 3a and Table 1), suggesting comparable intracellular processing and payload release for each of the examined sites on the time scale of the cytotoxicity assay (4 days). However, the cleavage of the VC-PABC linker in mouse plasma was distinctly dependent on the conjugation site (Table 1). Therefore, we selected the least stable C16 conjugate, Site A-C6-VC-PABC-Aur0101, as a substrate for enzymatic characterization assays. In a series of comparative assays, the substrate was incubated under the conditions described in the presence of purified Cathepsin B or plasma from mouse or human, followed by HIC analysis to assess the extent of VC-PABC linker cleavage and payload loss. The Site A-C6-VC-PABC-Aur0101 substrate underwent a complete cleavage in the presence of mouse or human Cathepsin B over a 20 h incubation at either pH 5.2 or 6.0; however, both enzymes showed negligible activity at pH 7.4 or higher (Table 2). This observation is consistent with the expectation that endosomal/lysosomal proteases, including Cathepsin B, have a pH optimum in the acidic range.[23] In contrast, incubation of the substrate in the mouse plasma at 37 °C for 20 h resulted in an efficient VC-PABC cleavage over a wide range of pH from 5.2 to 8.5 (Table 2). We did not detect any proteolytic activity upon incubation of the VC-PABC substrate in human plasma in vitro, suggesting that either human plasma does not contain the responsible hydrolase(s) or the human enzyme is inactive or inhibited under conditions used in the in vitro assay.

CSPC Exhibit 1004
Page 284 of 536

DOI: 10.1021/bc5005747
Bioconjugate Chem. 2014, 25, 649−659

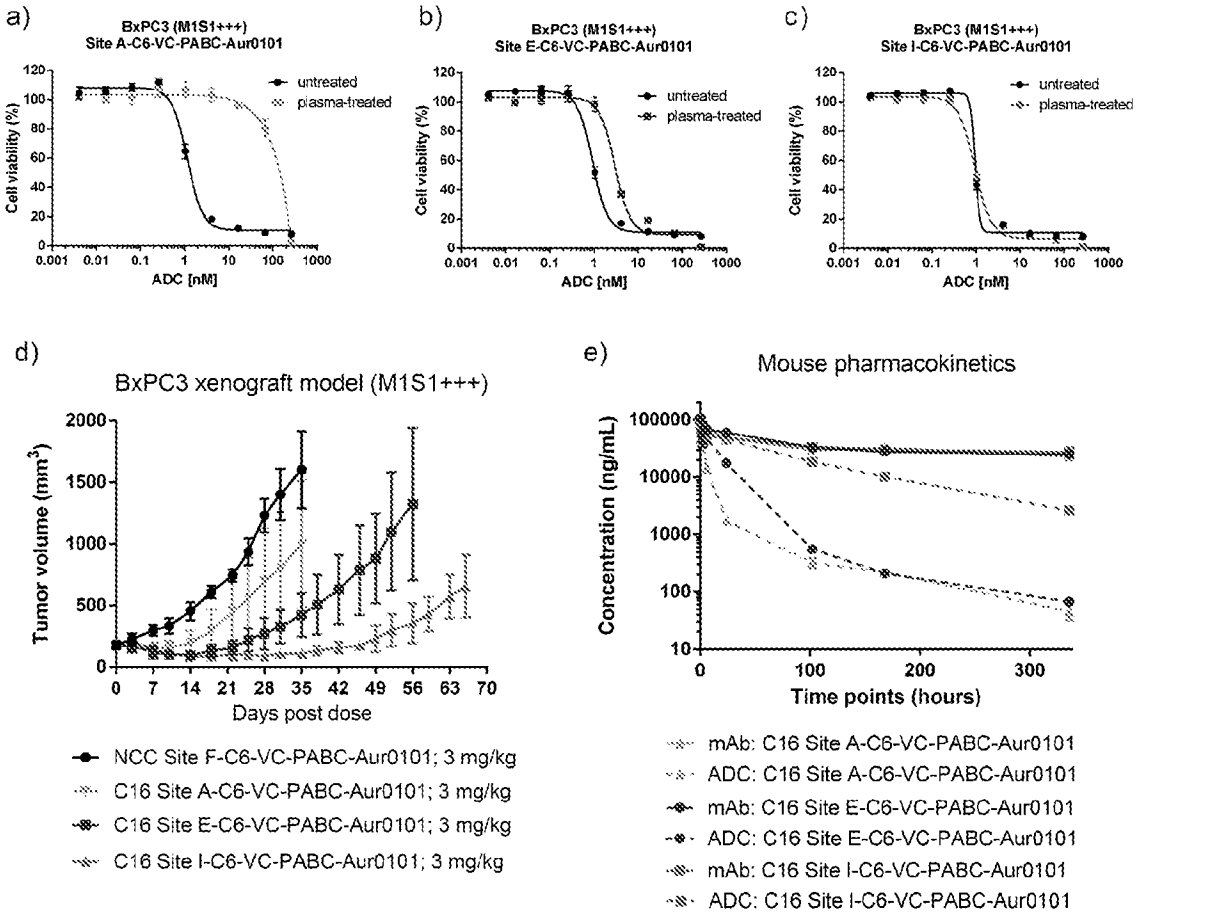


Figure 3. Comparative efficacy studies of cleavable ADCs. Comparison of in vitro cytotoxic activities of untreated and plasma-treated anti-M1S1 cleavable conjugates against BxPC3 cells (M1S1+++). (a) Plasma-sensitive C16 Site A-C6-VC-PABC-Aur0101 conjugate. (b) C16 Site E-C6-VC-PABC-Aur0101 conjugate with intermediate plasma stability. (c) Stable conjugate C16 Site I-C6-VC-PABC-Aur0101. (d) In vivo comparison of the three conjugates in the BxPC3 xenograft model, along with a negative control conjugate NCC Site F-C6-VC-PABC-Aur0101. All compounds were dosed at 3 mg/kg. (e) Mouse pharmacokinetic profiles of the three conjugates. Solid lines represent total antibody ELISA, while dashed lines show antidrug ELISA. All compounds were given as single dose at 3 mg/kg.

Table 2. Testing pH Dependence and Protease Inhibitor Sensitivity of the A-C6-VC-PABC-Aur0101 Linker Cleavage by Mouse and Human Cathepsin B in Comparison with Mouse and Human Plasma[a]

pH	inhibitor	mouse cathepsin B stability (%)	human cathepsin B stability (%)	mouse plasma stability (%)	human plasma stability (%)
5.2	-	0	0	47	100
6.0	-	0	0	45	100
7.4	-	95	94	47	100
8.5	-	100	100	42	100
6.0	E64, 10 μM	99	100	44	-
6.0	Leupeptin, 10 μM	90	76	44	-
6.0	Pefabloc, 1 mM	0	0	100	-

[a]The A-C6-VC-PABC-Aur0101 cleavage activity is expressed in terms of ADC stability values which are given as percentage. The incubation time was decreased to 20 h to capture any differences between Cathepsin B and plasma cleavage under various conditions.

To further investigate whether the cleavage of the VC-PABC linker in mouse plasma occurs through a Cathepsin B-independent mechanism, we employed a series of protease inhibition assays. The purified mouse and human Cathepsin B showed a reduced VC-PABC cleavage when incubated at pH 6.0 in the presence of protease inhibitor E64 (known to inhibit primarily cysteine proteases including Cathepsin B[14,24]) and Leupeptin (an inhibitor of cysteine and serine proteases[24]) (Table 2). In contrast, the addition of either E64 or Leupeptin to the substrate in mouse plasma had no effect on the extent of VC-PABC cleavage at either pH 6.0 or 7.4 (Tables 2 and 3). This observation further suggests that the enzymatic cleavage taking place in the mouse plasma is not mediated by Cathepsin B or a closely related cysteine protease. In further tests, the addition of Pefabloc, mainly a serine protease inhibitor,[24] had no effect on the VC-PABC cleavage by either mouse or human Cathepsin B at pH 6.0 (Table 2), but resulted in a significant inhibition of the cleavage in mouse plasma at both pH 6.0 and 7.4 (Table 2 and 3).

Among other serine protease inhibitors tested (Leupeptin, Antipain, Chymostatin, Aprotinin, Benzamidine, and 3,4-Dichloroisocoumarin[24,25]), only 3,4-Dichloroisocoumarin had a partial inhibitory effect on the VC-PABC cleavage in mouse plasma (Table 3). Inhibitors against cysteine-based hydrolases (E64, Leupeptin, Antipain, Chymostatin, and *N*-ethylmaleimide[24,25]) had no effect on the VC-PABC plasma cleavage, with the exception of partial inhibition by *N*-ethylmaleimide (Table 3). While a cysteine-based mechanism cannot be completely ruled out, it is possible that the partial sensitivity of the plasma enzyme to *N*-ethylmaleimide

DOI: 10.1021/bc5005747
Bioconjugate Chem. 2015, 26, 650-659
CSPC Exhibit 1004
Page 285 of 336

Table 3. Protease Inhibition Studies of the C6-VC-PABC-Aur0101 Cleavage in Mouse Plasma[a]

inhibitor	inhibitor specificity	C6-VC-PABC-Aur0101 stability in mouse plasma (%)
-	-	3
E64, 30 μM	Cys proteases and trypsin	3
Leupeptin, 100 μM	Cys & Ser proteases	4
Antipain, 100 μM	Cys & Ser proteases	4
Chymostatin, 100 μM	Cys & Ser proteases	6
N-Ethylmaleimide, 1 mM	Cys proteases	17
Aprotinin, 5 μM	Ser proteases	3
Pefabloc, 1 mM	Ser proteases	96
Benzamidine, 4 mM	Ser proteases	6
3,4-Dichloroisocoumarin, 1 mM	Ser proteases	28
Pepstatin A, 1 μM	Asp proteases	4
Bestatin, 135 μM	Metalloproteases	3
EDTA, 5 mM	Metalloproteases	5
Carboxypeptidase inhibitor, 10 μM	Carboxypeptidase A & B	4
α2-macroglobulin, 0.3 μM	Broad spectrum inhibitor	5

[a]The A-C6-VC-PABC-Aur0101 cleavage activity is expressed in terms of ADC stability values which are shown as percentage. All assays were carried out at pH 7.4.

might be due to reactivity with a cysteine, histidine, or the α-amino group of *N*-terminal residue.[26] Inhibitors of aspartate proteases (Pepstatin[24]), metalloproteases (Bestatin, EDTA[24]), and carboxypeptidases (carboxypeptidase inhibitor[25]), as well as the broad-spectrum inhibitor α2-macroglobulin[25] had no effect on the VC-PABC cleavage in mouse plasma (Table 3). These data suggest that the VC-PABC linker degradation in mouse plasma is most likely mediated by a serine hydrolase.

Interestingly, proteolysis of the Site A-C6-VC-PABC-Aur0101 conjugate by either mouse or human Cathepsin B is completely blocked upon the addition of plasma even when adjusted to pH 6.0 (Supporting Information Table 2). The loss of Cathepsin B activity in the presence of plasma could result from its inhibition or degradation by plasma components,[27] preference of Cathepsin B for other substrates that may be available in plasma, or its insufficient affinity toward the Site A-C6-VC-PABC-Aur0101 conjugate in the rich plasma environment. This observation further demonstrates that an enzyme other than Cathepsin B is likely responsible for VC-PABC cleavage in the plasma.

Taken together, our results suggest that the cleavage of the VC-PABC linker likely occurs by two independent enzymatic processes with unique characteristics: proteolysis by the lysosomal proteases such as Cathepsin B, most efficient under acidic conditions and effectively blocked by cysteine protease inhibitors, and in mouse plasma by a novel enzymatic activity attributed to an unidentified extracellular hydrolase. The plasma hydrolase activity shows less dependence on pH, and is sensitive to serine hydrolase inhibitors Pefabloc and 3,4-Dichloroisocoumarin. The existence of a distinct enzymatic process responsible for the VC-PABC linker instability in the plasma opens up the possibility to remedy this liability without affecting the desired ADC processing and payload release in the endosomal/lysosomal compartment of the target cell.

DISCUSSION AND CONCLUSIONS

The rapidly expanding field of antibody–drug conjugates for cancer therapy has relied on the properties of linkage chemistries which ideally would offer both a stable toxin attachment to the antibody while in the systemic circulation and an efficient release by intracellular proteases. Cleavable linker technologies designed to undergo drug release in response to pH or reducing environment show relatively poor in vivo stability compared to peptide-based linkers.[5,28,29] While the widely popular valine-citrulline based linkers have been thought to be stable in the plasma environment, payload loss has been reported to occur through the decoupling of thiosuccinimide linkages from conjugates generated through cysteine–maleimide methods.[9,30] The maleimide linkage stability was reported to be dependent on solvent accessibility and local environment, and has been demonstrated to be enhanced by forced or spontaneous maleimide ring opening.[9,31,32]

Alternative conjugation method utilizing microbial transglutaminase produces a site-specific and stable amide linkage between a primary amine of the linker-payload and a glutamine side chain on the antibody. The linkage remains intact upon prolonged exposure to plasma environment (both in vitro and in vivo) and allowed us to examine the stability of the remainder of the linker-payload. We report a wide range of plasma stabilities of ADCs bearing cleavable linker-payloads, with stability varying across specific locations throughout the antibody.

Our data suggest that the C6-VC-PABC-Aur0101 cleavage occurs most readily in mouse plasma, and is mediated by an alternative enzymatic entity than the endosomal/lysosomal protease Cathepsin B with altered pH preference and different protease inhibitor sensitivity. In the rat, the VC-PABC cleavage is more efficient in the circulation in vivo than in the plasma assays in vitro. In our experiments, we did not detect any VC-PABC proteolytic activity on the tested conjugates in human or cynomolgus monkey plasma in vitro; however, we observed some level of drug loss from a related C6-VC-PABC-MMAD conjugate in the monkey in vivo samples. While the problem of premature VC-PABC degradation in the circulation appears more severe in rodents than in primates so far, the time dependent toxin loss in the rodent plasma confounds understanding of relative efficacy and safety across various species. Clarifying these differences and controlling the cleavage mechanism to optimize ADC stability in the mouse and rat is essential since preclinical efficacy and safety studies typically utilize rodent species.

Our results demonstrate that site selection is an important step in the design of systemically stable cleavable auristatin-based conjugates, offering the means to overcome inherent linker instability. The VC-PABC linker proteolysis in the mouse plasma shows a strong dependence on the site of conjugation, implicating either local environment or steric hindrance by proximal antibody domains may play a role in protecting the VC-PABC linker from proteolytic cleavage. The site of attachment can have a dramatic impact on the conjugate stability both in vitro and in vivo, and consequently on conjugate potency. These observations are in line with previous studies describing the effect of conjugation site on ADC properties, including linker stability and drug exposure,[7,9] and further highlight the advantage of site-specific conjugation methods that permit generation of a homogeneous population of ADCs with the desired properties. We were able to identify positions on the antibody that are protective of the labile VC-PABC-containing linker, and narrowed down the potential hydrolases that are likely responsible for the cleavage in circulation. We expect that the VC-PABC degradation in the plasma is not unique to the transglutaminase-based cleavable conjugates, and that the cleavage will be observed at susceptible positions when other stable conjugation chemistries are utilized.[33] Future studies will focus on identification of the

CSPC Exhibit 1004
Page 286 of 336

DOI: 10.1021/bc5005747
Bioconjugate Chem. 2014, 25, 651−659

plasma hydrolase and deciphering how cleavable VC-PABC linkers can be further stabilized in circulation without compromising their intracellular processing and cytotoxic activity.

MATERIALS AND METHODS

Protein Purification. A glutamine tag was introduced at selected positions of anti-M1S1 C16 antibody through residue insertion or substitution using site directed mutagenesis as previously described.[7] The sites are as follows: Site A, light chain residues 200−202 replaced by LLQG tag; Site B, insertion of LLQG tag at position 160 in the heavy chain; Site C, insertion of LLQG tag at position 135 in the heavy chain; Site D, replacement of residue 447 with LLQGA tag in the heavy chain; Site E, heavy chain residues 190−192 replaced by LLQG tag; Site F, insertion of GGLLQGPP tag after residue 214 in the light chain; Site G, N297A deglycosylation mutant (conjugation happens at native Q295 on the heavy chain); Site H, N297Q mutant (conjugation happens on Q295 and Q297 on the heavy chain[34]); Site I, heavy chain residues 294−297 replaced with LLQG tag. Anti-M1S1 constructs were cloned into in-house expression plasmids and transiently expressed in HEK293 cells. Conditioned media was applied to Protein A MabSelect SuRe columns (GE Healthcare, Inc.) and washed with 140 mM NaCl, 2.7 mM KCl, and 10 mM PO_4^{-3} (1× PBS) until baseline was reached. Protein was eluted with 100 mM sodium citrate buffer, pH 3.5, and immediately neutralized with 800 mM sodium phosphate buffer, pH 7.4. Eluted protein was dialyzed into 1× PBS and stored at 4 °C.

CONJUGATION

For the conjugation of anti-M1S1 C16 constructs to C6-VC-PABC-Aur0101, the antibody concentration was adjusted to 5 mg/mL in buffer containing 25 mM Tris-HCl, pH 8.0, 150 mM sodium chloride. Payload was added in a 10- to 25-fold molar excess over antibody, and the enzymatic reaction was initiated by addition of 2% (w/v) bacterial transglutaminase (Ajinomoto Activa TI, Japan). Following incubation with shaking at 37 °C for 16−24 h, conjugates were purified using MabSelect SuRe (GE Healthcare, Inc.) following standard procedures. Alternatively, conjugates were purified using preparative Butyl Sepharose High Performance (Butyl HP, GE Healthcare Biosciences) by adjusting the reaction mixture to obtain a buffer composition of 0.75 M ammonium sulfate, 25 mM potassium phosphate, pH 7 (Buffer A). The material was applied to a Butyl HP column, washed with 5 column volumes of Buffer A, and eluted with a linear gradient into 25 mM potassium phosphate, pH 7. Fractions containing the ADC were pooled, dialyzed against PBS, concentrated using a 10 kDa Amicon Ultra centrifugal filter unit (Millipore Corporation), and sterile filtered through a 0.2 μm filter.

Hydrophobic Interaction Chromatography Analysis. Drug−antibody ratios (DAR) for purified conjugates and their metabolic products were evaluated using a TSK-GEL Butyl-NPR column (4.6 mm × 3.5 cm) (Tosoh Bioscience) on an Agilent HP 1100 HPLC (Agilent). The HIC method utilized a mobile phase of 1.5 M ammonium sulfate, 50 mM potassium phosphate, pH 7 for Buffer A, and 50 mM potassium phosphate, pH 7 with 20% isopropanol for Buffer B. Using a flow rate of 0.8 mL/min, ADC in 0.75 M ammonium sulfate was loaded onto the column, and eluted with a gradient consisting of a 2.5 min hold at 0% Buffer B, followed by a 35 min linear gradient into 100% Buffer B.

LC/MS Intact Mass Analysis. Prior to LC/MS analysis, conjugates and metabolites were deglycosylated with PNGase F (NEB, cat#P0704L) under nondenaturing conditions at 37 °C overnight. ADCs (500 ng) were loaded into a reverse phase column packed with a polymeric material (Michrom-Bruker, cat# CM8/00920/00). LC/MS analysis was performed using Agilent 1100 series HPLC system, comprising binary HPLC pump, degasser, thermostated auto sampler, column heater, and diode-array detector (DAD), coupled to an Orbitrap Velos Pro (Thermo Scientific) mass spectrometer with electrospray ion source. The mobile phases were composed of solvent A (water, 0.1% formic acid) and solvent B (acetonitrile, 0.1% formic acid). The HPLC was carried out using an increasing gradient of solvent B over a 30 min run, consisting of isocratic flow of 3% solvent B for 10 min, followed by a gradient up to 97% solvent B over 1 min, held at 97% solvent B for 2 min, and followed finally with an equilibration step at 3% solvent B for 17 min. The charge state envelopes corresponding to the ADCs were deconvoluted using ProMass software (Thermo Fisher Scientific) to determine the masses.

LC/MS/MS Analysis of ADC Tryptic Digestions. ADCs (100 μg) were solubilized in 0.2% RapiGest (Waters Corp, 186001861) in 20 mM ammonium bicarbonate. The samples were then incubated at 80 °C for 15 min. Dithiothreitol (DTT, 20 mM final concentration) was added and the samples were incubated at 60 °C for 30 min to reduce disulfide bonds. After the samples were cooled to room temperature, iodoacetamide (IAA, 15 mM final concentration) was added, and samples were incubated at room temperature for 30 min in the dark to alkylate reduced cysteines. Modified trypsin (Promega, cat#V5111) was added (1:100 enzyme/substrate) and the samples were incubated at 37 °C overnight. To hydrolyze the RapiGest prior to mass spectrometry analysis, TFA was added to a final concentration of 60 mM, and the solution was incubated at 37 °C for 45 min, and then centrifuged at 20 800 *g* at 4 °C for 30 min. Samples (2.5 μg of digested protein) were loaded into an Agilent Poroshell 120 C18 column (2.1 × 100 mm, 2.7 μm), and eluted at 45 °C with a flow rate of 0.3 mL/min. LC/MS/MS analysis was performed using Agilent 1100 series HPLC system, coupled to an Orbitrap Velos Pro (Thermo Scientific) mass spectrometer with electrospray ion source. Peptides were separated by gradient elution using water as mobile phase A, and acetonitrile as mobile phase B, both containing 0.1% formic acid. The gradient elution used was as follows: 0−2 min 3% B; 2−85 min 3−50% B; 83−83.1 min 50−95% B; 83.1−85 min 95% B; 85−85.1 min 95−3% B and 85.1−90 min 3% B. The Orbitrap Velos was operated in information dependent acquisition (IDA) mode with CID performed on the top 10 ions. The MS scan was performed in the Orbitrap at 100 000 resolution, whereas the fragment spectra were collected in the low pressure trap. Ion trap and Orbitrap maximal injection times were set to 50 and 500 ms, respectively. The ion target values were 30 000 for the ion trap, and 1 000 000 for the Orbitrap.

In Vitro Stability and Protease Inhibitor Assays. Plasma samples from mouse, rat, cynomolgus monkey, and human were purchased from BioreclamationIVT. In vitro stability assays were carried out by incubating 0.125 mg/mL of ADC in 62.5% (v/v) plasma diluted in 1× PBS. Protease inhibitors (Roche, Sigma) were added to plasma at appropriate concentrations as needed. In some assays, pH was adjusted by addition of 120 mM sodium acetate pH 5.2, 120 mM potassium phosphate pH 6.0 or 7.4, or 120 mM Tris HCl pH 8.5. Following incubation at 37 °C for 20 h − 4.5 days, samples were diluted with an equal volume of 1× PBS, and conjugates were isolated using MabSelect SuRe beads or M1S1 antigen coupled to CNBr-activated Sepharose

DOI: 10.1021/bc5005747
Bioconjugate Chem. 2015, 26, 656−659
CSPC Exhibit 1004
Page 287 of 336

(GE Healthcare, Inc.) following standard protocols. DAR values were assessed using HIC or mass spectrometric methods.

In Vivo Stability Assays. Plasma samples were obtained from mice 4.5 days following injection with 3 mg/kg cleavable ADCs. Samples were diluted with an equal volume of 1× PBS pH 7.4, and conjugates were isolated using MabSelect SuRe beads or M1S1 antigen coupled to CNBr-activated Sepharose (GE Healthcare, Inc.) following standard protocols. DAR values were assessed using HIC or mass spectrometric methods.

Enzymatic Assays. Purified recombinant mouse and human Cathepsin B were purchased from R&D Systems. Purified human Cathepsin B from liver was purchased from Sigma. Enzymes were activated in the presence of 1.2 mM L-cysteine and 0.75 mM EDTA at 40 °C for 10 min, and 0.5 ug/mL of enzyme was reacted with 0.125 mg/mL C16 Site A-C6-VC-PABC-Aur0101 substrate in one of the following buffers: 120 mM sodium acetate pH 5.2, 120 mM potassium phosphate pH 6.0 or 7.4, or 120 mM Tris HCl pH 8.5. Appropriate concentrations of protease inhibitors (Roche, Sigma) and 52.5% (v/v) mouse or human plasma (Bioreclamation) were added to reactions prior to the addition of substrate as desired. Following incubation at 37 °C for 20 h, conjugate was isolated using MabSelect SuRe beads or M1S1 antigen coupled to CNBr-activated Sepharose (GE Healthcare, Inc.) following standard protocols. DAR values were assessed using HIC or mass spectrometric methods.

In Vitro Cytotoxicity Assays. In vitro cytotoxicity studies of anti-M1S1 ADCs were performed on the high target-expressing pancreatic adenocarcinoma BxPC3 cell line (M1S1+++), and the target-negative colorectal adenocarcinoma SW620 cell line (M1S1-). Cells were seeded on white-walled clear-bottom plates at 2000 cells per well 24 h before treatment. Cells were treated with 4-fold serially diluted ADCs in triplicate. Cell viability was determined by CellTiter-Glo Luminescent Cell Viability Assay 96 (Promega, Madison, WI) 96 h after treatment. Relative cell viability was determined as percentage of untreated control. IC_{50} values were calculated by GraphPad Prism 5 software.

In Vivo Efficacy Studies. In vivo efficacy studies of ADCs with different stabilities were performed with the high target-expressing BxPC3 (M1S1+++) xenograft model. Two million BxPC3 cancer cells were implanted subcutaneously into 5−8 weeks old female CB17 SCID mice, and tumor growth was monitored until the tumor sizes reached around 200 mm^3. Animals were randomized by tumor sizes into groups of 4−5, and a single dose of either 3 mg/kg or 1.5 mg/kg of cleavable ADC was administered through bolus tail vein injection. Tumor volume was measured twice a week by a Caliper device and calculated with the following formula: Tumor volume = (length × $width^2$)/2. Animals were euthanized once tumor volumes reached 2000 mm^3.

Pharmacokinetics and in Vivo Stability Studies. For PK and stability experiments, compounds were dosed IV through the lateral tail vein at 3 mg/kg, and samples were withdrawn via retro-orbital bleed under isoflurane anesthesia at appropriate time points. For pharmacokinetic studies, a single intravenous dose of 3 mg/kg of ADC was administered into female CB17 SCID mice (n = 3). Stability samples were obtained from the same group at terminal bleeds.

Total Antibody PK Assay. Each well of a 96-well microtiter plate (NUNC) was coated with 100 uL of goat anti-human IgG antibody Fc specific (Pierce cat# 31125) at 1 ug/mL in 1× PBS (Cell Gro). The plates were incubated at 4−8 °C overnight. All washing steps were performed with a Biotek ELx405 plate washer with 1× PBS/0.05% Tween. After washing 3 times, plates were blocked with 200 uL of assay buffer (1× PBS/0.5% BSA/0.05% Polysorbate 20) and incubated for 1−2 h at room temperature with gentle agitation. Plates were washed 3 times and 100 μL of standards, controls, and samples diluted 1:100 in assay buffer were added to the corresponding wells. After a 2 h incubation with gentle agitation at room temperature, plates were washed 6 times before dispensing 100 μL of the detection antibody (anti-human IgG, Fab specific, HRP-labeled from Sigma, cat#A0293) diluted to 250 ng/mL in assay buffer. The plates were incubated for one more hour with gentle agitation at room temperature before washing 6 times. Then, 100 μL of TMB (KPL, SureBlue) was added to each well. Color development was allowed for approximately 5 min before stopping the reaction with 100 μL of 1 M phosphoric acid. Absorbance was measured at 450 nm with a reference at 650 nm on a SpectraMax 340 plate reader (Molecular Devices). SoftMax Pro 5.2 software was used to fit standard curves with a 4-parameter regression, and to calculate sample concentrations.

ADC PK Assay. Each well of a 96-well microtiter plate (NUNC) was coated with 100 μL of goat anti-human IgG antibody at 2 μg/mL in 1× PBS (Cell Gro). The plates were incubated at 4−8 °C overnight. All washing steps were performed on a Biotek ELx405 plate washer with 1× PBS/0.05% Tween. After washing 3 times, plates were blocked with 200 μL/well of assay buffer (1× PBS/0.5% BSA/0.05% Polysorbate 20) and incubated for 1−2 h at room temperature with gentle agitation. Plates were washed 3 times and 100 μL of standards, controls, and samples diluted 1:100 in assay buffer were added in duplicate to the corresponding wells. After a 2 h incubation with gentle agitation at room temperature, plates were washed 6 times before dispensing 100 μL of the detection antibody (biotinylated anti-MMAD monoclonal antibody, Pfizer) diluted to 4 μg/mL in assay buffer. The plates were incubated for 1.5 h with gentle agitation at room temperature before washing 6 times. Avidin-HRP (Vector, cat A-2004) was diluted to 0.25 μg/mL in assay buffer and 100 μL was dispensed into each well. Plates were incubated for another hour before washing 6 times. Then, 100 μL of TMB (KPL, SureBlue) was added to each well. Color development was allowed for approximately 5 min before stopping the reaction with 100 μL of 1 M phosphoric acid. Absorbance was measured at 450 nm with a reference at 650 nm on a SpectraMax 340 plate reader (Molecular Devices). SoftMax Pro 5.2 software was used to fit standard curves with a 4-parameter regression, and to calculate sample concentrations.

Chemical Synthesis. Synthesis of C6-VC-PABC-MMAD (AmCapValCitPABC-MMAD) was previously described.[7] Synthesis of C6-VC-PABC-Aur0101 (AmCapValCitPABC-Auristatin-0101) was as follows:

Fmoc-AmCapValCitPABA-OH (2). A solution of Fmoc-6-aminohexanoic acid (4.2 g, 11.40 mmol) in anhydrous *N,N*-dimethylformamide (50 mL) was treated with *N,N*-diisopropylethylamine (3.8 mL, 2.82 g, 21.8 mmol, 1.8 equiv) and HATU (5.6 g, 14.75 mmol, 1.25 equiv) and the mixture was stirred at room temperature for 10 min. L-Valyl-N^5-carbamoyl-*N*-[4-(hydroxymethyl)phenyl]-L-ornithinamide[11] (5.6 g, 14.75 mmol, 1.25 equiv) was then added to the mixture and stirring was continued for 15 h at room temperature. Dichloromethane was added to precipitate the product, which was filtered and air-dried to provide 5.9 g (100%) of the desired material as an off-white solid. This material was used directly in subsequent reactions without further purification. MS (ES) m/z: 715.6 $[M + H]^+$.

Fmoc-AmCapValCitPABC-PNP (3). A solution of FmocAmCapValCitPABA-OH (500 mg, 0.7 mmol) and bis(4-nitrophenyl)carbonate (638 mg, 2.1 mmol, 3 equiv) in anhydrous

DOI: 10.1021/bc5005747
Bioconjugate Chem. 2015, 26, 650−659
CSPC Exhibit 1004
Page 288 of 336

N,N-dimethylformamide (3 mL) was treated with *N,N*-diisopropylethylamine (365 μL, 270 mg, 2.1 mmol, 3 equiv) and the reaction was stirred at room temperature overnight. The reaction mixture was concentrated in vacuo and the resulting residue was purified by silica gel chromatography using gradient elution of 0−25% methanol in dichloromethane over 15 min, followed by isocratic elution of 25% methanol in dichloromethane. Pooled product-containing fractions were evaporated to provide 402 mg (68%) of the desired product as an off-white solid. MS (ES) m/z: 880.3 $[M + H]^+$.

*N-(6-Aminohexanoyl)-L-valyl-N-{4-[(8S,11S,12R)-11-[(2S)-butan-2-yl]-12-(2-{(2S)-2-[(1R,2R)-1-methoxy-2-methyl-3-oxo-3-{[(1S)-2-phenyl-1-(1,3-thiazol-2-yl)ethyl] amino}propyl]pyrrolidin-1-yl}-2-oxoethyl)-5,5,10-trimethyl-3,6,9-trioxo-8-(propan-2-yl)-2,13-dioxa-4,7,10-triazatetradec-1-yl]phenyl}-N^5-carbamoyl-L-ornithinamide (AmCapValCitPABC-Auristatin-0101, **5**).* A solution of 2-methylalanyl-*N*-[(3*R*,4*S*,5*S*)-3-methoxy-1-{(2*S*)-2-[(1*R*,2*R*)-1-methoxy-2-methyl-3-oxo-3-{[(1*S*)-2-phenyl-1-(1,3-thiazol-2-yl)ethyl]amino}propyl]pyrrolidin-1-yl}-5-methyl-1-oxoheptan-4-yl]-*N*-methyl-L-valinamide[10] (105 mg, 0.141 mmol), FmocAmCapValCitPABC-PNP (138 mg, 0.157 mmol), HOAt (6.40 mg, 0.047 mmol), and 2,6-lutidine (91 uL, 84 mg, 0.783 mmol) in *N,N*-dimethylformamide (1.4 mL) was heated at 45 °C for 21 h. Additional FmocAmCapValCitPABC-PNP (31 mg, 0.035 mmol), HOAt (3.83 mg, 0.028 mmol), and 2,6-lutidine (16 uL, 15 mg, 0.141 mmol) were then added, the reaction was heated at 40 °C for an additional 6 h, and then kept at room temperature overnight. LCMS analysis indicated that the reaction contained a mixture of compounds **4** and **5**. Piperidine (0.5 mL) was added and the reaction stirred at room temperature for 1 h. LCMS analysis indicated that the Fmoc-deprotection reaction was complete, and the reaction was concentrated and the residue was and purified by reverse phase chromatography over a 100 × 30 mm^2, 5 μm Phenomenex Luna C18 column using flow rate of 20 mL/min and gradient elution of 10−85% acetonitrile in water containing 0.02% trifluoracetic acid over 20 min. Pooled product-containing fractions were concentrated and lyophilized to provide 97 mg (54%) of the desired product (**5**) as white solid. MS (ES): m/z 1062.3$[M + H]^+$. This material was greater than 95% pure by analytical HPLC and the ^{1}H NMR was consistent with the assigned structure.

■ ASSOCIATED CONTENT

Ⓢ Supporting Information

Cytotoxicity of untreated and plasma-treated cleavable conjugates against the BxPC3 cell line (M1S1+++). Inhibition of Cathepsin B-catalyzed cleavage of the C16 Site A-C6-VC-PABC-Aur0101 substrate upon addition of mouse or human plasma. Stability analysis of the cleavable C16 Site A-C6-VC-PABC-Aur0101 conjugate using hydrophobic interaction chromatography. Mass spectrometric analysis of the cleavage product of C16 Site A-C6-VC-PABC-Aur0101 conjugate isolated from mouse plasma. Cytotoxicity assays of cleavable C6-VC-PABC-Aur0101 conjugates across various sites. Correlation between changes in IC_{50} values (efficacy) and changes in DAR (stability) for cleavable conjugates incubated in mouse plasma. Pharmacokinetic profiles of the humanized C16 Site D-C6-VC-PABC-MMAD conjugate in rat, and the chimeric C16 Site D-C6-VC-PABC-MMAD conjugate in cynomolgus monkey. This material is available free of charge via the Internet at http://pubs.acs.org.

■ AUTHOR INFORMATION

Corresponding Author

*E-mail: pavel.strop@pfizer.com. Phone: (650) 615-7355.

Author Contributions

Magdalena Dorywalska and Pavel Strop contributed equally to the work.

Notes

The authors declare the following competing financial interest(s): All authors are employees of Pfizer Inc.

■ ACKNOWLEDGMENTS

We would like to thank Michael Sherman Chin, Teresa Wong, and Colleen Brown for cell culture support, and Dan McDonough for help with ELISA assays. We also thank Janette Sutton for assistance with PK and stability experiments, and Eugenia Kraynov for help with PK studies.

■ REFERENCES

(1) Lambert, J. M. (2013) Drug-conjugated antibodies for the treatment of cancer. *Br. J. Clin. Pharmacol. 76*, 248−62.

(2) Sievers, E. L., and Senter, P. D. (2013) Antibody-drug conjugates in cancer therapy. *Annu. Rev. Med. 64*, 15−29.

(3) Panowksi, S., Bhakta, S., Raab, H., Polakis, P., and Junutula, J. R. (2014) Site-specific antibody drug conjugates for cancer therapy. *MAbs 6*, 34−45.

(4) Doronina, S. O., Toki, B. E., Torgov, M. Y., Mendelsohn, B. A., Cerveny, C. G., Chace, D. F., DeBlanc, R. L., Gearing, R. P., Bovee, T. D., Siegall, C. B., Francisco, J. A., Wahl, A. F., Meyer, D. L., and Senter, P. D. (2003) Development of potent monoclonal antibody auristatin conjugates for cancer therapy. *Nat. Biotechnol. 21*, 778−84.

(5) Sanderson, R. J., Hering, M. A., James, S. F., Sun, M. M., Doronina, S. O., Siadak, A. W., Senter, P. D., and Wahl, A. F. (2005) In vivo drug-linker stability of an anti-CD30 dipeptide-linked auristatin immunoconjugate. *Clin. Cancer. Res. 11*, 843−52.

(6) Strop, P., Dorywalska, M., Rajpal, A., Shelton, D. L., Liu, S.-H., Pons, J., and Dushin, R. (2012) Patent WO2012059882.

(7) Strop, P., Liu, S. H., Dorywalska, M., Delaria, K., Dushin, R. G., Tran, T. T., Ho, W. H., Farias, S., Casas, M. G., Abdiche, Y., Zhou, D., Chandrasekaran, R., Samain, C., Loo, C., Rossi, A., Rickert, M., Krimm, S., Wong, T., Chin, S. M., Yu, J., Dilley, J., Chaparro-Riggers, J., Filzen, G. F., O'Donnell, C. J., Wang, F., Myers, J. S., Pons, J., Shelton, D. L., and Rajpal, A. (2013) Location matters: site of conjugation modulates stability and pharmacokinetics of antibody drug conjugates. *Chem. Biol. 20*, 161−7.

(8) Farias, S. E., Strop, P., Delaria, K., Galindo Casas, M., Dorywalska, M., Shelton, D. L., Pons, J., and Rajpal, A. (2014) Mass spectrometric characterization of transglutaminase based site-specific antibody-drug conjugates. *Bioconjugate Chem. 25*, 240−50.

(9) Shen, B. Q., Xu, K., Liu, L., Raab, H., Bhakta, S., Kenrick, M., Parsons-Reponte, K. L., Tien, J., Yu, S. F., Mai, E., Li, D., Tibbitts, J., Baudys, J., Saad, O. M., Scales, S. J., McDonald, P. J., Hass, P. E., Eigenbrot, C., Nguyen, T., Solis, W. A., Fuji, R. N., Flagella, K. M., Patel, D., Spencer, S. D., Khawli, L. A., Ebens, A., Wong, W. L., Vandlen, R., Kaur, S., Sliwkowski, M. X., Scheller, R. H., Polakis, P., and Junutula, J. R. (2012) Conjugation site modulates the in vivo stability and therapeutic activity of antibody-drug conjugates. *Nat. Biotechnol. 30*, 184−9.

(10) Maderna, A., Doroski, M., Subramanyam, C., Porte, A., Leverett, C. A., Vetelino, B. C., Chen, Z., Risley, H., Parris, K., Pandit, J., Varghese, A. H., Shanker, S., Song, C., Sukuru, S. C., Farley, K. A., Wagenaar, M. M., Shapiro, M. J., Musto, S., Lam, M. H., Loganzo, F., and O'Donnell, C. J. (2014) Discovery of cytotoxic dolastatin 10 analogues with N-terminal modifications. *J. Med. Chem. 57*, 10527−43.

(11) Dubowchik, G. M., Firestone, R. A., Padilla, L., Willner, D., Hofstead, S. J., Mosure, K., Knipe, J. O., Lasch, S. J., and Trail, P. A. (2002) Cathepsin B-labile dipeptide linkers for lysosomal release of doxorubicin from internalizing immunoconjugates: model studies of enzymatic drug release and antigen-specific in vitro anticancer activity. *Bioconjugate Chem. 13*, 855−69.

(12) Toki, B. E., Cerveny, C. G., Wahl, A. F., and Senter, P. D. (2002) Protease-mediated fragmentation of p-amidobenzyl ethers: a new

CSPC Exhibit 1004
Page 280 of 336

DOI: 10.1021/bc5005747
Bioconjugate Chem. 2015, 26, 650−659

strategy for the activation of anticancer prodrugs. *J. Org. Chem. 67*, 1866–72.
(13) Doronina, S. O., Bovee, T. D., Meyer, D. W., Miyamoto, J. B., Anderson, M. E., Morris-Tilden, C. A., and Senter, P. D. (2008) Novel peptide linkers for highly potent antibody-auristatin conjugate. *Bioconjugate Chem. 19*, 1960–3.
(14) Sutherland, M. S., Sanderson, R. J., Gordon, K. A., Andreyka, J., Cerveny, C. G., Yu, C., Lewis, T. S., Meyer, D. L., Zabinski, R. F., Doronina, S. O., Senter, P. D., Law, C. L., and Wahl, A. F. (2006) Lysosomal trafficking and cysteine protease metabolism confer target-specific cytotoxicity by peptide-linked anti-CD30-auristatin conjugates. *J. Biol. Chem. 281*, 10540–7.
(15) Weidle, U. H., Tiefenthaler, G., and Georges, G. (2014) Proteases as activators for cytotoxic prodrugs in antitumor therapy. *Cancer Genomics Proteomics 11*, 67–79.
(16) Hook, V. Y. (2006) Unique neuronal functions of cathepsin L and cathepsin B in secretory vesicles: biosynthesis of peptides in neurotransmission and neurodegenerative disease. *Biol. Chem. 387*, 1429–39.
(17) Sundelof, J., Sundstrom, J., Hansson, O., Eriksdotter-Jonhagen, M., Giedraitis, V., Larsson, A., Degerman-Gunnarsson, M., Ingelsson, M., Minthon, L., Blennow, K., Kilander, L., Basun, H., and Lannfelt, L. (2010) Higher cathepsin B levels in plasma in Alzheimer's disease compared to healthy controls. *J. Alzheimers Dis. 22*, 1223–30.
(18) Vasiljeva, O., Reinheckel, T., Peters, C., Turk, D., Turk, V., and Turk, B. (2007) Emerging roles of cysteine cathepsins in disease and their potential as drug targets. *Curr. Pharm. Des. 13*, 387–403.
(19) Fonovic, M., and Turk, B. (2014) Cysteine cathepsins and extracellular matrix degradation. *Biochim. Biophys. Acta 1840*, 2560–70.
(20) Reiser, J., Adair, B., and Reinheckel, T. (2010) Specialized roles for cysteine cathepsins in health and disease. *J. Clin. Invest. 120*, 3421–31.
(21) Yan, S., and Sloane, B. F. (2003) Molecular regulation of human cathepsin B: implication in pathologies. *Biol. Chem. 384*, 845–54.
(22) Mohamed, M. M., and Sloane, B. F. (2006) Cysteine cathepsins: multifunctional enzymes in cancer. *Nat. Rev. Cancer 6*, 764–75.
(23) Guha, S., and Padh, H. (2008) Cathepsins: fundamental effectors of endolysosomal proteolysis. *Indian J. Biochem. Biophys. 45*, 75–90.
(24) Roche Molecular Biochemicals, *The Complete Guide for Protease Inhibition.*
(25) Sigma-Aldrich. (2009) Protease Inhibition and Detection. *Life Science BioFiles 4.*
(26) Smyth, D. G., Blumenfeld, O. O., and Konigsberg, W. (1964) Reactions of N-ethylmaleimide with peptides and amino acids. *Biochem. J. 91*, 589–95.
(27) Snellman, O., and Sylven, B. (1967) Haptoglobin acting as a natural inhibitor of cathepsin B activity. *Nature 216*, 1033.
(28) Ducry, L., and Stump, B. (2010) Antibody-drug conjugates: linking cytotoxic payloads to monoclonal antibodies. *Bioconjugate Chem. 21*, 5–13.
(29) Cardillo, T. M., Govindan, S. V., Sharkey, R. M., Trisal, P., and Goldenberg, D. M. (2011) Humanized anti-Trop-2 IgG-SN-38 conjugate for effective treatment of diverse epithelial cancers: preclinical studies in human cancer xenograft models and monkeys. *Clin. Cancer Res. 17*, 3157–69.
(30) Alley, S. C., Benjamin, D. R., Jeffrey, S. C., Okeley, N. M., Meyer, D. L., Sanderson, R. J., and Senter, P. D. (2008) Contribution of linker stability to the activities of anticancer immunoconjugates. *Bioconjugate Chem. 19*, 759–65.
(31) Tumey, L. N., Charati, M., He, T., Sousa, E., Ma, D., Han, X., Clark, T., Casavant, J., Loganzo, F., Barletta, F., Lucas, J., and Graziani, E. I. (2014) Mild method for succinimide hydrolysis on ADCs: impact on ADC potency, stability, exposure, and efficacy. *Bioconjugate Chem. 25*, 1871–80.
(32) Lyon, R. P., Setter, J. R., Bovee, T. D., Doronina, S. O., Hunter, J. H., Anderson, M. E., Balasubramanian, C. L., Duniho, S. M., Leiske, C. I., Li, F., and Senter, P. D. (2014) Self-hydrolyzing maleimides improve the stability and pharmacological properties of antibody-drug conjugates. *Nat. Biotechnol. 32*, 1059–62.
(33) Tian, F., Lu, Y., Manibusan, A., Sellers, A., Tran, H., Sun, Y., Phuong, T., Barnett, R., Hehli, B., Song, F., DeGuzman, M. J., Ensari, S., Pinkstaff, J. K., Sullivan, L. M., Biroc, S. L., Cho, H., Schultz, P. G., DiJoseph, J., Dougher, M., Ma, D., Dushin, R., Leal, M., Tchistiakova, L., Feyfant, E., Gerber, H. P., and Sapra, P. (2014) A general approach to site-specific antibody drug conjugates. *Proc. Natl. Acad. Sci. U. S. A. 111*, 1766–71.
(34) Jeger, S., Zimmermann, K., Blanc, A., Grünberg, J., Honer, M., Hunziker, P., Struthers, H., and Schibli, R. (2010) Site-specific and stoichiometric modification of antibodies by bacterial transglutaminase. *Angew. Chem. Int. Ed. Engl. 49*, 9995–9997.

CSPC Exhibit 1004
Page 290 of 336

DOI: 10.1021/bc5005747
Bioconjugate Chem. 2015, 26, 650−659

To: USPTOeAction@SeedIP.com,pairlinkdktg@seedip.com,
From: PAIR_eOfficeAction@uspto.gov
Cc: PAIR_eOfficeAction@uspto.gov
Subject: Private PAIR Correspondence Notification for Customer Number 500

Jan 17, 2020 03:30:27 AM

Dear PAIR Customer:

SEED INTELLECTUAL PROPERTY LAW GROUP LLP
701 FIFTH AVE
SUITE 5400
SEATTLE, WA 98104
UNITED STATES

The following USPTO patent application(s) associated with your Customer Number, 500 , have new outgoing correspondence. This correspondence is now available for viewing in Private PAIR.

The official date of notification of the outgoing correspondence will be indicated on the form PTOL-90 accompanying the correspondence.

Disclaimer:
The list of documents shown below is provided as a courtesy and is not part of the official file wrapper. The content of the images shown in PAIR is the official record.

Application	Document	Mailroom Date	Attorney Docket No.
15550995	CTNF	01/17/2020	850231.401USPC
	892	01/17/2020	850231.401USPC

To view your correspondence online or update your email addresses, please visit us anytime at https://sportal.uspto.gov/secure/myportal/privatepair.

If you have any questions, please email the Electronic Business Center (EBC) at EBC@uspto.gov with 'e-Office Action' on the subject line or call 1-866-217-9197 during the following hours:

Monday - Friday 6:00 a.m. to 12:00 a.m.

Thank you for prompt attention to this notice,

UNITED STATES PATENT AND TRADEMARK OFFICE

PATENT APPLICATION INFORMATION RETRIEVAL SYSTEM

PATENT

IN THE UNITED STATES PATENT AND TRADEMARK OFFICE

First Named Inventor	:	Chaohong Hu
Application No.	:	15/550,995
Filed	:	August 14, 2017
For	:	ANTIBODY-DRUG CONJUGATE
Examiner	:	Karen A Canella
Art Unit	:	1643
Docket No.	:	850231.401USPC
Date	:	March 26, 2020

Commissioner for Patents
P.O. Box 1450
Alexandria, VA 22313-1450

AMENDMENT

Commissioner for Patents:

In response to the Office Action dated January 17, 2020, please amend the application as follows:

Amendments to the Claims are reflected in the listing of claims which begins on page 2 of this paper.

Remarks begin on page 7 of this paper.

Amendments to the Claims:

This listing of claims will replace all prior versions, and listings, of claims in the application:

Listing of Claims:

1. (Canceled)

2. (Previously Presented) An antibody-drug conjugate or a pharmaceutically acceptable salt thereof, comprising an anti-epidermal growth factor receptor antibody covalently linked to a cytotoxic agent via a cleavable linker, wherein the anti-epidermal growth factor receptor antibody comprises a heavy chain and a light chain, wherein the heavy chain has a variable region comprising CDR1, CDR2 and CDR3 having sequences as shown in SEQ ID NOs: 5 to 7, and the light chain has a variable region comprising CDR1, CDR2 and CDR3 having sequences as shown in SEQ ID NOs: 12 to 14.

3. (Previously Presented) The antibody-drug conjugate or the pharmaceutically acceptable salt thereof according to claim 2, wherein FR1, FR2, FR3, FR4 of the variable region of the heavy chain of the anti-epidermal growth factor receptor antibody respectively comprise sequences as shown in SEQ ID NOs: 8 to 11.

4. (Currently Amended) The antibody-drug conjugate or the pharmaceutically acceptable salt thereof according to claim 2, wherein FR1, FR2, FR3, FR4 of the variable region of the light chain of the anti-epidermal growth factor receptor antibody respectively comprise sequences as shown in SEQ ID NOs: 15 to 18~~,~~.

5. (Previously Presented) The antibody-drug conjugate or the pharmaceutically acceptable salt thereof according to claim 2, wherein the heavy chain of the anti-epidermal growth factor receptor antibody has a constant region selected from the group consisting of

a human IgG constant region, a human IgM constant region, a human IgA constant region, and a human IgD constant region.

6. (Previously Presented) The antibody-drug conjugate or the pharmaceutically acceptable salt thereof according to claim 5, wherein the IgG is selected from the group consisting of IgG1, IgG2, IgG3 and IgG4.

7. (Currently Amended) The antibody-drug conjugate or the pharmaceutically acceptable salt thereof according to claim 5, wherein the constant region of the heavy chain of the anti-epidermal growth factor receptor antibody comprises an amino acid sequence as shown in SEQ ID NO: 3~~, or comprises a sequence with an identity of greater than 90%, 95%, or 99% to the sequence as shown in SEQ ID NO: 3~~.

8. (Previously Presented) The antibody-drug conjugate or the pharmaceutically acceptable salt thereof according to claim 2, wherein the light chain of the anti-epidermal growth factor receptor antibody has a constant region selected from the group consisting of a human lambda constant region, and a human kappa constant region.

9. (Currently Amended) The antibody-drug conjugate or the pharmaceutically acceptable salt thereof according to claim 8, wherein the constant region of the light chain of the anti-epidermal growth factor receptor antibody comprises an amino acid sequence as shown in SEQ ID NO: 4~~, or comprises a sequence with an identity of greater than 90%, 95%, or 99% to the sequence as shown in SEQ ID NO: 4~~.

10. (Previously Presented) The antibody-drug conjugate or the pharmaceutically acceptable salt thereof according to claim 2, which has a structure as shown in Formula I,

$$Ab\text{-}(L\text{-}D)_p$$

Formula I

wherein:

Ab represents the anti-epidermal growth factor receptor antibody;

L represents a cleavable linker;

D represents the cytotoxic agent;

p represents 1-9.

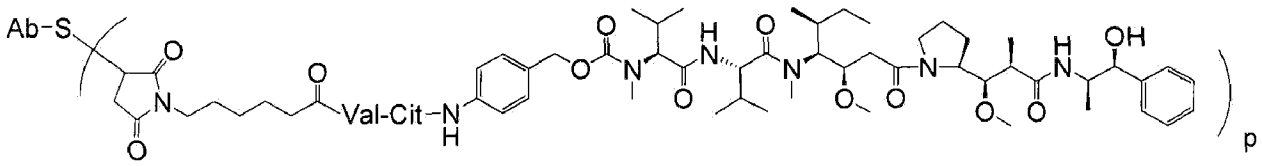
11. (Previously Presented) The antibody-drug conjugate or the pharmaceutically acceptable salt thereof according to claim 10, wherein the cytotoxic agent is selected from the group consisting of chemotherapeutic agents, radioisotopes, antibiotics, enzymes, and biologically active peptides.

12. (Previously Presented) The antibody-drug conjugate or the pharmaceutically acceptable salt thereof according to claim 11, wherein the cytotoxic agent is selected from the group consisting of Monomethyl auristatin E (MMAE), Monomethyl auristatin F (MMAF), maytansinoid alkaloids, Calicheamicin, duocarmycin MGBA, doxorubicin, ricin, diphtheria toxin, I131, and tumor necrosis factors.

13. (Canceled)

14. (Previously Presented) The antibody-drug conjugate or the pharmaceutically acceptable salt thereof according to claim 10, wherein the linker is selected from the group consisting of valine-citrulline (val-cit), alanine-phenylalanine (ala-phe), N-succinimidyl 4-(2-pyridylthio)valerate (SPP), and 6-maleimidocaproyl-valine-citrulline-p-aminobenzyloxycarbonyl (MC-vc-PAB).

15. (Previously Presented) The antibody-drug conjugate or the pharmaceutically acceptable salt thereof according to claim 10, which is:



wherein Ab represents the anti-epidermal growth factor receptor antibody, p is 1-8.

16. (Previously Presented) A composition, which comprises the antibody-drug conjugate or the pharmaceutically acceptable salt thereof according to claim 2, optionally, further comprises at least one pharmaceutically acceptable carrier, diluent or excipient.

17.-22. (Canceled)

23. (Previously Presented) A method for treatment of a disease associated with epidermal growth factor receptor (EGFR), comprising: administering to a subject in need a therapeutically effective amount of the antibody-drug conjugate or the pharmaceutically acceptable salt thereof according to claim 2.

24. (Previously Presented) The method according to claim 23, wherein the disease associated with epidermal growth factor receptor (EGFR) is a tumor associated with overexpression of EGFR.

25. (Previously Presented) A method for inhibiting tumor angiogenesis, delaying tumor progression, inhibiting tumor growth, or inhibiting tumor cell proliferation, comprising: administering to a subject in need a therapeutically effective amount of the antibody-drug conjugate or the pharmaceutically acceptable salt thereof according to claim 2.

26. (Original) The method according to claim 25, wherein the tumor is selected from colon cancer, rectal cancer, head and neck cancer, lung cancer, ovarian cancer, cervical cancer, bladder cancer, esophageal cancer, breast cancer, renal cancer, prostate cancer, gastric cancer, pancreatic cancer and brain glioma.

27. (Previously presented) The method according to claim 24, wherein the tumor is a tumor with KRAS gene mutation.

28. (Previously Presented) The method according to claim 24, wherein the tumor is a tumor with BRAF gene mutation.

29.-34. (Canceled)

35. (Previously Presented) The method according to claim 26, wherein the tumor is a tumor with KRAS gene mutation.

36. (Previously Presented) The method according to claim 26, wherein the tumor is a tumor with BRAF gene mutation.

37. (Previously Presented) The antibody-drug conjugate or the pharmaceutically acceptable salt thereof according to claim 10, wherein the linker is 6-maleimidocaproyl-valine-citrulline-p-aminobenzyloxycarbonyl (MC-vc-PAB).

REMARKS

Reconsideration of the present application in view of the above amendments and the following remarks are respectfully requested.

Claims 2-12, 14-16, 23-28, and 35-37 are pending. Claims 4, 7 and 9 have been amended. Such amendments have been made to facilitate allowance and without acquiescing to the rejections in the Office Action or disclaimers. No new matter has been added.

As an initial matter, Applicant thanks the Examiner for withdrawing the finality of the previous Office Action. Applicant also thanks the Examiner for allowing claims 27, 28, 35 and 36.

Rejections Under §103

Claims 2-12, 14-6, 23-26 and 37 are rejected under 35 U.S.C 103 as unpatentable over Tikhomirov (WO2015/000062, **D1**) in view of Liu (CN103772504, **D2**), Brand et al. (Cancer Biology & Therapy 11:777-92, 2011, **D3**), Chung et al. (New England Journal of Medicine 358:1109-17, 2008, **D4**) and Doronina et al. (Cancer Research 17:114-124, 2006, **D5**).

Applicant respectfully traverses this rejection. In its previous submission filed December 16, 2019, Applicant argued against the previous obviousness rejection over D1 in view of D2, D3 and D4, and submitted that (1) one of ordinary skill in the art would not have been motivated by the cited references to use a cleavable linker to arrive at the antibody-drug conjugate (ADC) or a pharmaceutically acceptable salt thereof as claimed in the present application, and (2) the ADC claimed in the present application is not obvious due to its unexpectedly superior property as demonstrated in Example 6 of the present application.

In this Office Action, in addition to D1 to D4, D5 is cited to support the assertion that it would have been *prima facie* obvious to use a cleavable linker rather than a non-cleavable linker in cases where the linked drug loses activity as a result of modification of the released drug such as MMAE.

Applicant respectfully disagrees and submits that one skilled in the art would not have been motivated by the cited references, including newly cited D5, to use a cleavable linker to arrive at the ADC or a pharmaceutically acceptable salt thereof as claimed in the present application. First, **D5** relates to enhanced activity of monomethylauristatin F through monoclonal antibody delivery and analysis of linker technology on efficacy and toxicity. The antibody used in D5 is an anti-CD30 antibody, cAC10. Because the target to which an ADC binds influences the efficacy of the ADC, and because the target of the ADC of D5 is different from the target of the claimed ADC of the present application, EGFR, D5 fails to provide a sufficient motivation for one of ordinary skill to use a cleavable linker to link an anti-EGFR antibody and MMAE together. Specifically, Polson *et al.*, Cancer Res 69:2358-64, 2009 (cited in the Office Action dated October 18, 2019) shows that the efficacies of ADCs with the same linker and drug combination were different if the targets of the ADCs were different. It further discloses:

> *In vitro* data suggest that the biology of the target, in particular, the extent of trafficking to the lysosomal compartment, will influence the effectiveness of the ADC (7-10). *In vivo*, the situation is even more complex; the extracellular microenvironment, and the intracellular trafficking of the target the longer exposure times (weeks instead of days), in combination with the linker-drug used, will determine where, to what extent, and in what form the cytotoxic drug is released and thus which linker-drug combinations are both effective and safe. *See* the first full paragraph in the right column on page 2358.

Thus, one skilled in the art would not have been motivated to use a cleavable linker with MMAE in an ADC with a target different from CD30 simply because D5 uses a cleavable linker and MMAE combination in an anti-CD30 ADC.

Second, even for the sake of argument assuming one had used a cleavable linker with MMAE, such a person would not have modified the ADC of D1 to substitute its antibody component with the antibody of D2. This is because Example 4 of D1 disclose that "Figure 13 shows that **conjugation of cetuximab to MMAE by a cleavable linker (valine-citrulline) potentiates its toxicity against normal cells and MDA-MB-468 cancer cells, whereas conjugation via non-cleavable linker (SMCC) potentiates anti-cancer activity**" (emphasis added). In addition, Example 4 of D1 further states:

> Thus, in these studies, only fully antagonistic anti-EGFR antibodies were not potentiated on normal cells by payload conjugation via non-cleavable linkers, whereas toxicity against normal cells of partial antagonist EGFR antibodies was potentiated by conjugation. Moreover, we subsequently tested the effect on this activity profile of the cleavable vs. non-cleavable linkers, while maintaining payload mechanism of action the same (i.e. anti-microtubule agent). The antibodies were conjugated via cleavable linker to anti-microtubule payload, MMAE as described by Doronina et al, Nature Biotechnology Nov 7, 2003, Vol 21: pp 778-784. Cleavable linker data demonstrate that **when the fully antagonistic antibodies are conjugated to their payloads via cleavable linkers, their toxicity against normal cells is potentiated**. Thus, **a safe anti-EGFR ADC should incorporate a strongly antagonistic anti-EGFR antibody linked to an anti-microtubule payload by a non-cleavable linker**. *See* the paragraph bridging pages 29 and 30 (emphasis added).

Thus, in view of the disclosure of D1, one of ordinary skill in the art would be discouraged from using a cleavable linker in incorporating a strongly antagonistic anti-EGFR antibody into an ADC due to potentiated toxicity against normal cells of such ADCs. Using a cleavable linker in generating anti-EGFR ADCs would eliminate or at least reduce the primary benefit of the invention disclosed in D1, that is, potentiating anti-cancer activities of ADCs without increasing their cytotoxicity against normal cells. As discussed in detail in Applicant's submission of December 16, 2019, cytotoxicity against normal cells of ADCs is a significant concern that resulted in dose reduction, discontinuation of treatment, and exploration of conjugates based on antibodies targeting mutated EGFR or with partial antagonistic activity against EGFR (*see* the paragraph bridging pages 11 and 12 of the previous response). Due to such a concern and because of the explicit teaching in the above-quoted paragraph of D1, even if one of ordinary skill in the art were to use an optional and less desirable cleavable linker (which is mentioned only once in D1), such a person would use it in combination with an antibody having partial antagonistic activity against EGFR, not a strongly antagonistic anti-EGFR antibody, such as the antibody of D2, which has higher binding affinity and ligand blocking abilities than cetuximab as acknowledged in the Office Action (*see* the last paragraph on page 7 of the Office Action). In addition, one skilled in the art would give more weight to D1 than D5 because unlike D5, the ADCs of D1 target the same EGFR protein as those claimed in the present application.

In addition to D5, the Office Action also cites Erickson *et al.* (Molecular Cancer Therapeutics 11: 1133-42, 2012, **D6**). **D6** relates to the effect of different linkers on target cell

catabolism and pharmacokinetics/pharmacodynamics of trastuzumab (anti-HER2 antibody) maytansinoid conjugates. Applicant is not very clear about the reason for citing D6 in the Office Action. D6 seems to be used in the Office Action to allege that it was known in the art that DM1 could be linked to either a cleavable linker or a non-cleavable linker whereas MMAE could only be linked to a cleavable linker. Again, as discussed above, the efficacy of an ADC is not only influenced by its linker and payload, but also by its target. Thus, one of ordinary skill in the art would not have combined a particular type of linker with a given payload to generate an ADC regardless the target of the ADC. One skilled in the art would also give more weight to D1 than D6 because unlike D6, the ADCs of D1 target the same EGFR protein as those claimed in the present application.

The Office Action further cites Dorywalska *et al.* (Bioconjugate Chemistry 26: 650-9, 2015, **D7**) to rebut Applicant's previous arguments related to toxicity against normal keratinocytes disclosed in D1. It is asserted in the Office Action that because the *in vitro* assay of D1 was done in the presence of 10% fetal bovine serum (FBS), and because D7 teaches that plasma from different sources comprise a factor, which cleaves VC-PABC resulting in drug loss from the ADC, one of skill in the art would "reasonably conclude that increased toxicity observed by Tikhomirov et al against keratinocytes in vitro on exposure to the cleavable DM1 conjugate was the result of exposure to untargeted DM1 rather than targeted DM1 relying on uptake by Her2 internalization" (*see* the first full paragraph on page 9 of the Office Action).

Applicant respectfully disagrees. **D7** relates to effect of attachment site on stability of cleavable antibody drug conjugates. D7 tested stability of the cleavable C6-VC-PABC-Aur0101 conjugate series in mouse, rat, cynomolgus monkey, and human plasma, and found that among the four sources of plasma, mouse plasma caused high levels of cleavage of ADCs, rat plasma caused low levels of cleavage, but cynomolgus monkey and human plasma caused practically no cleavage (*see* Table 1, the paragraph bridging pages 652 and 653). Nowhere in D7 shows that FBS caused cleavage of ADCs. In addition, because only mouse plasma among the 4 tested sources of serum caused significant cleavages of ADCs, one of ordinary skill in the art would not reasonably expect that another untested source of serum would also cause significant cleavages of ADCs. Accordingly, such a person would not interpret the toxicity against normal keratinocytes of ADCs with cleavable linkers disclosed D1 as resulting from the use of FBS in

its *in vitro* assay. In addition, it is worth noting that the Office Action seems to take an inconsistent position regarding D1: On one hand, it uses D1 as the primary reference to combine with the other cited references, but on the other hand, it cites D7 to discredit the primary teaching of D1.

In view of the above remarks, Applicant submits that this rejection has been overcome. Withdrawal of this rejection is respectfully requested.

Rejections Under §112

Claims 7 and 9 are rejected under 35 U.S.C. 112, first paragraph, as failing to meet the written description requirement due to their recitations of percentage sequence identity.

To facilitate allowance and without acquiescing to this rejection, Applicant has amended claims 7 and 9 to delete the recitations of percentage sequence identity. Accordingly, this rejection has been overcome.

The Director is authorized to charge any additional fees due by way of this Amendment, or credit any overpayment, to our Deposit Account No. 19-1090.

Respectfully submitted,

SEED Intellectual Property Law Group LLP

/Qing Lin/
Qing Lin, Ph.D.
Registration No. 53,937

QXL:bgh

701 Fifth Avenue, Suite 5400
Seattle, Washington 98104-7092
Phone: (206) 622-4900
Fax: (206) 682-6031

7177189.1

Electronic Acknowledgement Receipt

EFS ID:	38977742
Application Number:	15550995
International Application Number:	
Confirmation Number:	1813
Title of Invention:	Antibody-Drug Conjugate
First Named Inventor/Applicant Name:	Chaohong Hu
Customer Number:	500
Filer:	Qing Lin/Barbara Hannon
Filer Authorized By:	Qing Lin
Attorney Docket Number:	850231.401USPC
Receipt Date:	26-MAR-2020
Filing Date:	14-AUG-2017
Time Stamp:	16:00:58
Application Type:	U.S. National Stage under 35 USC 371

Payment information:

Submitted with Payment	no

File Listing:

Document Number	Document Description	File Name	File Size(Bytes)/ Message Digest	Multi Part /.zip	Pages (if appl.)
1		401USPC_RESP.pdf	236826 9f3955f07a9483d799a00287c12415455b266418	yes	11

	Multipart Description/PDF files in .zip description		
	Document Description	**Start**	**End**
	Amendment/Req. Reconsideration-After Non-Final Reject	1	1
	Claims	2	6
	Applicant Arguments/Remarks Made in an Amendment	7	11
Warnings:			
Information:			
	Total Files Size (in bytes):	236826	

This Acknowledgement Receipt evidences receipt on the noted date by the USPTO of the indicated documents, characterized by the applicant, and including page counts, where applicable. It serves as evidence of receipt similar to a Post Card, as described in MPEP 503.

New Applications Under 35 U.S.C. 111

If a new application is being filed and the application includes the necessary components for a filing date (see 37 CFR 1.53(b)-(d) and MPEP 506), a Filing Receipt (37 CFR 1.54) will be issued in due course and the date shown on this Acknowledgement Receipt will establish the filing date of the application.

National Stage of an International Application under 35 U.S.C. 371

If a timely submission to enter the national stage of an international application is compliant with the conditions of 35 U.S.C. 371 and other applicable requirements a Form PCT/DO/EO/903 indicating acceptance of the application as a national stage submission under 35 U.S.C. 371 will be issued in addition to the Filing Receipt, in due course.

New International Application Filed with the USPTO as a Receiving Office

If a new international application is being filed and the international application includes the necessary components for an international filing date (see PCT Article 11 and MPEP 1810), a Notification of the International Application Number and of the International Filing Date (Form PCT/RO/105) will be issued in due course, subject to prescriptions concerning national security, and the date shown on this Acknowledgement Receipt will establish the international filing date of the application.

PTO/SB/06 (09-11)
Approved for use through 1/31/2014. OMB 0651-0032
U.S. Patent and Trademark Office; U.S. DEPARTMENT OF COMMERCE
Under the Paperwork Reduction Act of 1995, no persons are required to respond to a collection of information unless it displays a valid OMB control number.

PATENT APPLICATION FEE DETERMINATION RECORD Substitute for Form PTO-875	Application or Docket Number 15/550,995	Filing Date 08/14/2017	☑ To be Mailed

ENTITY: ☐ LARGE ☑ SMALL ☐ MICRO

APPLICATION AS FILED - PART I

FOR	(Column 1) NUMBER FILED	(Column 2) NUMBER EXTRA		RATE ($)	FEE ($)
☐ BASIC FEE (37 CFR 1.16(a), (b), or (c))	N/A	N/A		N/A	
☐ SEARCH FEE (37 CFR 1.16(k), (i), or (m))	N/A	N/A		N/A	
☐ EXAMINATION FEE (37 CFR 1.16(o), (p), or (q))	N/A	N/A		N/A	
TOTAL CLAIMS (37 CFR 1.16(i))	minus 20 =	*		x $40 =	
INDEPENDENT CLAIMS (37 CFR 1.16(h))	minus 3 =	*		x $210 =	
☐ APPLICATION SIZE FEE (37 CFR 1.16(s))	If the specification and drawings exceed 100 sheets of paper, the application size fee due is $310 ($155 for small entity) for each additional 50 sheets or fraction thereof. See 35 U.S.C. 41(a)(1)(G) and 37 CFR 1.16(s).				
☐ MULTIPLE DEPENDENT CLAIM PRESENT (37 CFR 1.16(j))					
* If the difference in column 1 is less than zero, enter "0" in column 2.				TOTAL	

APPLICATION AS AMENDED - PART II

		(Column 1)		(Column 2)	(Column 3)			
AMENDMENT	03/26/2020	CLAIMS REMAINING AFTER AMENDMENT		HIGHEST NUMBER PREVIOUSLY PAID FOR	PRESENT EXTRA		RATE ($)	ADDITIONAL FEE ($)
	Total (37 CFR 1.16(i))	* 23	Minus	** 23	= 0		x $50 =	0
	Independent (37 CFR 1.16(h))	* 1	Minus	*** 3	= 0		x $230 =	0
	☐ Application Size Fee (37 CFR 1.16(s))							
	☐ FIRST PRESENTATION OF MULTIPLE DEPENDENT CLAIM (37 CFR 1.16(j))							
							TOTAL ADD'L FEE	0

		(Column 1)		(Column 2)	(Column 3)			
AMENDMENT		CLAIMS REMAINING AFTER AMENDMENT		HIGHEST NUMBER PREVIOUSLY PAID FOR	PRESENT EXTRA		RATE ($)	ADDITIONAL FEE ($)
	Total (37 CFR 1.16(i))	*	Minus	**	=		x $0 =	
	Independent (37 CFR 1.16(h))	*	Minus	***	=		x $0 =	
	☐ Application Size Fee (37 CFR 1.16(s))							
	☐ FIRST PRESENTATION OF MULTIPLE DEPENDENT CLAIM (37 CFR 1.16(j))							
							TOTAL ADD'L FEE	

* If the entry in column 1 is less than the entry in column 2, write "0" in column 3.	LIE
** If the "Highest Number Previously Paid For" IN THIS SPACE is less than 20, enter "20".	/ANGELA D JOHNSON/
*** If the "Highest Number Previously Paid For" IN THIS SPACE is less than 3, enter "3".	
The "Highest Number Previously Paid For" (Total or Independent) is the highest number found in the appropriate box in column 1.	

This collection of information is required by 37 CFR 1.16. The information is required to obtain or retain a benefit by the public which is to file (and by the USPTO to process) an application. Confidentiality is governed by 35 U.S.C. 122 and 37 CFR 1.14. This collection is estimated to take 12 minutes to complete, including gathering, preparing, and submitting the completed application form to the USPTO. Time will vary depending upon the individual case. Any comments on the amount of time you require to complete this form and/or suggestions for reducing this burden, should be sent to the Chief Information Officer, U.S. Patent and Trademark Office, U.S. Department of Commerce, P.O. Box 1450, Alexandria, VA 22313-1450. DO NOT SEND FEES OR COMPLETED FORMS TO THIS ADDRESS. **SEND TO: Commissioner for Patents, P.O. Box 1450, Alexandria, VA 22313-1450.**

If you need assistance in completing the form, call 1-800-PTO-9199 and select option 2.

UNITED STATES PATENT AND TRADEMARK OFFICE

UNITED STATES DEPARTMENT OF COMMERCE
United States Patent and Trademark Office
Address: COMMISSIONER FOR PATENTS
P.O. Box 1450
Alexandria, Virginia 22313-1450
www.uspto.gov

NOTICE OF ALLOWANCE AND FEE(S) DUE

500 7590 06/18/2020

SEED INTELLECTUAL PROPERTY LAW GROUP LLP
701 FIFTH AVE
SUITE 5400
SEATTLE, WA 98104

EXAMINER
CANELLA, KAREN A

ART UNIT	PAPER NUMBER
1643	

DATE MAILED: 06/18/2020

APPLICATION NO.	FILING DATE	FIRST NAMED INVENTOR	ATTORNEY DOCKET NO.	CONFIRMATION NO.
15/550,995	08/14/2017	Chaohong Hu	850231.401USPC	1813

TITLE OF INVENTION: Antibody-Drug Conjugate

APPLN. TYPE	ENTITY STATUS	ISSUE FEE DUE	PUBLICATION FEE DUE	PREV. PAID ISSUE FEE	TOTAL FEE(S) DUE	DATE DUE
nonprovisional	SMALL	$500	$0.00	$0.00	$500	09/18/2020

THE APPLICATION IDENTIFIED ABOVE HAS BEEN EXAMINED AND IS ALLOWED FOR ISSUANCE AS A PATENT. PROSECUTION ON THE MERITS IS CLOSED. THIS NOTICE OF ALLOWANCE IS NOT A GRANT OF PATENT RIGHTS. THIS APPLICATION IS SUBJECT TO WITHDRAWAL FROM ISSUE AT THE INITIATIVE OF THE OFFICE OR UPON PETITION BY THE APPLICANT. SEE 37 CFR 1.313 AND MPEP 1308.

THE ISSUE FEE AND PUBLICATION FEE (IF REQUIRED) MUST BE PAID WITHIN THREE MONTHS FROM THE MAILING DATE OF THIS NOTICE OR THIS APPLICATION SHALL BE REGARDED AS ABANDONED. THIS STATUTORY PERIOD CANNOT BE EXTENDED. SEE 35 U.S.C. 151. THE ISSUE FEE DUE INDICATED ABOVE DOES NOT REFLECT A CREDIT FOR ANY PREVIOUSLY PAID ISSUE FEE IN THIS APPLICATION. IF AN ISSUE FEE HAS PREVIOUSLY BEEN PAID IN THIS APPLICATION (AS SHOWN ABOVE), THE RETURN OF PART B OF THIS FORM WILL BE CONSIDERED A REQUEST TO REAPPLY THE PREVIOUSLY PAID ISSUE FEE TOWARD THE ISSUE FEE NOW DUE.

HOW TO REPLY TO THIS NOTICE:

I. Review the ENTITY STATUS shown above. If the ENTITY STATUS is shown as SMALL or MICRO, verify whether entitlement to that entity status still applies.

If the ENTITY STATUS is the same as shown above, pay the TOTAL FEE(S) DUE shown above.

If the ENTITY STATUS is changed from that shown above, on PART B - FEE(S) TRANSMITTAL, complete section number 5 titled "Change in Entity Status (from status indicated above)".

For purposes of this notice, small entity fees are 1/2 the amount of undiscounted fees, and micro entity fees are 1/2 the amount of small entity fees.

II. PART B - FEE(S) TRANSMITTAL, or its equivalent, must be completed and returned to the United States Patent and Trademark Office (USPTO) with your ISSUE FEE and PUBLICATION FEE (if required). If you are charging the fee(s) to your deposit account, section "4b" of Part B - Fee(s) Transmittal should be completed and an extra copy of the form should be submitted. If an equivalent of Part B is filed, a request to reapply a previously paid issue fee must be clearly made, and delays in processing may occur due to the difficulty in recognizing the paper as an equivalent of Part B.

III. All communications regarding this application must give the application number. Please direct all communications prior to issuance to Mail Stop ISSUE FEE unless advised to the contrary.

IMPORTANT REMINDER: Maintenance fees are due in utility patents issuing on applications filed on or after Dec. 12, 1980. It is patentee's responsibility to ensure timely payment of maintenance fees when due. More information is available at www.uspto.gov/PatentMaintenanceFees.

CSPC Exhibit 1004

PART B - FEE(S) TRANSMITTAL

Complete and send this form, together with applicable fee(s), by mail or fax, or via EFS-Web.

By mail, send to: Mail Stop ISSUE FEE
Commissioner for Patents
P.O. Box 1450
Alexandria, Virginia 22313-1450

By fax, send to: (571)-273-2885

INSTRUCTIONS: This form should be used for transmitting the ISSUE FEE and PUBLICATION FEE (if required). Blocks 1 through 5 should be completed where appropriate. All further correspondence including the Patent, advance orders and notification of maintenance fees will be mailed to the current correspondence address as indicated unless corrected below or directed otherwise in Block 1, by (a) specifying a new correspondence address; and/or (b) indicating a separate "FEE ADDRESS" for maintenance fee notifications.

CURRENT CORRESPONDENCE ADDRESS (Note: Use Block 1 for any change of address)

500 7590 06/18/2020

SEED INTELLECTUAL PROPERTY LAW GROUP LLP
701 FIFTH AVE
SUITE 5400
SEATTLE, WA 98104

Note: A certificate of mailing can only be used for domestic mailings of the Fee(s) Transmittal. This certificate cannot be used for any other accompanying papers. Each additional paper, such as an assignment or formal drawing, must have its own certificate of mailing or transmission.

Certificate of Mailing or Transmission

I hereby certify that this Fee(s) Transmittal is being deposited with the United States Postal Service with sufficient postage for first class mail in an envelope addressed to the Mail Stop ISSUE FEE address above, or being transmitted to the USPTO via EFS-Web or by facsimile to (571) 273-2885, on the date below.

(Typed or printed name)
(Signature)
(Date)

APPLICATION NO.	FILING DATE	FIRST NAMED INVENTOR	ATTORNEY DOCKET NO.	CONFIRMATION NO.
15/550,995	08/14/2017	Chaohong Hu	850231.401USPC	1813

TITLE OF INVENTION: Antibody-Drug Conjugate

APPLN. TYPE	ENTITY STATUS	ISSUE FEE DUE	PUBLICATION FEE DUE	PREV. PAID ISSUE FEE	TOTAL FEE(S) DUE	DATE DUE
nonprovisional	SMALL	$500	$0.00	$0.00	$500	09/18/2020

EXAMINER	ART UNIT	CLASS-SUBCLASS
CANELLA, KAREN A	1643	424-179100

1. Change of correspondence address or indication of "Fee Address" (37 CFR 1.363).

❑ Change of correspondence address (or Change of Correspondence Address form PTO/SB/122) attached.

❑ "Fee Address" indication (or "Fee Address" Indication form PTO/SB/47; Rev 03-09 or more recent) attached. **Use of a Customer Number is required.**

2. For printing on the patent front page, list

(1) The names of up to 3 registered patent attorneys or agents OR, alternatively,

(2) The name of a single firm (having as a member a registered attorney or agent) and the names of up to 2 registered patent attorneys or agents. If no name is listed, no name will be printed.

1 _____

2 _____

3 _____

3. ASSIGNEE NAME AND RESIDENCE DATA TO BE PRINTED ON THE PATENT (print or type)

PLEASE NOTE: Unless an assignee is identified below, no assignee data will appear on the patent. If an assignee is identified below, the document must have been previously recorded, or filed for recordation, as set forth in 37 CFR 3.11 and 37 CFR 3.81(a). Completion of this form is NOT a substitute for filing an assignment.

(A) NAME OF ASSIGNEE (B) RESIDENCE: (CITY and STATE OR COUNTRY)

Please check the appropriate assignee category or categories (will not be printed on the patent) : ❑ Individual ❑ Corporation or other private group entity ❑ Government

4a. Fees submitted: ❑ Issue Fee ❑ Publication Fee (if required) ❑ Advance Order - # of Copies _____

4b. Method of Payment: *(Please first reapply any previously paid fee shown above)*

❑ Electronic Payment via EFS-Web ❑ Enclosed check ❑ Non-electronic payment by credit card (Attach form PTO-2038)

❑ The Director is hereby authorized to charge the required fee(s), any deficiency, or credit any overpayment to Deposit Account No. _____

5. **Change in Entity Status** (from status indicated above)

❑ Applicant certifying micro entity status. See 37 CFR 1.29

❑ Applicant asserting small entity status. See 37 CFR 1.27

❑ Applicant changing to regular undiscounted fee status.

NOTE: Absent a valid certification of Micro Entity Status (see forms PTO/SB/15A and 15B), issue fee payment in the micro entity amount will not be accepted at the risk of application abandonment.
NOTE: If the application was previously under micro entity status, checking this box will be taken to be a notification of loss of entitlement to micro entity status.
NOTE: Checking this box will be taken to be a notification of loss of entitlement to small or micro entity status, as applicable.

NOTE: This form must be signed in accordance with 37 CFR 1.31 and 1.33. See 37 CFR 1.4 for signature requirements and certifications.

Authorized Signature _____ Date _____

Typed or printed name _____ Registration No. _____

UNITED STATES PATENT AND TRADEMARK OFFICE

UNITED STATES DEPARTMENT OF COMMERCE
United States Patent and Trademark Office
Address: COMMISSIONER FOR PATENTS
P.O. Box 1450
Alexandria, Virginia 22313-1450
www.uspto.gov

APPLICATION NO.	FILING DATE	FIRST NAMED INVENTOR	ATTORNEY DOCKET NO.	CONFIRMATION NO.
15/550,995	08/14/2017	Chaohong Hu	850231.401USPC	1813

500 7590 06/18/2020

SEED INTELLECTUAL PROPERTY LAW GROUP LLP
701 FIFTH AVE
SUITE 5400
SEATTLE, WA 98104

EXAMINER	
CANELLA, KAREN A	
ART UNIT	PAPER NUMBER
1643	

DATE MAILED: 06/18/2020

Determination of Patent Term Adjustment under 35 U.S.C. 154 (b)
(Applications filed on or after May 29, 2000)

The Office has discontinued providing a Patent Term Adjustment (PTA) calculation with the Notice of Allowance.

Section 1(h)(2) of the AIA Technical Corrections Act amended 35 U.S.C. 154(b)(3)(B)(i) to eliminate the requirement that the Office provide a patent term adjustment determination with the notice of allowance. See Revisions to Patent Term Adjustment, 78 Fed. Reg. 19416, 19417 (Apr. 1, 2013). Therefore, the Office is no longer providing an initial patent term adjustment determination with the notice of allowance. The Office will continue to provide a patent term adjustment determination with the Issue Notification Letter that is mailed to applicant approximately three weeks prior to the issue date of the patent, and will include the patent term adjustment on the patent. Any request for reconsideration of the patent term adjustment determination (or reinstatement of patent term adjustment) should follow the process outlined in 37 CFR 1.705.

Any questions regarding the Patent Term Extension or Adjustment determination should be directed to the Office of Patent Legal Administration at (571)-272-7702. Questions relating to issue and publication fee payments should be directed to the Customer Service Center of the Office of Patent Publication at 1-(888)-786-0101 or (571)-272-4200.

OMB Clearance and PRA Burden Statement for PTOL-85 Part B

The Paperwork Reduction Act (PRA) of 1995 requires Federal agencies to obtain Office of Management and Budget approval before requesting most types of information from the public. When OMB approves an agency request to collect information from the public, OMB (i) provides a valid OMB Control Number and expiration date for the agency to display on the instrument that will be used to collect the information and (ii) requires the agency to inform the public about the OMB Control Number's legal significance in accordance with 5 CFR 1320.5(b).

The information collected by PTOL-85 Part B is required by 37 CFR 1.311. The information is required to obtain or retain a benefit by the public which is to file (and by the USPTO to process) an application. Confidentiality is governed by 35 U.S.C. 122 and 37 CFR 1.14. This collection is estimated to take 30 minutes to complete, including gathering, preparing, and submitting the completed application form to the USPTO. Time will vary depending upon the individual case. Any comments on the amount of time you require to complete this form and/or suggestions for reducing this burden, should be sent to the Chief Information Officer, U.S. Patent and Trademark Office, U.S. Department of Commerce, P.O. Box 1450, Alexandria, Virginia 22313-1450. DO NOT SEND FEES OR COMPLETED FORMS TO THIS ADDRESS. SEND TO: Commissioner for Patents, P.O. Box 1450, Alexandria, Virginia 22313-1450. Under the Paperwork Reduction Act of 1995, no persons are required to respond to a collection of information unless it displays a valid OMB control number.

Privacy Act Statement

The Privacy Act of 1974 (P.L. 93-579) requires that you be given certain information in connection with your submission of the attached form related to a patent application or patent. Accordingly, pursuant to the requirements of the Act, please be advised that: (1) the general authority for the collection of this information is 35 U.S.C. 2(b)(2); (2) furnishing of the information solicited is voluntary; and (3) the principal purpose for which the information is used by the U.S. Patent and Trademark Office is to process and/or examine your submission related to a patent application or patent. If you do not furnish the requested information, the U.S. Patent and Trademark Office may not be able to process and/or examine your submission, which may result in termination of proceedings or abandonment of the application or expiration of the patent.

The information provided by you in this form will be subject to the following routine uses:

1. The information on this form will be treated confidentially to the extent allowed under the Freedom of Information Act (5 U.S.C. 552) and the Privacy Act (5 U.S.C 552a). Records from this system of records may be disclosed to the Department of Justice to determine whether disclosure of these records is required by the Freedom of Information Act.
2. A record from this system of records may be disclosed, as a routine use, in the course of presenting evidence to a court, magistrate, or administrative tribunal, including disclosures to opposing counsel in the course of settlement negotiations.
3. A record in this system of records may be disclosed, as a routine use, to a Member of Congress submitting a request involving an individual, to whom the record pertains, when the individual has requested assistance from the Member with respect to the subject matter of the record.
4. A record in this system of records may be disclosed, as a routine use, to a contractor of the Agency having need for the information in order to perform a contract. Recipients of information shall be required to comply with the requirements of the Privacy Act of 1974, as amended, pursuant to 5 U.S.C. 552a(m).
5. A record related to an International Application filed under the Patent Cooperation Treaty in this system of records may be disclosed, as a routine use, to the International Bureau of the World Intellectual Property Organization, pursuant to the Patent Cooperation Treaty.
6. A record in this system of records may be disclosed, as a routine use, to another federal agency for purposes of National Security review (35 U.S.C. 181) and for review pursuant to the Atomic Energy Act (42 U.S.C. 218(c)).
7. A record from this system of records may be disclosed, as a routine use, to the Administrator, General Services, or his/her designee, during an inspection of records conducted by GSA as part of that agency's responsibility to recommend improvements in records management practices and programs, under authority of 44 U.S.C. 2904 and 2906. Such disclosure shall be made in accordance with the GSA regulations governing inspection of records for this purpose, and any other relevant (i.e., GSA or Commerce) directive. Such disclosure shall not be used to make determinations about individuals.
8. A record from this system of records may be disclosed, as a routine use, to the public after either publication of the application pursuant to 35 U.S.C. 122(b) or issuance of a patent pursuant to 35 U.S.C. 151. Further, a record may be disclosed, subject to the limitations of 37 CFR 1.14, as a routine use, to the public if the record was filed in an application which became abandoned or in which the proceedings were terminated and which application is referenced by either a published application, an application open to public inspection or a issued patent.
9. A record from this system of records may be disclosed, as a routine use, to a Federal, State, or local law enforcement agency, if the USPTO becomes aware of a violation or potential violation of law or regulation.

Notice of Allowability	Application No. 15/550,995	Applicant(s) Hu, Chaohong	
	Examiner KAREN A CANELLA	Art Unit 1643	AIA (FITF) Status Yes

-- The MAILING DATE of this communication appears on the cover sheet with the correspondence address--

All claims being allowable, PROSECUTION ON THE MERITS IS (OR REMAINS) CLOSED in this application. If not included herewith (or previously mailed), a Notice of Allowance (PTOL-85) or other appropriate communication will be mailed in due course. **THIS NOTICE OF ALLOWABILITY IS NOT A GRANT OF PATENT RIGHTS.** This application is subject to withdrawal from issue at the initiative of the Office or upon petition by the applicant. See 37 CFR 1.313 and MPEP 1308.

1. ☑ This communication is responsive to the response filed 3-26-2020.
   ☐ A declaration(s)/affidavit(s) under **37 CFR 1.130(b)** was/were filed on _____.

2. ☐ An election was made by the applicant in response to a restriction requirement set forth during the interview on _____; the restriction requirement and election have been incorporated into this action.

3. ☑ The allowed claim(s) is/are See Continuation Sheet . As a result of the allowed claim(s), you may be eligible to benefit from the **Patent Prosecution Highway** program at a participating intellectual property office for the corresponding application. For more information, please see **http://www.uspto.gov/patents/init_events/pph/index.jsp** or send an inquiry to **PPHfeedback@uspto.gov.**

4. ☑ Acknowledgment is made of a claim for foreign priority under 35 U.S.C. § 119(a)-(d) or (f).

   Certified copies:

   a) ☑ All b) ☐ Some *c) ☐ None of the:

   1. ☑ Certified copies of the priority documents have been received.
   2. ☐ Certified copies of the priority documents have been received in Application No. _____ .
   3. ☐ Copies of the certified copies of the priority documents have been received in this national stage application from the International Bureau (PCT Rule 17.2(a)).

   * Certified copies not received: _____ .

Applicant has THREE MONTHS FROM THE "MAILING DATE" of this communication to file a reply complying with the requirements noted below. Failure to timely comply will result in ABANDONMENT of this application.
THIS THREE-MONTH PERIOD IS NOT EXTENDABLE.

5. ☐ CORRECTED DRAWINGS (as "replacement sheets") must be submitted.
   ☐ including changes required by the attached Examiner's Amendment / Comment or in the Office action of Paper No./Mail Date _____ .

   Identifying indicia such as the application number (see 37 CFR 1.84(c)) should be written on the drawings in the front (not the back) of each sheet. Replacement sheet(s) should be labeled as such in the header according to 37 CFR 1.121(d).

6. ☐ DEPOSIT OF and/or INFORMATION about the deposit of BIOLOGICAL MATERIAL must be submitted. Note the attached Examiner's comment regarding REQUIREMENT FOR THE DEPOSIT OF BIOLOGICAL MATERIAL.

Attachment(s)

1. ☐ Notice of References Cited (PTO-892)
2. ☐ Information Disclosure Statements (PTO/SB/08), Paper No./Mail Date _____.
3. ☐ Examiner's Comment Regarding Requirement for Deposit of Biological Material _____.
4. ☐ Interview Summary (PTO-413), Paper No./Mail Date. _____.
5. ☑ Examiner's Amendment/Comment
6. ☐ Examiner's Statement of Reasons for Allowance
7. ☐ Other _____.

/Karen A. Canella/
Primary Examiner, Art Unit 1643

Continuation of 3. The allowed claim(s) is/are: 2-12,14-16,23-28 and 35-37

EXAMINER'S AMENDMENT

An examiner's amendment to the record appears below. Should the changes and/or additions be unacceptable to applicant, an amendment may be filed as provided by 37 CFR 1.312. To ensure consideration of such an amendment, it MUST be submitted no later than the payment of the issue fee.

The application has been amended as follows:

In claim 4:

"18;" has been replaced by ---18---.

Any inquiry concerning this communication or earlier communications from the examiner should be directed to KAREN A CANELLA whose telephone number is (571)272-0828. The examiner can normally be reached on M-F 10-6:30.

Examiner interviews are available via telephone, in-person, and video conferencing using a USPTO supplied web-based collaboration tool. To schedule an interview, applicant is encouraged to use the USPTO Automated Interview Request (AIR) at http://www.uspto.gov/interviewpractice.

If attempts to reach the examiner by telephone are unsuccessful, the examiner's supervisor, Julie Wu can be reached on 571-272-5205. The fax phone number for the organization where this application or proceeding is assigned is 571-273-8300.

Information regarding the status of an application may be obtained from the Patent Application Information Retrieval (PAIR) system. Status information for published applications may be obtained from either Private PAIR or Public PAIR. Status information for unpublished applications is available through Private PAIR only. For more information about the PAIR system, see https://ppair-my.uspto.gov/pair/PrivatePair. Should you have questions on access to the Private PAIR system, contact the Electronic Business Center (EBC) at 866-217-9197 (toll-free). If you would like assistance from a USPTO Customer Service Representative or access to the automated information system, call 800-786-9199 (IN USA OR CANADA) or 571-272-1000.

KAREN A. CANELLA
Examiner
Art Unit 1643

/Karen A. Canella/
Primary Examiner, Art Unit 1643

Search Notes	Application/Control No.	Applicant(s)/Patent Under Reexamination
	15/550,995	Hu, Chaohong
	Examiner	Art Unit
	KAREN A CANELLA	1643

CPC - Searched*		
Symbol	**Date**	**Examiner**
A61K47/6889	01/08/2020	kac
A61K47/6849	01/08/2020	kac
A61K38/1808	01/08/2020	kac
A61K47/6889	06/13/2020	kac
A61K39/001104	06/13/2020	kac

CPC Combination Sets - Searched*		
Symbol	**Date**	**Examiner**

US Classification - Searched*			
Class	**Subclass**	**Date**	**Examiner**

* See search history printout included with this form or the SEARCH NOTES box below to determine the scope of the search.

/Karen A. Canella/ Primary Examiner, Art Unit 1643	

Search Notes	Application/Control No.	Applicant(s)/Patent Under Reexamination
	15/550,995	Hu, Chaohong
	Examiner	Art Unit
	KAREN A CANELLA	1643

Search Notes		
Search Notes	**Date**	**Examiner**
STN	03/16/2019	kac
West	03/31/2019	kac
inventor [DAV]	03/31/2019	kac
West	10/13/2019	kac
inventor [DAV]	10/13/2019	kac
West	01/08/2020	kac
inventor [DAV]	01/08/2020	kac
STNext	06/13/2020	kac
West	06/13/2020	kac
inventor [DAV]	06/13/2020	kac

Interference Search			
US Class/CPC Symbol	**US Subclass/CPC Group**	**Date**	**Examiner**
	West Interference	06/13/2020	kac

/Karen A. Canella/
Primary Examiner, Art Unit 1643

CSPC Exhibit 1004
Page 315 of 336

Issue Classification	Application/Control No.	Applicant(s)/Patent Under Reexamination
	15/550,995	Hu, Chaohong
	Examiner	**Art Unit**
	KAREN A CANELLA	1643

CPC								
Symbol							**Type**	**Version**
A61K	/	47	/	6811			F	2017-08-01
A61P	/	9	/	10			I	2018-01-01
A61P	/	35	/	00			I	2018-01-01
A61K	/	47	/	6803			I	2017-08-01
A61K	/	47	/	6851			I	2017-08-01
C07K	/	16	/	2863			I	2013-01-01
A61K	/	39	/	001104			I	2018-08-01
A61K	/	38	/	1808			I	2013-01-01
A61K	/	39	/	0011			I	2013-01-01
G01N	/	2030	/	8809			A	2013-01-01
A61K	/	2039	/	505			A	2013-01-01
C07K	/	2317	/	76			A	2013-01-01
C07K	/	2317	/	24			A	2013-01-01
C07K	/	2317	/	73			A	2013-01-01
G01N	/	2030	/	027			A	2013-01-01

CPC Combination Sets								
Symbol					**Type**	**Set**	**Ranking**	**Version**
	/		/					

NONE		**Total Claims Allowed:**	
(Assistant Examiner)	(Date)	23	
/Karen A. Canella/ Primary Examiner, Art Unit 1643	13 June 2020	O.G. Print Claim(s)	O.G. Print Figure
(Primary Examiner)	(Date)	1	none

Issue Classification	Application/Control No.	Applicant(s)/Patent Under Reexamination
	15/550,995	Hu, Chaohong
	Examiner	**Art Unit**
	KAREN A CANELLA	1643

INTERNATIONAL CLASSIFICATION				
CLAIMED				
A61K47/68	/	47	/	68
A61P35/00	/	35	/	00
A61K39/00	/	39	/	00
CPCONLY	/	NLY	/	

NON-CLAIMED				
A61P9/10	/	9	/	10
C07K16/28	/	16	/	28
A61K38/18	/	38	/	18
G01N30/88	/	30	/	88
G01N30/02	/	30	/	02

US ORIGINAL CLASSIFICATION	
CLASS	**SUBCLASS**

CROSS REFERENCES(S)						
CLASS	**SUBCLASS (ONE SUBCLASS PER BLOCK)**					

NONE (Assistant Examiner) (Date)	**Total Claims Allowed:** 23	
/Karen A. Canella/ Primary Examiner, Art Unit 1643 (Primary Examiner) 13 June 2020 (Date)	O.G. Print Claim(s) 1	O.G. Print Figure none

Issue Classification	Application/Control No.	Applicant(s)/Patent Under Reexamination
	15/550,995	Hu, Chaohong
	Examiner	**Art Unit**
	KAREN A CANELLA	1643

☐ Claims renumbered in the same order as presented by applicant ☐ CPA ☐ T.D. ☐ R.1.47

CLAIMS

Final	Original	Final	Original	Final	Original	Final	Original	Final	Original	Final	Original	Final	Original	Final	Original
-	1	9	10	-	19	21	28	14	37						
1	2	10	11	-	20	-	29								
2	3	11	12	-	21	-	30								
3	4	-	13	-	22	-	31								
4	5	12	14	16	23	-	32								
5	6	13	15	17	24	-	33								
6	7	15	16	18	25	-	34								
7	8	-	17	19	26	22	35								
8	9	-	18	20	27	23	36								

NONE (Assistant Examiner)	(Date)	**Total Claims Allowed:** 23	
/Karen A. Canella/ Primary Examiner, Art Unit 1643 (Primary Examiner)	13 June 2020 (Date)	O.G. Print Claim(s) 1	O.G. Print Figure none

WEST Search History

Hide Items | Restore | Clear | Close

DATE: Saturday, June 13, 2020

Hide?	Set Name	Query	Hit Count
DB=PGPB,USPT; PLUR=NO; OP=ADJ			
☐	L8	L7 and L2	1
☐	L7	L6 or L5	37
☐	L6	(SHANGHAI MIRACOGEN)![asn]	1
☐	L5	(Hu, Chaohong)[in]	36
☐	L4	L1 and L2	1
☐	L3	(A61K47/6851)![CPC,CPCL]	2749
☐	L2	(A61K39/001104)![CPC,CPCL]	198
☐	L1	(A61K47/6889)![CPC,CPCL]	1218

END OF SEARCH HISTORY

```
     (FILE 'HOME' ENTERED AT 03:11:37 ON 13 JUN 2020)
                D SET
                D CLUSTER

     FILE 'REGISTRY' ENTERED AT 03:11:52 ON 13 JUN 2020
L1             2 SEA FILE=REGISTRY NYDVH(.){1-}VIWSGGNTDYNTPFTS(.){1-}ALDYYDYEFA
                  Y/SQSP
                D LC TOT

     FILE 'CAPLUS' ENTERED AT 03:12:56 ON 13 JUN 2020
L2             3 SEA FILE=CAPLUS L1
                D TI BIB HITSEQ HITRN TOT

     FILE 'USPATFULL' ENTERED AT 03:15:15 ON 13 JUN 2020
L3             2 SEA FILE=USPATFULL L1
                D HITSTR 2
                D BIB HITSTR TOT

     FILE 'DGENE' ENTERED AT 03:20:17 ON 13 JUN 2020
                RUN GETSEQ
               ---------
L4            17 SEA FILE=DGENE NYDVH(.){1-}VIWSGGNTDYNTPFTS(.){1-}ALDYYDYEFAY/S
                  QSP
L5             0 SEA FILE=DGENE L4 AND @AD<20160216
L6             2 SEA FILE=DGENE L4 AND AD<20160216
                D BIB SEQ TOT

     FILE 'USGENE' ENTERED AT 03:25:32 ON 13 JUN 2020
                RUN GETSEQ
               ---------
L7             4 SEA FILE=USGENE NYDVH(.){1-}VIWSGGNTDYNTPFTS(.){1-}ALDYYDYEFAY/
                  SQSP
                D TI PN SEQN TOT
                D BIB 1-3
```

Bibliographic Data

Application No: 15/550,995

Foreign Priority claimed: (•) Yes ( ) No

35 USC 119 (a-d) conditions met: [✓] Yes [ ] No [ ] Met After Allowance

Verified and Acknowledged: /Karen A. Canella/ Examiner's Signature [ ] Initials

Title: Antibody-Drug Conjugate

FILING or 371(c) DATE	CLASS	GROUP ART UNIT	ATTORNEY DOCKET NO.
08/14/2017	424	1643	850231.401USPC
RULE			

APPLICANTS

SHANGHAI MIRACOGEN INC, SHANGHAI, CHINA

INVENTORS

Chaohong Hu SHANGHAI, CHINA

CONTINUING DATA

This application is a 371 of PCT/CN2016/073844 02/16/2016

FOREIGN APPLICATIONS

CHINA 201510085038.8 02/17/2015

IF REQUIRED, FOREIGN LICENSE GRANTED**

10/28/2017

**** SMALL ENTITY ****

STATE OR COUNTRY

CHINA

ADDRESS

SEED INTELLECTUAL PROPERTY LAW GROUP LLP
701 FIFTH AVE
SUITE 5400
SEATTLE, WA 98104
UNITED STATES

FILING FEE RECEIVED

$0

To: USPTOeAction@SeedIP.com,pairlinkdktg@seedip.com,
From: PAIR_eOfficeAction@uspto.gov
Cc: PAIR_eOfficeAction@uspto.gov
Subject: Private PAIR Correspondence Notification for Customer Number 500

Jun 18, 2020 09:34:58 AM

Dear PAIR Customer:

SEED INTELLECTUAL PROPERTY LAW GROUP LLP
701 FIFTH AVE
SUITE 5400
SEATTLE, WA 98104
UNITED STATES

The following USPTO patent application(s) associated with your Customer Number, 500 , have new outgoing correspondence. This correspondence is now available for viewing in Private PAIR.

The official date of notification of the outgoing correspondence will be indicated on the form PTOL-90 accompanying the correspondence.

Disclaimer:
The list of documents shown below is provided as a courtesy and is not part of the official file wrapper. The content of the images shown in PAIR is the official record.

Application	Document	Mailroom Date	Attorney Docket No.
15550995	NOA	06/18/2020	850231.401USPC

To view your correspondence online or update your email addresses, please visit us anytime at https://sportal.uspto.gov/secure/myportal/privatepair.

If you have any questions, please email the Electronic Business Center (EBC) at EBC@uspto.gov with 'e-Office Action' on the subject line or call 1-866-217-9197 during the following hours:

Monday - Friday 6:00 a.m. to 12:00 a.m.

Thank you for prompt attention to this notice,

UNITED STATES PATENT AND TRADEMARK OFFICE

PATENT APPLICATION INFORMATION RETRIEVAL SYSTEM

UNITED STATES PATENT AND TRADEMARK OFFICE

UNITED STATES DEPARTMENT OF COMMERCE
United States Patent and Trademark Office
Address: COMMISSIONER FOR PATENTS
P.O. Box 1450
Alexandria, Virginia 22313-1450
www.uspto.gov

APPLICATION NO.	FILING DATE	FIRST NAMED INVENTOR	ATTORNEY DOCKET NO.	CONFIRMATION NO.
15/550,995	08/14/2017	Chaohong Hu	850231.401USPC	1813

7590 07/29/2020

SEED INTELLECTUAL PROPERTY LAW GROUP LLP
701 FIFTH AVE
SUITE 5400
SEATTLE, WA 98104

EXAMINER	
CANELLA, KAREN A	
ART UNIT	PAPER NUMBER
1643	
NOTIFICATION DATE	DELIVERY MODE
07/29/2020	ELECTRONIC

NOTICE REQUIRING INVENTOR'S OATH OR DECLARATION

☑ An inventor's oath or declaration in compliance with 37 CFR 1.63 or substitute statement in compliance with 37 CFR 1.64 executed by or with respect to each inventor has not yet been submitted.

The inventor's oath or declaration or substitute statement dated _____ is defective. The inventor's oath or declaration does not comply with 37 CFR 1.63 or the substitute statement does not comply with 37 CFR 1.64 because it:

☐ does not include a statement that the person executing the oath or declaration or substitute statement believes the named inventor or joint inventor to be the original inventor or an original joint inventor of a claimed invention in the application for which the oath or declaration is being submitted.

☐ does not state that the application was made or was authorized to be made by the person executing the oath or declaration or substitute statement.

☐ does not acknowledge that any willful false statement made in such oath or declaration or substitute statement is punishable under section 1001 of title 18 by fine or imprisonment of not more than 5 years, or both.

☐ does not identify the person executing the oath or declaration or substitute statement by his or her legal name.

☐ does not identify the application to which the oath or declaration or substitute statement is directed.

☐ Other: _____

The substitute statement dated _____does not comply with 37 CFR 1.64 because it:

☐ does not identify the inventor with respect to whom the statement applies.

☐ does not identify the relationship to the non-signing inventor.

☐ does not identify the circumstances permitting execution of the statement.

☐ was signed by someone other than the applicant.

☐ Other: _____

An oath or declaration in compliance with 37 CFR 1.63, or a substitute statement in compliance with 37 CFR 1.64, executed by or with respect to each inventor MUST be filed **no later than the date on which the issue fee is paid.** See 35 U.S.C. 115(f). Failure to timely comply will result in ABANDONMENT of this application. This period for reply is not extendable under 37 CFR 1.136(a).

Questions relating to this Notice should be directed to the Application Assistance Unit at 571-272-4200.

(571)-272-4200 or 1(888)-786-0101
Patent Publication Branch
Office of Data Management

To: USPTOeAction@SeedIP.com,pairlinkdktg@seedip.com,
From: PAIR_eOfficeAction@uspto.gov
Cc: PAIR_eOfficeAction@uspto.gov
Subject: Private PAIR Correspondence Notification for Customer Number 500

Jul 30, 2020 03:56:45 AM

Dear PAIR Customer:

SEED INTELLECTUAL PROPERTY LAW GROUP LLP
701 FIFTH AVE
SUITE 5400
SEATTLE, WA 98104
UNITED STATES

The following USPTO patent application(s) associated with your Customer Number, 500 , have new outgoing correspondence. This correspondence is now available for viewing in Private PAIR.

The official date of notification of the outgoing correspondence will be indicated on the form PTOL-90 accompanying the correspondence.

Disclaimer:
The list of documents shown below is provided as a courtesy and is not part of the official file wrapper. The content of the images shown in PAIR is the official record.

Application	Document	Mailroom Date	Attorney Docket No.
15550995	M327	07/29/2020	850231.401USPC

To view your correspondence online or update your email addresses, please visit us anytime at https://sportal.uspto.gov/secure/myportal/privatepair.

If you have any questions, please email the Electronic Business Center (EBC) at EBC@uspto.gov with 'e-Office Action' on the subject line or call 1-866-217-9197 during the following hours:

Monday - Friday 6:00 a.m. to 12:00 a.m.

Thank you for prompt attention to this notice,

UNITED STATES PATENT AND TRADEMARK OFFICE

PATENT APPLICATION INFORMATION RETRIEVAL SYSTEM

PTO/AIA/01 (06-12)
Approved for use through 11/30/2020. OMB 0651-0032
U.S. Patent and Trademark Office; U.S. DEPARTMENT OF COMMERCE
Under the Paperwork Reduction Act of 1995, no persons are required to respond to a collection of information unless it displays a valid OMB control number.

DECLARATION (37 CFR 1.63) FOR UTILITY OR DESIGN APPLICATION USING AN APPLICATION DATA SHEET (37 CFR 1.76)

Title of Invention	ANTIBODY-DRUG CONJUGATE

As the below named inventor, I hereby declare that:

This declaration is directed to:

☐ The attached application, or

■ United States application or PCT international application number 15/550,995 filed on August 14, 2017.

The above-identified application was made or authorized to be made by me.

I believe that I am the original inventor or an original joint inventor of a claimed invention in the application.

I hereby acknowledge that any willful false statement made in this declaration is punishable under 18 U.S.C. 1001 by fine or imprisonment of not more than five (5) years, or both.

WARNING:

Petitioner/applicant is cautioned to avoid submitting personal information in documents filed in a patent application that may contribute to identity theft. Personal information such as social security numbers, bank account numbers, or credit card numbers (other than a check or credit card authorization form PTO-2038 submitted for payment purposes) is never required by the USPTO to support a petition or an application. If this type of personal information is included in documents submitted to the USPTO, petitioners/applicants should consider redacting such personal information from the documents before submitting them to the USPTO. Petitioner/applicant is advised that the record of a patent application is available to the public after publication of the application (unless a non-publication request in compliance with 37 CFR 1.213(a) is made in the application) or issuance of a patent. Furthermore, the record from an abandoned application may also be available to the public if the application is referenced in a published application or an issued patent (see 37 CFR 1.14). Checks and credit card authorization forms PTO-2038 submitted for payment purposes are not retained in the application file and therefore are not publicly available.

LEGAL NAME OF INVENTOR

Inventor: Chaohong HU Date (Optional): Aug. 18, 2020

Signature: Chaohong Hu

Note: An application data sheet (PTO/SB/14 or equivalent), including naming the entire inventive entity, must accompany this form or must have been previously filed. Use an additional PTO/AIA/01 form for each additional inventor.

This collection of information is required by 35 U.S.C. 115 and 37 CFR 1.63. The information is required to obtain or retain a benefit by the public which is to file (and by the USPTO to process) an application. Confidentiality is governed by 35 U.S.C. 122 and 37 CFR 1.11 and 1.14. This collection is estimated to take 1 minute to complete, including gathering, preparing, and submitting the completed application form to the USPTO. Time will vary depending upon the individual case. Any comments on the amount of time you require to complete this form and/or suggestions for reducing this burden, should be sent to the Chief Information Officer, U.S. Patent and Trademark Office, U.S. Department of Commerce, P.O. Box 1450, Alexandria, VA 22313-1450. DO NOT SEND FEES OR COMPLETED FORMS TO THIS ADDRESS. **SEND TO: Commissioner for Patents, P.O. Box 1450, Alexandria, VA 22313-1450.**

If you need assistance in completing the form, call 1-800-PTO-9199 and select option 2.

Electronic Patent Application Fee Transmittal

Application Number:	15550995
Filing Date:	14-Aug-2017
Title of Invention:	Antibody-Drug Conjugate
First Named Inventor/Applicant Name:	Chaohong Hu
Filer:	Qing Lin/Barbara Hannon
Attorney Docket Number:	850231.401USPC

Filed as Small Entity

Filing Fees for U.S. National Stage under 35 USC 371

Description	Fee Code	Quantity	Amount	Sub-Total in USD($)
Basic Filing:				
Pages:				
Claims:				
Miscellaneous-Filing:				
OATH/DECL > 30 MOS FROM 371 COMMENCEMENT	2617	1	70	70
Petition:				
Patent-Appeals-and-Interference:				
Post-Allowance-and-Post-Issuance:				

Description	Fee Code	Quantity	Amount	Sub-Total in USD($)
Extension-of-Time:				
Miscellaneous:				
			Total in USD ($)	**70**

Electronic Acknowledgement Receipt

EFS ID:	40310723
Application Number:	15550995
International Application Number:	
Confirmation Number:	1813
Title of Invention:	Antibody-Drug Conjugate
First Named Inventor/Applicant Name:	Chaohong Hu
Customer Number:	500
Filer:	Qing Lin/Barbara Hannon
Filer Authorized By:	Qing Lin
Attorney Docket Number:	850231.401USPC
Receipt Date:	18-AUG-2020
Filing Date:	14-AUG-2017
Time Stamp:	12:33:21
Application Type:	U.S. National Stage under 35 USC 371

Payment information:

Submitted with Payment	yes
Payment Type	CARD
Payment was successfully received in RAM	$70
RAM confirmation Number	E20208HC33433454
Deposit Account	
Authorized User	

The Director of the USPTO is hereby authorized to charge indicated fees and credit any overpayment as follows:

File Listing:

Document Number	Document Description	File Name	File Size(Bytes)/ Message Digest	Multi Part /.zip	Pages (if appl.)
1	Oath or Declaration filed	401USPC_DEC.pdf	445763 6d735b13c59c75ce2eca6456bea1c786aae9dec4	no	1
Warnings:					
Information:					
2	Fee Worksheet (SB06)	fee-info.pdf	30520 9b38fa80e8f3e943269e3afeaa7a9cab53767751	no	2
Warnings:					
Information:					
		Total Files Size (in bytes):	476283		

This Acknowledgement Receipt evidences receipt on the noted date by the USPTO of the indicated documents, characterized by the applicant, and including page counts, where applicable. It serves as evidence of receipt similar to a Post Card, as described in MPEP 503.

New Applications Under 35 U.S.C. 111

If a new application is being filed and the application includes the necessary components for a filing date (see 37 CFR 1.53(b)-(d) and MPEP 506), a Filing Receipt (37 CFR 1.54) will be issued in due course and the date shown on this Acknowledgement Receipt will establish the filing date of the application.

National Stage of an International Application under 35 U.S.C. 371

If a timely submission to enter the national stage of an international application is compliant with the conditions of 35 U.S.C. 371 and other applicable requirements a Form PCT/DO/EO/903 indicating acceptance of the application as a national stage submission under 35 U.S.C. 371 will be issued in addition to the Filing Receipt, in due course.

New International Application Filed with the USPTO as a Receiving Office

If a new international application is being filed and the international application includes the necessary components for an international filing date (see PCT Article 11 and MPEP 1810), a Notification of the International Application Number and of the International Filing Date (Form PCT/RO/105) will be issued in due course, subject to prescriptions concerning national security, and the date shown on this Acknowledgement Receipt will establish the international filing date of the application.

PART B - FEE(S) TRANSMITTAL

Complete and send this form, together with applicable fee(s), by mail or fax, or via EFS-Web.

By mail, send to: Mail Stop ISSUE FEE
Commissioner for Patents
P.O. Box 1450
Alexandria, Virginia 22313-1450

By fax, send to: (571)-273-2885

INSTRUCTIONS: This form should be used for transmitting the ISSUE FEE and PUBLICATION FEE (if required). Blocks 1 through 5 should be completed where appropriate. All further correspondence including the Patent, advance orders and notification of maintenance fees will be mailed to the current correspondence address as indicated unless corrected below or directed otherwise in Block 1, by (a) specifying a new correspondence address; and/or (b) indicating a separate "FEE ADDRESS" for maintenance fee notifications.

CURRENT CORRESPONDENCE ADDRESS (Note: Use Block 1 for any change of address)

500 7590 06/18/2020

SEED INTELLECTUAL PROPERTY LAW GROUP LLP
701 FIFTH AVE
SUITE 5400
SEATTLE, WA 98104

Note: A certificate of mailing can only be used for domestic mailings of the Fee(s) Transmittal. This certificate cannot be used for any other accompanying papers. Each additional paper, such as an assignment or formal drawing, must have its own certificate of mailing or transmission.

Certificate of Mailing or Transmission

I hereby certify that this Fee(s) Transmittal is being deposited with the United States Postal Service with sufficient postage for first class mail in an envelope addressed to the Mail Stop ISSUE FEE address above, or being transmitted to the USPTO via EFS-Web or by facsimile to (571) 273-2885, on the date below.

(Typed or printed name)
(Signature)
(Date)

APPLICATION NO.	FILING DATE	FIRST NAMED INVENTOR	ATTORNEY DOCKET NO.	CONFIRMATION NO.
15/550,995	08/14/2017	Chaohong Hu	850231.401USPC	1813

TITLE OF INVENTION: Antibody-Drug Conjugate

APPLN. TYPE	ENTITY STATUS	ISSUE FEE DUE	PUBLICATION FEE DUE	PREV. PAID ISSUE FEE	TOTAL FEE(S) DUE	DATE DUE
nonprovisional	SMALL	$500	$0.00	$0.00	$500	09/18/2020

EXAMINER	ART UNIT	CLASS-SUBCLASS
CANELLA, KAREN A	1643	424-179100

1. Change of correspondence address or indication of "Fee Address" (37 CFR 1.363).

☐ Change of correspondence address (or Change of Correspondence Address form PTO/SB/122) attached.

☐ "Fee Address" indication (or "Fee Address" Indication form PTO/SB/47; Rev 03-09 or more recent) attached. **Use of a Customer Number is required.**

2. For printing on the patent front page, list
(1) The names of up to 3 registered patent attorneys or agents OR, alternatively,
(2) The name of a single firm (having as a member a registered attorney or agent) and the names of up to 2 registered patent attorneys or agents. If no name is listed, no name will be printed.

1 Seed IP Law Group LLP
2
3

3. ASSIGNEE NAME AND RESIDENCE DATA TO BE PRINTED ON THE PATENT (print or type)

PLEASE NOTE: Unless an assignee is identified below, no assignee data will appear on the patent. If an assignee is identified below, the document must have been previously recorded, or filed for recordation, as set forth in 37 CFR 3.11 and 37 CFR 3.81(a). Completion of this form is NOT a substitute for filing an assignment.

(A) NAME OF ASSIGNEE: SHANGHAI MIRACOGEN INC

(B) RESIDENCE: (CITY and STATE OR COUNTRY): Shanghai, China

Please check the appropriate assignee category or categories (will not be printed on the patent) : ☐ Individual ☒ Corporation or other private group entity ☐ Government

4a. Fees submitted: ☒ Issue Fee ☐ Publication Fee (if required) ☐ Advance Order - # of Copies _____

4b. Method of Payment: *(Please first reapply any previously paid fee shown above)*

☒ Electronic Payment via EFS-Web ☐ Enclosed check ☐ Non-electronic payment by credit card (Attach form PTO-2038)

☒ The Director is hereby authorized to charge the required fee(s), any deficiency, or credit any overpayment to Deposit Account No. 19-1090

5. **Change in Entity Status** (from status indicated above)

☐ Applicant certifying micro entity status. See 37 CFR 1.29

☐ Applicant asserting small entity status. See 37 CFR 1.27

☐ Applicant changing to regular undiscounted fee status.

NOTE: Absent a valid certification of Micro Entity Status (see forms PTO/SB/15A and 15B), issue fee payment in the micro entity amount will not be accepted at the risk of application abandonment.
NOTE: If the application was previously under micro entity status, checking this box will be taken to be a notification of loss of entitlement to micro entity status.
NOTE: Checking this box will be taken to be a notification of loss of entitlement to small or micro entity status, as applicable.

NOTE: This form must be signed in accordance with 37 CFR 1.31 and 1.33. See 37 CFR 1.4 for signature requirements and certifications.

Authorized Signature /Qing Lin/ Date August 27, 2020

Typed or printed name Qing Lin, Ph.D. Registration No. 53,937

Electronic Patent Application Fee Transmittal

Application Number:	15550995
Filing Date:	14-Aug-2017
Title of Invention:	Antibody-Drug Conjugate
First Named Inventor/Applicant Name:	Chaohong Hu
Filer:	Qing Lin/Barbara Hannon
Attorney Docket Number:	850231.401USPC

Filed as Small Entity

Filing Fees for U.S. National Stage under 35 USC 371

Description	Fee Code	Quantity	Amount	Sub-Total in USD($)
Basic Filing:				
Pages:				
Claims:				
Miscellaneous-Filing:				
Petition:				
Patent-Appeals-and-Interference:				
Post-Allowance-and-Post-Issuance:				
UTILITY APPL ISSUE FEE	2501	1	500	500

Description	Fee Code	Quantity	Amount	Sub-Total in USD($)
Extension-of-Time:				
Miscellaneous:				
			Total in USD ($)	**500**

Electronic Acknowledgement Receipt

EFS ID:	40400180
Application Number:	15550995
International Application Number:	
Confirmation Number:	1813
Title of Invention:	Antibody-Drug Conjugate
First Named Inventor/Applicant Name:	Chaohong Hu
Customer Number:	500
Filer:	Qing Lin/Barbara Hannon
Filer Authorized By:	Qing Lin
Attorney Docket Number:	850231.401USPC
Receipt Date:	27-AUG-2020
Filing Date:	14-AUG-2017
Time Stamp:	14:56:59
Application Type:	U.S. National Stage under 35 USC 371

Payment information:

Submitted with Payment	yes
Payment Type	CARD
Payment was successfully received in RAM	$500
RAM confirmation Number	E20208QE57331762
Deposit Account	
Authorized User	

The Director of the USPTO is hereby authorized to charge indicated fees and credit any overpayment as follows:

File Listing:

Document Number	Document Description	File Name	File Size(Bytes)/ Message Digest	Multi Part /.zip	Pages (if appl.)
1	Issue Fee Payment (PTO-85B)	401USPC_ISS_FEE.pdf	400830 d58e7c29e47ba7d1ca11907244468a45460 3e23e	no	1
Warnings:					
Information:					
2	Fee Worksheet (SB06)	fee-info.pdf	30071 29d6fa1b9f2aeae6a472fa4861661cc52afe7 809	no	2
Warnings:					
Information:					
		Total Files Size (in bytes):	430901		

This Acknowledgement Receipt evidences receipt on the noted date by the USPTO of the indicated documents, characterized by the applicant, and including page counts, where applicable. It serves as evidence of receipt similar to a Post Card, as described in MPEP 503.

New Applications Under 35 U.S.C. 111

If a new application is being filed and the application includes the necessary components for a filing date (see 37 CFR 1.53(b)-(d) and MPEP 506), a Filing Receipt (37 CFR 1.54) will be issued in due course and the date shown on this Acknowledgement Receipt will establish the filing date of the application.

National Stage of an International Application under 35 U.S.C. 371

If a timely submission to enter the national stage of an international application is compliant with the conditions of 35 U.S.C. 371 and other applicable requirements a Form PCT/DO/EO/903 indicating acceptance of the application as a national stage submission under 35 U.S.C. 371 will be issued in addition to the Filing Receipt, in due course.

New International Application Filed with the USPTO as a Receiving Office

If a new international application is being filed and the international application includes the necessary components for an international filing date (see PCT Article 11 and MPEP 1810), a Notification of the International Application Number and of the International Filing Date (Form PCT/RO/105) will be issued in due course, subject to prescriptions concerning national security, and the date shown on this Acknowledgement Receipt will establish the international filing date of the application.

UNITED STATES PATENT AND TRADEMARK OFFICE

UNITED STATES DEPARTMENT OF COMMERCE
United States Patent and Trademark Office
Address: COMMISSIONER FOR PATENTS
P.O. Box 1450
Alexandria, Virginia 22313-1450
www.uspto.gov

APPLICATION NO.	ISSUE DATE	PATENT NO.	ATTORNEY DOCKET NO.	CONFIRMATION NO.
15/550,995	10/06/2020	10792370	850231.401USPC	1813

500 7590 09/16/2020

SEED INTELLECTUAL PROPERTY LAW GROUP LLP
701 FIFTH AVE
SUITE 5400
SEATTLE, WA 98104

ISSUE NOTIFICATION

The projected patent number and issue date are specified above.

Determination of Patent Term Adjustment under 35 U.S.C. 154 (b)
(application filed on or after May 29, 2000)

The Patent Term Adjustment is 225 day(s). Any patent to issue from the above-identified application will include an indication of the adjustment on the front page.

If a Continued Prosecution Application (CPA) was filed in the above-identified application, the filing date that determines Patent Term Adjustment is the filing date of the most recent CPA.

Applicant will be able to obtain more detailed information by accessing the Patent Application Information Retrieval (PAIR) WEB site (http://pair.uspto.gov).

Any questions regarding the Patent Term Extension or Adjustment determination should be directed to the Office of Patent Legal Administration at (571)-272-7702. Questions relating to issue and publication fee payments should be directed to the Application Assistance Unit (AAU) of the Office of Data Management (ODM) at (571)-272-4200.

APPLICANT(s) (Please see PAIR WEB site http://pair.uspto.gov for additional applicants):

Chaohong Hu, SHANGHAI, CHINA;
SHANGHAI MIRACOGEN INC, SHANGHAI, CHINA

The United States represents the largest, most dynamic marketplace in the world and is an unparalleled location for business investment, innovation, and commercialization of new technologies. The USA offers tremendous resources and advantages for those who invest and manufacture goods here. Through SelectUSA, our nation works to encourage and facilitate business investment. To learn more about why the USA is the best country in the world to develop technology, manufacture products, and grow your business, visit SelectUSA.gov

To: USPTOeAction@SeedIP.com,pairlinkdktg@seedip.com,
From: PAIR_eOfficeAction@uspto.gov
Cc: PAIR_eOfficeAction@uspto.gov
Subject: Private PAIR Correspondence Notification for Customer Number 500

Sep 17, 2020 04:15:51 AM

Dear PAIR Customer:

SEED INTELLECTUAL PROPERTY LAW GROUP LLP
701 FIFTH AVE
SUITE 5400
SEATTLE, WA 98104
UNITED STATES

The following USPTO patent application(s) associated with your Customer Number, 500 , have new outgoing correspondence. This correspondence is now available for viewing in Private PAIR.

The official date of notification of the outgoing correspondence will be indicated on the form PTOL-90 accompanying the correspondence.

Disclaimer:
The list of documents shown below is provided as a courtesy and is not part of the official file wrapper. The content of the images shown in PAIR is the official record.

Application	Document	Mailroom Date	Attorney Docket No.
15550995	ISSUE.NTF	09/16/2020	850231.401USPC

To view your correspondence online or update your email addresses, please visit us anytime at https://sportal.uspto.gov/secure/myportal/privatepair.

If you have any questions, please email the Electronic Business Center (EBC) at EBC@uspto.gov with 'e-Office Action' on the subject line or call 1-866-217-9197 during the following hours:

Monday - Friday 6:00 a.m. to 12:00 a.m.

Thank you for prompt attention to this notice,

UNITED STATES PATENT AND TRADEMARK OFFICE

PATENT APPLICATION INFORMATION RETRIEVAL SYSTEM